

UNIVERSITÀ
DEGLI STUDI
DI PADOVA

UNIVERSITÀ DEGLI STUDI DI PADOVA

DIPARTIMENTO DI CHIMICA BIOLOGICA

SCUOLA DI DOTTORATO DI RICERCA IN: BIOSCIENZE E BIOTECNOLOGIE

INDIRIZZO: BIOCHIMICA E BIOFISICA

CICLO XXIV

MASS SPECTROMETRY-BASED QUANTITATIVE PROTEOMICS TO STUDY PROTEOMES, PHOSPHOPROTEOMES AND INTERACTOMES

Direttore della Scuola: Ch.mo Prof. Giuseppe Zanotti

Coordinatore d'indirizzo: Ch.mo Prof. Maria Catia Sorgato

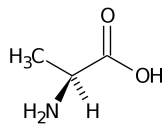
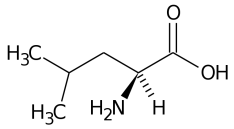
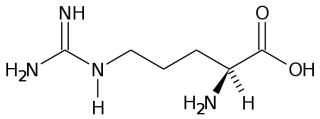
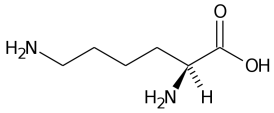
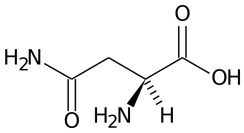
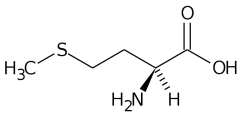
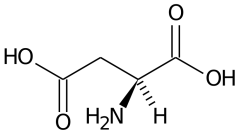
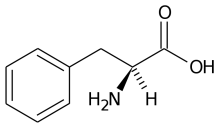
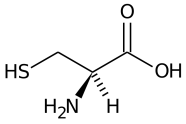
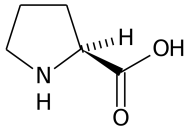
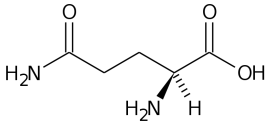
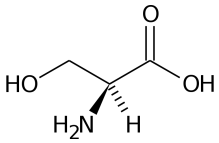
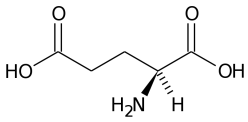
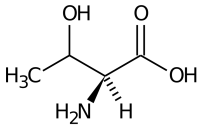
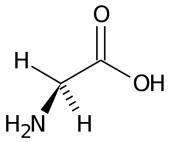
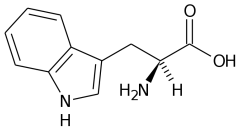
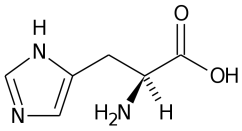
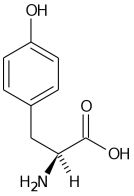
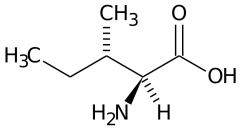
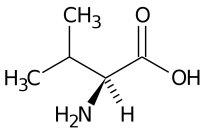
Supervisore: Dr. Giorgio Arrigoni

Dottorando: Cinzia Franchin

ABBREVIATIONS

1D-SDS PAGE	One Dimensional Sodium Dodecyl Sulfate-Polyacrylamide Gel Electrophoresis
2-DE	Two Dimensional Electrophoresis
ALP	Alkaline Phosphatase Activity
ATP	Adenosine-5'-triphosphate
BPC	Base Peak Chromatogram
BSA	Bovine Serum Albumin
BVIC	Bovine Interstitial Aortic Valve Cells
CID	Collision Induced Dissociation
CK2	Casein Kinase 2
CTRL	Control
E.C.	Enzyme Class
ETD	Electron Transfer Dissociation
GTP	Guanosine-5'-triphosphate
HPLC	High Performance Liquid Chromatography
IPI	International Protein Index
iTRAQ	Isobaric Tag for Relative and Absolute Quantitation
K_i	Inhibition Constant
LC	Liquid Chromatography
LC-MS	Liquid Chromatography-Mass Spectrometry
LC-MS/MS	Liquid Chromatography- Tandem Mass Spectrometry
LPS	Lipopolysaccharide
LPS-R	Lipopolysaccharide plus L-Arginine
LTQ	Linear Trap Quadrupole
MS	Mass Spectrometry
MSA	Multi Stage Activation
Q-TOF	Quadrupole-Time Of Flight
Q1	Quinalizarin
SCX	Strong Cation Exchange
SILAC	Stable Isotope Labeling with Amino Acids in Cell Colture
VIC	Interstitial Aortic Valve Cells

AMINO ACIDS

Alanine	Ala	A		A	Leucine	Leu	L	
Arginine	Arg	R		R	Lysine	Lys	K	
Asparagine	Asn	N		N	Methionine	Met	M	
Aspartic Acid	Asp	D		D	Phenylalanine	Phe	F	
Cysteine	Cys	C		C	Proline	Pro	P	
Glutamine	Gln	Q		Q	Serine	Ser	S	
Glutamic Acid	Glu	E		E	Threonine	Thr	T	
Glycine	Gly	G		G	Tryptophan	Trp	W	
Histidine	His	H		H	Tyrosine	Tyr	Y	
Isoleucine	Ile	I		I	Valine	Val	V	

CONTENTS

ABBREVIATIONS **2**

AMINO ACIDS **3**

CONTENTS **4**

ABSTRACT **6**

RIASSUNTO **7**

CHAPTER 1 ..... **8**

MASS SPECTROMETRY-BASED PROTEOMICS 8

1.1 Protein Analysis by Liquid Chromatography-Mass Spectrometry *9*

1.2 Mass Spectrometry-Based Quantitative Proteomic Approaches *10*

1.3 Label-Free Quantitative MS Analysis *11*

1.3.1 Relative quantification by peak intensity of LC-MS 12

1.3.2 Relative quantification by spectral count 14

1.3.3 Progenesis LC-MS 14

1.4 Quantitative MS Analyses Based on Stable Isotope Labeling *17*

1.4.1 Metabolic Labeling: SILAC 17

1.4.2 Enzymatic Labeling 20

1.4.3 Chemical Labeling: iTRAQ and TMT 21

1.5 Targeted Protein Quantification *23*

CHAPTER 2 ..... **26**

QUANTITATIVE PROTEOMICS ANALYSIS TO INVESTIGATE THE CALCIFICATION PROCESS IN CLONAL INTERSTITIAL AORTIC VALVE CELLS 26

2.1 Introduction *27*

2.1.1 Molecular Basis of Valvular Calcification 28

2.1.2 L-Arginine Metabolism is Involved in VIC Calcification 30

2.2 Aims of the Study *32*

2.3 SILAC analysis of BVIC *33*

2.3.1 Determination of the Incorporation Time 33

2.3.2 Arginine-to-Proline Conversion 34

2.3.3 SILAC Experimental Workflow 37

2.3.4 SILAC Results: Technical and Biological Reproducibility 38

2.3.5 SILAC Results: Bioinformatics and Pathway Analyses 42

2.4 iTRAQ Analysis of BVIC *45*

2.4.1 iTRAQ Experimental Workflow 45

2.4.2 iTRAQ Results: Technical Reproducibility 46

2.4.3 iTRAQ Results: Bioinformatics and Pathway Analyses 48

2.5 SILAC vs iTRAQ: Comparison of Methods *51*

2.6 Discussion *53*

2.7 Conclusions *58*

CHAPTER 3 ..... **59**

QUANTITATIVE PROTEOMICS ANALYSIS TO INVESTIGATE THE CK2-DEPENDENT INTERACTOMES AND PHOSPHOPROTEOMES 59

3.1 Introduction *60*

3.2 The Protein Kinase CK2 ..... *63*

3.3 CK2 as a Druggable Target *67*

3.4 Aims of the Study *70*

3.5 Label-Free MS Analysis of CK2 Interactomes *71*

3.5.1 Evaluation of System Reproducibility and Linearity 71

3.5.2 Experimental Workflow 74

3.5.3 Bioinformatics and Pathway Analyses 76

3.5.4 Discussion 78

3.5.5 Conclusions 81

3.6 SILAC Analyses of CK2-dependent Phosphoproteomes ... *82*
3.6.1 Global Protein Expression Analysis: Experimental Workflow ... 82
3.6.2 Evaluation of Labeling Efficiency ... 84
3.6.3 Global Protein Expression: Technical and Biological Reproducibility ... 86
3.6.4 Global Protein Expression: Bioinformatics and Pathway Analyses ... 94
3.6.5 Phosphoproteomics Analysis: Experimental Workflow ... 99
3.6.6 Phosphoproteomics: Technical and Biological Reproducibility ... 101
3.6.7 Phosphoproteomics: Bioinformatics and Pathway Analyses ... 106
3.6.8 Discussion ... 108
3.6.9 Conclusions ... 116

CHAPTER 4 ... 117
MATERIALS AND METHODS ... 117
4.1 Extraction of Cytosol and Nuclei from LAMA84 Cells ... *118*
4.2 Immunoprecipitation ... *118*
4.3 In-gel protein digestion ... *119*
4.4 SILAC on HEK 293 T Cells ... *119*
4.5 Phosphopeptides Enrichment with TiO_2 ... *120*
4.6 SILAC on Bovine Interstitial Aortic Valve Cells ... *121*
4.7 iTRAQ on Bovine Interstitial Aortic Valve Cells ... *122*
4.8 LC-MS/MS Analysis ... *123*
4.9 Data Analysis ... *124*

REFERENCES ... 126
PROTEIN DATA BANK (PDB) REFERENCES ... 135

APPENDIX ... 136
TABLE 1: List of Proteins Identified and quantified in SILAC BVIC experiment. ... *137*
TABLE 2: List of Proteins Identified and quantified in iTRAQ BVIC experiment. ... *150*
TABLE 3: List of Putative Interacting Partners of CK2. ... *170*
TABLE 4: Annotated List of Putative Interacting Partners of CK2. ... *173*
TABLE 5: Proteins Identified and Quantified in SILAC HEK 293 T - Global Protein Expression Analysis ... *177*
TABLE 6: Proteins Identified and Quantified in SILAC HEK 293 T - Phosphoproteome Analysis ... *215*

ABSTRACT

Over the past few years, mass spectrometry-based proteomics has been widely applied to the most diverse fields of biochemistry, biomedicine and biology, and several approaches have been developed to allow absolute and relative quantification of proteins in very complex mixtures. During my PhD, I have conducted three main studies, taking advantage of different quantitative proteomics techniques. In particular SILAC and iTRAQ approaches have been exploited to investigate the calcification process induced by endotoxin in clonal interstitial aortic valve cells, while SILAC and label-free quantitative approaches have been exploited to identify new potential interacting partners and substrates of the protein kinase CK2.

Calcific aortic valve disease represents the most common type of valvular disease and the first cause of surgical valve replacement in the industrialized world. No medical therapies are available to prevent or slow down calcium deposition within the valve leaflets, therefore surgery is the only possible treatment. To investigate the molecular mechanisms underlying the calcification process, SILAC and iTRAQ proteomics approaches have been applied to bovine interstitial aortic valve cells, a cellular model that is able to acquire a pro-calcific profile and drive matrix mineralization upon treatment with an inflammatory stimulus like the endotoxin lipopolysaccharide (LPS). The application to the same cellular model of two different quantitative technologies, led to the identification and relative quantification of hundreds of proteins, among which many showed a significant alteration in response to LPS. The acquired data suggest that cellular oxidoreductase activity, cytoskeletal and spliceosome regulation, glycolisis/gluconeogenesis, and arginine metabolism are altered during the acquisition of the pro-calcific profile. These results represent a starting point to investigate more in detail the molecular mechanisms that seem to be strongly involved in the calcification process induced by LPS.

The other projects described in this thesis focus on CK2, an essential, constitutively active and highly pleiotropic protein kinase. CK2, like many other kinases, is strongly involved in several cellular processes, and in particular it has been hypothesized that this enzyme plays a crucial role in the transduction of survival signals. However, a clear comprehension of the multiple roles played by this kinase within the cell has not been achieved. The aim of these projects was the identification of interacting partners and substrates of CK2 by means of proteomics approaches to try to shed some light on the functions performed by this kinase. In particular a combination of immunoprecipitation experiments and label-free quantitative analyses has been performed to identify new potential interacting partners of CK2, while the SILAC technology, in combination with the use of a specific and potent inhibitor of CK2, was exploited to identify new putative substrates of this kinase directly in a cellular system. The results obtained confirm the notion that CK2 plays a role in many fundamental cellular functions and clearly indicate a strong involvement of this kinase in the biological processes of protein biosynthesis and degradation. Moreover interesting aspects linked to phosphorylation/dephosphorylation turnover rates emerged from these analyses. A detailed discussion, from a technical and biological point of view, of the data collected is presented.

Finally, during my PhD I also collaborated to a project aiming at the identification of the primary molecular targets of antimicrobial photodynamic therapy. This work, not discussed in the thesis, has recently been submitted to the "Journal of Proteomics" with the title: "*Molecular Targets of Antimicrobial Photodynamic Therapy Identified by a Proteomic Approach*".

RIASSUNTO

Negli ultimi anni, la ricerca proteomica basata sulla spettrometria di massa è stata applicata in modo esponenziale ai più diversi campi della biochimica, biomedicina e biologia, permettendo il parallelo sviluppo di nuovi approcci per la quantificazione relativa e assoluta delle proteine.
Nel corso del mio dottorato, ho seguito lo sviluppo di tre progetti principali, sfruttando diverse tecniche di spettrometria quantitativa. In particolare, le tecnologie SILAC e iTRAQ sono state applicate allo studio del processo di calcificazione delle cellule interstiziali delle valvole aortiche, mentre i metodi SILAC e di quantificazione label-free sono stati sfruttati per l'identificazione di potenziali interattori e substrati della protein chinasi CK2.

La calcificazione delle valvole aortiche è una delle più comuni patologie valvolari e prima causa di sostituzione valvolare nei paesi industrializzati. A oggi sfortunatamente non esistono terapie che possano prevenire o curare la deposizione di calcio nelle valvole aortiche, e l'unica soluzione è l'intervento chirurgico. Per chiarire le basi molecolari di questo processo, abbiamo applicato le metodiche SILAC e iTRAQ ad un modello cellulare basato su cellule valvolari cardiache bovine (BVIC), in grado di acquisire un profilo pro-calcifico e favorire la mineralizzazione della matrice extra-cellulare in risposta ad uno stimolo infiammatorio come l'endotossina lipopolisaccaride (LPS). L'utilizzo di due diverse tecnologie allo stesso modello cellulare ha permesso l'identificazione, e la relativa quantificazione, di centinaia di proteine, parecchie delle quali mostrano una significativa alterazione in risposta al trattamento con LPS. L'analisi dei dati ha infatti rivelato l'alterazione di proteine appartenenti a diversi processi cellulari, quali la regolazione del citoscheletro, dei meccanismi ossidoriduttivi e dello spliceosoma, la via metabolica della glicolisi/gluconeogenesi, e il metabolismo dell'arginina, suggerendo il coinvolgimento di queste vie nel fenomeno della calcificazione delle valvole aortiche.
Questi risultati rappresentano perciò un punto di partenza per nuovi dettagliati studi dei meccanismi molecolari alla base della calcificazione valvolare indotta da LPS.

Gli altri progetti descritti in questa tesi sono focalizzato su CK2, una protein chinasi essenziale, altamente pleiotroica e costitutivamente attiva, fortemente implicata in una moltitudine di processi cellulari, in particolare nella trasduzione dei segnali di sopravvivenza, per la quale sembra giocare un ruolo chiave. Tuttavia una completa comprensione del ruolo che CK2 ricopre nei vari processi cellulari in cui è implicata non è ancora stata raggiunta, perciò questo lavoro ha come scopo l'identificazione di nuovi potenziali interattori e substrati di CK2, allo scopo di chiarire maggiormente la sua funzione all'interno della cellula. Nello specifico, abbiamo abbinato esperimenti d'immunoprecipitazione e analisi quantitativa label-free per lo studio delle proteine che interagiscono con CK2, mentre la tecnologia SILAC combinata con l'uso di un inibitore potente e specifico di CK2 è stata applicata alla ricerca di nuovi potenziali substrati di questa chinasi direttamente in un sistema cellulare. I risultati ottenuti confermano le conoscenze già note riguardo al coinvolgimento di CK2 in diversi processi essenziali per la vita cellulare, e fanno emergere chiaramente un coinvolgimento di primo piano di CK2 nei processi di biosintesi e degradazione proteica. Inoltre, l'analisi dei dati ha anche rivelato interessanti ed inattesi aspetti del turnover di fosforilazione/defosforilazione di proteine fosforilate da CK2. I dati ottenuti sono dettagliatamente presentati in questa tesi, da un punto di vista sia tecnico che biologico.

Infine, durante il dottorato ho anche collaborato alla realizzazione di un progetto volto all'identificazione di bersagli molecolari nella terapia fotodinamica antimicrobica, utilizzando un approccio proteomico. Da questa collaborazione, è nato un lavoro (non descritto in questa tesi) che è stato recentemente sottoposto a "Journal of Proteomics" con il titolo: "*Molecular Targets of Antimicrobial Photodynamic Therapy Identified by a Proteomic Approach*".

CHAPTER 1

MASS SPECTROMETRY-BASED PROTEOMICS

1.1 Protein Analysis by Liquid Chromatography-Mass Spectrometry

Nowadays, several mass spectrometry-based technologies are available for the analysis of proteins and many others are under development. In the past decade Liquid Chromatography-Mass Spectrometry (LC-MS) based quantitative proteomic approaches have become increasingly popular and discovery-based proteomics efforts led to global analyses and the possibility to quantify protein expression differences between samples.
Basically, protein analysis can be divided into 3 approaches, depending on the integrity of the proteins analyzed.

1. The most widely used approach is **bottom-up proteomics**, where proteins are digested and converted into relative small peptides for identification and quantification; this approach, combined with chromatographic steps, is applicable to very complex protein mixtures (like total lysates) and allows to identify and/or quantify up to thousands of proteins in a single analysis. Nevertheless this technology suffers of some important limitations, among which the main difficulties are related to the analysis of post-translational modifications (PTM) under normal Collision Induced Dissociation (CID) conditions, the loss of information regarding protein isoforms or splicing variants, and the often inadequate analysis of samples characterized by large dynamic ranges.

2. **Top-down proteomics** measures intact proteins to obtain information about the whole molecule. Such approach is usually applied to purified proteins or, at best, to simple protein mixtures. Since intact proteins are analyzed and fragmented, this method is particularly suitable to acquire information regarding the exact protein sequence (in case for example of splice variants) or the localization of PTMs. Main difficulties are related to the high charge state of ions produced in the analysis and the requirement of high resolution instruments that can support fragmentation technologies alternative to CID, such as Electron Capture Dissociation (ECD) or Electron Transfer Dissociation (ETD) (*McLafferty et al, J. Am. Soc. Mass Spectrom. 2001*; *Mikesh et al, Biochim. Biophys. Acta. 2006*). These fragmentation methods allow to obtain informative MS/MS spectra even from very large peptides and are particularly suitable for the analysis of high charge state molecules.

3. The last approach, **middle-down proteomics**, is halfway within the two previously described methods, because proteins are cleaved (chemically or enzymatically) to produce

large peptides (>3 kDa) (*Siuti et al, Nature Methods 2007*). This method takes advantage of ECD or ETD technologies and chromatographic separations, and can therefore be applied to relative complex mixtures. Although being introduced only recently, this approach seems promising overall applied to the analysis of integral membrane proteins or very basic proteins, where the classical bottom-up proteomics approach with trypsin digestion leads to poor results.

For all the projects described in this work we have used the bottom-up proteomics approach, and in particular, three LC-MS-based quantitative strategies have been exploited: SILAC, iTRAQ, and Label-free analysis. A description of the main quantitative MS technologies will be presented here, focusing in particular on the three selected methods.

1.2 Mass Spectrometry-Based Quantitative Proteomic Approaches

The relative quantification of peptides between different samples or biological conditions is usually based either on label-free or stable isotope labeling techniques (*Ong et al, Nat. Chem. Biol 2005*), and results are generally expressed as "-fold changes".

Label-free approaches have broader proteome coverage and wider dynamic range than stable isotope labeling methods, but the latter approaches offer higher precision and accuracy in quantification (*Bantscheff et al, Anal. Bioanal. Chem. 2007*). Both label-free and stable isotope labeling are usually used for the relative quantification of proteins, between two or more samples. However, if used in combination with appropriate internal standards they can also be exploited for the absolute quantification of proteins, i.e the determination of the exact protein/peptide amount or concentration in a given sample.

The high number of developed MS approaches is basically due to the high heterogeneity of the proteins/peptides physicochemical properties that produce large differences in MS response (*Bantscheff et al, Anal. Bioanal. Chem. 2007*). Therefore there is no recognized "one-size-fits-all" method good for every quantitative analysis, and the right approach has to be selected every time depending on the biological problem under investigation. Many factors can influence the MS measurement of protein samples, like digestion efficiency, LC separation, ionization efficiency, and ion suppression. In fact, signal intensity strongly depends on the amount of peptide that is ionized and on the ionization efficiency. Some tricks like low flow rates (e.g. 100 nl/min) (*Bantscheff et al, Anal. Bioanal. Chem. 2007*; *Schmidt et al, J. of Amer. Soc. for Mass Spec. 2003*) and internal standards can reduce the ion suppression problem (*Annesley, Clin. Chem. 2003*; *Elliott et al, J.*

Mass Spec. 2009). These elements are not the only ones that need to be considered when quantitative MS analyses are performed: reproducibility of the chromatographic steps, separation peak capacity, resolving power of the mass spectrometer and mass accuracy are also essential issues in LC-MS-based analysis.

1.3 Label-Free Quantitative MS Analysis

A conceptually simple and advantageous approach to compare two or more samples in a quantitative manner is the label-free analysis, an approach that does not require any modification of proteins, or peptides with stable isotope-containing compounds, or the addiction of heavy isotope-labeled internal standards to the sample. Moreover, label-free relative quantification requires only minimal sample manipulation and can be applied to any kind of biological material (i.e. cells, tissues, biological fluids) (*Xie et al, J. Biol. Chem. 2011*).

This technique is based on the comparison of samples that are analyzed under the same conditions by a liquid chromatography-mass spectrometry approach. With this method each sample is separately prepared and subjected to individual LC-MS or LC-MS/MS runs and the quantitative data is obtained by a direct comparison of the chromatographic traces intended as the sum of individual peptides that elute from the column and are registered by the mass spectrometer at any given time (see Fig.1).

After recording the chromatograms and the associated MS and MS/MS spectra, protein quantification is obtained mainly using two types of measurement: the first, more sophisticated and accurate method is based on the comparison of peptide peak areas or peak heights in chromatography, while the second is based on the spectral counting of identified proteins after MS/MS analysis. Label-free quantitation is preferably applicable when relatively large-abundance changes between samples are expected (*Xie et al, J. Biol. Chem. 2011*) because this technique is particularly sensitive to instrumental variations (described in the next two paragraphs) and sample complexity. Thus, compared with isotope-labeling methods, label-free experiments need to be more carefully controlled, especially regarding the LC and MS system performances. For these reasons label-free quantification requires an instrumental set-up characterized by high reproducibility; fortunately, in the last few years the development of increasingly reproducible nano-HPLC systems and of dedicated software and the advent of high resolution and high mass accuracy mass spectrometers, has improved the reliability and accuracy of label-free quantification technology.

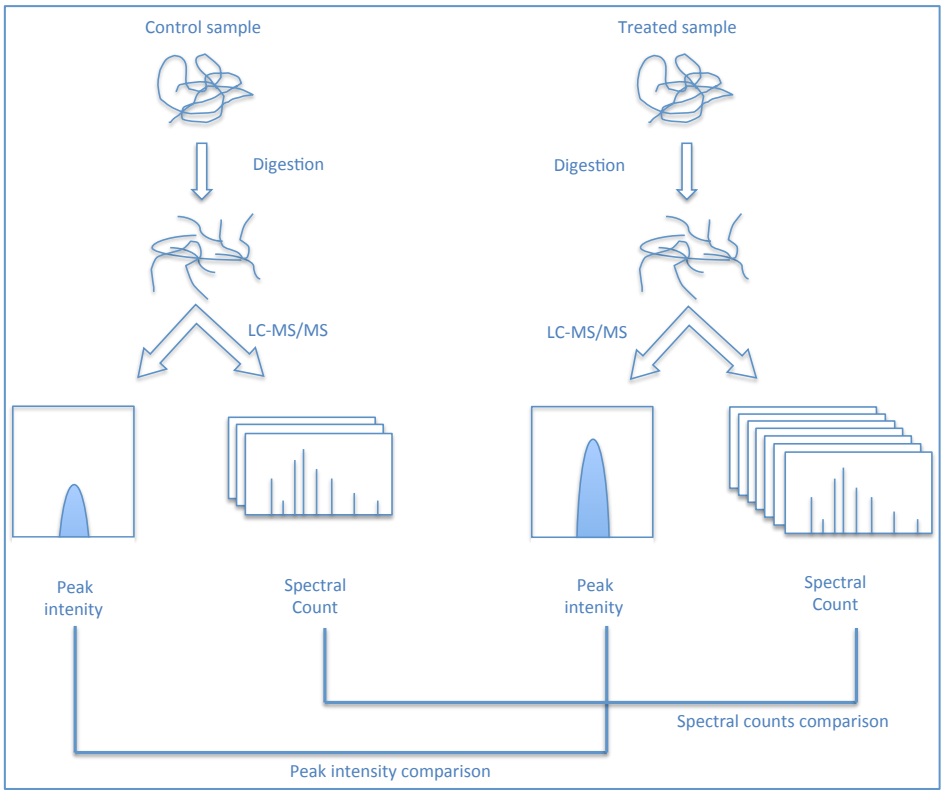


Figure 1 - Label-free quantitative analysis. Control and sample are separately prepared and subjected to LC-MS/MS analysis. Quantification is then based on the comparison of peak intensity of the same peptide, or on the spectral count of the same protein.

1.3.1 Relative quantification by peak intensity of LC-MS

It has been shown that a specific ion detected and recorded during a LC-MS run has a particular intensity at a particular retention time, and this intensity correlates with ion concentration (*Voyksner et al, Rapid Communication in Mass Spectrometry 1999*).

Peak intensity quantification is based on the comparison of mass scans and follows a long pipeline of analysis where MS peaks are detected and combined into chromatographic peaks for each LC-MS run (peak picking), isotopic pattern of each peptide is recognized, alignment of the features is performed across runs (supported sometimes by MS/MS information), identification of peptides is performed using search engines like Mascot against a specific database and eventually quantification of samples among runs is calculated. Several studies conducted on standard proteins like myoglobin (*Chelius et al, J. of Proteome Research 2002*) demonstrated that the extracted and calculated chromatographic areas of identified peptides proportionally increase and decrease with the concentration of the injected peptides. If the areas of the chromatographic peaks relative to all

identified myoglobin peptides are combined and plotted against the protein amount, it is notable that such peak area linearly correlates with the protein concentration. Unfortunately, this easy approach has some important limitations when applied to complex biological samples.

For example, samples can show differences in peak intensities of the peptides from run to run, that can be due to experimental variations such as differences in sample preparation, ionization differences, sample injection, and unstable temperature. A limitation of this technology is related to the algorithms used for peak picking and alignment of the features that show their weakness overall when low-intensity signals must be detected and processed.

One of the major problems of label-free quantification is the limited reproducibility of the LC separation carried out with flow rates in the nl/min range and with capillary C_{18} stationary phase columns, reproducibility that decreases proportionally with the increase of the run time. In fact, repeated injections of the same sample can display variations in elution time of the single components from seconds to minutes, leading to problems in peak alignment and thus resulting in large variability and inaccuracy in quantification (*Zhu et al, J. of Biomedicine and Biotechnology 2010*). Limited stability of nano-ESI ionization sources is another major cause of ion intensities fluctuations observable in repeated runs. Moreover, not all the peptides, even belonging to identical samples, necessarily appear in all the runs due to different ionization processes and ion suppression effects and sometimes inversion of retention times can occur during the LC separation of very complex mixtures; as a consequence several peptide signals do not have a partner in other comparing samples and the correct alignment of features among runs can be particularly difficult. These problems can be partially overcome by the application of a LC- system that exploits a Chip-based technology (such as the one we have used in our study) characterized by the absence of dead volumes in the hydraulic circuits and the high stability of spray conditions.

Software reliability in detecting and processing signals and LC system reproducibility are not the only factors influencing the outcome of a label-free quantitative analysis. Mass accuracy and resolution of the mass spectrometer used are essential factors for a successful analysis: they are essential for the correct alignment of features during the data-processing step because strongly facilitate feature extractions and comparison among samples. Moreover they help in distinguish signals due to co-eluting peptides with similar masses. Finally high mass accuracy strongly increases the possibility to correctly identify the proteins when MS/MS data are submitted to a search engine.

Considering all the above-mentioned problems related to data reproducibility and data processing and analysis, it is important to reduce the variability of the analysis as much as possible by using the correct technological precautions. At the same time, for a correct quantification process it is

essential to perform several biological as well as technical replicates (by analyzing the same sample several times under the same conditions) to obtain enough information for applying normalization and statistical models that will eventually lead to reliable quantitative results. Of course, the role of dedicated software that can correctly handle and compare LC-MS/MS data is of primary importance in the label-free quantitative analysis based on peak intensity.

1.3.2 Relative quantification by spectral count

The spectral counting approach, relatively quantify the proteins by comparing the number of identified MS/MS spectra from the same protein in each of the multiple LC-MS/MS. This method is based on the fact that, increasing a protein abundance, the number of its proteolytic peptides detected and fragmented into the mass spectrometer also increases, and this usually results in an increase of protein sequence coverage and total number of identified MS/MS spectra (spectral count) for each protein (*Washburn et al, Nature Biotechnology 2001*).

This method shows its main limitations in case of low abundant proteins, where the small number of spectral counts leads to a less robust or even unreliable quantitative measurement, overall when very complex samples are analyzed and undersampling is an issue (*Zhou et al, J. of Proteome Res. 2010*).

The advantage of using the spectral counting approach in place of the chromatographic peak intensity comparison, which requires delicate computer algorithms for aligning and comparing peaks, is that no specific tools or algorithms have been specially developed for spectral counting, due to its ease of implementation. However, also in this case normalization and statistical analysis of spectral counting datasets are necessary for reliable detection of protein changes in complex mixtures (*Dong, Science 2007*). It is important to highlight here that the spectral counting method, although easy to use and implement, leads to less confident quantitative results if compared with the peak intensity comparison method.

1.3.3 Progenesis LC-MS

Due to the limited requirements of sample manipulation and to its conceptual simplicity, label-free quantification approaches have becoming increasingly popular and the development of dedicated software and algorithms is constantly in evolution. Several specific software for label-free quantitative analysis are available, commercially or as open-source packages. Progenesis LC-MS

(*Nonlinear Dynamics*), SuperHirn (*Mueller et al, Proteomics 2007*) VIPER (*Monroe et al, Bioinformatics 2007*) or tools inserted in packages dedicated to quantitative proteomics data analysis like Mascot Distiller (Matrix Science), MaxQuant (*Cox et al, Nat. Biotechnol. 2008*), and OpenMS (www.openms.de) are only few examples of informatics tools that have been developed for this purpose. The data collected with a label-free approach and discussed in this thesis (see "*Label-free analysis of CK2 interactome*" chapter) have been analyzed using the commercial software Progenesis, therefore we will focus here on the description of the way this software works and deals with LC-MS/MS data, and how information regarding the relative quantification of proteins between samples is achieved.

Progenesis (Nonliner Dynamics, version 3.0) allows for relative protein quantification using the peak intensity approach of LC-MS data. In particular, the software combines and compares results from different LC-MS/MS runs, aligning them to compensate for between-run variations in the LC separation technique. The main steps of Progenesis LC-MS analysis are:

- Peak modeling: peaks are identified and peak models are created using a wavelet-based approach. This algorithm allows the retaining of the main quantification and positional information, reducing data files complexity.
- Run alignment: this is one of the most important steps because it allows to combine data from multiple LC-MS runs using retention time and mass information. The alignment is partially manually performed, creating several vectors based on visible spot maps that will be used by the software to perform the automatic alignment. The consensus map is then applied to all the features of the runs compensating for between-run variations in the LC separation technique.
- Peak picking: after the alignment, it is possible to create an aggregate data set to ensure a good match across all data files. The aggregate contains all the peak information from all the sample files, and it allows the detection of a single map of peptide ions, that is then applied to each sample. This is one of the limiting steps of the label-free analysis, because high sample complexity can lead to overlapping peptide ions.
- Ion abundance quantification: ion quantification is performed on MS scans using peak intensity quantification without considering the MS/MS information. This information can be added later, using a targeted inclusion list to improve the analysis and confirm the alignment. Data normalization is needed for final runs comparison.
- Statistical analysis of peptide ions: with this step, significant peptides are selected for identification through statistical tools like ANOVA, q-values, and power analysis.

- Peptide identification: all MS/MS data of peptides previously selected for identification are exported and used as input for search engines (e.g. mascot) and chosen databases.
- Review proteins of interest: quantitative data and qualitative fragmentation spectra are unified to obtain a peptide-based view of the identified proteins. Protein quantitation is based only on unique peptides to increase the reliability of the analysis, and an interesting option allows the selection of the best of these peptides and the creation of list of candidates for further SRM studies. This step also allows to filter the results deleting contaminants (e.g. keratins) and proteins under selected thresholds, or to apply more sophisticated filters. A final list of proteins with relative quantification and expression profiles is automatically created.
- Statistical analysis of protein data and report results: the last option of Progenesis is the multivariate statistical analysis on proteins measurement, a useful tool to generate a protein-based report of the experiment. Unfortunately this step, although very useful, is very slow and produces an extremely large report file that is difficult to manage for its size.

Once the list of proteins is ready, the discrimination between proteins that significantly change their expression between samples and false positives is needed. For this purpose a minimum threshold of fold-change has to be selected, and the choice is not standardized but is dependent on the instrumental and biological limits of the experiment performed, although in literature, the most used value of minimum fold-change is 1.5 (*Porteus et al, Appl. Microbiol. Biotechnol. 2011*). A big advantage of Progenesis is the fact that it can handle sets of LC-MS/MS data derived from a single sample subjected to multidimensional separation steps. Typical examples are the possibility to fractionate samples to be compared by 1D-SDS PAGE or Strong Cation Exchange (SCX) chromatography prior to LC-MS/MS analysis. Every fraction is analyzed independently from the others and, at the end of the process, Progenesis merges the data obtained from all the fractions into a single data set. Although very user-friendly, this software is a commercial product and therefore relies on algorithms and informatics tools that are not disclosed to be fully evaluated and optimized by the user. From one side therefore, Progenesis is very easy to use if compared to other non-commercial analogous software packages, but algorithms cannot be tuned using the specific characteristics of the instrumental set-up with which data are acquired.

1.4 Quantitative MS Analyses Based on Stable Isotope Labeling

Stable isotope labeling methods are based on the introduction of a modification in a protein or, more often, in a peptide sample, without changing the chemical properties of the labeled peptide compared to its native equivalent. The two peptides (labeled and unlabeled) should have the same chromatographic behavior and the same ionization characteristics in the MS, with a difference in mass due to the labels used (*Xie et al, J. Biol. Chem. 2011*). They can be therefore mixed before the analysis, remaining distinguishable by their masses. The intensities of the signals relative to the two peptides, as measured by MS, are therefore directly correlated with their abundance within the sample. The most used stable isotopes are ^{15}N, ^{13}C, and ^{18}O that can be incorporated into proteins or peptides by chemical, enzymatic, or metabolic reactions (*Zhang et al, J. Proteome Res. 2002*). After the labeling, samples are combined and analyzed simultaneously by LC-MS or LC-M/MS, so reducing the variability introduced by multiple injections of individual samples and enabling accurate quantification, more precise than that obtainable from the label-free approaches described above (*Xie et al, J. Biol. Chem. 2011*).

1.4.1 Metabolic Labeling: SILAC

The most used metabolic labeling approach is SILAC (Stable Isotope Labeling with Amino acids in Cell culture) that combined with high resolution and high accuracy mass spectrometers allows for the identification and quantification of hundreds or even thousands of proteins in a single experiment.

With this approach, cell lines are grown in a medium lacking one or more standard essential aminoacids (usually lysine and arginine) and supplemented with a non-radioactive, isotopically-labeled form of those aminoacids (usually containing ^{13}C and ^{15}N) (*Xie et al, J. Biol. Chem. 2011*). Thus, cells incorporate the "heavy" aminoacids during the synthesis of new proteins and such incorporation is carried on for several cell doublings. The growth of the cells maintained in this medium is not different from the growth in normal medium, as it is shown by cell morphology, doubling time, and ability to differentiate (*Ong et al, Mol. Cell. Proteomics 2002)*.

After harvesting, equal amounts of proteome belonging to the labeled and unlabeled cells are mixed at the level of either intact cells (i.e. the same number of cells from the two samples) or cell lysates

(i.e. equal amount of heavy and normal isotope-labeled proteins). The mixture is finally digested with one or more enzymes (usually trypsin) and analyzed using the mass spectrometer (*Xie et al, J. Biol. Chem. 2011*).

Every peptide will appear in the spectrum as a doublet: a light unlabeled peptide and a heavy labeled peptide. The signal intensities recorded by the MS are used for the quantification process. From the ratio measured for every peptide of a specific protein, it is possible to calculate the differential protein expression level in the two original conditions (*Ong et al, Mol. Cell. Proteomics 2002*).

Several labels (different forms of "heavy arginine, lysine and other aminoacids used less often like methionine or tyrosine) are available for the SILAC approach, allowing multiplex experiments where several samples or conditions are tested in parallel (*Xie et al, J. Biol. Chem. 2011*).

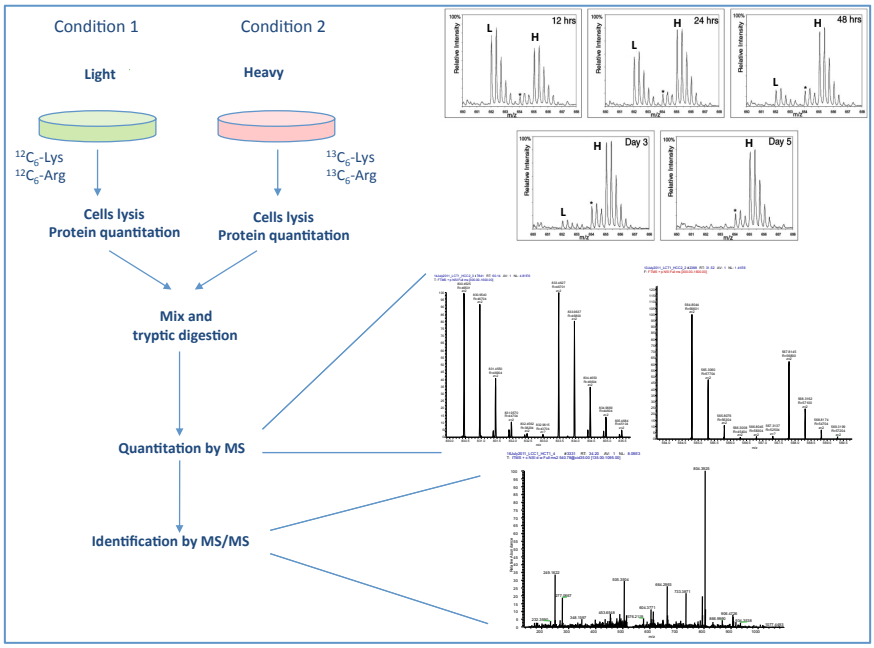


Figure 2 - SILAC experimental workflow (adapted from *Shao-En Ong, Molecular and Cellular Proteomics, 2002*)

SILAC is suitable for *in vivo* studies to quantify changes between samples (e.g. protein expression level or protein turnover) because isotopes are introduced in the cells trough a natural biosynthetic process, but this characteristic limits the applicability of this approach to tissues and biofluids analysis (*Xie et al, J. Biol. Chem. 2011*), although nowadays several studies on SILAC organisms are ongoing (e.g. SILAC mouse *Krüger et al, Cell. 2008*).

Differently to the label-free approach or other labeling-based methods, in SILAC experiments

samples are mixed at the beginning of the workflow, before any fractionation protocol and analysis, thus strongly reducing the variation due to repetitive runs or to the parallel processing of the samples to be compared. For this reason SILAC is recognized as the most accurate relative quantification method available for shotgun proteomics studies. The success of this approach is largely documented by the very high number of publications that have been produced employing this technology. However, as any other method, SILAC approach is not devoid of limits and drawbacks. Since samples are mixed and remain distinguishable during the MS analysis, this approach leads to an increased sample complexity and it usually requires preliminary fractionations and a high mass accuracy instruments for its successful application. Moreover, possible variations of physicochemical properties of labeled peptides caused by the heavy isotopes used, may result in retention time shifts during chromatographic separations, especially in experiments where deuterium is used as heavy element (*Zhang et al, Anal. Chem. 2001*). For this reason, proper informatics tools are needed to consider these shifts and correct the alignment of heavy/light peptide couples, and the accurate selection of heavy amino acids needs to be considered before starting a SILAC experiment. In fact, retention time shifts is not the only problem connected with the use of heavy amino acids. Another problem derives from the use of arginine as heavy amino acid. It has been shown that metabolic conversion of arginine to proline can occur in the cell, and in the case of heavy arginine conversion the resulting proline will be isotopically labeled. This effect can deeply affect the quantification of proline-containing peptides, overall when several proline residues are present within the same peptide (*Lössner et al, Anal. Biochem. 2011*). It is possible to significantly reduce this arginine to proline conversion by supplementing the standard SILAC medium with unlabeled proline. The high availability of proline induces cells to directly absorb it, without the need of metabolically producing that amino acid (*Lössner et al, Anal. Biochem. 2011*). Alternatively, if this metabolic conversion cannot be avoided because of limitations related to the particular experimental conditions, the problem can be bypassed by the use of lysine as the only heavy amino acid for cell labeling. This solution requires Lys-C as digesting enzyme in place of the more common (and definitely less expensive) trypsin. As a result, the average size of the peptides produced after protein digestion is bigger than that obtained with trypsin and MS analysis becomes less efficient because of the poorer fragmentation spectra obtainable under standard CID conditions. Another limit of the SILAC approach is the possible difficulty in correctly coupling light and heavy peptide pairs in very complex peptide mixtures. The software developed for SILAC analysis are designed to recognize for each peptide the correspondent heavy or light signal, with a shift in the m/z value that depends on the heavy amino acids contained in the sequence and the charge state of the peptide. This operation is often difficult because of the high number of signals in a small mass

range (samples with high complexity) or by a big difference in intensity between heavy and light peptides and can only be partially overcome by the use of high resolution instruments.
Finally, incomplete cell labeling represents an issue of potential strong impact on SILAC experiments. Before performing the actual experiment, every cell line needs to be properly tested to estimate the minimum number of cell doublings that are necessary to obtain the complete labeling of all proteins. In literature, an average of 5 to 7 (*Ong et al, Nat. Prot. 2006*) passages is reported to be enough, but the turnover rate of proteins in different cell lines or different growing conditions can dramatically change this value. Long cell culturing periods increase the costs of the experiment both in terms of material and time (*Chen, Analytica Chimica Acta 2008*).
When the quantification is performed and final results are reported, a minimum fold-change significance threshold needs to be selected: in literature various cases of the use of universal fold-change thresholds are reported and the most widely used threshold for SILAC analysis in literature is a 1.5 fold change. Many of these works do not consider differences due to experimental processes and limits. Other more accurate studies use a fitting of the distribution of all the ratio values, but this limits the statistic analysis to the null hypothesis. Standard methods as Bonferroni correction or q-value calculation are also used, but the best absolute threshold does not exist and it needs to be decided specifically for each single experiment and biological aspect under investigation (*Margolin et al, Plos one 2009*). Obviously, also for this approach, as already mentioned for the label-free methods, biological and technical replicates are necessary to increase statistical confidence and robustness of the quantification process.

1.4.2 Enzymatic Labeling

Enzymatic labeling exploits the incorporation of ^{18}O atoms into the carboxyl terminus of each proteolytic peptide during or after protein digestion catalyzed by trypsin (*Stewart et al, Rapid Commun. Mass Spec. 2001*) or other proteases (*Yao et al, J. Proteome Res 2003*) in presence of ^{18}O water ($H_2{}^{18}O$). Just like label-free approaches, the enzymatic labeling is also simple, relatively cheap and applicable to all types of biological samples, and many software are available for data analysis (*Qian et al, Mol. Cell. Proteomics 2005*). However, although this would appear as an economic alternative to other labeling techniques, many disadvantages are correlated with this method: different peptides often have different labeling efficiency, or are affected by incomplete labeling and ^{18}O back-exchange to ^{16}O (*Xie et al, J. Biol. Chem. 2011*). Recently, several studies reported an improved labeling efficiency obtained by adding boiling steps during the reaction (*Petritis et al, J. Proteome Res 2009*) or incubating directly the protease with peptides in presence

of $H_2{}^{18}O$ to prevent oxygen back conversion (*Qian et al, Mol. Cell. Proteomics 2005*; *Fenselau et al, J. Proteome Res. 2009*), but, probably because of these technical limitations, this quantitative method has never reached the popularity and the diffusion of other approaches.

1.4.3 Chemical Labeling: iTRAQ and TMT

Another stable isotope labeling strategy is based on chemical incorporation of isotope-containing tags into proteins or peptides. Several methods belonging to this class of labeling are currently used, but the first to be introduced was the isotope-coded affinity tag (ICAT) technology, based on reagents with a mass difference of 9 Da that react directly with the sulfhydryl group of cysteine residues (*Gygi et al, Nat. Biotech. 1999*). For this particular method, relative protein abundance is measured in MS mode. Recently, other reporters have been developed, allowing parallel analysis of multiple samples (*Bantscheff et al, Anal. Bioanal. Chem. 2007*).
Nowadays, the most used tags for peptide labeling are Isobaric Tags for Relative and Absolute Quantitation (iTRAQ) (*Ross et al, Mol. Cell. Proteomics 2004*; *Choe et al, Proteomics 2007*) and Tandem Mass Tags (TMT) (*Thompson et al, Anal. Chem. 2003*; *Dayon et al, Anal. Chem. 2008*), that specifically react with the free primary amine groups of tryptic peptides, i.e the N-terminus and the side chain of lysine residues. These reagents have the characteristic to be available in different isobaric forms so when a specific peptide is labeled with different tags, the final products will have the same mass, therefore appearing as a single peak during MS analysis and as a single peak during a chromatographic analysis, since the labeled peptides also have the same chromatographic behavior. However, upon fragmentation in MS/MS mode, the different tags generate specific reporter ions in a zone of the spectrum lacking the presence of sequence-specific fragments. The intensities of the reporter ions can then be used to quantify the relative abundance of the corresponding peptides. Using this strategy therefore, digested proteins from different samples are labeled with different reagents, samples are mixed and usually analyzed by LC-MS/MS. Fragmentation spectra are then used to identify the peptides and to quantify them thanks to the presence of the reporter ions.

Both iTRAQ and TMT reagents are composed of three distinct parts: the peptide reacting group, the reporter group and the balance group. Balance and reporter groups are designed in such a way that their total mass is constant. The specific design of iTRAQ reagents coupled to a generic peptide is shown in Fig. 3.

The iTRAQ kit is commercialized in four or eight different reagents isotopically enriched (e.g. iTRAQ 114.1, 115.1, 116.1, and 117.1 for the fourplex iTRAQ kit), while TMT can address the analysis of two to six samples in parallel.

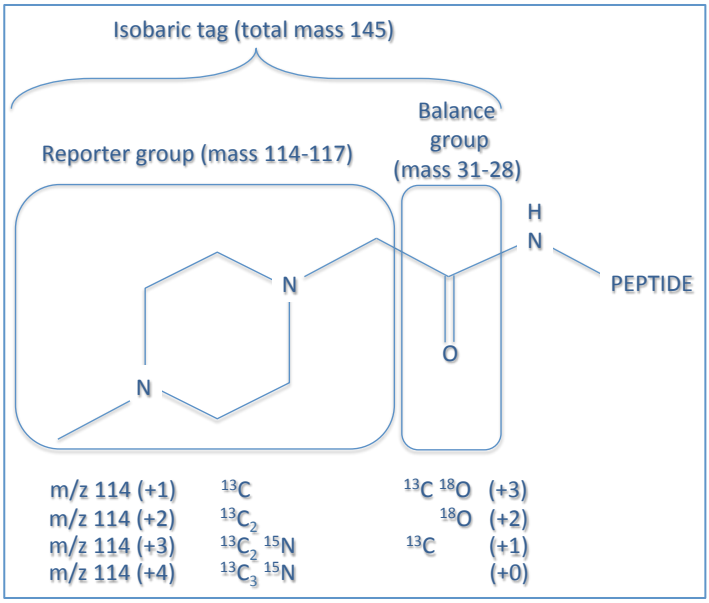


Figure 3 - Example of tetraplex isobaric tags.

These technologies are applicable to every kind of sample, but both require the ability to observe low mass over charge (*m/z*) fragment ions (i.e. the reporters), which limits the type of mass spectrometer that can be used (*Xie et al, J. Biol. Chem. 2011*).

A main advantage related to these methods is the fact that samples are mixed and analyzed in a single experiment. Up to 8 different samples can therefore be simultaneously analyzed and protein identification and quantification is achieved in a single step. Moreover, since peptides labeled with different tags are characterized by the same chromatographic behavior and by the same mass, mixing the sample before the analysis allows to increase the intensities of the signals.

Differently from the SILAC approach, for iTRAQ and TMT labeling is not performed on cells, but on peptides mixtures, thus they do not require the growth of cells with special expensive medium and heavy isotopes, that could in part affect cellular functions especially when the treatment is performed for long periods. However, these reagents are also expensive, especially considering the costs of a label-free approach, but the time saved and the possibility to multiplex makes in many cases iTRAQ or TMT very favorable strategies. The quantification process is also easier and more robust compared to SILAC, because peptide signals do not need to be correctly coupled at the MS

level and quantitative data are obtained directly from the MS/MS spectrum as intensities of reporter ions. Fragmentation spectra have a better signal-to-noise ratio compared with MS spectra, where background may strongly contribute to the total signal intensity and could lead to imprecise quantification, overall when low intensity signals are quantified. Therefore, iTRAQ and TMT technologies allow to obtain more precise quantifications (*Aggarwal et al, Brief. in Funct. Gen. and Proteomics 2006*). Thus, specific advantages for iTRAQ/TMT strategies include the preservation of post-translational modifications of peptides, an increased confidence on protein ID (due to a higher number of fragmented peptides compared to the SILAC approach, since the complexity of the sample is not affected), and a relatively easy data analysis without the need of complex software (*Chen, Analytica Chimica Acta 2008*). On the other hand, labeling with isobaric reagents occurs after protein extraction and digestion therefore the first part of the workflow of analysis must be conducted in parallel for all samples and this is a source of possible errors. Moreover, problems could be determined by a slight different labeling efficiency for the different reagents. This problem could be partially overcome by spiking a standard protein in equal amounts in all samples, before the digestion and the labeling process. In this way the quantitative values obtained for the internal standard can be used to normalize all other data. The presence in the MS spectrum of peptides with very similar masses could determine the co-selection of two or more peptides that, once fragmented, could lead to an incorrect quantification. As for all the other quantitative methods, also in this case quantification is obtained at the peptide level. Protein quantification is then obtained as an average or median value of all peptides belonging to the same protein. Moreover, as for every quantitative method, biological and technical replicates are necessary to achieve more confident and robust identifications and quantifications. iTRAQ and TMT experiments reported in literature usually consider a 1.5 fold change as the minimum threshold for significant difference between samples (*Aggarwal et al, Proteomics 2005*), however the correct threshold needs to be chosen for each specific experiment independently, taking into account systematic errors of the instruments used and all the limits connected with the biological samples under investigation.

1.5 Targeted Protein Quantification

In the past few years another class of quantitative proteomics approaches based on selected reaction monitoring (SRM) (or multiple reaction monitoring, MRM) has been developed to perform accurate quantification of selected analytes (*Xie et al, J. Biol. Chem. 2011*). SRM cannot be applied in a discovery study, because a list of known target ions to be measured is needed before starting the experiment. Thus, SRM is complementary to the shotgun method and is especially useful for the

quantification of low abundance proteins (that are scarcely detected with shotgun strategies) or for the confirmation of results obtained from discovery experiments (*Lange et al, Mol. Syst. Biol. 2008*).

The instrument required for targeted quantification is a triple quadrupole type, where the first quadrupole selects the precursor ion, that is then fragmented in the collision cell into ion fragments that are finally selected and analyzed in the last quadrupole. In particular the selected ions (generally unique peptides) are inserted as an input list of *m/z* values associated with the corresponding retention times, and for each ion one or several fragments are predicted. By monitoring only the predefined precursor-to-fragment ion transitions, a specific ion can be detected and quantified when it has the expected m/z value and produces the relative expected fragments (*Xie et al, J. Biol. Chem. 2011*). Considering and following only few transitions, the background noise is dramatically reduced, and the reproducibility is excellent, thanks also to the labeled synthetic peptides that can be used as internal standards (*Addona et al, Nat. Biotechnol. 2009*). Taking into account all these considerations, SRM is the quantitative proteomics method that has the highest sensitivity and the widest dynamic range that extends 4-5 orders of magnitude (*Duncan et al, Nat. Biotechnol. 2010*).

The possibility to absolute quantify proteins is one of the most important advantages of SRM and this service is achieved by the use of synthetic isotope-labeled target peptides in known concentration (*Gerber et al, PNAS 2003*): the native peptide concentration is determined by comparing ion intensities between labeled and unlabeled forms. However, this quantification may not reflect the true expression levels in the original sample, because the addition of internal standards after the enzymatic digestion does not correct for the variation occurring during sample preparation (*Havlis et al, Anal. Chem. 2004*). In this way, the quantitation is not really “absolute”. A solution to this problem is the addition of an isotope-labeled protein to the sample before starting its manipulation, combining the surrogate protein with the target one at the very beginning of the analytical process (*Xie et al, J. Biol. Chem. 2011*).

Generally, modified peptides cannot be detected by SRM unless specifically targeted. In fact, quantitative differences observed in the analysis of an unmodified peptide can be due to the change in abundance of the targeted protein in the samples or the (partial) modification of that particular peptide. Therefore, for reliable quantification, at least two peptides should be monitored for each targeted protein. If two peptides from the same protein reproducibly show divergent regulations, this could be indicative of the presence of post-translational modifications. SRM can also be applied to quantify peptides with post-translational modifications like phosphorylation (*Unwin et al, Mol. Cell Proteomics 2005*; Williamson et al, Mol. Cell. Proteomics 2006), ubiquitination (*Mollah et al,*

Rapid Commun. Mass Spectrom. 2007) or acetylation (*Griffiths et al, J. Am. Soc. Mass Spectrom. 2007*), provided that transitions for those peptides are established.

In conclusion, proteomics quantification is not a unique process, but it can involve relative and/or absolute abundance determinations across large sets of proteins. The most appropriate method needs to be selected depending on the biological problem under investigation and the sample available. As already mentioned, for the projects described in this thesis, we adopted SILAC, iTRAQ, and Label-free quantification strategies to performed our proteomic studies.

CHAPTER 2

QUANTITATIVE PROTEOMICS ANALYSIS TO INVESTIGATE THE CALCIFICATION PROCESS IN CLONAL INTERSTITIAL AORTIC VALVE CELLS

2.1 Introduction

Aortic valves are structures that are designed to work like one-way doors to allow the blood flow from one chamber or vessel to another, and then close to prevent the blood from regurgitating backward. The aortic valve consists of 3 half-moon–shaped pocket-like flaps of delicate tissue, named cusps, that are perfectly aligned when the valve is closed in order to separate the left ventricle from the aorta. Contractions of the ventricle (systole) pump the blood through the valve, opening the cusps, into the aortic system, while ventricle relaxing (diastole) induces the closure of the aortic valve, stopping the blood flow and bringing back the cusps to the original flat position. In this way the blood can flow from the left ventricle to the lungs through the left atrium across the mitral valve, thus refilling the ventricle for the next contraction (*Nishimura, Circulation 2002*). Several pathologies are associated to abnormalities of the cardiac valves, like valve stenosis (flow obstruction), valve regurgitation (a leakage backward), or combination of these two problems. These abnormalities usually cause a heart murmur and can easily be detected on physical examination with a stethoscope (*Nishimura, Circulation 2002*).

Other cardiac diseases are not due to a mechanical problem of the valves, but are caused by biological processes in the cardiac tissue. For example, the calcific degeneration of aortic valves is one of the most observed valvular diseases in the industrialized world (*Freeman et al, Circulation 2005*) that can also lead to valve stenosis (*Otto et al, Circulation 1997*; *Lindroos et al, Europ. Heart J. 1994*). Between the causes of aortic valve calcification there are high levels of low-density lipoprotein cholesterol (LDL) (*Pohle et al, Circulation 2001*), and some risk factors like age (over 65 years old, *Stewart et al, J. Am. Coll. Cardiol. 1997*), male gender, triglycerides, and smoking (*Mohler et al, Clin. Cardiol 1991*) that can increase the probability to develop aortic valvular diseases. Nowadays, there are no available therapies to prevent or reduce the calcium deposition on the valve leaflets, and the only possible treatment is surgery. Nevertheless, recent studies have challenged the idea of calcific aortic valve as an ineluctable and progressive phenomenon, and suggested a possible involvement of cell-driven processes in this disease (*O' Brien, Arterioscler. Thromb. Vasc. Biol. 2005*; *Demer et al, Circulation 2008*), opening the way to new therapeutic studies (*Otto, N. Eng. J. Med 2008*).

2.1.1 Molecular Basis of Valvular Calcification

In the past, the valvular calcification was considered as a degenerative disorder, involving the passive accumulation of calcium on the aortic valve tissue, but recently many studies have shown an active role of this biological process with a strong inflammation contribute in causing the calcification disease (*Kaden et al, J. Mol. Cell. Cardiol. 2004*; *Mohler et al, Circulation 2001*). A study on the inflammatory activation of human aortic valve interstitial cells in response to different stimuli (e.g. peptidoglycan (PGN) and lipopolysaccharide (LPS)) evidenced the activation of Toll-like receptors 2 and 4 that start the innate immunological response regulating the expression of proinflammatory mediators (*Meng et al, Am. J. Physiol. Cell. Physiol. 2008*). The same stimuli also up-regulate the expression of osteogenesis-associated factors (e.g. like BMP-2 and Runx2) supporting the idea that innate immunity is strongly involved in the aortic vale tissue inflammatory response and can contribute to the pathogenesis of valve leaflefts calcification (*Meng et al, Am. J. Physiol. Cell. Physiol. 2008*).

The largest fraction of the total cell population of the valve is composed of interstitial valve cells (VIC), with ultrastructural features that are intermediate between fibroblasts and vascular smooth muscle cells. Without a basal lamina VIC cells directly interact with collagen fibers, elastin microfibrils, and proteoglycans on the matrix (*Filip et al, Circulation Res. 1986*). Previous *in vitro and in vivo* experiments have shown that interstitial aortic valve cells from different animal species can acquire a pro-calcific profile and drive matrix mineralization in response to stimuli like inflammatory cytokines, modified lipids, reactive oxygen species (ROS), and other pathological factors (*O' Brien, Arterioscler. Thromb. Vasc. Biol. 2006*; *Akat et al, Heart 2009*). In fact, several studies conducted on calcific aortic valve lesions showed features typical of active pathobiological processes like chronic inflammation (*Otto et al, Circulation 1994*; *Olsson et al, J. Am. Coll. Cardiol. 1994*), lipoprotein deposition (*Walton et al, J. Pathol. 1970*; *Olsson et al, Arterioscler. Thromb. Vasc. Biol. 1999*), and renin-angiotensin system activation (*O' Brien et al, Circulation 2002*; *Helske et al, J. Am. Coll. Cardiol 2004*). Although the main effect of this disease is a dystrophic calcification, molecular patterns involved in bone remodeling, like features of mature lamellar bone and endochondral bone formation (*Mohler et al, Circulation 2001*), can also be involved in VIC calcification, including the expression of bone-related proteins like alkaline phosphatase, osteocalcin, and osteopontin (*Srivatsa et al, J. Clin. Invest. 1997*; *Caira et al, J. Am. Coll. Cardiol. 2006*).

Based on these evidences, the possibility to characterize the molecular pathways and mediators that control these complex phenomena could be extremely useful to identify new potential therapeutic

targets with the hope to develop treatments alternative to surgery. Considering that it had already been reported that VIC calcification is associated to an altered expression of some bone-related proteins, a proteomics approach is very useful to study the effect of calcifying agents at the protein expression level and on a large-scale. This goal was partially reached with a 2-D Gel

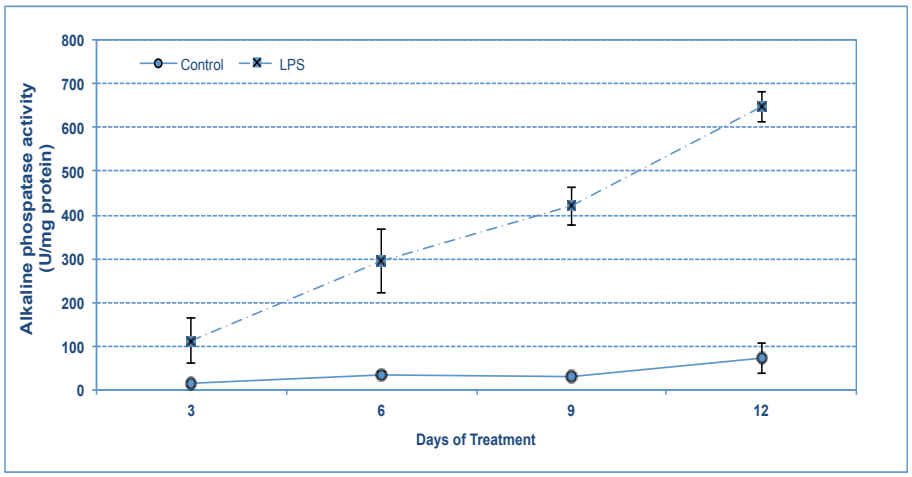


Figure 1 - ALP activity in clonal cells treated for 12 days with or without endotoxin (LPS, 100ng/ml). The graph is the result of 3 independent experiments.

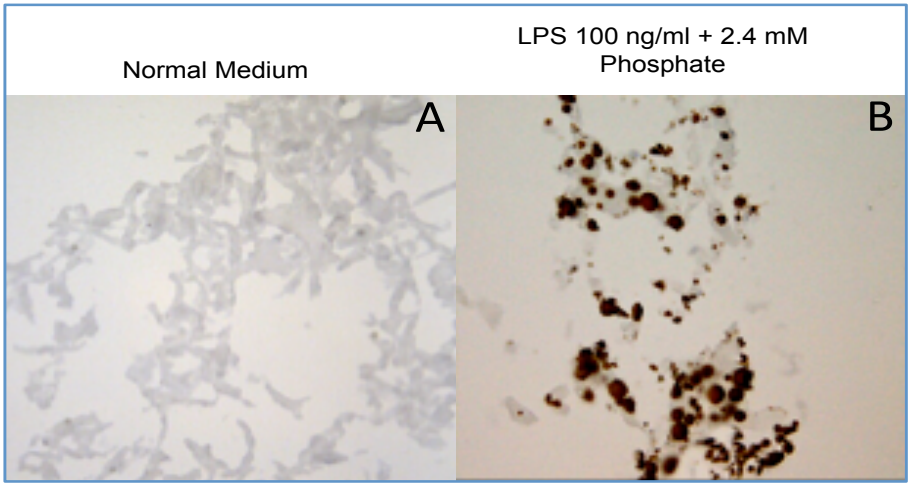


Figure 2 – Clonal subpopulation of LPS-sensitive BVIC seeded on microfibrillar type-I collagen matrix after cel treatment with (B) or without (A) endotoxin. Histochemical analysis of the calcium deposition performed with von Kossa Staining.

Electrophoresis proteomic analysis conducted by our group (*Bertacco et al, J. Proteome Res. 2010*) on a specific clonal population of bovine interstitial aortic valve cells (BVIC). This clone has been previously shown to express bone-related proteins (like osteocalcin), to display an increased alkaline phosphatase activity (ALP) (see Fig. 1), and to promote calcification of a tipe-I collagen matrix in response to lipopolysaccharide (LPS) endotoxin (see Fig. 2) (*Rattazzi et al, Arterioscler.*

Thromb. Vasc. Biol. 2008). LPS is a glycolipid composed of a hydrophilic polysaccharide moiety and hydrophobic domain known as lipid A (*Cuschieri et al, J. Leukoc. Biol. 2006*), and represents one of the major outer membrane components of Gram-negative bacteria (*Yue et al, BMC Genomics 2008*). LPS activates the macrophage response, producing proinflammatory cytokines (e.g. TNF-α) that help bacteria to invade host cells (*Cuschieri et al, J. Leukoc. Biol. 2006*). Thus, LPS is a perfect pro-inflammatory stimulus for *in vivo* and *in vitro* studies of the calcification model.

2.1.2 L-Arginine Metabolism is Involved in VIC Calcification

The 2-DE analysis allowed the identification of several proteins whose expression was significantly altered with the acquisition of a pro-calcific profile by the clonal BVIC treated with endotoxin. In particular, the altered proteins are involved in several cellular functions, like protein metabolism and transport, cell redox/nitric oxide homeostasis, chaperone-mediated folding, and cytoskeletal organization (*Bertacco et al, J. Proteome Res. 2010*). In particular the LPS treatment showed a reduced expression of proteins involved in nitric oxide synthase (NOS) bioactivity like Superoxide Dismutase (SOD [Cu-Zn]) and N(G),N(G)-dimethylarginine dimethylaminohydrolase 1 and 2 (DDAH-1 and DDAH-2). These findings appeared really interesting and suggested the involvement of L-arginine/ADMA (asymmetric dimethyl arginine) ratio in controlling the phenotypic profile of interstitial valve cells. ADMA (the physiological substrate of DDAH) competes with L-arginine (an immediate precursor of NO) for NOS activity (*Boger, Ann. Med. 2006*) and reduces nitric oxide synthesis. Therefore, some new experiments were performed to investigate the role of proteins involved in cell redox/NO homeostasis, recently found to be involved in valve degeneration (*Miller et al, J. Am. Coll. Cardiol 2008*; *Towler, J. Am. Coll. Cardiol 2008*). In particular, VIC cells were exposed to different concentrations of ADMA and L-arginine, to investigate the effects of these molecules on alkaline phosphatase (ALP) activity (one of the hallmark of interstitial aortic valve calcification) and matrix calcification. After 12 days of treatment with LPS, a dose-dependent effect of L-arginine in preventing ALP activity induction was found (see Fig. 3), while ADMA did not show any significant effect on ALP activity. Moreover, cells treated with L-arginine showed a significant decrease in calcification when exposed to endotoxin (see Fig. 4), suggesting that L-arginine exerts a protective effect against the calcification process induced by LPS (*Bertacco et al, J. Proteome Res. 2010)*. These findings suggested that L-Arginine might inhibit ALP increase through a positive effect on NO generation, opening a new scenario for the study of aortic valve calcification.

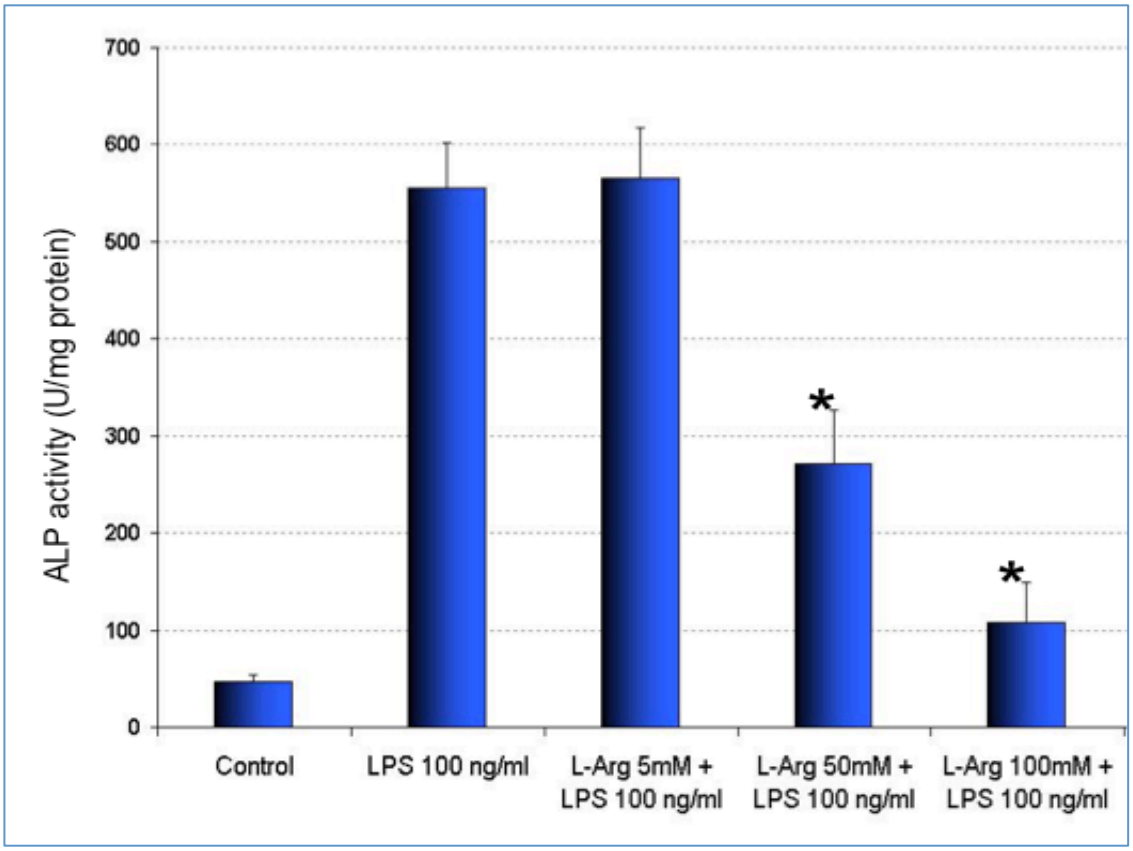


Figure 3 – Effect of L-Arg on ALP activity: increasing concentration of arginine administered together with LPS significantly inhibits the increase of alkaline phosphatase activity.

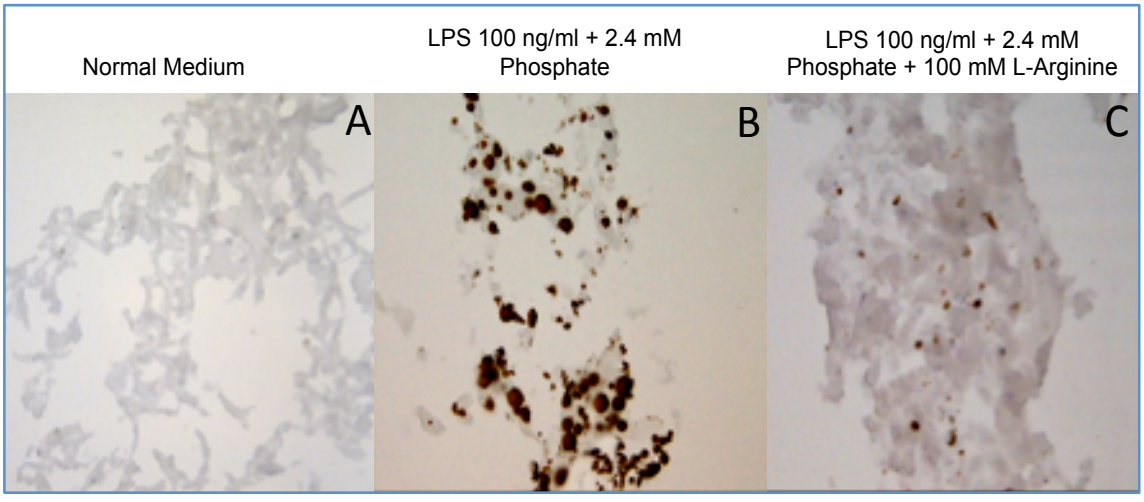


Figure 4 - Calcification of type-I collagen matrix after cell treatment with LPS (B), LPS combined with Arginine (C), and without treatment (A). Histochemical analysis of calcium deposition performed with von Kossa Staining.

2.2 Aims of the Study

Considering the very interesting information gained from our first 2-DE proteomics study on BVIC subjected to calcification stimuli, we decided to try to confirm and significantly expand the data already collected by applying alternative proteomics approaches to the same model. In particular we exploited two quantitative mass spectrometry-based proteomics approaches, SILAC and iTRAQ, to investigate the proteomes of bovine clonal interstitial valve cells treated with endotoxin (LPS) as a pro-calcific factor. Moreover, based on the information previously collected (*Bertacco et al, J. Proteome Res. 2010*) we have tried to gain additional information by adding to our model a combined treatment with LPS and L-arginine that showed a protective effect against the calcification process. This new treatment would allow to discriminate between proteins that respond to the LPS stimulus independently on the concomitant treatment with L-arginine from those proteins that under calcifying stimuli would change their expression level if not kept under "normal" conditions by the protective effect of L-arginine. Such an approach could be very useful to restrict the number of possible candidates to study as potential therapeutic targets. At the same time, the application of large-scale quantitative proteomics approaches such as SILAC and iTRAQ would strongly increase the proteome coverage with respect to the classical 2-DE approach, probably allowing to collect new quantitative data that would help to shed new light on the molecular mechanisms underlying the calcification process driven by endotoxin.

2.3 SILAC analysis of BVIC

As explained in the introduction, Bovine Interstitial Aortic Valve Cells (BVIC) were obtained from explants of intact aortic bovine valve leaflets and cloned by using a limited dilution technique. The selected clones show the expression of bone-related proteins (like osteocalcin), an increased alkaline phosphatase activity (ALP) and the ability to promote calcification of a collagen scaffold when subjected to treatment with the endotoxin lipopolysaccharide (LPS, 100 ng/mL) for a period of 12 days. They represent therefore a good model to investigate the calcification process driven by LPS.

The first proteomic approach we decided to use in this study is SILAC (Stable Isotope Labeling with Amino acid in Cell Culture), a method that, compared to the classical 2-DE approach was expected to lead to the identification of a much larger number of proteins and that could therefore be very useful to expand the data previously collected. The detailed protocol describing the cell growth conditions, the treatments, protein extraction, and the sample preparation for MS analysis is reported in section 4.6.

2.3.1 Determination of the Incorporation Time

Clonal bovine interstitial aortic valve cells used in this SILAC experiment showed the same characteristics of those used in the previous experiments, as described by Rattazzi (*Rattazzi et al, Artherioscler. Thromb. Vasc. 2008*). Cells were kept in culture for 8 passages, a number that was chosen after testing the labeling incorporation efficiency through repetitive measures at different time points of protein aliquots extracted from the heavy cells. Proteins extracted at different days of incubation were analyzed by LC-MS/MS to determine the time necessary for the complete labeling of proteins. In Fig. 5 a selected labeled ion of m/z 411.7230 (relative to the peptide LAEQAER belonging to 14-3-3 protein zeta/delta) is shown in comparison with the relative light peptide (m/z 408.7130). The percentage of labeling after 5, 12, and 18 days of culture is 91.6%, 96.8%, and 98.2% respectively. This last value corresponds to the 8^{th} splitting step. Analogous results were obtained for the great majority of peptides identified in these preliminary experiments.

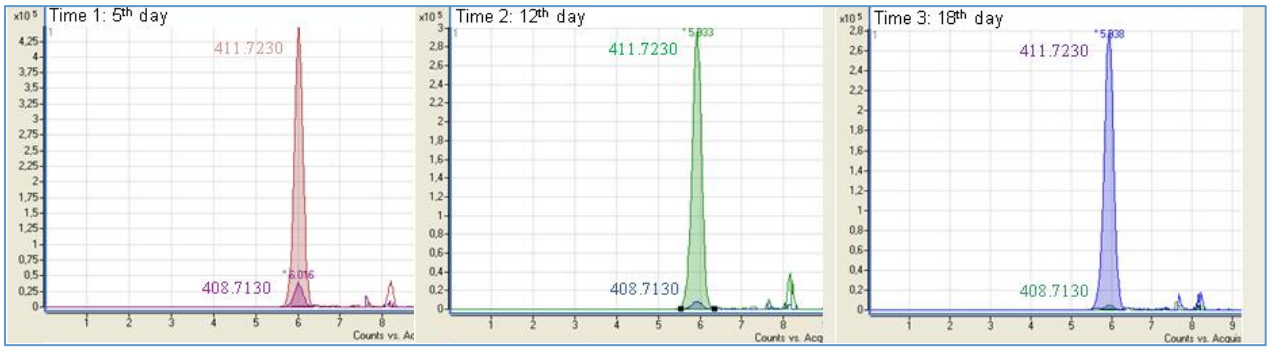


Figure 5 - Incorporation of heavy amino acids at different time points.

2.3.2 Arginine-to-Proline Conversion

In our first attempt to use the SILAC approach, we decided to apply the "classical" experimental set-up that requires the use of $^{13}C_6$-lysine and $^{13}C_6$-arginine as heavy amino acids. The use of both these amino acids in combination with trypsin as digesting enzyme, allows to obtain the maximum proteome coverage. However, we realized that this experimental set-up had a main drawback, represented by a massive arginine-to-proline conversion effect during the labeling process. This effect is determined by the metabolic synthesis within the cell of heavy proline ($^{13}C_5$-proline) from heavy arginine and, when present at high levels, leads to an incorrect heavy over light ratio in the MS analysis (*Lössner et al, Anal. Biochem. 2011*; *Blagoev et al, Methods 2006*). In fact, the accuracy of quantification is impaired by the incorporation within the proteins of heavy proline that results in additional satellite peaks due to heavy labeled proline-containing peptides. Although this is a known problem (*Lössner et al, Anal. Biochem. 2011*) and several algorithms have been proposed to correct SILAC data affected by the arginine-to-proline conversion (*Park et al, Nat. Methods 2009*; *Mortensen et al, J. Proteome Res.* 2010), the use of such open-source correcting algorithms is not trivial and requires the ability to manipulate large datasets while the outputs are often provided in formats that are not compatible with the use of commercial software as Proteome Discoverer, the informatics support we have used in all our studies. Moreover, the algorithms proposed are designed to specifically correct the data considering only a single satellite peak for proline-containing peptides. This design is based on the observation that the conversion is generally limited; therefore even for peptides containing several proline residues, the statistical probability to have two or more labeled prolines within the same peptide is very low. This approximation can be considered correct when cells that show the ability to convert arginine into proline are kept at confluence for a short time period, as reported in the great majority of SILAC-based proteomics

studies. In our case however, cells were kept at confluence and treated with LPS (or LPS plus L-arginine) for 12 days, therefore allowing the accumulation of heavy proline derived from the arginine metabolism. The amount of labeled proline within the cell is therefore not negligible and the rate and level of incorporation within proteins is such that a number of satellite peaks are often observable for peptides containing several prolines. Fig. 6 shows the MS spectrum of the peptide EMQ**P**TH**P**IR (m/z 557.792 Da) from 14-3-3 protein zeta/delta detected from cells labeled with $^{13}C_6$-arginine and $^{13}C_6$-lysine. The signal at m/z 560.302 is relative to the same peptide that has incorporated a significant proportion of heavy proline. As can be noted, using cells labeled in this way would lead to significant errors in the protein quantification process, since the contribution of peptides containing several proline residues would have a strong impact on the heavy over light ratio (H/L) calculated by the software for data analysis. An example of peptide containing several prolines is shown in Fig. 7. The MS spectrum shows a peak at m/z=935.048 relative to the triple-charged peptide SAGGSS**P**EGGEDSDREDGNYC**PP**VKR from Isoform 4 of Ran-binding protein 3. The expected heavy peptide (containing 1 "heavy" lysine and 2 "heavy" arginines) is visible with a lower intensity at m/z=941.04 and 2 satellite signals due to the same peptide containing 1 and 2 "heavy" prolines are also clearly visible. This peptide has a calculated heavy over light ratio equal to 0.713, but if we sum the contribution of all the "heavy" peaks, the ratio becomes greater than 1, dramatically changing the quantification.

To avoid the arginine-to-proline conversion problem, one of the most popular options is to use culturing media supplemented with proline (*Bendall et al, Mol. Cell. Proteomics 2008*) and with a lower content of arginine (*Blagoev et al, Methods 2006*), so to significantly reduce the conversion effect. However, in our case cells would no grow normally in such type of culture medium, therefore we decided to by-pass the problem by labeling the cells only with $^{13}C_6$-lysine (that is not converted into other amino acids) and digesting the proteins with Lys-C, a protease that cleaves after the lysine residues. Lys-C is a very specific protease but is usually less used compared to trypsin because is much more expensive and produces a higher number of large peptides. This results in lower quality MS/MS spectra under normal CID conditions, thus reducing the sequencing coverage.

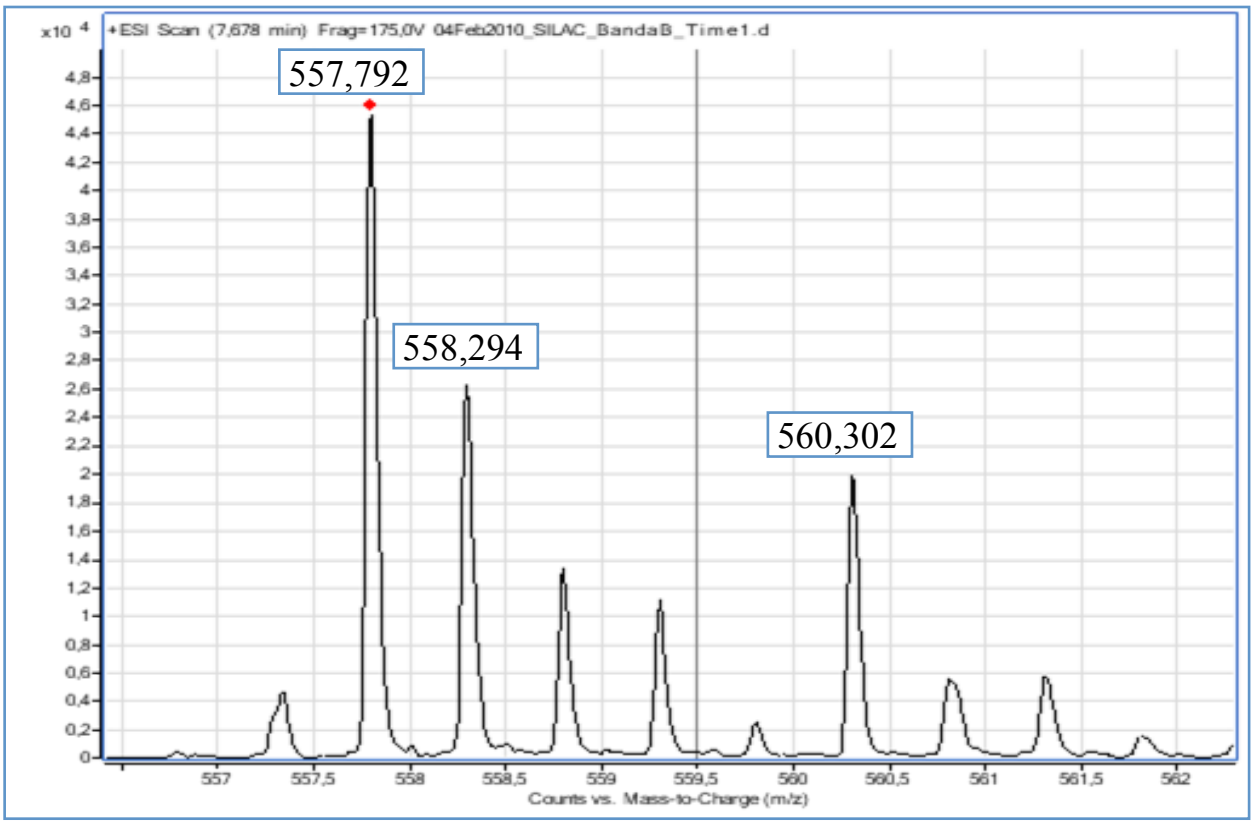


Figure 6 - Arginine to Proline conversion effect.

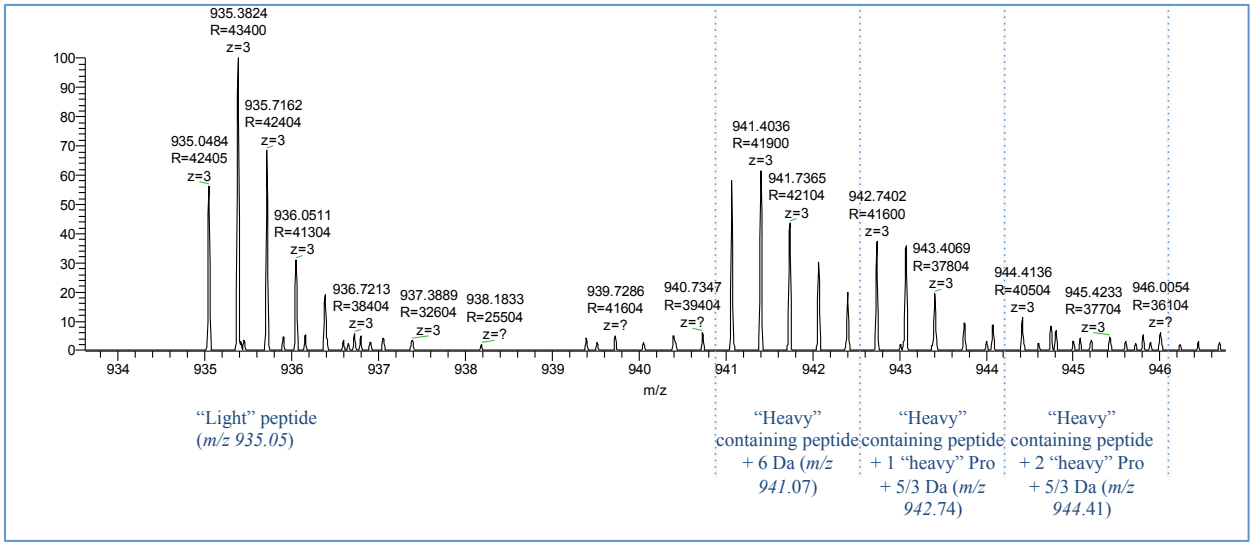


Figure 7 - Example of heavy proline contribution in peptide containing multiple prolines. Peptide sequence: SAGGSSPEGGEDSDREDGNYCPPVKR

2.3.3 SILAC Experimental Workflow

After the preliminary tests conducted to decide the best SILAC conditions, we chose to grow BVIC with $^{13}C_6$-Lys for 18 days before performing the treatment with LPS and a combination of LPS and L-arginine. The SILAC protocol used in this study is described in detail in section 4.6 and the experimental set-up is summarized in Fig. 8, where is reported also the swapping system. Shortly, we have grown 8 flasks of cells, 4 in normal medium and 4 in the SILAC medium (containing $^{13}C_6$-Lys). 2 batches of normal cells were treated with LPS, 1 batch was kept as control and 1 batch was treated with a combination of LPS and 50 mM L-arginine. The same treatments were also performed on the 4 batches of labeled cells. After the treatments, batches were pooled according to what is reported in Fig 8.

Thanks to this experimental set-up, LPS-treated cells will work as a common factor for the analysis of the diverse treatments and will therefore allow to directly compare the effect of LPS *vs* control and LPS *vs* LPS+arginine and, indirectly, the effect of L-arginine treatment *vs* control cells. At the same time, the use of a swapping system allows to immediately identify contaminants and partially labeled proteins. In fact, contaminants are usually proteins that come from the environment (such as keratins or serum proteins derived from the culturing medium) and do not come directly from the cells. In these cases, the incorporation of heavy amino acids do not occur, giving in the MS analysis singlet signals present only in the "light" form. This system has also the advantage of making easy the recognition of partially labeled proteins; in these cases, the "heavy" peptides show a lower intensity compared to the "light" ones, and such intensities are independent from the treatment. When measuring the Treated/Control ratios with the swapping system, partially labeled proteins show quantifications with opposite trend, and can therefore be easily discarded.

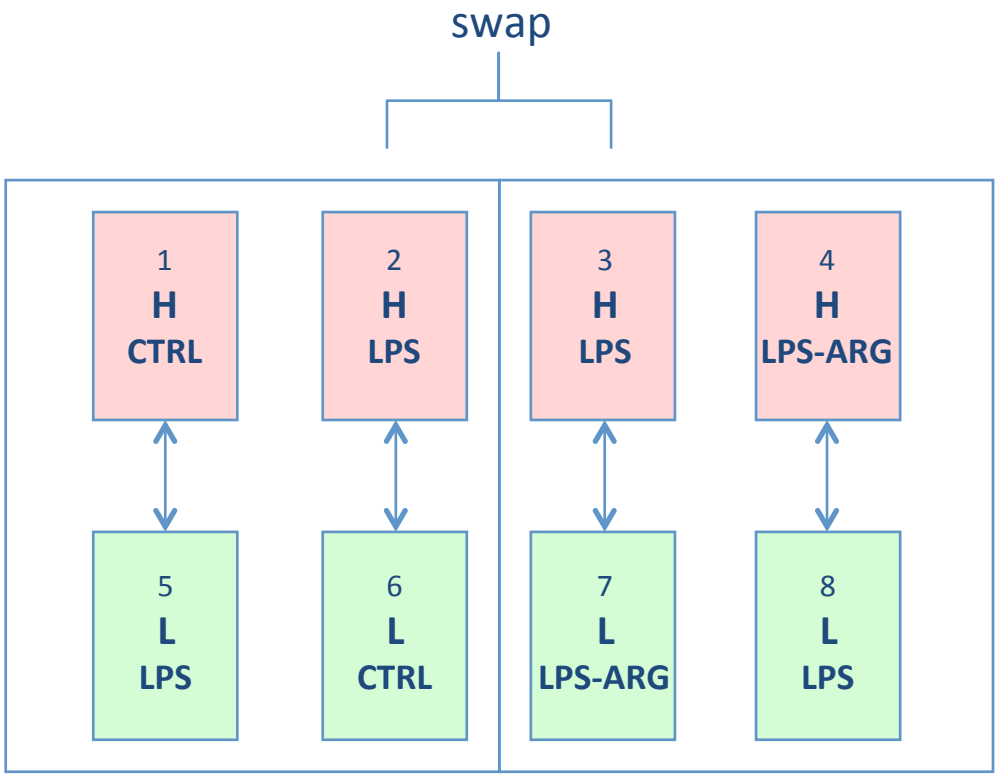


Figure 8 - SILAC experimental set-up

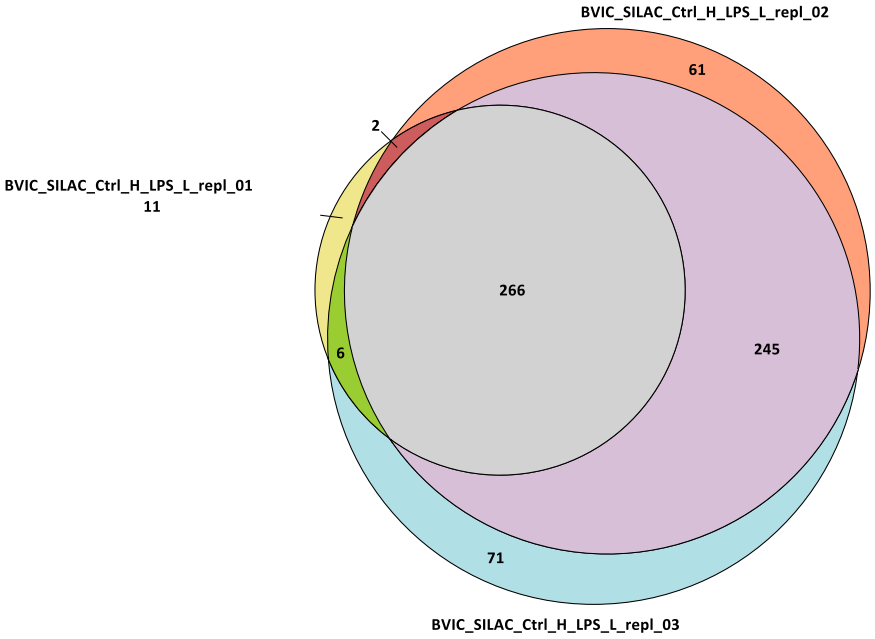
After 12 days of treatment cells were harvested, and lysed. Proteins extracted were carefully quantified and pooled in equal amounts according to the scheme reported in Fig 8. Proteins were separated by SDS-PAGE and digestion was performed in gel with Lys-C (see details in section 4.3). Peptide mixtures were analyzed by LC-MS/MS with a LTQ Orbitrap mass spectrometer and data acquired were searched and quantified using Mascot and Proteome Discoverer software (see the details of data analysis in sections 4.8 and 4.9). 3 technical replicates were performed for each biological replicate by running the same samples 3 times under the same analytical conditions. Thus a total of 84 LC-MS/MS runs were acquired in this experiment.

2.3.4 SILAC Results: Technical and Biological Reproducibility

With this SILAC experiment, a total of 820 proteins were identified with high confidence and relatively quantified using Mascot as search engine and Proteome Discoverer as quantification tool. The details regarding protein identification and quantification are described in section 4.9.

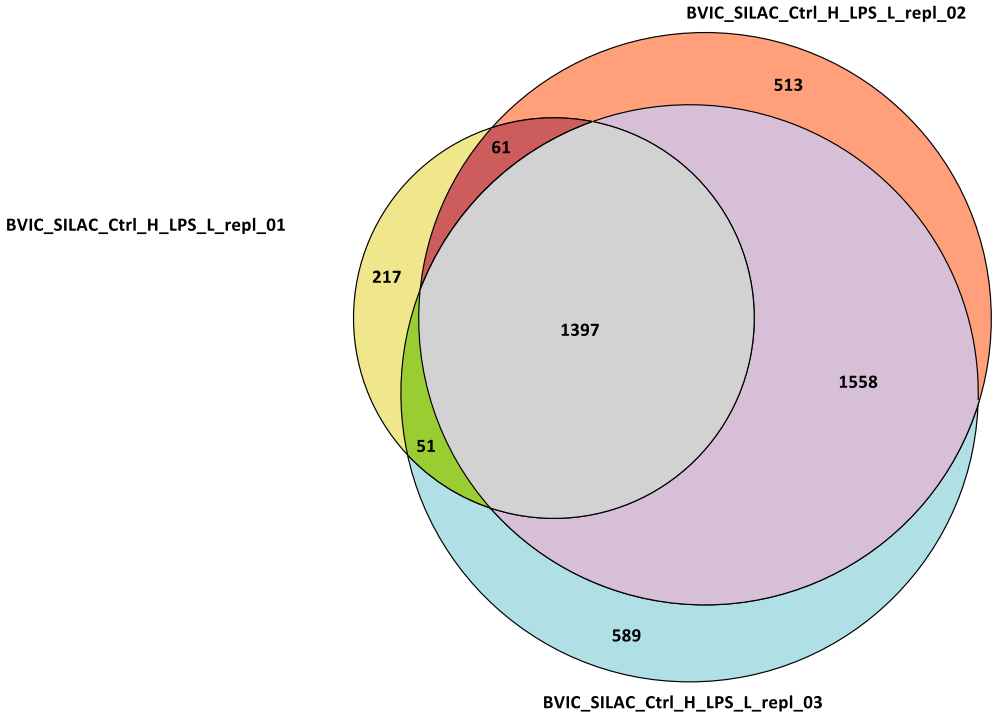
The technical reproducibility (in terms of protein identifications) achieved was evaluated and an example can be appreciated by looking at the Venn diagram reported in Fig. 9, where it is possible to see that 78% of the total proteins identified are in common between at least 2 technical replicates. Similar results were obtained also for the other biological replicates. These results show that undersampling of the MS/MS acquired is an issue although the chromatographic reproducibility of our system can be considered good.
Therefore the possibility to run the same sample more than once allows to increase the total number of identifications and, at the same time, to obtain a more confident quantification of proteins. Similar considerations apply when looking at the Venn diagram reported in Fig. 10, which shows the technical reproducibility at the peptide level. 70% of peptides were found in common to at least 2 technical replicates. As expected, this value is lower than the one found for proteins, since the undersampling effect is more evident at the peptide level, rather than at the protein level.
As it is possible to notice from these diagrams, one of the analyses led to a considerable smaller number of identifications, attributable to a not perfect tuning of the instrument. Technical replicates have therefore also the advantage of limiting the negative effects related to instrumental issues. All together, these data confirm that acquiring technical replicates is a good practice overall when very complex mixtures are analyzed.

We also evaluated the reproducibility of protein quantification between biological replicates. The data obtained from 2 biological replicates (as the average value of the 3 technical replicates) with the swapping system can be plotted as reported in Fig. 11. In this graph the ratio LPS/CTRL (as Heavy/Light) for each quantified protein is plotted against the ratio for the same proteins quantified in the swapping system (LPS/CTRL as Light/Heavy).
Ideally one would expect to find exactly the same value for each protein, therefore all the data in the graph would appear as distributed along the diagonal line (the green line in the graph).



	Exclusive	Total	Label	Description
	11	285	BVIC_SILAC_Ctrl_H_LPS_L_Repl_01	Repl_01
	61	574	BVIC_SILAC_Ctrl_H_LPS_L_Repl_02	Repl_02
	71	588	BVIC_SILAC_Ctrl_H_LPS_L_Repl_03	Repl_03
	2	268	BVIC_SILAC_Ctrl_H_LPS_L_Repl_01 / BVIC_SILAC_Ctrl_H_LPS_L_Repl_02	Repl_01 / Repl_02
	245	511	BVIC_SILAC_Ctrl_H_LPS_L_Repl_02 / BVIC_SILAC_Ctrl_H_LPS_L_Repl_03	Repl_02 / Repl_03
	6	272	BVIC_SILAC_Ctrl_H_LPS_L_Repl_01 / BVIC_SILAC_Ctrl_H_LPS_L_Repl_03	Repl_01 / Repl_03
	266	266	BVIC_SILAC_Ctrl_H_LPS_L_Repl_01 / BVIC_SILAC_Ctrl_H_LPS_L_Repl_02 / BVIC_SILAC_Ctrl_H_LPS_L_Repl_03	Repl_01 / Repl_02 / Repl_03
Sum	662			

Figure 9 - Example of technical replicates reproducibility for identified proteins.



	Exclusive	Total	Label	Description
	217	1726	BVIC_SILAC_Ctrl_H_LPS_L_Repl_01	Repl_01
	513	3529	BVIC_SILAC_Ctrl_H_LPS_L_Repl_02	Repl_02
	589	3595	BVIC_SILAC_Ctrl_H_LPS_L_Repl_03	Repl_03
	61	1458	BVIC_SILAC_Ctrl_H_LPS_L_Repl_01 / BVIC_SILAC_Ctrl_H_LPS_L_Repl_02	Repl_01 / Repl_02
	1558	2955	BVIC_SILAC_Ctrl_H_LPS_L_Repl_02 / BVIC_SILAC_Ctrl_H_LPS_L_Repl_03	Repl_02 / Repl_03
	51	1448	BVIC_SILAC_Ctrl_H_LPS_L_Repl_01 / BVIC_SILAC_Ctrl_H_LPS_L_Repl_03	Repl_01 / Repl_03
	1397	1397	BVIC_SILAC_Ctrl_H_LPS_L_Repl_01 / BVIC_SILAC_Ctrl_H_LPS_L_Repl_02 / BVIC_SILAC_Ctrl_H_LPS_L_Repl_03	Repl_01 / Repl_02 / Repl_03
Sum	4386			

Figure 10 - Example of technical replicates reproducibility for identified peptides.

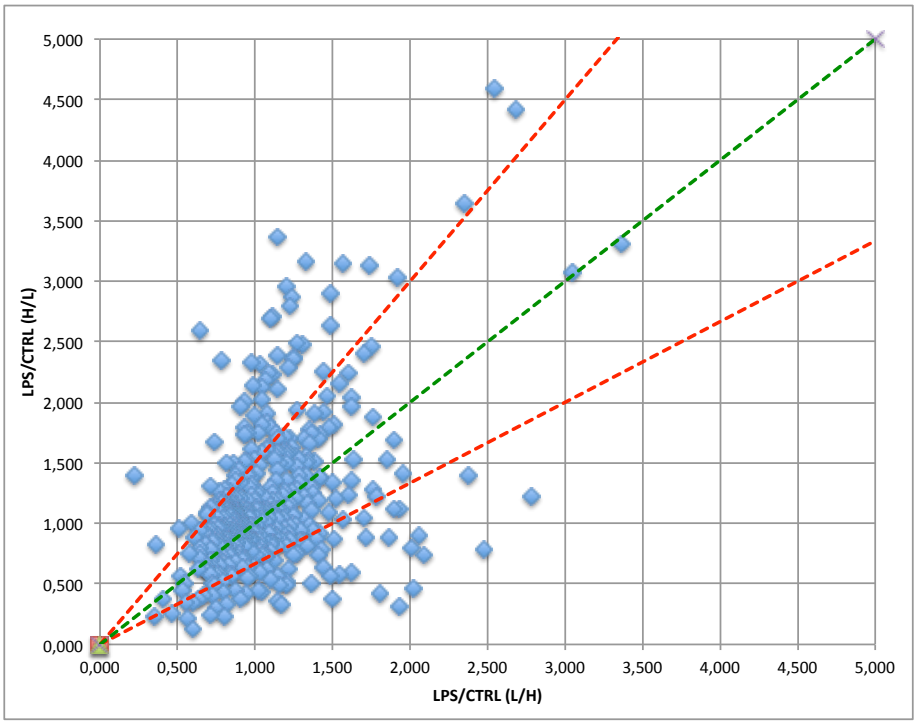


Figure 11 - SILAC quantification reproducibility test.

In our case, about 80% of protein quantifications showed a variability lower than 50%. This is a quite good result, considering the limits of the technique and the inevitable biological variability of the cellular system used. Proteins that showed a large difference in terms of quantification between biological replicates (those that in the graph appear outside the red lines) are mainly contaminant or partially labeled proteins that were therefore excluded from the following analyses. As can be also noticed, the great majority of ratios cluster around 1, further demonstrating that the experiment gave good technical results. Proteins showing a ratio LPS/CTRL significantly and reproducibly different from 1.0 (in this case a ratio >1.5 or <0.5) were those considered as altered for the following pathways analyses. Moreover only proteins found in at least two of the 3 technical replicates for each biological replicate were kept in our final list. Similar results were obtained by plotting with the same system the quantitative data from the other biological replicates (data not shown).

A list of all the proteins identified and quantified in this experiment is reported in Table 1 of "Appendix section". The quantification was performed using Proteome Discoverer software on proteins identified with at least 2 different unique peptides. In the table, proteins with an increased expression of at least 30% are colored in blue (in bold proteins with a difference of at least 50%), while proteins with a decreased expression are marked on magenta (again proteins with a difference

of at least 50% are bold). The same table reports also the quantitative data obtained from the experiment where LPS and L-Arginine were administered to the cells.

2.3.5 SILAC Results: Bioinformatics and Pathway Analyses

Proteome Discoverer software gives also the possibility to classify all the identified proteins according to their molecular functions, cellular components, and biological processes. The diagrams showing these classifications are reported in Fig. 12, 13, and 14.
This information is useful to verify if the analytical method used tends to enrich specific classes of proteins or if it can be considered unbiased. The classifications obtained for the identified proteins evidenced a rather homogeneous and equilibrated distribution between different cellular compartments and molecular processes and the various categories seem to well represent the common distribution of protein functions, with the most abundant classes represented by proteins with metabolic and catalytic activities. The presence of a not negligible proportion of proteins classified as "not annotated" is mostly due to an artifact derived from the use of IPI Bovine database, which contains a significant number of entries classified as "uncharacterized" proteins. In reality the large majority of these proteins are very well characterized and a simple BLAST analysis easily allows to retrieve the correct protein names and functions. On the other hand, the use of a specific, complete bovine database was for us a necessity, to make possible to compare the results obtained with different approaches.

Using the proteins included in the final list, a pathways analysis was performed with DAVID Bioinformatic Resources 6.7 (NIAID, NIH), using as input list 85 proteins significantly altered upon treatment with LPS (i.e. those that showed an altered expression level of at least 50% upon treatment with LPS), and as background list, all the proteins identified in this study. The results obtained suggest that several biological and molecular functions seem to be involved in the calcification process induced by LPS: chromosome organization, cellular oxidoreductase activity, cytoskeletal and spliceosome regulation, glycolysis/gluconeogenesis, and nitrogen and amines metabolism (see Fig. 15).
The results from the pathway analysis support the idea that nitrogen metabolism is involved in the calcification process driven by LPS. As reported before, a similar result emerged also from the data acquired with the classical 2-DE approach. The results obtained are discussed in detail in the discussion (section 2.6).

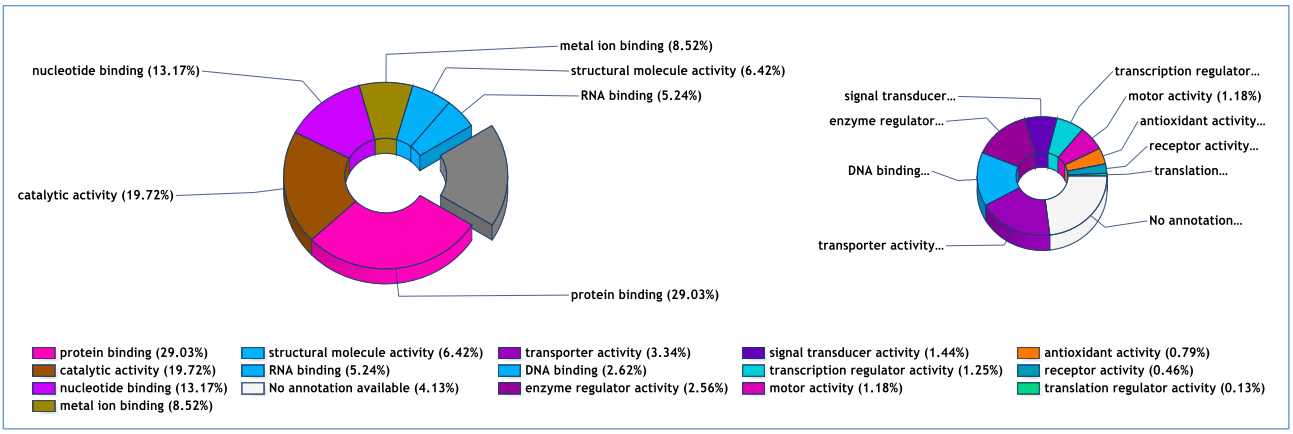


Figure 12 - Molecular function analysis.

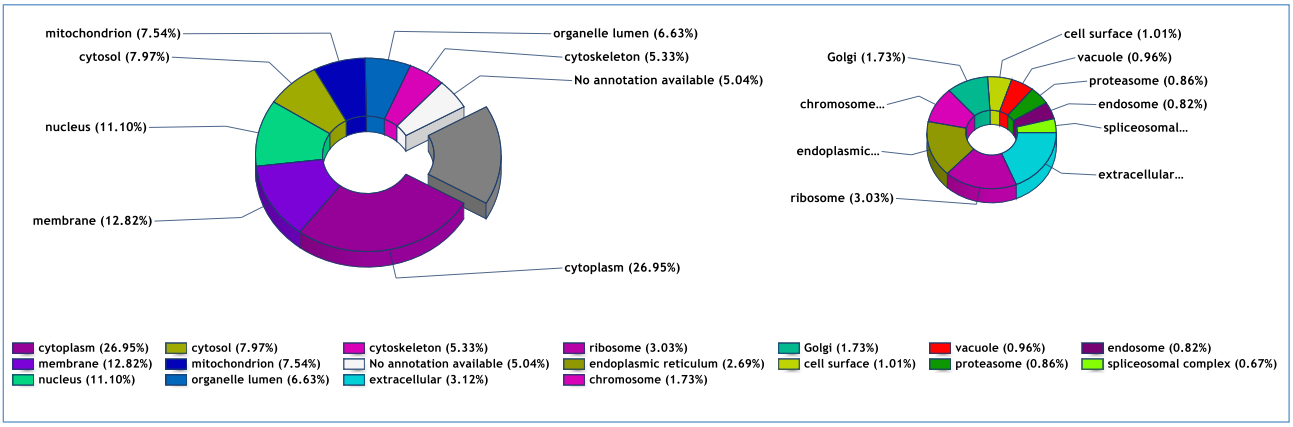


Figure 11 - Cellular component analysis.

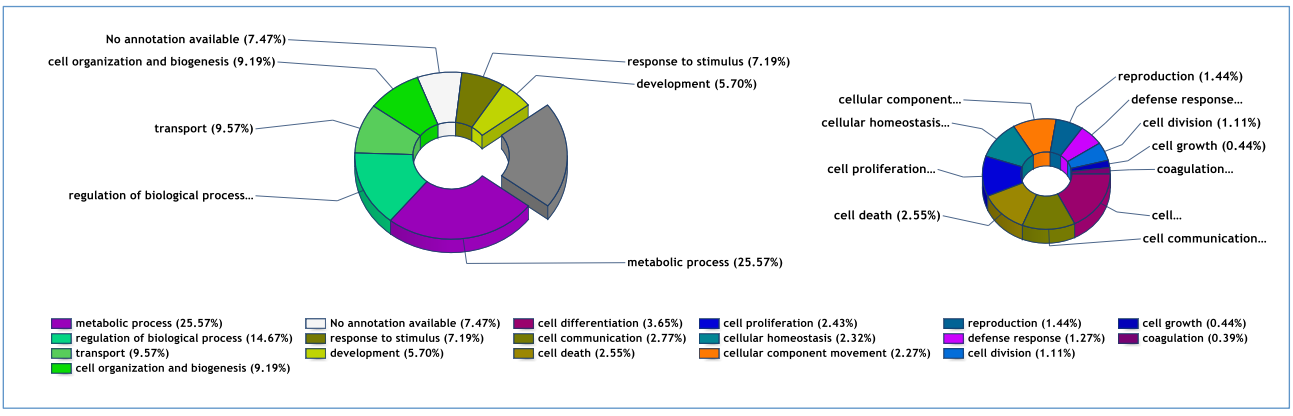
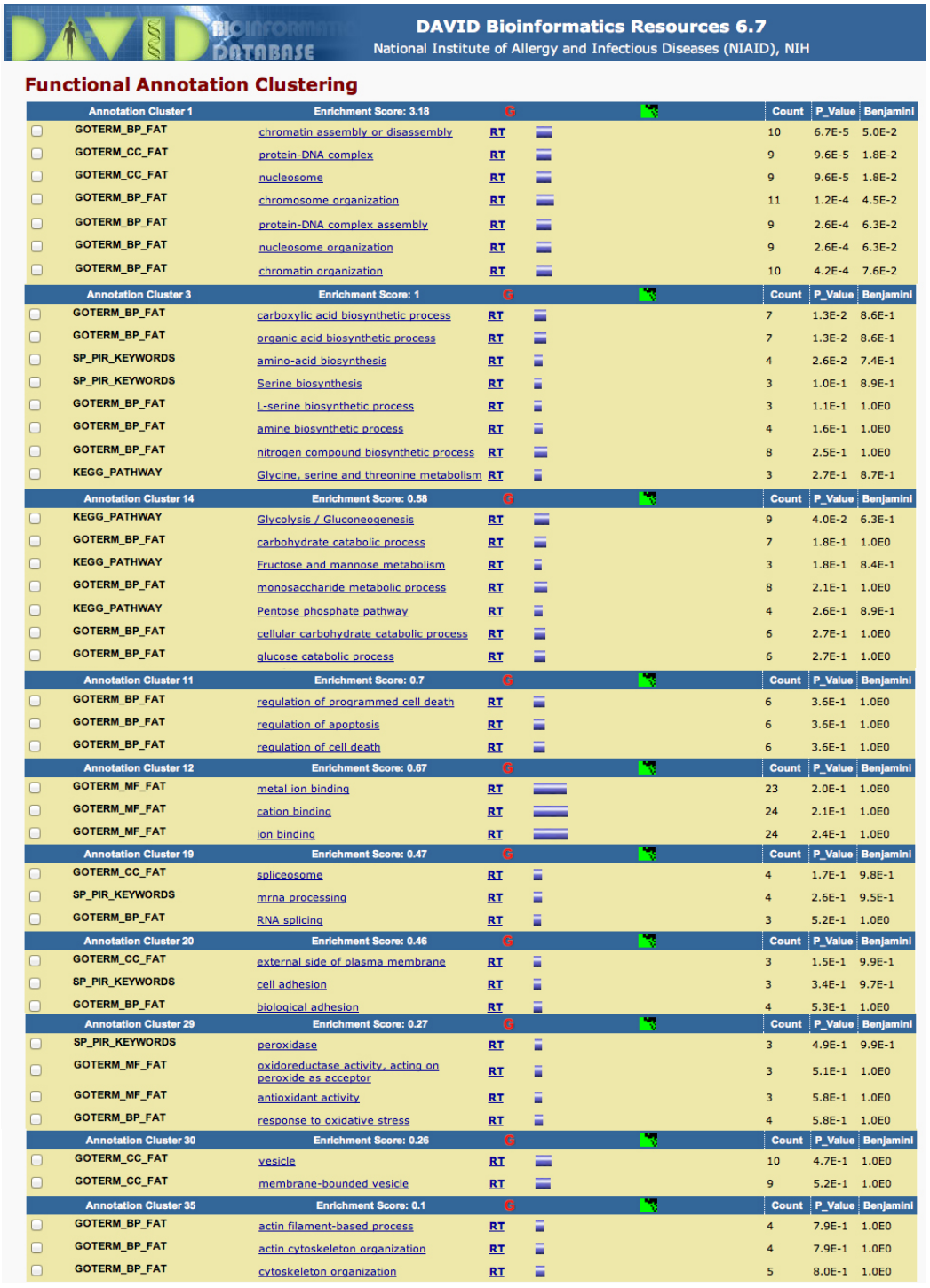


Figure 12 - Biological processes analysis.



DAVID Bioinformatics Resources 6.7
National Institute of Allergy and Infectious Diseases (NIAID), NIH

Functional Annotation Clustering

Annotation Cluster 1	Enrichment Score: 3.18			Count	P_Value	Benjamini
GOTERM_BP_FAT	chromatin assembly or disassembly	RT		10	6.7E-5	5.0E-2
GOTERM_CC_FAT	protein-DNA complex	RT		9	9.6E-5	1.8E-2
GOTERM_CC_FAT	nucleosome	RT		9	9.6E-5	1.8E-2
GOTERM_BP_FAT	chromosome organization	RT		11	1.2E-4	4.5E-2
GOTERM_BP_FAT	protein-DNA complex assembly	RT		9	2.6E-4	6.3E-2
GOTERM_BP_FAT	nucleosome organization	RT		9	2.6E-4	6.3E-2
GOTERM_BP_FAT	chromatin organization	RT		10	4.2E-4	7.6E-2
Annotation Cluster 3	**Enrichment Score: 1**			**Count**	**P_Value**	**Benjamini**
GOTERM_BP_FAT	carboxylic acid biosynthetic process	RT		7	1.3E-2	8.6E-1
GOTERM_BP_FAT	organic acid biosynthetic process	RT		7	1.3E-2	8.6E-1
SP_PIR_KEYWORDS	amino-acid biosynthesis	RT		4	2.6E-2	7.4E-1
SP_PIR_KEYWORDS	Serine biosynthesis	RT		3	1.0E-1	8.9E-1
GOTERM_BP_FAT	L-serine biosynthetic process	RT		3	1.1E-1	1.0E0
GOTERM_BP_FAT	amine biosynthetic process	RT		4	1.6E-1	1.0E0
GOTERM_BP_FAT	nitrogen compound biosynthetic process	RT		8	2.5E-1	1.0E0
KEGG_PATHWAY	Glycine, serine and threonine metabolism	RT		3	2.7E-1	8.7E-1
Annotation Cluster 14	**Enrichment Score: 0.58**			**Count**	**P_Value**	**Benjamini**
KEGG_PATHWAY	Glycolysis / Gluconeogenesis	RT		9	4.0E-2	6.3E-1
GOTERM_BP_FAT	carbohydrate catabolic process	RT		7	1.8E-1	1.0E0
KEGG_PATHWAY	Fructose and mannose metabolism	RT		3	1.8E-1	8.4E-1
GOTERM_BP_FAT	monosaccharide metabolic process	RT		8	2.1E-1	1.0E0
KEGG_PATHWAY	Pentose phosphate pathway	RT		4	2.6E-1	8.9E-1
GOTERM_BP_FAT	cellular carbohydrate catabolic process	RT		6	2.7E-1	1.0E0
GOTERM_BP_FAT	glucose catabolic process	RT		6	2.7E-1	1.0E0
Annotation Cluster 11	**Enrichment Score: 0.7**			**Count**	**P_Value**	**Benjamini**
GOTERM_BP_FAT	regulation of programmed cell death	RT		6	3.6E-1	1.0E0
GOTERM_BP_FAT	regulation of apoptosis	RT		6	3.6E-1	1.0E0
GOTERM_BP_FAT	regulation of cell death	RT		6	3.6E-1	1.0E0
Annotation Cluster 12	**Enrichment Score: 0.67**			**Count**	**P_Value**	**Benjamini**
GOTERM_MF_FAT	metal ion binding	RT		23	2.0E-1	1.0E0
GOTERM_MF_FAT	cation binding	RT		24	2.1E-1	1.0E0
GOTERM_MF_FAT	ion binding	RT		24	2.4E-1	1.0E0
Annotation Cluster 19	**Enrichment Score: 0.47**			**Count**	**P_Value**	**Benjamini**
GOTERM_CC_FAT	spliceosome	RT		4	1.7E-1	9.8E-1
SP_PIR_KEYWORDS	mrna processing	RT		4	2.6E-1	9.5E-1
GOTERM_BP_FAT	RNA splicing	RT		3	5.2E-1	1.0E0
Annotation Cluster 20	**Enrichment Score: 0.46**			**Count**	**P_Value**	**Benjamini**
GOTERM_CC_FAT	external side of plasma membrane	RT		3	1.5E-1	9.9E-1
SP_PIR_KEYWORDS	cell adhesion	RT		3	3.4E-1	9.7E-1
GOTERM_BP_FAT	biological adhesion	RT		4	5.3E-1	1.0E0
Annotation Cluster 29	**Enrichment Score: 0.27**			**Count**	**P_Value**	**Benjamini**
SP_PIR_KEYWORDS	peroxidase	RT		3	4.9E-1	9.9E-1
GOTERM_MF_FAT	oxidoreductase activity, acting on peroxide as acceptor	RT		3	5.1E-1	1.0E0
GOTERM_MF_FAT	antioxidant activity	RT		3	5.8E-1	1.0E0
GOTERM_BP_FAT	response to oxidative stress	RT		4	5.8E-1	1.0E0
Annotation Cluster 30	**Enrichment Score: 0.26**			**Count**	**P_Value**	**Benjamini**
GOTERM_CC_FAT	vesicle	RT		10	4.7E-1	1.0E0
GOTERM_CC_FAT	membrane-bounded vesicle	RT		9	5.2E-1	1.0E0
Annotation Cluster 35	**Enrichment Score: 0.1**			**Count**	**P_Value**	**Benjamini**
GOTERM_BP_FAT	actin filament-based process	RT		4	7.9E-1	1.0E0
GOTERM_BP_FAT	actin cytoskeleton organization	RT		4	7.9E-1	1.0E0
GOTERM_BP_FAT	cytoskeleton organization	RT		5	8.0E-1	1.0E0

Figure 15 –Pathway analysis performed with DAVID Bioinformatic Resources 6.7 (NIAID, NIH) software on proteins found to be altered upon treatment with LPS.

2.4 iTRAQ Analysis of BVIC

After applying the SILAC approach to our experimental model, we also decided to exploit the potential of a different mass spectrometry-based quantitative method applied to the same biological system. iTRAQ (Isobaric Tag for Relative and Absolute Quantitation) was applied to the same clone of BVIC cells used in the SILAC experiment. The iTRAQ protocol is sensibly different from SILAC: samples are lysed and prepared in a different manner, and this can affect the results in terms of both protein identification and quantification. Therefore we decided to apply two alternative and complementary methods to the same biological system, in order to confirm previous results and, possibly, collect more information about the calcification process of interstitial aortic valve cells induced by LPS.

2.4.1 iTRAQ Experimental Workflow

As in the SILAC experiment described above, cells were treated with LPS, LPS in combination with L-arginine, or left untreated and used as control. The detailed protocol describing the cell growth conditions, the treatments, protein extraction, and the sample preparation for MS analysis is reported in section 4.7.

For this experiment only one biological replicate was performed because preliminary tests on ALP activity showed a limited response of this batch of cells to LPS stimulus. So we preferred to perform the experiment only once and check whether our data would confirm the results obtained with the biochemical measurements.

After 12 days of treatment with LPS and LPS in combination with L-arginine, cells were lysed and proteins were extracted and carefully quantified to perform the iTRAQ protocol. iTRAQ experiment was performed by labeling the digested proteins belonging to control cells, LPS-treated cells, and LPS/L-arginine-treated cells respectively with 114, 115, and 117 tags (see Fig. 16).

Labeled samples were mixed together, fractionated by Strong Cation Exchange (SCX) chromatography and data were acquired in 3 technical replicates by LC-MS/MS on the LTQ-Orbitrap, using a scanning method that combines CID and HCD fragmentation on the same parent ions, so merging the good quality data of CID spectra (useful for the database search identification) with the quantitative data derived from the HCD spectra (*Köcher et al, J. Proteome Res. 2009*). Analysis of raw data files was performed with Mascot and Proteome Discoverer software and proteins were quantified and identified using the same Bovine IPI database used for the SILAC

experiment. This would allow us to easily compare the results obtained with the 2 approaches. A total of 15 LC-MS/MS analyses were performed for this iTRAQ experiment. Details about LC-MS/MS analyses are reported in section 4.8.

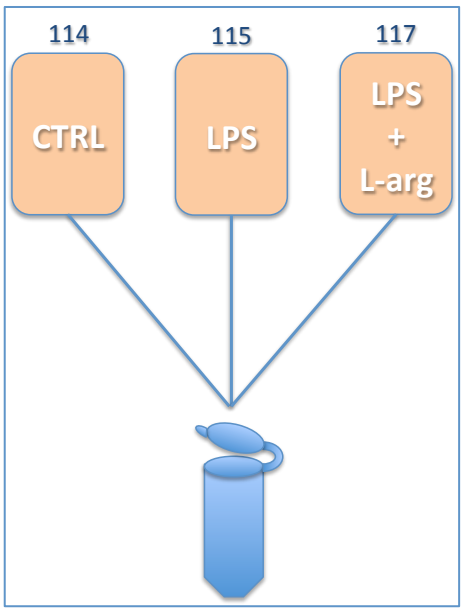
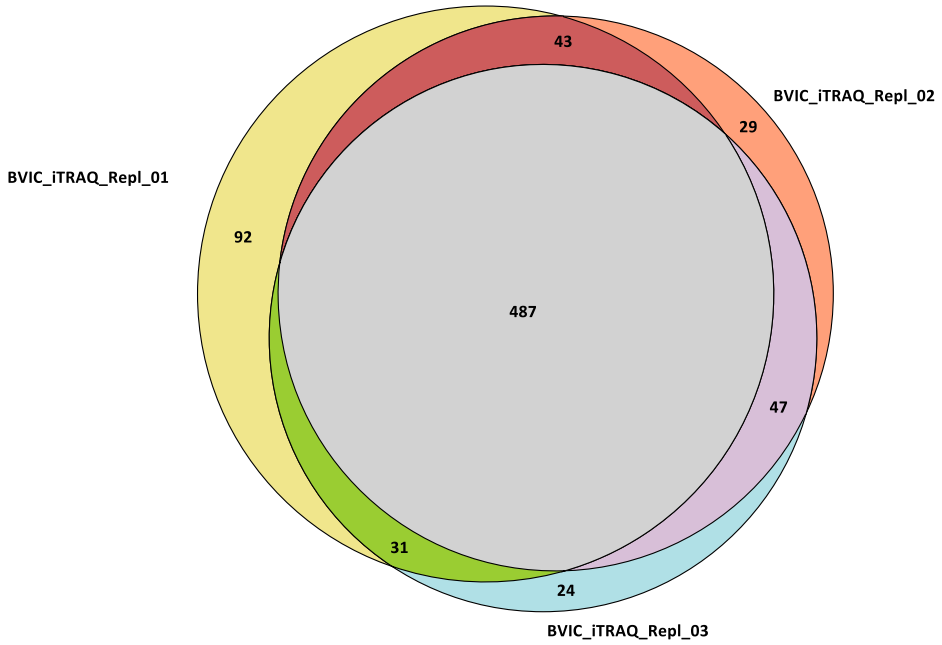


Figure 16 - iTRAQ experimental set-up

2.4.2 iTRAQ Results: Technical Reproducibility

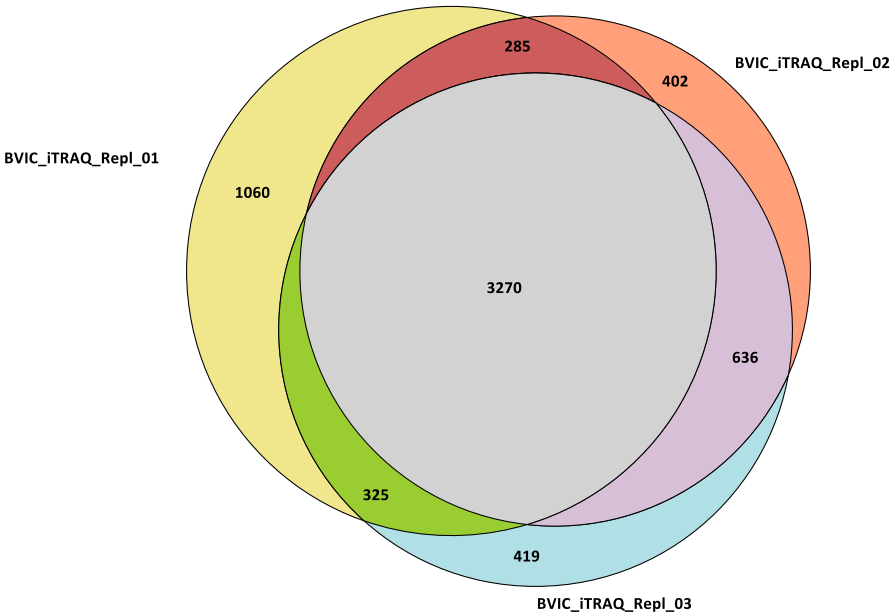
With this iTRAQ experiment, a total of 753 proteins were identified with high confidence and relatively quantified using Mascot as search engine and Proteome Discoverer as quantification tool. The details regarding protein identification and quantification are described in section 4.9.

81% of identified proteins were in common to at least 2 technical replicates, emphasizing the good reproducibility of our technical system (see Fig. 17). Reproducibility was tested also for the identified peptides (see Fig. 18), revealing that 71% of peptides were in common to at least two technical replicates. As expected, also in this case the same considerations about the undersampling effect already evidenced for the SILAC experiment, remain valid. However, differently from the SILAC study, in this experiment the tuning of the instrument was correct during all the three replicates, as it is shown by the homogeneous distribution of the number of proteins and peptides correlated with each replicate.



	Exclusive	Total	Label	Description
	92	653	BVIC_iTRAQ_Repl_01	Repl_01
	29	606	BVIC_iTRAQ_Repl_02	Repl_02
	24	589	BVIC_iTRAQ_Repl_03	Repl_03
	43	530	BVIC_iTRAQ_Repl_01 / BVIC_iTRAQ_Repl_02	Repl_01 / Repl_02
	47	534	BVIC_iTRAQ_Repl_02 / BVIC_iTRAQ_Repl_03	Repl_02 / Repl_03
	31	518	BVIC_iTRAQ_Repl_01 / BVIC_iTRAQ_Repl_03	Repl_01 / Repl_03
	487	487	BVIC_iTRAQ_Repl_01 / BVIC_iTRAQ_Repl_02 / BVIC_iTRAQ_R	Repl_01 / Repl_02 / Repl_03
Sum	753			

Figure 17 – Example of technical replicates reproducibility for identified proteins.



	Exclusive	Total	Label	Description
	1060	4940	BVIC_iTRAQ_Repl_01	Repl_01
	402	4593	BVIC_iTRAQ_Repl_02	Repl_02
	419	4650	BVIC_iTRAQ_Repl_03	Repl_03
	285	3555	BVIC_iTRAQ_Repl_01 / BVIC_iTRAQ_Repl_02	Repl_01 / Repl_02
	636	3906	BVIC_iTRAQ_Repl_02 / BVIC_iTRAQ_Repl_03	Repl_02 / Repl_03
	325	3595	BVIC_iTRAQ_Repl_01 / BVIC_iTRAQ_Repl_03	Repl_01 / Repl_03
	3270	3270	BVIC_iTRAQ_Repl_01 / BVIC_iTRAQ_Repl_02 / BVIC_iTRAQ_R	Repl_01 / Repl_02 / Repl_03
Sum	6397			

Figure 18 - Example of technical replicates reproducibility for identified peptides.

2.4.3 iTRAQ Results: Bioinformatics and Pathway Analyses

Quantification was performed on proteins with at least 2 different peptides and results were filtered in order to keep only the quantifications that showed a coefficient of variation (CV) lower than 50%. Quantification was performed by Proteome Discoverer based on the intensities of the reporter ions generated during the fragmentation of labeled peptides. With a single experiment we could therefore directly compare the effect of LPS *vs* control cells, as well as the effect of a combined treatment of LPS and L-arginine.

As previously illustrated in the SILAC results, Proteome Discoverer software gives also the possibility to classify all the identified proteins according to their molecular functions, cellular components, and biological processes. The diagrams showing these classifications are reported in Fig. 19, 20 and 21.
Also in this case, the classifications obtained for the identified proteins evidenced an equilibrated distribution between different cellular compartments and molecular processes. This result demonstrates that the method applied it is not biased toward a specific class of proteins, although, differently from the SILAC approach (where cells were lysed with SDS), here cells were lysed with a hypotonic buffer to avoid the presence of detergents that could give problems during the labeling phase with iTRAQ reagents. It seems therefore that the different sample preparation and protein fractionation methods applied, do not significantly affect the classes of proteins analyzable.

Proteins identified and quantified in this experiment are listed in Table 2 in the "Appendix" section, where proteins with an increased expression of at least 30% are colored in blue (in bold proteins with a difference of at least 50%), while downregulated proteins are marked on magenta (again proteins with a difference of at least 50% are bold).

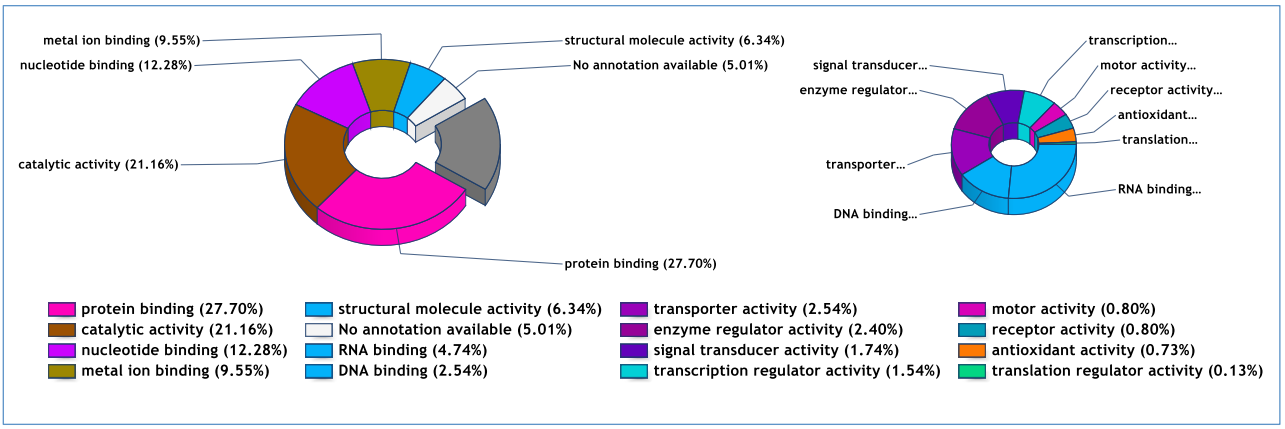


Figure 19 - Molecular function analysis.

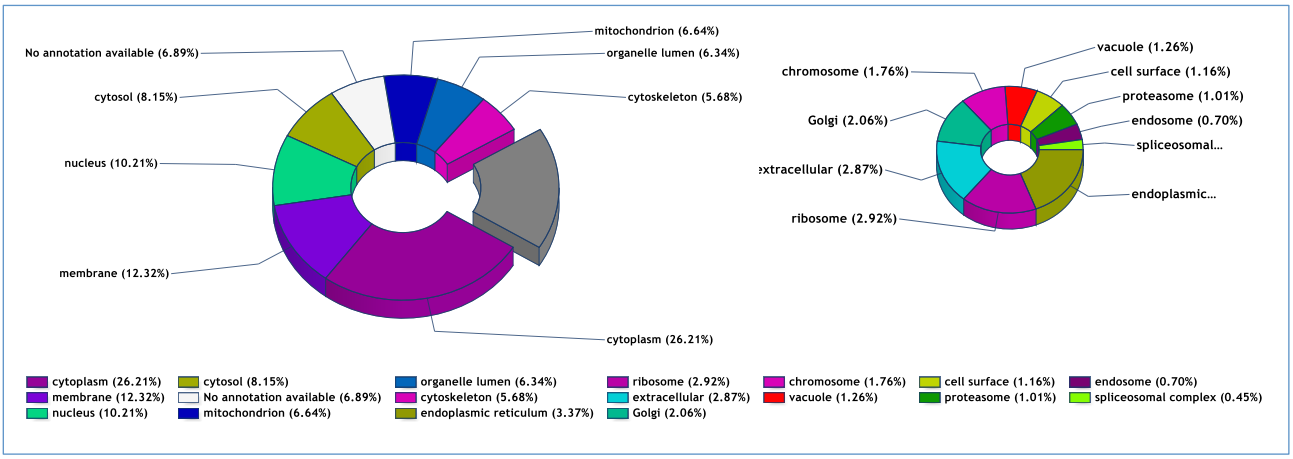


Figure 20 - Cellular components analysis.

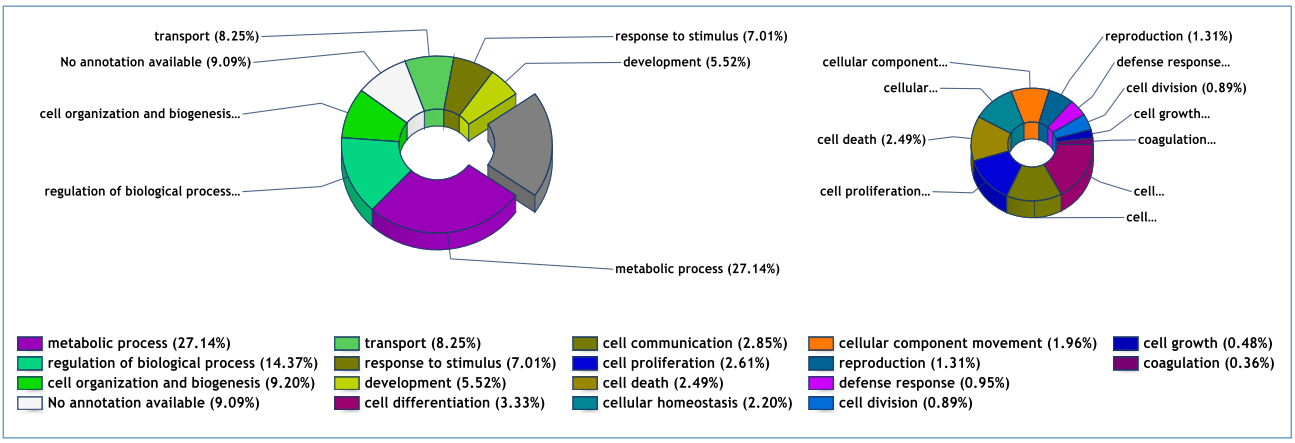


Figure 21 - Biological processes analysis.

A pathway analysis (DAVID) performed on the altered proteins against the total identified proteins highlighted the involvement of extracellular matrix proteins and protein oligomerization process (see Fig. 22) in the LPS-driven calcification of bovine aortic valve cells. In this case nitrogen metabolism (emerged from the SILAC and 2-DE experiments) does not emerge as a possible biological function implicated in the calcification process.

Biological results emerging from our SILAC and iTRAQ studies will be discussed in section 2.6, in order to produce a more comprehensive vision of the molecular changes occurring in aortic valve cells upon endotoxin stimulus and the potential role of L-arginine in preventing valve calcification.

Annotation Cluster 1	Enrichment Score: 1.91			Count	P_Value	Benjamini
GOTERM_CC_FAT	extracellular region part	RT		5	8.4E-3	4.4E-1
GOTERM_CC_FAT	proteinaceous extracellular matrix	RT		4	9.7E-3	2.8E-1
GOTERM_CC_FAT	extracellular matrix	RT		4	9.7E-3	2.8E-1
GOTERM_CC_FAT	extracellular region	RT		5	2.8E-2	4.8E-1
Annotation Cluster 2	**Enrichment Score: 1.18**			**Count**	**P_Value**	**Benjamini**
GOTERM_BP_FAT	protein homooligomerization	RT		3	1.9E-2	1.0E0
GOTERM_BP_FAT	protein oligomerization	RT		3	2.8E-2	9.9E-1
GOTERM_BP_FAT	protein complex assembly	RT		3	1.9E-1	1.0E0
GOTERM_BP_FAT	protein complex biogenesis	RT		3	1.9E-1	1.0E0
Annotation Cluster 3	**Enrichment Score: 0.89**			**Count**	**P_Value**	**Benjamini**
GOTERM_MF_FAT	metal ion binding	RT		9	1.1E-1	1.0E0
GOTERM_MF_FAT	cation binding	RT		9	1.4E-1	9.7E-1
GOTERM_MF_FAT	ion binding	RT		9	1.5E-1	9.5E-1
Annotation Cluster 4	**Enrichment Score: 0.15**			**Count**	**P_Value**	**Benjamini**
GOTERM_MF_FAT	purine nucleoside binding	RT		5	5.6E-1	1.0E0
GOTERM_MF_FAT	adenyl nucleotide binding	RT		5	5.6E-1	1.0E0
GOTERM_MF_FAT	nucleoside binding	RT		5	5.7E-1	1.0E0
GOTERM_MF_FAT	adenyl ribonucleotide binding	RT		4	7.1E-1	1.0E0
GOTERM_MF_FAT	purine nucleotide binding	RT		5	7.8E-1	1.0E0
GOTERM_MF_FAT	nucleotide binding	RT		6	8.2E-1	1.0E0
GOTERM_MF_FAT	purine ribonucleotide binding	RT		4	8.8E-1	1.0E0
GOTERM_MF_FAT	ribonucleotide binding	RT		4	8.8E-1	1.0E0

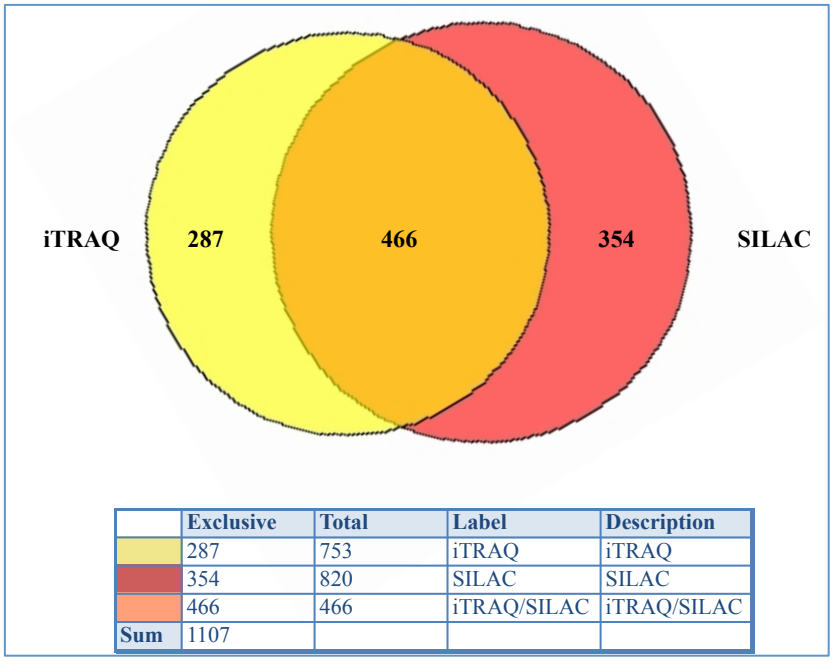
Figure 22 - Pathway analysis (DAVID Bioinformatic Resources 6.7, NIAID, NIH) of altered proteins identified and quantified with the iTRAQ experiment.

2.5 SILAC vs iTRAQ: Comparison of Methods

It is worth noting here that the two different methods applied to the same cellular system gave very similar results in terms of number and classes of proteins identified. However, when comparing the proteins identified in the 2 studies (see Fig. 23) it is possible to see that only 51% of proteins were found in common between the 2 different methods, thus highlighting the impact of lysis buffer and sample preparation on the final outcome of proteomics experiments.

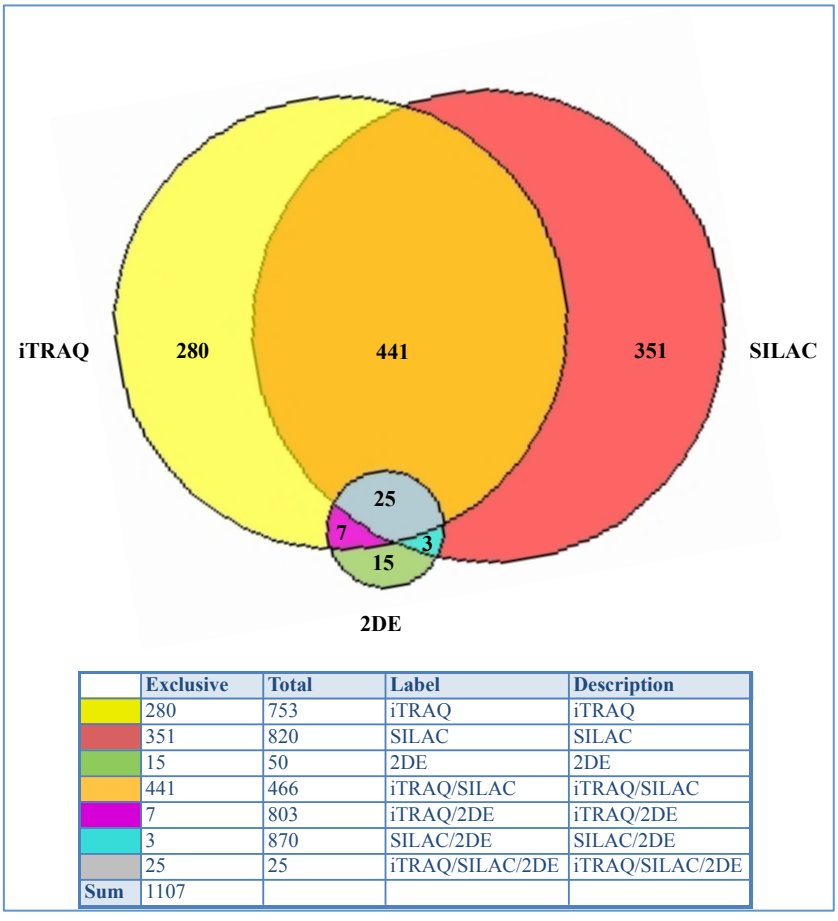
This data show that different workflows (SDS solubilization followed by SDS-PAGE separation for SILAC *vs* hypotonic solubilization followed by SCX fractionation for iTRAQ) lead to only partially overlapping results, making these strategies largely complementary. The same applies also to the 2-DE approach; Fig. 24 shows the number of proteins identified in common to all 3 approaches.
This comparison is not fair in terms of total number of proteins identified, since for the 2-DE approach only proteins that show an altered expression level are subjected to MS analysis, therefore their number is very limited compared to the MS-based approaches.
However, this diagram is very useful to highlight how different methods of analysis (requiring different protocols for protein extraction and fractionation) lead to very different results.

One method therefore does not exclude the others, thus supporting the idea that, whenever possible, more than one approach should be considered in order to gain as much information as possible on the particular biological problem under investigation.



	Exclusive	Total	Label	Description
	287	753	iTRAQ	iTRAQ
	354	820	SILAC	SILAC
	466	466	iTRAQ/SILAC	iTRAQ/SILAC
Sum	1107			

Figure 23 – Comparison of proteins identified with iTRAQ and SILAC methods.



	Exclusive	Total	Label	Description
	280	753	iTRAQ	iTRAQ
	351	820	SILAC	SILAC
	15	50	2DE	2DE
	441	466	iTRAQ/SILAC	iTRAQ/SILAC
	7	803	iTRAQ/2DE	iTRAQ/2DE
	3	870	SILAC/2DE	SILAC/2DE
	25	25	iTRAQ/SILAC/2DE	iTRAQ/SILAC/2DE
Sum	1107			

Figure 24 – Comparison of proteins identified with 3 different proteomic approaches.

2.6 Discussion

Besides all the technical considerations that were discussed above, the analysis of the results obtained with SILAC and iTRAQ approaches allowed us to gain information about the biological processes possibly involved in the LPS-driven calcification of clonal interstitial aortic valve cells. This first important consideration that is worth highlighting here, is the fact that in all our experiments alkaline phosphatase (ALP) shows an increased expression upon stimulation with LPS, confirming the data obtained by measuring the enzymatic activity of ALP. However, differently to what was reproducibly found in the previous study by 2-DE (*Bertacco et al, J. of Proteome Research 2010*) the batches of clonal cells used in our experiments did not show the capability of reducing ALP overexpression when stimulated with L-arginine. This effect is clearly visible by the relative expression level of ALP found in the various experiments: in the SILAC dataset ALP expression was strongly increased by the treatment (LPS/CTRL equal to 9.60) but the co-treatment with L-arginine did not inhibit the LPS effect on ALP expression, as it is shown by an LPS-R/LPS ratio equal to 1.10.

The same trend was also found in the iTRAQ study, where ALP expression is increased with endotoxin treatment (LPS/CTRL equal to 1.65), but is not inhibited by the concomitant treatment of LPS with L-arginine (LPS-R/CTRL equal to 1.66). The lower ratio found in the iTRAQ experiment confirmed the preliminary biochemical studies that showed a marked reduction of the ability of the cells to respond to LPS treatment and that led us to the decision of running the iTRAQ experiment in a single biological replicate. This problem was further confirmed by the fact that the number of proteins found to be altered in our iTRAQ experiment is considerably lower than that found in the SILAC study. The finding that the effect of LPS stimulation on ALP expression and activity was reduced compared to previously published data (*Bertacco et al, J. of Proteome Research 2010*) may be probably explained as an effect of cell senescence or by a possible contamination of clonal cells with pyrogenic agents, which could also explain the loss of susceptibility of the cells to L-arginine treatment. Several biochemical tests conducted on ALP activity on the same batch of cells were in agreement with our proteomics studies, showing that LPS stimulation was much less effective than usual and that L-arginine did not show any capability of inhibiting the increase of ALP activity.

We have already planned to repeat the same experiments using a new batch of clonal cells sensitive to LPS and L-arginine obtained directly from the aortic tissue. Unfortunately, the isolation and characterization of the correct clone population requires months of work and will not be discussed here.

Despite the limited sensitivity of the cells to LPS and L-arginine stimulations, both iTRAQ and SILAC experiments revealed a number of proteins that showed an altered expression level upon LPS treatment and, to a lesser extent, LPS combined with L-arginine treatment.

Several identified and quantified proteins found to be increased in the SILAC analysis confirmed the results previously obtained with the 2-DE analysis but, at the same time, many more proteins were identified, thus significantly increasing the data previously collected. In particular, beside the above-discussed alkaline phosphatase, Annexin A2, a calcium-dependent phospholipid binding protein that also modulates ALP expression in osteoblasts (*Gillette et al, J. Cell Sci. 2004*), showed an increased expression, confirming the data obtained by the 2-DE analysis. In contrast to what was found in the previous study (*Bertacco et al, J. of Proteome Research 2010*), cytoplasmic superoxide dismutase (SOD) did not show a reduced expression after the treatment with LPS, while the mitochondrial superoxide dismutase MnSOD (not previously identified) was found to be strongly upregulated. This suggests a strong increase of oxidative stress induced by the LPS during the calcification process, as already reported (*Miller et al, J Am Coll Cardiol. 2008*) and the increased expression of MnSOD could be explained as a defensive mechanism of the cells. In fact it was recently published that MnSOD exerts a protective effect against endothelial dysfunction in chronic heart failure and reduced mitochondrial isoform of SOD accelerates the progression of atherosclerosis in mice (*Miller et al, Am J Physiol Heart Circ Physiol. 2010*). This would also explain why the treatment with L-arginine did not inhibit the alteration of MnSOD, this being a protective factor for the cell. Although N(G),N(G)-dimethylarginine dimethylaminohydrolase 1 and 2 (DDAH1 and DDAH2, the enzymes that were found altered in the 2-DE study and suggested a correlation with NO synthesis) were not found in our analyses, the dysfunction of nitric oxide synthases, which produce superoxide instead of nitric oxide, (with consequent increased oxidative stress) has been suggested (*Miller et al, Am J Physiol Heart Circ Physiol. 2010*), thus further supporting the idea that NO production plays a key role in the molecular mechanisms involved in valve calcification.

Another result that confirms the 2-DE data is the up-regulation of HSP-70, which is probably correlated with the calcification process of aortic valve cells through the binding of the matrix protein Gla, an inhibitor of calcification which binds and inhibits bone morphogenetic protein (BMP)-2 and -4. The overexpression of HSP-70 could therefore enhance BMP activity and calcification (*Yao et al, Circ. Res. 2009*). High levels of HSP-70 were also found in cells treated with arginine.

In both SILAC and iTRAQ experiments, several proteins involved in chromosome organization, in particular histones, were found to be increased after endotoxin treatment, suggesting the idea that chromatin remodeling is activated during the process. The transcription factor Interleukin Enhancer-Binding Factor 2 (also known as NFAT), as well as Signal Transducer and Activator of Transcription (STAT1), which is strongly involved in cellular response to interferons, cytokines, and growth factors, were also found to be upregulated. Nucleosome structure remodeling, and consequently transcription activation, was also observed by Hurska in response to pro-inflammatory stimuli (*Hruska et al, Circulation Res 2005*). The alteration of the transcription system is probably correlated with the alterations found in the expression of some proteins of the splicing machinery: U2 small nuclear RNA auxiliary factor 2, arginine/serine rich splicing factor 1, and THO complex 4 showed an increased expression when cells were stimulated by LPS, consistently with the increased need of splicing of the mRNAs produced by increased gene transcription.

The increase in transcription and splicing requires more cellular energy, and this could explain the increased expression, revealed by SILAC, of proteins belonging to glycolysis and other energy-related proteins such as mitochondrial ATP synthase (the alteration of which was reduced by arginine treatment), aldehyde dehydrogenase, pyruvate dehydrogenase, phosphopglycerate kinase and triosephosphate isomerase (reported also in the previous work of *Bertacco et al, J. Pr. Res. 2010*), phosphoglycerate mutase, hexokinase, and mitochondrial adenylate kinase 2 (downregulated in presence of L-arginine). These last two proteins were already found to be correlated with aortic calcification (*Krog et al, Br. J. exp. Path 1987*) while correlations between glucose consumption and calcification were already reported in 2007 when Karsenty's laboratory established that the undercarboxylated form of osteocalcin (a pro-osteoblastic factor) has a positive effect on glucose metabolism (*Lee et al, Cell. 2007*) and, more recently, when it was reported that osteocalcin shifts cells toward glycolytic breakdown of glucose, in a HIF-1α–dependent manner, and stimulates calcification of cartilage and vasculature (*Idelevich et al, Arterioscler. Thromb. Vasc. Biol. 2011*).

The increased expression of proteins related to ATP production could also be explained by the increment of reactive oxygen species (ROS) inside the cells (as discussed above), that changes mitochondrial Ca^{2+} homeostasis, producing an unbalance in ionic gradients through mitochondrial membranes that influence ATP synthesis (*Brookes et al, Am. J. Physiol. Cell Physiol. 2004*). This hypothesis is supported by the altered expression of voltage-dependent ionic channels. Always related to increased ROS production, we found several peroxiredoxins (antioxidant enzymes) that increased their expression after LPS treatment, coherently with what already discussed about MnSOD. Two other important proteins emerging from this study are ERO1-like protein alpha and

Cathepsin D. The first one is an oxidoreductase enzyme with a strong oxidative activity in the endoplasmic reticulum and is responsible for the production of ROS, and the consequent increase of cellular oxidative stress (*Cabibbo et al, J. Biol. Chem. 2000*; *Appenzeller-Herzog et al, EMBO J. 2008*). ERO1-like protein alpha was found increased in cells treated with LPS, while a downregulation of its expression emerged in the cells treated with L-arginine, suggesting a possible role of this amino acid in reducing cellular stress caused by LPS treatment. The second, cathepsin D, a lysosomal acidic protease known to be involved in cancer and neurodegeneration (*Masson O et al, Biochimie. 2010*; *Steinfeld R. et al., Am. J. Hum. Genet. 2006*) was again upregulated by LPS while its increased expression was inhibited in presence of L-arginine. Another protein of the same family with a potent elastolytic activity, cathepsin S, has been already studied in correlation with aortic diseases, where it accelerates calcification in mice with chronic renal pathologies (*Aikawa et al, Circulation 2009*).

Other proteins found to be upregulated after treatment with endotoxin are involved in apoptosis regulation, coherently with the cell defense system against ROS activity. HSP-70 (discussed above), cadherin, catenin, several peroxiredoxins, and ADAMTSL4 show an altered expression upon LPS stimulation. In particular, cadherin (dowregulated by LPS treatment) and catenin are components of the cellular junctions: the first is a calcium dependent adhesion mediator of epithelial cells responsible for the correct orientation of mitotic spindle during asymmetric cell division in mammalian epithelia (den *Elzen et al, Molecular Biol. of the Cell 2009*), while catenin is strongly involved in the switch to osteoblastic-like phenotype (*Caverzasio, Rev. Med. Suisse Romande 2004*). ADAMTSL4, a protein that promotes apoptosis (*Liu et al, FEBS 2006*) was found positively altered after the stimulus, and this could indicate a cellular response to the biological stress in the direction of programmed cell death.

Interestingly, the acquisition of a calcific phenotype seems to be accompanied by a strong downregulation of several proteins involved in cytoskeletal structure and remodeling (e.g. cytoplasmic actin, alpha-actinin-1 and -4, ezrin, filamin-A and -1, microtubule associated protein 4, moesin, septin-11, and cytoplasmic tryptophanyl-tRNA synthase), suggesting a complete remodeling of the cellular structure that is probably due to the morphological phenotypic change to osteoblast-like cells. Moreover, changes in cytoskeleton structures drive also changes in the internal transport of vesicles, a really important mechanism for the calcification process because is required for the transport of calcium outside the cells to start matrix calcification.
Another protein found downregulated in our experiment is transgelin (SM22), an important marker of cellular morphology that, together with cytoskeletal proteins, suggest a strong cell response to

LPS, causing an evident change in cell function. Interestingly, the alteration of this protein seems to be blocked when cells are co-treated with LPS and L-arginine, supporting the notion that this amino acid tends to inhibit the acquisition of a calcific phenotype.

Moreover, in response to the calcification stimulus, cells seem to increase the production of pro-collagen factors, such as procollagen-lysine-2-oxoglutarate 5-dioxygenase 1, that was found increased after the treatment with LPS and is negatively affected by the presence of L-arginine. Other secreted proteins involved in matrix composition were found altered by the iTRAQ experiment, like SPARC (a secreted protein that has been discovered in bone cells and interacts with extracellular matrix, collagen and cytokines, *Brekken, Matrix. Biol. 2001*) and synaptic vesicle membrane protein VAT-1 homolog, a calcium-regulated keratinocyte activation protein that is involved in epidermal repair mechanisms (*Koch et al, Arch. Dermatol. Res. 2003*). Both these proteins were downregulated upon treatment with LPS. Moreover, collagen III alpha chains are altered by LPS treatment, while prolyl 4-hydroxylase subunit alpha-1 (a key enzyme in the biosynthesis of collagens), showed upon endotoxin stimulation an increased expression that is inhibited by the treatment with L-arginine, suggesting that mechanisms regulating the extracellular matrix might be strongly involved in the calcification process induced by LPS. Evidences of a role of collagen (especially isoform I) in the aortic calcification process have been reported in several studies (e.g. *Watson et al, Art., Thromb., and Vasc. Biol. 1998*; *Eriksen et al, Atherosclerosis.* 2006).

Few other interesting proteins like CD9 antigen, CD99 antigen-like protein, and prostaglandin G/H synthase 1 showed an altered expression upon LPS treatment. They are involved in cell adhesion and motility and in the regulation of cell proliferation (*Masellis-Smith et al, J- Immunol. 1994*; *Schenkel et al, Cell. Commun. Adhes. 2007*).

2.7 Conclusions

Summarizing, from our study, although conducted on a cellular model that was not as responsive to the selected stimuli as expected, we could identify several proteins whose expression level was altered by LPS treatment. Our data confirmed and supported the results previously obtained by a 2-DE approach using the same experimental model, and added new interesting connections to several cellular pathways that seem to be involved in aortic valve calcification, such as cellular oxidoreductase activity, cytoskeletal and spliceosome regulation, glycolisis/gluconeogenesis, and arginine metabolism, that was found to play a pivotal role during the calcification process induced by LPS. Obviously, selected and targeted functional studies will have to be performed in order to investigate the role of some of the proteins identified in these experiments. However, because of the low response to LPS stimulus of the clonal cells used in our study, we are planning to repeat the experiments starting from a new primary cell culture, hoping to obtain again a batch of cells sensitive to endotoxin stimulus and, most importantly, for which the treatment with L-arginine will inhibit the calcification process driven by LPS. The possibility to identify a class of proteins that upon calcifying stimulus change their expression level if not kept under "normal" conditions by the protective effect of arginine will allow to better focus further studies and to increase our understanding of the aortic valve calcification process induced by pro-inflammatory stimuli.

CHAPTER 3

QUANTITATIVE PROTEOMICS ANALYSIS TO INVESTIGATE THE CK2-DEPENDENT INTERACTOMES AND PHOSPHOPROTEOMES

3.1 Introduction

Protein phosphorylation is one of the most important covalent modifications in the cell and is essential for protein function and pathways regulation; in fact every organism, from bacteria to humans, exploits this post-translational modification to carry out the cellular activity. This reversible modification works like a molecular switch to regulate metabolic pathways, signaling process, intracellular transport, genic transcription, and cellular movement (*Petsko et al, Zanichelli 2006*).

The enzymes that are able to phosphorylate proteins adding a phosphate group to specific sites into the amino acid sequence are called kinases, while the enzymes performing the removal of the phosphate group are called phosphatases. The use of different enzymes for phosphorylation and dephosphorylation allows an independent control of these events that can be regulated by different stimuli (*Petsko et al, Zanichelli 2006*).

Genomic sequencing has revealed that 2-3% of all eukaryotic genes are likely to encode for protein kinases, and it has been suggested that 30% of all the proteins expressed in a eukaryotic cell is phosphorylated at some point, emphasizing the ubiquitous role of protein phosphorylation (*Hubbard, Trends Biochem. 1993*). Actually, in the last few years some high-throughput experimental studies by mass spectrometry showed a larger diffusion of protein phosphorylation, increasing the statistic reported above. Numerous large-scale phosphoproteomics experiments have been performed over the past few years by several groups (*Monetti et al, Nat. Methods 2011*; *Leemer et al, J. of Proteome Res 2008*; *Oppermann, Mol. Cell. Proteomics 2009*) and the results collected in specific databases like Phosida (Phosphorylation Site Database) (*Gnad et al, Genome Biology 2007*), PhosphoSitePlus (*Hornbeck et al, Proteomics 2004*), Phospho.ELM (*Dinkel et al, Nucl. Acids Res 2010*) or PhosphoPep (*Bodenmiller et al, Nature Biotechnology 2008*). More than 42900 eukaryotic non-redundant phosphosites are contained in Phospho.ELM for a total of about 8700 protein substrates and 300 different kinases, but the data stored in these databases are continuously updated, thanks to the contribution of an increasing number of scientific groups.

Considering the number of phosphoproteins identified until now and the total number of proteins of the human proteome (Ensemble 43.36) it is possible to estimate that the phosphorylation process involves almost 40% of the total human proteins, and this percentage seems to be continuously increasing.

The phosphate group used to phosphorylate proteins comes from the terminal phosphate of a nucleoside triphosphate, usually ATP, and the amino acid selected as the target of the

phosphorylation determines the class of the kinase. In fact, even if all protein kinases have the same function in the cell, they can be divided into different classes based on the substrate specificity. Due to the high pleiotropicity of the majority of them, it is more reasonable to classify these enzymes using the phospho-acceptor amino acid specificity, rather than substrate specificity (*Hunter, Methods in Enzymolgy 1991*).

The "Nomenclature Committee of the International Union of Biochemists" has recommended the following kinase classification:

1) serine/threonine kinases: enzymes involved in the transfer of a phosphate group from the nucleoside triphosphate to the hydrossilic group in side chain of serines and threonines, generating a phosphate ester (E.C. 2.7.1.0).
2) tyrosine kinases: the phosphate group is added to the phenolic group of tyrosines, creating a phosphate ester (E.C. 2.7.1.1).
3) histidine or arginine or lysine kinases: the adding of the phosphate group to these 3 amino acids lead to the formation of a phospho-amidate group in position 1 or 3 of histidines, on the guanidine group of arginines or on the amino group of lysines (E.C. 2.7.1.2).
4) cysteine kisases: a thioester is generated after the phosphorylation of an acceptor cysteine (E.C. 2.7.1.3).
5) aspartic or glutamic acid kinases: the phospho-acceptor group for the substrates of this class of kinases is the carboxylic group (E.C. 2.7.1.4).

In prokaryotes, kinases responsible for the phosphorylation of histidine and aspartic/glutamic acid residues are found together with serine/threonine and tyrosine kinases. However, in eukaryotes, kinases phosphorylating on serine, threonine, and tyrosine represent one of the largest protein families. In particular these enzymes are the third most common group coded in the human genome, accounting for 575 members (about 2% of the genome) and the substrates of this class of enzymes are definitely the most widely studied. Although these few hundreds kinases belong to different classes (as mentioned above) even within the same class the number of substrates recognized by each kinase is highly variable: some kinases are specific only for a single or few target proteins - like wee1 and MEK - while others can phosphorylate hundreds of different substrates, for example CK2 (*Litchfield, Biochem. J 2003*).

The phosphate addition to the side chain of serine, threonine, tyrosine, histidine, and aspartic/glutamic acid can deeply affect the structure/function relationship of the protein interested by the phosphorylation, for example through the conformational variation due to the new volume

and charge in the phospho-amino acid, or the creation of a new recognition site for other proteins that are able to interact with specific phospho-sequences (*Petsko et al, Zanichelli 2006*).
The frequency of phosphorylation changes depending on the amino acid and its accessibility in the protein structure. Some important observations about this topic were described by Olsen in a structural investigation of the phosphoproteome, demonstrating the role of hydrophilicity not only in the accessibility of phoshoresidues (even if this is an important requisite for the phosphorylation efficiency), but also in the amino acid phosphorylation preference: serine and threonine are more frequently phosphorylated (80% and 18%, respectively) than tyrosine (2%). Tyrosines, being more hydrophobic than serine and threonine, are usually located in less accessible regions of the protein, dramatically reducing the possibility of being phosphorylated by kinases (*Olsen et al, Cell 2006*).

In 1991, the first three-dimensional structure of the catalytic subunit of cAMP-dependent kinase (also called PKA) was solved *(Knighton et al, Science 1991)*. Since then, the comparison of different kinase structures has shown a high conservation between classes that can also explain the phosphorylation mechanism. Canonical kinases contain two main lobes: a β-sheets N-terminal region characterized by the presence of a single α-helix, essential for the enzyme activity, and a C-terminal region in which the most representative secondary structure is the α-helix. The C-terminal lobe is usually responsible for the catalytic activity, while the N-terminal part generally has a regulatory function. The connecting region between the two lobes is called hinge region and works as positioning site for the substrates (*Petsko et al, Zanichelli 2006*).
A high homology degree characterizes the primary structures of human kinases, supporting the idea of a similar activation state. Generally, kinases need to be activated by reversible modulation mechanisms, in response to cellular signals like hormones, growth factors, second messengers, metabolites, and other stimuli (*Petsko et al, Zanichelli 2006*). An exception is the protein kinase CK2 that is constitutively active inside the cell, i.e. no activation/deactivation mechanisms are known for this enzyme. Therefore, the above-mentioned factors can only modulate the activity of this kinase that remains always active (*Pinna, Acc. Chem. Res. 2003*).

3.2 The Protein Kinase CK2

Among protein kinases, CK2 has a special role due to its structural and functional characteristics.
CK2 was one of the first kinases to be discovered and originally its name was Casein Kinase II, because, in 1954, Burnett and Kennedy used artificial caseins as substrates to isolate enzymes from rat liver (*Burnett et al, J. Biol. Chem. 1954*). Nowadays, more than 300 substrates are known to be phosphorylated by CK2 (*Meggio et al, Faseb J. 2003*), but, although caseins are excellent *in vitro* substrates for this kinase, it's very unlikely that this class of proteins represent *in vivo* targets of this enzyme (*Pinna, Acc. Chem. Res. 2003*).
The enzymatic activity of CK2 is carried out by its catalytic subunit called CK2α, that bears the general structural features of the other kinases: a N-terminal region characterized by the presence of β-sheets with a single α-helix, essential for the enzyme activity, and a α-helix enriched C-terminal region, involved in the interactions with substrates. The C-terminal lobe is usually responsible for the catalytic activity and contains the activation loop (containing also the Tyr182, site of autophosphorylation) and the glycine loop, while the N-terminal part generally has a regulatory function and interacts with the activation loop locking it in a open position, essential to provide the fully active conformation of CK2 (*Sarno et al, J. of Biol. Chem. 2002*). The connecting region between the two lobes is called hinge region and works as positioning site for the substrates. All domains described are shown in Fig. 1.

It has been shown that in many organisms distinct isomeric forms of the catalytic subunit of CK2 exist, and in humans in particular, three catalytic isoforms, named CK2α, CK2α', and CK2α'' are expressed (*Litchfield, Biochem J. 2003*). While the first two isoforms are well characterized, less is known about the third one that was identified only recently.
Different genes encode for the different isoforms of the catalytic subunit, even if they are strictly correlated: in the catalytic site they reach 90% identity, explaining why their enzymatic properties are so similar *in vitro* (*Lietchfield et al, Mol. Cell. Biochem. 1993*). On the contrary, the C-terminal domains are totally different, but highly conserved among species, suggesting important functions related to this domain.

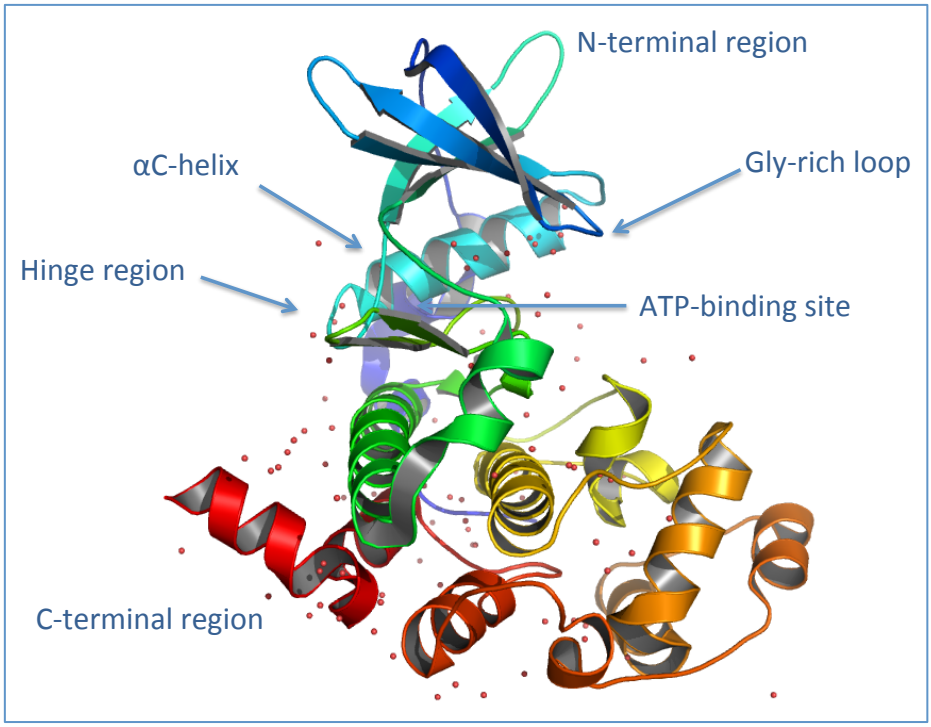


Figure 1 - 3D structure of the catalytic subunit of CK2 (pdb ref. 1JAM elaborated with MacPyMol, DeLano Scientific)

The activity of CK2α can be regulated either by the interaction with other proteins or co-factors or by the interaction with another CK2 subunit called CK2β, that has a regulatory function (*Litchfield, Biochem. J. 2003*). CK2β (see Fig. 2) is even more highly conserved between species than the catalytic subunits but, differently to CK2α, only one form of the β subunit has been discovered in humans, while, for other organisms such as plants, several isoforms of the β subunits are known (*Gietz et al, J. Biol. Chem. 1995*).

Also the regulatory subunit of CK2 (like its catalytic subunit) contains an autophosphorylation site that seems to be involved in the modulation of the activity of this kinase (*Zhang et al, Oncogene 2002*).

Even if the comprehensive understanding of the role of CK2β has not been achieved, many studies have shown that it stabilizes the catalytic subunit against denaturing agents, increasing the kinase activity toward most substrates (*Meggio et al, Eur. J. Biochem. 1992*); in particular, the C-terminal domain of the regulatory subunit was found to be important for this stimulatory effect (*Sarno et al, Biochemistry 2000*). Moreover, it has been found that CK2β cooperates in modulating substrate selectivity; this has been demonstrated for many CK2 cellular partners including for example p53 (*Filhol et al, J. Biol. Chem. 1992*), DNA topoisomerase II (*Bojanowski et al, J. Biol. Chem. 1993*), Fibroblast Growth Factor 2 (*Bonnet et al, J. Biol. Chem. 1996*).

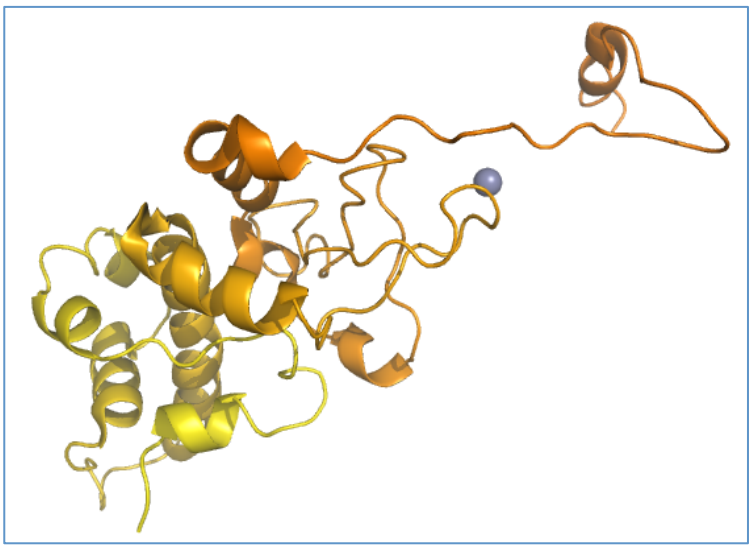


Figure 2 - 3D structure of regulatory subunit of CK2 (pdb ref 1JWH elaborated with MacPyMol, DeLano Scientific)

In this way, phosphorylation of these proteins is based not only on the consensus sequence recognition, but also on the formation of a molecular platform by the β subunit, which allows the docking and/or the recruitment of the substrates or other potential regulators (*Poletto et al, Biochemistry 2008*). This feature of CK2β is exploited when it interacts with the catalytic subunit to form the tetrameric holoenzyme (see Fig. 3), composed by two catalytic subunits linked to a central core of a CK2β dimer (*Niefind et al, the EMBO J. 2001*) that acts like a platform for the interactors of CK2.

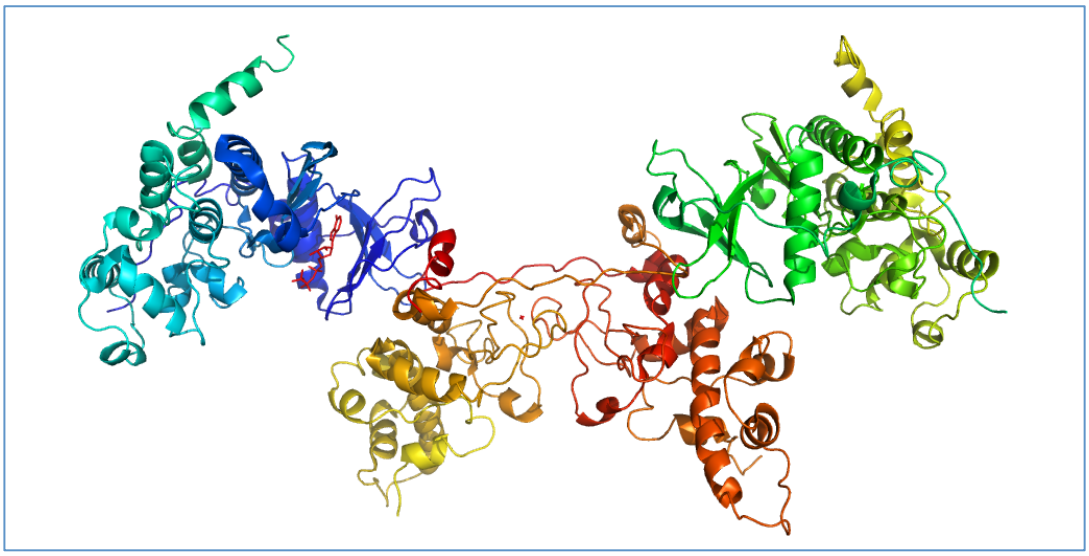


Figure 3 - 3D structure of human CK2 holoenzyme (pdb ref. 1JWH elaborated with MacPyMol, DeLano Scientific LLC)

Mammalian CK2 tetramer can contain two identical isoforms of CK2α (i.e. CK2α, CK2α', or CK2α") or different combinations of them. It has been shown that the catalytic subunits can exist and properly function also isolated from the β subunits, therefore not associated to form the tetrameric structure (*Litchfield et al, Mol. Cell. Biochem. 1993*), but once the complex with the regulatory subunits is created, the activity of CK2α can increase or decrease depending on the substrate. In fact, the substrates of CK2 can be divided into three different classes (*Marin et al, FEBS Letters 2000*):

1) Proteins that require for their phosphorylation only the catalytic subunit. For these substrates, the presence of the regulatory subunits can increase the efficiency but is not essential. Proteins belonging to this group are for example Inhibitor-2 of Protein Phosphatase I I-2 (*Marin et al, FEBS Letters 2000*), p23 (*Tosoni et al, Molecular and Cellular Biochemistry 2011*) and cdc37 (*Miyata et al, Molecular and Cellular Biochemistry 2008*).
2) Proteins that are not phosphorylated in the presence of the regulatory subunits and for which the β subunits consequently exert an inhibitory effect. Substrates belonging to this class are for example Calmodulin (*Marin et al, FEBS Letters 2000*) and MDM2 (*Pinna et al, Progress in Cell Cycle Res. 1997*).
3) Substrates that can be phosphorylated if the enzyme is in its tetrameric form, for which therefore the β subunits exert an activating effect (e. g. Rev, CREB, MS2-E7) (*Marin et al, FEBS Letters 2000*).

In contrast with the majority of the other cellular kinases, that exist in the cell in a stand-by mode and are transiently activated, CK2 is constitutively active and is regulated by covalent modifications and regulatory interactions with proteins and/or non-protein molecules (*Lietchfield, Biochem. J. 2003*). Evidence of possible roles for the two isolated subunits have led to the hypothesis of a balance between the expression of CK2α and CK2β and their localization into specific cellular compartments, which may contribute to the regulation of the enzymatic activity (*Faust et al, Cell Tissue Res. 2000*).

The specificity of CK2 is mainly directed to serine and threonine, even if in particular and very limited cases (especially in yeast) it is able to phosphorylate also tyrosine residues, therefore acquiring the role of dual-specificity kinase. A systematic screening of CK2 phosphorylation activity on synthetic peptides containing phosphorylatable serines, threonines, and tyrosines suggested that the kinetic parameters for serine-/threonine-containing peptides are much more

favorite compared to tyrosine-containing peptides (*Marin et al, J. Biol. Chem. 1999*). It is possible to define the minimum *consensus* sequence recognized by CK2 as S/T-x-x-E/D/pS/pT/pY, where x is any residue except basic aminoacids. Therefore CK2 is an acidophilic protein kinase that recognizes the target aminoacid (serine/threonine) when an acidic or phosphorylated residue is present in position +3, and such minimum *consensus* sequence is strongly reinforced by additional acidic residues around the phosphosite (*Sarno et al, J. of Biolog. Chem. 1996*). However, cases are known in which CK2 is not able to phosphorylate a substrate, even if it contains the correct *consensus* sequence, and cases in which CK2-dependent phosphorylations have been observed in the absence of the minimum *consensus* sequence, suggesting that other factors, probably related to the substrate's structural features, can influence the activity and substrate recognition (*Litchfield, Biochem. J. 2003*).

Such highly acidophilic *consensus* motif has been considered peculiar and strictly associated to protein kinase CK2 until the recent discovery of a new family of very acidophilic kinases: the Polo-like kinase (PLK) family, and in particular the members of the family named Polo-like kinases 2 and 3 (PLK2 and PLK3) (*Johnson et al, Biochemistry 2007*). The preference for acidic residues on all the positions encompassing the phosphoacceptor site suggests therefore a possible overlapping of substrate recognition between PLK2/PLK3 and protein kinase CK2.

Nowadays, more than 300 proteins are known to be phosphorylated by CK2, and the large majority of them are phosphorylated on serines and threonines (*Meggio et al, Faseb J. 2003*). It is quite interesting to note that CK2 substrates belong to very different protein classes, underlying the ubiquitous role of CK2 inside the cell and its wide effect on multiple cellular pathways.

3.3 CK2 as a Druggable Target

Inside the cell, CK2 is an essential protein, and the deletion of both its catalytic subunits is lethal (*Padmanabha et al, Mol. Cell. Biol. 1990*). In 1990 prof. Pinna curiously described CK2 as *an eminence grise* (*Pinna, Biochim. Biophys. Acta 1990*) that acts behind the scenes in such a way that it is indispensable, even if it does not apparently play any prominent role in the hierarchy of cellular functions. All these observations would support the idea that CK2 is of vital importance because of its pleiotropism: although a single phosphorylation might not be indispensable, the omission of all the tasks CK2 is in charged for would be fatal for the cell. It would be nice, however, to demonstrate that behind its randomness CK2 performs a number of global tasks that have specific means in regulating biological processes (*Pinna, J. Cell. Science 2002*).

Abnormalities in the natural role of kinases are often the cause of several human diseases, in particular cancer and tumor pathologies, the treatment of which used to be based on cytotoxic and hormonal agents until few years ago (*Battistutta, Cell. Mol. Life Sci. 2009*).

In the past two decades the development of inhibitors against kinases has grown exponentially, bringing this enzyme family on the second place of importance among the drug targets, after G-protein-coupled receptors (*Cohen, Nat. Rev. Drug Discov. 2002*). The choice of inhibiting the kinases is due to their high involvement in several key-role cellular processes, like signal transduction, apoptosis and cell proliferation. In fact, a lot of diseases, especially neoplasia, show high activity level of kinases. So, the development of selective and efficient inhibitors able to affect only single classes of kinases represents a perfect tool to better understand the role of each enzyme in the cell and create a library of compounds with high therapeutic potential.

CK2, like many other kinases, is strongly involved in several cellular processes, and in particular it has been hypothesized that this enzyme plays a crucial role in the transduction of survival signals, protecting the cells against stress conditions (*Ahmed et al, Trends Cell Biol. 2002*). CK2 is ubiquitous inside the cell, where it is localized both in the nucleus and in the cytoplasm, and its concentration dramatically increases in the nuclei of cancer cells, for example in prostatic, mammal gland, lung, and kidney tumors (*Battistutta, Cell. Mol. Life Sci. 2009*). Many studies demonstrated that overexpression of CK2 increases cell oncogenic potential by sensitizing cells to transformation by other oncogenic proteins, thus suggesting a strong anti-apoptotic potential for CK2. In fact, down-regulation of this kinase's activity decreases cellular proliferation and induces apoptosis in cancer cells (*Wang et al, Mol. Cell. Biochem. 2005*).

CK2 is a peculiar kinase because it can bind both ATP and GTP, and it is not inhibited by staurosporine, one of the most powerful kinase inhibitors (*Meggio et al, Eur. J. Biochem. 1995*). For this reason, it is possible to consider CK2 as a different kinase, with unique features that can be exploited to find specific inhibitors.

Nowadays several kinase inhibitors are used in clinical therapies and the majority of them are ATP-mimetic, therefore directed against the ATP (or GTP) binding site. The X-ray structures of kinase-inhibitor complexes have revealed that the structural elements around the ATP site are different enough between kinases to achieve a strong inhibition specificity. The shape and small size of the catalytic site of CK2 is essential for the inhibitors' selectivity against this enzyme (*Battistutta et al, Chem. Biol. 2005*) and these features have been exploited to design, develop and test a large array of ATP-mimetic inhibitors of CK2.

The majority of the CK2 inhibitors have been studied by crystallization of CK2α in complex with synthetic inhibitors that have been found in *in vitro* inhibition experiments to be efficient and

specific against CK2 compared with a panel of about 80 kinases representative of nearly all of the branches of the kinome (*Pagano et al, Biochem. J. 2008*). TBB (4,5,6,7-tetrabromo-1H-benzotriazole) and its derivatives DMAT (2-dimethylamino-4,5,6,7-tetrabromo-1H-benzimidazole) and TBI (4,5,6,7-tetrabromo-1H-benzimidazole) are the most used among the commercially available inhibitors (*Pagano et al, Biochem. J. 2008*). Unfortunately, these inhibitors where initially tested on a panel of only 30 kinases, and further studies performed on a larger panel revealed other more specific tetrabromo-benzimidazole derivatives inhibitors (*Pagano et al, Biochem. J. 2008*). In contrast, other commercially available CK2 inhibitors, like quercetin, apigenin and emodin (1,3,8-trihydroxy-6-methyl-anthraquinone), do not display a selectivity comparable with TBB e DMAT (*Sarno et al, Biochem J. 2003*).

Another more potent, cell permeable and selective inhibitor designed by virtual screening is the anthraquinone quinalizarin (Q1) (1,2,5,8-tetrahydroxyanthraquinone), the efficiency and selectivity of which have been tested on a panel of almost 90 kinases (*Cozza et al, Biochem. J 2009*). Q1 (see Fig. 4) is a powerful, cell permeable inhibitor of CK2, with the lowest inhibition constant among the anthraquinones ($K_i \cong 50$ nM) and with the lowest promiscuity score (*Sarno et al, Curr. Top Med. Chem. 2011*), characteristics that make Q1 one of the most selective CK2 inhibitors found so far. For these reasons we have selected the inhibitor Q1 to conduct the study described in this thesis.

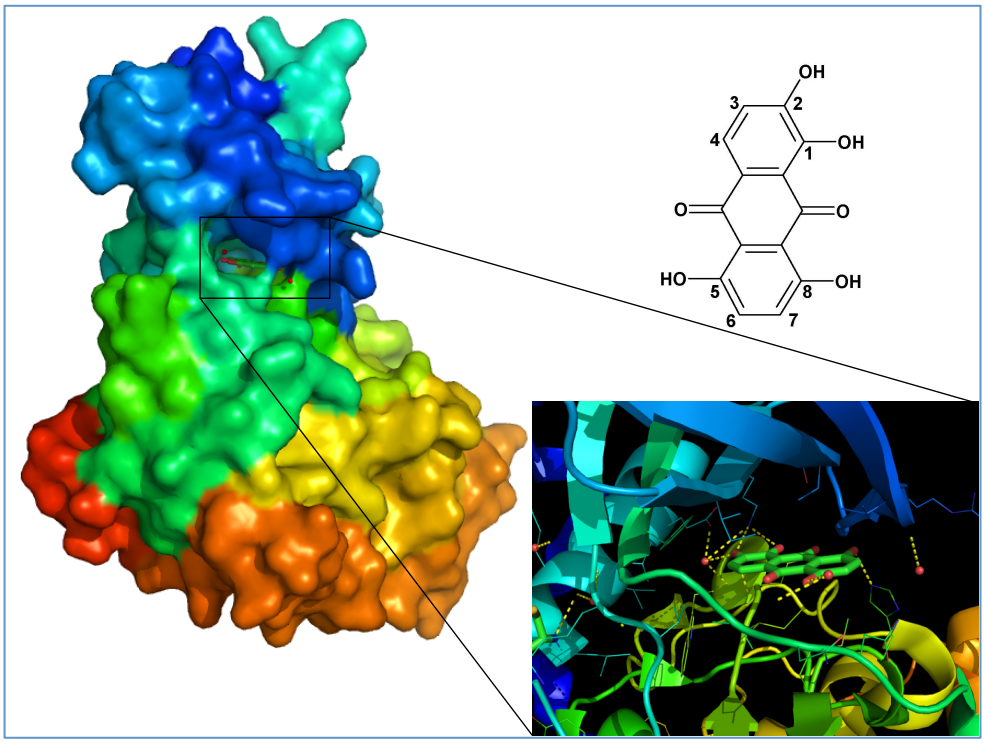


Figure 4 - 3D structure of CK2α from *Zea mais* in complex with quinalizarin (pdb ref. 3FL5, elaborated with MacPyMol (DeLano Scientific LLC))

Recently, the discovery of a novel class of potent tricyclic ATP-competitive CK2 inhibitors has opened the way for the therapeutic targeting of CK2 in humans for the treatment of cancer (*Battistutta et al, Biochemistry 2011*). An analogue of this class of inhibitors, CX-4945 (5-(3-chlorophenylamino)benzo[c][2,6]-naphthyridine-8-carboxylic acid), displays very good pharmacological properties and *in vivo* efficacy, and is now under evaluation in clinical trials for the treatments of solid tumors (*Pierre et al, J. Med. Chem. 2011*; *Siddiqui-Jain et al, Cancer Res. 2010*).

3.4 Aims of the Study

Although CK2 is one of the most pleiotropic protein kinases with a growing list of more than 300 physiological substrates identified so far, the role of this enzyme within the cell is far from being completely understood. It is known that CK2 is involved in a wide range of cellular pathways and activities and it is also for this reason that it is extremely difficult to grasp the real role played by this kinase in the cell. To try to elucidate this aspect and shed some light on the main cellular functions in which CK2 is involved, we decided to apply large-scale proteomics and phosphoproteomics approaches to detect proteins that stably interact with CK2 and to identify putative *in vivo* substrates of this pleiotropic kinase. The possibility to gain information about proteins that interact and/or are substrates of CK2 will help to better understand the role played by this kinase in the cell and will hopefully be useful to pinpoint new cellular activities that are influenced by this enzyme.

The first part of this chapter will focus on the identification of new interacting partners of CK2 by a label-free quantitative approach. In the second part of the chapter, the search for new possible substrates of CK2 directly in a cellular system by means of SILAC technology will be presented.

3.5 Label-Free MS Analysis of CK2 Interactomes

The first part of this project aimed at the identification of molecular partners of the protein kinase CK2, i.e. proteins that can stably interact with this protein kinase and that therefore might be substrates or play a role in the modulation of its cellular activity. To investigate this aspect we decided to apply a mass spectrometry-based label-free quantitative approach to proteins that were co-immunoprecipitated with CK2α subunit (see details of this proteomic approach in section 1.3). The possibility to use a very specific and efficient antibody produced *in-house* against the catalytic subunit of CK2 made possible to combine a classical co-immunoprecipitation experiment with the identification of proteins by a proteomic approach. This strategy has been widely used to identify interacting partners of a specific protein, but suffers from a main limitation, i.e. the difficulty in distinguishing among all identified proteins those that are real interacting partners of the target protein and those that are simply contaminants. To overcome this problem it is therefore necessary to exploit a quantitative technique; in this case we have chosen a quantitative label-free approach.
To perform a reliable quantitative label-free analysis it is necessary to use a high resolution and high mass accuracy mass spectrometer coupled with a highly reproducible LC system. Such instrumental set-up allows to obtain high quality LC-MS/MS data that can be aligned and compared by dedicated software to gain qualitative and quantitative information regarding the samples analyzed. The instrument chosen for this study is the Agilent Technology 6520 Accurate-Mass Q-TOF Mass Spectrometer coupled online with a nano-HPLC (1200 series, Agilent Technologies) by a Chip Cube interface. This particular interface requires the use of a chip-based chromatographic system that integrates a nano-column, an enrichment column and a spray emitter into a compact system, thus reducing the presence of dead volumes and assuring highly reproducible chromatographic analyses.

3.5.1 Evaluation of System Reproducibility and Linearity

Before starting the actual experiment, reproducibility and linearity of our LC-MS system were tested by repeated analyses of tryptic digested Bovine Serum Albumin (BSA) as a standard sample. BSA was analyzed in different amounts to verify the linear response of the instrument to the protein concentration and the reproducibility of the chromatographic system.

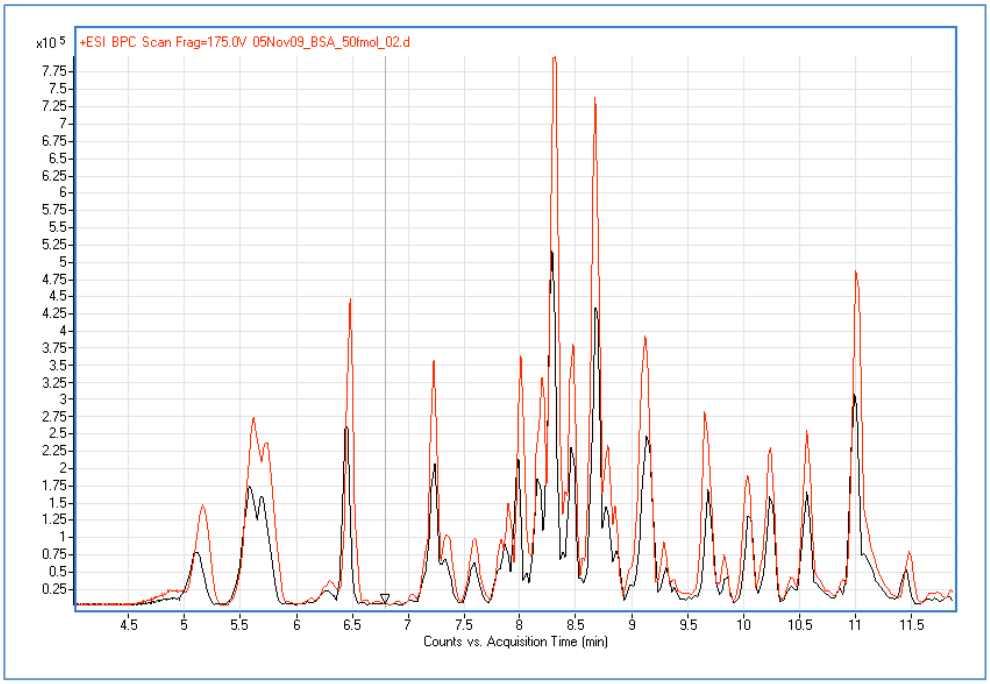


Figure 5 - Base Peak Chromatograms (BPC) of 30 fmol (black curve) and 50 fmol (red curve) of tryptic digested BSA.

Fig. 5 shows the Base Peak Chromatograms (BPC) relative to 30 fmols (black curve) and 50 fmols (red curve) of digested BSA injected in our system and eluted in 15 min with a linear gradient of acetonitrile. The chromatographic traces are obviously extremely similar and the peak intensity is proportional to the amount of protein loaded onto the system. This feature can be tested across several orders of magnitude of protein concentration to define the limits of the instrument in terms of linear response. Thus, we performed a more detailed test by analyzing different quantities of BSA (from 0.1 to 100 fmols) in triplicate to assess the sensitivity and the linear response of the mass spectrometer as well as the reproducibility of the LC system. Details about the conditions applied to the LC-MS/MS analyses are reported in section 4.8.

The results were plotted in a graph (see Fig. 6) that shows how the instrument is characterized by an excellent linear response over a wide range spanning 3 orders of magnitude, resulting in a correlation score R^2 of 0.99967. Each test sample was analyzed in triplicate and the reproducibility of the MS signals obtained is extremely high as can be appreciated by the very small error bars in the graph.

We also wanted to test the reproducibility of the LC system that has a strong impact on the label-free quantitative analyses because can greatly affect the alignment of LC-MS data performed by dedicated software. We decided therefore to evaluate the maximum shift in retention time observed

for repeated injections during the chromatographic separation. Fig. 7 shows the maximum variation of retention times measured for 6 selected BSA ions.

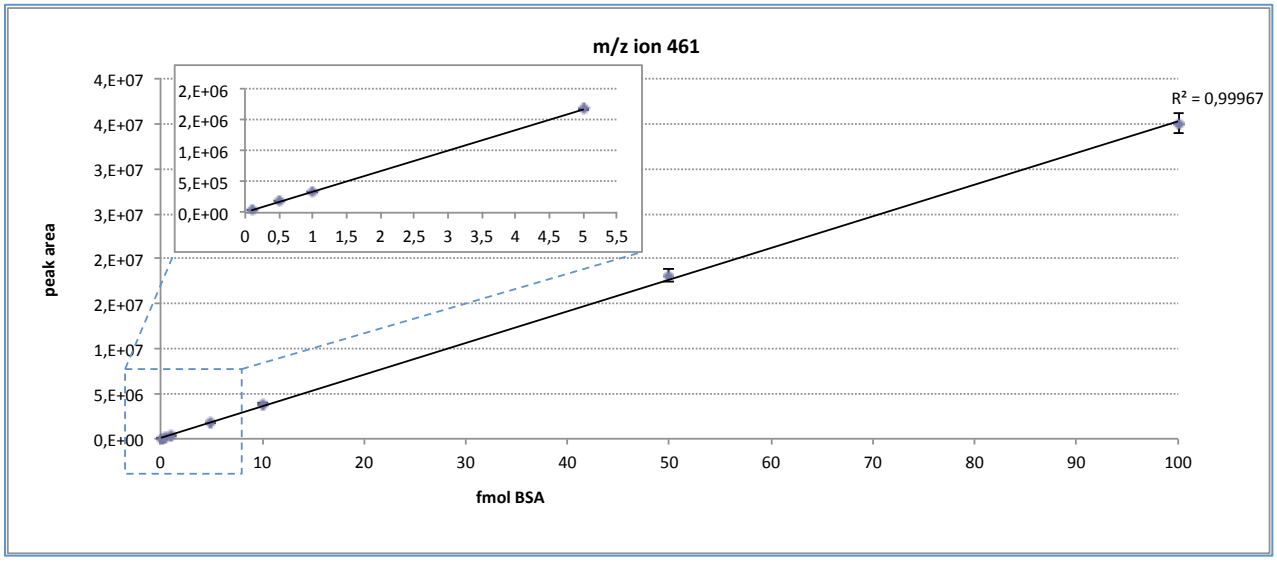


Figure 6 – Linear response of the 6520 Q-TOF mass spectrometer (Agilent Technologies) across different orders of magnitude of standard protein injected into the system. In the small panel, an enlarged view of the first part of the graph is displayed, highlighting an excellent linear response even for really low amounts of standard protein.

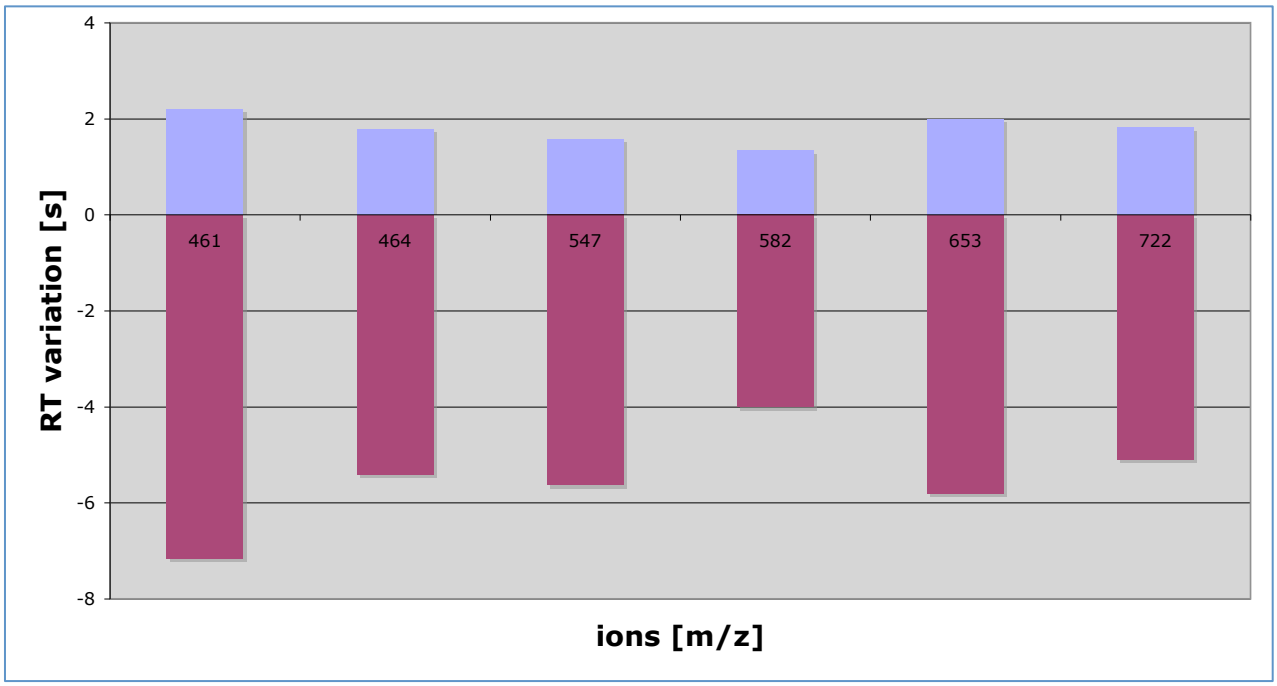


Figure 7 - Retention time variation measured for different LC-MS analyses of the standard protein BSA (six BSA ions are shown).

The resulting histograms show that our system is characterized by a very high reproducibility since less than 10 seconds of variation in retention time (RT) could be observed for all standard ions in multiple runs.

Testing the linear response and reproducibility of the mass spectrometer and the reliability of the LC system allowed us to gain important information that are necessary for the correct settings of the software used for the data analysis. Obviously for our label-free experiment we analyzed all samples using the same chromatographic and instrumental conditions, so we were able to use the information gained in the preliminary tests for the correct setting of the software parameters.

3.5.2 Experimental Workflow

After the necessary preliminary tests that guaranteed optimal conditions to perform a label-free analysis, the actual study was conducted on protein mixtures derived from immunoprecipitation experiments performed with a specific antibody against the catalytic subunit of protein kinase CK2.

Immunoprecipitation of CK2α in complex with its interactors was performed on total protein extracts from LAMA cells (see details in section 4.2) using the serum from a rabbit that was immunized against the C-terminal region of CK2α and, as control, using the serum from the same rabbit before the immunization. We chose to use an antiserum instead of the purified antibody to purposely create a "dirty" system, with a high degree of contamination that would be very useful to test the capabilities of our label-free approach in distinguishing contaminant proteins from real interactors of CK2. Samples obtained from the immunoprecipitation and the control experiments were loaded onto a SDS-PAGE.

The gel reported in Fig. 8 shows the proteins that were immunoprecipitated using the antiserum against the C-terminal region of the catalytic subunit α of CK2 (lane 1), and with the serum from the same rabbit before immunization (lane 2).

The two patterns are extremely similar due to the use of a not purified antibody, a system that introduced a high degree of contamination. The only visible differences between the two lanes are two bands whose molecular weights correspond to CK2 α and β subunits. Nonetheless, proteins that were unspecifically immunoprecipitated can be distinguished with a quantitative label-free analysis thanks to its differential processing: contaminant proteins are in fact expected to be found in the two gel lanes in very similar amount, while proteins that specifically bind (directly or indirectly) to CK2α will be present in significantly different amount in the two gel lanes. Thus the

final list of putative interactors of CK2 will be compiled using only the proteins that show a significant difference in abundance between the two immunoprecipitated samples.

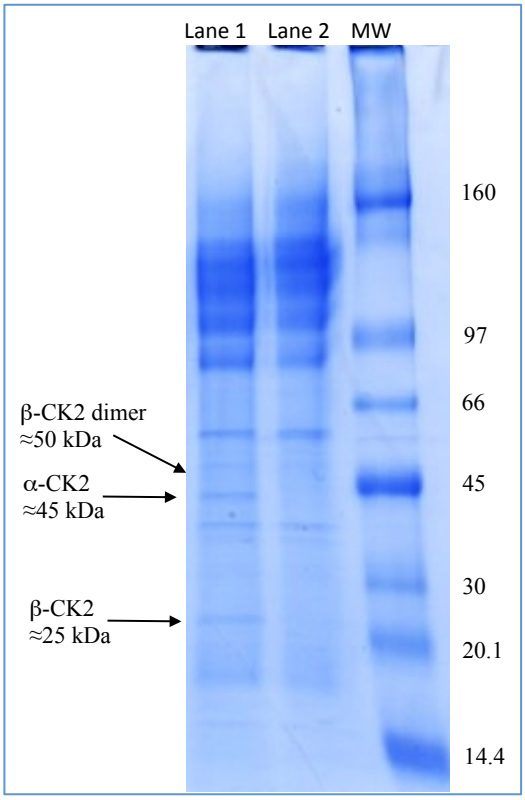


Figure 8 - SDS-PAGE of proteins immunoprecipitated with a CK2 alpha antiserum and with a control serum: lane 1 contains proteins immunoprecipitated using the antiserum against the C-terminal region of α-CK2; lane 2 contains proteins immunoprecipitated using the serum from the same rabbit before the immunization with α-CK2 peptide. MW: markers for molecular weights [kDa].

Gel lanes were cut in 10 slices in order to reduce the complexity of the samples thus improving the efficiency of data analysis. Proteins were digested in-gel with trypsin and the resulting peptide mixtures were analyzed by LC-MS/MS on the Agilent Q-TOF (details are reported in section 4.8) using the instrumental and chromatographic conditions that were used to test the reliability of the LC-MS system, as described above. Each sample (i.e. peptide mixtures from each gel slice) was analyzed in triplicate to increase the robustness of the quantification process. So a total of 60 LC-MS/MS runs were acquired. The comparative analysis of the LC-MS/MS data was performed using Progenesis LC-MS software (see section 4.9 for details).

The same experiment was repeated also with the purified antibody (instead of the antiserum) and the immunoprecipitation was performed using protein extracts from nuclei and from cytosol separately (for details see the protocol in the sections 4.1). To identify contaminant proteins a parallel immunoprecipitation conducted without the purified antibody was performed as control. Also in this case gel lanes were cut in 10 slices, digested (see section 4.3), analyzed by LC-MS/MS

and finally processed with Progenesis (a detailed description of how Progenesis works is reported in the section 1.3.3).

3.5.3 Bioinformatics and Pathway Analyses

The results obtained after the analysis with Progenesis (from both experiments) are summarized in Table 3 in the "Appendix" section. The list contains only the proteins that were identified with high confidence with at least two unique peptides and with a difference in abundance of at least 100% (max fold change>2) between the sample immunoprecipitated with the antibody (or antiserum) and the control sample.

The first observation that can be done by looking at the data reported in this table is that both CK2 subunits (α and β) appear in the list as highly enriched. This result was obviously expected in an immunoprecipitation experiment performed with an antibody directed against the catalytic subunit of CK2. The presence of the β subunit is also perfectly normal considering that the interaction between CK2 α and β is very stable, therefore CK2β subunit represents the first and more obvious interacting partner of CK2α. Thus the presence of CK2 in our final list confirms that the antibody used was efficient and that the immunoprecipitation experiment worked properly. Beside the expected presence of CK2, the final list of putative interacting partners of this protein kinase reveals the presence of several other interesting proteins that will be discussed in detail in the next section.

To gain a global vision of the functions of the putative partners of CK2 and therefore to gain information about biological processes in which CK2 is probably involved, a pathway analysis was performed using the bioinformatics tool DAVID Bioinformatics Resources 6.7 (NIAID, NIH). A snapshot of the results obtained is shown in Fig. 9.

The pathway analysis clustered proteins into functional groups, suggesting the involvement of CK2 in a number of processes such as RNA splicing, RNA localization and transport, protein synthesis and glucose metabolism, thus supporting the idea of a transversal role of CK2 across several main cellular processes.

Since the number of proteins identified in this experiment is not high, it was possible to screen the literature and exploit several bioinformatics tools to individually analyze each candidate interacting partner in order to find correlations with CK2 (either phosphorylations or interactions) and information regarding their cellular localization and cellular functions. This research was mainly based on the use of some free online databases like PhosphoSitePlus (*Hornbeck et al, Proteomics*

2004), IntAct (*Kerrien et al, Nucl. Acids Res. 2012*), UniProtKB (*The Uniprot Consortium, Nucleic Acids Res. 2011*), and Phospho.ELM (*Dinkel et al, Nucl. Acids Res. 2010*), and three main papers where information about interacting partners of CK2 could be easily retrieved (*Meggio et al, Faseb J. 2003*; *Arrigoni et al, J. Proteome Res. 2008*; *Gavin et al, Nature 2002*). All these information are collected in Table 4 in the "Appendix" section and will be discussed in the following paragraph.

DAVID Bioinformatics Resources 6.7
National Institute of Allergy and Infectious Diseases (NIAID), NIH

Functional Annotation Clustering

	Annotation Cluster 1	Enrichment Score: 8.24	G		Count	P_Value	Fold Change	Benjamini
	GOTERM_BP_FAT	RNA splicing, via transesterification reactions	RT		10	5.8E-9	1.7E1	5.5E-7
	GOTERM_BP_FAT	RNA splicing, via transesterification reactions with bulged adenosine as nucleophile	RT		10	5.8E-9	1.7E1	5.5E-7
	GOTERM_BP_FAT	nuclear mRNA splicing, via spliceosome	RT		10	5.8E-9	1.7E1	5.5E-7
	Annotation Cluster 2	**Enrichment Score: 6.24**	G		Count	P_Value	Fold Change	Benjamini
	GOTERM_CC_FAT	cytosolic ribosome	RT		8	3.4E-8	2.4E1	1.1E-6
	KEGG_PATHWAY	Ribosome	RT		8	6.3E-7	1.5E1	2.5E-5
	SP_PIR_KEYWORDS	ribosomal protein	RT		8	1.0E-6	1.5E1	1.4E-5
	GOTERM_MF_FAT	structural constituent of ribosome	RT		8	5.0E-6	1.1E1	2.5E-4
	Annotation Cluster 3	**Enrichment Score: 4.29**	G		Count	P_Value	Fold Change	Benjamini
	GOTERM_CC_FAT	intracellular organelle lumen	RT		20	3.8E-5	2.7E0	4.2E-4
	GOTERM_CC_FAT	organelle lumen	RT		20	5.2E-5	2.7E0	5.3E-4
	GOTERM_CC_FAT	membrane-enclosed lumen	RT		20	6.8E-5	2.6E0	6.5E-4
	Annotation Cluster 4	**Enrichment Score: 3.89**	G		Count	P_Value	Fold Change	Benjamini
	SP_PIR_KEYWORDS	glycolysis	RT		5	7.5E-6	3.9E1	8.3E-5
	GOTERM_BP_FAT	glycolysis	RT		5	3.1E-5	2.7E1	2.2E-3
	GOTERM_BP_FAT	glucose catabolic process	RT		5	7.1E-5	2.2E1	4.4E-3
	GOTERM_BP_FAT	hexose catabolic process	RT		5	1.4E-4	1.8E1	7.9E-3
	GOTERM_BP_FAT	monosaccharide catabolic process	RT		5	1.6E-4	1.8E1	7.3E-3
	GOTERM_BP_FAT	alcohol catabolic process	RT		5	2.6E-4	1.6E1	1.1E-2
	GOTERM_BP_FAT	cellular carbohydrate catabolic process	RT		5	3.1E-4	1.5E1	1.2E-2
	KEGG_PATHWAY	Glycolysis / Gluconeogenesis	RT		5	4.3E-4	1.3E1	5.6E-3
	GOTERM_BP_FAT	carbohydrate catabolic process	RT		5	8.0E-4	1.2E1	2.6E-2
	Annotation Cluster 5	**Enrichment Score: 3.14**	G		Count	P_Value	Fold Change	Benjamini
	GOTERM_BP_FAT	glucose metabolic process	RT		6	2.9E-4	1.0E1	1.2E-2
	GOTERM_BP_FAT	hexose metabolic process	RT		6	8.3E-4	8.0E0	2.6E-2
	GOTERM_BP_FAT	monosaccharide metabolic process	RT		6	1.6E-3	6.9E0	4.0E-2
	Annotation Cluster 6	**Enrichment Score: 2.17**	G		Count	P_Value	Fold Change	Benjamini
	GOTERM_BP_FAT	establishment of RNA localization	RT		4	6.1E-3	1.1E1	1.2E-1
	GOTERM_BP_FAT	RNA transport	RT		4	6.1E-3	1.1E1	1.2E-1
	GOTERM_BP_FAT	nucleic acid transport	RT		4	6.1E-3	1.1E1	1.2E-1
	GOTERM_BP_FAT	RNA localization	RT		4	6.7E-3	1.0E1	1.3E-1
	GOTERM_BP_FAT	nucleobase, nucleoside, nucleotide and nucleic acid transport	RT		4	9.3E-3	9.0E0	1.7E-1
	Annotation Cluster 7	**Enrichment Score: 2.07**	G		Count	P_Value	Fold Change	Benjamini
	GOTERM_CC_FAT	eukaryotic translation initiation factor 3 complex	RT		3	1.6E-3	4.8E1	1.4E-2
	SP_PIR_KEYWORDS	Initiation factor	RT		3	9.7E-3	2.0E1	7.0E-2
	GOTERM_BP_FAT	translational initiation	RT		3	1.3E-2	1.7E1	2.1E-1
	GOTERM_MF_FAT	translation initiation factor activity	RT		3	2.6E-2	1.2E1	3.0E-1

Figure 9 - Pathway analysis performed on proteins listed in table 1.

3.5.4 Discussion

The first data that emerges from the pathway analysis is the strong involvement of CK2 in all the main biological processes of the protein synthesis, from gene transcription to protein degradation. In fact, several DNA binding proteins were found among the probable interactors of CK2, like several isoforms of histones, Interleukin enhancer-binding factor 2 (ILF2 also known as NFAT), and the proliferation-associated protein 2G4 (PA2G4), that are all involved in the regulation of gene transcription. The involvement of CK2 in regulating the transcription is a well known fact and several examples of gene transcription activation by CK2 are reported in literature: CK2-dependent phosphorylation of the antioxidant-activated transcription factor Nrf2 regulates the induction of cytoprotective genes against chemical toxicity and oxidative injuries (*Apopa et al, J. Biochem. Mol. Toxicol. 2008*); in the same way CK2 activity has been found to positively induce the transcription of CTCF (*El-Kady et al, FEBS Lett. 2005*), and RNA pol III (*Johnston et al, Mol. Cell Biol. 2002*) by stabilizing transcription complexes.

CK2 is also known to participate in the regulation of the splicing mechanism by interacting and phosphorylating several splicing factors like hPrp3p, that is important for the assembly of the spliceosome (*Lehnert et al, Oncogene 2008*), and the pre-mRNA splicing activator factor RNPS1 (*Trembley et al, Mol. Cell. Biol. 2005*). Our study identified other proteins involved in the splicing process, thus confirming this notion and enriching the limited data reported in literature so far. For example, we found Heterogeneous Nuclear Ribonucleoprotein K (hnRNP K), that is known to be phosphorylated by CK2. This protein influences the pre-mRNA splicing (*Mikula et al, Biochim. Biophys Acta 2006*) and participates also in the processes of transcription, translation, and signal transduction. Several other Heterogeneous Nuclear Ribonucleoproteins were found specifically immunoprecipitated in our study, like the isoforms AB, L, D, U, and H1, that have not been correlated with CK2 yet, and A2B1, C, and A1, that were already known to be phosphorylated by CK2. The identification of hnRNPs is important to correlate CK2 activity to the mRNA splicing process, and this result is further confirmed by other identified proteins such as spliceosome RNA helicases BAT1 and DDX5, cleavage and polyadenylation specificity factor CPSF6, and splicing factor SFRS3.

The involvement of CK2 in transcription and translation could be expected considering the nuclear localization of this kinase; but CK2 is also present in the cytoplasm, where interacts with other proteins involved in protein synthesis and degradation. In fact, several proteins belonging to these two cellular processes emerged from our study: eight ribosomal proteins, mainly belonging to the 60S ribosomal subunit, were identified. Among these, 60S acidic ribosomal protein P0 had already

been reported as interacting partner of CK2 in yeast, and CK2 is also responsible for its phosphorylation (*Meggio et al, Faseb J. 2003*). We found also three subunits of the Eukaryotic Initiation Factor 3. This very large complex (about 800 kDa, 13 subunits eIF3a-m) was the first endogenous substrate of CK2 to be identified (*Pinna, Cell. Molec. Biol. Res. 1994*) and plays an essential role in the mammalian protein synthesis, promoting the binding between initiator methionyl-tRNA and the mRNA to the 40S ribosomal subunit, to form the 48S initiation complex (*Chaudhuri et al, J. Biol. Chem. 1999*). The eIF3 complex also prevents premature association of the 40S and 60S ribosomal subunits, and in previous studies the ability of eIF3 to bind the 40S subunit in absence of other initiation factor thanks to its loosely associated eIF3j subunit has been reported (*Fraser et al, J. Biol. Chem. 2004*). Further experiments aiming at confirming the interaction between CK2α and eIF3j and the phosphorylation of this subunit have been done and are currently ongoing in our laboratory.
We also found in the list of the identified proteins three elongation factors (eEF1-A1, eEF1-B2, and eEF1-G). eEF1-A1 in particular is essential for the correct binding of the aminoacyl-tRNA to the A-site of the ribosome (*Maruyama et al, Clin. Exp. Immunol. 2007*), and it was apparently never been related to CK2 before. Finally, two synthetases related to protein synthesis and folding were found: CARS and WARS, as well as mitochondrial 60 kDa heat shock protein.
Our results confirm the active participation of CK2 in the whole life of proteins, and the cycle is concluded by the background knowledge about the interaction of CK2 with several proteins responsible for protein degradation, like ubiquitin and proteasome regulatory subunits (*Arrigoni et al, J. Proteome Res. 2008*).

The label-free analysis allowed the identification of another really important class of proteins that are involved in the cellular response to stress, such as Peroxiredoxin-1, that is important for the elimination of peroxides generated during cellular metabolism, Heat Shock Cognate 71 kDa protein and mitochondrial stress-70 protein, that can act also as chaperones and are well known substrates and interactors of CK2. The implication of CK2 in the context of cellular stress does not come as a surprise because it was already demonstrated in cellular systems subjected to stress conditions like heat and UV irradiation (*Gerber et al, J. Biol. Chem 2000*). In these experiments the investigators also observed a subcellular relocalization of nuclear CK2 to the nucleolus in response to stress stimuli. Moreover, several evidences suggested that CK2 plays an important role in the regulation of apoptotic mechanisms by acting as an apoptosis suppressor through the regulation of a variety of agents including removal of survival factors, chemical and physical agents, and death receptor ligands (*Ahmad et al, Adv. Enz. Regul. 2008*). In this study however, we did not identify proteins

belonging to the apoptosis machinery. Interestingly, we also found two 14-3-3 proteins (zeta/delta and gamma), that are involved in the regulation of a wide spectrum of general and specialized signaling pathways. These data confirm the role of CK2 in signaling regulation and especially its involvement in important pathways such as Wnt signaling (*Seldin et al, Mol. Cell. Biochem. 2005*) and cell growth (*Ahmed, Crit. Rev. Eukaryot Gene Expr. 1999*).

CK2 seemed to interact also with several structural proteins, such as cytoplasmic Actin 1 (an important housekeeping gene) and Echinoderm Microtubule-associated protein-like 4, supporting the notion that this kinase is involved in the regulation of actin and tubulin structures. This involvement is reported in literature where an emerging role of CK2 in the regulation of cell polarity, cell morphology and cytoskeleton organization is described (*Canton et al, Cell Signal. 2006*).

The last class of proteins found to interact with CK2 were those related to metabolic processes, especially glycolysis. One of these proteins is Alpha-Enolase 1 (ENO1), that was already known to be phosphorylated and interact with CK2, and that is involved not only in glycolysis but also in several other biological processes like cell growth control, hypoxia tolerance and allergic response (*Sedoris et al, BMC Cancer 2010*; *Lee et al, Yonsei Med J. 2008*). We identified also other glycolytic enzymes: Phosphoglycerate kinase I (PGK1) and Fructose-bisphosphate aldolase A that plays a role also in gluconeogenesis and may also work as scaffolding protein. Finally, our analysis highlighted the presence of Glyceraldehyde 3-phosphate dehydrogenase (GAPDH), another important housekeeping enzyme, that catalyzes the first step of glycolysis, converting D-glyceraldehyde 3-phosphate (G3P) into 3-phospho-D-glyceroyl phosphate. GAPDH was also found to participate in nuclear events including transcription, RNA transport, DNA replication and apoptosis (*Tisdale, J. Biol. Chem. 2002*).
Only limited information about the involvement of CK2 in glycolysis can be found in literature (just one main work describing the regulatory phosphorylation of Phosphoglucose isomerase (PGI) by CK2; *Yanagawa et al, J. Biol. Chem. 2005*), but information about the role of CK2 in the other processes that involve the proteins just described is well known. For example, CK2–PTEN is a negative modulating pathway of Phosphatidylinositol-3-kinase (PI3K) that plays a central role in PAF-induced systemic anaphylaxis (*Kang et al, The J. of Immunology 2011*), highlighting the involvement of CK2 in the allergic response. Another process where CK2 activity is critical is the hypoxia response: hypoxia conditions induce CK2 to phosphorylate and activate Histone Deacetylases (HADCs), thus contributing to tumor growth and vasculogenesis (*Pluemsampant et al,*

Int. J. Cancer 2008). Altogether these findings assign to CK2 a key role as mediator in tumor progression under hypoxia condition, supporting the possible future application of CK2 inhibitors in cancer therapy.

3.5.5 Conclusions

The search for interacting partners of CK2 led to the identification of a number of proteins, only part of which were already known to interact or be related to this protein kinase. Our results confirmed the notion that CK2 plays important roles inside the cell, highlighting once again the ubiquitous involvement of this kinase in many essential cellular processes. In particular, the data collected in this study support the idea that CK2 participates to all the main steps of protein life, from gene transcription to translation, from protein folding to protein degradation. Beside this key processes, the data collected support also the previous knowledge about the role that CK2 plays in other cellular events such as metabolic pathways, stress response, apoptosis, and modulation of cellular structure and motility through the regulation of cytoskeletal proteins.

As for all high-throughput approaches, the results obtained must be confirmed by independent methods, therefore it will be necessary to perform further experiments to confirm the interaction between CK2 and the candidate interacting partners found in this study. Alternative approaches such as classical biochemical methods (immunoprecipitations and co-immunopreocipitations) or biophysical methods (Surface Plasmon Resonance, florescence spectroscopy) could be used. These will also be useful to evaluate whether the detected interactions are directed or mediated by other proteins belonging to the complexes to which CK2 takes part. One of the proteins we have identified in this study, EIF3j, raised particular interest in our group and it is now under investigation. We could already confirm that EIF3j indeed interacts with CK2 (probably through other subunits of the EIF3 complex) and is also phosphorylated *in vitro* and *in vivo* by this protein kinase (data not shown). Further studies aiming at elucidating the functional role of this phosphorylation are ongoing.

3.6 SILAC Analyses of CK2-dependent Phosphoproteomes

While the first part of this project aimed at the identification of new potential interactors of CK2, the second part of the chapter is focused on identification of new possible substrates of this enzyme directly in a cellular system. The possibility to gain information about substrates of CK2 will help to better understand the role played by this kinase in the cell and will hopefully be useful to determine new cellular activities that are strongly influenced by this enzyme.

To achieve this result, we decided to apply a large-scale phosphoproteomics approach using the SILAC technology in combination with the specific inhibition of CK2.

The combination of these methodologies with the high resolution and high mass accuracy mass spectrometer LTQ-Orbitrap (Thermo Scientific) allows the identification and the quantification of hundreds of proteins for each experiment. The results obtained are divided in two main parts: data relative to a global protein expression analysis and data relative to the specific phosphoproteomics analysis.

3.6.1 Global Protein Expression Analysis: Experimental Workflow

To study the phosphoproteome depending on CK2, we chose to perform a SILAC experiment on a cell culture of Human Embryonic Kidney (HEK) 293 T cells, a widely used cell line for SILAC experiments. Details of the cell growth and SILAC procedure are described in section 4.4.

Fig. 10 represents the experimental set-up, where cells treated for 3 hours with 50 μM quinalizarin are shown as T flasks, in opposition to untreated control (C) cells. The scheme also shows the swapping system used: in order to obtain results independent from the presence of the isotopically-labeled amino acids, the experiment was performed twice, once treating the heavy (H) cells and one treating the light (L) cells. In this way 6 biological replicates were obtained in total.

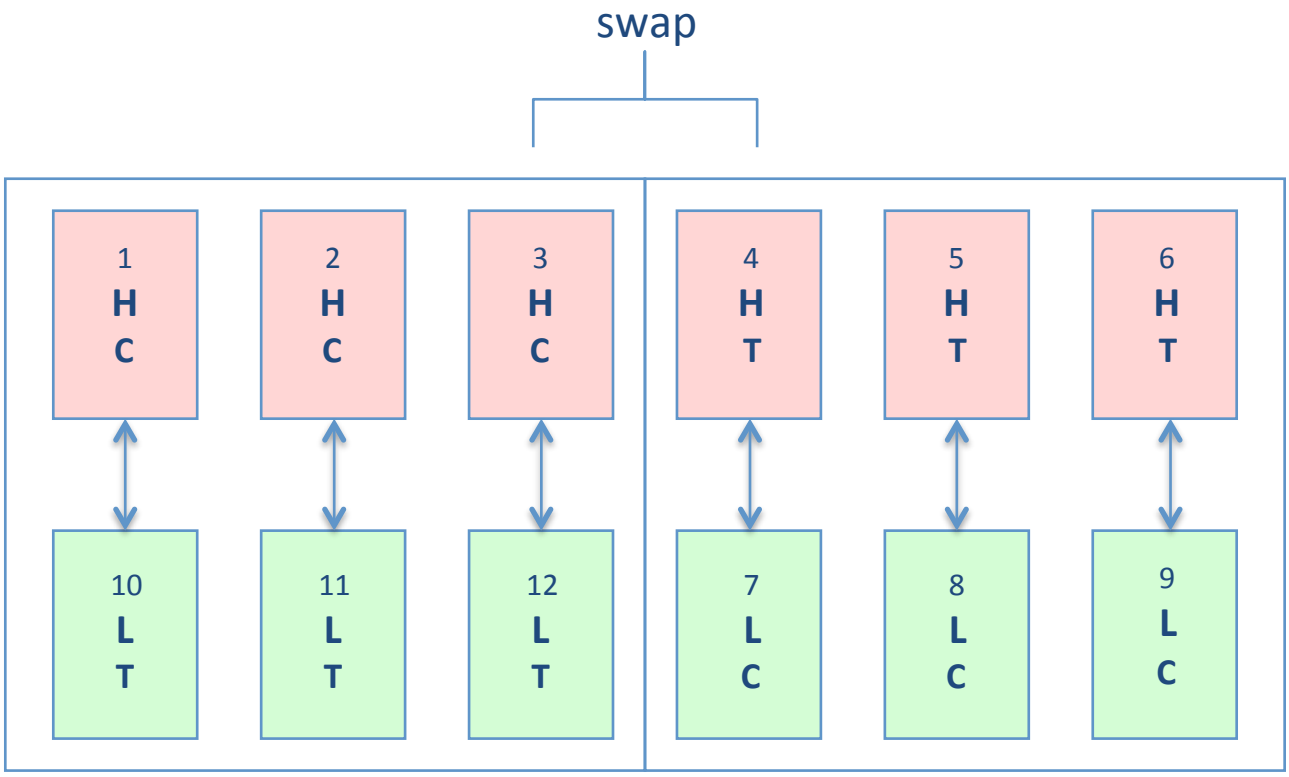


Figure 10 - SILAC experimental set-up

After the treatment cells were harvested, lysed, proteins were carefully quantified and, for the total protein expression analysis, 30 μg of total protein extract from each sample were mixed according to the scheme reported in Fig. 10. Two randomly chosen Control samples (heavy and light) and two Treated samples (heavy and light) were also mixed in equal amounts to check the labeling efficiency of our system. Samples were then run onto a 1D-SDS-PAGE, gel lanes were cut into 5 slices, proteins digested with trypsin (see details in section 4.3) and analyzed by LC-MS/MS (details in section 4.8). Each sample was run a first time, data obtained were searched with Mascot and an excluding list was created by Proteome Discoverer based on all the peptides that were positively identified. The same sample was then analyzed again under the same conditions but excluding all the peptides inserted into the list from the precursor selection. Details about Mascot search and quantification with Proteome Discoverer are reported in section 4.9. A total of 60 LC-MS/MS runs were performed to acquire the SILAC data relative to the global protein expression analysis.

3.6.2 Evaluation of Labeling Efficiency

Before starting the analysis of the whole set of samples, the two test samples with light and heavy treated or untreated proteins were analyzed by LC-MS/MS, to check the labeling efficiency. The heavy over light ratio of identified and quantified proteins was plotted in a histogram to evaluate its distribution (see Fig. 11).

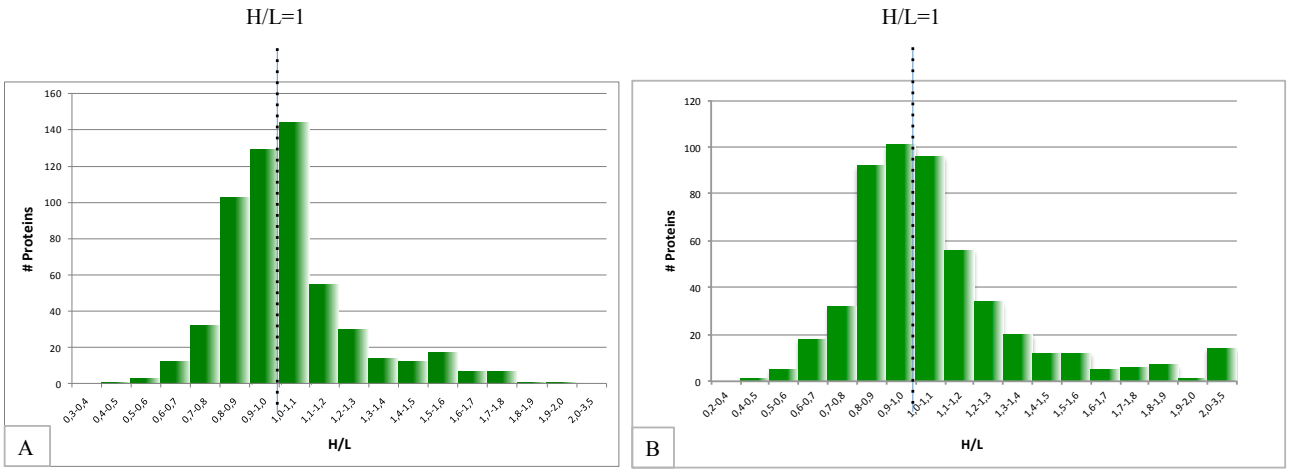


Figure 11 – Heavy over light ratio distribution of proteins identified and quantified in the test samples: (A) heavy control + light control; (B) heavy treated + light treated.

Histograms show a Gaussian distribution for the test samples: ideally, all the ratios should be 1 because no differences should exist between the pair of samples in each couple. In practice, a slight difference among the samples is always present due to the biological and technical variability of the approach. In this case, the Gaussian distribution of both the histograms is centered on 1, indicating that the very large majority of quantified proteins were correctly labeled. Notably, the distribution of the heavy over light ratios of proteins obtained from untreated cells (histogram A) is narrower than the distribution observed for proteins derived from treated cells (histogram B). Looking at the tails of both histograms, it is very clear that the treated cells show a higher number of proteins with high values of heavy over light ratios. This effect could be explained by a limited reproducibility of the treatment with quinalizarin, therefore the 2 treated samples that were mixed for this test already showed a slight difference at the protein expression level. This also immediately indicates that the treatment has an effect at the protein expression level, although the time of the treatment was limited to only 3 hours.

Another way to represent the labeling efficiency is shown in Fig. 12: here the heavy over light ratios were plotted in a logarithmic scale.

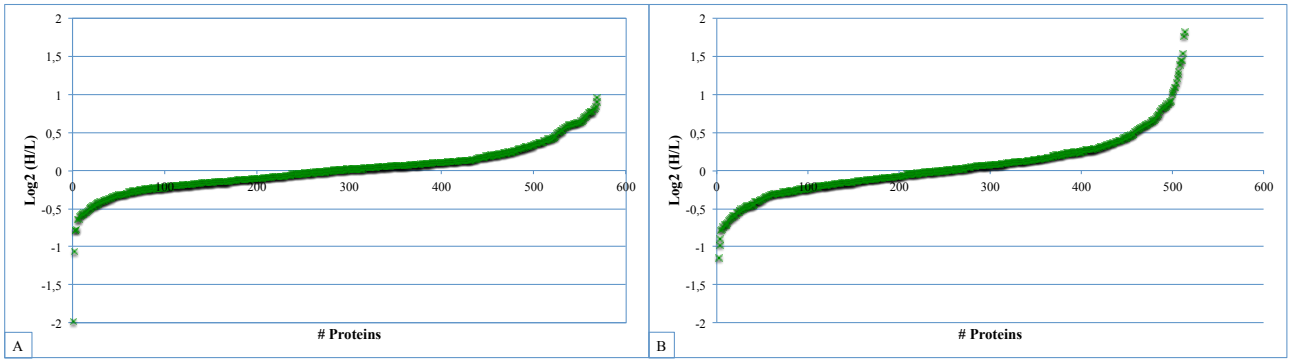


Figure 12 – Logarithmic distribution of heavy over light ratios from test samples: (A) heavy control + light control; (B) heavy treated + light treated.

For both curves the inflection point and the large majority of values are distributed around zero on the x axis. This is the value that corresponds to a heavy over light ratio of 1.0 in Fig. 11. This again demonstrates that most of the heavy and light signals have comparable intensities. In Fig. 12A, it is possible to note the symmetry of the curve and how all values are included in the interval between -1.0 and +1.0, meaning that for all the identified proteins the difference in expression level between heavy and light proteins was lower than ±100%, while for over 90% of quantified proteins the H/L values were included in the interval ±30%.

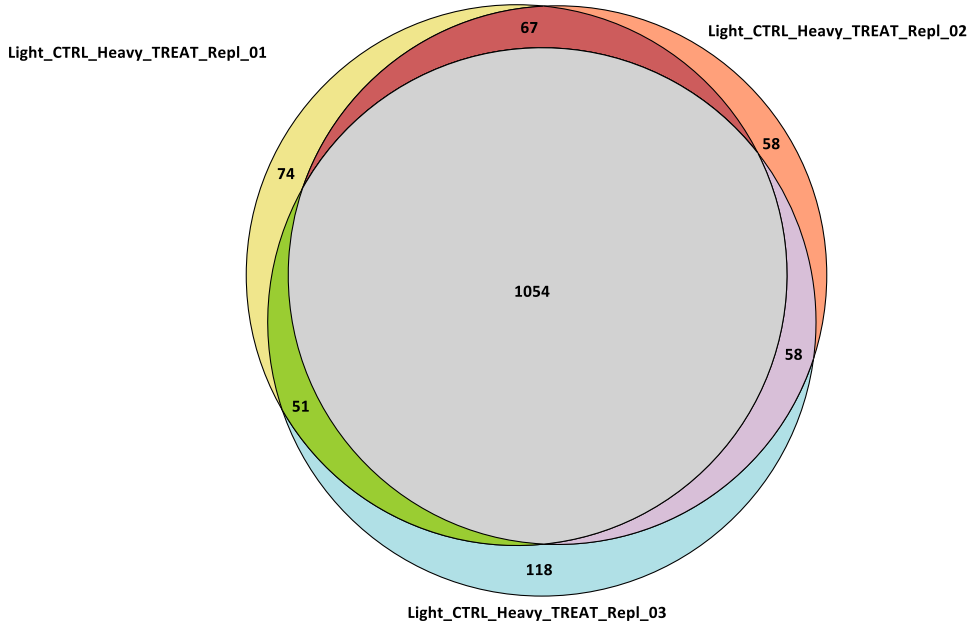
This difference is clearly higher in the case of the sample treated with Q1 (see Fig. 12B), where the values of heavy over light ratio encompass the -1.0 - +2.0 interval. This asymmetrical distribution confirms that the treatment has an effect at the protein expression level, mainly by altering it in a positive way. However, this effect should not appear in this test because the 2 mixed samples were treated exactly in the same way. Thus this first result highlights that the reproducibility of the treatment is limited and cells respond to the presence of the inhibitor in a different manner.

The labeling efficiency test was useful not only to highlight these phenomena, but also to set a minimum threshold above which the difference in expression level of a protein can be considered as significant. For the experiments described below, we have chosen to consider as significantly altered proteins for which the treatment has induced a variation of their expression level of at least 100%.

3.6.3 Global Protein Expression: Technical and Biological Reproducibility

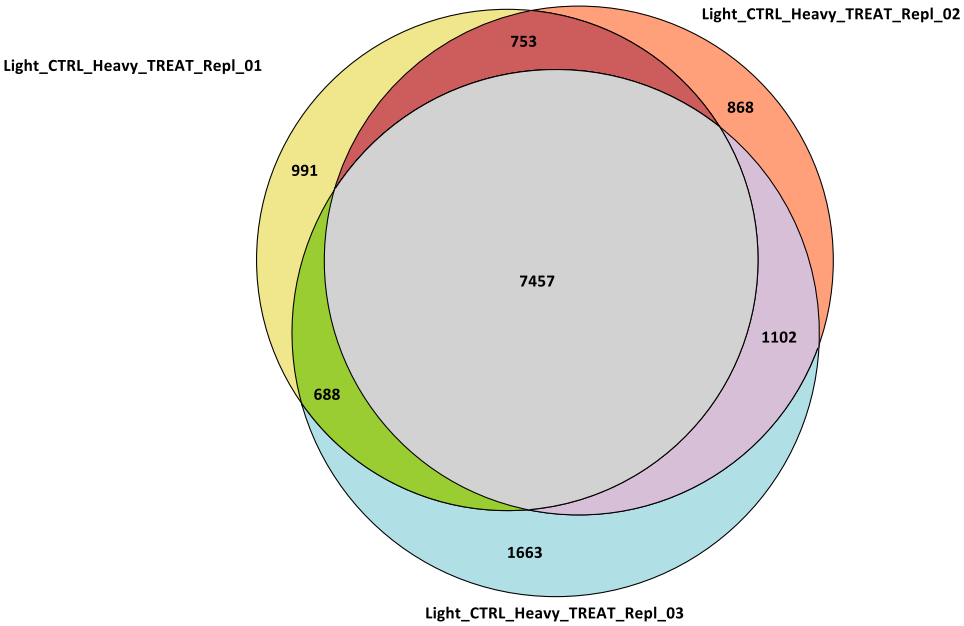
Once the labeling was tested and the significant cut-off was decided, we proceeded with the analysis of the 6 samples corresponding to 6 different biological replicates as indicated in Fig. 10. This first part of the project aimed at the identification of global proteomics changes at the protein expression level in cells treated with the CK2 inhibitor quinalizarin (Q1). Only in the second part of the project (that will be discussed later) we focused on the analysis of phosphopeptides.
From all the samples, 1685 proteins were identified with high confidence, for a total of 15828 unique peptides. 1307 proteins were also quantified in at least 3 biological replicates and 54 proteins were found to be significantly altered upon treatment with Q1. We decided to be stringent and consider only proteins with a variation of at least 100% calculated as the median value obtained from all the quantified biological replicates. The results of this analysis are reported in Table 5 in the Appendix section.
The high reproducibility (in terms of protein identifications) achieved across the different biological replicates can be appreciated by looking at the Venn diagram reported in Fig. 13, where it is possible to see that 83% of the identified proteins are in common between at least 2 biological replicates. For the sake of clarity, a Venn diagram reporting the results from only 3 replicates is shown, but similar results were obtained also for the other biological replicates (data not shown).

Similar considerations can be applied when looking at the Venn diagram reported in Fig. 14, which shows the reproducibility of our analyses at the peptide level. 74% of identified peptides were found in common to at least 2 biological replicates. As expected, this value is lower than the one found for proteins, since the undersampling effect is more evident at the peptide level, rather than at the protein level.



	Exclusive	Total	Label	Description
	74	1246	Light_CTRL_Heavy_TREAT_Repl_01	Repl_01
	58	1237	Light_CTRL_Heavy_TREAT_Repl_02	Repl_02
	118	1281	Light_CTRL_Heavy_TREAT_Repl_03	Repl_03
	67	1121	Light_CTRL_Heavy_TREAT_Repl_01 / Light_CTRL_Heavy_TREAT_Repl_02	Repl_01 / Repl_02
	58	1112	Light_CTRL_Heavy_TREAT_Repl_02 / Light_CTRL_Heavy_TREAT_Repl_03	Repl_02 / Repl_03
	51	1105	Light_CTRL_Heavy_TREAT_Repl_01 / Light_CTRL_Heavy_TREAT_Repl_03	Repl_01 / Repl_03
	1054	1054	Light_CTRL_Heavy_TREAT_Repl_01 / Light_CTRL_Heavy_TREAT_Repl_02 / Light_CTRL_Heavy_TREAT_Repl_03	Repl_01 / Repl_02 / Repl_03
Sum	1480			

Figure 13 - Reproducibility across 3 biological replicates for identified proteins.



	Exclusive	Total	Label	Description
	991	9889	Light_CTRL_Heavy_TREAT_Repl_01	Repl_01
	868	10180	Light_CTRL_Heavy_TREAT_Repl_02	Repl_02
	1663	10910	Light_CTRL_Heavy_TREAT_Repl_03	Repl_03
	753	8210	Light_CTRL_Heavy_TREAT_Repl_01 / Light_CTRL_Heavy_TREAT_Repl_02	Repl_01 / Repl_02
	1102	8559	Light_CTRL_Heavy_TREAT_Repl_02 / Light_CTRL_Heavy_TREAT_Repl_03	Repl_02 / Repl_03
	688	8145	Light_CTRL_Heavy_TREAT_Repl_01 / Light_CTRL_Heavy_TREAT_Repl_03	Repl_01 / Repl_03
	7457	7457	Light_CTRL_Heavy_TREAT_Repl_01 / Light_CTRL_Heavy_TREAT_Repl_02 / Light_CTRL_Heavy_TREAT_Repl_03	Repl_01 / Repl_02 / Repl_03
Sum	13522			

Figure 14 - Reproducibility across 3 biological replicates for identified peptides.

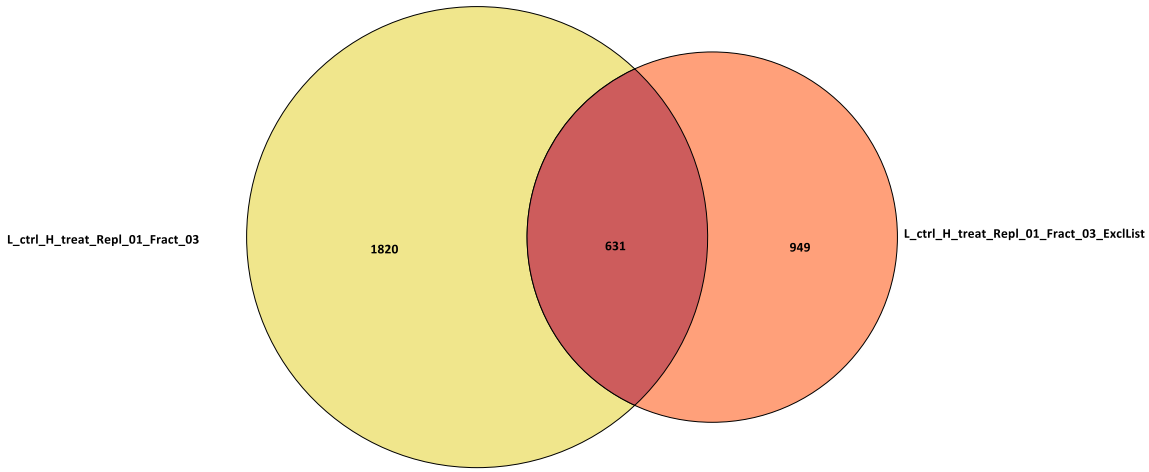
In this experiment, unlike the method applied and described in the previous chapter, we did not run 3 technical replicates for each sample but decided to analyze each sample twice. After the first analysis, an excluding list was created and used for the second analysis. In this way, we could increase the number of precursors that were selected and quantified in MS mode, and consequently, the number of the identified proteins and the sequence coverage were also increased, thus improving the robustness of quantification.

The advantage obtained by using the exclusion list can be deduced from the Venn diagram in Fig. 15, where peptides (identified form a single gel slice of a sample) identified in the first analysis are compared to those identified in the second analysis with the excluding list. It is immediately possible to notice that the number of peptides in the first run is higher than in the second run, but only 19% of all identified peptides were found in both analyses and 28% of peptides were identified only thanks to the use of the exclusion list.

Using this approach it was possible to increase the number of identified peptides per protein as well as the total number of identified proteins (see Fig. 16). In fact in the second run we could identify and quantify 64 new proteins present probably in lower concentrations and that would not be identified without using the exclusion list method. Analogous results were obtained from all the other gel slices from all samples (data not shown).

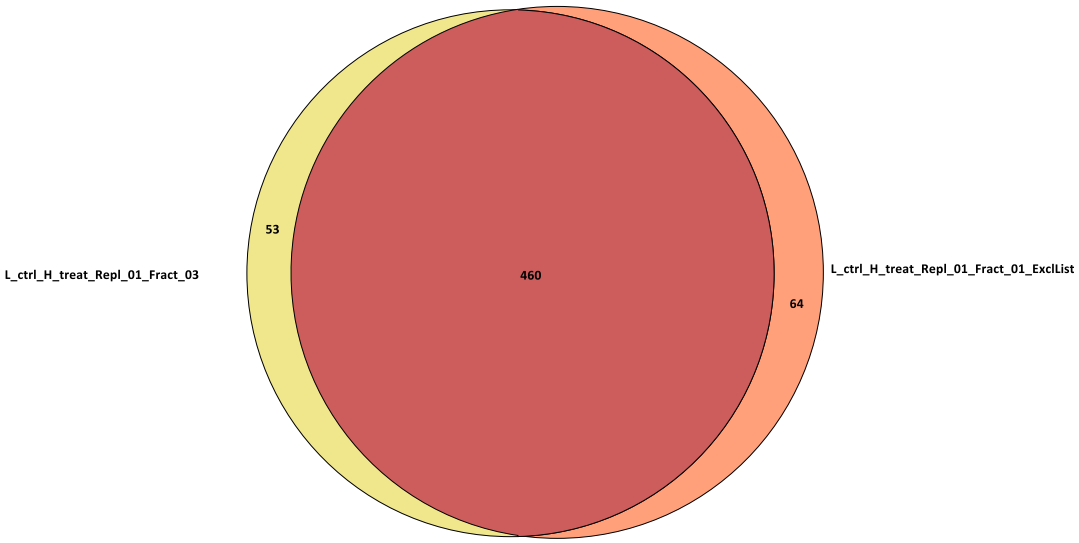
The advantage of this approach that increases sequence coverage, is particularly useful in the analysis of phosphopeptides, because it increases the possibility to correlate changes in the phosphorylation state with changes in protein expression level by a direct comparison of quantified peptides and phosphopeptides belonging to the same protein. This aspect will be discussed later in more detail.

Another way to evaluate the reproducibility of the results obtained across biological replicates is the logarithmic plot of the heavy over light ratios. Fig. 17 shows the trend of heavy over light ratios for 3 out of the 6 biological replicates. The 3 replicates shown refers to the 3 samples where the treated cells were grown in the heavy medium and the control cells in the light one, therefore the heavy over light ratio is the equivalent of a Treatment over Control ratio, as reported in the figure. As it is possible to see, the curves are very similar but not symmetrical, with the logarithmic values spanning between -2.0 and +6.0. Few proteins have a logarithmic ratio lower than -2.0 and these are specifically due to contaminant proteins such as keratins. The resulting asymmetry and in particular the right part of the curves indicate an increased expression of several proteins due to the treatment of cells with quinalizarin, while only very few proteins showed a significant decrement of their expression level.



	Exclusive	Total	Label	Description
	1820	2451	Light_CTRL_Heavy_TREAT_Repl_01_Fract_03	Repl_01_Fract_03
	949	1580	Light_CTRL_Heavy_TREAT_Repl_01_Fract_03_ExclList	Repl_01_Fract_03_ExclList
	631	631	Light_CTRL_Heavy_TREAT_Repl_01_Fract_03 / Light_CTRL_Heavy_TREAT_Repl_01_Fract_03_ExclList	Repl_01_Fract_03 / Repl_01_Fract_03_ExclList
Sum	3400			

Figure 15 – Overlap of peptides identified from the same sample in two different analyses, with and without the use of exclusion list.



	Exclusive	Total	Label	Description
	53	513	Light_CTRL_Heavy_TREAT_Repl_01_Fract_03	Repl_01_Fract_03
	64	524	Light_CTRL_Heavy_TREAT_Repl_01_Fract_03_ExclList	Repl_01_Fract_03_ExclList
	460	460	Light_CTRL_Heavy_TREAT_Repl_01_Fract_03 / Light_CTRL_Heavy_TREAT_Repl_01_Fract_03_ExclList	Repl_01_Fract_03 / Repl_01_Fract_03_ExclList
Sum	577			

Figure 16 - Overlap of proteins identified from the same sample in two different analyses, with and without the use of exclusion list.

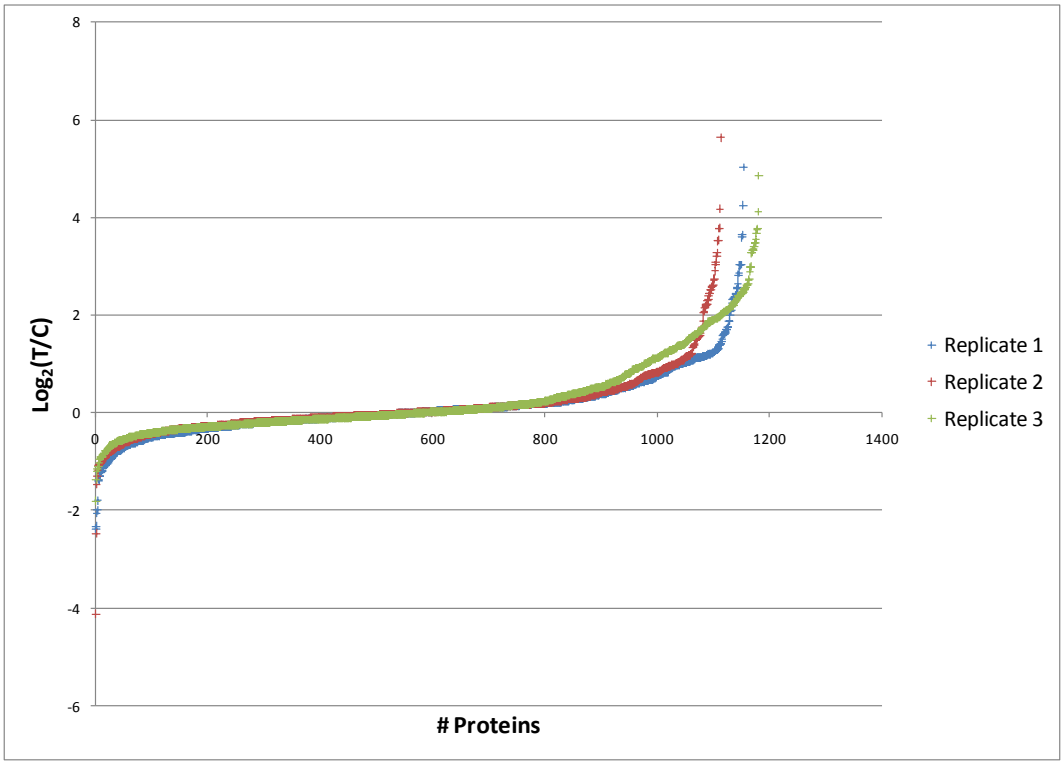


Figure 17 - Logarithmic distribution of treated over control ratios of 3 biological replicates.

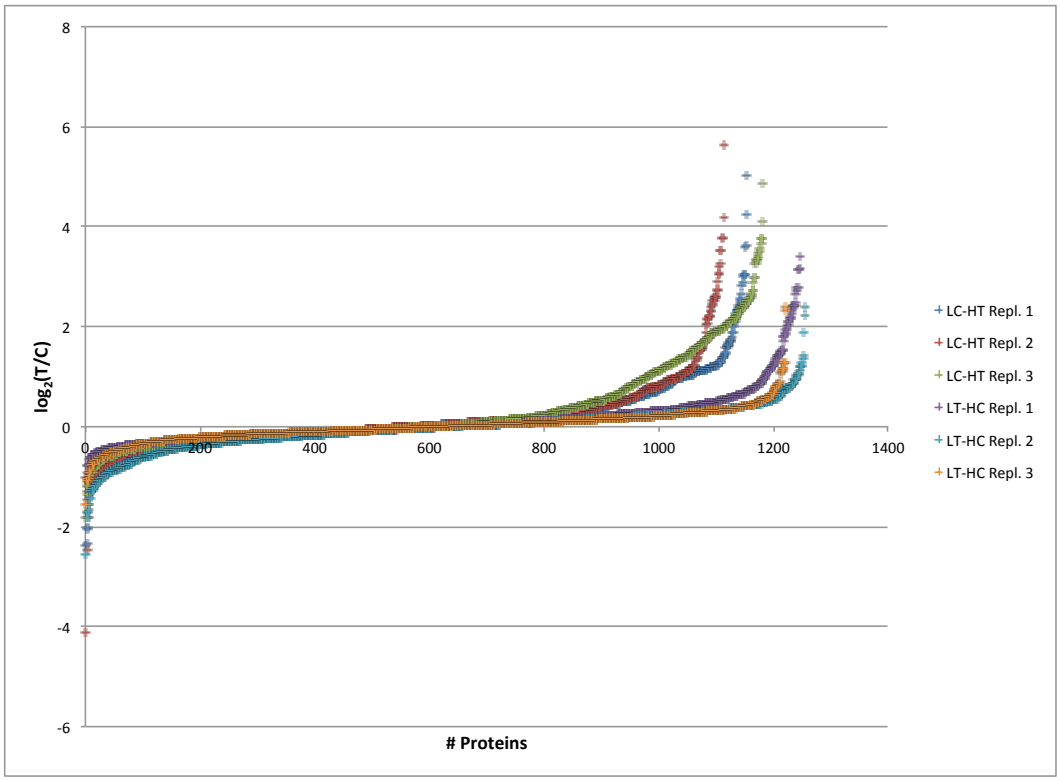


Figure 18 - Logarithmic distribution of treated over control ratios for all the 6 replicates.

When observing the trend of logarithmic ratios for all 6 biological replicates, other considerations can be done. Fig. 18 shows the trend of Log2 values of the Treatment/Control ratios for all 6 replicates.
Here it is possible to observe that the 6 replicates tend to cluster in 2 separate groups. One group composed of the 3 replicates in which the heavy cells were treated with Q1, and the second group due to the replicates in which the treatment was administered to the light cells. Both these clusters suggest a remarkable upregulation effect on a number of proteins, an effect induced by the treatment with quinalizarin; however, the number of proteins quantified in each batch was slightly different (probably because of a less sensitive tuning of the instrument) and this could in part explain the fact that the 2 groups overlap only partially. What it is important to note is that the slopes of the right parts of the curves are sensibly different between the 2 clusters. This reflects the fact that a larger number of proteins showed a significantly increased expression level in the biological replicates where the heavy cells were treated with Q1 as compared to the replicates in which the light cells were treated with the inhibitor. Exactly the same trend is observable for the quantified peptides of all the 6 replicates (data not shown). This evidence suggests once again that the experiment, although performed with all possible precautions, gave results that are only partially reproducible, thus leading to an increased complexity of acquired data.

A severe problem we encountered when examining the data, was related to the quantification distribution across biological replicates, that we observed to be not homogeneous. Two main behaviors can be observed by analyzing the quantification data:

1. A not negligible number of proteins showed a significant altered expression level in few of the biological replicates, but not in the others. Generally, the first 3 replicates are concordant in the majority of the cases; replicate 1 of the light treated cells is also often concordant with the previous ones (but not always), while the last 2 replicates (Light Treat/Heavy Ctrl Replicate 2 and 3) usually diverge. This effect can be attributable to a different response of the cells to the treatment with Q1, therefore to a limited reproducibility of the biological effects induced by the inhibitor.
2. Several proteins showed an altered expression level (upregulation or downregulation) in few replicates and exactly the opposite trend (downregulation or upregulation) in other replicates.

Some examples of these behaviors can be seen in Table 1 where, for example, several ribosomal proteins were found altered in 4 biological replicates while in the other 2 replicates they appear to be not affected by the treatment with Q1.
In other cases, like for Cellular retinoic acid-binding protein 2 or Histone-binding protein RBBP7, the second behavior emerges. In this case the expression level of the proteins decreases in the 3 replicates where treated cells where heavy labeled, and increases of the same amount in the swapped replicates.

This second effect is probably due to an incomplete labeling of proteins with heavy amino acids. In fact, looking at the mass spectra relative to these cases, we realized that the light signals were always higher than the heavy ones. This clearly indicates an incomplete labeling of those particular proteins, though cells were grown in the heavy medium for a number of cell doublings much higher than the one suggested in literature for the same cell line.
This incomplete labeling seems to be in contrast to what was found in the preliminary experiments described above (section 3.6.2), where the results of the test samples did not evidence this problem. However, in that case we performed a less deep analysis, without running the samples in duplicate with the excluding lists. Therefore the number of proteins identified in that case was lower than what has been found in the actual experiment, thus the incomplete labeling was probably less evident. Moreover, this effect dramatically emerges when replicates with the swapping system are analyzed, since those particular proteins characterized by an incomplete labeling appear with opposite quantifications if the treatment is administered to the heavy cells or to the light cells.
This incomplete labeling (very difficult to explain considering that cells were grown in heavy medium for almost one month) could be classified as a technical problem that can be easily faced by simply not keeping into account the proteins that show this behavior. However, this effect cannot be easily disregarded because it may strongly affect the results of our analyses. Examples of how the incomplete labeling can affect the quantification of proteins altered by the treatment are reported in Fig. 19. There it is possible to see how light proteins that decreased after the treatment might reach the same signal intensity of the heavy control proteins (see Fig. 19 panel 1), and, on the same way, heavy proteins that increased after the inhibition with quinalizarin may reach a signal intensity comparable with the light untreated proteins (see Fig. 19 panel 2). Thus, in these particular cases, only proteins with a large difference between the heavy and light signal due to the treatment could show a significant alteration. The data we collected is therefore affected by this phenomenon and it is probable that information regarding altered expression levels of proteins belonging to this category can be lost during data analysis.

ACCESSION	DESCRIPTION	Heavy Treat/Light Ctrl Replicate 1	Heavy Treat/Light Ctrl Replicate 2	Heavy Treat/Light Ctrl Replicate 3	Light Treat/Heavy Ctrl Replicate 1	Light Treat/Heavy Ctrl Replicate 2	Light Treat/Heavy Ctrl Replicate 3
IPI01014951.1	163 kDa protein	1,267	0,941	**6,625**	0,738	**0,285**	**0,589**
IPI00185374.4	26S proteasome non-ATPase regulatory subunit 12	1,349	1,383	**2,487**	1,027	0,734	0,836
IPI00975963.1	29 kDa protein	**2,400**	**2,033**	**3,423**	1,125	0,838	0,951
IPI00165360.5	3-mercaptopyruvate sulfurtransferase	0,722	**0,654**	0,671	1,155	1,115	1,186
IPI00025091.3	40S ribosomal protein S11	**4,303**	**2,995**	**4,837**	**2,349**	0,873	1,301
IPI00013917.3	40S ribosomal protein S12	**2,308**	**1,965**	**3,049**	1,239	0,749	0,949
IPI00221089.5	40S ribosomal protein S13	**4,969**	**4,237**	**11,200**	**2,849**	1,048	1,441
IPI00026271.5	40S ribosomal protein S14	**2,314**	**1,859**	**4,168**	**1,676**	0,786	1,096
IPI00221091.9	40S ribosomal protein S15a	**5,337**	**4,124**	**10,048**	**2,172**	0,873	1,136
IPI00221092.8	40S ribosomal protein S16	**2,467**	**2,865**	**5,878**	**1,525**	0,976	1,210
IPI00013296.3	40S ribosomal protein S18	**2,286**	**2,330**	**4,186**	1,364	0,785	1,033
IPI00215780.5	40S ribosomal protein S19	**2,349**	**2,324**	**5,274**	1,387	0,843	1,173
IPI00013485.3	40S ribosomal protein S2	**2,104**	**2,059**	**3,812**	**1,556**	0,983	1,247
IPI00012493.1	40S ribosomal protein S20	**1,600**	1,425	**2,540**	**1,547**	1,028	1,244
IPI00937239.2	40S ribosomal protein S21	1,134	0,966	1,277	0,716	**0,546**	**0,602**
IPI00012750.3	40S ribosomal protein S25	**3,052**	**2,224**	**5,738**	**1,612**	1,024	1,223
IPI00655650.2	40S ribosomal protein S26	**7,072**	**4,427**	**9,725**	**2,867**	1,136	1,478
IPI00719622.1	40S ribosomal protein S28	**1,936**	**1,783**	**2,040**	1,192	0,883	0,948
IPI00182289.6	40S ribosomal protein S29	**2,107**	**2,210**	**4,868**	1,167	0,732	1,218
IPI00011253.3	40S ribosomal protein S3	**2,117**	**2,194**	**3,721**	1,245	0,807	0,999
IPI00419880.6	40S ribosomal protein S3a	**2,347**	**1,767**	**5,751**	1,239	0,687	0,842
IPI00217030.10	40S ribosomal protein S4, X isoform	**4,530**	**3,648**	**7,857**	**2,215**	0,909	1,326
IPI00008433.4	40S ribosomal protein S5	**2,249**	**2,089**	**4,040**	1,181	0,721	0,929
IPI00021840.1	40S ribosomal protein S6	**3,019**	**2,332**	**2,234**	**1,650**	1,123	1,074
IPI00013415.1	40S ribosomal protein S7	**2,493**	**1,822**	**2,301**	**1,640**	0,843	1,059
IPI00216587.9	40S ribosomal protein S8	**5,123**	**4,985**	**10,293**	**2,747**	0,832	**1,503**
IPI00221088.5	40S ribosomal protein S9	**3,393**	**2,802**	**5,480**	**1,706**	0,788	1,079
IPI00029997.1	6-phosphogluconolactonase	**0,608**	**0,527**	**0,534**	1,131	1,039	1,093
IPI00412607.6	60S ribosomal protein L35	**2,329**	**2,102**	**2,345**	1,434	0,759	0,722
IPI00215790.6	60S ribosomal protein L38	**1,919**	**2,064**	**2,586**	**2,046**	0,731	0,755
IPI01013446.1	cDNA FLJ51947, highly similar to Epididymal secretory protein E1	**0,590**	**0,600**	**0,552**	1,495	**2,451**	**1,723**
IPI00908883.3	cDNA FLJ55002, highly similar to Alpha-centractin	**1,559**	1,449	**2,439**	0,937	0,740	0,715
IPI00216088.3	Cellular retinoic acid-binding protein 2	**0,559**	**0,557**	**0,536**	1,402	**1,615**	1,379
IPI00007673.4	Coiled-coil-helix-coiled-coil-helix domain-containing protein 2, mitochondrial	**0,501**	0,890	**0,409**	**2,461**	**2,861**	**2,762**
IPI00220416.3	Cytochrome b-c1 complex subunit 7	**3,810**	**4,483**	**2,605**	**3,484**	**2,354**	**2,452**
IPI00395865.4	Histone-binding protein RBBP7	**0,409**	**0,595**	0,723	**1,683**	**1,723**	**2,126**

Table 1 – Example of opposite quantification trends detected in the protein expression SILAC analysis.

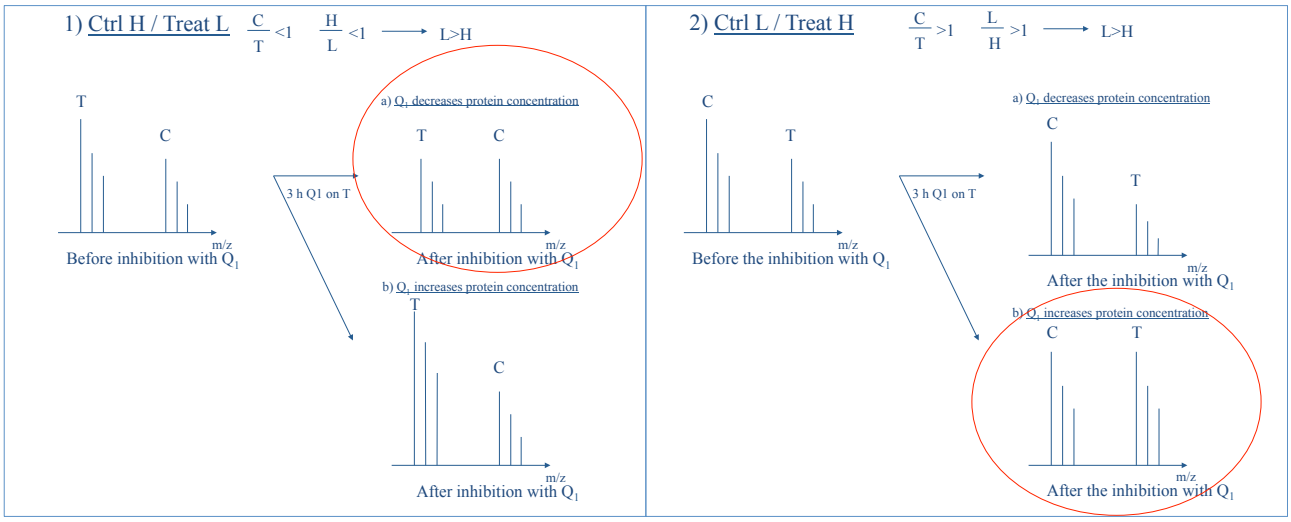


Figure 19 – Two possible cases of loss of information due to incomplete protein labeling.

3.6.4 Global Protein Expression: Bioinformatics and Pathway Analyses

The data analysis performed with Proteome Discoverer gave us also information about the molecular function of the identified proteins (see Fig. 20), the cellular component in which they are localized (see Fig. 21), and the biological processes in which they are involved (see Fig. 22), interesting data to evaluate the presence of bias during sample preparation, such as the enrichment of particular classes of proteins.

The classifications obtained for the identified proteins highlight a rather homogeneous and equilibrated distribution between different cellular compartments and molecular processes, and the various categories seem to well represent the common distribution of protein functions, with the most abundant classes represented by proteins with metabolic and protein binding activities. Moreover, the majority of the proteins have a cytoplasmic localization. The presence of a not negligible proportion of proteins classified as "not annotated" (about 4%) is mostly due to an artifact derived from the use of IPI Human database (as previously described for the SILAC experiment performed on BVIC cells), which contains a significant number of entries classified as "uncharacterized" proteins. In reality, many of these proteins are very well characterized and a simple BLAST analysis easily allows to retrieve the correct protein names and functions.

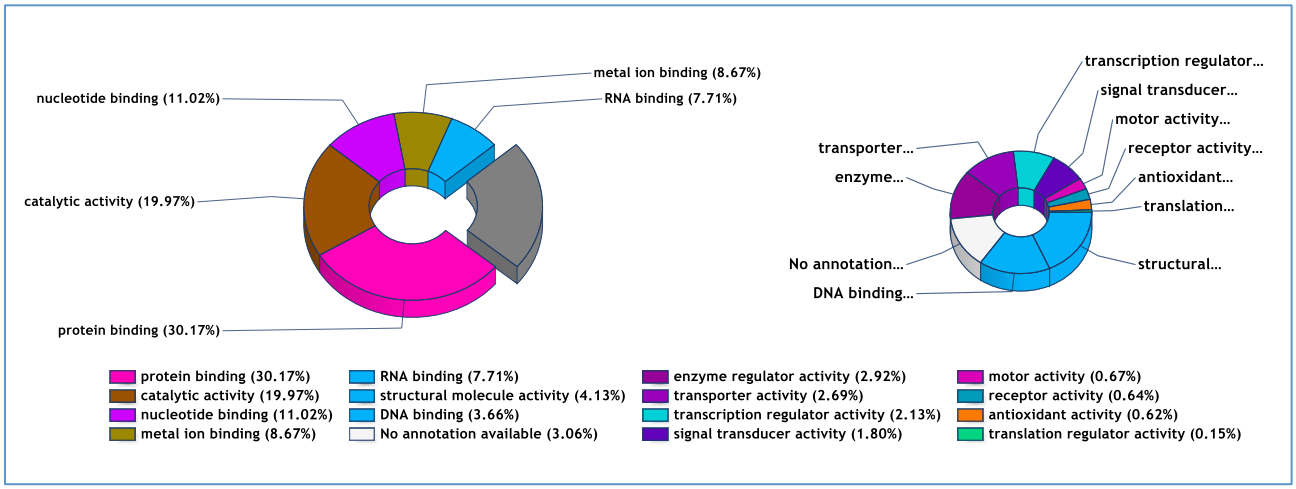


Figure 20 - Molecular function analysis.

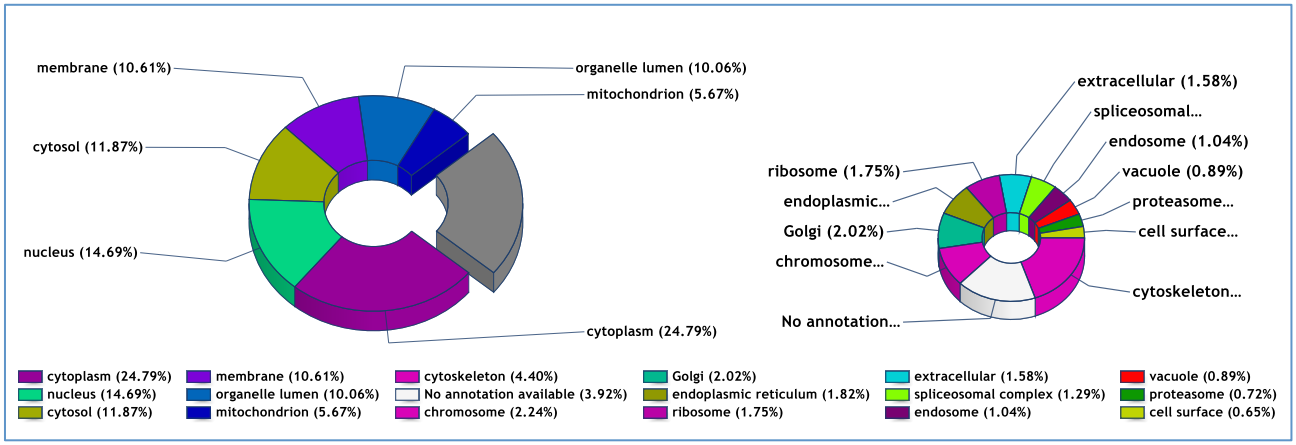


Figure 21 - Cellular component analysis.

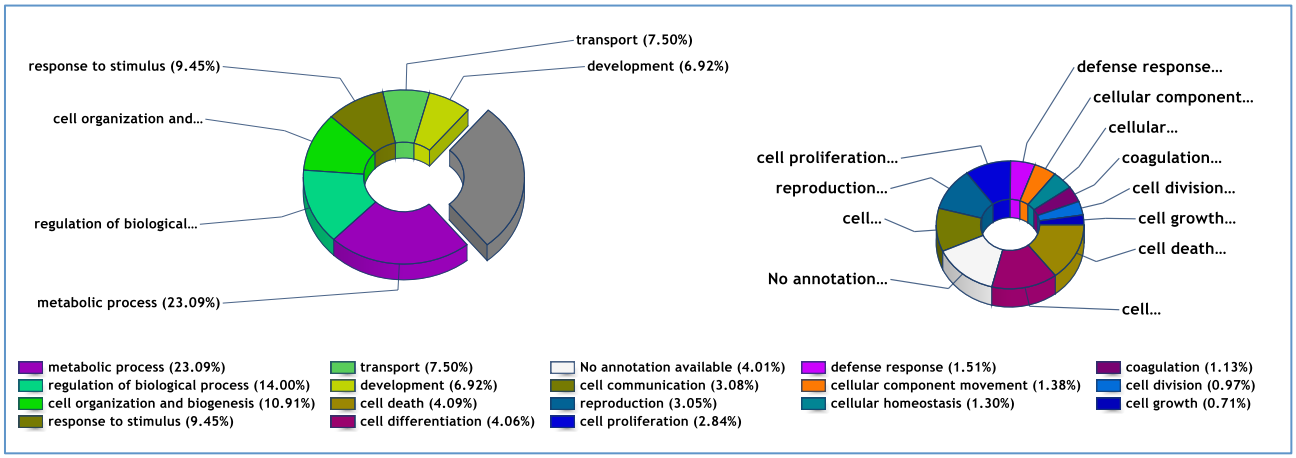
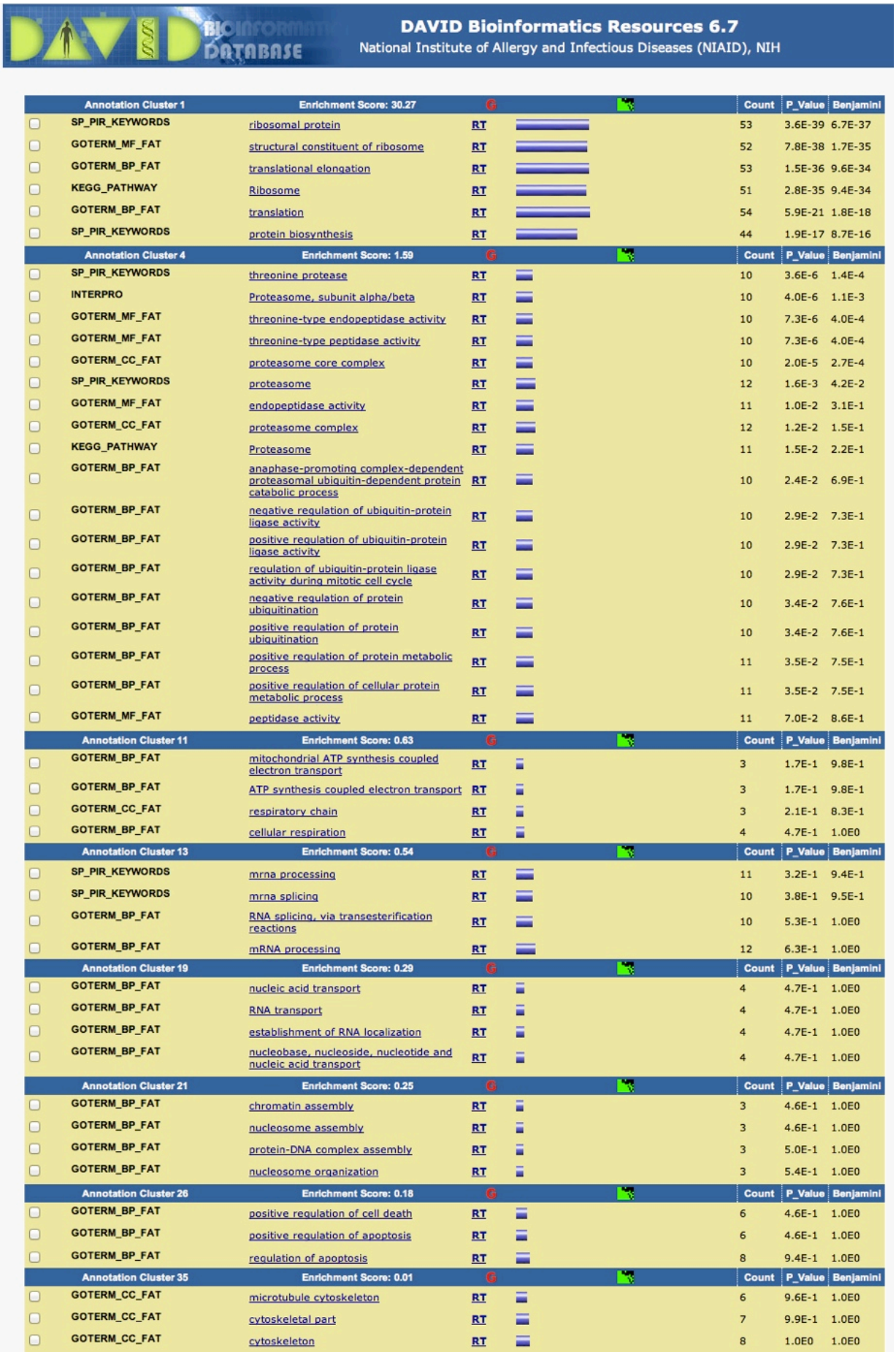


Figure 22 - Biological processes analysis.

To partially avoid the above described problems (i.e. the limited reproducibility of the biological effects exerted by the treatment with Q1 and the incomplete labeling of a number of proteins) we performed a pathways analysis with the DAVID Bioinformatic Resources 6.7 (NIAID, NIH) software, using as background list all the proteins identified and quantified in this study, and as input list only the proteins that showed an altered expression level of at least 100% in all 6 biological replicates.

The results obtained suggested that two main cellular complexes seem to be strongly altered in response to the treatment with the CK2 inhibitor: ribosomes and proteasomes (see Fig. 23). This information confirmed the results previously discussed in the section relative to the label-free analysis of CK2 interacting partners that suggested a strong correlation of CK2 with all stages of protein life, including synthesis and degradation.
In particular, Fig. 24 and 25 evidenced which subunits of the ribosome and proteasome complexes were found altered in this study.

Interestingly all the proteins of the core of the proteasome are upregulated, as well as many proteins of the 60 S and 40 S ribosomal subunits. Besides these two main molecular complexes, other proteins showed an altered expression level upon treatment with Q1 and will be discussed in detail in the discussion section.



Annotation Cluster 1	Enrichment Score: 30.27		Count	P_Value	Benjamini
SP_PIR_KEYWORDS	ribosomal protein	RT	53	3.6E-39	6.7E-37
GOTERM_MF_FAT	structural constituent of ribosome	RT	52	7.8E-38	1.7E-35
GOTERM_BP_FAT	translational elongation	RT	53	1.5E-36	9.6E-34
KEGG_PATHWAY	Ribosome	RT	51	2.8E-35	9.4E-34
GOTERM_BP_FAT	translation	RT	54	5.9E-21	1.8E-18
SP_PIR_KEYWORDS	protein biosynthesis	RT	44	1.9E-17	8.7E-16
Annotation Cluster 4	**Enrichment Score: 1.59**		**Count**	**P_Value**	**Benjamini**
SP_PIR_KEYWORDS	threonine protease	RT	10	3.6E-6	1.4E-4
INTERPRO	Proteasome, subunit alpha/beta	RT	10	4.0E-6	1.1E-3
GOTERM_MF_FAT	threonine-type endopeptidase activity	RT	10	7.3E-6	4.0E-4
GOTERM_MF_FAT	threonine-type peptidase activity	RT	10	7.3E-6	4.0E-4
GOTERM_CC_FAT	proteasome core complex	RT	10	2.0E-5	2.7E-4
SP_PIR_KEYWORDS	proteasome	RT	12	1.6E-3	4.2E-2
GOTERM_MF_FAT	endopeptidase activity	RT	11	1.0E-2	3.1E-1
GOTERM_CC_FAT	proteasome complex	RT	12	1.2E-2	1.5E-1
KEGG_PATHWAY	Proteasome	RT	11	1.5E-2	2.2E-1
GOTERM_BP_FAT	anaphase-promoting complex-dependent proteasomal ubiquitin-dependent protein catabolic process	RT	10	2.4E-2	6.9E-1
GOTERM_BP_FAT	negative regulation of ubiquitin-protein ligase activity	RT	10	2.9E-2	7.3E-1
GOTERM_BP_FAT	positive regulation of ubiquitin-protein ligase activity	RT	10	2.9E-2	7.3E-1
GOTERM_BP_FAT	regulation of ubiquitin-protein ligase activity during mitotic cell cycle	RT	10	2.9E-2	7.3E-1
GOTERM_BP_FAT	negative regulation of protein ubiquitination	RT	10	3.4E-2	7.6E-1
GOTERM_BP_FAT	positive regulation of protein ubiquitination	RT	10	3.4E-2	7.6E-1
GOTERM_BP_FAT	positive regulation of protein metabolic process	RT	11	3.5E-2	7.5E-1
GOTERM_BP_FAT	positive regulation of cellular protein metabolic process	RT	11	3.5E-2	7.5E-1
GOTERM_MF_FAT	peptidase activity	RT	11	7.0E-2	8.6E-1
Annotation Cluster 11	**Enrichment Score: 0.63**		**Count**	**P_Value**	**Benjamini**
GOTERM_BP_FAT	mitochondrial ATP synthesis coupled electron transport	RT	3	1.7E-1	9.8E-1
GOTERM_BP_FAT	ATP synthesis coupled electron transport	RT	3	1.7E-1	9.8E-1
GOTERM_CC_FAT	respiratory chain	RT	3	2.1E-1	8.3E-1
GOTERM_BP_FAT	cellular respiration	RT	4	4.7E-1	1.0E0
Annotation Cluster 13	**Enrichment Score: 0.54**		**Count**	**P_Value**	**Benjamini**
SP_PIR_KEYWORDS	mrna processing	RT	11	3.2E-1	9.4E-1
SP_PIR_KEYWORDS	mrna splicing	RT	10	3.8E-1	9.5E-1
GOTERM_BP_FAT	RNA splicing, via transesterification reactions	RT	10	5.3E-1	1.0E0
GOTERM_BP_FAT	mRNA processing	RT	12	6.3E-1	1.0E0
Annotation Cluster 19	**Enrichment Score: 0.29**		**Count**	**P_Value**	**Benjamini**
GOTERM_BP_FAT	nucleic acid transport	RT	4	4.7E-1	1.0E0
GOTERM_BP_FAT	RNA transport	RT	4	4.7E-1	1.0E0
GOTERM_BP_FAT	establishment of RNA localization	RT	4	4.7E-1	1.0E0
GOTERM_BP_FAT	nucleobase, nucleoside, nucleotide and nucleic acid transport	RT	4	4.7E-1	1.0E0
Annotation Cluster 21	**Enrichment Score: 0.25**		**Count**	**P_Value**	**Benjamini**
GOTERM_BP_FAT	chromatin assembly	RT	3	4.6E-1	1.0E0
GOTERM_BP_FAT	nucleosome assembly	RT	3	4.6E-1	1.0E0
GOTERM_BP_FAT	protein-DNA complex assembly	RT	3	5.0E-1	1.0E0
GOTERM_BP_FAT	nucleosome organization	RT	3	5.4E-1	1.0E0
Annotation Cluster 26	**Enrichment Score: 0.18**		**Count**	**P_Value**	**Benjamini**
GOTERM_BP_FAT	positive regulation of cell death	RT	6	4.6E-1	1.0E0
GOTERM_BP_FAT	positive regulation of apoptosis	RT	6	4.6E-1	1.0E0
GOTERM_BP_FAT	regulation of apoptosis	RT	8	9.4E-1	1.0E0
Annotation Cluster 35	**Enrichment Score: 0.01**		**Count**	**P_Value**	**Benjamini**
GOTERM_CC_FAT	microtubule cytoskeleton	RT	6	9.6E-1	1.0E0
GOTERM_CC_FAT	cytoskeletal part	RT	7	9.9E-1	1.0E0
GOTERM_CC_FAT	cytoskeleton	RT	8	1.0E0	1.0E0

Figure 23 - Patway analysis of altered proteins identified by SILAC experiment.

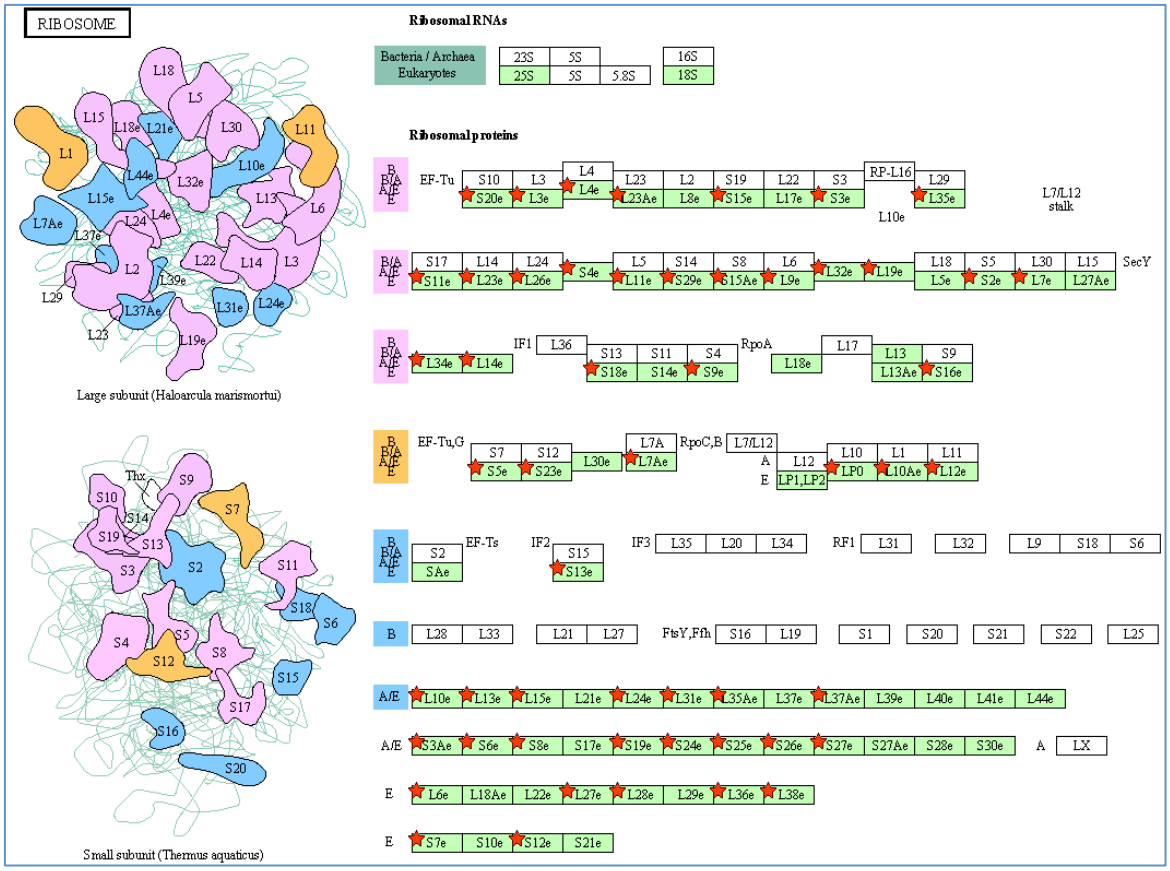


Figure 24 - Proteins found to be altered in the ribosome are marked with a red star.

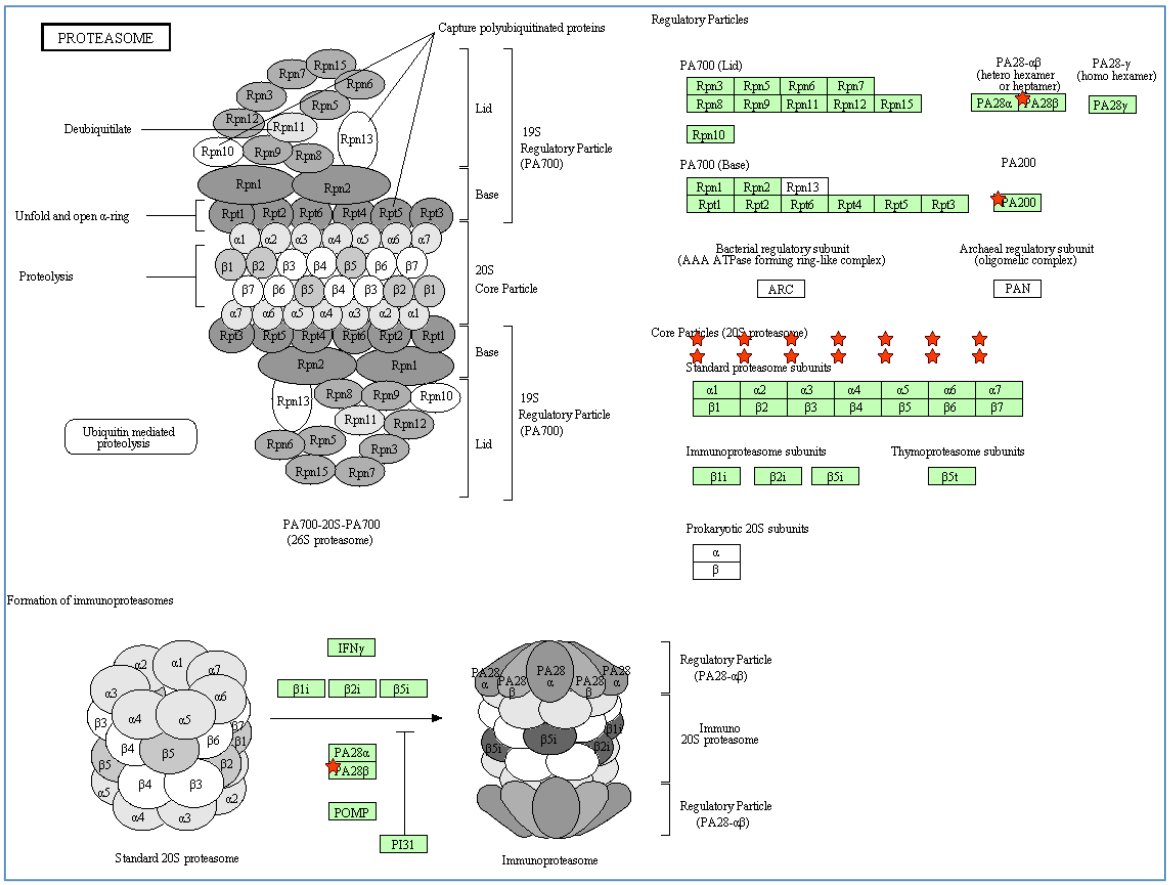


Figure 25 - Proteasome subunits found to be altered are marked with red stars.

3.6.5 Phosphoproteomics Analysis: Experimental Workflow

The second part of the SILAC experiment focused on the phosphopeptides analysis, with the aim of identifying new putative substrates of CK2 directly in a cellular system. For this purpose the same samples used for the global protein expression analysis described above, were also used to identify, at the protein phosphorylation level, changes induced by the treatment with the specific inhibitor of CK2. Thanks to this experimental approach, phosphopeptides (and therefore phosphoproteins) that show a difference in their phosphorylation state upon treatment with the inhibitor can be classified as (directly or indirectly) regulated by the activity of protein kinase CK2.

To perform this part of the project, 200 μg of each sample (as described in Fig. 10) were subjected to a phosphopeptides enrichment step with titanium dioxide (the detailed protocol is described in section 4.5) without any prior fractionation. The phosphopeptides enrichment step facilitates the specific detection of this low abundant class of peptides by reducing the interfering presence of non-phosphorylated peptides in the mixtures. As already mentioned, the samples we used were the same used for the expression analysis, thus the final experiment was still composed of 6 biological replicates. However, to increase the precision of the approach and obtain more accurate quantitative results, we exploited the data acquired during the first phase of the project to recalculate the quantities of proteins derived from heavy and light cells that was necessary to mix in equal amounts. In particular, from the data acquired in the global protein expression analysis it was possible to estimate the errors that were made during the protein quantification process with colorimetric methods (such as Lowry, Bradford or BCA methods), and calculate the new volumes of samples that needed to be mixed in order to obtain a more accurate ratio 1:1 of heavy/light proteins. This step is usually not necessary, since a simple normalization procedure can be applied post-acquisition in order to correct for possible errors derived from an imprecise mixing of heavy and light protein pools. However, generally speaking, the normalization process of a dataset can be correctly done only when the observed changes (of protein expression or phosphorylation) pertain to a small minority of all measured events. In this particular case, we originally expected to identify a quite large proportion of the phosphoproteome to be affected by the treatment with Q1. This consideration was based on the evidence that CK2 seems to be responsible for about 20% of the entire human phosphoproteome (*Salvi et al, Bioch. Biophys. Acta 2009*). Therefore, if this were the expected situation, it would not have been possible to apply to our dataset a post-acquisition normalization procedure. Thanks to this correction step, we expected to obtain more accurate quantifications, thus reducing the cutoff to apply in order to consider a phosphopeptide as significantly altered by the treatment. We have estimated that a 50% difference at the

phosphopeptide level is a safe threshold above which to consider a phosphorylation event as influenced by the treatment.

Always from a technical point of view, the mass spectrometry analysis was performed on the LTQ-Orbitrap running every sample 3 times with three different fragmentation methods: MS^2, MS^3, and MSA.
The first is the classical approach, where the selected parent ion is fragmented, and in the case of phosphopeptides, the fragmentation often results in the neutral loss of phosphoric acid and in the lack of ions derived from the peptide backbone.
The problem of the poor phosphopeptides backbone fragmentation can be overcome by generating MS^3 spectra in a data-dependent manner upon detection of the neutral loss of a phosphoric acid in MS^2 spectra.
With the multistage activation (MSA) approach, the neutral loss product ion in the MS^2 spectrum is activated and fragmented without an additional isolation cycle. The final spectrum is therefore the composition of the signals of the product ions of the neutral loss fragment, and the initial MS^2 product ions, since they are trapped together. These last two strategies require additional cycle time on the instrument, resulting in a reduced number of spectra that can be measured in the same amount of time.
In literature are reported several studies that have been done to investigate the advantages or disadvantages linked to this 3 different scanning methods when applied to the analysis of phosphopeptides. However the results are quite controversial and a definite answer regarding the approach to apply to obtain the best possible results has not been given (*Ulintz et al, J. Proteome Res. 2009*; *Jiang et al, Anal. Chem. 2010*; *Boersema et al, J. Mass Spectr. 2009*).

We decided that the best way to increase the depth of our analysis was to exploit all 3 approaches and combine the results obtained. Indeed, this allowed us to improve the number of phosphopeptide identifications, thus increasing the quantity and quality of the acquired data, as will be discussed in the next paragraphs. Moreover, as it was done for the global protein expression analysis, each sample was run with the same fragmentation method twice, using an exclusion list in the second run to improve the detection of low abundance peptides. Thus, 6 LC-MS/MS runs were performed for each biological replicate, resulting in a total of 36 LC-MS/MS runs. These analyses led to the highly confident identification of 1957 proteins and 85210 peptides. Differently to the protein expression analysis, where it is considered a positive hit a protein identified with at least 2 unique peptides, here proteins were considered as correctly identified even if a single unique peptide per protein was identified with high confidence. This is a perfectly normal procedure when dealing with

phosphoproteomics studies where the redundancy of peptides identified per protein is strongly reduced.

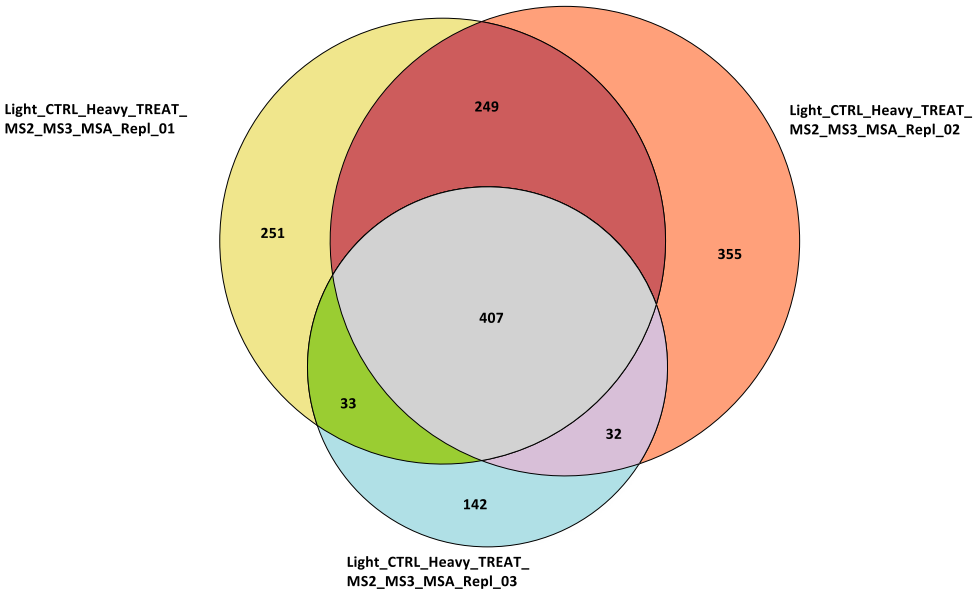
To further increase the number and quality of phosphopeptide identifications, we also decided to analyze the data with two different search engines, Mascot and Sequest that are known to give only partially overlapping results when used to process the same set of data (*Kapp et al, Proteomics 2005*; *Millioni et al, PlosOne 2011*). The results obtained with all these combined approaches were finally analyzed with Proteome Discoverer.

3.6.6 Phosphoproteomics: Technical and Biological Reproducibility

From these analyses, we found that 85% of the identified proteins were phosphoproteins, for a total of 6498 unique phosphopeptides, thus indicating that the phosphopeptide enrichment step was quite efficient. Moreover, 917 of the identified phosphoproteins were also quantified and are reported in Table 6 of the Appendix section (phosphopeptides are not shown for space reason). Considering the enormous amount of data collected and its complexity (phosphopeptides must be manually verified since often a single phosphopeptide is identified per protein), the detailed analysis of the acquired data is still ongoing. Nevertheless, it was still possible to extract some important preliminary results, especially regarding the technical approaches used, rather than the biological aspects.

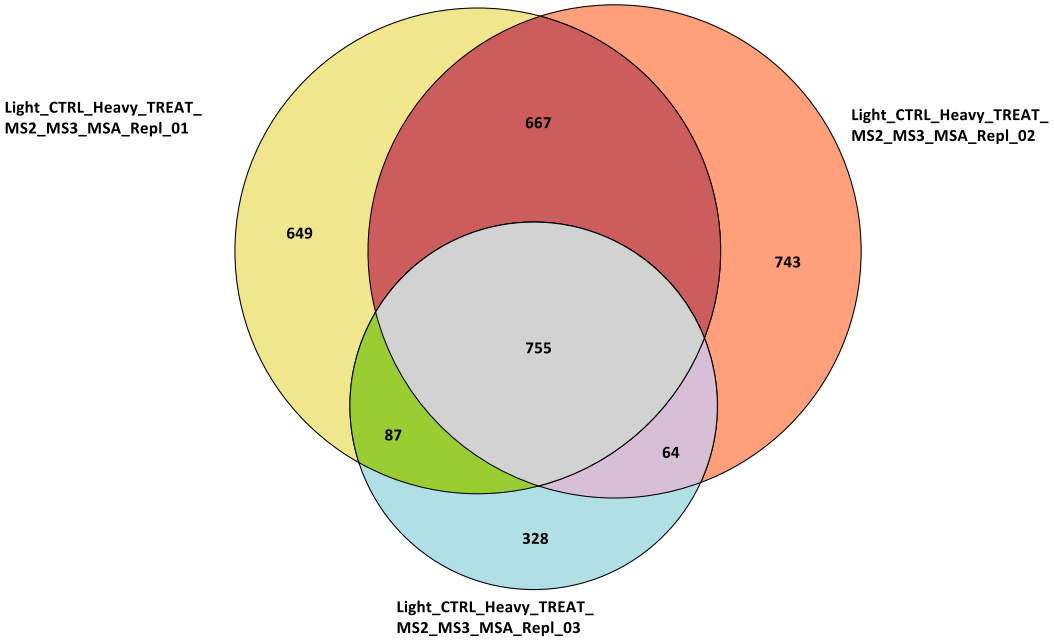
The reproducibility of the analyses across biological replicates in terms of protein identifications was again evaluated thanks to Proteome Discoverer software, as previously described. Fig. 26 shows the overlap of identified proteins from 3 biological replicates, where the number of proteins identified in each replicate was obtained as a combination of all proteins identified with the different scanning methods (MS^2, MS^3 and MSA).

The first obvious consideration that can be done by looking at the Venn diagram is that one of the 3 replicates led to the identification of a considerably lower number of proteins, possibly because of instrumental issues or, more probably, because a technical problem occurred during the phosphopeptide enrichment step, a procedure that is not trivial to perform. The second obvious observation is that only 49% of identified proteins were in common to at least 2 biological replicates. This variability was probably introduced during the phosphopeptides enrichment step. As just mentioned, such procedure cannot be considered easy to perform, since it requires the use of self-made micro-columns, a probable source of variability that can be only partially limited by the use of multiple biological replicates.



	Exclusive	Total	Label	Description
	251	940	Light_CTRL_Heavy_TREAT_MS2_MS3_MSA_Repl_01	Repl_01
	355	1043	Light_CTRL_Heavy_TREAT_MS2_MS3_MSA_Repl_02	Repl_02
	142	614	Light_CTRL_Heavy_TREAT_MS2_MS3_MSA_Repl_03	Repl_03
	249	656	Light_CTRL_Heavy_TREAT_MS2_MS3_MSA_Repl_01 / Light_CTRL_Heavy_TREAT_MS2_MS3_MSA_Repl_02	Repl_01 / Repl_02
	32	439	Light_CTRL_Heavy_TREAT_MS2_MS3_MSA_Repl_02 / Light_CTRL_Heavy_TREAT_MS2_MS3_MSA_Repl_03	Repl_02 / Repl_03
	33	440	Light_CTRL_Heavy_TREAT_MS2_MS3_MSA_Repl_01 / Light_CTRL_Heavy_TREAT_MS2_MS3_MSA_Repl_03	Repl_01 / Repl_03
	407	407	Light_CTRL_Heavy_TREAT_MS2_MS3_MSA_Repl_01 / Light_CTRL_Heavy_TREAT_MS2_MS3_MSA_Repl_02 / Light_CTRL_Heavy_TREAT_MS2_MS3_MSA_Repl_03	Repl_01 / Repl_02 / Repl_03
Sum	1469			

Figure 26 - Example of reproducibility at the protein identification level across biological replicates.



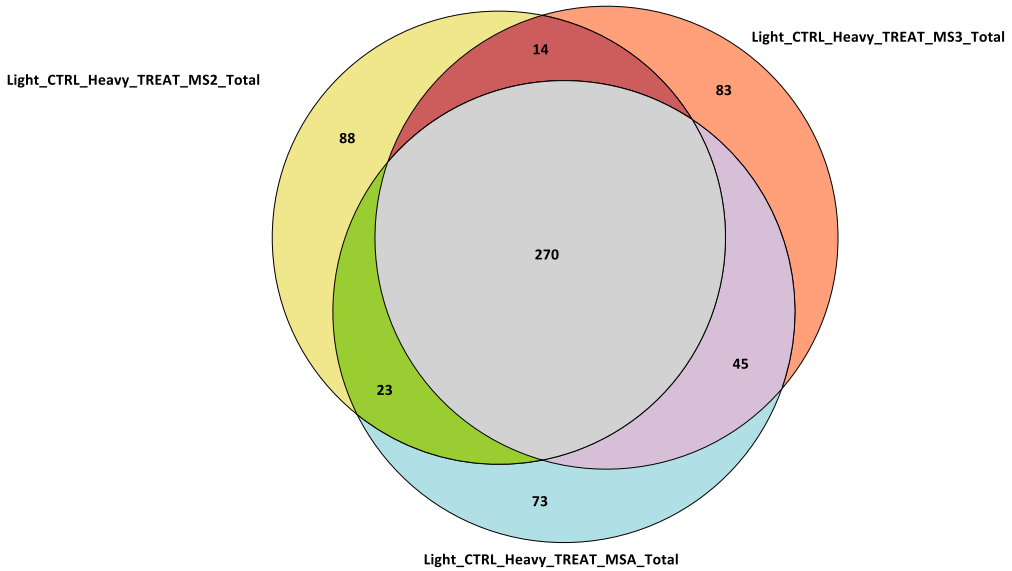
	Exclusive	Total	Label	Description
	649	2158	Light_CTRL_Heavy_TREAT_MS2_MS3_MSA_Repl_01	Repl_01
	743	2229	Light_CTRL_Heavy_TREAT_MS2_MS3_MSA_Repl_02	Repl_02
	328	1234	Light_CTRL_Heavy_TREAT_MS2_MS3_MSA_Repl_03	Repl_03
	667	1422	Light_CTRL_Heavy_TREAT_MS2_MS3_MSA_Repl_01 / Light_CTRL_Heavy_TREAT_MS2_MS3_MSA_Repl_02	Repl_01 / Repl_02
	64	819	Light_CTRL_Heavy_TREAT_MS2_MS3_MSA_Repl_02 / Light_CTRL_Heavy_TREAT_MS2_MS3_MSA_Repl_03	Repl_02 / Repl_03
	87	842	Light_CTRL_Heavy_TREAT_MS2_MS3_MSA_Repl_01 / Light_CTRL_Heavy_TREAT_MS2_MS3_MSA_Repl_03	Repl_01 / Repl_03
	755	755	Light_CTRL_Heavy_TREAT_MS2_MS3_MSA_Repl_01 / Light_CTRL_Heavy_TREAT_MS2_MS3_MSA_Repl_02 / Light_CTRL_Heavy_TREAT_MS2_MS3_M	Repl_01 / Repl_02 / Repl_03
Sum	3293			

Figure 27 - Example of biological replicates of identified peptides.

Similar considerations can be applied also at the peptide level: Fig. 27 shows the Venn diagram of the identified peptides from the same 3 biological replicates reported in the previous diagram. Here the overlap between at least 2 replicates is 48%, perfectly comparable with the value found for proteins, since the redundancy of peptides identified per protein is strongly reduced when dealing with phosphoproteomics studies where only one high confidence peptide is sufficient to identify a protein.

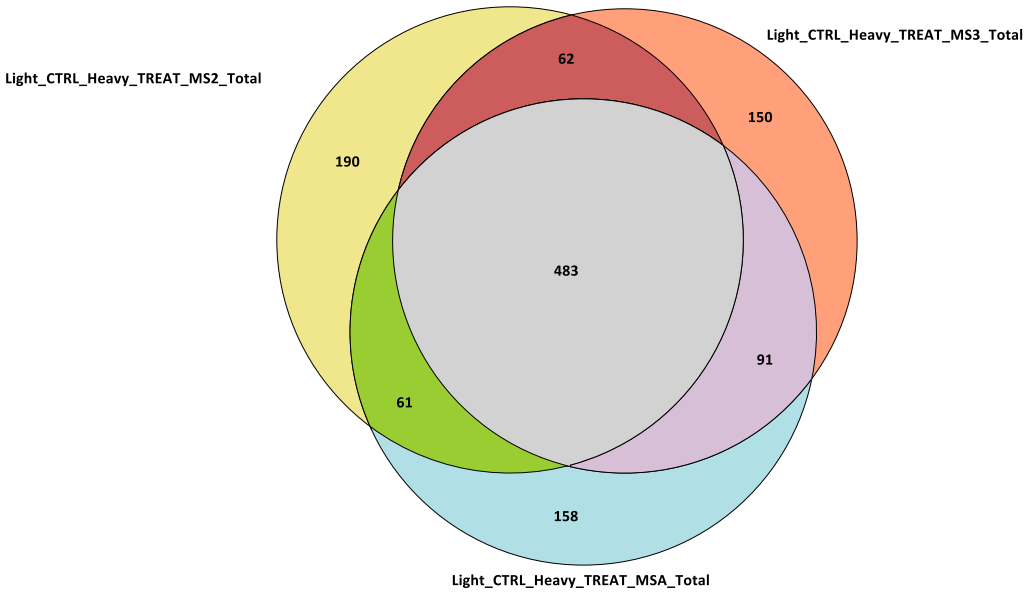
Another information that could be extracted from the phosphopeptides analysis was the differential protein detection between the 3 fragmentation technologies (see Fig. 28).
The Venn diagram shows that 59% of proteins were identified by at least 2 different scanning methods, while the rest was found only with a single approach. Thus, 13% of proteins could be found only by each specific approach.
Similar considerations can be applied to the peptides (the majority of which are phosphopeptides) identified by MS^2, MS^3, and MSA scanning approaches (see Fig. 29). The Venn diagram shows that the total number of peptides that was identified with each scanning method is very similar but only 40% of peptides were identified by all three fragmentation strategies. Both MS^3 and MSA alone led to the identification of 13% of the peptides while MS^2 fragmentation worked a bit better, leading to the identification of 16% of peptides. Thus the selection of only one scanning method would have led to the loss of about 25% of all identified peptides. Therefore this homogeneous distribution between the 3 methodologies perfectly justifies the use of a combination of them to obtain a more comprehensive analysis.

As described in the previous part of this chapter, further analyses to evaluate the relevance of the exclusion list at the protein and peptide identification level can be performed (see Fig. 30, 31, and 32).



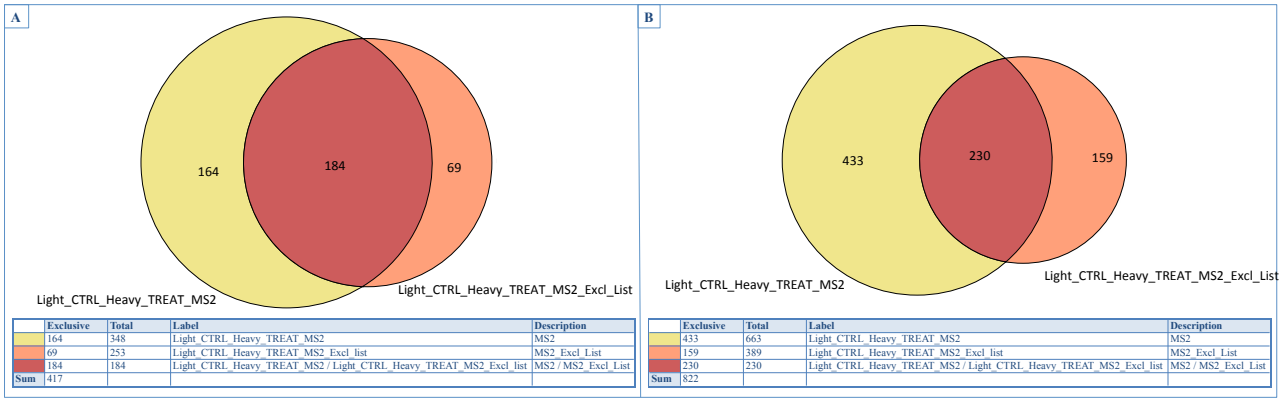
	Exclusive	Total	Label	Description
	88	395	Light_CTRL_Heavy_TREAT_MS2_Total	MS2
	83	412	Light_CTRL_Heavy_TREAT_MS3_Total	MS3
	73	411	Light_CTRL_Heavy_TREAT_MSA_Total	MSA
	14	284	Light_CTRL_Heavy_TREAT_MS2_Total / Light_CTRL_Heavy_TREAT_MS3_Total	MS2 / MS3
	45	315	Light_CTRL_Heavy_TREAT_MS3_Total / Light_CTRL_Heavy_TREAT_MSA_Total	MS3 / MSA
	23	293	Light_CTRL_Heavy_TREAT_MS2_Total / Light_CTRL_Heavy_TREAT_MSA_Total	MS2 / MSA
	270	270	Light_CTRL_Heavy_TREAT_MS2_Total / Light_CTRL_Heavy_TREAT_MS3_Total / Light_CTRL_Heavy_TREAT_MSA_Total	MS2 / MS3 / MSA
Sum	596			

Figure 28 – Comparison of proteins identified with different fragmentation methods (MS^2, MS^3, MSA).



	Exclusive	Total	Label	Description
	190	796	Light_CTRL_Heavy_TREAT_MS2_Total	MS2
	150	786	Light_CTRL_Heavy_TREAT_MS3_Total	MS3
	158	793	Light_CTRL_Heavy_TREAT_MSA_Total	MSA
	62	545	Light_CTRL_Heavy_TREAT_MS2_Total / Light_CTRL_Heavy_TREAT_MS3_Total	MS2 / MS3
	91	574	Light_CTRL_Heavy_TREAT_MS3_Total / Light_CTRL_Heavy_TREAT_MSA_Total	MS3 / MSA
	61	544	Light_CTRL_Heavy_TREAT_MS2_Total / Light_CTRL_Heavy_TREAT_MSA_Total	MS2 / MSA
	483	483	Light_CTRL_Heavy_TREAT_MS2_Total / Light_CTRL_Heavy_TREAT_MS3_Total / Light_CTRL_Heavy_TREAT_MSA_Total	MS2 / MS3 / MSA
Sum	1195			

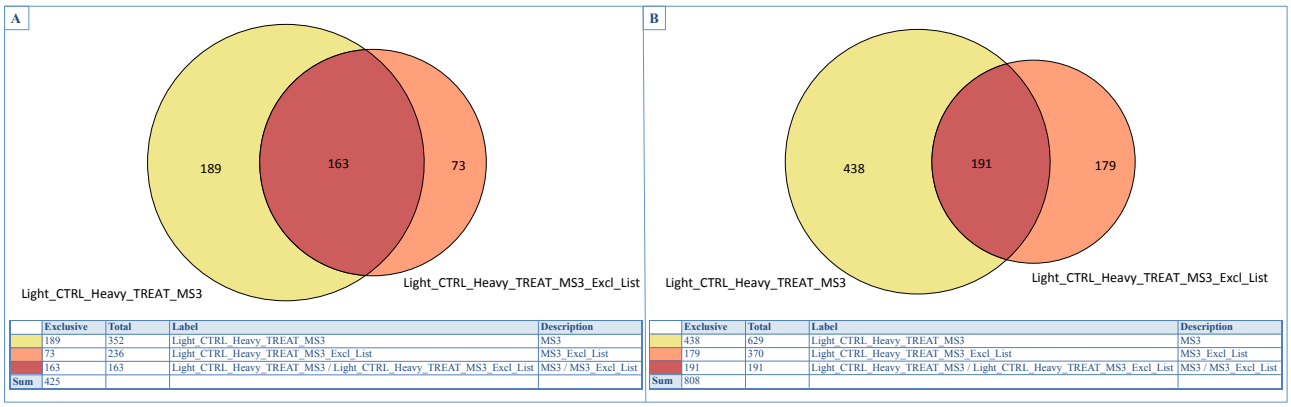
Figure 29 - Comparison of peptides identified with different fragmentation methods (MS^2, MS^3, MSA).



	Exclusive	Total	Label	Description
	164	348	Light_CTRL_Heavy_TREAT_MS2	MS2
	69	253	Light_CTRL_Heavy_TREAT_MS2_Excl_list	MS2_Excl_List
	184	184	Light_CTRL_Heavy_TREAT_MS2 / Light_CTRL_Heavy_TREAT_MS2_Excl_list	MS2 / MS2_Excl_List
Sum	417			

	Exclusive	Total	Label	Description
	433	663	Light_CTRL_Heavy_TREAT_MS2	MS2
	159	389	Light_CTRL_Heavy_TREAT_MS2_Excl_list	MS2_Excl_List
	230	230	Light_CTRL_Heavy_TREAT_MS2 / Light_CTRL_Heavy_TREAT_MS2_Excl_list	MS2 / MS2_Excl_List
Sum	822			

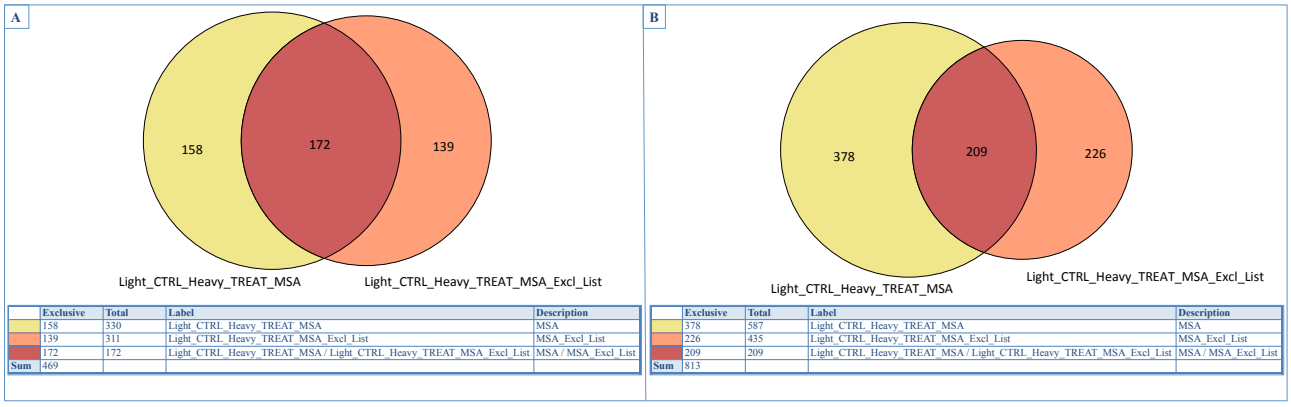
Figure 30 – Overlapping proteins (A) and peptides (B) identified by two LC-MS/MS analyses of the same fraction, based on MS^2 fragmentation, with or without the use of exclusion list.



	Exclusive	Total	Label	Description
	189	352	Light_CTRL_Heavy_TREAT_MS3	MS3
	73	236	Light_CTRL_Heavy_TREAT_MS3_Excl_List	MS3_Excl_List
	163	163	Light_CTRL_Heavy_TREAT_MS3 / Light_CTRL_Heavy_TREAT_MS3_Excl_List	MS3 / MS3_Excl_List
Sum	425			

	Exclusive	Total	Label	Description
	438	629	Light_CTRL_Heavy_TREAT_MS3	MS3
	179	370	Light_CTRL_Heavy_TREAT_MS3_Excl_List	MS3_Excl_List
	191	191	Light_CTRL_Heavy_TREAT_MS3 / Light_CTRL_Heavy_TREAT_MS3_Excl_List	MS3 / MS3_Excl_List
Sum	808			

Figure 31 – Overlapping proteins (A) and peptides (B) identified by two LC-MS/MS analyses of the same fraction, based on MS^3 fragmentation, with or without the use of exclusion list.



	Exclusive	Total	Label	Description
	158	330	Light_CTRL_Heavy_TREAT_MSA	MSA
	139	311	Light_CTRL_Heavy_TREAT_MSA_Excl_List	MSA_Excl_List
	172	172	Light_CTRL_Heavy_TREAT_MSA / Light_CTRL_Heavy_TREAT_MSA_Excl_List	MSA / MSA_Excl_List
Sum	469			

	Exclusive	Total	Label	Description
	378	587	Light_CTRL_Heavy_TREAT_MSA	MSA
	226	435	Light_CTRL_Heavy_TREAT_MSA_Excl_List	MSA_Excl_List
	209	209	Light_CTRL_Heavy_TREAT_MSA / Light_CTRL_Heavy_TREAT_MSA_Excl_List	MSA / MSA_Excl_List
Sum	813			

Figure 32 – Overlapping proteins (A) and peptides (B) identified by two LC-MS/MS analyses of the same fraction, based on MSA fragmentation, with or without the use of exclusion list.

The three Venn diagrams show that in average only 40% of proteins were found in common when the same sample was analyzed twice, with an without an excluding list. Therefore this approach

resulted in a 60% increase of protein identifications. A similar consideration is valid at the peptide level, where the average number of peptides found in common between the two LC-MS/MS analyses is lower (26%). Thus, analyzing each sample a second time after having excluded the peptides detected in the first analysis, led to a relevant increase in peptide and protein identifications as well as in sequence coverage.

A last consideration can be done by comparing the proteins identified with the global protein expression analysis with those identified with the phosphoproteomics approach. Since the phosphopeptide enrichment allows to explore a different portion of the proteome, we expected a rather small overlapping between the two groups and the Venn diagram reported in Fig. 33 confirmed this hypothesis, showing that only 7.7% of the proteins were in common between the two analyses.



	Exclusive	Total	Label	Description
	1404	1685	Global expression analysis	Global expression analysis
	1676	1957	Phosphoproteome analysis	Phosphoproteome analysis
	281	281	Global expression analysis/Phosphoproteome analysis	Global expression analysis/Phosphoproteome analysis
Sum	1107			

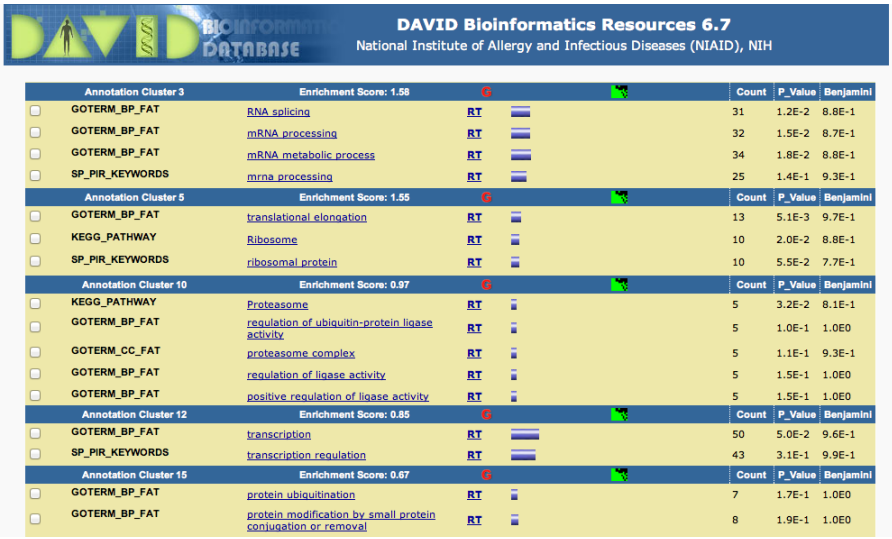
Figure 33 – Comparison of proteins identified from the global protein expression analysis and the phosphoproteomics analysis.

3.6.7 Phosphoproteomics: Bioinformatics and Pathway Analyses

Although, as I mentioned before, the detailed analysis of phosphopeptides and phosphoproteins identified in this project is still ongoing, a preliminary analysis of the data relative to the phosphopeptides show that we could identify 6498 unique phosphopeptides for a total of 9756 phosphosites on serine, threonine, and tyrosine distributed as follows: 69% phosphoserines, 25.5% phosphothreonines, and 4.5% phosphotyrosines. This distribution is in agreement with what is found in all phosphopeptide databases and shows a strong dominance of phosphoserine peptides over the other two categories, reflecting the notion that serine is by far the most favorite target of

protein kinases within the cell (*Hanks et al, Science 1988*). We also gained information about the number of phosphosites per peptide: 4090 of the identified peptides are mono-phosphorylated (63%), 1694 are *bis*-phosphorylated (26%), 512 peptides contain 3 phosphosites (8%), and the rest of peptides showed an higher number of phosphorylations.

Beside the detailed analysis of phosphopeptides that will hopefully lead to the identification of several new *in vivo* substrates of CK2, a pathway analysis was performed with DAVID Bioinformatic Resources software, using as background list all the proteins identified and quantified in the phosphoproteomics experiment and as input list 121 proteins that were quantified in at least 3 biological replicates and showed an altered expression and/or phosphorylation level of at least 50% upon treatment with quinalizarin. The result is displayed in Fig. 34.



DAVID Bioinformatics Resources 6.7
National Institute of Allergy and Infectious Diseases (NIAID), NIH

Annotation Cluster 3	Enrichment Score: 1.58			Count	P_Value	Benjamini
GOTERM_BP_FAT	RNA splicing	RT		31	1.2E-2	8.8E-1
GOTERM_BP_FAT	mRNA processing	RT		32	1.5E-2	8.7E-1
GOTERM_BP_FAT	mRNA metabolic process	RT		34	1.8E-2	8.8E-1
SP_PIR_KEYWORDS	mrna processing	RT		25	1.4E-1	9.3E-1
Annotation Cluster 5	**Enrichment Score: 1.55**			**Count**	**P_Value**	**Benjamini**
GOTERM_BP_FAT	translational elongation	RT		13	5.1E-3	9.7E-1
KEGG_PATHWAY	Ribosome	RT		10	2.0E-2	8.8E-1
SP_PIR_KEYWORDS	ribosomal protein	RT		10	5.5E-2	7.7E-1
Annotation Cluster 10	**Enrichment Score: 0.97**			**Count**	**P_Value**	**Benjamini**
KEGG_PATHWAY	Proteasome	RT		5	3.2E-2	8.1E-1
GOTERM_BP_FAT	regulation of ubiquitin-protein ligase activity	RT		5	1.0E-1	1.0E0
GOTERM_CC_FAT	proteasome complex	RT		5	1.1E-1	9.3E-1
GOTERM_BP_FAT	regulation of ligase activity	RT		5	1.5E-1	1.0E0
GOTERM_BP_FAT	positive regulation of ligase activity	RT		5	1.5E-1	1.0E0
Annotation Cluster 12	**Enrichment Score: 0.85**			**Count**	**P_Value**	**Benjamini**
GOTERM_BP_FAT	transcription	RT		50	5.0E-2	9.6E-1
SP_PIR_KEYWORDS	transcription regulation	RT		43	3.1E-1	9.9E-1
Annotation Cluster 15	**Enrichment Score: 0.67**			**Count**	**P_Value**	**Benjamini**
GOTERM_BP_FAT	protein ubiquitination	RT		7	1.7E-1	1.0E0
GOTERM_BP_FAT	protein modification by small protein conjugation or removal	RT		8	1.9E-1	1.0E0

Figure 34 - Pathway analysis of the proteins found to be altered in the phosphoproteomics analysis

Also in this case, as it was already found for the proteins identified in the global protein expression analysis and in the study of interacting partners of CK2, the results suggest that the treatment of the cells with an inhibitor of CK2 mainly affects the expression level and the phosphorylation of proteins involved in biosynthesis (ribosome) and degradation (proteasome) of proteins, together with other biological processes such as transcription and splicing.

3.6.8 Discussion

The aim of this study was the investigation of the molecular response of cells to CK2 inhibition, using a SILAC approach. The basic idea was the identification of proteins that change their expression level and/or their phosphorylation state upon the treatment with a specific, cell permeable and potent inhibitor of the protein kinase CK2. The data obtained from these experiments can be used to highlight cellular processes in which CK2 is strongly involved and, overall, to compile a list of proteins the phosphorylation of which is, directly or indirectly, regulated by the activity of this protein kinase.

The analysis of the data obtained from the global protein expression analysis and overall from the phosphoproteomics analysis was extremely difficult and is partially still in progress. Beside the expected biological variability, we realized that the treatment of cells with Q1 does not give highly reproducible results in terms of protein expression level across different biological replicates, therefore this lack of reproducibility obviously affects also the data acquired in the phosphoproteomics experiments. Moreover we needed to cope with other issues that have been poorly discussed in literature. In particular from a quantitative point of view, the analysis of the data obtained in these experiments is complicated by several factors:

1. We observed an unexpected incomplete labeling of proteins, despite the high number of cell doublings (definitely higher than the one suggested in literature for the same cell line) that becomes evident only when the analysis is performed with a swapping system.

2. A variation of the phosphorylation state of phosphopeptides could be only apparent and not substantial, since it could simply be related to a change in expression of the proteins they belong to, rather than a real variation of their phosphorylation level. Thus, an important issue is the correlation between data regarding the phosphorylation level and data regarding the global protein expression. Of course this approach is applicable only to those proteins that have been identified and quantified in both the experiments and the very small overlap between proteins identified in the global expression analysis and in the phosphoproteomics analysis makes this correlation possible only for a small fraction of proteins. For the other proteins could be applicable an alternative normalization strategy that takes advantage of the possible detection and quantification in the same experiment of phosphopeptides and non-phosphorylated peptides that belong to the same protein. In this case, the unmodified peptides can be used as internal standards to highlight possible variations in the expression

of the whole protein. Obviously, this complication works in two ways: if a significant variation of phosphorylation level could be only apparent, on the other hand also the lack of variation could be only an apparent effect.

3. We observed another important effect with a strong impact on the protein quantification. Specifically in the datasets relative to the phosphopeptide analysis, a strong arginine-to-proline conversion effect can be observed (details about the arginine-to-proline conversion effect are described in section 2.3.2). Such effect was present also in the dataset relative to the global protein expression analysis but in that case it had a much smaller impact and led to errors in the quantification process that could be quantifiable in about 10-15% (data not shown). In the phosphoproteomics analysis, the arginine-to-proline conversion leads sometimes to quantification errors of the order of 50% or more. This difference can be easily explained considering that a large proportion of the phosphopeptides we have identified are particularly rich in proline residues and this makes this effect very evident. It is therefore important to correct the acquired data with suitable informatics tools in order to avoid gross quantification errors and reduce the complexity of the data analysis.

All these problems, very rarely discussed in literature, seriously limited the reliability of the quantification process, thus making a comprehensive analysis of the data very difficult.
Nonetheless, based on the datasets that could be reliably quantified, it was possible to extract few preliminary considerations from the global protein expression analysis as well as the phosphoproteomics analysis.
Collectively taken, the data once again suggest a strong involvement of CK2 in all aspects of cell life and in particular in the complex biological process of protein synthesis and degradation. In fact, we observed a significant overexpression of proteins belonging to the ribosome and proteasome complexes in response to quinalizarin treatment: whether this increment is due to an increased expression of those proteins or to a reduced degradation, remains to be investigated. It is important to highlight here that the observed effect on ribosomal and proteasomal proteins could be simply attributable to an unspecific cytotoxic effect of the inhibitor, rather than to a specific effect related to the inhibition of CK2. However, this is not the first time that a strong increase in abundance of ribosomal proteins is observed in response to CK2 inhibition: a study conducted by the group of Silvio Perea on NCI-H125 cell line highlighted that protein translation was the most affected process (23% of total identified proteins) after treatment with CIGB-300, a cyclic peptide that inhibits CK2 activity (*Rodríguez-Ulloa et al, J. Proteome Res, 2010*). The fact that two inhibitors

with completely different physicochemical properties, induce a similar effect on different cells, suggest that the observed alterations are probably related to the specific inhibition of the kinase rather than to an unspecific cytotoxicity.

Considering that our data show a remarkable increased abundance of ribosomal proteins, it could be very interesting to further investigate this aspect and to verify if a higher number of functional ribosomes is indeed present in treated cells as compared to untreated cells.

In our study other proteins involved in the process of protein biosynthesis were also found altered, such as several isoforms of eukaryotic translation elongation factors, eukaryotic translation initiation factors, and proteins belonging to the chaperonins containing TCP1 complex.

The same proteins were found to be altered also in the phosphoprotein analysis, where several phosphopeptides showed a decrease in their phosphorylation state upon treatment with Q1.

Another cellular complex found positively altered after the treatment was the proteasome, where all the proteins constituting its core, together with few other regulatory proteins, were found upregulated. The same trend was observed also for the phosphopeptides of some proteasomal subunits quantified in the phosphoproteomic experiment. In this case the increased phosphorylation observed in these peptides is probably due to the increased expression of the proteins rather than to a direct increase in phosphorylation activity. This is just an example of a quite common situation observed for several other phosphopeptides. This underlines the need to normalize all the phosphopeptides quantifications on the basis of the correlated protein expression, to discriminate whether the observed alteration of phosphopeptides is related to an alteration of the whole protein expression or to a real change in the phosphorylation state.

Other interesting proteins that emerged from our analysis are involved in the regulation of transcription, such as CREB regulated transcription coactivator 2, zinc finger E-box binding homeobox 2, interferon regulatory factor 2 binding protein 1, and heterogeneous nuclear ribonucleoprotein U, a protein specifically involved in mRNA stability. All this data confirm and integrate the results obtained with our interactome analysis and support the notion that CK2 plays a pivotal role on protein synthesis and degradation.

If pathway analyses confirmed other data already discussed in this thesis, the preliminary analysis of phosphopeptides identified in the phosphoproteomics approach suggested really interesting observations. When we planned and designed this phosphoproteomics experiment, we expected that the analysis would cluster the detected phosphopeptides into two main categories: phosphopeptides with phosphosites that are not affected (directly or indirectly) by CK2 activity should not change their phosphorylation state upon quinalizarin treatment, while phosphopeptides the phosphorylation

of which is dependent (directly or indirectly) by CK2 should show a decreased MS signal caused by the inhibition of CK2. A schematic representation of these situations is reported in Fig. 35.

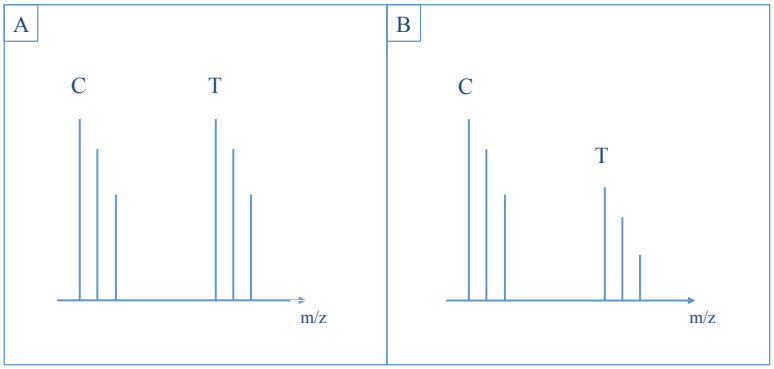


Figure 35 - Expected cases of phosphopeptides MS signals.

What we really obtained with this phosphoproteomics approach is a much more complicated scenario in which the two previously described cases can be observed together with several other interesting (but not easy to explain) situations.

Fig. 36 schematically shows 6 different situations that we have found analyzing the dataset, i.e. six classes of phosphopeptides displaying different phosphorylation behaviors in response to CK2 inhibition with quinalizarin:

1. Peptides with phosphosites that do not display the *consensus* sequence recognized by CK2 and that, as expected, did not change their phosphorylation state. This group of peptides can be classified as phosphorylated independently by the activity of CK2. Panel 1 of Fig. 36 shows an exemplificative case: the peptide VVVsPTKK derived from the protein Nucleolin is phosphorylated on a Serine with a *consensus* sequence different from the one recognized by CK2, and its phosphorylation state was not affected by the treatment with quinalizarin. In fact, we found that the treatment over control ratio for this phosphopeptide was 1.044. This is just an example of a rather common situation that can be found by looking at the entire dataset collected in our experiment.

2. Peptides with a strong *consensus* sequence for CK2 that, as expected, showed a decreased phosphorylation upon treatment with Q1. An example is reported in Fig. 36, panel 2: the

peptide GSGTAsDDEFENLR from E3 ubiquitin-protein ligase showed a significant reduced phosphorylation after treatment with the inhibitor. Up to now, E3 ubiquitin-protein ligase was not known to be phosphorylated by CK2, thus the identification of a phosphosite recognizable by the kinase and that reduces its phosphorylation in response to CK2 inhibition could add a novel protein to the list of substrates of CK2. This is the class of phosphopeptides we are more interested in, since our main goal is the identification of as many as possible new substrates of CK2, directly in a cellular system.

3. Peptides that have a CK2 *consensus* sequence and that are known to be phosphorylated by this kinase but that did not show any significant change in their phosphorylation level. An example can be seen in Fig. 36, panel 3 that reports the case of Heat Shock Protein HSP 90-beta of which we identified the phosphopeptide EKEIsDDEAEEEKGEK (known to be phosphorylated by CK2 - *information from PhosphoSitePlus Database*). The best hypothesis that could explain this situation is that the duration of the treatment with the inhibitor was too short compared to the turnover of dephosphorylation for that specific phosphosite. Therefore, although CK2 is responsible for that specific phosphorylation event, the lack of dephosphorylation results in an unchanged phosphorylation upon inhibition. Apparently, a large set of peptides identified in this study show this behavior, suggesting a particularly slow phosphorylation/dephosphorylation turnover (this point is discussed more in detail in the last paragraph).

4. *Bis*-phosphorylated peptides with 2 phosphosites in hierarchical positions (both recognized by CK2) that, after treatment with quinalizarin, showed a decreased phosphorylation, with a concomitant increment of the corresponding *mono*-phosphorylated peptides. An example is serine/arginine repetitive matrix protein 1 (see Fig. 36, panel 4). The identified peptide KEtEsEAEDNLDDLEK has two phosphosites, both of them recognized by CK2 and that showed two different behaviors upon treatment with quinalizarin. As expected for a CK2 substrate, the *bis*-phosphorylated peptide showed a significant decrease in its phosphorylation level (Treatment/Control=0.5). However, the *mono*-phosphorylated peptide increased after treatment with CK2 inhibitor with exactly the opposite trend (Treatment/Control=1.5). This higher level of *mono*-phosphorylated peptide does not depend on new phosphorylation events, but rather on the dephosphorylation of the *bis*-phosphorylated peptide that leads to an accumulation of the *mono*-phosphorylated one. Looking at the phosphosites, we can see that the serine is phosphorylated in both the *mono*-

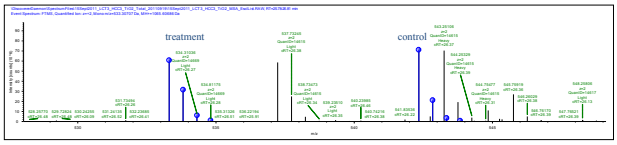
and *bis*-phosphorylated sequence: we can therefore deduce that the phosphorylation state of this residue did not change with the treatment. On the other hand, threonine was subjected to a reduction in phosphorylation, indicating that these two residues have independent and different turnover of dephosphorylation. Moreover, it is possible to speculate that being the phosphorylation of serine more stable, this residue could play a role as primer for the subsequent phosphorylation of the threonine. Therefore both the phosphorylations on threonine and serine are due to CK2 which probably acts with two subsequent catalytic reactions by phosphorylating the serine in the first step, and the threonine immediately after. Peptides belonging to this class can be classified as putative substrates of CK2 *in vivo*.

5. *Bis*-phosphorylated peptides with phosphosites in adjacent positions (both recognized by CK2) that decreased upon CK2 inhibition and for which the corresponding *mono*-phosphorylated peptides could not be identified. This case is similar to the previous one, but this time the phosphopeptides contain two phosphosites in adjacent position and only the *bis*-phosphorylated sequence was observed. The *bis*-phosphorylated peptide (see Fig. 36, panel 5) DIEIstEEEKDTGDLKDSSLLK belongs to La-related protein 7 and is a perfect example of this class of peptides: treatment with quinalizarin resulted in a decreased phosphorylation of both phosphosites, suggesting that probably the two residues are phosphorylated during the same reaction by the kinase and dephosphorylated with the same turnover by the phosphatase. Also this class of peptides can be classified as putative substrates of CK2 *in vivo*.

6. Peptides with phosphosites displaying a *consensus* sequence for more than one kinase and that showed a significant variation of their phosphorylation state after treatment with quinalizarin. An example of this particular case can be seen on Fig. 36, panel 6. Programmed cell death protein 4 contains a phosphopeptide, (R)KRFVsEGDGGR, that in literature is reported to be phosphorylated *in vitro* by Akt (*Palamarchuk et al, Cancer Ref. 2005*). And indeed this peptide displays the *consensus* sequence for Akt, with the basic residues upstream the phosphosite. However, looking at the region downstream the phosphoserine it is clear that also the *consensus* sequence for CK2 is present. Thus, the altered phosphorylation in response to the treatment with Q1 suggests that, under our experimental conditions, the phosphorylation of this serine is catalyzed directly by CK2 or, alternatively, that this phosphorylation event indirectly depends on CK2, probably through a CK2-dependent regulation of Akt activity (*Di Maira et al, Cell Death Differ. 2005*).

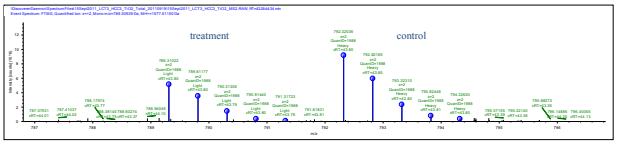
1. Protein not Phosphorylated by CK2

Peptide Sequence	Ratio T/C	Protein
VVVsPTKK	1.044	Nucleolin



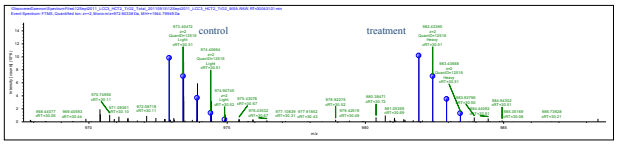
2. Protein Phosphorylated by CK2 (Novel Substrate of CK2)

Peptide Sequence	Ratio T/C	Protein
GSGTAsDDEFENLR	0.390	E3 ubiquitin-protein ligase HUWE1



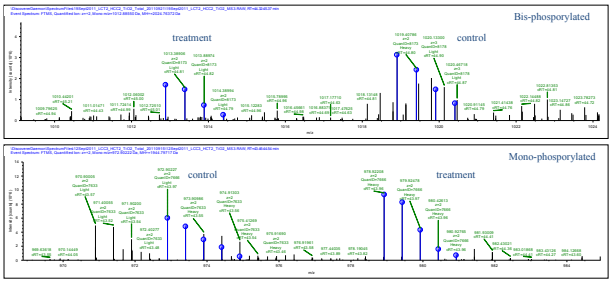
3. Protein Known to be Phosphorylated by CK2

Peptide Sequence	Ratio T/C	Protein
EKEIsDDEAEEEKGEK	0.871	Heat shock protein HSP 90-beta



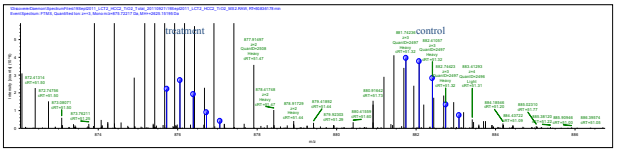
4. Protein with 2 Hierarchical Phosphosites Phosphorylated by CK2

Peoptide Sequence	Ratio T/C	Protein
KETEsEAEDNLDDLEK	1.500	Serine/arginine repetitive matrix protein 1
KEtEsEAEDNLDDLEK	0.500	Serine/arginine repetitive matrix protein 1



5. Protein with Adjacent Phosphoresidues Phosphorylated by CK2

Peptide Sequence	Ratio T/C	Protein
DIEIstEEEKDTGDLKDSSLLK	0.600	La-related protein 7



6. Protein Phosphorylated by Other Kinases: Correct Assignment

Peptide Sequence	Ratio T/C	Protein
(R)KRFVsEGDGGR	0.218	Programmed cell death protein 4

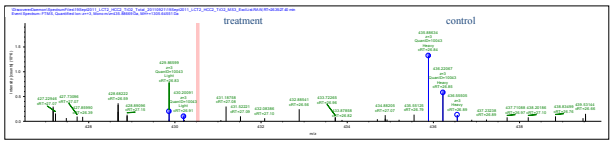


Figure 36 - Examples of classes of phosphopeptides found in our analysis. Phosphorylated residues are marked in red. Ratios Treatment/Control are written in Blue if a significant increased in phosphorylation is measured after treatment with quinalizarin. Ratios Treatment/Control are written in Magenta if a significant decreased phosphorylation is measured after treatment with quinalizarin.

The situation described above shows that the inhibition of CK2 results in a complex alteration of the phosphorylation network within the cell and that significant variations of phosphorylation events often require to be correctly interpreted. As mentioned before, the detailed analysis of the results obtained from our phosphoproteomics study is still ongoing but we hope to successfully compile a list of new putative substrates of CK2 and also to retrieve other interesting information

regarding for example the phosphorylation/dephosphorylation turnover, or the attribution to a specific kinase of promiscuous phosphorylation sites.

Our analysis revealed that about 18% of the identified phosphorylation sites display the classical *consensus* sequence for CK2 (an acidic or phosphorylated residue in position +3 downstream the phosphosite, often supported by other acidic residues in the nearby region). This percentage is in good agreement with what was found by Salvi in a bioinformatics analysis of very large sets of phosphopeptides retrieved from several databases (*Salvi et al, Bioch. Biophys. Acta 2009*).

Very interestingly, a preliminary screening of the quantitative values measured in our phosphoproteomics study for these phosphopeptides reveals that the large majority of phosphorylation events ascribable to CK2 do not show any significant change upon treatment with the inhibitor. These somehow unexpected results find support in a really old hypothesis formulated in the 1980s by Cohen about the physiological meaning of CK2-dependent phosphorylation. After a thorough investigation of several phosphorylation events dependent by CK2, Cohen found that none of these phosphorylations changed the activities of the substrate proteins, while CK2 seemed to act as a primer to trigger subsequent phosphorylations mediated by other kinases (*Woodgett et al, Biochim Biophys Acta 1984*; *Cohen et al, Phil. Trans. R. Soc. Lond 1983*). Moreover, other experiments showed that CK2-dependent phosphosites tend to be fully phosphorylated under every condition, thus indicating a high stability of these phosphorylation events and suggesting that these sites might be poor substrates for protein phosphatases and therefore be characterized by slow phosphorylation/dephosphorylation turnover rate *in vivo* (*Picton et al, FEBS Lett. 1982*; *Agostinis et al, Biochem J. 1987*). Of course these observations were based on a very limited number of substrates of CK2. However, more recently a similar idea was also mentioned in a large-scale study published by Gygi (*Wu et al, Nat. Methods 2011*), where phosphosites surrounded by acidic residues appear to have higher stoichiometry of phosphorylation and higher occupancy with respect to the other phosphosites, therefore supporting the idea that phosphorylations mediated by acidophilic protein kinases are probably dephosphorylated with slow turnover rate. The preliminary results obtained from our phosphoproteomics analysis indicate that indeed this seems to be the case for protein kinase CK2.

3.6.9 Conclusions

Our quantitative proteomics approaches aiming at the identification of substrates and interacting partners of the protein kinase CK2, has led to the acquisition of a very large amount of data that need to be carefully evaluated. All the evidences collected in these studies, both at the protein expression level and at the phosphorylation level, indicate that CK2 plays a major role in the cell by participating to many key biological processes with particular reference to those that regulate the life of proteins. Moreover, our data strongly suggest that phosphorylations mediated by CK2 are particularly stable and have slow dephosphorylation rates.

This last aspect will make difficult to compile a list of new substrates of CK2 (as we expected to do when we designed and performed the experiments), since only few phosphopeptides with a consensus sequence for CK2 seem to be significantly affected by a 3-hour treatment with the inhibitor of this kinase. It will be therefore very interesting to repeat the same study but increasing the time of the treatment with the inhibitor up to 24 hours. This will probably allow to find many more peptides the phosphorylation of which is affected by the inhibition of CK2, thus increasing the number of proteins that can be classified as substrates of CK2 directly in a cellular system.

As widely discussed, the approaches used in this study are not devoid of technical problems that affect the quantification procedures and limit the reliability of the results. Nevertheless all the data presented in this thesis were carefully evaluated and only very solid results were reported. However, for future analogous applications it will be important to take into account all the above-mentioned aspects and find appropriate solutions. For example, to avoid the problem of arginine-to-proline conversion it would be possible to use only isotopically-labeled lysine, and digest proteins with Lys-C peptidase. In this case, the confident identification of phosphopeptides could be more difficult because of the larger size of peptides, but the possibility to analyze phosphopeptides with alternative fragmentation methods such as Electron Transfer Dissociation (ETD) could overcome these problems. An alternative valid strategy could also be the application of a Super-SILAC approach (*Geiger et al, Nature Methods, 2010*) that should allow to avoid the main quantification problems discussed above.

CHAPTER 4

MATERIALS AND METHODS

4.1 Extraction of Cytosol and Nuclei from LAMA84 Cells

LAMA84 cells were harvested (about $3x10^6$ cells) and washed 3 times with PBS 1X and resuspended for 5 min on ice in 1 ml of 20 mM TRIS HCl pH 8, 1% NP-40, complete proteases inhibitors (Roche) 1 tablet/5ml, phosphatases inhibitors cocktail I 1:50.
After dilution with water to double the volume, cells were pipetted 10 times with 23G-needle syringe to break the cellular membranes but not nuclei. Nuclei were separated by centrifugation for 10 min at 4°C and 100xg from cytoplasm and membranes. The supernatant was then collected and ultracentrifuged for 1h at 4°C and 150000xg to obtain the cytosolic fraction (supernatant) and discard cell membranes, while nuclei were lysate with 300 µl of 0.5% Triton X-100, complete proteases inhibitors (Roche) 1 tablet/10ml, phosphatases inhibitors cocktail I 1:100, and centrifuged for 15 min at 4°C and 16000xg to remove nuclear membranes.
Cytosol and nuclei extracts were finally used for immunoprecipitation with antibodies against the C-terminal region of CK2 catalytic subunit. The immunoprecipitation protocol is described in the next section.

4.2 Immunoprecipitation

LAMA84 cells were lysed with a buffer containing 20 mM Tris-HCl pH 7.5, 50 mM NaCl, 1 mM EDTA, 0.5% Triton X-100, 10% Glycerol, complete proteases inhibitors EDTA-free (Roche) 1 tablet/10 ml.
200-800 µg of protein lysates were immunoprecipitated with 0.5-2 µg of a specific antibody produced in house against the alpha subunit of CK2. To allow the antibody-proteins complex formation the incubation was carried on under rotation overnight at 4°C. Control samples were obtained by treating samples in exactly the same way but without the addition of the antibody.
The day after a solution 1/1 (v/v) of sepharose-Protein A (Invitrogen) was added to the samples and left at 4°C under rotation for other 40 min. Proteins bound to the complex Sepharose Protein A-Antibody were isolated by 3 steps of centrifugation (at 4°C for 3 min and 3.5 x g), washing every time with 50 mM Tris-HCl pH 7.5. Immunoprecipitated proteins were finally dissolved in sample buffer (0.6 M Tris-HCl pH 7.8, 2% SDS, 20% glycerol, 5 mM 2-mercaptoethanol, pyronin in traces), boiled for 3 min at 100°C to break immunoglobulines, and loaded onto a 11% polyacrylamide gel for SDS-PAGE analysis. Gel lanes were cut in 10 slices, proteins digested as described in section 4.3 and samples were finally analysed by LC-MS/MS.

4.3 In-gel protein digestion

Gel lanes were divided into slices of approximately 1 cm and each slice was cut in smaller pieces of about 1 mm^2. After destaining and dehydration with several changes of acetonitrile (ACN, Sigma) and 50 mM NH_4HCO_3 (Sigma), gel pieces were reduced with 10 mM dithiothreitol (DTT, Fluka) in 50 mM NH_4HCO_3 for 1h at 56°C, and alkylated with 55 mM iodoacetamide (Sigma) in 50 mM NH_4HCO_3 for 45 min in a dark place at room temperature.

After 4 steps of washing alternatively with 25 mM NH_4HCO_3 and acetonitrile, samples were digested overnight at 37°C with 10-15 µl of 12.5 ng/µl Trypsin (Promega) in 25 mM NH_4HCO_3, and the peptides extracted with 3 changes of 50% ACN, 0.1% formic acid (FA, Fluka).

Samples were dried under vacuum and dissolved in 0.1% FA for the MS analysis.

Digestion with Lys-C enzyme was performed as described above, simply replacing Trypsin with a solution 12.5 ng/µl of Lys-C (Promega) in 25 mM Tris-HCl pH 8.5.

4.4 SILAC on HEK 293 T Cells

The SILAC experiment was performed in cell culture of Human Embryonic Kidney (HEK) 293 T cells, grown in DMEM with 1 mM L-glutamine, 1% penicillin/streptomycin, 10% dialyzed Fetal Bovine Serum, lacking the two standard amino acids Arginine and Lysine.

The experiment was based on 12 parallel cultures, 6 of them contained the normal amino acids Arginine and Lysine (light cells) and the other 6 were supplemented with non-radioactive isotopically-labeled ($^{13}C_6$) form of the same amino acids (heavy cells). The growth of the cells maintained in this medium was not different from the growth in normal medium, as it was shown by cell morphology and doubling time. Using $^{13}C_6$-Arginine and $^{13}C_6$-Lysine (Cambridge Isotope Laboratories), the difference in mass between a peptide containing one of this amino acids and the light one will be equal to 6.02 Da. Cells were maintained in culture for 4 weeks in 6-wells plate to ensure the complete incorporation of the heavy amino acids, and then expanded in 15 ml flasks, for a total of 8 splitting steps. Once confluence was reached (about 10^6 cells for flask) 3 light flasks and 3 heavy flasks were treated for 3 hours with 50 µM Quinalizarin dissolved in dimethyl sulfoxide (DMSO), and the remaining 6 flasks were treated with the same volume of DMSO without inhibitor.

After the treatment cells were washed twice with Phosphate Buffered Saline (PBS) and one time with Washing Buffer (5 mM Tris-HCl, 250 mM sucrose) and harvested using scrapers and 500 µl

ipotonic lysis buffer containing 10 mM Tris-HCl pH 7.9, 10 mM KCl, 0.1mM EDTA, 0.1 mM EGTA, complete proteases inhibitors EDTA-free (Roche) 1 tablet/10 ml, phosphatases inhibitors cocktail I 1:100.

Cells were transferred on 2 ml tubes, freezed and thawed twice, sonicated 3 times and eventually centrifuged for 15 minutes at 14000xg. The insoluble pellet was discarded and the supernatant was stored at -80°C for the further ultracentrifugation to separate soluble proteins from membranes.

The ultracentrifugation of the lysate was performed at 100000xg for 1 hour at 4°C and the pellet obtained was dissolved in 100 µl of lysis buffer containing 50 mM TRIS-HCl pH 7.5, 1% SDS, complete proteases inhibitors EDTA-free (Roche) 1 tablet/10 ml, phosphatases inhibitors cocktail I 1:100.

Finally, both cytosolic and the membrane (pellet) fractions were kept at -80°C until use.

The protein lysate was then quantified using the Micro-Lowry Peterson's Modification Total Protein Kit (Sigma). 30 µg of proteins from heavy cells were mixed with 30 µg of proteins from light cells in order to obtain 6 independent replicates and mixed samples were loaded onto a SDS-PAGE using a 4-12% polyacrylamide precast gel (NuPAGE Bis-Tris Gel, Invitrogen), at 200 V constant for 1 hour. The gel was coloured for 1 h with Colloidal Coomassie Stain (Invitrogen) and destained overnight in water. Gel lanes were then divided into 5 slices and digested with trypsin as described in section 4.3. The samples were eventually dried and dissolved in 0.1% FA for the MS analysis.

4.5 Phosphopeptides Enrichment with TiO_2

Protein samples obtained in the SILAC experiment with HEK 293 T cells were also phosphoenriched to perform a phosphopeptide analysis.

Phosphopeptide enrichment was done with home made affinity chromatography micro-columns prepared by inserting 1.2 mg of TiO_2 into Stage Tips (C18 material, Proxeon). Columns were conditioned twice (50 µl) with acetonitrile and then twice (50 µl) with 80% ACN, 6% TFA (Loading/Washing buffer). 200 µg of total samples were dissolved in 60 µl of Loading buffer and slowly loaded onto the micro-column. The resin was washed with washing buffer four times (50 µl each time) and twice with 0.1% TFA (50 µl each time).

Phoshopeptides were finally eluted with 50 µl of 5% ammonium hydroxide freshly prepared. A last passage of elution from the C18 filter was performed with 50% ACN, 0.1% FA and sample was then dried in speedvac and resuspended in 0.1% FA for MS analysis.

4.6 SILAC on Bovine Interstitial Aortic Valve Cells

Primary aortic BVIC cell lines were obtained from explants of intact aortic bovine valve leaflets and cultured in DMEM containing 4.5 g/L glucose plus 20% Fetal Bovine Serum (FBS), 100 U/mL penicillin, and 100 μg/mL streptomycin. Collected cells were cloned using a limited dilution technique (*Rattazzi et al, Artherioscler. Thromb. Vasc. 2008*).

Two BVIC cell cultures were grown using Dulbecco's Modified Eagle Medium (DMEM) lacking L-lysine and containing 1% L-glutammine, dialysed FBS 10% (Invitrogen), 1% penicillin, and 1% streptomycin. In the first culture (light culture) $^{12}C_6$ Lysine (0.798 mM, Sigma) was added, while in the second one (heavy culture) $^{13}C_6$ Lysine (0.798 mM, Cambridge Isotope Laboratories) was added. Cells were cultured under these conditions for eight splitting passages, then the two cultures were expanded in order to obtain 8 final flasks. Once the cells reached confluence four flasks (two light and two heavy) were treated with LPS (100 ng/ml), two flasks (one light and one heavy) were treated with LPS (100 ng/ml) combined with 50 mM L-arginine, and the remaining two flasks (one light and one heavy) were not treated (CTRL). After 12 days of treatment, cells were harvested scraping with 600 μl of 0.9% NaCl, 1% TRITON X-100. The sample was further treated with 300 μl of lysis buffer containing 50 mM Tris pH 7, 1% SDS and complete proteases inhibitors EDTA-free (Roche) 1 tablet/10 ml.

Cells were transferred in 2 ml tubes, freezed and thawed twice, sonicated 2 times and eventually centrifuged for 15 minutes at 13000 x g. The supernatant was transferred in another tube and both the supernatant and the pellet were stocked at -80° until use.

The four supernatants were then quantified using the Micro-Lowry Peterson's Modification Total Protein Kit (Sigma) and samples were then mixed in equal amount (50 μg per sample) in the following way: heavy untreated proteins with light proteins treated with LPS; heavy proteins treated with LPS with light untreated proteins; heavy proteins treated with LPS with light proteins treated with LPS plus L-arginine; and light proteins treated with LPS with heavy proteins treated with LPS plus L-arginine. Protein pools were run in a homemade 11% polyacrylamide gel at 200 V for 1 hour. The gel was coloured for 1 h with Colloidal Coomassie Stain (Invitrogen) and destained overnight in water. Gel lanes were divided into 7 slices and digested following the protocol described in section 4.3 using Lys-C as proteolitic enzyme.

4.7 iTRAQ on Bovine Interstitial Aortic Valve Cells

Primary aortic BVIC cell lines were obtained as described in the previous section. Selected clonal cells were seeded in 100 mm Petri dishes and brought to confluence. From this point, cells were treated with DMEM, 5% FBS, 100 U/mL penicillin, and 100 μg/mL streptomycin supplemented with LPS (100 ng/mL; *E. coli*), with LPS plus arginine (50 mM), or without LPS as a control. After 12 days of treatment, cells were lysed directly into the flasks using a hypotonic buffer containing 25 mM Triethylammonium bicarbonate (TEAB, Sigma), 0.01% SDS, proteases inhibitors cocktail 1 tablet/10 ml (Roche).

Samples were sonicated and protein quantitation based on Micro-Lowry Peterson's Modification Total Protein Kit (Sigma) was performed for all the samples and 230 μg of proteins for each tube were collected in new tubes and precipitated with six volumes of acetone (-20°C) overnight. After 10 minutes of centrifugation at 13000 rpm, the acetone was removed and protein pellets dissolved in 100 μl of dissolution buffer (0.5 M TEAB, 0.1% SDS) for a final concentration of 2 mg/ml. The complete dissolution was achieved by adding aliquots of 20 μl per time, vortexing and sonicating. After dissolution samples were centrifuged at 13000 rpm for 10 minutes to remove possible particles and the solutions were transferred into new tubes.

A new protein quantitation with the Lowry kit was performed: 50 μg of each sample were used for the iTRAQ labelling and 0.75 pmol of alcohol dehydrogenase (ADH, *S. cerevisiae*) were added at each sample as internal standard to check the digestion and normalize data during the analysis.

2 μl of reducing agent (iTRAQ Reagent Multi-Plex Kit, AB Sciex) were added to each sample and the reaction was carried out for 1 hour at 60°C.

Alkylation of cysteines was then performed adding 1 μl of alkylating agent (iTRAQ Reagent Multi-Plex Kit, AB Sciex), and leaving samples to react for 10 minutes at room temperature.

Sequencing grade modified Trypsin (Promega) was added in 25:1 w/w ratio to the samples, and the digestion was carried out overnight at 37 °C.

Before performing the labeling with the iTRAQ reagents, 1 μl of each sample was cleaned and desalted with ZipTip (Millipore) and tested on the Orbitrap to check the completeness of digestion.

Samples were then labeled following the commercial iTRAQ protocol (AB Sciex) setting up the experiment as follow: Control sample was labeled with 114 tag; LPS treated sample was labeled with 115 tag; LPS + Arginine treated sample was labled with 177 tag.

After the labeling with the iTRAQ tags, 1 μl of each sample was cleaned and desalted again with ZipTip (Millipore) and tested on the Orbitrap, this time to check the completeness of the labeling

procedure. After LC-MS/MS, data were searched with Mascot, using iTRAQ 4plex labeling of N-terminus and Lysine as variable modification, in order to estimate the amount of unlabeled peptides identified. Only if the labeling was satisfactory (i.e. no unlabeled peptides were identified in the run), samples were pooled and subjected to SCX fractionation.
Strong Cation Exchange (SCX) step was performed using a SCX cartridge (AB Sciex) according to the manufacturer instructions. Elution of peptides was carried out in a step-wise mode, by using the following concentrations of KCl: 50, 100, 150, 200, and 350 mM.
Samples were desalted with Sep-Pak C18 Cartridges (Waters), dried under vacuum and finally resuspended for MS analysis in 20 ml of 0.1% FA.

4.8 LC-MS/MS Analysis

Samples from SILAC and iTRAQ experiments were run in an LTQ-Orbitrap XL mass spectrometer (ThermoScientific) coupled with a nano-HPLC Ultimate 3000 (Dionex). Samples were loaded onto a homemade pico-frit column packed with C18 material and separated using a 90 min linear gradient of acetonitrile/0.1% formic acid (from 0% to 50% acetonitrile in 60 min), at a flow rate of 250 nl/min. Capillary voltage was set at around 1.3-1.5 kV and source temperature at 200 °C.
For SILAC experiments, the instrument was operating in a data dependent mode according to the following method: a full scan at 60000 resolution on the Orbitrap, followed by 4 MS/MS scans on the most intense ions in the linear trap.
For iTRAQ experiments, the instrument was operating in a data dependent mode according to the following method: a full scan at 60000 resolution on the Orbitrap was followed by 3 MS/MS scans on the 3 most intense ions acquired with CID fragmentation in the linear trap. On the same ions a further HCD fragmentation was performed with detection on the Orbitrap, to allow the recording of the low molecular weight ions necessary for the quantification procedure.

Samples for label-free quantification experiments were analyzed by LC-MS/MS on a 6520 Q-TOF mass spectrometer (Agilent Technologies) coupled to a chip-based chromatographic interface. A Large Capacity Chip (C18, 150 mm x 75 mm) with an enrichment column (C18, 9 mm, 160 nl volume) was used to separate peptides at a flow rate of 0.5 ml/min. Water/0.1% formic acid and acetonitrile/0.1% formic acid were used as eluents A and B, respectively. The chromatographic separation was achieved with a gradient of eluent B from 3% to 50% in 15 min. Mass spectra were recorded in a data dependent mode: MS/MS spectra of the 3 most intense ions were acquired for each MS scan in the range of 350-2400 Da. Scan speed was set to 4 MS spectra/sec and 3 MS/MS

spectra/sec. Each sample was analyzed in triplicate under the same conditions to increase the robustness of the quantification procedure. Quantification was achieved using the software Progenesis LC-MS.

4.9 Data Analysis

Raw data files from ThermoScientific instruments were directly analyzed with the software Proteome Discoverer 1.3 (ThermoScientific).

For SILAC and iTRAQ experiments appropriate workflows were set in order to identify and quantify the proteins, using Mascot, version 2.2.4 (Matrix Science, London, UK) as search engine.

For SILAC experiments, the following databases were used: IPI_Bovine (version 3.73 2011.11.25, 30403 sequences) for experiments on BVIC cells, IPI_Human (version 3.87 2011.09.29, 91464 sequences) for experiments on HEK293T cells. Enzyme specificity was set to trypsin or Lys-C with 1 missed cleavage. 2 missed cleavages were allowed in case of phosphopeptide analysis. Mass tolerance window was set to 5 ppm for parent mass and to 0.6 Da for fragment ions. Carbamidomethylation of cysteine residues was set as fixed modification and methionine oxidation as variable modification. $^{13}C_6$-Lys only (for BVIC studies) or $^{13}C_6$-Lys and $^{13}C_6$-Arg (for studies on HEK293T cells) were set also as variable modifications. Identical settings were also used with Sequest (2011.05.26 released version, 93289 sequences) when phosphopeptide analysis was conducted. Proteome Discoverer automatically merges the results of Mascot and Sequest search engines.

For iTRAQ experiments, the following parameters were set: IPI_Bovine database (version 3.73 2011.11.25, 30403 sequences); enzyme specificity was set to trypsin with up to 1 missed cleavage. Mass tolerance window was to 10 ppm for parent mass and to 0.6 Da for fragment ions. Methyltiocysteine was set as fixed modification and methionine oxidation as variable modification. iTRAQ 4plex labeling of N-terminus and Lys residues were set as static modifications. Proteome Discoverer automatically takes care of connecting CID and HCD spectra of the same parent ions, thus providing at the same time reliable identification of peptide sequence and quantification of iTRAQ reporter ions.

Proteome Discoverer calculates a False Discovery Rate (FDR) based on the parallel search against randomized databases, or using the Percolator algorithm. Only peptides classified as medium or high confidence (95% and 99% confidence respectively) were considered as positive hits.

For each MS/MS run, quantification of proteins was obtained as a result of the median value of all peptides identified for a specific protein. Only unique peptides were considered for quantification

purposes and (except for phosphoproteomics studies) only proteins identified with at least 2 unique peptides were considered.
In case of technical and biological replicates, the final quantification values were obtained as median value of all replicates. For SILAC experiments with swapping of the labels, contradicting quantification results, due to contaminants or incomplete labelling, were removed from the list of identified proteins.

For label-free experiments, LC-MS/MS raw data files acquired with the Q-TOF mass spectrometer were directly analyzed with Progenesis LC-MS software (NonLinear Dynamic) connected to a Mascot Search engine for the identification of the proteins. Progenesis LC-MS general pipeline is described in section 1.3.3.
In our study, each gel lane was divided in 10 slices, so Progenesis performed 10 different analyses by comparing proteins immunoprecipitated in presence or absence of the antibody. All analyses were eventually merged into a single file containing information about both protein identification and quantification. The resulting list of identified and relatively quantified proteins was filtered in order to keep only proteins identified with at least 2 peptides (with significant Mascot score) and that showed at least a 2-fold change between sample and control.

REFERENCES

Addona TA, Abbatiello SE, Schilling B, Skates SJ, Mani DR, Bunk DM, Spiegelman CH, Zimmerman LJ, Ham AJ, Keshishian H, Hal SC, Allen S, Blackman RK, Borchers CH, Buck C, Cardasis HL, Cusack MP, Dodder NG, Gibson BW, Held JM, Hiltke T, Jackson A, Johansen EB, Kinsinger CR, Li J, Meesri M, Neubert TA, Niles RK, Pulsipher TC, Ransohoff D, Rodriguez H, Rudnick PA, Smith D, Tabb DL, Tegeler TJ, Variyath AM, Vega-Montoto LJ, Wahlander A, Waldemarson S, Wang M, Whiteaker JR, Zhao L, Anderson NL, Fisher SJ, Liebler DC, Paulovich AG, Regnier FE, Tempst P, Carr SA, *Multi-site assesment of the precision and reproducibility of multiple raction monitoring-based measurements of proteins in plasma*, Nat. Biotechnol. 27: 663-641 (2009)

Aggarwal K, Choe LH, Lee KH, *Quantitative analysis of protein expression using amine-specific isobaric tags in Escherichia coli cells expressing rhsA elements*, Proteomics 5: 2297-2308 (2005)

Aggarwal K, Choe LH, Lee KH, *Shotgun proteomics using the iTRAQ isobaric tags*, Briefings in functional genomics and proteomics 5(2): 112-120 (2006)

Agostinis P, Goris J, Pinna LA, Merlevede W, *Regulation of casein kinase 2 by phosphorylation/dephosphorylation*, Biochem. J. 248: 785-789 (1987)

Ahmad KA, Wang G, Unger G, Slaton J, Ahmed K, *Protein kinase CK2- A key suppressor of apoptosis*, Adv. Enzyme Regul. 48: 179-187 (2008)

Ahmed K, Gerber DA, Cochet C, *Joining the cell survival squad: an emergency role for protein kinase CK2*, Trends Cell Biol. 12: 226-230 (2002)

Ahmed K, *Nuclear matrix and protein kinase CK2 signaling*, Crit. Rev. Eukaryot. Gene Expr. 9(3-4): 329-336 (1999)

Aikawa E, Aikawa M, Libby P, Figueiredo JL, Rusanescu G, Iwamoto Y, Fukudo D, Kohler RH, Shi GP, Jaffer FA, Weissleder R, *Arterial and aortic valve calcification abolished by elastolytic cathepsin S deficiency in chronic renal disease*, Circulation 119(13): 1785-1794 (2009)

Akat K, Borggrefe M, Kaden JJ, *Aortic valve calcification: basic science to clinical practice*, Heart 95: 616-623 (2009)

Annesley TM, *Ion suppression in mass spectrometry*, Clinical Chem. 49(7): 1041-1044 (2003)

Apopa PL, He X, Ma Q, *Phosphorylation of Nrf2 in the transcription activation domain by casein kinase 2 (CK2) is critical for the nuclear translocation and transcription activation function of Nrf2 in IMR-32 neuroblastoma cells*, J. Biochem. Mol. Toxicol. 22(1): 63-76 (2008)

Appenzeller-Herzog C, Riemer J, Christensen B, Soerensen ES, Ellgaard L, *A novel disulphide switch mechanism in Ero1alpha balances ER oxidation in human cells*, EMBO J. 27: 2977-2987 (2008)

Arrigoni G, Pagano MA, Sarno S, Cesaro L, James P, Pinna LA, *Mass spectrometry analysis of a protein kinase CK2β subunit interactome isolated from mouse brain by affinity chromatography*, J. Proteome Research 7: 990-1000 (2008)

Bantscheff M, Schirle M, Sweetman G, Rick J, Kuster B, *Quantitative mass spectrometry in proteomics: a critical review*, Anal. Bioanal. Chem. 389(4): 1017-1031 (2007)

Battistutta R, Cozza G, Pierre F, Papinutto E, Lolli G, Sarno S, o'Brien SE, Siddiqui-Jain A, Haddach M, Anderes K, Ryckman DM, Meggio F, Pinna LA, *Unprecedented selectivity and structural determinants of a new class of protein kinase CK2 inhibitors in clinical trials for the treatment of cancer*, Biochemistry 50: 8478-8488 (2011)

Battistutta R, Mazzorana M, Sarno S, Kazimierczuk Z, Zanotti G, Pinna LA, *Inspecting the structure-activity relationship of protein kinase CK2 inhibitors derived from tetrabromo-benzimidazole*, Chem. Biol. 12(11): 1211-1219 (2005)

Battistutta R, *Structural bases of protein kinase CK2 inhibition*, Cell. Mol. Life Sci. 66: 1868-1889 (2009)

Bendall SC, Hughes C, Stewart MH, Doble B, Bhatia M, Lajoie GA, *Prevention of amino acid conversion in SILAC experiments with embryonic stem cells*, Mol. Cell. Proteomics 7: 1587-1597 (2008)

Bertacco E, Millioni R, Arrigoni G, Faggin E, Iop L, Puato M, Pinna LA, Tessari P, Pauletto P, Rattazzi M, *Proteomic analysis of clonal interstitial aortic valve cells acquiring a pro-calcific profile*, J. of Proteome Research 9: 5913-5921 (2010)

Blagoev B, Mann M, *Quantitative proteomics to study mitogen-activated protein kinases*, Methods 40: 243-250 (2006)

Bodenmiller B, Campbell D, Gerrits B, Lam H, Jovanovic M, Picotti P, Schlapbach R, Aebersold R, *PhosphoPep—a database of protein phosphorylation sites in model organism*, Nat. Biotechnol. 26(12): 1339-1340 (2008)

Boersema PJ, Mohammed S, Heck AJ, *Phosphopeptide fragmentation and analysis by mass spectrometry*, J. Mass Spectrometry 44(6): 861-878 (2009)

Boger RH, *Asymmetric dimethylarginine (ADMA): a novel risk marker in cardiovascular medicine and beyond*, Ann. Med. 38(2): 126-136 (2006)

Bojanowski K, Filhol O, Cochet C, Chambaz EM, Larsen AK, *DNA topoisomerase II and casein kinase II associate in a molecular complex that is catalytically active*, J. Biol. Chem. 268: 22920-22926 (1993)

Bonnet H, Filhol O, Truchet I, Brethenou P, Cochet C, Amalric F, Bouche G, *Fibroblast growth factor-2 binds to the regulatory β subunit of CK2 and directly stimulates CK2 activity toward nucleolin*, J. Biol. Chem. 271: 24781-24787 (1996)

Brekken RA, Sage EH, *SPARC, a matricellular protein: at the crossroads of cell-matrix communication*, Matrix Biol. 19:816-827 (2001)

Brookes PS, Yoon Y, Robotham JL, Anders MW, Shey-Shing S, *Calcium, ATP, and ROS: a mitochondrial love-hate triangle*, Am. J. Physiol. Cell Physiol. 287: C817-C833 (2004)

Brown KM, Gilmartin GM, *A mechanism for the regulation of pre-mRNA 3' processing by human cleavage factor Im*, Mol. Cell 12: 1467-1476 (2003)

Burnett G, Kennedy EP, *The enzymatic phosphorylation of proteins*, J. Biol. Chem. 211: 969-980 (1954)

Cabibbo A, Pagani M, Fabbri M, Rocchi M, Farmery MR, Bulleid NJ, Sitia R, *ERO1-L, a human protein that favors disulphide bond formation in the endoplasmic reticulum*, J. Biol. Chem. 275: 4827-4833 (2000)

Caira FC, Stock SR, Gleason TG, McGee EC, Huang J, Bonow RO, Spelsberg TC, McCarthy PM, Rahimtoola SH, Rajamannan NM, *Human degenerative valve disease is associated with up-regulation of low-density lipoprotein receptor-related protein 5 receptor-mediated bone formation*, J. Am. Coll. Cardiol. 47: 1707-1712 (2006)

Canton DA, Litchfield DW, *The shape of thing to come: an emerging role for protein kinase CK2 in the regulation of cell morphology and the cytoskeleton*, Cell Signal. 18(3): 267-275 (2006)

Caverzasio J, *Wnt/LRP5, a new regulation oteoblastic pathway involved in reaching peak bone masses*, Rev. Med. Suisse Romande 124(2): 81-82 (2004)

Chaudhuri J, Chowdhury D, Maitra U, *Distinct functions of eukaryotic translation initiation factors eIF1A and eIF3 in the formation of the 40 S ribosomal preinitiation complex*, J. Biol. Chem. 274: 17975-17980 (1999)

Chelius D, Bondarenko PV, *Quantitative profiling of proteins in complex mixtures using liquid chromatography and mass spectrometry*, Journal of Proteome Research 1(4): 317-323 (2002)

Chen CHW, *Review of a current role of mass spectrometry for proteome research*, Analytica Chimica Acta 624: 16-36 (2008)

Choe L, D'ascenzo M, Relkin NR, Pappin D, Ross P, Williamson B, Guertin S, Pribil P, Lee KH, *8-plex quantitation of changes in cerebrosinal fluid protein expression in subjects undergoing intravenous immunoglobulin treatment for Alzheimer's disease*, Proteomics 7: 3651-3660 (2007)

Cohen P, Goldstone T, *Protein phosphorylation and the control of glycogen metabolism in skeletal muscle [and discussion]*, Phil. Trans. R. Soc. Lond. B 302: 13-25 (1983)

Cohen P, *Protein kinases: the major drug targets of the twenty-first century?*, Nat. Rev. Drug Discov. 1: 309-315 (2002)

Cox J, Mann M, *MaxQuant enables high peptide identification rates, individualized p.p.b.-range mass accuracies and proteome-wide protein quantification*, Nat. Biotechnol. 26: 1367-1372 (2008)

Cozza G, Mazzorana M, Papinutto E, Bain J, Elliott M, Di Maira G, Gianoncelli A, Pagano MA, Sarno S, Ruzzene M, Battistutta R, Meggio F, Moro S, Zagotto G, Pinna LA, *Quinalizarin as a potent, selective and cell-permeable inhibitor of protein kinase CK2*, Biochem. J. 421: 387-395 (2009)

Cuschieri J, Billigren J, Maier RV, *Endotoxin tolerance attenuates LPS-induced TLR4 mobilization to lipid rafts: a condition reversed by PKC activation*, J. Leukoc. Biol. 80: 1289-1297 (2006)

Dayon L, Hainard A, Licker V, Turck N, Kuhn K, Hochstrasser DF, Burkhard PR, Sanchez JC, *Relative quantification of proteins in human cerebrospinal fluids by MS/MS using 6-plex isobaric tags*, Anal. Chem. 80: 2921-2931 (2008)

Demer LL, Tintut Y, *Vascular calcification: pathobiology of a multifaceted disease*, Circulation 117: 2938-2948 (2008)

den Elzen N, Buttery CV, Maddugoda MP, Ren G, Yap AS, *Cadherin adhesion receptors orient the mitotic spindle during symmetric cell division in mammalian epithelia*, Molecular Biology of the Cell 20: 3740-3750 (2009)

Di Maira G, Salvi M, Arrigoni G, Marin O, Sarno S, Brustolon F, Pinna LA, Ruzzene M, *Protein kinase CK2 phosphorylates and upregulates Akt/PKB*, Cell Death Differ. 12(6): 668-677 (2005)

Dinkel H, Chica C, Via A, Gould CM, Jensen LJ, Gibson TJ, Diella F, *Phospho.ELM: a database of phosphorylation sites-update 2011*, Nucl. Acids Res. doi: 10.1093/nar/gkq1104 (2010)

Dong MQ, Venable JD, Au N, Xu T, Park SK, Cociorva D, Johnson JR, Dillin A, Yates III JR, *Quantitative mass spectrometry identifies insulin signaling targets in C. elegans*, Science 317(5838): 660-663 (2007).

Duncan MW, Aebersold R, Caprioli RM, *The pros and cons of peptide-centric proteomics*, Nature Biotechnologies 28: 659-664 (2010)

El-Kady A, Klenova E, *Regulation of the transcription factor, CTCF, by phosphorylation with protein kinase CK2*, FEBS Letters 579(6): 1424-1434 (2005)

Elliott MH, Smith DS, Parker CE, Borchers C, *Current trends in quantitative proteomics*, J. Mass Spectrom 44(12): 1637-1660 (2009)

Eriksen HA, Satta J, Risteli J, Veijola M, Väre P, Soini Y*, Type I and type III collagen synthesis and composition in the valve matrix in aortic valve stenosis*, Atherosclerosis 189(1): 91-98 (2006)

Faust M, Montenarh M, *Subcellular localization of protein kinase CK2. A key to its function?* Cell Tissue Res. 301: 329-340 (2000)

Fenselau C, Yao X, *$^{18}O_2$-labeling in quantitative proteomic strategies: a status report*, J. Proteome Res 8: 2140-2143 (2009)

Feo S, Arcuri D, Piddini E, Passantino R, Giallongo A, *ENO1 gene product binds to the c-myc promoter and acts as a transcriptional repressor: relationship with Myc promoter-binding protein 1 (MBP-1)*, FEBS Lett. 473: 47-52 (2000)

Filhol O, Baudier J, Delphin C, Loue-Mackenbach P, Chambaz EM, Cochet C, *Casein kinase II and the tumor suppressor protein P53 associate in a molecular complex which is negatively regulated upon P53 phosphorylation*, J. Biol. Chem. 267: 20577-20583 (1992)

Filip DA, Radu A, Simionescu M, *Interstitial cells of the heart valves possess characteristics similar to smooth muscle cells*, Circulation Res. 59: 310-320 (1986)

Fleckner J, Zhang M, Valcarcel J, Green MR, *U2AF65 recruits a novel human DEAD box protein required for the U2 snRNP-branchpoint interaction*, Genes Dev. 11: 1864-1872 (1997)

Fraser CS, Lee JY, Mayeur GL, Bushell M, Doudna JA, Hershey JW, *The j-subunit of human translation initiation factor eIF3 is required for the stable binding of eIF3 and its subcomplexes to 40 S ribosomal subunits in vitro*, J. Biol. Chem. 279: 8946-8956 (2004)

Freeman RV, Otto CM, *Spectrum of calcific aortic valve disease: pathogenesis, disease progression, and treatment strategies*, Circulation 111: 3316-3326 (2005)

Gavin AC, Bösche M, Krause R, Grandi P, Marzloch M, Bauer A, Schults J, Rick JM, Michon AM, Cruciat CM, Remor M, Höfert C, Schelder M, Brajenovic M, Ruffner H, Merino A, Klein K, Hudak M, Dickson D, Rudi T, Gnau V, Bauch A, Bastuck S, Huhse B, Leutwein C, Heurtier MA, Copley RR, Edelmann A, Querfurth E, Rybin V, Drewes G, Raida M, Bouwmeester T, Bork P, Seraphin B, Kuster B, Neubauer G, Superti-Furga G, *Functional organization of the yeast proteome by systematic analysis of protein complexes*, Nature 415: 141-147 (2002)

Geiger T, Cox J, Ostasiewicz P, Wisniewski JR, Mann M, *Super-SILAC mix for quantitative proteomics of human tumor tissue*, Nature Methods 7(5): 383-387 (2010)

Gerber DA, Souquere-Besse S, Puvion F, Dubois MF, Bensaude O, Cochet C, *Heat-induced relocalization of protein kinase CK2. Implication of CK2 in the context of cellular stress*, J. Biol. Chem. 275(31): 23919-23926 (2000)

Gerber SA, Rush J, Stemman O, Kirschner MW, Gygi SP, *Absolute quantification of proteins and phosphoproteins from cell lysates by tandem MS*, Proc. Natl. Acad. Sci. U.S.A. 100(12): 6940-6945 (2003)

Gietz RD, Graham KC, Litchfield DW, *Interactions between the subunits of casein kinase II*, J. Biol. Chem 270: 13017-13021 (1995)

Gillette JM, Nielsen-Preiss SM, *The role of annexin 2 in osteoblastic mineralization*, J. Cell Sci. 117(Pt 3): 441-449 (2004)

Gnad F, Ren S, Cox J, Olsen JV, Macek B, Oroshi M, Mann M, *PHOSIDA (phosphorylation site database): management, structural and evolutionary investigation, and prediction of phosphosites*, Genome Biology 8:R250 doi:10.1186/gb-2007-8-11-r250 (2007)

Griffiths JR, Unwin RD, Evans CA, Leech SH, Corfe BM, Whetton AD, *The application of a hypothesis-driven strategy to the sensitive detection and location of acetylated lysine residues*, J. Am. Soc. Mass Spectrom. 18: 1423-1428 (2007)

Gygi SP, Rist B, Gerber SA, Turecek F, Gelb MH, Aebersold R, *Quantitative analysis of complex protein mixtures using isotope-coded affinity tags*, Nature Biotechnology 17: 994-999 (1999)

Hanks SK, Quinn AM, Hunter T, *The protein kinase family: conserved features and deduced phylogeny of the catalytic domains*, Science 241(4861): 42-52 (1988)

Havlis J, Shevchenko A, *Absolute quantification of proteins in solutions and in polyacrylamide gels by mass spectrometry*, Anal. Chem. 76: 3029-3036 (2004)

Helske S, Lindsted KA, Laine M, Mayranpaa M, Werkkala K, Lommi J, Turto H, Kupari M, Kovanen PT, *Induction of loal angiotensin II-producing systems in stenotic aortic valves*, J. Am. Coll. Cardiol. 44: 1859-1866 (2004)

Hornbeck PV, Chabra I, Kornhauser JM, Skrzypek E, Zhang B, *PhosphoSite: a bioinformatics resource dedicated to physiological protein phosphorylation*, Proteomics 4(6): 1551-1561 (2004)

Hruska KA, Mathew S, Saab G, *Bone morphogenetic proteins in vascular calcification*, Circulation Research 97: 105-114 (2005)

Hubbard MJ, Cohen P, *On target with a new mechanism for the regulation of protein phosphorylation*, Trends Biochem. Sci. 18: 172–177 (1993)

Hunter T, *Protein-kinase classification,* Methods in Enzymology 200: 3-37 (1991)

Idelevich A, Rais Y, Monsonego-Ornan E, *Bone Gla protein increases HIF-1alpha-dependent glucose metabolism and induces cartilage and vascular calcification*, Arterioscler. Thromb. Vasc. Biol. 31(9): e55-71 (2011)

Ito S, Tan LJ, Andoh D, Narita T, Seki M, Hirano Y, Narita K, Kuraoka I, Hiraoka Y, Tanaka K, *MMXD, a TFIIH-independent XPD-MMS19 protein complex involved in chromosome segregation*, Mol. Cell 39: 632-640 (2010)

Jiang X, Ye M, Han G, Dong X, Zou H, *Classification filtering strategy to improve the coverage and sensitivity of phosphoproteome analysis*, Anal. Chem. 82(14): 6168-6175 (2010)

Jin Y, Dai MS, Lu SZ, Xu Y, Luo Z, Zhao Y, Lu H, *14-3-3 gamma binds to MDMX that is phosphorylated by UV-activated Chk1, resulting in p53 activation*, EMBO J. 25: 1207-1218 (2006)

Johnson EF, Stewart KD, Woods KW, Giranda VL, Luo Y, *Pharmacological and functional comparison of the Polo-like kinase family: insight into inhibitor and substrate specificity*, Biochemistry 46(33): 9551-9563 (2007)

Johnston IM, Allison SJ, Morton JP, Schramm L, Scott PH, White RJ, *CK2 forms a stable complex with TFIIIB and activates RNA polymerase III transcription in human cells*, Mol. Cell Biol. 22(11): 3757-3768 (2002)

Kaden JJ, Bickelhaupt S, Grobholz R, Haase KK, Sarikoc A, Kilic R, Brueckmann M, Lang S, Zahn I, Vahl C, Hagl S, Dempfle CE, Borggrefe M, *Receptor activator of nuclear factor kappa B ligand and osteoprotegerin regulate aortic valve calcification*, J. Mol. Cell. Cardiol. 36: 57-66 (2004)

Kang NI, Yoon HY, Kim HA, Kim KJ, Han MK, Lee YR, Hwang PH, Soh BY, Shin SJ, Im SY, Lee HK, *Protein kinase CK2/PTEN pathway plays a key role in platelet-activating factor-mediated murine anaphylactic shock*, The J. of Immunology 186(11): 6625-6632 (2011)

Kapp EA, Schütz F, Connolly LM, Chakel JA, Meza JE, Miller CA, Fenyo D, Eng JK, Adkins JN, Omenn GS, Simpson RJ, *An evaluation, comparison, and accurate benchmarking of several publicly available MS/MS search algorithms: sensitivity and specificity analysis*, Proteomics 5(13): 3475-3490 (2005)

Kar A, Fushimi K, Zhou X, Ray P, Shi C, Chen X, Liu Z, Chen S, Wu JY, *RNA helicase p68 (DDX5) regulates tau exon 10 splicing by modulating a stem-loop structure at the 5′ splice site*, Mol. Cell. Biol. 31: 1812-1821 (2011)

Kemp MG, Mason AC, Carreira A, Reardon JT, Haring SJ, Borgstahl GE, Kowalczykowski SC, Sancar A, Wold MS, *An alternative form of replication protein a expressed in normal human tissues supports DNA repair*, J. Biol. Chem. 285: 4788-4797 (2010)

Kerrien S, Aranda B, Breuza L, Bridge A, Broackes-Carter F, Chen C, Duesbury M, Dumousseau M, Feuermann M, Hinz U, Jandrasits C, Jimenez RC, Khadake J, Mahadevan U, Masson P, Pedruzzi I, Pfeiffenberger E, Porras P, Raghunath A, Roechert B, Orchard S, Hermjakob H, *The IntAct molecular interaction database in 2012,* Nucleic Acids Res. 40: D841-D846 (2012)

Kim CS, Seol SK, Song OK, Park JH, Jang SK, *An RNA-binding protein, hnRNP A1, and a scaffold protein, septin 6, facilitate hepatitis C virus replication*, J. Virol. 81: 3852-3865 (2007)

Kim JH, Paek KY, Choi K, Kim TD, Hahm B, Kim KT, Jang SK, *Heterogeneous nuclear ribonucleoprotein C modulates translation of c-myc mRNA in a cell cycle phase-dependent manner*, Mol. Cell. Biol. 23: 708-720 (2003)

Knighton DR, Zheng JH, Ten Eych LF, Ashford VA, Xuong NH, Taylor SS, Sowadsky JM, *Crystal structure of the catalytic subunit of cyclic adenosine monophosphate-dependent protein kinase,* Science 253: 407-414 (1991)

Koch J, Foekens J, Timmermans M, Wirzbach A, Kramer MD, Schaefer BM, *Human VAT-1: a calcium-regulated activation marker of human epithelial cells*, Arch. Dermatol. Res 295: 203-210 (2003)

Köcher T, Pichler P, Schutzbier M, Stingl C, Kaul A, Teucher N, Hasenfuss G, Penninger JM, Mechtler K, *High precision quantitative proteomics using iTRAQ on an LTQ Orbitrap: a new mass spectrometric method combining the benefits of all*, J. Proteome Res. 8(10): 4743-4752 (2009)

Krog M, Ejerblad S, Johansson H, Wilander E, Ågren A, *Hexokinase and adenylate kinase activities in aorta, heart muscle and skeletal muscle from uraemic rats*, Br. J. Exp. Path. 68: 331-341 (1987)

Krüger M, Moser M, Ussar S, Thievessen I, Luber CA, Forner F, Schmidt S, Zanivan S, Fässler R, Mann M, *SILAC mouse for quantitative proteomics uncovers kindlin-3 as an essential factor for red blood cell function*, Cell. 134(2): 353-364 (2008)

Lange V, Picotti P, Domon B, Aebersold R, *Selected reaction monitoring for quantitative proteomics: a tutorial*, Molecular System Biology 4:222 (2008)

Lee HA, Kwon B, Hur GY, Choi SJ, Nahm DH, Park HS, *Isotype and IgG subclass distribution of autoantibody response to alpha-enolase protein in adult patients with severe asthma*, Yonsei Med. J. 49(6): 923-930 (2008)

Lee NK, Sowa H, Hinoi E, Ferron M, Ahn JD, Confavreux C, Dacquin R, Mee PJ, McKee MD, Jung DY, Zhang Z, Kim JK, Mauvais-Jarvis F, Ducy P, Karsenty G, *Endocrine regulation of energy metabolism by the skeleton*, Cell. 130(3): 456-469 (2007)

Leemer S, Pinkse MW, Mohammed S, van Breukelen B, den Hertog J, Slijper M, Heck AJ, *Online automated in vivo zebrafish phosphoproteomics: from large-scale analysis down to a single embryo*, J. of Proteome Res. 7(4): 1555-1564 (2008)

Lehnert S, Götz C, Kartarius S, Schäfer B, Montenarh M, *Protein kinase CK2 interacts with the splicing factor hPrp3p*, Oncogene 27(17): 2390-2400 (2008)

Lindroos M, Kupari M, Valvanne J, Strandberg T, Heikkilä J, Tilvis R, *Factors associated with calcific aortic valve degeneration in the elderly*, European Heart J. 15: 865-870 (1994)

Litchfield DW, Lüscher B, *Casein kinase II in signal transduction and cell cycle regulation*, Mol. Cell. Biochem. 127(128): 187-200 (1993)

Litchfield DW, *Protein kinase CK2: structure, regulation and role in cellular decisions of life and death,* Biochem. J. 369: 1-15 (2003)

Liu J, Guo Q, Chen B, Yu Y, Lu H, Li YY, *Cathepsin B and its interacting proteins, bikunin and TSRC1, correlate with TNF-induced apoptosis of ovarian cancer cells OV-90*, FEBS Lett. 580: 245-250 (2006)

Lössner C, Warnken U, Pscherer A, Schnölzer M, *Preventing arginine-to-proline conversion in a cell-line-indipendent manner during cell cultivation under stable isotope labelling by amino acids in cell culture (SILAC) conditions*, Anal. Biochem. 412(1): 123-125 (2011)

Margolin AA, Ong SE, Schenone M, Gould R, Schreiber SL, Carr SA, Golub TR, *Empirical bayes analysis of quantitative proteomics experiments*, Plos One 4(10): e7454 (2009)

Marin O, Meggio F, Sarno S, Cesaro L, Pagano MA, Pinna LA, *Tyrosine versus serine/threonine phosphorylation by protein kinase casein kinase-2. A study with peptide substrates derived from immunophilin Fpr3*, J. Biol. Chem. 274(41): 29260-29265 (1999)

Marin O, Sarno S, Boschetti M, Pagano MA, Meggio F, Ciminale V, D'agostino DM, Pinna LA, *Unique features of HIV-1 Rev protein phosphorylation by protein kinase CK2 ('casein kinase-2')*, FEBS Letters 481: 63-67 (2000)

Maruyama T, Nara K, Yoshikawa H, Suzuki N, *Txk, a member of the non-receptor tyrosine kinase of the Tec family, forms a complex with poly(ADP-ribose) polymerase 1 and elongation factor 1alpha and regulates interferon-gamma gene transcription in Th1 cells*, Clin. Exp. Immunol. 147: 164-175 (2007)

Masellis-Smith A, Shaw AR, *CD9-regulated adhesion. Anti-CD9 monoclonal antibody induce pre-B cell adhesion to bone marrow fibroblasts through de novo recognition of fibronectin*, J. Immunol. 152: 2768-2777 (1994)

Masson O, Bach AS, Derocq D, Prébois C, Laurent-Matha V, Pattingre S, Liaudet-Coopman E, *Pathophysiological functions of cathepsin D: targeting its catalytic activity versus its protein binding activity?*, Biochimie. 92(11): 1635-

1643 (2010)

McLafferty FW, Horn DM, Breuker K, Ge Y, Lewis MA, Cerda B, Zubarev RA, Carpenter BK, *Electron capture dissociation of gaseous multiply charged ions by Fourier-transform ion cyclotron resonance*, J. Am. Soc. Mass Spectrom. 12(3): 245-249 (2001)

Meggio F, Boldyreff B, Marin O, Pinna LA, Issinger OG, *Role of the β subunit of the casein kinase-2 on the stability and specificity of the recombinant reconstituted holoenzyme*, Eur. J. Biochem. 204: 293-297 (1992)

Meggio F, Donella Deana A, Ruzzane M, Brunati AM, Cesaro L, Guerra B, Meyer T, Mett H, Fabbro D, Furet P, Dobrowolska G, Pinna LA, *Different susceptibility of protein kinases to staurosporine inhibition. Kinetic studies and molecular bases for the resistance of protein kinase CK2*, Eur. J. Biochem. 234: 317-322 (1995)

Meggio F, Pinna LA, *One-thousand-and-one substrates of protein kinase CK2?*, Faseb J. 17: 349-368 (2003)

Meng X, Ao L, Song Y, Babu A, Yang X, Maorong W, Weyant J, Dinarello A, Cleveland JC Jr, Fullerton DA, *Expression of functional Toll-like receptors 2 and 4 in human aortic valve interstitial cells: potential roles in aortic valve inflammation and stenosis*, Am. J. Physiol. Cell. Physiol. 294: C29-C35 (2008)

Mi J, Guo C, Brautigan DL, Larner JM, *Protein phosphatase-1alpha regulates centrosome splitting through Nek2*, Cancer Res. 67: 1082-1089 (2007)

Mikesh LM, Ueberheide B, Chi A, Coon JJ, Syka JE, Shabanowitz J, Hunt DF, *The utility of ETD mass spectrometry in proteomic analysis*, Biochim. Biophys. Acta. 1764(12): 1811-1822 (2006)

Mikula M, Karczmarski J, Dzwonek A, Rubel T, Hennig E, Dadlez M, Bujnicki JM, Bomsztyk K, Ostrowski J, *Casein kinases phosphorylate multiple residues spanning the entire hnRNP K length*, Biochim. Biophys. Acta 1764(2): 299-306 (2006)

Miller JD, Chu Y, Brooks RM, Richenbacher WE, Pena-Silva R, Heistad DD, *Dysregulation of antioxidant mechanisms contributes to increased oxidative stress in calcific aortic valvular stenosis in humans*, J. Am. Coll. Cardiol. 52(10): 843-850 (2008)

Miller JD, Peotta VA, Chu Y, Weiss RM, Zimmerman K, Brooks RM, Heistad DD, *MnSOD protects against COX1-mediated endothelial dysfunction in chronic heart failure*, Am. J. Physiol. Heart Circ. Physiol. 298(5): H1600-1607 (2010)

Millioni R, Tolin S, Puricelli L, Sbrignadello S, Fadini GP, Tessari P, Arrigoni G, *High abundance proteins depletion vs low abundance proteins enrichment: comparison of methods to reduce the plasma proteome complexity*, PLoS One 6(5): e19603 (2011)

Miyata Y, Nishida E, *Evaluating CK2 activity with the antibody specific for the CK2-phosphorylated form of a kinase-targeting cochaperone Cdc37*, Molecular and Cellular Biochemistry 316: 127-134 (2008)

Mohler ER III, Gannon F, Reynolds C, Zimmerman R, Keane MG, Kaplan FS, *Bone formation and inflammation in cardiac valves*, Circulation 103(11): 1522-1528 (2001)

Mohler ER, Sheridan MJ, Nichols R, Harvey WP, Waller BF, *Development and progression of aortic valve stenosis: atherosclerosis risk factors-a causal relationship? A clinical morphologic study*, Clin. Cardiol. 14: 995-999 (1991)

Mollah S, Wertz IE, Phung Q, Arnott D, Dixit VM, Lill JR, *Targeted mass spectrometric strategy for global mapping of ubiquitination on proteins*, Rapid Commun. Mass Spectrom. 21: 3357-3364 (2007)

Monetti M, Nagaraj N, Sharma K, Mann M, *Large-scale phosphosite quantification in tissue by a spike-in SILAC method*, Nat. Methods 8(8): 655-658 (2011)

Monroe ME, Tolic´, Jaitly N, Shaw JL, Adkins JN, Smith RD, *VIPER: an advanced software package to support high-throughput LC-MS peptide identification*, Bioinformatics 23(15): 2021-2023 (2007)

Mortensen P, Gouw JW, Olsen JV, Ong SE, Rigbolt KT, Bunkenborg J, Cox J, Foster LJ, Heck AJ, Blagoev B, Andersen JS, Mann M, *MSQuant, an open source platform for mass spectrometry-based quantitative proteomics*, J. Proteome Res. 9: 393-403 (2010)

Mueller LN, Rinner O, Schmidt A, Letarte S, Bodenmiller B, Brusniak MY, Vitek O, Aebersold R, Muller M, *SuperHirn - a novel tool for high resolution LC-MS-based peptide/protein profiling*, Proteomics 7**:** 3470-3480 (2007)

Niefind K, Guerra B, Ermakowa I, Issinger OG, *Crystal structure of human protein kinase CK2: insights into basic properties of the CK2 holoenzyme*, EMBO J. 20(19): 5320-5331 (2001)

Nishimura RA, *Aortic valve disease,* Circulation 106: 770-772 (2002)

O' Brien KD, *Pathogenesis of calcific aortic valve disease: a disease process comes of age (and a good deal more)*, Arterioscler. Thromb. Vasc. Biol. 26: 1721-1728 (2006)

O'Brien KD, Shavelle DM, Caulfield MT, McDonald TO, Olin-Lewis K, Otto CM, Probstfield JL, *Association of angiotensin-converting enzyme with low-density lipoprotein in aortic valvular lesions and in human plasma*, Circulation 106: 2224-2230 (2002)

Obsilova V, Vecer J, Herman P, Pabianova A, Sulc M, Teisinger J, Boura E, Obsil T, *14-3-3 protein interacts with nuclear localization sequence of forkhead transcription factor FoxO4*, Biochemistry 44: 11608-11617 (2005)

Olsen JV, Blagoev B, Gnad F, Macek B, Kumar C, Mortensen P, Mann M, *Global, in vivo, and site-specific phosphorylation dynamics in signaling networks*, Cell 127: 635-648 (2006)

Olsson M, Rosenqvist M, Nilsson J, *Expression of HLA-DR antigen and smooth muscle cell differentiation markers by valvular fibroblasts in degenerative aortic stenosis*, J. Am. Coll. Cardiol. 24: 1664-1671 (1994)

Olsson M, Thyberg J, Nilsson J, *Presence of oxidized low density lipoprotein in nonrheumatic stenotic aortic valves*, Arterioscler. Thromb. Vasc. Biol. 19:1218-1222 (1999)

Ong SE, Blagoev B, Kratchmarova I, Kristensen DB, Steen H, Pandey A, Mann M, *Stable isotope labeling by amino acids in cell culture, SILAC, as a simple and accurate approach to expression proteomics*, Mol. Cell. Proteomics 1(5): 376-386 (2002)

Ong SE, Mann M, *A pratical recipe for stable isotope labelling by amino acids in cell culture (SILAC)*, Nature Protocols 1(6): 2650-2660 (2006)

Ong SE, Mann M, *Mass spectrometry-based proteomics turns quantitative*, Nat. Chem. Biol. 1(5): 252-262 (2005)

Oppermann FS, Gnad F, Olsen JV, Hornberger R, Greff Z, Kéri G, Mann M, Daub H, *Large-scale proteomics analysis of the human kinome*, Mol. Cell. Proteomics 8(7): 1751-1764 (2009)

Otto CM, Burwash IG, Legget ME, Munt BI, Fujioka M, Healy NL, Kraft CD, Miyake-Hull CY, Schwaegler RG, *Prospective study of asymptomatic valvular aortic stenosis. Clinical, echocardiographic, and exercise predictors of outcome*, Circulation 95: 2262-2270 (1997)

Otto CM, *Calcific aortic stenosis-time to look more closely at the valve*, N. Eng. J. Med. 359: 1395-1398 (2008)

Otto CM, Kuusisto J, Reichenbach DD, Gown AM, O'Brien KD, *Characteriaztion of the early lesion of "degenerative" valvular aortic stenosis. Histological and immunohistochemical studies*, Circulation 90: 844-853 (1994)

Padmanabha R, Chen-Wu JLP, Hanna DE, Glover CVC, *Isolation, sequencing and disruption of the yeast CKA2 gene: Casein Kinase II is essential for viability in Saccharomyces cerevisiae*, Mol. Cell. Biol. 10: 4089-4099 (1990)

Pagano MA, Bain J, Kazimierczuk Z, Sarno S, Ruzzene M, Di Maira G, Elliott M, Orzeszko A, Cozza G, Meggio F, Pinna LA, *The selectivity of inhibitors of protein kinase CK2: an update*, Biochem. J. 415: 353-365 (2008)

Palamarchuk A, Efanov A, Maximov V, Aqeilan RI, Croce CM, Pekarsky Y, *Akt phosphorylates and regulates Pdcd4 tumor suppressor protein*, Cancer Res. 65(24): 11282-11286 (2005)

Park SK, Liao L, Kim JY, Yates 3rd JR, *A computational approach to correct arginine-to-proline conversion in quantitative proteomics*, Nat. Methods 6: 184-185 (2009)

Paul S, Dansithong W, Kim D, Rossi J, Webster NJ, Comai L, Reddy S, *Interaction of muscleblind, CUG-BP1 and hnRNP H proteins in DM1-associated aberrant IR splicing*, EMBO J. 25: 4271-4283 (2006)

Petritis BO, Qian WJ, Camp DG, 2nd, Smith RD, *A simple procedure for effective quenching of trypsin activity and prevention of ^{18}O-labeling back-exchange*, J. Proteome Res 8(5): 2157-2163 (2009)

Petsko G, Ringe D, *Struttura e funzione delle proteine* , Zanichelli (2006)

Picton C, Woodgett J, Hemmings B, Cohen P, *Phosphorylation of site 5 by glycogen synthase kinase-5 (casein kinase-II) is a prerequisite for phosphorylation of sites 3 by glycogen synthase kinase-3*, FEBS Lett. 150(1): 191-196 (1982)

Pierre F, Chua PC, O'Brien SE, Siddiqui-Jain A, Bourbon P, Haddach M, Michaux J, Nagasawa J, Schwaebe MK, Stefan E, Vialettes A, Whitten JP, Chen TK, Darjania L, Stansfield R, Anderes K, Bliesath J, Drygin D, Ho C, Omori M, Proffitt C, Streiner N, Trent K, Rice WG, Ryckman DM, *Discovery and SAR of 5-(3-Chlorophenylamino)benzol[c][2,6]-naphthyridine-8-carboxylic Acid (CX-4945), the first clinical stage inhibitor of protein kinase CK2 for the treatment of cancer*, J. Med. Chem. 54:635-654 (2011)

Pinna LA, *A historical view of protein-kinase CK2*. Cellular & Molecular Biology Research, 40(5-6): 383-390 (1994)

Pinna LA, *Casein kinase 2: an 'eminence grise' in cellular regulation?*, Biochim. Biophys. Acta., 1054(3): 267-284

(1990)

Pinna LA, Meggio F, *Protein kinase CK2 ("casein kinase-2") and its implication in cell division and proliferation*, Progress in Cell Cycle Research 3: 77-97 (1997)

Pinna LA, *Protein kinase CK2: a challenge to canons*, J. of Cell Science 115: 3873-3878 (2002)

Pinna LA, *The raison d'être of constitutvely active protein kinases: the lesson of CK2*, Acc. Chem. Res. 36: 378-384 (2003)

Pluemsampant S, Safronova OS, Nakahama K, Morita I*, Protein kinase CK2 is a key activator of histone deacetylase in hypoxia-associated tumors*, Int. J. Cancer 122(2): 333-341 (2008)

Pohle K, Mäffert R, Ropers D, Moshage W, Stilianakis N, DanielWG, Achenbach S, *Progression of aortic valve calcification: association with coronary atherosclerosis and cardiovascular risk factors*, Circulaton 104: 1927-1932 (2001)

Poletto G, Vilardell J, Marin O, Pagano MA, Cozza G, Sarno S, Falqués, Itarte E, Pinna LA, Meggio F, *The regulatory β subunit of protein kinase CK2 contributes to the recognition of the substrate consensus sequence. A study with an eIF2β-derived peptide*, Biochemistry 47: 8317-8325 (2008)

Porteus B, Kocharunchitt C, Nilsson RE, Ross T, Bowman JP, *Utility of gel-free, label-free shotgun proteomics approaches to invedstigate microorganism*, Appl. Microbiol. Biotechnol. 90: 407-416 (2011)

Qian WJ, Monroe ME, Liu T, Jacobs JM, Anderson GA, Shen Y, Moore RJ, Anderson DJ, Zhang R, Calvano SE, Lowry SF, Xiao W, Moldawer LL, Davis RW, Tompkins RG, Camp DG, Smith RD, *Quantitative proteome analysis of human plasma following in vivo lipopolysaccharide administration using $^{16}O/^{18}O$ labeling and the accurate mass and time tag approach*, Mol. Cell. Proteomics, 4(5): 700-709 (2005)

Rattazzi M, Iop L, Faggin E, Bertacco E, Zoppellaro G, Baesso I, Puato M, Torregrossa G, Fadini GP, Agostini C, Gerosa G, Sartore S, Pauletto P, *Clones of interstitial cells from bovine aortic valve exhibit different calcifying potential when exposed to endotoxin and phosphate*, Artherioscler. Thromb. Vasc. Biol. 28: 2165-2172 (2008)

Rodríguez-Ulloa A, Ramos Y, Gil J, Perera Y, Castellanos-Serra L, García Y, Betancourt L, Besada V, González LJ, Fernández-de-Cossio J, Sanchez A, Serrano JM, Farina H, Alonso DF, Acevedo BE, Padrón G, Musacchio A, Perea SE, *Proteomic profile regulated by the anticancer peptide CIGB-300 in non-small cell lung cancer (NSCLC) cells*, J. Proteome Res. 9: 5473-5483 (2010)

Ross PL, Huang YN, archese JN, Williamson B, Parker K, Hattan S, Khainovski N, Pillai S, Dey S, Daniels S, Purkayastha S, Juhasz P, Martin S, Bartlet-Jones M, He F, Jacobson A, Pappin DJ, *Multiplexed protein quantitation in Saccharomyces cerevisiae using amine-reactive isobaric tagging reagents*, Mol. Cell. Proteomics 3: 1154-1169 (2004)

Salvi M, Sarno S, Cesaro L, Nakamura H, Pinna LA, *Extraordinary pleiotropy of protein kinase CK2 revealed by weblogo phosphoproteome analysis*, Biochimica et Biophysica Acta 1793: 847-859 (2009)

Sarno S, De Moliner E, Ruzzene M, Pagano MA, Battistutta R, Bain J, Fabbro D, Schoepfer J, Elliott M, Furet P, Meggio F, Zanotti G, Pinna LA, *Biochemical and three-dimensional-structural study of the specific inhibition of protein kinase CK2 by [5-oxo-5,6-dihydroindolo-(1,2-a)quinazolin-7-yl]acetic acid (IQA)*, Biochem J. 374: 639-646 (2003)

Sarno S, Ghisellini P, Pinna LA, *Unique activation mechanism of protein kinase CK2*, J. of Biol. Chem. 277(25): 22509-22514 (2002)

Sarno S, Marin O, Boschetti M, Pagano MA, Meggio F, Pinna LA, *Cooperative modulation of protein kinase CK2 by separate domains of its regulatory β-subunit*, Biochemistry 39: 12324-12329 (2000)

Sarno S, Papinutto E, Franchin C, Bain J, Elliott M, Meggio F, Kazimierczuk Z, Orzeszko A, Zanotti G, Battistutta R, Pinna LA, *ATP site-directed inhibitors of protein kinase CK2: an update*, Curr. Top Med. Chem. 11(11): 1340-1351 (2011)

Sarno S, Vaglio P, Meggio F, Issinger OG, Pinna LA, *Protein kinase CK2 mutants defective in substrate recognition*, The Journal of Biological Chemistry 271(18): 10595-10601 (1996)

Schenkel AR, Dufour EM, Chew TW, Sorg E, Muller WA, *The murine CD99-related molecule CD99-like 2 (CD99L2) is an adhesion molecule involved in the inflammatory response*, Cell Commun. Adhes. 14: 227-237 (2007)

Schmidt A, Karas M, Dülcks T, *Effect of different solution flow rates on analyte ion signals in nano-ESI MS, or: when does ESI turn into nano-ESI?*, J. of the American Society for Mass Spectrometry 14(5): 492-500 (2003)

Sedoris KC, Thomas SD, Miller DM, *Hypoxia induces differential translation of enolase/MBP-1*, BMC Cancer 10: 157 (2010)

Seldin DC, Landesman-Bollag E, Farago M, Currier N, Lou D, Dominquez I, *CK2 as a positive regulator of Wnt signalling and tumorigenesis*, Mol. Cell Biochem. 274(1-2): 63-67 (2005)

Siddiqui-Jain A, Drygin D, Streiner N, Chua PC, Pierre F, O'Brien SE, Bliesath J, Omori M, Huser N, Ho C, Proffitt C, Schwaebe MK, Ryckman DM, Rice WG, Anderes K, *CX-4945, an orally bioavailable selective inhibitor of protein kinase CK2, inhibits prosurvival and angiogenic signalling and exhibits antitumor efficacy*, Cancer Res 70: 10288-10298 (2010)

Siuti N, Kelleher NL, *Decoding protein modifications using top-down mass spectrometry*, Nature Methods 4(10): 817-821 (2007)

Srivatsa SS, Harrity PJ, Maercklein PB, Kleppe L, Veinot J, Edwards WD, Johnson CM, Fitzpatrick LA, *Increased cellular expression of matrix proteins that regulate mineralization is associated with calcification of native human and porcine xenograft bioprosthetic heart valves*, J. Clin. Invest. 99: 996-1009 (1997)

Steinfeld R, Reinhardt K, Schreiber K, Hillebrand M, Kraetzner R, Bruck W, Saftig P, Gartner J, *Cathepsin D deficiency is associated with a human neurodegenerative disorder*, Am. J. Hum. Genet. 78(6): 988-998 (2006)

Stewart BF, Siscovick D, Lind BK, Gardin JM, Gottdiener JS, Smith VE, Kitzman DW, Otto CM, *Clinical factors associated with calcific aortic valve disease. Cardiovascular Health Study*, J. Am. Coll. Cardiol. 29: 630-634 (1997)

Stewart II, Thomson T, Figeys D, *^{18}O labeling: a tool for proteomics*, Rapid Commun. Mass Spectrom. 15: 2456-2465 (2001)

The Uniprot Consortium, *Ongoing and future developments at the Universal Protein* Resource, Nucleic Acids Res. 39: D214-D219 (2011)

Thompson A, Schäfer J, Kuhn K, Kienle S, Schwarz J, Schimidt G, Neumann T, Hamon C, *Tandem mass tags: a novel quantification strategy for comparative analysis of complex protein mixtures by MS/MS*, Anal. Chem. 75: 1895-1904 (2003)

Tisdale EJ, *Glyceraldehyde-3-phosphate dehydrogenase is phosphorylated by protein kinase Ciota /lambda and plays a role in microtubule dynamics in the early secretory pathway*, J. Biol. Chem. 277: 3334-3341 (2002)

Tosoni K, Costa A, Sarno S, D'Alessandro S, Sparla F, Pinna LA, Zottini M, Ruzzene M, *The p23 co-chaperone protein is a novel substrate of CK2 in Arabidopsis*, Molecular and Cellular Biochemistry 356: 245-254 (2011)

Towler DA, *Oxidation, inflammation, and aortic valve calcification peroxide paves an osteogenic path*, J. Am. Coll. Cardiol. 52(10): 851-854 (2008)

Trembley JH, Tatsumi S, Sakashita E, Loyer P, Slaughter CA, Suzuki H, Endo H, Kidd VJ, Mayeda A, *Activation of Pre-mRNA splicing by human RNPS1 is regulated by CK2 phosphorylation*, Mol. Cell Biol. 25(4): 1446-1457 (2005)

Ulintz PJ, Yocum AK, Bodenmiller B, Aebersold R, Andrews PC, Nesvizhskii AI, *Comparison of MS^2-only, MSA, and MS^2/MS^3 methodologies for phosphopeptide identification*, J. Proteome Res. 8(2): 887-899 (2009)

Unwin RD, Griffiths JR, Leverentz MK, Grallert A, Hagan IM, Whetton AD, *Multiple reaction monitoring to identify sites of protein phosphorylation with high sensitivity*, Mol. Cell Proteomics 4: 1134-1144 (2005)

Voyksner RD, Lee H, *Investigating the use of octupole ion guide for ion storage and high-pass mass filtering to improve the quantitative performance of electrospray ion trap mass spectrometry*, Rapid Communication in Mass Spectrometry 13(14): 1427-1437 (1999)

Walton KW, Williamson N, Johnson AG, *The pathogenesis of artherosclerosis of the mitral and aortic valves*, J. Pathol. 101: 205-220 (1970)

Wang G, Unger G, Ahmad KA, Slaton JW, Ahmed K, *Downregulation of CK2 induces apoptosis in cancer cells-a potential approach to cancer therapy*, Mol. Cell. Biochem. 274: 77-84 (2005)

Washburn MP, Wolters D, Yates III JR, *Large-scale analysis of the yeast proteome by multidimensional protein identification technology*, *Nature Biotechnology* 19(3): 242-247 (2001)

Watson KE, Parhami F, Shim V, Demer LL, *Fibronectin and collagen I matrixes promote calcification of vascular cells in vitro, whereas collagen IV matrix is inhibitory*, Arterios. Thromb. Vasc. Biol. 18: 1964-1971 (1998)

Weidensdorfer D, Stoehr N, Baude A, Lederer M, Koehn M, Schierhorn A, Buchmeier S, Wahle E, Huettelmaiery S, *Control of c-myc mRNA stability by IGF2BP1-associated cytoplasmic RNPs*, RNA 15: 104-115 (2009)

Williamson BL, Marchese J, Morrice NA, *Automated identification and quantification of protein phosphorylation sites by LC/MS on a hybrid triple quadrupole linear ion trap mass spectrometer*, Mol. Cell Proteomics 5: 337-346 (2006)

Woodgett JR, Cohen P, *Multisite phosphorylation of glycogen synthase. Molecular basis for the substrate specificity of*

glycogen synthase kinase-3 and casein kinase II (glycogen synthase kinase-5), Biochim. Biophys. Acta. 788(3): 339-347 (1984)

Wu R, Haas W, Dephore N, Huttlin EL, Zhai B, Sowa ME, Gygi SP, *A large-scale method to measure absolute protein phosphorylation stoichiometries*, Nat. Methods 8(8): 677-683 (2011)

Xie F, Liu T, Q WJ, Petyuk VA, Smith RD, *Liquid chromatography-mass spectrometry-based quantitative proteomics*, The Journal of Biological Chemistry 286(29): 25443-25449 (2011)

Yanagawa T, Funasaka T, Tsutsumi S, Raz T, Tanaka N, Raz A, *Differential regulation of phosphoglucose isomerase/autocrine motility factor activities by protein kinase CK2 phosphorylation*, j. Biol. Chem. 280(11): 10419-10426 (2005)

Yao X, Afonso C, Fenselau C, *Dissection of proteolytic ^{18}O labeling: endoprotease-catalyzed ^{16}O-to-^{18}O exchange of truncated peptide substrates*, J. Proteome Res. 2: 147-152 (2003)

Yao Y, Watson AD, Ji S, Bostrom K, *Heat shock protein 70 enhances vascular bone morphogenetic protein-4 signaling by binding matrix Gla protein*, Circ. Res. 105(6): 575-584 (2009)

Yue G, Shi G, Azaro MA, Yang Qm Hu G, Luo M, Yin K, Nagele RG, Fine DH, Yang JM, Li H, *Lipopolysaccharide (LPS) potentiates hydrogen peroxide toxicity in T98G astrocytoma cells by suppression of anti-oxidative and growth factor gene expression*, BMC Genomics 9:608-620 (2008)

Zhang C, Vilk G, Canton DA, Litchfield DW, *Phosphorylation regulates the stability of the regulatory CK2beta subunit*, Oncogene 21: 3754-3764 (2002)

Zhang R, Regnier FE, *Minimizing resolution of isotopically coded peptides in comparative proteomics*, J. Proteome Res 1: 139-147 (2002)

Zhang R, Sioma CS, Wang S, Regnier FE, *Fractionation of isotopically labelled peptides in quantitative proteomics*, Anal. Chem. 73(21): 5142-5149 (2001)

Zhou JY, Schepmoes AA, Zhang X, Moore RJ, Monroe ME, Lee JH, Camp DG, Smith RD, Qian WJ, *Improved LC-MS/MS spectral counting by recovering low scoring spectra matched to confidently identified peptide sequences*, J. Proteome Res. 9(11): 5698-5704 (2010)

Zhu W, Smith JW, Huang CM, *Mass spectrometry-based label-free quantitative proteomics*, J. of Biomedicine and Biotechnology doi:10.1155/2010/840518 (2010))

Protein Data Bank (PDB) References

1JAM – Battistutta R, De Moliner E, Sarno S, Zanotti G, Pinna LA, *Crystal structure of apo-form of Z. Mays CK2 protein kinase alpha subunit*, DOI:10.2210/pdb1jam/pdb deposited on 2001-05-31

1JWH – Niefind K, Guerra B, Ermakowa I, Issinger OG, *Crystal structure of human protein kinase CK2 holoenzyme*, DOI:10.2210/pdb1jwh/pdb deposited on 2001-09-04

3FL5 – Mazzorana M, Franchin C, Battistutta R, *Protein kinase CK2 in complex with the inhibitor Quinalizarin*, DOI:10.2210/pdb3fl5/pdb deposited on 2008-12-18

APPENDIX

TABLE 1: List of Proteins Identified and quantified in SILAC BVIC experiment.

ACCESSION	DESCRIPTION	LPS/CTRL AVERAGE	LPS+R/LPS AVERAGE
P61603	10 kDa heat shock protein, mitochondrial OS=Bos taurus GN=HSPE1 PE=2 SV=2 - [CH10_BOVIN]	0,921	0,894
P68250	14-3-3 protein beta/alpha OS=Bos taurus GN=YWHAB PE=1 SV=2 - [1433B_BOVIN]	0,996	1,022
P62261	14-3-3 protein epsilon OS=Bos taurus GN=YWHAE PE=2 SV=1 - [1433E_BOVIN]	0,971	1,042
Q3SZI4	14-3-3 protein theta OS=Bos taurus GN=YWHAQ PE=2 SV=1 - [1433T_BOVIN]	1,015	1,167
P63103	14-3-3 protein zeta/delta OS=Bos taurus GN=YWHAZ PE=1 SV=1 - [1433Z_BOVIN]	1,035	0,863
Q865A2	2'-5'-oligoadenylate synthetase OS=Bos taurus GN=OAS1 PE=2 SV=1 - [Q865A2_BOVIN]	1,185	0,751
Q3T030	26S protease regulatory subunit 6B OS=Bos taurus GN=PSMC4 PE=2 SV=1 - [PRS6B_BOVIN]	1,038	1,175
Q2KIW6	26S protease regulatory subunit S10B OS=Bos taurus GN=PSMC6 PE=2 SV=1 - [PRS10_BOVIN]	1,049	1,112
Q2HJD7	3-hydroxyisobutyrate dehydrogenase, mitochondrial OS=Bos taurus GN=HIBADH PE=2 SV=1 - [3HIDH_BOVIN]	0,924	0,988
Q3T0R7	3-ketoacyl-CoA thiolase, mitochondrial OS=Bos taurus GN=ACAA2 PE=2 SV=1 - [THIM_BOVIN]	0,956	0,950
Q56JX8	40S ribosomal protein S13 OS=Bos taurus GN=RPS13 PE=2 SV=3 - [RS13_BOVIN]	0,929	0,900
Q56K10	40S ribosomal protein S15 OS=Bos taurus GN=RPS15 PE=2 SV=3 - [RS15_BOVIN]	1,025	0,902
Q76I82	40S ribosomal protein S15a OS=Bos taurus GN=RPS15A PE=2 SV=1 - [RS15A_BOVIN]	1,045	0,886
Q3T0X6	40S ribosomal protein S16 OS=Bos taurus GN=RPS16 PE=2 SV=3 - [RS16_BOVIN]	0,967	0,869
A5PK63	40S ribosomal protein S17 OS=Bos taurus GN=RPS17 PE=2 SV=1 - [RS17_BOVIN]	0,973	0,904
Q32PD5	40S ribosomal protein S19 OS=Bos taurus GN=RPS19 PE=2 SV=3 - [RS19_BOVIN]	0,977	0,909
O18789	40S ribosomal protein S2 OS=Bos taurus GN=RPS2 PE=2 SV=2 - [RS2_BOVIN]	0,960	0,906
Q3T199	40S ribosomal protein S23 OS=Bos taurus GN=RPS23 PE=2 SV=1 - [RS23_BOVIN]	1,026	0,888
Q56JU9	40S ribosomal protein S24 OS=Bos taurus GN=RPS24 PE=2 SV=2 - [RS24_BOVIN]	0,980	0,897
Q56JX5	40S ribosomal protein S25 OS=Bos taurus GN=RPS25 PE=2 SV=1 - [RS25_BOVIN]	0,958	0,889
Q3T0B7	40S ribosomal protein S27-like OS=Bos taurus GN=RPS27L PE=3 SV=3 - [RS27L_BOVIN]	1,139	1,059
Q3T169	40S ribosomal protein S3 OS=Bos taurus GN=RPS3 PE=2 SV=1 - [RS3_BOVIN]	1,117	1,020
Q56JV9	40S ribosomal protein S3a OS=Bos taurus GN=RPS3A PE=2 SV=3 - [RS3A_BOVIN]	0,970	0,921
P79103	40S ribosomal protein S4 OS=Bos taurus GN=RPS4 PE=2 SV=3 - [RS4_BOVIN]	0,965	0,918
Q5E995	40S ribosomal protein S6 OS=Bos taurus GN=RPS6 PE=2 SV=1 - [RS6_BOVIN]	0,866	0,899
A6H769	40S ribosomal protein S7 OS=Bos taurus GN=RPS7 PE=2 SV=1 - [RS7_BOVIN]	0,951	0,900
Q5E958	40S ribosomal protein S8 OS=Bos taurus GN=RPS8 PE=2 SV=3 - [RS8_BOVIN]	0,953	0,959
A6QLG5	40S ribosomal protein S9 OS=Bos taurus GN=RPS9 PE=2 SV=1 - [RS9_BOVIN]	0,936	0,911
Q05927	5'-nucleotidase OS=Bos taurus GN=NT5E PE=1 SV=2 - [5NTD_BOVIN]	**1,880**	1,083
Q3ZCI4	6-phosphogluconate dehydrogenase, decarboxylating OS=Bos taurus GN=PGD PE=2 SV=2 - [Q3ZCI4_BOVIN]	0,964	0,891

P31081	60 kDa heat shock protein, mitochondrial OS=Bos taurus GN=HSPD1 PE=1 SV=2 - [CH60_BOVIN]	0,867	0,837
Q95140	60S acidic ribosomal protein P0 OS=Bos taurus GN=RPLP0 PE=2 SV=3 - [RLA0_BOVIN]	0,960	0,910
P42899	60S acidic ribosomal protein P2 OS=Bos taurus GN=RPLP2 PE=3 SV=1 - [RLA2_BOVIN]	0,795	1,093
Q9XSI3	60S ribosomal protein L10 OS=Bos taurus GN=RPL10 PE=2 SV=4 - [RL10_BOVIN]	1,022	0,973
Q5E9E6	60S ribosomal protein L10a OS=Bos taurus GN=RPL10A PE=2 SV=3 - [RL10A_BOVIN]	0,970	0,921
Q3T087	60S ribosomal protein L11 OS=Bos taurus GN=RPL11 PE=2 SV=3 - [RL11_BOVIN]	1,015	0,901
Q56JZ1	60S ribosomal protein L13 OS=Bos taurus GN=RPL13 PE=2 SV=3 - [RL13_BOVIN]	0,972	0,917
Q3T057	60S ribosomal protein L23 OS=Bos taurus GN=RPL23 PE=2 SV=2 - [RL23_BOVIN]	1,003	0,911
Q24JY1	60S ribosomal protein L23a OS=Bos taurus GN=RPL23A PE=2 SV=1 - [RL23A_BOVIN]	0,940	0,958
Q56K03	60S ribosomal protein L27a OS=Bos taurus GN=RPL27A PE=2 SV=3 - [RL27A_BOVIN]	0,973	0,900
Q58DW3	60S ribosomal protein L29 OS=Bos taurus GN=RPL29 PE=2 SV=3 - [RL29_BOVIN]	0,944	0,892
Q56JX3	60S ribosomal protein L31 OS=Bos taurus GN=RPL31 PE=2 SV=1 - [RL31_BOVIN]	0,991	0,907
Q3MHM7	60S ribosomal protein L35 OS=Bos taurus GN=RPL35 PE=2 SV=3 - [RL35_BOVIN]	0,981	0,887
Q3T171	60S ribosomal protein L36 OS=Bos taurus GN=RPL36 PE=3 SV=3 - [RL36_BOVIN]	0,950	0,901
Q58DW0	60S ribosomal protein L4 OS=Bos taurus GN=RPL4 PE=2 SV=3 - [RL4_BOVIN]	0,929	0,943
Q58DW5	60S ribosomal protein L5 OS=Bos taurus GN=RPL5 PE=2 SV=3 - [RL5_BOVIN]	1,048	1,044
Q58DQ3	60S ribosomal protein L6 OS=Bos taurus GN=RPL6 PE=2 SV=3 - [RL6_BOVIN]	0,940	1,058
Q58DT1	60S ribosomal protein L7 OS=Bos taurus GN=RPL7 PE=2 SV=1 - [RL7_BOVIN]	0,981	0,912
Q2TBQ5	60S ribosomal protein L7a OS=Bos taurus GN=RPL7A PE=2 SV=3 - [RL7A_BOVIN]	0,990	0,955
Q3T0S6	60S ribosomal protein L8 OS=Bos taurus GN=RPL8 PE=2 SV=3 - [RL8_BOVIN]	0,948	0,921
Q3SYR7	60S ribosomal protein L9 OS=Bos taurus GN=RPL9 PE=2 SV=1 - [RL9_BOVIN]	0,959	0,912
Q0VCX2	78 kDa glucose-regulated protein OS=Bos taurus GN=HSPA5 PE=2 SV=1 - [GRP78_BOVIN]	0,761	0,978
Q29RZ0	Acetyl-CoA acetyltransferase, mitochondrial OS=Bos taurus GN=ACAT1 PE=2 SV=1 - [THIL_BOVIN]	1,368	1,038
Q17QB3	Acid ceramidase OS=Bos taurus GN=ASAH1 PE=2 SV=3 - [ASAH1_BOVIN]	**3,332**	0,695
Q3SZC6	Acidic leucine-rich nuclear phosphoprotein 32 family member B OS=Bos taurus GN=ANP32B PE=2 SV=1 - [AN32B_BOVIN]	**1,680**	0,917
A7MB62	Actin-related protein 2 OS=Bos taurus GN=ACTR2 PE=1 SV=1 - [ARP2_BOVIN]	0,879	1,077
Q3MHR7	Actin-related protein 2/3 complex subunit 2 OS=Bos taurus GN=ARPC2 PE=1 SV=1 - [ARPC2_BOVIN]	0,868	1,176
Q3T035	Actin-related protein 2/3 complex subunit 3 OS=Bos taurus GN=ARPC3 PE=1 SV=3 - [ARPC3_BOVIN]	0,826	1,020
Q3SYX9	Actin-related protein 2/3 complex subunit 5 OS=Bos taurus GN=ARPC5 PE=1 SV=3 - [ARPC5_BOVIN]	0,909	1,133
P60712	Actin, cytoplasmic 1 OS=Bos taurus GN=ACTB PE=1 SV=1 - [ACTB_BOVIN]	**0,665**	1,376
Q56JW4	Adenine phosphoribosyltransferase OS=Bos taurus GN=APRT PE=2 SV=1 - [APT_BOVIN]	**1,554**	0,898
Q3MHL4	Adenosylhomocysteinase OS=Bos taurus GN=AHCY PE=2 SV=3 - [SAHH_BOVIN]	1,069	1,101
P08166	Adenylate kinase 2, mitochondrial OS=Bos taurus GN=AK2 PE=1 SV=2 - [KAD2_BOVIN]	**1,637**	**0,649**
A6QLB7	Adenylyl cyclase-associated protein OS=Bos taurus GN=CAP1 PE=2 SV=1 - [A6QLB7_BOVIN]	0,735	1,047
P84080	ADP-ribosylation factor 1 OS=Bos taurus GN=ARF1 PE=1 SV=2 - [ARF1_BOVIN]	1,006	0,988

Q3SZF2	ADP-ribosylation factor 4 OS=Bos taurus GN=ARF4 PE=2 SV=3 - [ARF4_BOVIN]	0,998	1,042
Q2TBW6	ADP-ribosylation factor-like protein 3 OS=Bos taurus GN=ARL3 PE=2 SV=1 - [ARL3_BOVIN]	0,911	1,054
Q3ZCJ2	Alcohol dehydrogenase [NADP+] OS=Bos taurus GN=AKR1A1 PE=2 SV=1 - [AK1A1_BOVIN]	**1,578**	1,015
P20000	Aldehyde dehydrogenase, mitochondrial OS=Bos taurus GN=ALDH2 PE=1 SV=2 - [ALDH2_BOVIN]	**1,653**	0,917
P09487	Alkaline phosphatase, tissue-nonspecific isozyme OS=Bos taurus GN=ALPL PE=1 SV=2 - [PPBT_BOVIN]	**9,593**	1,143
Q3B7N2	Alpha-actinin-1 OS=Bos taurus GN=ACTN1 PE=2 SV=1 - [ACTN1_BOVIN]	**0,514**	**2,296**
A5D7D1	Alpha-actinin-4 OS=Bos taurus GN=ACTN4 PE=2 SV=1 - [ACTN4_BOVIN]	1,101	1,382
Q9XSJ4	Alpha-enolase OS=Bos taurus GN=ENO1 PE=1 SV=4 - [ENOA_BOVIN]	1,359	1,087
A1L5B6	Annexin 5 OS=Bos taurus GN=ANXA5 PE=2 SV=1 - [A1L5B6_BOVIN]	0,678	1,064
P46193	Annexin A1 OS=Bos taurus GN=ANXA1 PE=2 SV=2 - [ANXA1_BOVIN]	1,476	0,956
P27214	Annexin A11 OS=Bos taurus GN=ANXA11 PE=1 SV=1 - [ANX11_BOVIN]	1,124	0,765
P04272	Annexin A2 OS=Bos taurus GN=ANXA2 PE=1 SV=2 - [ANXA2_BOVIN]	**1,663**	1,078
P13214	Annexin A4 OS=Bos taurus GN=ANXA4 PE=1 SV=2 - [ANXA4_BOVIN]	1,063	0,991
P79134	Annexin A6 OS=Bos taurus GN=ANXA6 PE=1 SV=2 - [ANXA6_BOVIN]	0,951	1,139
Q95L54	Annexin A8 OS=Bos taurus GN=ANXA8 PE=2 SV=1 - [ANXA8_BOVIN]	**1,502**	**0,620**
Q2YDH6	AP-3 complex subunit sigma-1 OS=Bos taurus GN=AP3S1 PE=2 SV=1 - [AP3S1_BOVIN]	0,849	1,289
Q6QRN6	Apolipoprotein A-I-binding protein OS=Bos taurus GN=APOA1BP PE=2 SV=1 - [AIBP_BOVIN]	0,805	1,133
P12344	Aspartate aminotransferase, mitochondrial OS=Bos taurus GN=GOT2 PE=1 SV=2 - [AATM_BOVIN]	0,911	0,860
Q1RMN0	Aspartylglucosaminidase OS=Bos taurus GN=AGA PE=2 SV=1 - [Q1RMN0_BOVIN]	1,170	0,776
P19483	ATP synthase subunit alpha, mitochondrial OS=Bos taurus GN=ATP5A1 PE=1 SV=1 - [ATPA_BOVIN]	1,424	0,971
P13619	ATP synthase subunit b, mitochondrial OS=Bos taurus GN=ATP5F1 PE=1 SV=2 - [AT5F1_BOVIN]	1,255	1,041
P00829	ATP synthase subunit beta, mitochondrial OS=Bos taurus GN=ATP5B PE=1 SV=2 - [ATPB_BOVIN]	1,325	1,001
P13620	ATP synthase subunit d, mitochondrial OS=Bos taurus GN=ATP5H PE=1 SV=2 - [ATP5H_BOVIN]	1,405	1,009
Q00361	ATP synthase subunit e, mitochondrial OS=Bos taurus GN=ATP5I PE=1 SV=2 - [ATP5I_BOVIN]	1,467	0,974
Q28852	ATP synthase subunit g, mitochondrial OS=Bos taurus GN=ATP5L PE=1 SV=3 - [ATP5L_BOVIN]	1,351	0,984
P05631	ATP synthase subunit gamma, mitochondrial OS=Bos taurus GN=ATP5C1 PE=1 SV=3 - [ATPG_BOVIN]	1,458	0,965
Q0IIK5	ATP-dependent RNA helicase DDX1 OS=Bos taurus GN=DDX1 PE=2 SV=1 - [DDX1_BOVIN]	0,904	1,250
Q5E9F1	B-cell receptor-associated protein 31 OS=Bos taurus GN=BCAP31 PE=2 SV=1 - [Q5E9F1_BOVIN]	0,894	0,718
P61283	Barrier-to-autointegration factor OS=Bos taurus GN=BANF1 PE=3 SV=1 - [BAF_BOVIN]	1,155	1,159
A5D7U5	Beta-galactosidase OS=Bos taurus GN=GLB1 PE=2 SV=2 - [A5D7U5_BOVIN]	1,210	0,906
Q0VCK0	Bifunctional purine biosynthesis protein PURH OS=Bos taurus GN=ATIC PE=2 SV=1 - [PUR9_BOVIN]	0,893	1,037
P80724	Brain acid soluble protein 1 OS=Bos taurus GN=BASP1 PE=1 SV=3 - [BASP1_BOVIN]	0,938	1,288
Q3B7N0	Cadherin-13 OS=Bos taurus GN=CDH13 PE=2 SV=1 - [CAD13_BOVIN]	**0,563**	1,264
A5PJZ1	Calcium-binding mitochondrial carrier protein SCaMC-1 OS=Bos taurus GN=SLC25A24 PE=2 SV=1 - [SCMC1_BOVIN]	1,362	0,843
Q3T168	Calcyclin-binding protein OS=Bos taurus GN=CACYBP PE=2 SV=1 - [CYBP_BOVIN]	0,790	0,794

Q27971	Calpain-2 catalytic subunit OS=Bos taurus GN=CAPN2 PE=2 SV=2 - [CAN2_BOVIN]	0,668	1,125
A7LFP6	Calpastatin OS=Bos mutus grunniens GN=CAST PE=2 SV=1 - [A7LFP6_BOSMU]	1,109	0,892
Q32L92	Calponin-3 OS=Bos taurus GN=CNN3 PE=2 SV=1 - [CNN3_BOVIN]	1,253	**1,903**
A5D7J6	CALR protein OS=Bos taurus GN=CALR PE=2 SV=1 - [A5D7J6_BOVIN]	1,484	1,050
Q9TSB1	Calvasculin (Fragments) OS=Bos taurus PE=1 SV=1 - [Q9TSB1_BOVIN]	1,494	1,038
A7Z066	Canx protein OS=Bos taurus GN=canx PE=2 SV=1 - [A7Z066_BOVIN]	1,174	0,819
P68399	Casein kinase II subunit alpha OS=Bos taurus GN=CSNK2A1 PE=1 SV=1 - [CSK21_BOVIN]	1,161	0,889
Q3MHM6	Catenin alpha-1 OS=Bos taurus GN=CTNNA1 PE=2 SV=1 - [CTNA1_BOVIN]	1,417	0,770
Q9BGU5	Cathepsin D (Fragment) OS=Bos taurus GN=cat-D PE=2 SV=1 - [Q9BGU5_BOVIN]	**2,999**	0,705
Q3T0I2	Cathepsin H OS=Bos taurus GN=CTSH PE=2 SV=1 - [CATH_BOVIN]	0,848	0,870
P79132	Caveolin-1 OS=Bos taurus GN=CAV1 PE=2 SV=1 - [CAV1_BOVIN]	0,893	1,300
Q66WT7	Caveolin-2 OS=Bos taurus GN=CAV2 PE=1 SV=1 - [CAV2_BOVIN]	0,964	1,225
A6H7C4	CBX3 protein OS=Bos taurus GN=CBX3 PE=2 SV=1 - [A6H7C4_BOVIN]	**1,998**	1,182
P30932	CD9 antigen OS=Bos taurus GN=CD9 PE=2 SV=2 - [CD9_BOVIN]	1,231	0,837
B6VAP7	CDC42 protein OS=Bos taurus GN=CDC42 PE=2 SV=1 - [B6VAP7_BOVIN]	1,025	1,208
Q05B71	CDGSH iron sulfur domain-containing protein 2 OS=Bos taurus GN=CISD2 PE=2 SV=1 - [CISD2_BOVIN]	0,721	0,752
Q5EAB4	Chitinase domain-containing protein 1 OS=Bos taurus GN=CHID1 PE=2 SV=1 - [CHID1_BOVIN]	0,731	0,873
Q5E9B7	Chloride intracellular channel protein 1 OS=Bos taurus GN=CLIC1 PE=2 SV=3 - [CLIC1_BOVIN]	1,288	1,042
Q9XSA7	Chloride intracellular channel protein 4 OS=Bos taurus GN=CLIC4 PE=2 SV=3 - [CLIC4_BOVIN]	0,818	1,125
Q08E32	CHMP4B protein OS=Bos taurus GN=CHMP4B PE=2 SV=2 - [Q08E32_BOVIN]	1,188	1,081
Q3T0S7	Chromosome 14 open reading frame 166 ortholog OS=Bos taurus GN=C10H14ORF166 PE=2 SV=1 - [Q3T0S7_BOVIN]	0,964	1,354
Q29RK1	Citrate synthase, mitochondrial OS=Bos taurus GN=CS PE=2 SV=1 - [CISY_BOVIN]	0,928	0,860
Q3ZCA2	Cleavage and polyadenylation specificity factor subunit 5 OS=Bos taurus GN=NUDT21 PE=2 SV=1 - [CPSF5_BOVIN]	**1,681**	0,922
Q2HJ57	Coactosin-like protein OS=Bos taurus GN=COTL1 PE=2 SV=3 - [COTL1_BOVIN]	**3,569**	1,256
P53620	Coatomer subunit gamma OS=Bos taurus GN=COPG PE=1 SV=1 - [COPG_BOVIN]	0,936	1,075
Q5E9F7	Cofilin-1 OS=Bos taurus GN=CFL1 PE=2 SV=3 - [COF1_BOVIN]	0,913	0,995
Q148F1	Cofilin-2 OS=Bos taurus GN=CFL2 PE=2 SV=1 - [COF2_BOVIN]	**0,500**	**1,605**
P02453	Collagen alpha-1(I) chain OS=Bos taurus GN=COL1A1 PE=1 SV=3 - [CO1A1_BOVIN]	0,755	**0,482**
P02465	Collagen alpha-2(I) chain OS=Bos taurus GN=COL1A2 PE=1 SV=2 - [CO1A2_BOVIN]	0,829	**0,632**
Q08E14	Collagen, type III, alpha 1 OS=Bos taurus GN=COL3A1 PE=2 SV=1 - [Q08E14_BOVIN]	1,074	0,671
Q1RMR3	Cortactin OS=Bos taurus GN=CTTN PE=2 SV=1 - [Q1RMR3_BOVIN]	0,791	1,094
O02751	Craniofacial development protein 2 OS=Bos taurus GN=CFDP2 PE=1 SV=2 - [CFDP2_BOVIN]	**1,885**	1,196
A7MBJ5	Cullin-associated NEDD8-dissociated protein 1 OS=Bos taurus GN=CAND1 PE=2 SV=1 - [CAND1_BOVIN]	0,976	1,092
Q3MHY1	Cysteine and glycine-rich protein 1 OS=Bos taurus GN=CSRP1 PE=2 SV=3 - [CSRP1_BOVIN]	0,861	**1,854**
Q32LE9	Cysteine and glycine-rich protein 2 OS=Bos taurus GN=CSRP2 PE=2 SV=3 - [CSRP2_BOVIN]	1,240	**1,983**

Q0VFX8	Cysteine-rich protein 2 OS=Bos taurus GN=CRIP2 PE=2 SV=1 - [CRIP2_BOVIN]	0,708	1,008
P23004	Cytochrome b-c1 complex subunit 2, mitochondrial OS=Bos taurus GN=UQCRC2 PE=1 SV=2 - [QCR2_BOVIN]	1,205	1,020
P00129	Cytochrome b-c1 complex subunit 7 OS=Bos taurus GN=UQCRB PE=1 SV=3 - [QCR7_BOVIN]	1,181	0,951
P00423	Cytochrome c oxidase subunit 4 isoform 1, mitochondrial OS=Bos taurus GN=COX4I1 PE=1 SV=1 - [COX41_BOVIN]	1,107	1,028
P00428	Cytochrome c oxidase subunit 5B, mitochondrial OS=Bos taurus GN=COX5B PE=1 SV=2 - [COX5B_BOVIN]	1,090	1,021
P04038	Cytochrome c oxidase subunit 6C OS=Bos taurus GN=COX6C PE=1 SV=2 - [COX6C_BOVIN]	1,134	0,984
Q2TBX1	Cytokine induced protein 29 kDa OS=Bos taurus GN=CIP29 PE=2 SV=1 - [Q2TBX1_BOVIN]	1,211	1,023
P00727	Cytosol aminopeptidase OS=Bos taurus GN=LAP3 PE=1 SV=3 - [AMPL_BOVIN]	**2,104**	0,685
B7XA48	Cytosolic aspartate aminotransferase OS=Bubalus bubalis GN=ast1 PE=2 SV=1 - [B7XA48_BUBBU]	1,419	1,165
Q3ZC84	Cytosolic non-specific dipeptidase OS=Bos taurus GN=CNDP2 PE=2 SV=1 - [CNDP2_BOVIN]	1,060	1,252
Q5EAD2	D-3-phosphoglycerate dehydrogenase OS=Bos taurus GN=PHGDH PE=2 SV=3 - [SERA_BOVIN]	**0,477**	0,979
C0L633	Ddx3y (Fragment) OS=Bos taurus PE=2 SV=1 - [C0L633_BOVIN]	0,856	0,964
Q5E9D5	Destrin OS=Bos taurus GN=DSTN PE=2 SV=3 - [DEST_BOVIN]	**0,452**	1,382
Q3T0Z7	Dihydropteridine reductase OS=Bos taurus GN=QDPR PE=2 SV=1 - [DHPR_BOVIN]	0,942	0,950
O02675	Dihydropyrimidinase-related protein 2 OS=Bos taurus GN=DPYSL2 PE=2 SV=1 - [DPYL2_BOVIN]	0,677	0,913
P23196	DNA-(apurinic or apyrimidinic site) lyase OS=Bos taurus GN=APEX1 PE=1 SV=2 - [APEX1_BOVIN]	1,298	1,224
A7MBI5	DPYSL3 protein OS=Bos taurus GN=DPYSL3 PE=2 SV=1 - [A7MBI5_BOVIN]	**0,642**	1,121
Q5E9R3	EH domain-containing protein 1 OS=Bos taurus GN=EHD1 PE=2 SV=1 - [EHD1_BOVIN]	0,966	1,419
Q2KJ47	EH-domain containing 2 OS=Bos taurus GN=EHD2 PE=2 SV=1 - [Q2KJ47_BOVIN]	0,938	1,286
A7E394	EIF6 protein (Fragment) OS=Bos taurus GN=EIF6 PE=2 SV=1 - [A7E394_BOVIN]	1,231	1,027
Q2KJE4	Electron transfer flavoprotein subunit alpha, mitochondrial OS=Bos taurus GN=ETFA PE=2 SV=1 - [ETFA_BOVIN]	1,264	0,899
P68103	Elongation factor 1-alpha 1 OS=Bos taurus GN=EEF1A1 PE=2 SV=1 - [EF1A1_BOVIN]	0,721	1,072
Q3SYU2	Elongation factor 2 OS=Bos taurus GN=EEF2 PE=2 SV=3 - [EF2_BOVIN]	0,920	0,910
B8Y9S9	Embryo-specific fibronectin 1 transcript variant OS=Bos taurus PE=2 SV=1 - [B8Y9S9_BOVIN]	0,853	0,767
P81623	Endoplasmic reticulum resident protein 29 OS=Bos taurus GN=ERP29 PE=1 SV=2 - [ERP29_BOVIN]	0,792	0,678
Q3T0L2	Endoplasmic reticulum resident protein 44 OS=Bos taurus GN=ERP44 PE=2 SV=1 - [ERP44_BOVIN]	0,674	0,718
Q95M18	Endoplasmin OS=Bos taurus GN=HSP90B1 PE=2 SV=1 - [ENPL_BOVIN]	1,330	0,931
A5PJN2	ERO1-like protein alpha OS=Bos taurus GN=ERO1L PE=2 SV=1 - [ERO1A_BOVIN]	**1,507**	**0,486**
Q3T0U3	Es1 protein OS=Bos taurus GN=ES1 PE=2 SV=1 - [Q3T0U3_BOVIN]	0,794	0,914
Q1JPA2	Eukaryotic translation elongation factor 1 gamma (Fragment) OS=Bos taurus GN=EEF1G PE=2 SV=1 - [Q1JPA2_BOVIN]	0,999	1,187
Q3MHP6	Eukaryotic translation initiation factor 4B OS=Bos taurus GN=EIF4B PE=2 SV=1 - [Q3MHP6_BOVIN]	0,823	**1,803**
Q6EWQ7	Eukaryotic translation initiation factor 5A-1 OS=Bos taurus GN=EIF5A PE=2 SV=3 - [IF5A1_BOVIN]	0,882	0,886
P31976	Ezrin OS=Bos taurus GN=EZR PE=1 SV=2 - [EZRI_BOVIN]	**0,524**	0,822
A4FUA8	F-actin-capping protein subunit alpha-1 OS=Bos taurus GN=CAPZA1 PE=2 SV=1 - [CAZA1_BOVIN]	1,001	1,014
P79136	F-actin-capping protein subunit beta OS=Bos taurus GN=CAPZB PE=1 SV=1 - [CAPZB_BOVIN]	0,948	1,036

P55052	Fatty acid-binding protein, epidermal OS=Bos taurus GN=FABP5 PE=1 SV=4 - [FABP5_BOVIN]	**0,475**	1,020
Q8WMQ6	Filamin A (Fragment) OS=Bos taurus PE=2 SV=1 - [Q8WMQ6_BOVIN]	**0,534**	**1,885**
Q95LH5	Filamin-1 (Fragment) OS=Bos taurus PE=2 SV=1 - [Q95LH5_BOVIN]	**0,573**	**2,003**
A6QPJ6	FKBP7 protein OS=Bos taurus GN=FKBP7 PE=2 SV=1 - [A6QPJ6_BOVIN]	0,990	1,030
P52556	Flavin reductase OS=Bos taurus GN=BLVRB PE=1 SV=2 - [BLVRB_BOVIN]	1,439	0,754
A6QLL8	Fructose-bisphosphate aldolase OS=Bos taurus GN=ALDOA PE=2 SV=1 - [A6QLL8_BOVIN]	1,390	1,027
Q148D3	Fumarate hydratase OS=Bos taurus GN=FH PE=2 SV=1 - [Q148D3_BOVIN]	0,721	1,121
A5D7A2	GARS protein OS=Bos taurus GN=GARS PE=2 SV=1 - [A5D7A2_BOVIN]	**0,385**	1,278
Q3SX14	Gelsolin OS=Bos taurus GN=GSN PE=2 SV=1 - [GELS_BOVIN]	0,909	1,138
P41541	General vesicular transport factor p115 OS=Bos taurus GN=USO1 PE=1 SV=1 - [USO1_BOVIN]	0,967	1,065
Q0VCH9	GLI pathogenesis-related 2 OS=Bos taurus GN=GLIPR2 PE=2 SV=1 - [Q0VCH9_BOVIN]	0,745	0,886
A4FUZ1	GLO1 protein OS=Bos taurus GN=GLO1 PE=2 SV=1 - [A4FUZ1_BOVIN]	0,987	0,801
A7MBI6	GLOD4 protein OS=Bos taurus GN=GLOD4 PE=2 SV=1 - [A7MBI6_BOVIN]	0,816	0,873
Q08DV2	Glucosamine-phosphate N-acetyltransferase 1 OS=Bos taurus GN=GNPNAT1 PE=2 SV=1 - [Q08DV2_BOVIN]	0,905	1,383
Q3ZBD7	Glucose-6-phosphate isomerase OS=Bos taurus GN=GPI PE=2 SV=3 - [G6PI_BOVIN]	1,054	1,066
Q28034	Glucosidase 2 subunit beta OS=Bos taurus GN=PRKCSH PE=2 SV=1 - [GLU2B_BOVIN]	1,076	0,992
Q2KHZ8	Glucosylceramidase OS=Bos taurus GN=GBA PE=2 SV=1 - [GLCM_BOVIN]	**1,908**	1,141
P00366	Glutamate dehydrogenase 1, mitochondrial OS=Bos taurus GN=GLUD1 PE=1 SV=2 - [DHE3_BOVIN]	1,349	**0,617**
Q58DA7	Glutaredoxin-3 OS=Bos taurus GN=GLRX3 PE=2 SV=1 - [GLRX3_BOVIN]	0,951	1,034
Q5E9G0	Glutathione S-transferase A4 OS=Bos taurus GN=GSTA4 PE=2 SV=1 - [GSTA4_BOVIN]	0,749	1,002
Q9N0V4	Glutathione S-transferase Mu 1 OS=Bos taurus GN=GSTM1 PE=1 SV=3 - [GSTM1_BOVIN]	**0,593**	0,925
Q0VCE1	Glutathione S-transferase omega 1 OS=Bos taurus GN=GSTO1 PE=2 SV=1 - [Q0VCE1_BOVIN]	0,908	1,002
P28801	Glutathione S-transferase P OS=Bos taurus GN=GSTP1 PE=1 SV=2 - [GSTP1_BOVIN]	0,807	1,135
Q0VCM4	Glycogen phosphorylase, liver form OS=Bos taurus GN=PYGL PE=2 SV=1 - [PYGL_BOVIN]	1,132	0,944
Q3T054	GTP-binding nuclear protein Ran OS=Bos taurus GN=RAN PE=2 SV=3 - [RAN_BOVIN]	1,222	0,914
Q3T0D7	GTP-binding protein SAR1a OS=Bos taurus GN=SAR1A PE=2 SV=1 - [SAR1A_BOVIN]	0,782	0,734
P08760	GTP:AMP phosphotransferase mitochondrial OS=Bos taurus GN=AK3 PE=1 SV=3 - [KAD3_BOVIN]	0,845	1,108
Q3SZ00	HADHA protein OS=Bos taurus GN=HADHA PE=2 SV=1 - [Q3SZ00_BOVIN]	**2,054**	0,686
Q08E18	HDGF protein OS=Bos taurus GN=HDGF PE=2 SV=1 - [Q08E18_BOVIN]	1,165	1,235
Q2YDE6	HDLBP protein (Fragment) OS=Bos taurus GN=HDLBP PE=2 SV=1 - [Q2YDE6_BOVIN]	1,050	1,058
Q27965	Heat shock 70 kDa protein 1B OS=Bos taurus GN=HSPA1B PE=2 SV=1 - [HS71B_BOVIN]	**2,049**	**1,515**
A7E3S8	Heat shock 70kD protein binding protein OS=Bos taurus GN=ST13 PE=2 SV=1 - [A7E3S8_BOVIN]	0,866	0,956
P19120	Heat shock cognate 71 kDa protein OS=Bos taurus GN=HSPA8 PE=1 SV=2 - [HSP7C_BOVIN]	0,889	1,119
Q76LV2	Heat shock protein HSP 90-alpha OS=Bos taurus GN=HSP90AA1 PE=2 SV=3 - [HS90A_BOVIN]	1,004	0,839
Q76LV1	Heat shock protein HSP 90-beta OS=Bos taurus GN=HSP90AB1 PE=2 SV=3 - [HS90B_BOVIN]	1,229	1,041

Q148C9	Heme-binding protein 1 OS=Bos taurus GN=HEBP1 PE=2 SV=1 - [HEBP1_BOVIN]	1,129	0,895
P01966	Hemoglobin subunit alpha OS=Bos taurus GN=HBA PE=1 SV=2 - [HBA_BOVIN]	**24,653**	**0,039**
D3YC70	Heparin-binding protein (Fragment) OS=Bos gaurus frontalis PE=2 SV=1 - [D3YC70_BOSGF]	0,984	0,958
Q08DU9	Heterochromatin protein 1-binding protein 3 OS=Bos taurus GN=HP1BP3 PE=2 SV=1 - [HP1B3_BOVIN]	1,334	1,163
Q3ZC44	Heterogeneous nuclear ribonucleoprotein A/B OS=Bos taurus GN=HNRNPAB PE=2 SV=1 - [Q3ZC44_BOVIN]	1,161	1,163
P09867	Heterogeneous nuclear ribonucleoprotein A1 OS=Bos taurus GN=HNRNPA1 PE=1 SV=2 - [ROA1_BOVIN]	**1,602**	0,744
A5D9H5	Heterogeneous nuclear ribonucleoprotein D OS=Bos taurus GN=HNRPD PE=2 SV=1 - [A5D9H5_BOVIN]	**1,557**	0,911
Q3T0D0	Heterogeneous nuclear ribonucleoprotein K OS=Bos taurus GN=HNRNPK PE=2 SV=1 - [HNRPK_BOVIN]	1,410	0,904
Q2HJ60	Heterogeneous nuclear ribonucleoproteins A2/B1 OS=Bos taurus GN=HNRNPA2B1 PE=2 SV=1 - [ROA2_BOVIN]	**1,849**	1,074
Q5W5U3	Hexokinase 1 OS=Bos taurus GN=HK1 PE=2 SV=1 - [Q5W5U3_BOVIN]	**2,357**	0,934
P10103	High mobility group protein B1 OS=Bos taurus GN=HMGB1 PE=1 SV=3 - [HMGB1_BOVIN]	**1,755**	0,951
A7MAZ5	HIST1H1D protein OS=Bos taurus GN=HIST1H1D PE=2 SV=1 - [A7MAZ5_BOVIN]	**1,895**	0,801
P62958	Histidine triad nucleotide-binding protein 1 OS=Bos taurus GN=HINT1 PE=1 SV=2 - [HINT1_BOVIN]	0,904	1,146
Q0IIJ2	Histone H1.0 OS=Bos taurus GN=H1F0 PE=2 SV=3 - [H10_BOVIN]	**1,678**	0,979
P02253	Histone H1.1 (Fragment) OS=Bos taurus PE=1 SV=1 - [H11_BOVIN]	**2,255**	0,842
Q17QG8	Histone H2A OS=Bos taurus GN=H2AFX PE=2 SV=1 - [Q17QG8_BOVIN]	**1,763**	0,862
Q2HJ65	Histone H2A OS=Bos taurus GN=H2AFY PE=2 SV=1 - [Q2HJ65_BOVIN]	1,439	1,298
A4IFU5	Histone H2A OS=Bos taurus GN=HIST3H2A PE=2 SV=1 - [A4IFU5_BOVIN]	**1,562**	0,850
P0C0S9	Histone H2A type 1 OS=Bos taurus PE=1 SV=2 - [H2A1_BOVIN]	**1,625**	0,834
P62808	Histone H2B type 1 OS=Bos taurus PE=1 SV=2 - [H2B1_BOVIN]	**1,667**	0,865
P68432	Histone H3.1 OS=Bos taurus PE=1 SV=2 - [H31_BOVIN]	**1,670**	0,878
P62803	Histone H4 OS=Bos taurus PE=1 SV=2 - [H4_BOVIN]	**1,587**	0,861
A3KMV6	HNRNPR protein OS=Bos taurus GN=HNRNPR PE=2 SV=1 - [A3KMV6_BOVIN]	1,396	1,132
Q2HJH4	HNRPDL protein (Fragment) OS=Bos taurus GN=HNRPDL PE=2 SV=1 - [Q2HJH4_BOVIN]	1,310	0,954
Q3T179	HSPD1 protein (Fragment) OS=Bos taurus GN=HSPD1 PE=2 SV=1 - [Q3T179_BOVIN]	0,822	0,789
Q9GJT9	Hypoxanthine phosphoribosyltransferase (Fragment) OS=Bos taurus GN=HPRT PE=2 SV=1 - [Q9GJT9_BOVIN]	1,291	**0,631**
P80746	Integrin alpha-V OS=Bos taurus GN=ITGAV PE=1 SV=3 - [ITAV_BOVIN]	**1,684**	0,990
P53712	Integrin beta-1 OS=Bos taurus GN=ITGB1 PE=1 SV=3 - [ITB1_BOVIN]	0,923	1,045
Q2T9Y9	Interleukin enhancer binding factor 2, 45kDa OS=Bos taurus GN=ILF2 PE=2 SV=1 - [Q2T9Y9_BOVIN]	1,366	1,052
Q9XSG3	Isocitrate dehydrogenase [NADP] cytoplasmic OS=Bos taurus GN=IDH1 PE=2 SV=1 - [IDHC_BOVIN]	0,858	1,023
Q04467	Isocitrate dehydrogenase [NADP], mitochondrial OS=Bos taurus GN=IDH2 PE=1 SV=2 - [IDHP_BOVIN]	0,759	1,174
A7MB48	KTN1 protein OS=Bos taurus GN=KTN1 PE=2 SV=1 - [A7MB48_BOVIN]	0,904	0,942
Q8HYY3	L-caldesmon OS=Bos taurus PE=2 SV=1 - [Q8HYY3_BOVIN]	1,117	1,497
A0A1F3	L-lactate dehydrogenase A chain OS=Bos mutus grunniens GN=LDHA PE=2 SV=3 - [LDHA_BOSMU]	1,372	1,068
A0FH34	L-lactate dehydrogenase OS=Bos mutus grunniens PE=2 SV=1 - [A0FH34_BOSMU]	0,806	1,219

Q3SZI2	Lamin A/C OS=Bos taurus GN=LMNA PE=2 SV=1 - [Q3SZI2_BOVIN]	1,297	1,062
Q3T0U1	LDLR chaperone MESD OS=Bos taurus GN=MESDC2 PE=2 SV=1 - [MESD_BOVIN]	1,017	0,938
Q95M12	Legumain OS=Bos taurus GN=LGMN PE=1 SV=1 - [LGMN_BOVIN]	**1,566**	**0,335**
Q0VCA3	LETM1 and EF-hand domain-containing protein 1, mitochondrial OS=Bos taurus GN=LETM1 PE=2 SV=1 - [LETM1_BOVIN]	1,373	1,016
Q5E9X4	Leucine-rich repeat-containing protein 59 OS=Bos taurus GN=LRRC59 PE=2 SV=1 - [LRC59_BOVIN]	1,070	1,094
Q1JPB0	Leukocyte elastase inhibitor OS=Bos taurus GN=SERPINB1 PE=2 SV=2 - [ILEU_BOVIN]	1,074	1,082
A6QLZ0	LGALS3 protein OS=Bos taurus GN=LGALS3 PE=2 SV=1 - [A6QLZ0_BOVIN]	**2,083**	0,749
Q3B7M5	LIM and SH3 domain protein 1 OS=Bos taurus GN=LASP1 PE=2 SV=1 - [LASP1_BOVIN]	0,710	1,412
A5PJY0	LMAN1 protein OS=Bos taurus GN=LMAN1 PE=2 SV=1 - [A5PJY0_BOVIN]	1,082	0,981
A7YY47	LMNB1 protein OS=Bos taurus GN=LMNB1 PE=2 SV=1 - [A7YY47_BOVIN]	**2,434**	0,997
A6QR15	LOC535277 protein OS=Bos taurus GN=LOC535277 PE=2 SV=1 - [A6QR15_BOVIN]	0,747	**1,602**
Q59HJ6	Lon protease homolog, mitochondrial OS=Bos taurus GN=LONP1 PE=1 SV=1 - [LONM_BOVIN]	0,842	0,951
Q865V6	Macrophage-capping protein OS=Bos taurus GN=CAPG PE=2 SV=1 - [CAPG_BOVIN]	0,711	0,907
Q3T145	Malate dehydrogenase, cytoplasmic OS=Bos taurus GN=MDH1 PE=2 SV=3 - [MDHC_BOVIN]	0,947	0,890
Q32LG3	Malate dehydrogenase, mitochondrial OS=Bos taurus GN=MDH2 PE=2 SV=1 - [MDHM_BOVIN]	0,993	1,006
Q148E3	MAP1B protein (Fragment) OS=Bos taurus GN=MAP1B PE=2 SV=1 - [Q148E3_BOVIN]	0,854	0,845
A4IF82	MATR3 protein OS=Bos taurus GN=MATR3 PE=2 SV=1 - [A4IF82_BOVIN]	1,451	1,000
P80513	Mesencephalic astrocyte-derived neurotrophic factor OS=Bos taurus GN=MANF PE=1 SV=2 - [MANF_BOVIN]	1,312	0,890
A5PK67	MGC165862 protein OS=Bos taurus GN=MGC165862 PE=4 SV=1 - [A5PK67_BOVIN]	**2,469**	0,718
A1Z1N7	Micromolar calcium-activated neutral protease 1 large subunit OS=Bos mutus grunniens GN=CAPN1 PE=2 SV=2 - [A1Z1N7_BOSMU]	0,796	1,032
P36225	Microtubule-associated protein 4 OS=Bos taurus GN=MAP4 PE=1 SV=1 - [MAP4_BOVIN]	0,733	1,343
Q3ZBD9	Microtubule-associated protein RP/EB family member 1 OS=Bos taurus GN=MAPRE1 PE=2 SV=3 - [MARE1_BOVIN]	1,109	0,958
Q1P9Q3	Mitochondrial aconitase 2 (Fragment) OS=Bos taurus GN=ACO2 PE=4 SV=1 - [Q1P9Q3_BOVIN]	1,029	1,000
Q3T0I5	Mitochondrial fission 1 protein OS=Bos taurus GN=FIS1 PE=2 SV=1 - [FIS1_BOVIN]	0,842	0,746
Q2HJ49	Moesin OS=Bos taurus GN=MSN PE=2 SV=3 - [MOES_BOVIN]	1,147	1,307
Q27991	Myosin-10 OS=Bos taurus GN=MYH10 PE=2 SV=2 - [MYH10_BOVIN]	0,934	**1,567**
Q1RMX7	N-acetylneuraminic acid synthase OS=Bos taurus GN=NANS PE=2 SV=1 - [Q1RMX7_BOVIN]	1,142	1,051
Q1JPF2	NADH dehydrogenase (Ubiquinone) 1 alpha subcomplex, 9, 39kDa (Fragment) OS=Bos taurus GN=NDUFA9 PE=2 SV=1 - [Q1JPF2_BOVIN]	0,787	1,040
P07514	NADH-cytochrome b5 reductase 3 OS=Bos taurus GN=CYB5R3 PE=1 SV=2 - [NB5R3_BOVIN]	0,833	0,902
Q1RMM9	NAGA protein OS=Bos taurus GN=NAGA PE=2 SV=1 - [Q1RMM9_BOVIN]	1,014	**0,621**
Q5E9A1	Nascent polypeptide-associated complex subunit alpha OS=Bos taurus GN=NACA PE=1 SV=1 - [NACA_BOVIN]	0,973	1,025
P02316	Non-histone chromosomal protein HMG-14 OS=Bos taurus GN=HMGN1 PE=1 SV=2 - [HMGN1_BOVIN]	**1,626**	**0,631**
O02717	Non-muscle myosin heavy chain (Fragment) OS=Bos taurus PE=2 SV=2 - [O02717_BOVIN]	0,738	**1,503**
P07857	Non-specific lipid-transfer protein OS=Bos taurus GN=SCP2 PE=1 SV=2 - [NLTP_BOVIN]	0,880	0,832
A7E357	NOP58 protein (Fragment) OS=Bos taurus GN=NOP58 PE=2 SV=1 - [A7E357_BOVIN]	1,279	1,142

Q32KP9	Nuclear transport factor 2 OS=Bos taurus GN=NUTF2 PE=2 SV=1 - [NTF2_BOVIN]	0,819	1,079
Q29S11	Nuclear ubiquitous casein and cyclin-dependent kinases substrate OS=Bos taurus GN=NUCKS1 PE=2 SV=1 - [NUCKS_BOVIN]	1,404	**1,544**
P67808	Nuclease-sensitive element-binding protein 1 OS=Bos taurus GN=YBX1 PE=2 SV=3 - [YBOX1_BOVIN]	0,902	0,887
D3U796	Nucleophosmin OS=Bos taurus GN=NPM PE=4 SV=1 - [D3U796_BOVIN]	1,002	1,031
Q3T0Q4	Nucleoside diphosphate kinase B OS=Bos taurus GN=NME2 PE=2 SV=1 - [NDKB_BOVIN]	0,844	1,126
Q2HJ33	Obg-like ATPase 1 OS=Bos taurus GN=OLA1 PE=2 SV=1 - [OLA1_BOVIN]	1,027	1,209
Q3ZCF5	Ornithine aminotransferase, mitochondrial OS=Bos taurus GN=OAT PE=2 SV=1 - [OAT_BOVIN]	1,042	1,243
Q8MJ50	Osteoclast-stimulating factor 1 OS=Bos taurus GN=OSTF1 PE=2 SV=1 - [OSTF1_BOVIN]	0,896	0,948
A6QL77	P4HA1 protein OS=Bos taurus GN=P4HA1 PE=2 SV=1 - [A6QL77_BOVIN]	1,299	0,828
A6H7J6	P4HB protein OS=Bos taurus GN=P4HB PE=2 SV=1 - [A6H7J6_BOVIN]	**1,577**	0,853
A5PK55	PARVA protein OS=Bos taurus GN=PARVA PE=2 SV=1 - [A5PK55_BOVIN]	1,031	1,165
A5D7E8	PDIA3 protein OS=Bos taurus GN=PDIA3 PE=2 SV=1 - [A5D7E8_BOVIN]	1,315	0,894
A6QNL5	PDIA6 protein (Fragment) OS=Bos taurus GN=PDIA6 PE=2 SV=1 - [A6QNL5_BOVIN]	1,342	0,881
A6H7E3	PDZ and LIM domain 1 OS=Bos taurus GN=PDLIM1 PE=2 SV=1 - [A6H7E3_BOVIN]	1,419	**1,883**
Q861V9	Peptidyl-prolyl cis-trans isomerase (Fragment) OS=Bos taurus PE=2 SV=1 - [Q861V9_BOVIN]	1,002	1,004
P80311	Peptidyl-prolyl cis-trans isomerase B OS=Bos taurus GN=PPIB PE=1 SV=4 - [PPIB_BOVIN]	0,799	0,986
Q08E11	Peptidyl-prolyl cis-trans isomerase C OS=Bos taurus GN=PPIC PE=2 SV=1 - [PPIC_BOVIN]	0,863	0,855
Q2HJ89	Peptidyl-prolyl cis-trans isomerase FKBP10 OS=Bos taurus GN=FKBP10 PE=2 SV=1 - [FKB10_BOVIN]	1,039	0,822
P18203	Peptidyl-prolyl cis-trans isomerase FKBP1A OS=Bos taurus GN=FKBP1A PE=1 SV=2 - [FKB1A_BOVIN]	1,139	0,884
P26884	Peptidyl-prolyl cis-trans isomerase FKBP3 OS=Bos taurus GN=FKBP3 PE=1 SV=2 - [FKBP3_BOVIN]	1,177	1,061
Q5E947	Peroxiredoxin-1 OS=Bos taurus GN=PRDX1 PE=2 SV=1 - [PRDX1_BOVIN]	1,170	0,815
Q9BGI3	Peroxiredoxin-2 OS=Bos taurus GN=PRDX2 PE=2 SV=1 - [PRDX2_BOVIN]	1,401	1,008
Q9BGI1	Peroxiredoxin-5, mitochondrial OS=Bos taurus GN=PRDX5 PE=2 SV=2 - [PRDX5_BOVIN]	1,428	1,069
O77834	Peroxiredoxin-6 OS=Bos taurus GN=PRDX6 PE=1 SV=3 - [PRDX6_BOVIN]	0,920	1,461
Q32PF3	PEST proteolytic signal-containing nuclear protein OS=Bos taurus GN=PCNP PE=2 SV=1 - [PCNP_BOVIN]	1,329	1,335
P13696	Phosphatidylethanolamine-binding protein 1 OS=Bos taurus GN=PEBP1 PE=1 SV=2 - [PEBP1_BOVIN]	0,750	1,101
Q08DP0	Phosphoglucomutase-1 OS=Bos taurus GN=PGM1 PE=2 SV=1 - [PGM1_BOVIN]	0,788	1,273
Q3T0P6	Phosphoglycerate kinase 1 OS=Bos taurus GN=PGK1 PE=2 SV=3 - [PGK1_BOVIN]	**1,790**	0,958
Q3SZ62	Phosphoglycerate mutase 1 OS=Bos taurus GN=PGAM1 PE=2 SV=3 - [PGAM1_BOVIN]	1,450	1,086
A6QR28	Phosphoserine aminotransferase OS=Bos taurus GN=PSAT1 PE=2 SV=1 - [A6QR28_BOVIN]	**0,288**	0,706
A7E3Q8	Plastin-3 OS=Bos taurus GN=PLS3 PE=2 SV=1 - [PLST_BOVIN]	**0,543**	1,090
A7MB83	PLOD2 protein OS=Bos taurus GN=PLOD2 PE=2 SV=1 - [A7MB83_BOVIN]	1,375	1,052
A1L578	Polymerase I and transcript release factor OS=Bos taurus GN=PTRF PE=2 SV=1 - [A1L578_BOVIN]	0,926	1,227
Q8WN55	Polypyrimidine tract-binding protein 1 OS=Bos taurus GN=PTBP1 PE=2 SV=1 - [PTBP1_BOVIN]	1,364	0,996
Q3MHF7	PRDX3 protein OS=Bos taurus GN=PRDX3 PE=2 SV=1 - [Q3MHF7_BOVIN]	1,096	0,923

Q2TBX2	Prefoldin subunit 3 OS=Bos taurus GN=VBP1 PE=2 SV=1 - [PFD3_BOVIN]	0,927	0,914
Q8HYI9	Prefoldin subunit 5 OS=Bos taurus GN=PFDN5 PE=2 SV=1 - [PFD5_BOVIN]	0,924	0,853
Q2NL01	Probable glutathione peroxidase 8 OS=Bos taurus GN=GPX8 PE=2 SV=1 - [GPX8_BOVIN]	1,171	1,400
O77588	Procollagen-lysine,2-oxoglutarate 5-dioxygenase 1 OS=Bos taurus GN=PLOD1 PE=2 SV=2 - [PLOD1_BOVIN]	**2,242**	**0,665**
P02584	Profilin-1 OS=Bos taurus GN=PFN1 PE=1 SV=2 - [PROF1_BOVIN]	0,837	1,104
Q2HJ97	Prohibitin-2 OS=Bos taurus GN=PHB2 PE=2 SV=1 - [PHB2_BOVIN]	1,347	0,682
Q3SYY3	Prolyl 4-hydroxylase, alpha polypeptide II OS=Bos taurus GN=P4HA2 PE=2 SV=1 - [Q3SYY3_BOVIN]	1,397	**0,630**
Q29626	Prostacyclin synthase OS=Bos taurus GN=PTGIS PE=1 SV=1 - [PTGIS_BOVIN]	**0,650**	0,950
O62664	Prostaglandin G/H synthase 1 OS=Bos taurus GN=PTGS1 PE=2 SV=2 - [PGH1_BOVIN]	**11,281**	0,791
Q2KJE7	Proteasome (Prosome, macropain) activator subunit 1 (PA28 alpha) OS=Bos taurus GN=PSME1 PE=2 SV=1 - [Q2KJE7_BOVIN]	1,233	0,896
Q1JP95	Proteasome 26S ATPase subunit 3 (Fragment) OS=Bos taurus GN=PSMC3 PE=2 SV=1 - [Q1JP95_BOVIN]	1,074	1,122
A1L5B1	Proteasome 26S non-ATPase subunit 7 (Fragment) OS=Bos taurus GN=PSMD7 PE=2 SV=1 - [A1L5B1_BOVIN]	0,976	1,031
Q5E9G3	Proteasome activator complex subunit 2 OS=Bos taurus GN=PSME2 PE=1 SV=3 - [PSME2_BOVIN]	1,427	0,759
A7E3D5	Proteasome subunit alpha type (Fragment) OS=Bos taurus GN=PSMA7 PE=2 SV=1 - [A7E3D5_BOVIN]	1,073	1,058
Q3T0X5	Proteasome subunit alpha type-1 OS=Bos taurus GN=PSMA1 PE=1 SV=1 - [PSA1_BOVIN]	1,091	1,001
Q3ZCK9	Proteasome subunit alpha type-4 OS=Bos taurus GN=PSMA4 PE=1 SV=1 - [PSA4_BOVIN]	1,191	1,030
Q5E987	Proteasome subunit alpha type-5 OS=Bos taurus GN=PSMA5 PE=1 SV=1 - [PSA5_BOVIN]	1,117	1,048
Q2YDE4	Proteasome subunit alpha type-6 OS=Bos taurus GN=PSMA6 PE=1 SV=1 - [PSA6_BOVIN]	1,122	1,029
Q2TBX6	Proteasome subunit beta type-1 OS=Bos taurus GN=PSMB1 PE=1 SV=1 - [PSB1_BOVIN]	1,129	0,930
P33672	Proteasome subunit beta type-3 OS=Bos taurus GN=PSMB3 PE=1 SV=3 - [PSB3_BOVIN]	1,090	0,964
Q29RV1	Protein disulfide-isomerase A4 OS=Bos taurus GN=PDIA4 PE=2 SV=1 - [PDIA4_BOVIN]	**1,509**	0,908
Q5E946	Protein DJ-1 OS=Bos taurus GN=PARK7 PE=2 SV=1 - [PARK7_BOVIN]	0,924	1,224
A4FV37	Protein kinase C delta-binding protein OS=Bos taurus GN=PRKCDBP PE=2 SV=1 - [PRDBP_BOVIN]	0,775	1,264
P60902	Protein S100-A10 OS=Bos taurus GN=S100A10 PE=1 SV=2 - [S10AA_BOVIN]	1,349	1,177
P79342	Protein S100-A13 OS=Bos taurus GN=S100A13 PE=3 SV=2 - [S10AD_BOVIN]	1,018	0,733
P35466	Protein S100-A4 OS=Bos taurus GN=S100A4 PE=1 SV=2 - [S10A4_BOVIN]	1,465	1,013
P15246	Protein-L-isoaspartate(D-aspartate) O-methyltransferase OS=Bos taurus GN=PCMT1 PE=1 SV=2 - [PIMT_BOVIN]	0,919	1,109
P55859	Purine nucleoside phosphorylase OS=Bos taurus GN=PNP PE=1 SV=3 - [PNPH_BOVIN]	1,272	0,897
Q0II59	Pyridoxal kinase OS=Bos taurus GN=PDXK PE=2 SV=1 - [PDXK_BOVIN]	**3,062**	0,792
Q5E9K3	Pyridoxine-5'-phosphate oxidase OS=Bos taurus GN=PNPO PE=2 SV=1 - [PNPO_BOVIN]	**1,529**	**0,551**
Q58DT4	Pyrroline-5-carboxylate reductase 1, mitochondrial OS=Bos taurus GN=PYCR1 PE=2 SV=1 - [P5CR1_BOVIN]	**0,391**	0,829
P11966	Pyruvate dehydrogenase E1 component subunit beta, mitochondrial OS=Bos taurus GN=PDHB PE=1 SV=2 - [ODPB_BOVIN]	**1,649**	0,950
A5D984	Pyruvate kinase OS=Bos taurus GN=PKM2 PE=2 SV=1 - [A5D984_BOVIN]	1,135	1,250
P50397	Rab GDP dissociation inhibitor beta OS=Bos taurus GN=GDI2 PE=2 SV=3 - [GDIB_BOVIN]	0,827	1,159
Q32LP2	Radixin OS=Bos taurus GN=RDX PE=2 SV=1 - [RADI_BOVIN]	1,362	0,916

Q3T0M7	Ran-specific GTPase-activating protein OS=Bos taurus GN=RANBP1 PE=2 SV=1 - [RANG_BOVIN]	0,921	1,235
Q5E9C0	Ras suppressor protein 1 OS=Bos taurus GN=RSU1 PE=2 SV=1 - [RSU1_BOVIN]	0,824	1,252
P62998	Ras-related C3 botulinum toxin substrate 1 OS=Bos taurus GN=RAC1 PE=1 SV=1 - [RAC1_BOVIN]	0,860	0,903
Q0IIG7	Ras-related protein Rab-5A OS=Bos taurus GN=RAB5A PE=2 SV=1 - [RAB5A_BOVIN]	1,076	0,957
Q58DS9	Ras-related protein Rab-5C OS=Bos taurus GN=RAB5C PE=2 SV=1 - [RAB5C_BOVIN]	0,971	0,978
Q3T0F5	Ras-related protein Rab-7a OS=Bos taurus GN=RAB7A PE=2 SV=1 - [RAB7A_BOVIN]	0,699	0,824
P61223	Ras-related protein Rap-1b OS=Bos taurus GN=RAP1B PE=2 SV=1 - [RAP1B_BOVIN]	1,254	0,932
Q29RM3	Receptor expression-enhancing protein 5 OS=Bos taurus GN=REEP5 PE=2 SV=1 - [REEP5_BOVIN]	0,822	0,738
Q2TBH2	Related RAS viral (R-ras) oncogene homolog OS=Bos taurus GN=RRAS PE=2 SV=1 - [Q2TBH2_BOVIN]	1,072	0,933
P19803	Rho GDP-dissociation inhibitor 1 OS=Bos taurus GN=ARHGDIA PE=1 SV=3 - [GDIR1_BOVIN]	1,013	1,066
Q3T114	Ribonuclease UK114 OS=Bos taurus GN=HRSP12 PE=2 SV=3 - [UK114_BOVIN]	1,055	1,024
Q0QEV5	Ribosomal protein L18 (Fragment) OS=Bos taurus GN=RPL18 PE=2 SV=1 - [Q0QEV5_BOVIN]	0,985	0,928
A2VE06	Ribosomal protein S4, Y-linked 1 OS=Bos taurus GN=RPS4Y1 PE=2 SV=1 - [A2VE06_BOVIN]	1,000	0,974
Q3SWZ6	Ribosome maturation protein SBDS OS=Bos taurus GN=SBDS PE=2 SV=1 - [SBDS_BOVIN]	1,068	**0,606**
A6QLW3	RPRD1B protein OS=Bos taurus GN=RPRD1B PE=2 SV=1 - [A6QLW3_BOVIN]	1,351	0,728
Q1RMR8	RTN4 protein OS=Bos taurus GN=RTN4 PE=2 SV=1 - [Q1RMR8_BOVIN]	**0,614**	0,854
Q862H7	S100A11 protein (Fragment) OS=Bos taurus GN=S100A11 PE=2 SV=1 - [Q862H7_BOVIN]	0,850	0,951
A6QQP4	SCARB2 protein OS=Bos taurus GN=SCARB2 PE=2 SV=1 - [A6QQP4_BOVIN]	0,752	0,857
A6QNM0	Septin 7 OS=Bos taurus GN=SEPT7 PE=2 SV=1 - [A6QNM0_BOVIN]	0,804	1,247
A2VE99	Septin-11 OS=Bos taurus GN=SEPT11 PE=2 SV=1 - [SEP11_BOVIN]	0,694	1,321
Q2NKY7	Septin-2 OS=Bos taurus GN=SEPT2 PE=2 SV=1 - [SEPT2_BOVIN]	0,775	1,346
Q3SZ20	Serine hydroxymethyltransferase, mitochondrial OS=Bos taurus GN=SHMT2 PE=2 SV=1 - [GLYM_BOVIN]	1,274	0,733
O97658	Serine protease (Fragment) OS=Bos taurus GN=HTRA PE=2 SV=1 - [O97658_BOVIN]	**1,746**	0,870
Q2KJH6	Serpin H1 OS=Bos taurus GN=SERPINH1 PE=2 SV=1 - [SERPH_BOVIN]	**0,650**	1,043
Q05FF2	Signal transducer and activator of transcription 1 OS=Bos taurus GN=STAT1 PE=2 SV=1 - [Q05FF2_BOVIN]	**1,830**	0,774
Q862H8	Similar to 40S ribosomal protein SA (P40) (Fragment) OS=Bos taurus PE=2 SV=1 - [Q862H8_BOVIN]	0,909	0,758
Q862L6	Similar to ribosomal protein L12 (Fragment) OS=Bos taurus PE=2 SV=1 - [Q862L6_BOVIN]	0,963	0,888
Q862E3	Similar to ribosomal protein L17 (Fragment) OS=Bos taurus PE=2 SV=1 - [Q862E3_BOVIN]	0,934	0,927
Q861S4	Similar to ribosomal protein L21 (Fragment) OS=Bos taurus PE=2 SV=1 - [Q861S4_BOVIN]	0,970	0,914
Q862D6	Similar to ribosomal protein L30 (Fragment) OS=Bos taurus PE=2 SV=1 - [Q862D6_BOVIN]	0,947	0,875
Q862B7	Similar to ribosomal protein S14 (Fragment) OS=Bos taurus PE=2 SV=1 - [Q862B7_BOVIN]	0,974	0,901
Q862S8	Similar to ribosomal protein S18 (Fragment) OS=Bos taurus PE=2 SV=1 - [Q862S8_BOVIN]	0,915	0,915
Q862Q9	Similar to ubiquitin-conjugating enzyme E2 variant 2 (Fragment) OS=Bos taurus PE=2 SV=1 - [Q862Q9_BOVIN]	0,875	0,965
Q3ZBX5	Small inducible cytokine subfamily E, member 1 (Endothelial monocyte-activating) OS=Bos taurus GN=SCYE1 PE=2 SV=2 - [Q3ZBX5_BOVIN]	0,911	1,110
Q3SZF8	Small nuclear ribonucleoprotein Sm D2 OS=Bos taurus GN=SNRPD2 PE=3 SV=1 - [SMD2_BOVIN]	1,242	0,987

A6H788	SNRPA1 protein OS=Bos taurus GN=SNRPA1 PE=2 SV=1 - [A6H788_BOVIN]	1,388	0,843
A4IFN6	SNX18 protein OS=Bos taurus GN=SNX18 PE=2 SV=1 - [A4IFN6_BOVIN]	**1,506**	1,246
Q0VCY7	Splicing factor, arginine/serine-rich 1 OS=Bos taurus GN=SFRS1 PE=2 SV=1 - [SFRS1_BOVIN]	1,426	0,826
Q1RMK4	SPTBN1 protein (Fragment) OS=Bos taurus GN=SPTBN1 PE=2 SV=1 - [Q1RMK4_BOVIN]	**0,663**	0,909
Q3MHW4	SQRDL protein OS=Bos taurus GN=SQRDL PE=2 SV=1 - [Q3MHW4_BOVIN]	**2,059**	1,060
A8E4P3	STOM protein OS=Bos taurus GN=STOM PE=2 SV=1 - [A8E4P3_BOVIN]	**1,821**	**0,422**
Q3ZCH0	Stress-70 protein, mitochondrial OS=Bos taurus GN=HSPA9 PE=2 SV=1 - [GRP75_BOVIN]	0,672	1,068
Q3SZ45	Stromal cell-derived factor 2 OS=Bos taurus GN=SDF2 PE=2 SV=1 - [SDF2_BOVIN]	1,061	1,000
A7YWC6	SUB1 protein OS=Bos taurus GN=SUB1 PE=2 SV=1 - [A7YWC6_BOVIN]	1,411	1,183
P50227	Sulfotransferase 1A1 OS=Bos taurus GN=SULT1A1 PE=1 SV=2 - [ST1A1_BOVIN]	**2,192**	0,955
A4URH1	Superoxide dismutase (Fragment) OS=Bos taurus GN=SOD1 PE=2 SV=1 - [A4URH1_BOVIN]	1,131	1,143
P41976	Superoxide dismutase [Mn], mitochondrial OS=Bos taurus GN=SOD2 PE=2 SV=1 - [SODM_BOVIN]	**24,758**	1,149
A7E355	SYNCRIP protein (Fragment) OS=Bos taurus GN=SYNCRIP PE=2 SV=1 - [A7E355_BOVIN]	1,047	1,154
Q3ZBH0	T-complex protein 1 subunit beta OS=Bos taurus GN=CCT2 PE=2 SV=3 - [TCPB_BOVIN]	0,797	1,147
Q2T9X2	T-complex protein 1 subunit delta OS=Bos taurus GN=CCT4 PE=2 SV=3 - [TCPD_BOVIN]	0,865	1,049
Q3ZCI9	T-complex protein 1 subunit theta OS=Bos taurus GN=CCT8 PE=2 SV=3 - [TCPQ_BOVIN]	0,861	1,055
Q3MHL7	T-complex protein 1 subunit zeta OS=Bos taurus GN=CCT6A PE=2 SV=3 - [TCPZ_BOVIN]	0,803	1,053
O97680	Thioredoxin OS=Bos taurus GN=TXN PE=3 SV=3 - [THIO_BOVIN]	1,075	**0,631**
P35705	Thioredoxin-dependent peroxide reductase, mitochondrial OS=Bos taurus GN=PRDX3 PE=1 SV=2 - [PRDX3_BOVIN]	**1,887**	0,793
Q0II43	Thioredoxin-like 1 OS=Bos taurus GN=TXNL1 PE=2 SV=1 - [Q0II43_BOVIN]	1,073	0,947
Q0Z7W6	Thioredoxin-related transmembrane protein 1 OS=Bos taurus GN=TMX1 PE=2 SV=1 - [TMX1_BOVIN]	1,137	0,836
Q3T0I4	THO complex subunit 4 OS=Bos taurus GN=THOC4 PE=2 SV=1 - [THOC4_BOVIN]	1,445	0,927
Q3ZBV8	Threonyl-tRNA synthetase, cytoplasmic OS=Bos taurus GN=TARS PE=2 SV=1 - [SYTC_BOVIN]	0,680	1,124
Q0II79	TLN1 protein (Fragment) OS=Bos taurus GN=TLN1 PE=2 SV=1 - [Q0II79_BOVIN]	1,044	1,326
Q2TBL6	Transaldolase OS=Bos taurus GN=TALDO1 PE=2 SV=1 - [TALDO_BOVIN]	**0,628**	0,752
Q9TS87	Transgelin OS=Bos taurus GN=TAGLN PE=1 SV=4 - [TAGL_BOVIN]	**0,365**	**2,332**
Q5E9F5	Transgelin-2 OS=Bos taurus GN=TAGLN2 PE=2 SV=3 - [TAGL2_BOVIN]	0,819	1,365
Q3ZBT1	Transitional endoplasmic reticulum ATPase OS=Bos taurus GN=VCP PE=1 SV=1 - [TERA_BOVIN]	1,195	0,865
A7E3W4	Transketolase OS=Bos taurus GN=TKT PE=2 SV=1 - [A7E3W4_BOVIN]	0,974	1,370
A6QLP7	Translocon-associated protein subunit alpha OS=Bos taurus GN=SSR1 PE=2 SV=1 - [SSRA_BOVIN]	1,108	1,238
Q5E971	Transmembrane emp24 domain-containing protein 10 OS=Bos taurus GN=TMED10 PE=2 SV=1 - [TMEDA_BOVIN]	1,041	0,975
O46629	Trifunctional enzyme subunit beta, mitochondrial OS=Bos taurus GN=HADHB PE=2 SV=1 - [ECHB_BOVIN]	**1,807**	0,737
Q5E956	Triosephosphate isomerase OS=Bos taurus GN=TPI1 PE=2 SV=3 - [TPIS_BOVIN]	1,445	0,951
Q5KR49	Tropomyosin alpha-1 chain OS=Bos taurus GN=TPM1 PE=2 SV=1 - [TPM1_BOVIN]	1,123	**1,566**
P17248	Tryptophanyl-tRNA synthetase, cytoplasmic OS=Bos taurus GN=WARS PE=1 SV=3 - [SYWC_BOVIN]	**0,358**	**0,650**

P81947	Tubulin alpha-1B chain OS=Bos taurus PE=1 SV=2 - [TBA1B_BOVIN]	0,782	0,940
Q2KJD0	Tubulin beta-5 chain OS=Bos taurus GN=TUBB5 PE=2 SV=1 - [TBB5_BOVIN]	0,843	0,980
Q2HJ81	Tubulin beta-6 chain OS=Bos taurus GN=TUBB6 PE=2 SV=1 - [TBB6_BOVIN]	0,752	0,905
Q3SYU8	Tumor protein D52-like 2 OS=Bos taurus GN=TPD52L2 PE=2 SV=1 - [Q3SYU8_BOVIN]	0,875	0,795
Q24JZ8	U2 small nuclear RNA auxiliary factor 2 OS=Bos taurus GN=U2AF2 PE=2 SV=1 - [Q24JZ8_BOVIN]	**1,560**	0,820
A5D987	Ubiquitin carrier protein OS=Bos taurus GN=UBE2N PE=2 SV=1 - [A5D987_BOVIN]	0,965	1,044
P62990	Ubiquitin OS=Bos taurus GN=RPS27A PE=1 SV=1 - [UBIQ_BOVIN]	**1,518**	0,929
A3KMV5	Ubiquitin-like modifier-activating enzyme 1 OS=Bos taurus GN=UBA1 PE=2 SV=1 - [UBA1_BOVIN]	1,123	1,132
P12378	UDP-glucose 6-dehydrogenase OS=Bos taurus GN=UGDH PE=1 SV=2 - [UGDH_BOVIN]	**0,653**	0,811
Q2KIW9	UMP-CMP kinase OS=Bos taurus GN=CMPK1 PE=2 SV=2 - [KCY_BOVIN]	0,815	1,118
A1A4Q2	UPF0566 protein OS=Bos taurus PE=2 SV=1 - [U566_BOVIN]	0,875	1,316
Q07130	UTP--glucose-1-phosphate uridylyltransferase OS=Bos taurus GN=UGP2 PE=1 SV=2 - [UGPA_BOVIN]	1,172	1,008
Q2HJG5	Vacuolar protein sorting-associated protein 35 OS=Bos taurus GN=VPS35 PE=2 SV=1 - [VPS35_BOVIN]	0,875	1,056
P48818	Very long-chain specific acyl-CoA dehydrogenase, mitochondrial OS=Bos taurus GN=ACADVL PE=2 SV=3 - [ACADV_BOVIN]	0,922	1,078
Q0VCY1	Vesicle-associated membrane protein-associated protein A OS=Bos taurus GN=VAPA PE=2 SV=1 - [VAPA_BOVIN]	0,975	0,964
A2VDZ9	Vesicle-associated membrane protein-associated protein B OS=Bos taurus GN=VAPB PE=2 SV=1 - [VAPB_BOVIN]	0,933	0,894
P48616	Vimentin OS=Bos taurus GN=VIM PE=1 SV=3 - [VIME_BOVIN]	0,902	0,845
Q2PQT6	Vinculin (Fragment) OS=Bos taurus PE=2 SV=1 - [Q2PQT6_BOVIN]	**0,484**	1,362
P45879	Voltage-dependent anion-selective channel protein 1 OS=Bos taurus GN=VDAC1 PE=1 SV=3 - [VDAC1_BOVIN]	1,389	**0,588**
P68002	Voltage-dependent anion-selective channel protein 2 OS=Bos taurus GN=VDAC2 PE=2 SV=2 - [VDAC2_BOVIN]	**1,800**	**0,570**
Q9MZ13	Voltage-dependent anion-selective channel protein 3 OS=Bos taurus GN=VDAC3 PE=2 SV=1 - [VDAC3_BOVIN]	1,443	0,733
Q0III5	YARS protein OS=Bos taurus GN=YARS PE=2 SV=1 - [Q0III5_BOVIN]	**0,614**	0,827
A7Z057	YWHAG protein OS=Bos taurus GN=YWHAG PE=2 SV=1 - [A7Z057_BOVIN]	1,156	1,045
O97764	Zeta-crystallin OS=Bos taurus GN=CRYZ PE=2 SV=2 - [QOR_BOVIN]	0,817	1,062
Q08DQ6	Zyxin OS=Bos taurus GN=ZYX PE=2 SV=1 - [Q08DQ6_BOVIN]	1,041	**1,709**

TABLE 2: List of Proteins Identified and quantified in iTRAQ BVIC experiment.

ACCESSION	DESCRIPTION	LPS/CTRL	LPS-R/LPS
IPI00702858.2	10 kDa heat shock protein, mitochondrial	0,799	1,308
IPI01028291.1	11 kDa protein	1,153	1,194
IPI00696435.1	14-3-3 protein epsilon	1,027	0,937
IPI00693106.2	14-3-3 protein gamma	1,006	0,970
IPI00707320.1	14-3-3 protein theta	0,953	0,854
IPI00703110.1	14-3-3 protein zeta/delta	0,993	0,948
IPI00716355.4	170 kDa protein	1,006	0,900
IPI00687413.3	2-oxoglutarate dehydrogenase, mitochondrial	1,044	1,074
IPI00696901.2	2-oxoisovalerate dehydrogenase subunit beta, mitochondrial	0,996	1,006
IPI00701790.7	26S protease regulatory subunit 6A	0,898	0,971
IPI00718026.1	26S protease regulatory subunit 6B	0,974	0,839
IPI00693210.3	26S protease regulatory subunit 7	0,882	0,934
IPI00717227.1	26S protease regulatory subunit 8	0,931	1,048
IPI00710615.2	26S proteasome non-ATPase regulatory subunit 2	1,040	0,887
IPI00707518.2	26S proteasome non-ATPase regulatory subunit 3	0,904	0,931
IPI00697833.1	26S proteasome non-ATPase regulatory subunit 6	0,993	0,902
IPI00687921.3	3-hydroxyacyl-CoA dehydratase 3	1,146	1,054
IPI00699128.2	3-hydroxyacyl-CoA dehydrogenase type-2	1,061	1,041
IPI00697138.1	3-ketoacyl-CoA thiolase, mitochondrial	0,918	1,124
IPI00730144.2	3'-phosphoadenosine 5'-phosphosulfate synthase 2	1,075	1,151
IPI00703131.5	4-trimethylaminobutyraldehyde dehydrogenase	1,084	0,922
IPI01028051.1	40 kDa protein	1,025	**1,526**
IPI00701135.1	40S ribosomal protein S10	0,927	1,077
IPI00689811.3	40S ribosomal protein S11	1,113	0,837
IPI00713536.1	40S ribosomal protein S12	1,015	0,991
IPI00688727.3	40S ribosomal protein S13	0,981	0,961
IPI00704074.2	40S ribosomal protein S15	0,956	0,967
IPI00689728.3	40S ribosomal protein S17	0,983	1,011
IPI00689850.3	40S ribosomal protein S18	0,960	1,019
IPI00707431.3	40S ribosomal protein S19	0,922	0,940
IPI00695732.1	40S ribosomal protein S2	1,040	0,875
IPI00715091.1	40S ribosomal protein S20	0,950	0,937
IPI00691584.1	40S ribosomal protein S25	0,946	0,932

IPI00694688.3	40S ribosomal protein S26	0,937	1,010
IPI00685601.3	40S ribosomal protein S3	0,975	0,935
IPI00712833.3	40S ribosomal protein S3a	0,975	1,013
IPI00702348.2	40S ribosomal protein S5	0,957	0,982
IPI00702948.1	40S ribosomal protein S6	1,019	0,888
IPI00694243.3	40S ribosomal protein S7	1,015	1,032
IPI00696508.2	40S ribosomal protein S8	1,016	0,922
IPI00694565.1	40S ribosomal protein S9	0,982	1,084
IPI00709865.3	40S ribosomal protein SA	0,950	0,902
IPI00698673.2	5'-nucleotidase	1,087	1,125
IPI00691031.4	55 kDa protein	0,823	1,018
IPI00718220.4	6-phosphofructokinase, liver type	1,263	0,973
IPI00701642.5	6-phosphogluconate dehydrogenase, decarboxylating	1,037	0,951
IPI00727043.1	6-phosphogluconolactonase	0,979	1,051
IPI01002905.1	60 kDa heat shock protein, mitochondrial	0,886	1,025
IPI00703564.2	60S acidic ribosomal protein P0	0,901	1,089
IPI00702456.1	60S acidic ribosomal protein P2	0,940	1,125
IPI00708210.2	60S ribosomal protein L10	0,988	0,973
IPI00710091.2	60S ribosomal protein L10a	1,040	1,025
IPI00688640.3	60S ribosomal protein L11	0,879	1,078
IPI00700975.1	60S ribosomal protein L12	0,887	1,063
IPI00714042.2	60S ribosomal protein L13	0,997	1,016
IPI00712384.3	60S ribosomal protein L13a	0,994	0,983
IPI00712641.3	60S ribosomal protein L14	0,959	1,076
IPI00709409.5	60S ribosomal protein L15	0,941	1,016
IPI00689565.3	60S ribosomal protein L17	1,011	0,943
IPI00718379.3	60S ribosomal protein L18	0,983	1,184
IPI00710859.3	60S ribosomal protein L19	0,911	1,015
IPI00695041.2	60S ribosomal protein L23	1,015	0,855
IPI00706607.1	60S ribosomal protein L23a	0,984	1,193
IPI00685352.1	60S ribosomal protein L24	1,049	0,886
IPI00685484.1	60S ribosomal protein L26	1,003	0,984
IPI00707537.3	60S ribosomal protein L28	1,070	1,020
IPI00698932.3	60S ribosomal protein L29	1,001	1,074
IPI00687634.2	60S ribosomal protein L3	1,016	1,079
IPI00689092.1	60S ribosomal protein L31	0,928	1,163
IPI00716860.3	60S ribosomal protein L36	0,855	0,931
IPI00699827.3	60S ribosomal protein L4	0,970	1,009

IPI00716609.3	60S ribosomal protein L5	1,027	0,895
IPI00717048.2	60S ribosomal protein L6	0,967	0,992
IPI00714181.1	60S ribosomal protein L7	0,943	1,015
IPI00691853.4	60S ribosomal protein L7a	1,004	1,061
IPI00698077.3	60S ribosomal protein L8	0,927	0,987
IPI00702292.3	78 kDa APAMIN binding protein	1,081	0,944
IPI00717234.3	78 kDa glucose-regulated protein	0,944	0,954
IPI01028441.1	8 kDa protein	1,054	0,911
IPI00999284.1	A-kinase anchor protein 2	1,170	0,747
IPI00711918.5	Acetyl-CoA acetyltransferase, mitochondrial	1,024	1,132
IPI00685191.3	Acetyl-Coenzyme A acetyltransferase 2	1,320	1,053
IPI00685320.4	Acid ceramidase	1,080	1,229
IPI00699002.1	Acidic leucine-rich nuclear phosphoprotein 32 family member B	1,310	0,914
IPI00690870.2	Aconitate hydratase, mitochondrial	0,903	1,169
IPI00729166.5	ACSL4 protein (Fragment)	**1,589**	1,061
IPI00867472.1	Actin-related protein 2	0,940	0,917
IPI00693939.4	Actin-related protein 2/3 complex subunit 1B	0,964	0,879
IPI00715364.1	Actin-related protein 2/3 complex subunit 2	1,067	1,015
IPI00711750.2	Actin-related protein 2/3 complex subunit 3	0,868	1,154
IPI00708767.5	Actin-related protein 2/3 complex subunit 4	0,955	0,884
IPI00716307.2	Actin-related protein 2/3 complex subunit 5	0,890	0,844
IPI00714052.3	Actin-related protein 3	0,900	0,961
IPI00698900.1	Actin, cytoplasmic 1	0,923	1,034
IPI00692609.1	Actin, gamma-enteric smooth muscle	0,830	1,015
IPI00685776.1	Acyl carrier protein, mitochondrial	0,927	1,091
IPI00717758.2	Acyl-CoA synthetase family member 2, mitochondrial	0,875	1,203
IPI00695419.2	Acyl-CoA-binding protein	1,052	1,010
IPI00867404.1	ADAMTSL4 protein	**1,538**	0,982
IPI00686658.1	Adenine phosphoribosyltransferase	1,310	0,874
IPI00714294.3	Adenosylhomocysteinase	1,026	1,007
IPI00691361.3	Adenylyl cyclase-associated protein 1	0,973	1,065
IPI00706451.3	ADP-ribosylation factor 4	0,993	0,925
IPI00705378.2	ADP/ATP translocase 3	0,966	1,070
IPI01000167.1	AHNAK nucleoprotein	0,899	0,962
IPI00689965.4	AHNAK nucleoprotein 2	0,890	0,902
IPI00824539.2	AHNAK nucleoprotein, partial	0,918	0,971
IPI00686984.3	Alcohol dehydrogenase [NADP+]	1,009	1,027
IPI00705226.4	Aldehyde dehydrogenase, mitochondrial	1,220	1,115

IPI00705186.1	Aldehyde oxidase	0,928	0,883
IPI00700920.1	Aldo-keto reductase family 1, member B1	0,784	0,866
IPI00712164.1	Aldose 1-epimerase	1,037	1,035
IPI00702768.5	Alkaline phosphatase, tissue-nonspecific isozyme	**1,650**	1,002
IPI00695489.1	Alpha-1-antiproteinase	0,870	1,077
IPI00707101.1	Alpha-2-HS-glycoprotein	0,792	1,282
IPI00871133.1	Alpha-2-macroglobulin	0,822	0,847
IPI00712562.1	Alpha-actinin-1	0,695	1,066
IPI00713468.1	Alpha-actinin-4	0,958	0,961
IPI00688530.1	Alpha-crystallin B chain	**0,548**	1,234
IPI00707095.3	Alpha-enolase	1,138	0,983
IPI00726194.5	alpha-galactosidase A	1,296	1,120
IPI00697359.3	Alpha-N-acetylgalactosaminidase	1,221	0,929
IPI00698059.2	Amine oxidase [flavin-containing] A	1,279	1,004
IPI00703345.2	Annexin A1	1,112	0,837
IPI00706002.2	Annexin A2	1,145	0,995
IPI00686981.2	Annexin A4	0,904	0,933
IPI00692093.3	Annexin A5	0,804	0,983
IPI00868644.1	Annexin A6	0,992	1,018
IPI00694787.3	Annexin A7	0,982	1,010
IPI00699333.1	Annexin A8	1,188	0,859
IPI00845219.1	AP-2 complex subunit beta	0,977	0,980
IPI00700286.1	Arginyl-tRNA synthetase, cytoplasmic	1,043	0,866
IPI00716331.3	Asparagine synthetase [glutamine-hydrolyzing]	0,676	0,985
IPI00694612.3	Aspartate aminotransferase, cytoplasmic	1,032	1,009
IPI00713137.1	Aspartate aminotransferase, mitochondrial	0,848	1,206
IPI00696237.3	Aspartyl aminopeptidase	0,844	1,099
IPI00715362.1	Aspartyl-tRNA synthetase, cytoplasmic	1,031	0,999
IPI00693170.2	Aspartylglucosaminidase	1,036	1,140
IPI00694295.1	ATP synthase subunit alpha, mitochondrial	1,005	1,277
IPI00717884.1	ATP synthase subunit beta, mitochondrial	0,996	1,175
IPI00712252.2	ATP synthase subunit d, mitochondrial	1,017	1,147
IPI00714379.2	ATP synthase subunit O, mitochondrial	1,069	1,263
IPI00705528.1	ATP synthase-coupling factor 6, mitochondrial	0,990	1,444
IPI00714708.1	ATP-dependent RNA helicase A	0,979	1,142
IPI00717362.1	Barrier-to-autointegration factor	1,085	1,163
IPI00704694.3	BCL2-like 13	0,972	0,919
IPI00905257.2	beta actin	0,963	0,940

IPI00699237.1	Beta-galactosidase	1,083	1,051
IPI00702413.3	Beta-hexosaminidase subunit alpha	1,163	0,981
IPI00706203.3	beta-hexosaminidase subunit beta preproprotein	1,148	1,005
IPI00724051.2	Bifunctional purine biosynthesis protein PURH	0,948	0,951
IPI00716881.2	Biphenyl hydrolase-like	1,020	1,091
IPI00705815.2	Brain acid soluble protein 1	0,881	1,043
IPI00826794.1	bucentaur-2	1,082	0,941
IPI00690393.3	C-type mannose receptor 2	1,054	0,977
IPI00711008.1	Cadherin-13	0,749	1,063
IPI00699719.6	calcium channel, voltage-dependent, alpha 2/delta subunit 1	1,207	1,136
IPI00704434.4	Calcium/calmodulin-dependent protein kinase II delta	0,975	1,093
IPI00695508.4	Calmodulin	0,941	1,150
IPI00696263.1	Calpain small subunit 1	0,932	1,046
IPI00708219.2	Calpain-1 catalytic subunit	0,974	0,834
IPI00695673.4	Calpain-2 catalytic subunit	0,994	1,032
IPI00688469.1	calponin 3 isoform 1	0,957	1,046
IPI00687658.3	Calponin-2	0,940	1,180
IPI00691963.1	Calreticulin	1,067	1,004
IPI00716493.1	Calumenin	0,993	0,954
IPI01001835.1	cAMP-dependent protein kinase, regulatory subunit alpha 2	0,989	1,063
IPI00715046.1	Canopy 2 homolog	1,020	1,064
IPI00871078.1	Canx protein	1,122	0,883
IPI00697781.1	CAP1 protein-like	0,832	0,867
IPI01000621.1	carbonic anhydrase IX-like isoform 3	1,239	**1,796**
IPI00716785.2	Carnitine O-palmitoyltransferase 2, mitochondrial	1,063	0,968
IPI00867349.1	CAST protein (Fragment)	0,844	0,998
IPI00705932.2	Catalase	1,170	0,871
IPI00715690.1	Catenin alpha-1	1,085	1,023
IPI00718444.5	catenin delta-1	1,075	0,981
IPI00692061.2	Cathepsin B	1,147	0,965
IPI00709876.1	Caveolin-1	0,968	1,025
IPI00723023.3	CBX3 protein	1,259	0,811
IPI00686645.2	CD9 antigen	1,313	1,160
IPI00686662.4	CD99 antigen-like	1,155	1,396
IPI00710012.4	chaperonin containing TCP1, subunit 5	0,944	0,913
IPI00693645.3	Chloride intracellular channel protein 1	1,119	0,958
IPI00717902.4	Chloride intracellular channel protein 4	0,929	0,980
IPI00699260.1	Citrate synthase, mitochondrial	0,887	1,100

IPI00688816.1	Clathrin heavy chain 1	0,946	1,024
IPI00718757.5	Coactosin-like protein	1,012	1,045
IPI00712785.2	Coatomer subunit beta	0,896	1,063
IPI00706476.3	Coatomer subunit beta'	0,939	0,843
IPI00706192.1	Coatomer subunit delta	1,099	0,837
IPI00696888.3	Coatomer subunit epsilon	1,280	0,928
IPI00717350.3	Coatomer subunit gamma	0,983	1,004
IPI00699700.2	Cofilin-1	0,923	0,882
IPI00707857.2	Collagen alpha-1(I) chain	1,022	0,947
IPI01003695.1	collagen alpha-1(V) chain-like	0,995	0,784
IPI00708244.1	Collagen alpha-2(I) chain	1,050	0,994
IPI00731432.2	Collagen, type III, alpha 1	1,357	0,841
IPI00700909.1	COP9 signalosome complex subunit 4	0,899	1,071
IPI00695379.1	Craniofacial development protein 2	0,991	1,175
IPI00708129.1	Cystatin-B	1,128	1,078
IPI00718193.2	Cysteine and glycine-rich protein 1	0,937	0,921
IPI00717036.3	Cysteine and glycine-rich protein 2	0,667	1,131
IPI00695536.2	Cysteine-rich protein 1	0,757	0,933
IPI00693776.2	Cysteine-rich protein 2	0,895	0,860
IPI00685808.1	cytochrome b-c1 complex subunit 2, mitochondrial-like	0,786	1,127
IPI00708779.1	Cytochrome c oxidase subunit 2	0,998	1,154
IPI00724136.3	Cytochrome P450, subfamily IIIA, polypeptide 4	0,998	0,872
IPI01002580.1	cytoskeleton-associated protein 4	1,099	1,043
IPI00694082.1	Cytosolic non-specific dipeptidase	0,887	1,093
IPI00702726.5	Cytosolic phospholipase A2	1,269	1,034
IPI00699717.2	D-3-phosphoglycerate dehydrogenase	0,850	0,851
IPI00905293.2	Ddx3y (Fragment)	0,846	1,096
IPI00716534.4	DEAD (Asp-Glu-Ala-Asp) box polypeptide 1	1,028	0,957
IPI00688878.1	Dehydrogenase/reductase SDR family member 7B	1,001	1,091
IPI00698435.2	Destrin	0,676	0,877
IPI00704993.1	dihydrolipoyl dehydrogenase, mitochondrial	0,865	1,354
IPI00692907.2	Dihydrolipoyllysine-residue succinyltransferase component of 2-oxoglutarate dehydrogenase complex, mitochondrial	0,901	1,104
IPI00698338.3	Dihydropyrimidinase-related protein 2	0,811	0,908
IPI00999424.1	DNA topoisomerase II, beta isozyme, partial	1,265	0,911
IPI00715890.2	DNA-(apurinic or apyrimidinic site) lyase	1,234	0,950
IPI00693977.1	Dolichyl-diphosphooligosaccharide--protein glycosyltransferase subunit 2	0,985	1,032
IPI00867334.1	DPP7 protein	1,173	1,027
IPI00687539.2	DPYSL3 protein	0,936	0,841

IPI00693929.3	Dynactin subunit 2	0,934	0,855
IPI00693516.1	Dynein light chain 1, cytoplasmic	0,968	0,960
IPI00843257.2	EF-hand domain-containing protein D2	1,017	1,022
IPI00707316.1	EH domain-containing protein 1	1,064	1,062
IPI00707559.3	Electron transfer flavoprotein subunit alpha, mitochondrial	1,037	0,999
IPI00712775.1	Elongation factor 1-alpha 1	0,837	0,997
IPI00685732.2	Elongation factor 1-beta	0,994	0,959
IPI00706632.1	Elongation factor 1-gamma	0,994	0,977
IPI00707751.3	Elongation factor 2	0,923	0,890
IPI00696052.1	Elongation factor Tu, mitochondrial	0,946	1,058
IPI00714673.3	Embryo-specific fibronectin 1 transcript variant	0,939	1,019
IPI00702891.2	Endoplasmic reticulum resident protein 29	0,980	0,853
IPI00687688.1	Endoplasmic reticulum resident protein 44	0,979	0,946
IPI00701876.1	Enoyl-CoA hydratase, mitochondrial	0,972	1,151
IPI00711862.1	Epididymal secretory protein E1	1,228	0,993
IPI00697691.3	erythrocyte membrane protein band 4.1-like 2	1,038	1,016
IPI00698793.1	Eukaryotic initiation factor 4A-I	1,070	0,993
IPI00711238.2	Eukaryotic initiation factor 4A-II	1,016	1,053
IPI00714818.1	Eukaryotic translation initiation factor 3 subunit H	0,984	1,071
IPI00700182.1	Eukaryotic translation initiation factor 4B	0,984	1,157
IPI00704728.2	Eukaryotic translation initiation factor 5A-1	0,938	0,992
IPI00713369.4	exportin-1	1,256	0,961
IPI00694641.2	Ezrin	0,803	0,887
IPI00694110.3	F-actin-capping protein subunit alpha-1	1,030	1,108
IPI00696451.3	F-actin-capping protein subunit alpha-2	0,910	1,136
IPI00706815.1	Fascin homolog 1, actin-bundling protein	1,270	0,980
IPI00705734.2	Fatty acid-binding protein, epidermal	**0,664**	0,791
IPI00702650.1	FGF-2 binding protein	1,140	1,076
IPI01002732.1	filamin B, beta isoform 2	1,056	1,074
IPI00971572.3	filamin-A	0,741	0,990
IPI00718510.2	Flavin reductase	1,192	0,831
IPI00692676.2	Four and a half LIM domains protein 2	**0,628**	1,094
IPI00704584.3	Fructose-1,6-bisphosphatase 1	1,063	1,374
IPI00852561.1	Fructose-bisphosphate aldolase	1,215	1,040
IPI00867095.1	Fructose-bisphosphate aldolase	1,237	0,948
IPI00690094.2	Galectin-1	1,001	0,970
IPI00715562.5	Galectin-3-binding protein	1,077	1,007
IPI00733616.2	Gamma-interferon-inducible lysosomal thiol reductase	1,259	1,045

IPI00715439.3	GCN1 general control of amino-acid synthesis 1-like 1	1,018	1,044
IPI00694255.2	Gelsolin	0,869	1,038
IPI00702314.1	General vesicular transport factor p115	1,097	0,877
IPI00713484.4	GLO1 protein	0,867	0,952
IPI00826614.2	glucose-6-phosphate dehydrogenase isoform 2	1,020	0,959
IPI00714446.3	Glucose-6-phosphate isomerase	1,171	0,956
IPI00692278.1	Glucosidase 2 subunit beta	1,059	0,810
IPI01003725.1	glucosidase, alpha; neutral AB isoform 1	0,954	0,961
IPI00717765.2	Glucosylceramidase	1,233	1,135
IPI00708246.1	Glutaminyl-tRNA synthetase	0,887	0,989
IPI00702151.3	Glutathione S-transferase Mu 1	1,090	0,911
IPI00686173.2	Glutathione S-transferase P	0,926	0,946
IPI00713814.2	Glyceraldehyde-3-phosphate dehydrogenase	1,236	0,943
IPI00685482.3	Glycogen phosphorylase, liver form	1,095	0,924
IPI00907362.1	Glycyl-tran synthetase (Fragment)	0,667	0,891
IPI00712620.2	Glycylpeptide N-tetradecanoyltransferase	1,102	0,777
IPI01001508.1	Golgi apparatus protein 1	1,093	0,861
IPI01002344.1	golgi autoantigen, golgin subfamily b, macrogolgin 1-like	0,912	1,042
IPI00701994.1	GrpE protein homolog 1, mitochondrial	0,940	1,183
IPI00705941.3	GTP-binding nuclear protein Ran	0,996	0,902
IPI00717465.1	GTP-binding protein SAR1a	0,862	1,128
IPI00706808.2	Guanine nucleotide-binding protein G(I)/G(S)/G(O) subunit gamma-2	1,085	1,069
IPI00703160.2	Guanine nucleotide-binding protein G(I)/G(S)/G(T) subunit beta-1	1,013	1,025
IPI00712819.2	Guanine nucleotide-binding protein G(I)/G(S)/G(T) subunit beta-2	0,959	0,920
IPI00718393.1	Guanine nucleotide-binding protein subunit alpha-14	1,081	1,045
IPI00700792.3	Guanine nucleotide-binding protein subunit beta-2-like 1	0,982	1,042
IPI00691968.4	GUSB protein	1,208	1,098
IPI00689641.3	H1 histone family, member X-like	1,260	1,013
IPI00696488.1	hCG1994130-like	0,992	0,959
IPI00700035.1	Heat shock 70 kDa protein 1B	1,146	1,128
IPI00708526.2	Heat shock cognate 71 kDa protein	0,977	1,019
IPI00708342.1	heat shock protein 70-like	1,238	1,336
IPI00704110.3	Heat shock protein beta-6	0,938	0,932
IPI00699622.3	Heat shock protein HSP 90-alpha	0,973	0,949
IPI00709435.3	Heat shock protein HSP 90-beta	0,994	0,922
IPI00701120.3	Heme-binding protein 1	0,929	1,179
IPI01000857.1	heparan sulfate proteoglycan 2	1,008	0,966
IPI00696746.1	Hepatoma-derived growth factor	1,041	1,078

IPI00706671.2	Heterochromatin protein 1-binding protein 3	1,165	1,193
IPI00692235.1	Heterogeneous nuclear ribonucleoprotein A1	1,157	1,012
IPI00696554.1	Heterogeneous nuclear ribonucleoprotein K	1,130	1,012
IPI00697891.4	heterogeneous nuclear ribonucleoprotein L	1,109	1,027
IPI00826962.3	heterogeneous nuclear ribonucleoprotein M isoform 2	1,234	1,025
IPI00688257.4	Heterogeneous nuclear ribonucleoprotein U	1,298	1,016
IPI00695201.4	Heterogeneous nuclear ribonucleoproteins A2/B1	1,122	1,196
IPI00687211.1	Hexokinase 1	1,241	1,058
IPI00703727.1	histone cluster 1, H1b-like	1,347	1,224
IPI00702167.2	histone cluster 1, H1e-like	1,303	1,201
IPI00712163.1	histone cluster 1, H2ag-like	1,077	1,088
IPI00705104.5	Histone H1.0	1,106	1,208
IPI00712399.2	Histone H2A	0,980	1,373
IPI00698339.3	Histone H2A	1,133	1,218
IPI00693947.1	Histone H2B	1,314	**1,550**
IPI00705000.1	Histone H2B	1,161	1,220
IPI00697542.2	HNRPDL protein	1,167	0,840
IPI00718101.3	Hsp90 co-chaperone Cdc37	0,981	0,941
IPI00712538.4	HtrA serine peptidase 1	1,120	1,373
IPI00702040.2	Hydroxysteroid (17-beta) dehydrogenase 4	0,981	1,017
IPI01000273.1	hypothetical protein, partial	**1,588**	0,970
IPI00686225.4	Hypoxanthine-guanine phosphoribosyltransferase	1,373	0,820
IPI00687334.4	Inner membrane protein, mitochondrial	1,092	1,124
IPI00687219.4	Inorganic pyrophosphatase	1,071	0,984
IPI00707643.3	Integrin alpha-V	1,147	1,031
IPI00703559.1	Integrin-linked protein kinase	0,931	0,953
IPI00715132.1	Interleukin enhancer binding factor 2, 45kDa	1,114	0,978
IPI01002098.2	Interleukin enhancer binding factor 3 isoform c (Fragment)	1,061	1,192
IPI00825494.4	IQ motif containing GTPase activating protein 1	0,978	1,011
IPI00699016.2	Isocitrate dehydrogenase [NAD] subunit alpha, mitochondrial	1,066	1,052
IPI01028293.1	isocitrate dehydrogenase [NADP] cytoplasmic	0,969	0,967
IPI00714468.2	Isocitrate dehydrogenase [NADP], mitochondrial	0,816	1,153
IPI00704257.2	Isoform 1 of Cell division control protein 42 homolog	0,987	0,887
IPI00695660.4	Isoform 1 of Integrin beta-1	0,965	1,070
IPI00685721.1	Isoform 1 of PDZ and LIM domain protein 7	0,743	1,081
IPI00718311.3	Isoform 1 of Proactivator polypeptide	0,968	1,115
IPI00715226.4	Isoform 1 of Protein-L-isoaspartate(D-aspartate) O-methyltransferase	0,981	1,035
IPI00742580.1	Isoform 2 of 40S ribosomal protein S24	0,933	1,089

IPI00829526.1	Isoform 2 of Cytosol aminopeptidase	1,180	0,903
IPI00697756.2	Isoform 2 of Myosin-Ic	0,972	1,077
IPI00714405.3	Isoform 2 of Tropomyosin alpha-3 chain	0,939	1,154
IPI00703268.2	Isoform 2 of Tropomyosin beta chain	0,787	1,133
IPI01017561.2	Isoform 3 of Microtubule-associated protein 4	0,844	0,930
IPI00691138.3	Isoform AK2B of Adenylate kinase 2, mitochondrial	1,057	0,912
IPI00706541.1	Isoform B of Phosphate carrier protein, mitochondrial	0,982	0,957
IPI00714725.1	Isoform Beta-2 of F-actin-capping protein subunit beta	0,974	0,961
IPI00760445.2	Isoform Cytoplasmic+peroxisomal of Peroxiredoxin-5, mitochondrial	0,976	1,132
IPI00691827.2	Isoform Liver of ATP synthase subunit gamma, mitochondrial	1,013	1,201
IPI00760424.3	Isoform Short of 14-3-3 protein beta/alpha	0,873	0,890
IPI00716013.2	Isoform Smooth muscle of Myosin light polypeptide 6	0,839	1,136
IPI00701608.1	Isoform V3 of Versican core protein	0,856	0,828
IPI00695838.2	KN motif and ankyrin repeat domain-containing protein 2	1,180	0,869
IPI00867199.1	KTN1 protein	1,034	1,047
IPI00686760.1	L-caldesmon	0,883	1,038
IPI00906445.1	L-lactate dehydrogenase	1,209	0,944
IPI00760524.3	L-lactate dehydrogenase B chain	0,933	0,915
IPI00714765.2	LanC lantibiotic synthetase component C-like 1	1,057	0,949
IPI00714481.2	LDLR chaperone MESD	0,989	0,964
IPI00692681.1	Leucine-rich repeat-containing protein 59	0,941	0,999
IPI00712013.3	leucyl-cystinyl aminopeptidase-like	0,802	1,205
IPI00686735.1	LIM and SH3 domain protein 1	0,876	1,012
IPI00854503.1	LMAN1 protein	1,055	0,923
IPI00709524.3	LMO7 protein	0,893	0,998
IPI00685576.1	Lon protease homolog, mitochondrial	0,938	1,062
IPI00687044.3	Lupus La protein homolog	1,037	1,009
IPI00695601.1	Lysosomal alpha-glucosidase	1,191	1,090
IPI00705699.1	Lysosomal alpha-mannosidase	1,265	0,977
IPI00687092.1	Lysosomal protective protein	1,026	1,088
IPI00842574.1	lysosomal-associated membrane protein 2 isoform 2	**0,638**	0,721
IPI00705401.3	Lysosome-associated membrane glycoprotein 1	0,812	0,916
IPI00718673.3	M-RIP protein	0,877	0,854
IPI00694142.3	Macrophage migration inhibitory factor	**1,645**	1,024
IPI00693691.1	Macrophage-capping protein	0,810	1,035
IPI00709302.2	Major vault protein	1,032	1,076
IPI00699109.3	Malate dehydrogenase, cytoplasmic	0,906	1,048
IPI00712250.1	Malate dehydrogenase, mitochondrial	0,870	1,114

IPI00714950.5	Malic enzyme	1,153	0,992
IPI00732135.3	MAP2K1 protein	1,000	0,957
IPI00786391.1	MHC class I antigen (Fragment)	1,192	0,997
IPI00697813.3	microtubule-associated protein 1A-like	1,179	0,923
IPI00712266.1	Mitochondrial inner membrane protein OXA1L	1,206	1,183
IPI00697915.2	Mitochondrial trifunctional protein, beta subunit	1,039	1,279
IPI00713672.3	Mitogen-activated protein kinase 1	1,015	0,848
IPI00727417.4	Moesin	1,032	1,043
IPI01000866.1	myoferlin isoform 2	1,046	0,961
IPI00687409.3	Myosin regulatory light chain 12B	0,892	1,101
IPI00709219.1	Myosin-10	1,010	1,108
IPI00713054.3	Myosin-Id	1,168	1,094
IPI01001130.1	myosin, heavy chain 9, non-muscle	0,860	1,083
IPI00703141.1	N-acetylgalactosamine-6-sulfatase	1,189	1,067
IPI00703612.3	N-acetylglucosamine-6-sulfatase	1,213	1,052
IPI00718600.4	N-acylglucosamine 2-epimerase	0,883	0,938
IPI00715415.1	N(G),N(G)-dimethylarginine dimethylaminohydrolase 2	0,983	1,075
IPI00689030.2	NADH dehydrogenase [ubiquinone] 1 alpha subcomplex subunit 5	0,946	1,101
IPI00868665.1	NADH-cytochrome b5 reductase 3	0,968	0,956
IPI00698385.1	Nascent polypeptide-associated complex subunit alpha	0,837	1,003
IPI01000029.2	nestin	**0,660**	1,240
IPI00693385.3	niban protein-like	1,135	0,979
IPI00700403.2	Nipsnap homolog 3A	1,002	1,199
IPI01002058.1	NME1-NME2 protein-like	0,949	0,974
IPI00722271.2	Nucleobindin-1	0,961	1,073
IPI01003576.1	nucleolar protein 58	1,066	1,117
IPI00971535.1	nucleolin	1,005	1,019
IPI00689902.1	Nucleophosmin	0,953	1,122
IPI00968635.1	nucleosome assembly protein 1-like 1 isoform 1	0,869	1,021
IPI00843042.2	Nucleosome assembly protein 1-like 4	0,938	1,069
IPI00724124.1	Obg-like ATPase 1	1,088	0,976
IPI00708018.2	Oligoribonuclease, mitochondrial (Fragment)	1,095	1,109
IPI00707351.2	Ornithine aminotransferase, mitochondrial	0,776	1,201
IPI00689005.7	palladin, cytoskeletal associated protein	0,965	0,954
IPI00709294.1	Palmitoyl-protein thioesterase 1	1,130	1,292
IPI00687999.4	Parathymosin	1,000	0,956
IPI00694169.4	paxillin-like	0,923	1,089
IPI00712021.2	PDCD6 protein	0,973	1,111

IPI00700710.2	PDZ and LIM domain protein 1	1,016	0,944
IPI00697285.3	Peptidyl-prolyl cis-trans isomerase A	0,922	0,944
IPI00702098.4	Peptidyl-prolyl cis-trans isomerase B	0,998	0,948
IPI00699838.3	Peptidyl-prolyl cis-trans isomerase C	0,911	1,043
IPI00697856.1	Peptidyl-prolyl cis-trans isomerase FKBP10	1,164	0,921
IPI00689629.1	Peptidyl-prolyl cis-trans isomerase FKBP11	1,074	0,933
IPI00698916.2	Peptidyl-prolyl cis-trans isomerase FKBP1A	0,972	0,897
IPI00712144.1	Peptidyl-prolyl cis-trans isomerase FKBP2	1,251	1,172
IPI00693278.1	Peptidyl-prolyl cis-trans isomerase FKBP9	1,060	0,921
IPI00686092.1	Peroxiredoxin-1	0,999	0,959
IPI00713112.1	Peroxiredoxin-2	1,146	0,985
IPI00691994.1	Peroxiredoxin-4	0,990	1,270
IPI00689857.2	Peroxiredoxin-6	1,080	0,982
IPI00704735.2	Phosphatidylethanolamine-binding protein 1	0,866	1,077
IPI00701244.3	Phosphatidylinositol 4-kinase alpha	0,862	1,063
IPI00704159.4	phosphoglucomutase 2	1,066	1,032
IPI00693718.2	Phosphoglucomutase 3	1,154	1,056
IPI00701643.2	Phosphoglucomutase-1	0,931	1,011
IPI00710895.3	Phosphoglycerate kinase 1	1,429	0,938
IPI00698589.3	Phosphoglycerate mutase 1	1,236	0,969
IPI00712643.3	Phospholipase B-like 1	0,902	0,941
IPI00711106.2	Phospholipase D3	0,983	0,904
IPI00867128.1	Phosphoserine aminotransferase	0,854	0,819
IPI00701167.2	Phosphoserine phosphatase	0,793	0,966
IPI00788547.1	Plastin-3	0,692	1,040
IPI00692295.1	Platelet-activating factor acetylhydrolase IB subunit beta	0,930	1,023
IPI00687560.1	Poly(rC)-binding protein 1	1,015	0,925
IPI00705440.1	Polyadenylate-binding protein 1	1,039	1,029
IPI00883444.1	polymerase I and transcript release factor isoform 2	1,007	1,155
IPI00712263.2	Polypyrimidine tract-binding protein 1	1,151	1,058
IPI00786471.2	Polyubiquitin-B	1,005	1,002
IPI00708597.1	PRA1 family protein 3	1,005	0,950
IPI00883375.1	PRDX3 protein	0,978	0,965
IPI00693034.1	Pro-cathepsin H	0,930	1,081
IPI01017582.2	probable transcription factor PML	1,168	1,050
IPI00718774.2	Procollagen-lysine,2-oxoglutarate 5-dioxygenase 1	0,981	0,903
IPI00694107.2	Profilin-1	1,012	0,942
IPI00688006.1	Prohibitin	1,023	1,059

IPI00700678.2	Prolyl 4-hydroxylase subunit alpha-1	**1,653**	0,814
IPI00838420.3	prolyl 4-hydroxylase subunit alpha-2 isoform 2	1,204	0,796
IPI00691552.1	Prolyl endopeptidase	0,883	0,792
IPI00685444.1	Prostacyclin synthase	0,794	1,045
IPI00712216.2	Prostaglandin E synthase 3	1,145	1,115
IPI00688636.4	Prostaglandin G/H synthase 1	1,332	1,174
IPI00905104.3	Proteasome 26S non-ATPase subunit 11	1,015	0,934
IPI00707279.1	Proteasome activator complex subunit 1	1,205	0,962
IPI00697970.2	Proteasome activator complex subunit 2	1,069	1,047
IPI00687075.1	Proteasome subunit alpha type-1	0,946	1,035
IPI00713535.3	Proteasome subunit alpha type-2	0,947	1,186
IPI00705531.1	Proteasome subunit alpha type-4	0,927	1,017
IPI00707875.1	Proteasome subunit alpha type-5	1,158	0,877
IPI00715748.1	Proteasome subunit alpha type-6	1,056	1,125
IPI00695078.2	Proteasome subunit alpha type-7	0,910	1,048
IPI00722440.1	Proteasome subunit beta type-1	0,945	1,083
IPI00712187.2	Proteasome subunit beta type-7	0,884	1,017
IPI00709465.1	Protein disulfide-isomerase	1,235	0,890
IPI00706136.2	Protein disulfide-isomerase A4	1,166	0,912
IPI01017790.1	protein disulfide-isomerase A6	1,181	0,952
IPI00702765.1	Protein DJ-1	0,981	0,859
IPI00716264.2	Protein kinase C delta-binding protein	0,910	1,198
IPI00685792.2	Protein S100-A10	1,115	1,136
IPI00705400.2	Protein S100-A13	0,934	1,053
IPI00698663.2	Protein S100-A4	1,135	1,060
IPI00692963.3	Protein transport protein Sec23A	1,036	0,914
IPI00687313.5	Protein transport protein Sec61 subunit alpha isoform 1	1,181	1,047
IPI00717573.2	Purine nucleoside phosphorylase	0,985	1,015
IPI00702401.3	Putative phospholipase B-like 2	1,127	1,034
IPI00701044.3	Pyridoxal kinase	**1,828**	0,747
IPI00694230.1	Pyrroline-5-carboxylate reductase 1, mitochondrial	0,745	0,998
IPI00715345.3	Pyruvate carboxylase, mitochondrial	0,718	1,230
IPI00694488.1	Pyruvate dehydrogenase E1 component subunit alpha, somatic form, mitochondrial	1,056	1,187
IPI00703729.1	Pyruvate dehydrogenase E1 component subunit beta, mitochondrial	1,076	1,126
IPI00839408.2	Pyruvate kinase	1,088	0,963
IPI00904243.1	Pyruvate kinase (Fragment)	1,082	1,315
IPI00698594.1	Rab GDP dissociation inhibitor alpha	1,105	0,985
IPI00713760.3	Rab GDP dissociation inhibitor beta	0,966	0,934

IPI00829520.1	RAB1A, member RAS oncogene family	0,883	0,873
IPI00711368.1	Radixin	1,013	1,005
IPI00696011.1	Ragulator complex protein LAMTOR2	0,995	1,027
IPI00700672.3	Ras suppressor protein 1	0,916	0,998
IPI00695221.3	Ras-related protein Rab-11A	1,006	0,956
IPI00727050.2	Ras-related protein Rab-1B	0,979	1,029
IPI00694198.1	Ras-related protein Rab-5C	1,059	1,044
IPI00704752.1	Ras-related protein Rab-7a	0,752	1,127
IPI00695776.1	Ras-related protein Rap-1b	0,961	0,993
IPI00847093.1	RCN1 protein	0,703	1,120
IPI00695166.3	Receptor expression-enhancing protein 5	0,934	1,100
IPI00686255.3	Reticulocalbin 2, EF-hand calcium binding domain	0,864	1,178
IPI00708234.3	Reticulocalbin-3	1,174	1,048
IPI00692627.3	Retinal dehydrogenase 1	0,766	0,759
IPI00716328.5	Rho GDP-dissociation inhibitor 1	0,950	0,895
IPI00842262.4	rho GTPase-activating protein 1	0,937	1,020
IPI00712042.1	Ribonuclease/angiogenin inhibitor 1	0,994	0,892
IPI00714344.2	ribosomal protein L18a-like	1,239	0,966
IPI00699826.1	ribosomal protein L9-like	0,946	1,050
IPI00904537.2	ribosomal protein S4, X-linked X-like	1,002	0,983
IPI00705463.4	RNA-binding protein FUS	1,064	0,863
IPI00867372.1	RPS6KA3 protein	1,131	1,185
IPI00730691.2	RTN4 protein	0,860	1,082
IPI00689436.3	S-formylglutathione hydrolase	0,852	0,973
IPI00867366.1	SCARB2 protein	0,956	1,015
IPI00702565.1	SEC22 vesicle trafficking protein homolog B	0,949	0,952
IPI01003866.1	SEC31 homolog A	0,982	0,936
IPI00825603.3	septin 9	1,154	0,862
IPI00718654.1	Serine hydroxymethyltransferase, mitochondrial	1,069	0,985
IPI00692211.3	Serine/arginine-rich splicing factor 1	1,141	1,129
IPI00688887.3	Serine/threonine-protein phosphatase 2A 65 kDa regulatory subunit A alpha isoform	1,018	0,968
IPI00707577.2	Serine/threonine-protein phosphatase 2A activator	1,135	0,877
IPI00708693.1	Serine/threonine-protein phosphatase 2A catalytic subunit alpha isoform	0,925	0,952
IPI00699798.1	Serine/threonine-protein phosphatase PP1-beta catalytic subunit	0,985	1,128
IPI00686948.1	Serpin B6	1,071	0,976
IPI00694938.1	Serpin H1	0,875	0,852
IPI01028455.1	Serum albumin	0,722	1,271
IPI00705229.2	Seryl-tRNA synthetase, cytoplasmic	0,809	0,935

IPI00728768.1	SET translocation	1,173	1,121
IPI00694580.1	SH3 domain-binding glutamic acid-rich-like protein 3	0,967	1,132
IPI00718020.1	Short-chain specific acyl-CoA dehydrogenase, mitochondrial	1,006	1,192
IPI00867096.1	Sideroflexin-3	0,961	1,137
IPI00693755.3	Similar to S100 calcium-binding protein A11 (Fragment)	0,924	0,993
IPI00705159.3	Sodium/potassium-transporting ATPase subunit alpha-1	0,982	1,093
IPI00698975.3	SPARC	**0,572**	0,911
IPI00690141.1	Spliceosome RNA helicase DDX39B	1,229	0,837
IPI00699430.1	SQRDL protein	1,214	1,123
IPI00695802.3	Staphylococcal nuclease domain-containing protein 1	1,035	0,920
IPI00710834.4	STOM protein	1,136	0,950
IPI00692247.1	Stress-70 protein, mitochondrial	0,771	0,959
IPI00717685.1	Stress-induced-phosphoprotein 1	1,054	1,062
IPI00692468.1	Superoxide dismutase [Mn], mitochondrial	1,267	1,154
IPI00867022.1	Surfeit locus protein 4	1,150	0,904
IPI00689789.3	synaptic vesicle membrane protein VAT-1 homolog	0,686	0,978
IPI00999412.2	synaptonemal complex protein SC65-like, partial	1,177	0,981
IPI01003325.1	synaptotagmin binding, cytoplasmic RNA interacting protein isoform 1	1,044	1,011
IPI00686546.5	T-complex protein 1 subunit beta	0,947	1,001
IPI00841695.1	T-complex protein 1 subunit delta	0,965	1,025
IPI00700509.2	T-complex protein 1 subunit eta	0,942	0,937
IPI00714624.1	T-complex protein 1 subunit gamma	0,975	0,890
IPI00710726.3	T-complex protein 1 subunit theta	0,821	1,055
IPI00689377.3	T-complex protein 1 subunit zeta	0,944	1,070
IPI00685123.3	talin-1	0,942	0,980
IPI00688409.4	tankyrase 1 binding protein 1, 182kDa	1,032	1,018
IPI00924157.2	thiolester containing protein II-like, partial	1,405	0,923
IPI00712196.2	Thioredoxin	1,075	0,903
IPI00699038.4	thioredoxin domain-containing protein 5	0,951	0,848
IPI00696824.1	Thioredoxin-dependent peroxide reductase, mitochondrial	1,259	1,144
IPI00710588.1	THO complex subunit 4	1,184	1,007
IPI00711455.1	Threonyl-tRNA synthetase, cytoplasmic	0,946	0,808
IPI00691137.2	Thymosin beta-4	**0,602**	1,135
IPI00709756.4	TMEM43 protein	1,018	0,974
IPI00722240.4	TMX3 protein	0,948	1,087
IPI00711241.2	Transaldolase	1,032	0,891
IPI00699220.1	Transcription elongation factor B (SIII), polypeptide 2	1,251	0,897
IPI00686932.2	Transforming growth factor beta-1-induced transcript 1 protein	0,920	0,941

IPI00688998.3	Transforming protein RhoA	1,012	0,967
IPI00717279.5	Transgelin	**0,619**	0,962
IPI00702028.2	Transgelin-2	0,961	0,938
IPI00710727.1	Transitional endoplasmic reticulum ATPase	0,951	0,952
IPI00712420.1	Translocator protein	1,192	0,923
IPI00717836.3	Transmembrane emp24 domain-containing protein 10	1,021	0,980
IPI01017656.1	transmembrane emp24 domain-containing protein 4	1,119	1,165
IPI00689711.1	Transmembrane emp24 domain-containing protein 9	1,149	1,061
IPI00706942.3	Triosephosphate isomerase	1,234	0,979
IPI00906033.3	tropomyosin 2, beta-like isoform 1	0,876	1,007
IPI00708322.1	Tropomyosin alpha-1 chain	0,668	1,117
IPI00704325.1	Tryptophanyl-tRNA synthetase, cytoplasmic	0,852	0,777
IPI00721706.3	tubulin alpha-1B chain	0,886	0,891
IPI00700865.4	Tubulin alpha-1B chain	1,139	0,837
IPI00697107.2	Tubulin beta-2B chain	1,072	0,759
IPI00706594.1	Tubulin beta-2C chain	0,981	1,004
IPI00708046.1	Tubulin beta-5 chain	0,950	0,930
IPI00712127.3	Tubulin beta-6 chain	0,802	0,990
IPI00699740.2	Tubulin tyrosine ligase-like family, member 12	1,007	0,889
IPI00687540.2	Tyrosyl-tRNA synthetase, cytoplasmic	0,903	0,865
IPI00685112.6	ubiquitin specific peptidase 5 (isopeptidase T) isoform 2	1,032	0,944
IPI00711977.1	Ubiquitin-conjugating enzyme E2 L3	1,094	0,840
IPI00703470.2	Ubiquitin-conjugating enzyme E2 N	1,106	0,927
IPI00712671.1	UDP-glucose 6-dehydrogenase	0,929	0,889
IPI00999392.1	UDP-glucose glycoprotein glucosyltransferase 1	0,841	0,920
IPI00717207.3	UMP-CMP kinase	0,893	0,885
IPI00695852.3	Uncharacterized protein	0,738	**1,563**
IPI00689750.1	Uncharacterized protein	1,065	**1,531**
IPI00699808.3	Uncharacterized protein	1,082	1,463
IPI00692457.1	Uncharacterized protein	0,904	1,367
IPI00698430.1	Uncharacterized protein	0,807	1,331
IPI00705979.1	Uncharacterized protein	1,100	1,287
IPI00691433.1	Uncharacterized protein	0,947	1,276
IPI01017864.1	Uncharacterized protein	1,148	1,258
IPI00908135.2	Uncharacterized protein	0,955	1,254
IPI00905120.1	Uncharacterized protein	0,966	1,230
IPI00704977.4	Uncharacterized protein	**0,645**	1,227
IPI00711664.2	Uncharacterized protein	0,782	1,197

IPI00827006.2	Uncharacterized protein	1,215	1,192
IPI00701347.1	Uncharacterized protein	0,917	1,175
IPI00702365.1	Uncharacterized protein	0,953	1,171
IPI00924056.1	Uncharacterized protein	1,144	1,158
IPI00695331.1	Uncharacterized protein	0,996	1,153
IPI00867041.1	Uncharacterized protein	0,951	1,135
IPI00705248.2	Uncharacterized protein	0,987	1,133
IPI00698179.3	Uncharacterized protein	0,820	1,130
IPI00841240.2	Uncharacterized protein	0,976	1,129
IPI00696729.2	Uncharacterized protein	1,005	1,126
IPI00697783.3	Uncharacterized protein	1,007	1,125
IPI00843025.1	Uncharacterized protein	0,983	1,118
IPI00904774.1	Uncharacterized protein	0,846	1,117
IPI00841960.2	Uncharacterized protein	0,940	1,116
IPI00904104.1	Uncharacterized protein	1,017	1,112
IPI00694637.2	Uncharacterized protein	1,170	1,112
IPI00702457.1	Uncharacterized protein	1,075	1,110
IPI00690667.9	Uncharacterized protein	1,097	1,108
IPI00717554.3	Uncharacterized protein	1,078	1,106
IPI00717116.4	Uncharacterized protein	0,983	1,101
IPI00725254.2	Uncharacterized protein	1,440	1,100
IPI00707369.4	Uncharacterized protein	1,092	1,099
IPI00691896.4	Uncharacterized protein	1,002	1,099
IPI00701107.1	Uncharacterized protein	1,022	1,098
IPI00685613.1	Uncharacterized protein	0,970	1,098
IPI00688960.4	Uncharacterized protein	1,049	1,097
IPI00734138.2	Uncharacterized protein	1,081	1,095
IPI00691772.4	Uncharacterized protein	0,961	1,082
IPI00847122.2	Uncharacterized protein	1,085	1,081
IPI00692453.2	Uncharacterized protein	0,998	1,080
IPI00713881.2	Uncharacterized protein	0,983	1,075
IPI00714628.3	Uncharacterized protein	1,321	1,074
IPI00707201.2	Uncharacterized protein	1,017	1,071
IPI00707040.2	Uncharacterized protein	0,830	1,068
IPI00697568.3	Uncharacterized protein	0,967	1,066
IPI00710041.3	Uncharacterized protein	1,051	1,064
IPI00914500.1	Uncharacterized protein	0,952	1,060
IPI00691941.2	Uncharacterized protein	0,960	1,060

IPI00698213.3	Uncharacterized protein	1,101	1,059
IPI00838361.2	Uncharacterized protein	0,867	1,057
IPI00720815.3	Uncharacterized protein	0,897	1,055
IPI00730808.3	Uncharacterized protein	1,141	1,055
IPI01017728.2	Uncharacterized protein	0,725	1,054
IPI00825112.2	Uncharacterized protein	1,086	1,053
IPI00694835.4	Uncharacterized protein	1,197	1,052
IPI00838947.2	Uncharacterized protein	0,998	1,043
IPI00696325.1	Uncharacterized protein	1,230	1,038
IPI00725325.1	Uncharacterized protein	1,091	1,032
IPI00694851.1	Uncharacterized protein	1,095	1,026
IPI00690785.2	Uncharacterized protein	1,097	1,025
IPI00709240.2	Uncharacterized protein	0,976	1,023
IPI00711537.1	Uncharacterized protein	1,177	1,023
IPI00701183.2	Uncharacterized protein	1,125	1,018
IPI00727017.1	Uncharacterized protein	0,911	1,017
IPI00706784.1	Uncharacterized protein	1,150	1,016
IPI00866823.1	Uncharacterized protein	0,871	1,013
IPI00825390.3	Uncharacterized protein	0,928	1,008
IPI00700324.4	Uncharacterized protein	1,277	1,006
IPI00691090.3	Uncharacterized protein	1,001	1,005
IPI00703856.2	Uncharacterized protein	1,424	1,004
IPI00692544.1	Uncharacterized protein	1,164	1,001
IPI00688378.2	Uncharacterized protein	1,176	0,999
IPI00722050.4	Uncharacterized protein	0,761	0,996
IPI00699994.1	Uncharacterized protein	0,997	0,995
IPI00730219.2	Uncharacterized protein	1,189	0,993
IPI00908057.1	Uncharacterized protein	0,867	0,992
IPI00689444.2	Uncharacterized protein	0,883	0,992
IPI00685232.2	Uncharacterized protein	0,941	0,991
IPI00714855.2	Uncharacterized protein	0,922	0,991
IPI00721832.2	Uncharacterized protein	0,727	0,990
IPI00905569.1	Uncharacterized protein	1,005	0,986
IPI00702545.1	Uncharacterized protein	1,264	0,984
IPI00700851.2	Uncharacterized protein	1,063	0,984
IPI00914517.1	Uncharacterized protein	1,001	0,983
IPI00696708.3	Uncharacterized protein	1,051	0,981
IPI00703423.1	Uncharacterized protein	0,953	0,981

IPI00726312.3	Uncharacterized protein	0,920	0,978
IPI00716694.1	Uncharacterized protein	1,135	0,975
IPI00905408.1	Uncharacterized protein	1,173	0,972
IPI00686498.3	Uncharacterized protein	1,066	0,972
IPI00694267.3	Uncharacterized protein	0,911	0,972
IPI00691512.3	Uncharacterized protein	1,042	0,970
IPI00701999.2	Uncharacterized protein	0,937	0,968
IPI00839653.2	Uncharacterized protein	**0,380**	0,968
IPI01028037.1	Uncharacterized protein	1,024	0,965
IPI00908241.1	Uncharacterized protein	0,957	0,962
IPI00699124.2	Uncharacterized protein	1,237	0,962
IPI00906322.1	Uncharacterized protein	1,005	0,960
IPI00852512.1	Uncharacterized protein	1,127	0,956
IPI00685676.2	Uncharacterized protein	1,004	0,954
IPI00702461.2	Uncharacterized protein	1,000	0,952
IPI00732001.3	Uncharacterized protein	0,898	0,951
IPI00708684.2	Uncharacterized protein	0,893	0,950
IPI00704118.2	Uncharacterized protein	1,034	0,944
IPI00709361.1	Uncharacterized protein	0,996	0,937
IPI00713575.5	Uncharacterized protein	0,807	0,935
IPI00689218.3	Uncharacterized protein	1,094	0,933
IPI00904110.1	Uncharacterized protein	1,026	0,933
IPI00716130.1	Uncharacterized protein	1,060	0,932
IPI00734427.3	Uncharacterized protein	0,971	0,926
IPI00908231.1	Uncharacterized protein	**1,747**	0,921
IPI00718698.2	Uncharacterized protein	1,000	0,916
IPI00842075.1	Uncharacterized protein	1,011	0,911
IPI00843078.2	Uncharacterized protein	1,007	0,908
IPI00692516.2	Uncharacterized protein	1,083	0,906
IPI00714910.5	Uncharacterized protein	1,107	0,904
IPI00692865.2	Uncharacterized protein	1,124	0,903
IPI00690816.4	Uncharacterized protein	0,945	0,900
IPI00687601.2	Uncharacterized protein	0,964	0,889
IPI00718678.3	Uncharacterized protein	1,058	0,885
IPI00695031.5	Uncharacterized protein	0,984	0,883
IPI00710247.1	Uncharacterized protein	1,100	0,880
IPI00826022.4	Uncharacterized protein	1,084	0,879
IPI00709621.1	Uncharacterized protein	1,328	0,870

IPI00711789.4	Uncharacterized protein	0,731	0,859
IPI00691523.1	Uncharacterized protein	1,022	0,852
IPI00904732.1	Uncharacterized protein	1,001	0,847
IPI00867179.1	Uncharacterized protein	0,872	0,847
IPI00704480.3	Uncharacterized protein	1,211	0,837
IPI00692739.3	Uncharacterized protein	1,182	0,816
IPI00695425.1	Uncharacterized protein	0,983	0,801
IPI00713573.3	Uncharacterized protein	1,050	0,723
IPI00714359.3	Uncharacterized protein	1,359	0,681
IPI00707132.2	Uncharacterized protein (Fragment)	0,977	1,203
IPI00702412.3	Uncharacterized protein (Fragment)	0,686	1,197
IPI00843121.3	Uncharacterized protein (Fragment)	1,106	1,182
IPI00701919.4	Uncharacterized protein (Fragment)	1,103	1,101
IPI00838035.2	Uncharacterized protein (Fragment)	0,960	1,077
IPI00907801.1	Uncharacterized protein (Fragment)	1,102	1,045
IPI00686802.2	Uncharacterized protein (Fragment)	1,027	0,986
IPI00713306.5	Uncharacterized protein (Fragment)	0,953	0,978
IPI00711216.1	UPF0556 protein C19orf10 homolog	0,988	1,107
IPI00714864.1	Uroporphyrinogen decarboxylase	1,192	0,972
IPI00689863.2	UTP--glucose-1-phosphate uridylyltransferase	1,109	0,879
IPI00999882.1	utrophin-like	1,160	0,972
IPI00708797.2	UV excision repair protein RAD23 homolog B	0,883	1,054
IPI00686074.3	V-type proton ATPase catalytic subunit A	0,887	0,955
IPI00688522.2	V-type proton ATPase subunit B, brain isoform	0,863	1,061
IPI00695642.1	Vacuolar protein sorting-associated protein 35	0,962	1,143
IPI00696178.3	Very long-chain specific acyl-CoA dehydrogenase, mitochondrial	0,945	1,114
IPI00716830.3	Vesicle-associated membrane protein-associated protein A	0,865	0,939
IPI00689228.3	Vimentin	1,062	1,096
IPI00826289.7	vinculin isoform 2	0,769	0,939
IPI00712934.2	Vitronectin	1,004	**1,871**
IPI00703129.3	Voltage-dependent anion-selective channel protein 1	0,931	0,974
IPI00687246.2	Voltage-dependent anion-selective channel protein 2	1,041	1,058
IPI00716638.7	WD repeat-containing protein 1	1,034	0,992
IPI00695367.3	Xanthine dehydrogenase/oxidase	1,397	1,015
IPI00705781.3	Zyxin	0,842	0,952

TABLE 3: List of Putative Interacting Partners of CK2.

Proteins have been filtered for a minimum max fold change equal to 2.

ACCESSION	DESCRIPTION	PEPTIDE COUNT	PEPTIDES USED FOR QUANITATION	CONFIDENCE SCORE	MAX FOLD CHANGE
IPI00168728.1	IGHG3 FLJ00385 protein (Fragment)	2	2	72,41	29,89313942
IPI00016613.2	CSNK2A1 CSNK2A1 protein	12	10	389,91	20,04765931
IPI00010865.1	CSNK2B Casein kinase II subunit beta	3	3	104,57	18,8355688
IPI00020602.1	CSNK2A2 Casein kinase II subunit alpha'	7	4	191,64	14,49011359
IPI00217030.10	RPS4X 40S ribosomal protein S4, X isoform	5	4	113,59	8,344036218
IPI00027423.3	PPP1CA protein phosphatase 1, catalytic subunit, alpha isoform 3	3	3	95,22	7,486647749
IPI00001466.2	EML4 Echinoderm microtubule-associated protein-like 4	13	12	321,2	6,358604388
IPI00654777.2	EIF3F cDNA FLJ36192 fis, clone TESTI2027450, highly similar to Eukaryotic translation initiation factor 3 subunit 5	2	2	92,29	5,305279614
IPI00027443.5	CARS cysteinyl-tRNA synthetase isoform c	5	5	84,82	5,174219848
IPI00398625.5	HRNR Hornerin	17	17	303,64	4,609352401
IPI00007188.5	SLC25A5 ADP/ATP translocase 2	3	3	73,09	4,524956984
IPI00012998.2	CPSF6 Isoform 1 of Cleavage and polyadenylation specificity factor subunit 6	7	7	221,91	4,429745822
IPI00396378.3	HNRNPA2B1 Isoform B1 of Heterogeneous nuclear ribonucleoproteins A2/B1	11	8	256,27	4,213231122
IPI00647650.3	EIF3H Eukaryotic translation initiation factor 3, subunit 3 gamma, 40kDa, isoform CRA_b	2	2	97,72	4,201924711
IPI00376798.3	RPL11 Isoform 1 of 60S ribosomal protein L11	3	2	153,68	4,141549406
IPI00396485.3	EEF1A1 Elongation factor 1-alpha 1	9	3	366,49	3,969314756
IPI00008530.1	RPLP0 60S acidic ribosomal protein P0	5	5	180	3,864048442
IPI00216592.2	HNRNPC Isoform C1 of Heterogeneous nuclear ribonucleoproteins C1/C2	9	9	242,4	3,851671809
IPI00215719.6	RPL18 60S ribosomal protein L18	2	2	44,35	3,735313112
IPI00217053.6	PRRC1 Isoform 3 of Protein PRRC1	4	4	157,07	3,697064914
IPI00334587.1	HNRNPAB Isoform 2 of Heterogeneous nuclear ribonucleoprotein A/B	3	2	125,86	3,66735887
IPI00220642.7	YWHAG 14-3-3 protein gamma	3	1	79,12	3,666287882
IPI00215965.3	HNRNPA1 Isoform A1-B of Heterogeneous nuclear ribonucleoprotein A1	10	8	301,61	3,578960228
IPI00295400.1	WARS Isoform 1 of Tryptophanyl-tRNA synthetase, cytoplasmic	5	5	157,71	3,511286061
IPI00465028.7	RCTPI1;TPI1 triosephosphate isomerase 1 isoform 2	2	2	25,07	3,364652583

IPI00010303.1	SERPINB4 Serpin B4	4	4	87,67	3,312835655
IPI00641829.5	BAT1 Isoform 2 of Spliceosome RNA helicase BAT1	2	2	65,15	3,201041176
IPI00027834.3	HNRNPL Heterogeneous nuclear ribonucleoprotein L	2	2	60,69	3,12457241
IPI00020127.1	RPA1 Replication protein A 70 kDa DNA-binding subunit	7	7	189,18	2,991266202
IPI00220740.1	NPM1 Isoform 2 of Nucleophosmin	2	2	45,51	2,933193851
IPI00028888.1	HNRNPD Isoform 1 of Heterogeneous nuclear ribonucleoprotein D0	4	4	140,76	2,904375648
IPI00021266.1	RPL23A 60S ribosomal protein L23a	2	2	38,41	2,804619721
IPI00290461.3	EIF3J Eukaryotic translation initiation factor 3 subunit J	5	5	81,8	2,799872012
IPI00000874.1	PRDX1 Peroxiredoxin-1	2	2	48,09	2,788838562
IPI00465361.4	RPL13 60S ribosomal protein L13	4	3	98,57	2,664698051
IPI00216049.1	HNRNPK Isoform 1 of Heterogeneous nuclear ribonucleoprotein K	5	5	113,13	2,647313248
IPI00219018.7	GAPDH Glyceraldehyde-3-phosphate dehydrogenase	6	5	216,94	2,59118413
IPI00026272.2	HIST1H2AE;HIST1H2AB;HIST1H2AD;HIST1H2AK;HIST1H2AL;HIST1H2AM;HIST1H2AJ;HIST1H2AI;HIST1H2AG Histone H2A type 1-B/E	2	2	55,82	2,552858568
IPI00011268.2	RALY RNA binding protein, autoantigenic (HnRNP-associated with lethal yellow homolog (Mouse)), isoform CRA_a (Fragment)	3	3	73,57	2,489303372
IPI00003865.1	HSPA8 Isoform 1 of Heat shock cognate 71 kDa protein	12	7	399,5	2,463322446
IPI00021439.1	ACTB Actin, cytoplasmic 1	13	1	540,44	2,457953708
IPI00479217.1	HNRNPU Isoform Short of Heterogeneous nuclear ribonucleoprotein U	8	8	221,6	2,380321613
IPI00030179.3	RPL7P32;RPL7 60S ribosomal protein L7	5	2	165,14	2,371963403
IPI00646304.4	PPIB Peptidyl-prolyl cis-trans isomerase B	5	5	160,97	2,370332193
IPI00003918.6	RPL4 60S ribosomal protein L4	5	5	150,3	2,360308303
IPI00017617.1	DDX5 Probable ATP-dependent RNA helicase DDX5	3	3	106,68	2,331237571
IPI00465439.5	ALDOA Fructose-bisphosphate aldolase A	4	4	178,66	2,326268546
IPI00005198.2	ILF2 Interleukin enhancer-binding factor 2	3	3	138,69	2,289706176
IPI00299000.5	PA2G4 Proliferation-associated protein 2G4	6	6	164,36	2,285557484
IPI00007765.5	HSPA9 Stress-70 protein, mitochondrial	6	5	170,75	2,262335033
IPI00410693.4	SERBP1 SERPINE1 mRNA binding protein 1, isoform CRA_d	5	5	184,28	2,228234724
IPI00000875.7	TUT1;EEF1G cDNA FLJ56389, highly similar to Elongation factor 1-gamma	2	2	31,12	2,227613715
IPI00178440.3	EEF1B2 Elongation factor 1-beta	2	1	37,35	2,207714794
IPI00169383.3	PGK1 Phosphoglycerate kinase 1	2	1	47,23	2,20057822
IPI00021263.3	YWHAZ 14-3-3 protein zeta/delta	4	4	127,33	2,179143719

IPI00465248.5	ENO1 Isoform alpha-enolase of Alpha-enolase	2	2	52,89	2,165466334
IPI00013881.6	HNRNPH1 Heterogeneous nuclear ribonucleoprotein H	5	5	74,24	2,165449878
IPI00010204.1	SFRS3 Splicing factor, arginine/serine-rich 3	2	2	42,27	2,135453127
IPI00011416.2	ECH1 Delta(3,5)-Delta(2,4)-dienoyl-CoA isomerase, mitochondrial	2	1	52,13	2,122382683
IPI00069693.4	- Putative uncharacterized protein RPL14P1	2	2	36,46	2,094414608
IPI00644570.1	- 18 kDa protein	2	1	64,76	2,058228663
IPI00784154.1	HSPD1 60 kDa heat shock protein, mitochondrial	5	4	189,49	2,048808807

TABLE 4: Annotated List of Putative Interacting Partners of CK2.

Information about function, relation with CK2 and eventual phosphorylation are collected from the literature.

ACCESSION	DESCRIPTION	FUNCTION	CELLULAR LOCALIZATION	PHOSPHORYLATED BY CK2	RELATED TO CK2
Proteins involved in signaling pathways					
IPI00016613.2	CSNK2A1 CSNK2A1 protein	Catalytic subunit of a constitutively active serine/threonine-protein kinase complex that phosphorylates a large number of substrates containing acidic residues C-terminal to the phosphorylated serine or threonine. CK2 regulates several cellular processes, such as cell cycle progression, apoptosis and transcription, and it is also involved in viral infection. It partecipates in Wnt signaling.	ubiquitarious	yes	yes
IPI00010865.1	CSNK2B Casein kinase II subunit beta	Regulatory subunit of CK2 complex. It plays a complex role in regulating the basal catalytic activity of the alpha subunit. It partecipates in Wnt signaling.	ubiquitarious	yes	yes
IPI00020602.1	CSNK2A2 Casein kinase II subunit alpha'	Catalytic subunit of a constitutively active serine/threonine-protein kinase complex that phosphorylates a large number of substrates containing acidic residues C-terminal to the phosphorylated serine or threonine. CK2 regulates several cellular processes, such as cell cycle progression, apoptosis and transcription, and it is also involved in viral infection. It partecipates in Wnt signaling.	ubiquitarious	yes	yes
IPI00021263.3	YWHAZ 14-3-3 protein zeta/delta	Adapter protein implicated in the regulation of a wide spectrum of both general and specialized signaling pathways. Binds to a large number of partners, usually by recognition of a phosphoserine or phosphothreonine motif. Binding generally results in the modulation of the activity of the binding partner. (*Obsilova et al, Biochemistry 2005*)	cytoplasm - melaosome	no	no
IPI00220642.7	YWHAG 14-3-3 protein gamma	Adapter protein implicated in the regulation of a wide spectrum of both general and specialized signaling pathways. Binds to a large number of partners, usually by recognition of a phosphoserine or phosphothreonine motif. Binding generally results in the modulation of the activity of the binding partner. (*Jin et al, EMBO J. 2006*; *Obsilova et al, Biochemistry 2005*)	cytoplasm	no	no
Proteins involved in synthesis					
IPI00654777.2	EIF3F cDNA FLJ36192 fis, clone TESTI2027450, highly similar to Eukaryotic translation initiation factor 3 subunit 5	Component of the eukaryotic translation initiation factor 3 (eIF-3) complex, which is required for several steps in the initiation of protein synthesis. EIF3 was the first endogenous sustrate of CK2 to be identified. (*Pinna, Cell. Molec. Biol. Res. 1994*)	cytoplasm	no	yes
IPI00647650.3	EIF3H Eukaryotic translation initiation factor 3, subunit 3 gamma, 40kDa, isoform CRA_b	Component of the eukaryotic translation initiation factor 3 (eIF-3) complex, which is required for several steps in the initiation of protein synthesis. EIF3 was the first endogenous sustrate of CK2 to be identified. (*Pinna, Cell. Molec. Biol. Res. 1994*)	nucleus - cytoplasm	yes	yes
IPI00290461.3	EIF3J Eukaryotic translation initiation factor 3 subunit J	Component of the eukaryotic translation initiation factor 3 (eIF-3) complex, which is required for several steps in the initiation of protein synthesis. This subunit binds directly within the mRNA entry channel of the 40S ribosome to the aminoacyl (A) site. It may regulate the interaction between the 43S PIC and mRNA. EIF3 was the first endogenous sustrate of CK2 to be identified. (*Pinna, Cell. Molec. Biol. Res. 1994*)	cytoplasm	no	no
IPI00396485.3	EEF1A1 Elongation factor 1-alpha 1	This protein promotes the GTP-dependent binding of aminoacyl-tRNA to the A-site of ribosomes during protein biosynthesis. With PARP1 and TXK, forms a complex that acts as a T helper 1 (Th1) cell-specific transcription factor and binds the promoter of IFN-gamma to directly regulate its transcription. In this way, it is importantly involved in Th1 cytokine production. (*Maruyama et al, Clin. Exp. Immunol. 2007*)	cytoplasm - nucleus	no	no
IPI00178440.3	EEF1B2 Elongation factor 1-beta	EF-1-beta and EF-1-delta stimulate the exchange of GDP bound to EF-1-alpha to GTP.	cytoplasm	yes	no
IPI00000875.7	TUT1;EEF1G cDNA FLJ56389, highly similar to Elongation factor 1-gamma	Probably plays a role in anchoring the complex to other cellular components.	cytoplasm	yes	yes
IPI00217030.10	RPS4X 40S ribosomal protein S4, X isoform	Structural constituent of ribosome responsible of the rRNA binding.	ribosome	no	no
IPI00376798.3	RPL11 Isoform 1 of 60S ribosomal protein L11	Binds to 5S ribosomal RNA. Required for rRNA maturation and formation of the 60S ribosomal subunits.	nucleus	no	no
IPI00021266.1	RPL23A 60S ribosomal protein L23a	This protein binds to a specific region on the 26S rRNA.	ribosome	no	no
IPI00003918.6	RPL4 60S ribosomal protein L4	Structural constituent of ribosome responsible of the RNA binding.	ribosome	no	no

IPI00215719.6	RPL18 60S ribosomal protein L18	Structural constituent of ribosome responsible of the RNA binding.	cytoplasm	no	no
IPI00465361.4	RPL13 60S ribosomal protein L13	A component of the 60S ribosomal subunit. Binds proteins.	ribosome	no	no
IPI00030179.3	RPL7P32;RPL7 60S ribosomal protein L7	Binds to G-rich structures in 28S rRNA and in mRNAs. Plays a regulatory role in the translation apparatus; inhibits cell-free translation of mRNAs.	ribosome	no	no
IPI00008530.1	RPLP0 60S acidic ribosomal protein P0	Structural constituent of ribosome with RNA and protein binding activity.	cytoplasm - nucleus	yes	yes
IPI00027443.5	CARS cysteinyl-tRNA synthetase isoform c	Enzyme involved in protein binding, homodimerization activity, cysteine-tRNA ligase activity, metal ion binding, nucleotide binding, ATP binding, ligase activity, and tRNA binding.	cytoplasm	no	no
IPI00295400.1	WARS Isoform 1 of Tryptophanyl-tRNA synthetase, cytoplasmic	Synthetase with regulative activity on ERK, Akt, and eNOS activation pathways that are associated with angiogenesis, cytoskeletal reorganization and shear stress-responsive gene expression.	cytoplasm	yes	no
IPI00027423.3	PPP1CA protein phosphatase 1, catalytic subunit, alpha isoform 3	May play an important role in dephosphorylating substrates such as the postsynaptic density-associated Ca2+/calmodulin dependent protein kinase II. Component of the PTW/PP1 phosphatase complex, which plays a role in the control of chromatin structure and cell cycle progression during the transition from mitosis into interphase. Regulates NEK2 function in terms of kinase activity and centrosome number and splitting, both in the presence and absence of radiation-induced DNA damage. (*Mi et al, Cancer Res. 2007*)	cytoplasm - nucleus	no	no
IPI00646304.4	PPIB Peptidyl-prolyl cis-trans isomerase B	PPIases accelerate the folding of proteins. It catalyzes the cis-trans isomerization of proline imidic peptide bonds in oligopeptides.	endoplasmatic reticulum - melanosome	no	no
IPI00784154.1	HSPD1 60 kDa heat shock protein, mitochondrial	Implicated in mitochondrial protein import and macromolecular assembly. May facilitate the correct folding of imported proteins. May also prevent misfolding and promote the refolding and proper assembly of unfolded polypeptides generated under stress conditions in the mitochondrial matrix.	mitochondria	no	no
Cytoskeletal/Structural proteins					
IPI00001466.2	EML4 Echinoderm microtubule-associated protein-like 4	May modify the assembly dynamics of microtubules, such that microtubules are slightly longer, but more dynamic. Strongly overexpressed during mitosis.	cytoskeleton	no	no
IPI00021439.1	ACTB Actin, cytoplasmic 1	Highly conserved protein involved in cell motility and ubiquitously expressed in all eukaryotic cells.	cytoskeleton	yes	yes
IPI00398625.5	HRNR Hornerin	Possess nucleoside-triphosphatase activity and calcium ion binding. May play a role in cornification. Belong to epidermic cells. Probably hornerin is a contaminant.	cytoplasmic granules	no	no
Proteins binding DNA/RNA, transcription factors and related proteins					
IPI00012998.2	CPSF6 Isoform 1 of Cleavage and polyadenylation specificity factor subunit 6	Component of the cleavage factor Im complex (CFIm) that plays a key role in pre-mRNA 3'-processing. Involved in association with NUDT21/CPSF5 in pre-MRNA 3'-end poly(A) site cleavage and poly(A) addition. CPSF6 binds to cleavage and polyadenylation RNA substrates and promotes RNA looping. (*Brown et al, Moll. Cell 2003*)	nucleus	no	no
IPI00396378.3	HNRNPA2B1 Isoform B1 of Heterogeneous nuclear ribonucleoproteins A2/B1	Involved with pre-mRNA processing. Forms complexes (ribonucleosomes) with at least 20 other different hnRNP and heterogeneous nuclear RNA in the nucleous.	nucleus	yes	yes
IPI00216592.2	HNRNPC Isoform C1 of Heterogeneous nuclear ribonucleoproteins C1/C2	Binds pre-mRNA and nucleates the assembly of 40S hnRNP particles. Single HNRNPC tetramers bind 230-240 nucleotides. Trimers of HNRNPC tetramers bind 700 nucleotides. May play a role in the early steps of spliceosome assembly and pre-mRNA splicing. Interacts with poly-U tracts in the 3'-UTR or 5'-UTR of mRNA and modulates the stability and the level of translation of bound mRNA molecules. (*Kim et al, Mol. Cell Biol. 2003*)	nucleus	yes	no
IPI00334587.1	HNRNPAB Isoform 2 of Heterogeneous nuclear ribonucleoprotein A/B	Binds single-stranded RNA. Has a high affinity for G-rich and U-rich regions of hnRNA. Also binds to APOB mRNA transcripts around the RNA editing site.	nucleus	no	no
IPI00215965.3	HNRNPA1 Isoform A1-B of Heterogeneous nuclear ribonucleoprotein A1	Involved in the packaging of pre-mRNA into hnRNP particles, transport of poly(A) mRNA from the nucleus to the cytoplasm and may modulate splice site selection. May play a role in HCV RNA replication. (*Kim et al, J. Virol. 2007*)	nucleus	yes	no
IPI00027834.3	HNRNPL Heterogeneous nuclear ribonucleoprotein L	This protein is a component of the heterogeneous nuclear ribonucleoprotein (hnRNP) complexe which provide the substrate for the processing events that pre-mRNAs undergo before becoming functional, translatable mRNAs in the cytoplasm.	nucleus	no	no
IPI00028888.1	HNRNPD Isoform 1 of Heterogeneous nuclear ribonucleoprotein D0	Binds with high affinity to RNA molecules that contain AU-rich elements (AREs) found within the 3'-UTR of many proto-oncogenes and cytokine mRNAs. Also binds to double- and single-stranded DNA sequences in a specific manner and functions a transcription factor.	nucleus	no	no

IPI00216049.1	HNRNPK Isoform 1 of Heterogeneous nuclear ribonucleoprotein K	One of the major pre-mRNA-binding proteins. Binds tenaciously to poly(C) sequences. Likely to play a role in the nuclear metabolism of hnRNAs, particularly for pre-mRNAs that contain cytidine-rich sequences. Can also bind poly(C) single-stranded DNA. Involved in the regulation of transcription, translation, nuclear transport, and signal transduction.	nucleus	yes	yes
IPI00479217.1	HNRNPU Isoform Short of Heterogeneous nuclear ribonucleoprotein U	Component of the CRD-mediated complex that promotes MYC mRNA stabilization. Binds to pre-mRNA. Has high affinity for scaffold-attached region (SAR) DNA. Binds to double- and single-stranded DNA and RNA. (*Weidensdorfer et al, Rna 2009*)	nucleus - cell surface	no	no
IPI00013881.6	HNRNPH1 Heterogeneous nuclear ribonucleoprotein H	This protein is a component of the heterogeneous nuclear ribonucleoprotein (hnRNP) complexe which provide the substrate for the processing events that pre-mRNAs undergo before becoming functional, translatable mRNAs in the cytoplasm. Mediates pre-mRNA alternative splicing regulation. Inhibits insulin receptor (IR) pre-mRNA exon 11 inclusion in myoblast, together with CUGBP1. Binds to the IR RNA. Binds poly(RG). (*Paul et al, EMBO J 2006*)	nucleus	no	no
IPI00641829.5	BAT1 Isoform 2 of Spliceosome RNA helicase BAT1	Component of the THO subcomplex of the TREX complex. The TREX complex specifically associates with spliced mRNA. Splice factor that is required for the first ATP-dependent step in spliceosome assembly and for the interaction of U2 snRNP with the branchpoint. (*Fleckner et al, Genes Dev. 1997*)	nucleus - spliceosome	no	no
IPI00020127.1	RPA1 Replication protein A 70 kDa DNA-binding subunit	Plays an essential role in several cellular processes in DNA metabolism including replication, recombination and DNA repair. Binds and subsequently stabilizes single-stranded DNA intermediates and thus prevents complementary DNA from reannealing. (*Kemp et al, J. Biol. Chem. 2010*)	nucleus	no	no
IPI00017617.1	DDX5 Probable ATP-dependent RNA helicase DDX5	Involved in the alternative regulation of pre-mRNA splicing; its RNA helicase activity is necessary for increasing tau exon 10 inclusion and occurs in a RBM4-dependent manner. Binds to the tau pre-mRNA in the stem-loop region downstream of exon 10. The rate of ATP hydrolysis is highly stimulated by single-stranded RNA. (*Kar et al, Mol. Cell. Biol. 2011*)	nucleus	no	no
IPI00005198.2	ILF2 Interleukin enhancer-binding factor 2	Appears to function predominantly as a heterodimeric complex with ILF3. This complex may regulate transcription of the IL2 gene during T-cell activation. It can also promote the formation of stable DNA-dependent protein kinase holoenzyme complexes on DNA.	nucleus	no	no
IPI00299000.5	PA2G4 Proliferation-associated protein 2G4	May play a role in a ERBB3-regulated signal transduction pathway. Seems be involved in growth regulation. Inhibits transcription of some E2F1-regulated promoters, probably by recruiting histone acetylase (HAT) activity. Binds RNA. Associates with 28S, 18S and 5.8S mature rRNAs, several rRNA precursors and probably U3 small nucleolar RNA. May be involved in regulation of intermediate and late steps of rRNA processing. May be involved in ribosome assembly.	cytoplasm - nucleus	no	no
IPI00410693.4	SERBP1 SERPINE1 mRNA binding protein 1, isoform CRA_d	SERPINE1 is a predicted RNA-binding protein. May specifically binds the mRNA of type-1 plasminogen activator inhibitor (PAI-1), and is thought to be involved in regulation of mRNA stability.	cytoplasm - nucleus - plasma membrane	no	no
IPI00010204.1	SFRS3 Splicing factor, arginine/serine-rich 3	May be involved in RNA processing in relation with cellular proliferation and/or maturation.	nucleus	no	no
IPI00220740.1	NPM1 Isoform 2 of Nucleophosmin	Involved in diverse cellular processes such as ribosome biogenesis, centrosome duplication, protein chaperoning, histone assembly, cell proliferation, and regulation of tumor suppressors p53/TP53 and ARF.	nucleus - centrosomes	yes	no
IPI00026272.2	HIST1H2AE;HIST1H2AB;HIST1H2AD;HIST1H2AK;HIST1H2AL;HIST1H2AM;HIST1H2AJ;HIST1H2AI;HIST1H2AG Histone H2A type 1-B/E	Core component of nucleosome.	nucleus	no	no
IPI00011268.2	RALY RNA binding protein, autoantigenic (HnRNP-associated with lethal yellow homolog (Mouse)), isoform CRA_a (Fragment)	Probable-RNA binding protein. Could be a heterogeneous nuclear ribonucleoprotein (hnRNP). May be involved in pre-mRNA splicing.	nucleus	no	no
Proteins involved in metabolic processes					
IPI00465028.7	RCTPI1;TPI1 triosephosphate isomerase 1 isoform 2	Possess isomerase activity.	cytoplasm	no	no
IPI00465439.5	ALDOA Fructose-bisphosphate aldolase A	Plays a key role in glycolysis and gluconeogenesis. In addition, may also function as scaffolding protein	cytoplasm	no	no
IPI00219018.7	GAPDH Glyceraldehyde-3-phosphate dehydrogenase	Glyceraldehyde-3-phosphate dehydrogenase is a key enzyme in glycolysis that catalyzes the first step of the pathway by converting D-glyceraldehyde 3-phosphate (G3P) into 3-phospho-D-glyceroylphosphate. Participates in nuclear events including transcription, RNA transport, DNA replication and apoptosis. (*Tisdale, J. Biol. Chem 2002*)	cytoplasm - nucleus - membranes	no	no
IPI00169383.3	PGK1 Phosphoglycerate kinase 1	In addition to its role as a glycolytic enzyme, it seems that PGK-1 acts as a polymerase alpha cofactor protein (primer recognition protein).	cytoplasm	no	no
IPI00465248.5	ENO1 Isoform alpha-enolase of Alpha-enolase	Multifunctional enzyme that, as well as its role in glycolysis, plays a part in several cellular processes such as growth control, hypoxia tolerance and allergic responses. May also function in the intravascular and	cytoplasm	yes	yes

		pericellular fibrinolytic system due to its ability to serve as a receptor and activator of plasminogen on the cell surface of several cell-types such as leukocytes and neurons. Stimulates immunoglobulin production. (*Feo et al, FEBS letter 2000*)			
IPI00011416.2	ECH1 Delta(3,5)-Delta(2,4)-dienoyl-CoA isomerase, mitochondrial	Catalyzes the isomerization of 3-trans,5-cis-dienoyl-CoA to 2-trans,4-trans-dienoyl-CoA.	mitochondria	no	no
IPI00007188.5	SLC25A5 ADP/ATP translocase 2	Catalyzes the exchange of cytoplasmic ADP with mitochondrial ATP across the mitochondrial inner membrane. As part of the mitotic spindle-associated MMXD complex it may play a role in chromosome segregation. (*Ito et al, Mol. Cell. 2010*)	mitochondrion inner membrane	no	yes
Proteins involved in cellular stress response					
IPI00003865.1	HSPA8 Isoform 1 of Heat shock cognate 71 kDa protein	Possess chaperone activity. Involved in stress response of the cell.	cytoplasm - nucleus	yes	yes
IPI00007765.5	HSPA9 Stress-70 protein, mitochondrial	Implicated in the control of cell proliferation and cellular aging. May also act as a chaperone.	mitochondria	yes	yes
IPI00410693.4	SERBP1 SERPINE1 Plasminogen activator inhibitor 1 RNA-binding protein	SERPINE1 is a predicted RNA-binding protein. May specifically binds the mRNA of type-1 plasminogen activator inhibitor (PAI-1), and is thought to be involved in regulation of mRNA stability.	cytoplasm - nucleus - plasma membrane	no	no
IPI00000874.1	PRDX1 Peroxiredoxin-1	Involved in redox regulation of the cell. Reduces peroxides with reducing equivalents provided through the thioredoxin system but not from glutaredoxin. May play an important role in eliminating peroxides generated during metabolism. Might participate in the signaling cascades of growth factors and tumor necrosis factor-alpha by regulating the intracellular concentrations of H2O2.	cytoplasm - melaosome	no	no
Various proteins					
IPI00217053.6	PRRC1 Isoform 3 of Protein PRRC1	Belongs to the PRRC1 family. 5 isoforms of the human protein are produced by alternative splicing.	golgy apparatus	no	no
IPI00010303.1	SERPINB4 Serpin B4	May act as a protease inhibitor to modulate the host immune response against tumor cells.	cytoplasm	no	no
Unknown proteins					
IPI00069693.4	- Putative uncharacterized protein RPL14P1	unknown	unknown	no	no
IPI00644570.1	- 18 kDa protein	unknown	unknown	no	no
IPI00168728.1	IGHG3 FLJ00385 protein (Fragment)	unknown	unknown	no	no

TABLE 5: Proteins Identified and Quantified in SILAC HEK 293 T - Global Protein Expression Analysis

ACCESSION	DESCRIPTION	Heavy Treat/Light Ctrl Replicate 1	Heavy Treat/Light Ctrl Replicate 2	Heavy Treat/Light Ctrl Replicate 3	Light Treat/Heavy Ctrl Repicate 1	Light Treat/Heavy Ctrl Replicate 2	Light Treat/Heavy Ctrl Replicate 3	MEDIAN
IPI00296635.5	1,4-alpha-glucan-branching enzyme		0,881	0,883		1,043		0,883
IPI00220362.5	10 kDa heat shock protein, mitochondrial	1,159	0,992	0,975	0,860	0,985	0,962	0,980
IPI00917777.1	116 kDa U5 small nuclear ribonucleoprotein component isoform b	1,165	1,174	**1,559**	1,095	0,919	1,033	1,130
IPI01011924.1	117 kDa protein	0,933	0,880	1,010	1,072	1,007	1,091	1,009
IPI00797738.1	12 kDa protein		1,233	0,936		1,197	1,216	1,206
IPI01012543.1	131 kDa protein		1,106	0,983	0,841	0,884	0,857	0,884
IPI01010578.1	137 kDa protein	1,397	**2,291**	**1,677**	1,430	0,893		1,430
IPI00299977.1	14 kDa phosphohistidine phosphatase	1,142	1,025	0,925	0,846	0,974	1,139	1,000
IPI00216319.3	14-3-3 protein eta	1,004	0,959	1,005	0,837	0,893	0,861	0,926
IPI00220642.7	14-3-3 protein gamma	1,038	1,035	1,053	0,801	0,871	0,863	0,953
IPI00018146.1	14-3-3 protein theta	1,027	1,018	0,998	0,832	0,943	0,910	0,970
IPI00021263.3	14-3-3 protein zeta/delta	1,046	1,036	0,999	0,835	0,953	0,922	0,976
IPI00030877.2	15 kDa selenoprotein isoform 1 precursor	0,961	1,002	1,126	0,820	0,750	0,854	0,907
IPI00916994.1	16 kDa protein	1,170		0,893	0,936	0,941	1,083	0,941
IPI01014951.1	163 kDa protein	1,267	0,941	**6,625**	0,738	**0,285**	**0,589**	0,839
IPI00966782.1	17 kDa protein	0,793	0,872	0,761	1,045	1,197	1,145	0,958
IPI00927715.1	21 kDa protein		**6,613**	**13,406**	**4,473**			**6,613**
IPI01012847.1	21 kDa protein		1,268	1,093	1,001		0,991	1,047
IPI00977126.1	21 kDa protein	0,950	0,926	0,969		0,866	0,871	0,926
IPI00878075.1	23 kDa protein	0,976	1,006	0,925	0,815	0,867	0,882	0,904
IPI01014410.1	25 kDa protein			0,963	1,174	1,178	1,092	1,133
IPI00797249.1	26 kDa protein	0,995	0,999	0,812	0,883	1,013	1,079	0,997
IPI00021435.3	26S protease regulatory subunit 7	1,176	1,224	**2,630**	1,229	0,817	1,009	1,200
IPI00926977.1	26S protease regulatory subunit S10B	1,361	1,193	**1,666**	1,107	0,799	0,844	1,150
IPI00003565.1	26S proteasome non-ATPase regulatory subunit 10	1,195	1,139	1,013	0,842	1,142	0,935	1,076
IPI00185374.4	26S proteasome non-ATPase regulatory subunit 12	1,349	1,383	**2,487**	1,027	0,734	0,836	1,188
IPI00024821.1	26S proteasome non-ATPase regulatory subunit 14		0,970		1,498		1,263	1,263
IPI00012268.3	26S proteasome non-ATPase regulatory subunit 2	1,216	1,171	**2,324**	1,258	0,913	1,028	1,193
IPI00014151.3	26S proteasome non-ATPase regulatory subunit 6	1,199	1,126	**1,940**	1,247	0,962	1,070	1,163
IPI00019927.2	26S proteasome non-ATPase regulatory subunit 7	1,426	**1,512**	**2,488**	1,102	0,746	0,868	1,264
IPI00005050.1	28S ribosomal protein S14, mitochondrial	**2,187**		**7,431**	**1,508**			**2,187**
IPI00014812.1	28S ribosomal protein S21, mitochondrial	**3,343**			1,215	0,810	1,000	1,108

IPI00006606.1	28S ribosomal protein S26, mitochondrial				**1,605**	1,214	1,489	1,489
IPI00022276.3	28S ribosomal protein S28, mitochondrial				1,026	0,830	0,897	0,897
IPI00020495.1	28S ribosomal protein S36, mitochondrial	**1,987**				1,326	1,226	1,326
IPI01009970.1	29 kDa protein	**0,345**			**1,734**	**2,270**	**1,844**	**1,789**
IPI00975963.1	29 kDa protein	**2,400**	**2,033**	**3,423**	1,125	0,838	0,951	**1,579**
IPI00013860.3	3-hydroxyisobutyrate dehydrogenase, mitochondrial	1,234	1,059	1,169	**0,609**	0,888		1,059
IPI00001539.8	3-ketoacyl-CoA thiolase, mitochondrial	1,044	1,087	1,000	1,012	1,166		1,044
IPI00165360.5	3-mercaptopyruvate sulfurtransferase	0,722	**0,654**	0,671	1,155	1,115	1,186	0,918
IPI01011685.1	31 kDa protein	1,436	**2,038**		1,171	0,744		1,303
IPI01017942.1	34 kDa protein	0,736	0,937	0,984	1,168	1,111	1,094	1,039
IPI01015264.1	34 kDa protein	0,844	0,905	1,210	0,945	0,835	0,847	0,876
IPI00946527.1	35 kDa protein	0,875	0,885	0,907	0,978	1,128	1,083	0,943
IPI01015060.1	39S ribosomal protein L12, mitochondrial	1,360	0,965	0,892	1,147	1,375	1,104	1,126
IPI00479877.4	4-trimethylaminobutyraldehyde dehydrogenase	1,023	1,017	0,970	0,851	1,049	1,031	1,020
IPI00008438.1	40S ribosomal protein S10	**2,284**	0,934	**5,570**	1,144	0,743	1,005	1,074
IPI00025091.3	40S ribosomal protein S11	**4,303**	**2,995**	**4,837**	**2,349**	0,873	1,301	**2,672**
IPI00013917.3	40S ribosomal protein S12	**2,308**	**1,965**	**3,049**	1,239	0,749	0,949	**1,602**
IPI00221089.5	40S ribosomal protein S13	**4,969**	**4,237**	**11,200**	**2,849**	1,048	1,441	**3,543**
IPI00026271.5	40S ribosomal protein S14	**2,314**	**1,859**	**4,168**	**1,676**	0,786	1,096	**1,767**
IPI00479058.2	40S ribosomal protein S15	**2,132**	**2,013**		**1,550**	0,870	1,148	**1,550**
IPI00221091.9	40S ribosomal protein S15a	**5,337**	**4,124**	**10,048**	**2,172**	0,873	1,136	**3,148**
IPI00221092.8	40S ribosomal protein S16	**2,467**	**2,865**	**5,878**	**1,525**	0,976	1,210	**1,996**
IPI00221093.7	40S ribosomal protein S17	**1,565**	1,225	**3,204**	1,111	0,705	0,926	1,168
IPI00013296.3	40S ribosomal protein S18	**2,286**	**2,330**	**4,186**	1,364	0,785	1,033	**1,825**
IPI00215780.5	40S ribosomal protein S19	**2,349**	**2,324**	**5,274**	1,387	0,843	1,173	**1,855**
IPI00013485.3	40S ribosomal protein S2	**2,104**	**2,059**	**3,812**	**1,556**	0,983	1,247	**1,807**
IPI00012493.1	40S ribosomal protein S20	**1,600**	1,425	**2,540**	**1,547**	1,028	1,244	1,486
IPI00937239.2	40S ribosomal protein S21	1,134	0,966	1,277	0,716	**0,546**	**0,602**	0,841
IPI00218606.7	40S ribosomal protein S23	**5,329**	**12,204**		**1,726**	0,989	**1,592**	**1,726**
IPI00012750.3	40S ribosomal protein S25	**3,052**	**2,224**	**5,738**	**1,612**	1,024	1,223	**1,918**
IPI00655650.2	40S ribosomal protein S26	**7,072**	**4,427**	**9,725**	**2,867**	1,136	1,478	**3,647**
IPI00719622.1	40S ribosomal protein S28	**1,936**	**1,783**	**2,040**	1,192	0,883	0,948	1,487
IPI00182289.6	40S ribosomal protein S29	**2,107**	**2,210**	**4,868**	1,167	0,732	1,218	**1,663**
IPI00011253.3	40S ribosomal protein S3	**2,117**	**2,194**	**3,721**	1,245	0,807	0,999	**1,681**
IPI00419880.6	40S ribosomal protein S3a	**2,347**	**1,767**	**5,751**	1,239	0,687	0,842	**1,503**
IPI00217030.10	40S ribosomal protein S4, X isoform	**4,530**	**3,648**	**7,857**	**2,215**	0,909	1,326	**2,932**
IPI00008433.4	40S ribosomal protein S5	**2,249**	**2,089**	**4,040**	1,181	0,721	0,929	**1,635**

IPI00021840.1	40S ribosomal protein S6	**3,019**	**2,332**	**2,234**	**1,650**	1,123	1,074	**1,942**
IPI00013415.1	40S ribosomal protein S7	**2,493**	**1,822**	**2,301**	**1,640**	0,843	1,059	**1,731**
IPI00216587.9	40S ribosomal protein S8	**5,123**	**4,985**	**10,293**	**2,747**	0,832	**1,503**	**3,866**
IPI00221088.5	40S ribosomal protein S9	**3,393**	**2,802**	**5,480**	**1,706**	0,788	1,079	**2,254**
IPI00979423.1	44 kDa protein	1,057	1,055	1,434	1,125	0,943	0,974	1,056
IPI01016024.1	45 kDa protein	1,078	1,061	1,061	0,831	0,977	0,904	1,019
IPI01015447.1	47 kDa protein	1,010	0,980	**2,004**				1,010
IPI00177965.5	5'-nucleotidase domain-containing protein 1	0,759	0,744	0,765	1,203	1,161	1,175	0,963
IPI01013537.1	50 kDa protein	0,875	0,867	0,857	0,923	1,016	1,028	0,899
IPI00925539.1	57 kDa protein	0,791	1,244		0,780			0,791
IPI00009790.1	6-phosphofructokinase type C	**1,636**	**1,576**	**2,756**	1,057	1,155	0,994	1,365
IPI01012504.1	6-phosphogluconate dehydrogenase, decarboxylating	0,964	1,018	0,964	0,928	1,033	1,009	0,986
IPI00029997.1	6-phosphogluconolactonase	**0,608**	**0,527**	**0,534**	1,131	1,039	1,093	0,823
IPI00784154.1	60 kDa heat shock protein, mitochondrial	0,979	0,894	0,944	0,920	0,938	0,961	0,941
IPI01012685.1	60 kDa protein			0,962	0,986	0,681	0,826	0,894
IPI00008530.1	60S acidic ribosomal protein P0	**3,281**	**2,646**	**3,375**	**2,629**	0,847	1,014	**2,637**
IPI00008527.3	60S acidic ribosomal protein P1	0,968	1,084	0,917	**1,808**	**2,075**	1,386	1,235
IPI00008529.1	60S acidic ribosomal protein P2	1,279	1,213	1,136	1,132	1,188	0,943	1,162
IPI00853161.4	60S ribosomal protein L10	**2,454**	**2,114**	**2,273**	**2,132**			**2,203**
IPI00412579.6	60S ribosomal protein L10a	**14,731**	**11,602**	**12,746**	**6,542**			**12,174**
IPI00465361.4	60S ribosomal protein L13	**8,196**	**21,982**	**9,988**	**5,188**	1,312	**1,779**	**6,692**
IPI00413324.6	60S ribosomal protein L17	**2,619**	**2,533**	**2,139**	**1,644**	1,004	0,968	**1,891**
IPI00025329.1	60S ribosomal protein L19	**3,278**	**2,892**	**4,327**				**3,278**
IPI00219153.4	60S ribosomal protein L22	1,021	**1,506**	**3,020**	1,316	**0,647**	0,818	1,169
IPI00010153.5	60S ribosomal protein L23	**1,579**	**1,749**	**1,727**	**1,549**	0,894	1,015	**1,564**
IPI00021266.1	60S ribosomal protein L23a	**2,006**	**1,733**	**2,406**	1,208	0,667	0,838	1,471
IPI00027270.1	60S ribosomal protein L26	**2,303**		**3,102**		**0,637**	1,150	**1,727**
IPI00219155.5	60S ribosomal protein L27	**5,874**	**5,256**	**5,532**	**3,837**	1,029	**1,736**	**4,547**
IPI00182533.5	60S ribosomal protein L28		**4,891**	**1,736**	**5,037**	**2,031**		**3,461**
IPI00651660.1	60S ribosomal protein L3 isoform b	**5,460**	**3,365**	**2,863**	**6,201**			**4,413**
IPI00026302.3	60S ribosomal protein L31	**2,452**	**2,266**	**4,267**	**1,672**	0,862	1,115	**1,969**
IPI00219160.3	60S ribosomal protein L34	**6,259**	**14,253**	**5,797**	**3,525**			**6,028**
IPI00412607.6	60S ribosomal protein L35	**2,329**	**2,102**	**2,345**	1,434	0,759	0,722	**1,768**
IPI00029731.8	60S ribosomal protein L35a	**18,110**	**45,479**	**28,971**	**7,575**			**23,540**
IPI00216237.5	60S ribosomal protein L36	**8,152**	**6,713**	**9,325**	**5,397**	**0,479**		**6,713**
IPI00414860.6	60S ribosomal protein L37a		**9,032**		**3,680**	0,968	1,406	**2,543**
IPI00215790.6	60S ribosomal protein L38	**1,919**	**2,064**	**2,586**	**2,046**	0,731	0,755	**1,983**
IPI00003918.6	60S ribosomal protein L4	**4,843**	**3,420**		**8,709**			**4,843**

IPI00031691.1	60S ribosomal protein L9	**18,948**	**13,797**	**17,323**	**6,888**			**15,560**
IPI00003362.3	78 kDa glucose-regulated protein	0,946	0,956	0,905	1,050	1,143	1,087	1,003
IPI01011937.1	83 kDa protein	0,822		**1,610**	1,380	0,967	0,902	0,967
IPI01010478.1	92 kDa protein			0,846	0,885	1,035	0,910	0,898
IPI00020075.4	Abhydrolase domain-containing protein 10, mitochondrial	1,253	1,255	1,119	0,805	0,919	0,904	1,019
IPI01014863.1	Acetyl-CoA acetyltransferase, cytosolic	0,806	0,777	0,797	1,133	1,235	1,187	0,970
IPI00030363.1	Acetyl-CoA acetyltransferase, mitochondrial	1,138	0,943	0,940	1,084	1,079	1,081	1,080
IPI00165393.1	Acidic leucine-rich nuclear phosphoprotein 32 family member E	1,025	1,017	0,982	0,852	0,988	0,930	0,985
IPI00017855.1	Aconitate hydratase, mitochondrial	0,845	0,912	0,810	0,739	0,949	0,859	0,852
IPI00005159.3	Actin-related protein 2	**2,049**			1,215		1,092	1,215
IPI00005162.3	Actin-related protein 2/3 complex subunit 3	**2,047**	**1,944**	1,444	**1,571**	**1,665**	1,276	**1,618**
IPI00554811.2	Actin-related protein 2/3 complex subunit 4	**2,159**	**1,996**	1,410	1,347	1,379	1,128	1,394
IPI00414554.5	Actin-related protein 2/3 complex subunit 5-like protein	**1,947**	**1,888**	1,291	**1,515**	1,422	1,138	1,468
IPI00028091.3	Actin-related protein 3	**2,188**		1,445	1,427	1,403	1,172	1,427
IPI00021439.1	Actin, cytoplasmic 1	0,889	0,906	0,990	0,999	1,032	1,009	0,994
IPI00221222.7	Activated RNA polymerase II transcriptional coactivator p15	0,716	0,865	**1,502**	1,017	0,904	0,890	0,897
IPI00022442.2	Acyl carrier protein, mitochondrial	1,101	0,801			1,193	1,112	1,106
IPI00333838.1	Acyl-coenzyme A thioesterase 1	1,093		**0,433**		1,391	1,469	1,242
IPI00930594.1	acyl-coenzyme A thioesterase 13 isoform 2				**1,812**	**2,210**	**1,783**	**1,812**
IPI00337741.4	Acylamino-acid-releasing enzyme	0,970	0,947	0,931	1,026	0,993	1,055	0,982
IPI00221117.3	Acylphosphatase-1	1,157	1,049	0,915	0,923	1,166	1,018	1,033
IPI00305469.4	adapter molecule crk isoform b	0,742	0,790	0,839			1,256	0,815
IPI00218693.8	Adenine phosphoribosyltransferase	0,918	0,891	0,805	0,967	1,214	1,099	0,943
IPI00012007.6	Adenosylhomocysteinase	1,081	0,995	1,014	0,936	0,984	0,950	0,990
IPI00018342.5	Adenylate kinase isoenzyme 1	0,883	0,910	0,828	1,019	1,194	1,132	0,965
IPI00641992.4	Adenylosuccinate synthetase	1,069	1,102	1,015	0,855	1,006	0,936	1,011
IPI00215914.5	ADP-ribosylation factor 1	**0,582**	0,815	0,956	1,035	1,032	0,996	0,976
IPI00215918.3	ADP-ribosylation factor 4	**0,549**	0,720	1,057	0,990	0,824	0,886	0,855
IPI00215919.5	ADP-ribosylation factor 5	**0,475**	**0,579**	0,928	1,105	0,837	0,883	0,860
IPI00215920.8	ADP-ribosylation factor 6				1,171	**0,646**	0,819	0,819
IPI00003326.4	ADP-ribosylation factor-like protein 2	0,922	1,115	1,059	0,836	1,004	0,942	0,973
IPI00003327.1	ADP-ribosylation factor-like protein 3	0,817	0,896	0,811	0,964	1,096	1,027	0,930
IPI00296913.1	ADP-sugar pyrophosphatase	1,105	1,101	1,022	0,899	0,961	1,016	1,019
IPI00007188.6	ADP/ATP translocase 2	**5,813**	**6,159**	**6,575**	**3,786**	0,919	1,443	**4,800**
IPI00019326.1	Adrenodoxin, mitochondrial	0,931	0,719	0,784	0,672	0,821	0,815	0,799
IPI00027442.4	Alanyl-tRNA synthetase, cytoplasmic	0,954	0,957	0,924	0,915	1,137	1,012	0,956
IPI00220271.3	Alcohol dehydrogenase [NADP+]	0,868	0,876	**0,557**	1,143	**1,755**	**1,576**	1,009

IPI00746777.3	Alcohol dehydrogenase class-3	1,042	1,130	0,918	0,787	0,994	0,914	0,956
IPI00103467.5	Aldehyde dehydrogenase X, mitochondrial	0,989	0,928	0,960	0,931	1,019	1,071	0,975
IPI00006663.1	Aldehyde dehydrogenase, mitochondrial	0,987	0,966	0,904	0,902	1,066	1,121	0,977
IPI00413641.7	Aldose reductase	0,981	0,907	0,870	0,820	1,112	1,018	0,944
IPI00909239.1	alpha-actinin-1 isoform c	1,011	1,017	1,010	0,853	0,942	0,910	0,976
IPI00013808.1	Alpha-actinin-4	0,994	0,965	1,016	0,862	0,945	0,933	0,955
IPI00025869.1	Alpha-galactosidase A	0,973	0,912	0,852	0,787	1,152	1,038	0,943
IPI00029534.1	Amidophosphoribosyltransferase	1,092	0,944	0,975	0,925	1,002	0,965	0,970
IPI00006252.3	Aminoacyl tRNA synthase complex-interacting multifunctional protein 1		1,233		1,206	0,920	1,013	1,110
IPI00642211.3	Aminopeptidase B	0,889	0,850	0,881	0,971	1,023	1,061	0,930
IPI00218918.5	Annexin A1	0,736	0,734	0,843	1,138	1,468	1,278	0,990
IPI00329801.12	Annexin A5	1,005	0,987	1,004	0,885	1,053	0,968	0,996
IPI00221226.7	Annexin A6	0,758	1,025	**3,288**	0,847	1,010	0,949	0,980
IPI00940656.2	ANP32A protein	0,929	0,962	0,942	0,853	1,118	1,000	0,952
IPI00922006.2	AP-1 complex subunit sigma-2				1,089	0,816	0,976	0,976
IPI00556297.1	Arginine/serine-rich splicing factor 6 variant (Fragment)	1,005	1,263	**2,321**	0,803	**0,560**	0,767	0,904
IPI00953925.1	Aryl hydrocarbon receptor interacting protein		**0,648**		1,031	0,958	0,942	0,950
IPI00306960.3	Asparaginyl-tRNA synthetase, cytoplasmic	**1,549**	1,046	0,794	1,195	1,477	1,299	1,247
IPI00219029.3	Aspartate aminotransferase, cytoplasmic	0,845	0,816	0,804	1,060	1,239	1,171	0,953
IPI00018206.4	Aspartate aminotransferase, mitochondrial	1,290	1,128	1,027	0,858	1,012	0,909	1,019
IPI00216951.2	Aspartyl-tRNA synthetase, cytoplasmic	**1,551**	1,239	**2,455**	1,210	0,946	1,052	1,224
IPI00014850.4	Astrocytic phosphoprotein PEA-15	1,023	0,988	0,886		**1,761**		1,006
IPI00440493.2	ATP synthase subunit alpha, mitochondrial	**2,014**	**1,958**	**2,113**	1,272	0,895	1,000	**1,615**
IPI00303476.1	ATP synthase subunit beta, mitochondrial	1,362	1,219	1,398	0,993	0,856	0,930	1,106
IPI00024920.1	ATP synthase subunit delta, mitochondrial	**1,772**	1,496	1,342		1,000	0,967	1,342
IPI00176527.1	ATP synthase subunit epsilon-like protein, mitochondrial			**3,835**		1,181	1,002	1,181
IPI00007611.1	ATP synthase subunit O, mitochondrial	**8,164**	**8,181**		**4,113**			**8,164**
IPI00303207.3	ATP-binding cassette sub-family E member 1	0,823	1,060		1,327	0,897	0,892	0,897
IPI00844578.1	ATP-dependent RNA helicase A	1,413	**1,626**	**2,897**	1,274	0,862	1,173	1,343
IPI00985384.1	ATP-dependent RNA helicase DDX3X isoform 3	**1,671**	1,359	**3,731**	1,133	**0,607**	1,217	1,288
IPI00026087.1	Barrier-to-autointegration factor	**4,993**	**4,691**	1,256	**4,794**	**5,305**	**4,987**	**4,890**
IPI00006952.3	Beta-lactamase-like protein 2	0,850		0,732	0,859	0,900	1,221	0,859
IPI00011619.4	Bifunctional 3'-phosphoadenosine 5'-phosphosulfate synthase 1	**0,586**	**1,723**	0,779	1,137	1,117		1,117
IPI00013452.11	Bifunctional aminoacyl-tRNA synthetase	**1,589**	1,239	**3,044**	1,054	0,903	0,976	1,147
IPI00551024.5	Bifunctional ATP-dependent dihydroxyacetone kinase/FAD-AMP lyase (cyclizing)	1,083	0,922	0,896	1,033	1,011	1,053	1,022
IPI00011307.4	Bifunctional methylenetetrahydrofolate	0,854	0,965	1,122	0,868	0,938	0,959	0,948

	dehydrogenase/cyclohydrolase, mitochondrial							
IPI00477231.3	Bifunctional protein NCOAT		**0,481**	**0,651**	0,975		1,332	0,813
IPI00289499.3	Bifunctional purine biosynthesis protein PURH	0,957	0,941	0,901	0,930	1,110	1,029	0,949
IPI00294158.1	Biliverdin reductase A	0,933	0,991	0,777	1,021	1,110	1,107	1,006
IPI00221231.3	Bis(5'-nucleosyl)-tetraphosphatase [asymmetrical]	0,968	1,068	0,959	0,813	1,038	1,025	0,997
IPI00219575.5	Bleomycin hydrolase	0,787	0,815	0,836	1,349	1,454	1,276	1,056
IPI00032900.1	BolA-like protein 1	0,705		**0,637**	1,158	1,382	1,223	1,158
IPI00301434.4	BolA-like protein 2	0,888	0,845	0,792	0,876	1,137	1,149	0,882
IPI00983406.1	branched-chain-amino-acid aminotransferase, cytosolic isoform 5				1,058	1,174	1,246	1,174
IPI00060715.1	BTB/POZ domain-containing protein KCTD12	0,772	0,847	0,955	1,003	1,137	1,151	0,979
IPI00218342.10	C-1-tetrahydrofolate synthase, cytoplasmic	**2,038**	1,340	1,029	**1,625**	**1,557**	1,306	1,448
IPI00871174.2	C-Myc-binding protein	0,814	0,859	0,805	1,331	1,170	1,338	1,014
IPI00554626.3	C-terminal-binding protein 1 isoform 2	0,866		1,039	1,050	1,096		1,044
IPI00032561.1	Calcium-binding protein 39	1,041	1,070	0,894	0,972	0,939	0,904	0,956
IPI00304409.3	Calcium-regulated heat stable protein 1	0,860	0,844	0,807	1,027	1,264	1,147	0,944
IPI00977736.1	calcyclin-binding protein isoform 2	0,902	0,859	0,887	1,106	0,949	1,122	0,925
IPI00075248.11	Calmodulin	0,950	1,009	1,099	0,818	0,922	0,908	0,936
IPI00941747.1	Calnexin	1,118	0,964	1,495	1,156	0,837	0,954	1,041
IPI00025084.3	Calpain small subunit 1	**0,473**	0,750	0,891	0,825	0,909	0,823	0,824
IPI00011285.1	Calpain-1 catalytic subunit		0,676			1,201	0,706	0,706
IPI00020599.1	Calreticulin	1,033	1,017	0,777	0,848	1,037	1,200	1,025
IPI00031570.1	Cancer-related nucleoside-triphosphatase	0,853		**2,780**	**1,675**	**1,717**	1,479	**1,675**
IPI00218414.5	Carbonic anhydrase 2	0,897	0,860	0,843	1,019	1,184	1,099	0,958
IPI00219669.5	Carbonic anhydrase-related protein	0,771	0,720	0,689	1,277	1,460	1,353	1,024
IPI00295386.7	Carbonyl reductase [NADPH] 1	1,031	0,981	0,911	0,909	1,090	1,056	1,006
IPI00383046.3	Carboxymethylenebutenolidase homolog	1,008	1,247	1,024				1,024
IPI00020602.1	Casein kinase II subunit alpha'	1,053	0,920	1,349	0,841	0,786	0,923	0,921
IPI00010865.1	Casein kinase II subunit beta	0,837	0,884	1,092	1,085	1,009	0,987	0,998
IPI00292140.4	Caspase-3	1,094	1,072	1,078	0,885	0,980	0,975	1,026
IPI00984217.2	Catenin (Cadherin-associated protein), alpha 1, 102kDa, isoform CRA_c			1,176	1,073	0,751		1,073
IPI00103047.1	Cation transport regulator-like protein 2	0,934	0,980	0,938	0,904	1,032	1,022	0,959
IPI00017672.4	cDNA FLJ25678 fis, clone TST04067, highly similar to PURINE NUCLEOSIDE PHOSPHORYLASE	0,807	0,766	0,760	1,142	1,364	1,275	0,975
IPI01015295.1	cDNA FLJ30049 fis, clone ADRGL1000033, highly similar to 26S proteasome non-ATPase regulatory subunit 3	1,455	1,214	**2,413**	1,078	0,788	0,898	1,146
IPI01011483.1	cDNA FLJ30614 fis, clone CTONG2001139		1,148	**1,534**	0,945	**0,586**	0,777	0,945
IPI00954146.2	cDNA FLJ31682 fis, clone NT2RI2005335,	0,694	0,745	1,148	0,823	**0,545**	0,845	0,784

	highly similar to MMS19-like protein							
IPI00939530.1	cDNA FLJ34106 fis, clone FCBBF3008073, highly similar to SPLICING FACTOR, ARGININE/SERINE-RICH 7	0,781	1,283	**2,851**	1,009	0,728	0,945	0,977
IPI00385786.3	cDNA FLJ35170 fis, clone PLACE6012942, highly similar to SPLICING FACTOR, ARGININE/SERINE-RICH 2	1,046	1,113	**1,578**	0,798	0,710	0,897	0,971
IPI00879876.1	cDNA FLJ36221 fis, clone THYMU2000950, highly similar to Eukaryotic translation initiation factor 3 subunit 6-interacting protein	1,328	1,010		0,718	**0,322**	**0,463**	0,718
IPI01013880.1	cDNA FLJ37277 fis, clone BRAMY2012581, highly similar to Coronin-7			0,708	1,074		**1,765**	1,074
IPI00640037.2	cDNA FLJ38496 fis, clone FELIV1000137, highly similar to 60S RIBOSOMAL PROTEIN L5	1,138	1,092	1,411	1,048	1,049	1,021	1,070
IPI00894104.2	cDNA FLJ39381 fis, clone PERIC2000422, highly similar to HEAT repeat-containing protein 2		1,094	**1,850**	0,832	**0,340**		0,963
IPI00445741.3	cDNA FLJ43165 fis, clone FCBBF3002163, highly similar to Homo sapiens chromosome condensation-related SMC-associated protein 1	1,494	1,494	**2,143**	**1,504**	0,851	0,862	1,494
IPI00903231.1	cDNA FLJ45471 fis, clone BRSTN2016892, highly similar to COMM domain-containing protein 3	1,091	0,950		0,922	0,745	0,862	0,922
IPI00334291.9	cDNA FLJ45970 fis, clone PLACE7016526, highly similar to Lon protease homolog, mitochondrial	1,472	1,001	1,101	1,200	0,904	1,263	1,150
IPI00922787.1	cDNA FLJ50123		0,887	0,736	1,314	**1,526**	1,407	1,314
IPI01010287.1	cDNA FLJ51031, highly similar to ATP-dependent RNA helicase DDX1	**1,726**	**1,965**	**4,018**	1,258	0,815	0,997	1,492
IPI00942143.2	cDNA FLJ51069, highly similar to DNA mismatch repair protein Msh2	1,499	1,350	**2,179**	0,981	0,819		1,350
IPI00879681.4	cDNA FLJ51385, highly similar to Ran GTPase-activating protein 1	**0,548**	0,865	1,068	0,981	**0,571**	0,998	0,923
IPI00925572.1	cDNA FLJ51387, highly similar to Asparagine synthetase	0,832	0,942	0,759	0,823	0,956	1,106	0,887
IPI00909703.2	cDNA FLJ51518, highly similar to Annexin A11	**0,250**		**5,957**	0,863	0,858	0,876	0,863
IPI01014435.1	cDNA FLJ51696, highly similar to Ras-related protein Rap-1b	1,396	1,304	1,372	1,105	1,157	1,047	1,230
IPI01011723.1	cDNA FLJ51704, highly similar to ADP-ribosylation factor-like protein 1	**0,658**		0,917	1,128	1,050	0,963	0,963
IPI00872780.2	cDNA FLJ51794, highly similar to Annexin A4	1,101	1,499		0,924	0,724	0,832	0,924
IPI00964716.1	cDNA FLJ51799, highly similar to Sorting nexin-2	**0,139**	0,708	**0,458**	0,899	0,768	0,711	0,710
IPI00946636.2	cDNA FLJ51804, highly similar to Vacuolar ATP synthase catalytic subunit A, ubiquitous isoform	0,993	1,007	1,122	0,997	0,995	0,933	0,996
IPI01013974.1	cDNA FLJ51852, highly similar to Homo sapiens ADP-ribosylhydrolase like 2 (ADPRHL2), mRNA	0,955		1,073		0,848	0,790	0,901
IPI00878876.1	cDNA FLJ51872, highly similar to Small nuclear ribonucleoprotein Sm D3	1,470	**1,734**	**2,538**	1,153	0,790	1,001	1,311
IPI00966238.2	cDNA FLJ51907, highly similar to Stress-70 protein, mitochondrial	1,085	1,088	1,122	0,783	0,905	0,809	0,995
IPI01013446.1	cDNA FLJ51947, highly similar to Epididymal secretory protein E1	**0,590**	**0,600**	**0,552**	1,495	**2,451**	**1,723**	1,047

IPI00922554.1	cDNA FLJ51996, highly similar to Deoxyribonuclease-2-alpha	0,938	0,900	0,833	0,975	1,123	1,135	0,956
IPI00909562.1	cDNA FLJ52462, moderately similar to Mus musculus proteasome (prosome, macropain) 26S subunit, non-ATPase, 8 (Psmd8), mRNA	1,264			1,304	1,275	1,074	1,270
IPI00910487.1	cDNA FLJ52569, highly similar to Collagen-binding protein 2	1,187	1,107	0,931	1,156	1,408	1,103	1,131
IPI01013988.1	cDNA FLJ52696, highly similar to Eukaryotic translation initiation factor 3 subunit 5	1,154	1,010	**1,896**	0,734	**0,503**	**0,578**	0,872
IPI00910706.1	cDNA FLJ52710, highly similar to Abhydrolase domain-containing protein 14B	0,975	0,931	0,983	0,912	1,134	0,936	0,955
IPI00843996.1	cDNA FLJ52832, highly similar to Splicing factor, arginine/serine-rich 3	1,131	1,362	**2,856**	1,119	**0,650**	0,863	1,125
IPI01010035.1	cDNA FLJ52928, highly similar to COP9 signalosome complex subunit 2	0,831	0,962	1,366	0,898	0,854	0,950	0,924
IPI01014777.1	cDNA FLJ53007, highly similar to UBA/UBX 33.3 kDa protein	**0,570**	0,781	0,830	1,383	1,163	1,329	0,996
IPI00909623.1	cDNA FLJ53072, highly similar to Calponin-3		**2,206**	1,114	0,996	1,002	0,789	1,002
IPI01014074.1	cDNA FLJ53296, highly similar to Serine/threonine-protein phosphatase 2A 65 kDa regulatory subunit A alpha isoform	0,746	0,806	0,874	0,950	0,937	0,987	0,906
IPI00893431.2	cDNA FLJ53410, highly similar to Eukaryotic translation initiation factor 3 subunit 9	1,311	1,010		0,832	**0,477**	**0,604**	0,832
IPI00981395.1	cDNA FLJ53442, highly similar to Poly (ADP-ribose) polymerase 1	1,159	1,100	**3,864**	0,810	**0,517**	0,670	0,955
IPI00909232.1	cDNA FLJ53542, highly similar to Heterogeneous nuclear ribonucleoproteins C	**1,758**	**9,554**	**4,247**	1,191	0,762	0,979	1,474
IPI01012205.1	cDNA FLJ53863, highly similar to Cystathionine beta-synthase	0,871	0,830	0,795	1,107	1,088	1,100	0,980
IPI01013280.1	cDNA FLJ54090, highly similar to 4F2 cell-surface antigen heavy chain	**1,566**	1,369	**1,517**	**1,602**	0,911	0,865	1,443
IPI01011531.1	cDNA FLJ54149, highly similar to Annexin A7	0,670			0,810	0,842	0,741	0,775
IPI00794622.2	cDNA FLJ54300, highly similar to Homo sapiens queuine tRNA-ribosyltransferase domain containing 1 (QTRTD1), mRNA	0,898	0,752		0,956		0,905	0,902
IPI00925511.1	cDNA FLJ54314, highly similar to Glutaminyl-tRNA synthetase	1,313	0,973	**2,138**	1,007	0,823	0,885	0,990
IPI00795318.2	cDNA FLJ54365, highly similar to DNA replication licensing factor MCM4	1,043	1,107	1,414	0,862	0,893	0,996	1,019
IPI00925850.2	cDNA FLJ54572, highly similar to Lysosomal alpha-mannosidase	1,209	1,143		0,852			1,143
IPI00908883.3	cDNA FLJ55002, highly similar to Alpha-centractin	**1,559**	1,449	**2,439**	0,937	0,740	0,715	1,193
IPI00017799.5	cDNA FLJ55158, highly similar to Thioredoxin, mitochondrial	**1,829**	0,937	**2,207**	0,744		**1,744**	**1,744**
IPI00100748.4	cDNA FLJ55382, highly similar to Hsp70-binding protein 1	0,901	1,043	1,063	0,815	0,820	0,835	0,868
IPI01009614.1	cDNA FLJ55450, highly similar to Eukaryotic translation initiation factor 3 subunit 8		0,845	**2,975**	0,835	**0,455**	**0,623**	0,835
IPI00013214.2	cDNA FLJ55599, highly similar to DNA replication licensing factor MCM3	**1,670**	1,410	1,494	0,891	0,914	0,909	1,162
IPI01010195.1	cDNA FLJ55629, highly similar to Transcription elongation factor SPT5	**0,424**	**0,580**	1,049	0,825	0,778		0,778
IPI01018954.1	cDNA FLJ56214, highly similar to Trifunctional enzyme subunit beta, mitochondrial	1,221	1,211		0,784	**0,653**	0,705	0,784
IPI00789674.2	cDNA FLJ56271, highly similar to Coatomer subunit beta	1,002	1,088	**1,547**	0,797	**0,629**	0,751	0,899

IPI00793119.2	cDNA FLJ56274, highly similar to Transketolase	1,137	1,137	1,083	1,057	1,151	0,978	1,110
IPI00550882.3	cDNA FLJ56298, highly similar to Pyrroline-5-carboxylate reductase 1	**2,274**			**1,574**	0,784		**1,574**
IPI00644653.1	cDNA FLJ56337, highly similar to High mobility group protein B1	1,226	1,193	**1,736**	1,262	1,186	1,153	1,210
IPI00394838.3	cDNA FLJ56442, highly similar to ATP-citrate synthase	1,236	1,115	1,443	1,024	1,095	1,038	1,105
IPI00909004.1	cDNA FLJ56541, highly similar to Ubiquilin-2	0,669	**0,559**	0,861	1,411			0,765
IPI01012490.1	cDNA FLJ56675, highly similar to Activator of 90 kDa heat shock protein ATPase homolog 1	0,744	0,814	1,009	0,913	0,767	0,925	0,863
IPI00909890.1	cDNA FLJ58049, highly similar to RNA-binding protein FUS	**1,547**	0,919	**2,598**	1,202	0,898	1,279	1,241
IPI01015427.1	cDNA FLJ58247, highly similar to 26S protease regulatory subunit 4	**1,508**	1,435	**2,347**	1,109	0,807	0,814	1,272
IPI01015278.1	cDNA FLJ58314, highly similar to Mitogen-activated protein kinase 1			0,936		1,146	1,137	1,137
IPI01013559.1	cDNA FLJ58502, highly similar to Protein disulfide-isomerase A6	0,912	1,023	0,944	0,883	0,977	1,062	0,960
IPI00980890.2	cDNA FLJ58780, highly similar to Homo sapiens lysosomal-associated membrane protein 2 (LAMP2), transcript variant LAMP2B, mRNA	1,120	1,093	0,989	1,041	1,137	0,969	1,067
IPI00909622.1	cDNA FLJ58787, highly similar to Cleavage stimulation factor 64 kDa subunit	0,819		0,866	0,833	1,258		0,849
IPI00909208.1	cDNA FLJ58832, highly similar to Heterogeneous nuclear ribonucleoprotein A3	**2,158**	**2,271**	**5,091**	1,206	0,881	0,989	**1,682**
IPI00909336.1	cDNA FLJ59092	1,042	0,974	0,885	0,814	0,980	1,050	0,977
IPI01010489.1	cDNA FLJ59093, highly similar to DnaJ homolog subfamily B member 1	1,455	**1,697**			1,390		1,455
IPI00908588.1	cDNA FLJ59206, highly similar to Eukaryotic translation initiation factor 4B	1,307	1,218	0,886	0,952	0,800	1,203	1,078
IPI00798375.2	cDNA FLJ59357, highly similar to Probable ATP-dependent RNA helicase DDX5	**2,194**	1,297	**3,829**	1,301	0,696	0,995	1,299
IPI01013271.1	cDNA FLJ59601, highly similar to Pyridoxine-5'-phosphate oxidase	0,923		0,881	0,930	1,107	1,179	0,930
IPI00011876.3	cDNA FLJ59758, highly similar to S-methyl-5-thioadenosine phosphorylase	0,883	0,837	0,802	1,061	1,192	1,149	0,972
IPI00908647.1	cDNA FLJ59942, highly similar to Prostaglandin E synthase 3	0,886	1,080	1,064	0,769	0,983	0,877	0,934
IPI00917623.1	cDNA FLJ59957, highly similar to Translin	0,917	0,956	0,957	0,940	1,075	1,014	0,956
IPI00644220.4	cDNA FLJ60139, highly similar to Homo sapiens HIV TAT specific factor 1 (HTATSF1), mRNA	1,060	0,766	1,014	0,771	1,027	0,808	0,911
IPI01015383.1	cDNA FLJ60587, highly similar to Glomulin		0,797		0,899	0,689	0,887	0,842
IPI00983652.2	cDNA FLJ61021, highly similar to Far upstream element-binding protein 1	1,221	1,176	**1,918**	1,163	0,956	1,215	1,196
IPI00383581.4	cDNA FLJ61290, highly similar to Neutral alpha-glucosidase AB	**0,545**	**0,533**	**0,532**	**1,555**	**1,903**		**0,545**
IPI00745502.2	cDNA FLJ75514, highly similar to S.scrofa putative 26S protease subunit	1,369	1,278	**2,579**	1,105	0,871	0,951	1,192
IPI00640902.1	cDNA FLJ75987, highly similar to Homo sapiens zinc finger and BTB domain containing 8 opposite strand (ZBTB8OS), mRNA	1,028	0,931	0,809	0,910	1,088		0,931
IPI00947554.1	cDNA FLJ90669 fis, clone PLACE1005519, moderately similar to Homo sapiens STE20-like kinase 3 (mst-3) mRNA	0,744	0,982	1,141	0,939	0,851	0,983	0,961
IPI01012004.1	cDNA PSEC0175 fis, clone OVARC1000169,	1,023	0,982	0,924	0,884	0,988	1,025	0,985

	highly similar to Protein disulfide-isomerase A3							
IPI01015888.1	cDNA, FLJ78845, highly similar to Medium-chain specific acyl-CoA dehydrogenase, mitochondrial	1,019	0,912	0,934	0,871	1,011	0,987	0,960
IPI01010797.1	cDNA, FLJ96158, highly similar to Homo sapiens calpain 2, (m/II) large subunit (CAPN2), mRNA	0,672	0,681	0,755		1,009	1,056	0,755
IPI00216088.3	Cellular retinoic acid-binding protein 2	**0,559**	**0,557**	**0,536**	1,402	**1,615**	1,379	0,969
IPI00025974.3	Charged multivesicular body protein 4b	1,002	0,933		0,846	1,094	0,959	0,959
IPI00100796.4	Charged multivesicular body protein 5	0,753	**0,574**	0,712		1,222	1,491	0,753
IPI00010896.3	Chloride intracellular channel protein 1	0,889	0,834	0,807	1,029	1,203	1,182	0,959
IPI00001960.4	Chloride intracellular channel protein 4	0,809	0,796	0,741	1,250	1,389	1,269	1,029
IPI00297579.4	Chromobox protein homolog 3	0,744	0,823	0,822	0,790	0,829	0,952	0,822
IPI01015600.1	CIP29 protein		**6,067**		1,462	**0,604**		1,462
IPI00383539.5	Citrate synthase	1,193	1,120	0,965	0,992	1,165	1,085	1,102
IPI00646917.1	Cleavage and polyadenylation specificity factor subunit 5	1,350	**1,937**	**4,195**	1,148	0,789	1,090	1,249
IPI00017704.3	Coactosin-like protein	0,931	0,933	0,888	0,919	1,099	1,021	0,932
IPI00295851.4	Coatomer subunit beta	0,795	0,931	**1,839**	0,833	**0,405**	**0,663**	0,814
IPI00514053.1	Coatomer subunit delta		**5,415**		0,882	0,718	0,831	0,857
IPI00399318.1	coatomer subunit epsilon isoform b				0,868	**0,538**	0,877	0,868
IPI00783982.1	Coatomer subunit gamma	0,758	0,850	**1,632**	0,859	**0,444**	0,694	0,804
IPI00032851.1	Coatomer subunit zeta-1	**0,515**	0,696	0,915	0,971	0,896	0,965	0,906
IPI00012011.6	Cofilin-1	0,892	0,968	0,910	0,966	1,037	0,955	0,961
IPI00413344.3	Cofilin-2	0,983	0,996	1,064	0,874	0,997	0,871	0,989
IPI00006378.3	Coiled-coil domain-containing protein 72			**1,583**	0,961	0,915		0,961
IPI00007673.4	Coiled-coil-helix-coiled-coil-helix domain-containing protein 2, mitochondrial	**0,501**	0,890	**0,409**	**2,461**	**2,861**	**2,762**	**1,675**
IPI00395372.2	Coiled-coil-helix-coiled-coil-helix domain-containing protein 5	0,897	0,900	0,756		1,080	1,228	0,900
IPI00291136.4	Collagen alpha-1(VI) chain	0,815	0,716		0,840			0,815
IPI00014230.1	Complement component 1 Q subcomponent-binding protein, mitochondrial	1,011	1,100	1,050	0,726	0,830	0,905	0,958
IPI00549389.3	Conserved hypothetical protein	**0,652**	0,827	0,945	0,980	0,860	0,946	0,902
IPI00171844.3	COP9 signalosome complex subunit 4	0,898	0,883	1,167	0,957	0,990	0,964	0,961
IPI00009958.6	COP9 signalosome complex subunit 5	1,154			0,816	0,804	0,837	0,827
IPI00377080.1	COP9 signalosome complex subunit 8 isoform 2	0,759	0,812	1,098	0,932	0,877	0,947	0,905
IPI00917016.2	copine-1 isoform c	0,736	0,722	0,825	1,231	1,389	1,312	1,028
IPI00024403.1	Copine-3	**0,199**	0,955	**19,750**	0,993	0,980	0,947	0,968
IPI00093057.6	Coproporphyrinogen-III oxidase, mitochondrial	0,957	0,875	0,827	1,104	1,316	1,146	1,031
IPI00855846.1	Costars family protein C6orf115	1,073	1,035	1,011	0,831	0,950	0,862	0,980
IPI00022977.1	Creatine kinase B-type	1,070	1,069	1,025	0,840	0,963	0,923	0,994
IPI00004839.1	Crk-like protein	0,939	0,981	0,787	1,305	1,241	1,073	1,027

IPI00290142.5	CTP synthase 1	1,064	0,905	0,954	0,886	1,101	1,106	1,009
IPI00023530.7	Cyclin-dependent kinase 5	1,290		1,011	0,962	1,009	1,124	1,011
IPI00908512.2	cystathionine gamma-lyase isoform 3	0,820	0,947	0,871	1,010	1,265	1,112	0,978
IPI00021828.1	Cystatin-B	0,955	1,007	0,997	0,911	0,987	0,924	0,971
IPI00002824.7	Cysteine and glycine-rich protein 2	**2,609**	**0,613**		1,142	**0,536**	0,686	0,686
IPI00220416.3	Cytochrome b-c1 complex subunit 7	**3,810**	**4,483**	**2,605**	**3,484**	**2,354**	**2,452**	**3,045**
IPI00218144.3	Cytochrome c oxidase copper chaperone	0,685		**0,645**	**1,888**	1,226		0,955
IPI00017510.3	Cytochrome c oxidase subunit 2	**5,782**	**9,193**		**6,880**	**2,540**	**3,450**	**5,782**
IPI00006579.1	Cytochrome c oxidase subunit 4 isoform 1, mitochondrial	0,872	0,710	0,732	**2,318**	1,339	1,277	1,075
IPI00025086.4	Cytochrome c oxidase subunit 5A, mitochondrial	**1,771**	**1,582**	**1,538**	1,457	1,332	1,224	1,498
IPI00021785.2	Cytochrome c oxidase subunit 5B, mitochondrial		1,247	1,029	**1,962**	1,281	1,437	1,281
IPI00015972.1	Cytochrome c oxidase subunit 6C	**8,126**	**10,075**	**8,466**	**5,364**			**8,296**
IPI01014268.1	Cytochrome c oxidase subunit 7A2, mitochondrial	**7,280**	**8,478**	**13,648**				**8,478**
IPI00008485.1	Cytoplasmic aconitate hydratase	0,819	**0,564**	0,671	1,151	1,333	1,349	0,985
IPI00456969.1	Cytoplasmic dynein 1 heavy chain 1		**1,796**	**3,443**	**2,497**	0,742	1,220	**1,796**
IPI00011200.5	D-3-phosphoglycerate dehydrogenase	0,738	0,924	1,195	0,852	**0,576**	0,746	0,799
IPI00293867.7	D-dopachrome decarboxylase	0,900	0,883	0,864	0,995	1,158	1,091	0,947
IPI00152692.2	D-tyrosyl-tRNA(Tyr) deacylase 1		**1,667**	1,295		1,080	0,995	1,187
IPI00012197.1	dCTP pyrophosphatase 1	0,752	0,725	0,790	1,208	1,409	1,459	0,999
IPI00011416.2	Delta(3,5)-Delta(2,4)-dienoyl-CoA isomerase, mitochondrial	1,126	1,093	1,160	0,857	1,084	1,021	1,089
IPI00171856.1	Deoxyhypusine hydroxylase		0,783	0,793	0,956	1,199	1,212	0,956
IPI00845388.1	destrin isoform b	0,911	0,897	0,903	0,890	0,938	1,105	0,907
IPI00031836.3	Developmentally-regulated GTP-binding protein 1	1,443	**2,059**	1,402	1,347	0,916	1,024	1,375
IPI00030357.7	Dihydrofolate reductase	1,118	1,083	1,051	**0,655**	0,814	0,978	1,015
IPI00021338.2	Dihydrolipoyllysine-residue acetyltransferase component of pyruvate dehydrogenase complex, mitochondrial	1,294	1,118	**1,787**	0,965	0,829	0,683	1,041
IPI00420108.6	Dihydrolipoyllysine-residue succinyltransferase component of 2-oxoglutarate dehydrogenase complex, mitochondrial	**2,650**				**1,784**	0,749	**1,784**
IPI00014439.4	Dihydropteridine reductase			0,994	0,797	0,938		0,938
IPI00106642.4	Dihydropyrimidinase-like 2	1,376	0,892		1,142	0,903	0,914	0,914
IPI00335509.3	Dihydropyrimidinase-related protein 5		0,886			1,280	1,318	1,280
IPI00984865.2	Diphthine synthase	**0,636**			0,710	0,816		0,710
IPI00293464.5	DNA damage-binding protein 1	0,960	0,976	1,046	0,974	1,015	1,070	0,996
IPI00556021.3	DNA polymerase (Fragment)	0,676	0,743	0,892	1,253	1,020	1,298	0,956
IPI00008436.4	DNA polymerase epsilon subunit 4	0,898	1,059	1,070	1,060	1,112	1,202	1,065
IPI00032387.1	DNA replication complex GINS protein PSF1	**0,632**	0,737	0,785	0,782	1,238	1,126	0,784
IPI00007146.3	DNA replication complex GINS protein PSF2	0,863	0,852	0,844	1,012	1,155	1,098	0,937

IPI00031517.1	DNA replication licensing factor MCM6	1,049	1,096	1,423	0,914	0,819	0,916	0,983
IPI00215911.3	DNA-(apurinic or apyrimidinic site) lyase	1,297	1,219	1,044	1,317	1,280	1,289	1,284
IPI00556199.1	DNA-directed RNA polymerase II subunit RPB11-b2	0,963			1,018	0,858	1,055	0,991
IPI00007283.1	DNA-directed RNA polymerase II subunit RPB4	0,971	1,056	1,339	0,749	0,787	0,816	0,894
IPI00218895.6	DNA-directed RNA polymerase II subunit RPB7	0,991	1,022		0,870	0,679	**0,643**	0,870
IPI00291093.3	DNA-directed RNA polymerases I, II, and III subunit RPABC1	1,134	1,349	**2,083**		0,757	0,943	1,134
IPI00003311.1	DNA-directed RNA polymerases I, II, and III subunit RPABC5	0,976		**1,861**	1,225	0,901	1,093	1,093
IPI00012535.1	DnaJ homolog subfamily A member 1				0,764	**0,501**	**0,658**	**0,658**
IPI00794610.2	dnaJ homolog subfamily C member 7 isoform 2				0,951	0,690	0,923	0,923
IPI00003438.2	DnaJ homolog subfamily C member 8	0,960			1,253	1,457	1,301	1,277
IPI00018671.1	Dual specificity protein phosphatase 3	**0,552**	0,696	0,970	0,955	1,023	0,773	0,864
IPI00914026.1	dynactin subunit 1 isoform 4			**3,040**	0,883	**0,427**		0,883
IPI00019329.1	Dynein light chain 1, cytoplasmic	1,080	1,145	1,080	0,891	0,814	0,799	0,985
IPI00062037.1	Dynein light chain 2, cytoplasmic	0,999	1,118	1,187	0,971	0,828	0,795	0,985
IPI00019495.1	Dynein light chain Tctex-type 1	**1,516**	1,322	1,199	1,090	1,103	0,853	1,151
IPI00292354.8	E3 ubiquitin-protein ligase RNF181				1,187	1,278	1,191	1,191
IPI00940851.1	ELAV-like protein 1	**1,536**	**1,768**	**3,722**	1,153	0,785	1,037	1,344
IPI00010810.1	Electron transfer flavoprotein subunit alpha, mitochondrial	1,043	0,944	0,827	1,012	1,199	1,143	1,028
IPI00396485.3	Elongation factor 1-alpha 1	1,124	1,154	0,826	**1,966**	**1,759**	**1,526**	1,340
IPI00014424.1	Elongation factor 1-alpha 2	1,155			**2,313**	**2,102**	**1,890**	**1,996**
IPI00178440.3	Elongation factor 1-beta	1,197	1,363	1,354	1,237	1,002	1,178	1,217
IPI00937615.2	Elongation factor 1-gamma	1,198	1,471	**1,603**	1,118	0,834	0,933	1,158
IPI00186290.6	Elongation factor 2	1,257	1,145	0,951	1,232	1,437	1,162	1,197
IPI00976226.1	Enabled-like protein variant hMenaDv6	**0,567**	**0,637**	1,297	1,168		1,255	1,168
IPI00019169.3	endophilin-A2 isoform 1	0,854	0,956	1,055			1,128	1,006
IPI00024911.1	Endoplasmic reticulum resident protein 29	1,339	1,037	0,824	1,008	1,119	1,236	1,078
IPI00401264.5	Endoplasmic reticulum resident protein 44	0,950	0,962	0,922	1,002	1,208	1,038	0,982
IPI00027230.3	Endoplasmin	1,049	0,978	0,869	0,891	1,048	1,012	0,995
IPI00029631.1	Enhancer of rudimentary homolog	0,965	1,210	**3,462**	0,754	**0,550**	0,712	0,859
IPI00791152.1	enhancer of yellow 2 transcription factor homolog isoform 2	0,731	0,888	0,922	0,897	0,944	0,951	0,910
IPI00024993.4	Enoyl-CoA hydratase, mitochondrial	1,015	0,941	1,002	0,942	1,043	1,054	1,008
IPI00010951.2	Epiplakin	**0,575**	**0,482**	**0,662**	0,918	0,690	0,840	0,676
IPI00386755.2	ERO1-like protein alpha	0,990	0,967	0,877	0,820	0,927	0,960	0,943
IPI00025491.1	Eukaryotic initiation factor 4A-I	0,929	1,137	1,343	0,864	0,735	0,917	0,923
IPI00009328.4	Eukaryotic initiation factor 4A-III	1,135	1,374	**1,918**	1,192	0,694	0,974	1,164
IPI00909083.1	eukaryotic peptide chain release factor GTP-binding subunit ERF3A isoform 2	0,975	0,741	0,762	0,978	1,049	1,021	0,977

IPI00003588.1	Eukaryotic translation elongation factor 1 epsilon-1	**2,023**	**1,624**	**3,236**	1,040	0,864	0,935	1,332
IPI00015077.1	Eukaryotic translation initiation factor 1	0,910	1,075	1,312	0,950	0,862	0,741	0,930
IPI00232533.5	Eukaryotic translation initiation factor 1A, X-chromosomal	1,359	1,093	**1,726**	0,804	**0,571**	**0,596**	0,949
IPI00219678.3	Eukaryotic translation initiation factor 2 subunit 1	**1,831**	**1,678**		1,178		0,929	1,428
IPI00297982.7	Eukaryotic translation initiation factor 2 subunit 3		1,380		**1,554**		1,310	1,380
IPI00013068.1	Eukaryotic translation initiation factor 3 subunit E	1,421	1,161		0,771	**0,303**	**0,485**	0,771
IPI00290460.3	Eukaryotic translation initiation factor 3 subunit G	0,832	**1,697**		0,884	**0,620**	0,745	0,832
IPI00012795.3	Eukaryotic translation initiation factor 3 subunit I	**3,794**	0,929		0,745	**0,355**	**0,411**	0,745
IPI00033143.1	Eukaryotic translation initiation factor 3 subunit K	1,121	0,944	**1,545**	0,808	**0,569**	0,693	0,876
IPI00102069.5	Eukaryotic translation initiation factor 3 subunit M		1,042		0,799	**0,556**	**0,644**	0,722
IPI00022648.2	Eukaryotic translation initiation factor 5	0,953	0,836	1,155	0,690	**0,547**	**0,636**	0,763
IPI00010105.1	Eukaryotic translation initiation factor 6	0,878	0,921	0,843	0,956	1,012	1,030	0,938
IPI00968296.1	Eukaryotic translation termination factor 1, isoform CRA_b	0,927	0,930	0,755	1,199	1,123	1,013	0,972
IPI00644775.2	Exosome complex exonuclease RRP46	**1,962**	**2,099**	**1,657**				**1,962**
IPI00298961.3	Exportin-1	**0,603**	0,944	1,460	0,693	**0,343**	**0,560**	**0,648**
IPI00640703.3	Exportin-5	0,780	1,087	1,153	0,773	**0,497**	0,779	0,780
IPI00302458.10	Exportin-7	1,139	1,193	1,316	0,765	0,674	0,760	0,952
IPI00306290.5	Exportin-T	0,955	0,993	0,945	0,871	1,088	1,028	0,974
IPI00843975.1	Ezrin	1,354	1,284	1,104	1,446	1,316	1,281	1,300
IPI00005969.3	F-actin-capping protein subunit alpha-1	0,883	0,832	0,900	0,975	1,218	1,028	0,937
IPI00026182.5	F-actin-capping protein subunit alpha-2	0,877	0,755			1,193		0,877
IPI00026970.4	FACT complex subunit SPT16	**0,626**	0,788	**1,635**	0,751	**0,537**	**0,632**	0,692
IPI00005154.1	FACT complex subunit SSRP1	**0,644**	0,803	**1,685**	0,729	**0,542**	0,680	0,705
IPI00914971.1	farnesyl pyrophosphate synthase isoform b	1,045	0,986	1,014	0,860	1,140	0,963	1,000
IPI00163187.10	Fascin	0,871	0,741	0,725	1,128	1,342	1,159	1,000
IPI00026781.3	Fatty acid synthase	0,845	0,903	1,334	0,992	0,871	0,953	0,928
IPI00007797.3	Fatty acid-binding protein, epidermal	0,997	0,975	0,918	0,879	1,032	0,959	0,967
IPI00554521.2	Ferritin heavy chain	1,292	1,133	1,240	0,822	0,688	0,809	0,978
IPI00647507.1	FK506 binding protein 1A, 12kDa	1,041	0,998	0,963	0,872	1,034	0,945	0,981
IPI00026215.1	Flap endonuclease 1	0,806	0,970	1,310	1,055	0,948	1,060	1,012
IPI00783862.2	Flavin reductase	0,844	0,862	0,790	1,032	1,304	1,200	0,947
IPI00643324.1	Four and a half LIM domains 1	0,948	0,907	0,735	1,001	1,111	0,916	0,932
IPI01014927.1	Fructose-bisphosphate aldolase	1,104	0,994	1,046	1,448	1,441	1,140	1,122
IPI00465439.5	Fructose-bisphosphate aldolase A	1,210	1,026	1,105	1,426	1,299	1,073	1,158
IPI00031708.1	Fumarylacetoacetase	1,069	1,030	0,832	1,056	1,227	1,089	1,063
IPI00329742.2	Fumarylacetoacetate hydrolase domain-containing protein 2A	0,783	0,731		1,151	1,116	1,258	1,116

IPI00914953.1	G-rich sequence factor 1 isoform 2	**0,607**		0,732	1,257	1,273	**1,552**	1,257
IPI00940264.1	Galactokinase	0,855	0,845	0,732	1,231	1,430	1,246	1,043
IPI00219219.3	Galectin-1	0,728	**0,664**	0,713	1,208	1,288	1,097	0,912
IPI00023549.5	Galectin-related protein	0,798	0,824	0,693	1,031	1,263	1,047	0,928
IPI00026358.3	Gamma-aminobutyric acid receptor-associated protein-like 2	0,958	1,081	1,111	0,986	0,827	0,872	0,972
IPI00215881.3	Gamma-crystallin D	1,089		0,896	0,770	0,917	0,875	0,896
IPI00216171.3	Gamma-enolase	**0,559**	0,786	0,757	1,088	1,263	1,320	0,937
IPI00013832.3	GatC-like protein	1,074		0,889	1,042	0,960		1,001
IPI00291783.4	Gem-associated protein 5			**1,785**	0,916	0,799	0,939	0,927
IPI00016725.2	General transcription factor 3C polypeptide 4	0,962	1,080	1,113	0,859	0,689	0,854	0,911
IPI00978910.1	Glia maturation factor beta	0,953	0,791	1,115	0,790	0,835	0,853	0,844
IPI00061525.3	Glucosamine 6-phosphate N-acetyltransferase	1,400	1,298	0,942	1,038	1,331	1,199	1,248
IPI00009305.1	Glucosamine-6-phosphate isomerase 1	0,748	0,762	0,706	1,003	1,168	1,152	0,882
IPI00027497.5	Glucose-6-phosphate isomerase	1,167	1,145	1,114	0,916	1,027	0,928	1,071
IPI00792916.2	glucosidase 2 subunit beta isoform 2	0,878	**0,581**	0,941	**0,664**	0,982	0,980	0,910
IPI00010130.3	Glutamine synthetase			1,036	**1,667**	1,177		1,177
IPI00219025.3	Glutaredoxin-1	0,788	0,763	0,751	1,141	1,338	1,244	0,965
IPI00008552.6	Glutaredoxin-3	0,809	0,839	0,808	0,882	1,017	0,984	0,860
IPI00333763.7	Glutaredoxin-related protein 5, mitochondrial	1,047	1,049	0,834	0,835	0,889	0,805	0,862
IPI00927606.1	Glutathione peroxidase 1	1,159	1,072	0,927	0,699	1,064	0,948	1,006
IPI00984060.1	glutathione S-transferase Mu 2 isoform 2	0,839	0,762	0,782	1,126	1,260	1,166	0,983
IPI00246975.8	Glutathione S-transferase Mu 3	0,832	0,783	0,803	1,062	1,299	1,090	0,947
IPI00019755.3	Glutathione S-transferase omega-1	0,929	0,882	0,901	1,027	1,225	1,105	0,978
IPI00219757.13	Glutathione S-transferase P	0,956	0,940	0,851	0,909	1,111	1,039	0,948
IPI00010706.1	Glutathione synthetase	1,030	1,016	1,010	0,849	0,975	0,939	0,992
IPI00219018.7	Glyceraldehyde-3-phosphate dehydrogenase	1,071	1,281	1,415	1,164	1,092	0,856	1,128
IPI00011604.2	Glycine cleavage system H protein, mitochondrial			0,889	0,846	1,061		0,889
IPI00157144.2	glycogen [starch] synthase, muscle isoform 2		**1,515**	**1,760**		1,222		**1,515**
IPI00004358.4	Glycogen phosphorylase, brain form	1,080	1,102	1,109	0,875	1,020	0,979	1,050
IPI00943894.1	glycogen phosphorylase, liver form isoform 2	0,980	0,962	0,998	1,014	1,115	1,069	1,006
IPI00783097.4	Glycyl-tRNA synthetase	0,855	0,943	0,928	1,063	1,017	1,137	0,980
IPI00037448.3	Glyoxylate reductase/hydroxypyruvate reductase	1,081	1,078	0,984	0,838	1,120	1,019	1,048
IPI00029079.5	GMP synthase [glutamine-hydrolyzing]	0,719	0,798	0,791	0,962	1,136	1,062	0,880
IPI00009315.6	Golgi resident protein GCP60	**0,640**	0,740	0,987		1,117	0,795	0,795
IPI00029557.3	GrpE protein homolog 1, mitochondrial	1,016	1,024	0,956	0,840	0,959	1,029	0,988
IPI00643041.3	GTP-binding nuclear protein Ran	1,078	1,009	0,958	0,954	1,022	0,999	1,004
IPI00016669.1	GTP-binding protein Rheb	1,008	1,197	0,921	0,906	0,876	0,928	0,925

IPI00015954.1	GTP-binding protein SAR1a	**0,653**	0,873				0,916	0,873
IPI00002149.1	GTP-binding protein SAR1b	**0,436**	**0,665**	**0,652**	1,242	1,178	1,134	0,900
IPI00000005.1	GTPase NRas	0,930	1,053	0,874	0,981	0,828	0,846	0,902
IPI00848226.1	Guanine nucleotide-binding protein subunit beta-2-like 1	1,303	1,229	**1,501**	1,044	0,833	0,839	1,137
IPI00328868.3	HCLS1-binding protein 3	**0,487**	**0,468**			1,310	1,259	0,873
IPI00304925.5	Heat shock 70 kDa protein 1A/1B	0,763	0,867	0,892	0,999	1,169	1,128	0,945
IPI00002966.2	Heat shock 70 kDa protein 4	0,961	0,892	0,946	0,926	1,124	1,038	0,954
IPI00295485.4	Heat shock 70 kDa protein 4L	0,894	0,847	0,931	0,931	1,045	1,016	0,931
IPI00025512.2	Heat shock protein beta-1	**0,385**	**0,441**	**0,563**	1,236	1,028	1,005	0,784
IPI00098827.1	Heat shock protein beta-11	0,999	0,975	0,987	0,826	0,948	0,964	0,970
IPI00414676.6	Heat shock protein HSP 90-beta	0,818	0,842	0,947	0,934	0,984	1,019	0,941
IPI00644697.2	HEBP2 protein (Fragment)	1,130	1,040	0,956	0,863	1,049	1,068	1,044
IPI00148063.1	Heme-binding protein 1	0,808	0,961	0,865	1,147	1,180	1,161	1,054
IPI00020956.1	Hepatoma-derived growth factor	0,918	0,903	**0,520**	**1,597**	**1,773**	1,378	1,148
IPI00011913.1	Heterogeneous nuclear ribonucleoprotein A0	**2,042**	**2,109**	**4,139**	1,132	0,760	0,950	**1,587**
IPI00003881.5	Heterogeneous nuclear ribonucleoprotein F	1,150	1,192	1,177	0,830	0,762	0,865	1,008
IPI00304692.1	Heterogeneous nuclear ribonucleoprotein G	**3,084**	**5,107**	**11,706**	**1,725**	0,821	1,160	**2,404**
IPI00013881.6	Heterogeneous nuclear ribonucleoprotein H	1,482	1,440	**2,014**	1,023	0,770	0,971	1,231
IPI00026230.1	Heterogeneous nuclear ribonucleoprotein H2				1,229	0,858	0,974	0,974
IPI00027834.3	Heterogeneous nuclear ribonucleoprotein L	**1,555**	1,413	**4,565**	1,384	0,875	1,005	1,398
IPI00930205.1	heterogeneous nuclear ribonucleoprotein Q isoform 5	**1,728**	**1,671**	**2,630**	1,115	0,895	1,029	1,393
IPI00219344.4	Hippocalcin-like protein 1				**0,598**	**0,170**	**0,344**	**0,344**
IPI00239077.5	Histidine triad nucleotide-binding protein 1	1,059	0,996	0,881	0,870	1,163	1,060	1,028
IPI00000335.1	Histidine triad nucleotide-binding protein 2, mitochondrial	0,863	0,822	0,701	0,982	1,114	1,118	0,923
IPI00651621.1	Histone acetyltransferase 1, isoform CRA_b	**0,459**	0,693	0,777	1,021	0,733	0,903	0,755
IPI00972999.1	Histone deacetylase	0,898			1,027	0,979		0,979
IPI00013774.1	Histone deacetylase 1	0,969	0,954			0,987	0,928	0,961
IPI00217465.5	Histone H1.2	1,157	**6,162**		0,835	**0,418**	**0,505**	0,835
IPI00021924.1	Histone H1x	**2,192**			**2,709**	1,467	**1,824**	**2,008**
IPI00081836.3	Histone H2A type 1-H	1,192	**2,140**	**2,717**	1,256	0,831	0,950	1,224
IPI00018278.3	Histone H2A.V	1,239	1,093	1,098	1,166	1,134	1,226	1,150
IPI00018534.4	Histone H2B type 1-L	**1,593**	**4,378**	**3,015**	0,973	**0,644**	0,718	1,283
IPI00003935.6	Histone H2B type 2-E	**1,781**	**1,916**	**3,878**		**0,560**	0,695	**1,781**
IPI00171611.7	Histone H3.2	1,222	**1,766**	**3,497**	1,114	0,675	0,778	1,168
IPI00453473.6	Histone H4	1,473	**1,902**	**4,364**	0,963	**0,575**	**0,651**	1,218
IPI00395865.4	Histone-binding protein RBBP7	**0,409**	**0,595**	0,723	**1,683**	**1,723**	**2,126**	1,203
IPI00032826.1	Hsc70-interacting protein	0,993	0,962	1,171	0,822	0,814	0,874	0,918

IPI00013122.1	Hsp90 co-chaperone Cdc37	0,680	0,859	0,835	0,859	1,032	0,989	0,859
IPI00549672.2	HSPC027	1,166	1,169	**2,179**	1,108	0,830	0,910	1,137
IPI01012145.1	Hydroxymethylbilane synthase	0,810	0,834	0,865	0,909	1,082	1,018	0,887
IPI00218493.7	Hypoxanthine-guanine phosphoribosyltransferase	1,043	1,043	0,962	0,834	0,975	0,903	0,969
IPI00000877.1	Hypoxia up-regulated protein 1	0,950	0,930	0,902	0,834	0,977	0,982	0,940
IPI00002214.1	Importin subunit alpha-2	**0,647**	0,745	0,977	1,030	0,799	0,872	0,836
IPI00299033.1	Importin subunit alpha-3	**0,649**			1,093	0,903	1,100	0,998
IPI00012578.1	Importin subunit alpha-4	0,814			0,897	0,835	0,870	0,853
IPI00001639.2	Importin subunit beta-1	1,008	1,164	1,047	0,943	0,877	1,040	1,024
IPI00301107.7	Importin-11	**0,648**	0,845	0,905	0,850	0,751	0,856	0,847
IPI00007402.3	Importin-7	0,883	0,959	1,085	0,840	0,828	0,859	0,871
IPI00185146.5	Importin-9	0,762	0,878	1,353	0,806	**0,315**	**0,597**	0,784
IPI00015018.1	Inorganic pyrophosphatase	0,952	0,931	0,825	0,994	1,189	1,096	0,973
IPI00018783.1	Inosine triphosphate pyrophosphatase	0,674	0,685	**0,665**	1,090	1,280	1,068	0,877
IPI00291510.3	Inosine-5'-monophosphate dehydrogenase 2	**4,205**	**2,963**	**11,110**	**2,084**	**1,918**	1,247	**2,524**
IPI00220373.5	Insulin-degrading enzyme	0,910	0,955	1,025	0,990	1,052	1,029	1,008
IPI00008557.6	Insulin-like growth factor 2 mRNA-binding protein 1	1,416	1,364	**2,952**	1,315	0,912	1,214	1,340
IPI00005198.2	Interleukin enhancer-binding factor 2	**1,527**	**1,695**	**2,219**	1,366	0,995	1,245	1,447
IPI00376195.5	Iron-sulfur cluster assembly 2 homolog, mitochondrial	0,896		0,918	0,680	0,843	0,875	0,875
IPI00304082.8	Isochorismatase domain-containing protein 1	0,989	0,903	1,030	1,010	0,957	1,058	1,000
IPI01015385.1	Isocitrate dehydrogenase	1,119	1,003	1,019	0,858	1,084	0,953	1,011
IPI00027223.2	Isocitrate dehydrogenase [NADP] cytoplasmic	0,982	0,923	0,791	1,006	1,134	1,048	0,994
IPI00016736.1	Isoform 1 of 1-phosphatidylinositol-4,5-bisphosphate phosphodiesterase gamma-1				0,950	1,142	1,044	1,044
IPI00651738.1	Isoform 1 of 1,2-dihydroxy-3-keto-5-methylthiopentene dioxygenase	0,800	0,854	0,711	0,697	1,063	0,996	0,827
IPI00000816.1	Isoform 1 of 14-3-3 protein epsilon	1,021	1,024	1,008	0,831	0,923	0,900	0,965
IPI00017726.1	Isoform 1 of 3-hydroxyacyl-CoA dehydrogenase type-2	0,945	0,916	0,991	0,904	1,029	1,037	0,968
IPI00607799.5	Isoform 1 of 3-hydroxybutyrate dehydrogenase type 2	1,067	1,066	1,076	0,785	1,216	0,939	1,066
IPI00419802.4	Isoform 1 of 3-hydroxyisobutyryl-CoA hydrolase, mitochondrial			0,774		1,035	1,134	1,035
IPI00300567.1	Isoform 1 of 3,2-trans-enoyl-CoA isomerase, mitochondrial	1,001	1,017	0,940	0,749	0,978	0,876	0,959
IPI00410214.1	Isoform 1 of 3'(2'),5'-bisphosphate nucleotidase 1	0,878	0,954	0,920	0,866	1,022	1,001	0,937
IPI00332371.9	Isoform 1 of 6-phosphofructokinase, liver type	**2,196**	**1,923**	**4,057**	1,291	1,240	1,045	**1,607**
IPI00743142.2	Isoform 1 of 6-phosphofructokinase, muscle type	**2,173**	**1,648**	**2,983**	1,306		0,855	**1,648**
IPI00024933.3	Isoform 1 of 60S ribosomal protein L12	**12,030**	**9,695**	**10,643**	**5,557**	1,353	**2,194**	**7,626**
IPI00003627.1	Isoform 1 of Actin-like protein 6A				1,181	1,089	1,120	1,120
IPI00550234.4	Isoform 1 of Actin-related protein 2/3 complex subunit 5	**2,237**		1,439	1,341	1,223	1,045	1,341

IPI00010182.4	Isoform 1 of Acyl-CoA-binding protein	0,922	0,945	0,815	0,904	1,193	1,137	0,933
IPI00032879.1	Isoform 1 of Adenylate kinase isoenzyme 6	0,855	0,839	0,884	0,741	0,795	0,925	0,847
IPI00942092.1	Isoform 1 of Adenylosuccinate lyase	1,053	1,104	1,085	0,819	0,979	0,879	1,016
IPI00008274.8	Isoform 1 of Adenylyl cyclase-associated protein 1	0,978	0,922	1,280	0,975	1,019	0,916	0,976
IPI00021685.1	Isoform 1 of ADP-ribosylation factor-like protein 6	0,762	0,934	0,895	**1,799**	**1,851**	**1,552**	1,243
IPI00028277.8	Isoform 1 of Alpha-ketoglutarate-dependent dioxygenase FTO	**0,584**	0,708	0,889	0,819	0,822	0,924	0,820
IPI00455315.4	Isoform 1 of Annexin A2	**0,483**	0,965	**5,258**	0,952	0,960	0,910	0,956
IPI00553153.2	Isoform 1 of ATPase inhibitor, mitochondrial	**1,598**	1,208	1,038	0,880	1,234	0,924	1,123
IPI00413587.2	Isoform 1 of BH3-interacting domain death agonist	0,795	0,827	0,944	0,820	0,763	0,847	0,823
IPI00184821.1	Isoform 1 of Bifunctional coenzyme A synthase	0,702	0,695	0,796	1,379	1,231	1,337	1,014
IPI00002203.6	Isoform 1 of BRCA2 and CDKN1A-interacting protein	0,858	0,837	0,824	0,986	1,064	1,126	0,922
IPI00941900.1	Isoform 1 of Calumenin	1,075	0,668	0,883	0,683	1,016	1,034	0,950
IPI00299177.4	Isoform 1 of Cat eye syndrome critical region protein 5	0,850	0,693	0,738	1,074	1,059	1,215	0,954
IPI00295857.7	Isoform 1 of Coatomer subunit alpha		1,474	**2,481**	0,765	**0,454**	**0,660**	0,765
IPI00375957.3	Isoform 1 of COMM domain-containing protein 6	0,997		**1,860**	0,818	0,703	0,695	0,818
IPI00016746.1	Isoform 1 of Core-binding factor subunit beta	0,789		0,949	0,796	0,916	0,785	0,796
IPI00658109.1	Isoform 1 of Creatine kinase U-type, mitochondrial	**1,983**	**1,723**	1,149	1,215	1,260		1,260
IPI00100160.3	Isoform 1 of Cullin-associated NEDD8-dissociated protein 1	1,213	1,135	1,235	0,980	0,822	0,904	1,057
IPI00942408.1	Isoform 1 of Cyclin-dependent kinase inhibitor 2A, isoforms 1/2/3	0,811	0,856	0,881	0,884	1,163	1,120	0,882
IPI00015897.2	Isoform 1 of Cysteine and histidine-rich domain-containing protein 1	0,904	0,976	0,853	1,047	1,369	1,159	1,011
IPI00177728.3	Isoform 1 of Cytosolic non-specific dipeptidase	0,867	0,811	0,755	0,932	1,302	1,108	0,899
IPI00007926.1	Isoform 1 of Deoxyribonucleoside 5'-monophosphate N-glycosidase	1,121	1,099	1,003	1,026	1,186	0,905	1,062
IPI00748700.2	Isoform 1 of DNA replication complex GINS protein PSF3	0,905	0,855	1,037	0,952	1,124	1,023	0,987
IPI00031614.2	Isoform 1 of DNA replication complex GINS protein SLD5	**0,561**		0,899		**1,961**	1,144	1,022
IPI00299904.3	Isoform 1 of DNA replication licensing factor MCM7	1,092	1,088	1,494	0,768	0,845	0,919	1,004
IPI00296337.2	Isoform 1 of DNA-dependent protein kinase catalytic subunit	**3,681**	**2,868**	**9,660**	**1,590**	0,837	1,019	**2,229**
IPI00003406.4	Isoform 1 of Drebrin	0,749	**0,540**	1,345	0,913	0,791	0,873	0,832
IPI00456925.3	Isoform 1 of Drebrin-like protein		**0,612**	0,688	1,088	0,959	0,867	0,867
IPI00643583.2	Isoform 1 of Dynein light chain roadblock-type 1	1,043	1,002	0,941	1,193	1,324	1,160	1,101
IPI00004902.1	Isoform 1 of Electron transfer flavoprotein subunit beta	1,021	0,886	0,865	1,038	1,218	1,065	1,029
IPI00376317.4	Isoform 1 of Enhancer of mRNA-decapping protein 4			1,158	0,960	**0,447**	**0,593**	0,777
IPI00038378.5	Isoform 1 of Enolase-phosphatase E1	1,007	0,932	0,844	0,826	1,091	1,243	0,969

IPI00411704.9	Isoform 1 of Eukaryotic translation initiation factor 5A-1	1,365	1,208	1,120	0,935	0,904	0,915	1,028
IPI00377261.1	Isoform 1 of Far upstream element-binding protein 3		0,747		**1,668**	0,928		0,928
IPI00031564.1	Isoform 1 of Gamma-glutamylcyclotransferase	0,852	0,896	0,824	0,942	1,173	1,111	0,919
IPI00219673.6	Isoform 1 of Glutathione S-transferase kappa 1	**5,678**	**5,974**	**4,806**	**4,462**	**4,675**	**4,692**	**4,749**
IPI00514126.2	Isoform 1 of Glycogen debranching enzyme	1,234	1,173	1,235	1,166	1,327	1,238	1,234
IPI00021327.3	Isoform 1 of Growth factor receptor-bound protein 2	0,936	0,976	1,008	0,851	1,102	0,861	0,956
IPI00789618.2	Isoform 1 of Guanosine-3',5'-bis(diphosphate) 3'-pyrophosphohydrolase MESH1	**1,932**	0,728	0,745		1,274		1,009
IPI00872352.1	Isoform 1 of HD domain-containing protein 2	0,928	0,823	0,789	0,869	1,139	0,961	0,899
IPI00100984.4	Isoform 1 of HEAT repeat-containing protein 3	0,735	0,796	1,022	0,882	0,758	0,853	0,825
IPI00003865.1	Isoform 1 of Heat shock cognate 71 kDa protein	1,066	1,083	1,187	0,805	0,814	0,867	0,967
IPI00784295.2	Isoform 1 of Heat shock protein HSP 90-alpha	0,820	0,821	0,905	0,977	1,032	1,092	0,941
IPI00007764.4	Isoform 1 of Hematological and neurological expressed 1 protein	0,886	**0,588**	**0,631**	0,991	1,329	1,078	0,938
IPI00939776.1	Isoform 1 of Hepatoma-derived growth factor-related protein 2	0,740	**0,470**			1,392		0,740
IPI00216049.1	Isoform 1 of Heterogeneous nuclear ribonucleoprotein K	1,233	1,287	**2,159**	1,200	0,829	1,067	1,217
IPI00012074.3	Isoform 1 of Heterogeneous nuclear ribonucleoprotein R	**1,609**	**1,664**	**3,244**	1,372	0,937	1,192	1,490
IPI00294398.2	Isoform 1 of Hydroxyacyl-coenzyme A dehydrogenase, mitochondrial	**1,607**	**1,533**	0,918	0,897	0,992	0,816	0,955
IPI00414384.1	Isoform 1 of Hydroxysteroid dehydrogenase-like protein 2	1,162	1,225	1,261	0,989			1,193
IPI00156374.6	Isoform 1 of Importin-4	**0,624**	0,799	1,073	0,872	**0,590**	0,788	0,794
IPI00793443.2	Isoform 1 of Importin-5	0,718	0,912	1,158	0,738	**0,630**	0,694	0,728
IPI00301109.4	Isoform 1 of Inorganic pyrophosphatase 2, mitochondrial	1,228	1,027	0,998	0,903	0,945	0,956	0,977
IPI00658000.3	Isoform 1 of Insulin-like growth factor 2 mRNA-binding protein 3	1,392	1,313	**2,974**	1,469	0,844	1,142	1,353
IPI00872292.1	Isoform 1 of Intraflagellar transport protein 27 homolog	0,984	0,985	0,834	0,870	1,033	1,003	0,985
IPI00551022.3	Isoform 1 of Isochorismatase domain-containing protein 2, mitochondrial	0,908	0,768	0,820	0,931	1,114	1,114	0,920
IPI00030702.1	Isoform 1 of Isocitrate dehydrogenase [NAD] subunit alpha, mitochondrial	1,062	1,099	1,156	1,017	1,052	1,229	1,080
IPI00645307.2	Isoform 1 of Isopentenyl-diphosphate Delta-isomerase 1	1,102	0,998	**0,613**	0,787	1,010	0,856	0,927
IPI00143921.9	Isoform 1 of KDEL motif-containing protein 2	1,078	1,416			1,297		1,297
IPI00555734.3	Isoform 1 of L-asparaginase	1,010	0,922	0,828	0,824	0,975	0,813	0,875
IPI00217966.9	Isoform 1 of L-lactate dehydrogenase A chain	1,149	1,102	1,087	0,848	0,978	0,919	1,032
IPI00219077.4	Isoform 1 of Leukotriene A-4 hydrolase	0,929	0,933	0,935	0,977	1,152	1,014	0,956
IPI00000861.1	Isoform 1 of LIM and SH3 domain protein 1	0,851	0,825			1,492	1,149	1,000
IPI00219861.3	Isoform 1 of Low molecular weight phosphotyrosine protein phosphatase	0,841	0,829	0,819	1,001	1,107	1,103	0,921
IPI00059762.5	Isoform 1 of Lysophospholipase-like protein 1	0,860	1,043	0,990	0,862		0,755	0,862

IPI00101782.3	Isoform 1 of Mannose-1-phosphate guanyltransferase alpha	0,890		0,686	1,121	1,250	1,462	1,121
IPI00030920.2	Isoform 1 of Mannose-1-phosphate guanyltransferase beta	1,138			0,992	1,170	1,296	1,154
IPI00219358.7	Isoform 1 of Mannose-6-phosphate isomerase	0,763	0,750	0,832	1,001	1,137	1,241	0,916
IPI00005948.1	Isoform 1 of Methylthioribose-1-phosphate isomerase	1,015	1,015	1,046	0,755	0,932	0,928	0,973
IPI00032409.1	Isoform 1 of Mitogen-activated protein-binding protein-interacting protein	1,119	1,236	1,119	0,948	0,978	0,870	1,048
IPI00397526.3	Isoform 1 of Myosin-10	1,292	1,220	**1,847**	1,147	0,952	0,945	1,183
IPI00337335.8	Isoform 1 of Myosin-14	0,929	1,077	1,204	0,924	0,898	0,714	0,926
IPI00019502.3	Isoform 1 of Myosin-9	1,132	1,188	**1,539**	1,170	1,023	1,030	1,151
IPI00386189.2	Isoform 1 of N-alpha-acetyltransferase 15, NatA auxiliary subunit	1,074	1,126	0,961	0,887	0,779	0,838	0,924
IPI00301051.3	Isoform 1 of NHL repeat-containing protein 2	0,873	0,831	0,849	0,747	1,019	1,111	0,861
IPI00456663.1	Isoform 1 of Nitrilase homolog 1	0,950	0,901	0,954	0,989	1,200	1,112	0,971
IPI00100197.3	Isoform 1 of NSFL1 cofactor p47	0,803	0,790	1,015	0,952	1,046	0,994	0,973
IPI00179953.2	Isoform 1 of Nuclear autoantigenic sperm protein	0,980	0,769	0,866	0,824	1,054	1,022	0,923
IPI00183500.2	Isoform 1 of Nuclear cap-binding protein subunit 2	1,126	1,334	**2,424**	0,942	0,751	0,981	1,053
IPI00304267.3	Isoform 1 of Nucleoredoxin			**0,642**	1,191	1,468	1,417	1,304
IPI00290416.3	Isoform 1 of Obg-like ATPase 1	0,926	0,944	0,882	0,960	1,072	1,049	0,952
IPI00783302.1	Isoform 1 of Pentatricopeptide repeat-containing protein 3, mitochondrial		**2,191**		1,257	0,748		1,257
IPI00941201.1	Isoform 1 of Peptidyl-prolyl cis-trans isomerase NIMA-interacting 4	**2,305**	**2,282**	**1,869**	**3,083**	0,990	1,172	**2,076**
IPI00300952.3	Isoform 1 of Peptidyl-prolyl cis-trans isomerase-like 3	1,066	1,108	1,053	1,020	1,154	1,126	1,087
IPI00334907.3	Isoform 1 of Phosphatidylinositol transfer protein beta isoform	0,731	0,892	0,844	0,943	1,121	1,107	0,918
IPI00797038.1	Isoform 1 of Phosphoenolpyruvate carboxykinase [GTP], mitochondrial	0,734	0,727	0,743		1,065	1,244	0,743
IPI00219526.6	Isoform 1 of Phosphoglucomutase-1	0,939	0,904	0,943	0,855	1,032	0,976	0,941
IPI00218728.4	Isoform 1 of Platelet-activating factor acetylhydrolase IB subunit alpha	1,020	0,911	1,064	0,823	0,886	0,985	0,948
IPI00179964.5	Isoform 1 of Polypyrimidine tract-binding protein 1	0,957	1,120	**2,085**	1,337	0,763	1,138	1,129
IPI00163381.4	Isoform 1 of Prolyl 3-hydroxylase 1	0,874	1,056	1,092				1,056
IPI00030243.1	Isoform 1 of Proteasome activator complex subunit 3	1,012	0,960	1,422	0,890	0,865	0,989	0,975
IPI00005260.4	Isoform 1 of Proteasome activator complex subunit 4			**4,224**		**1,897**	**1,828**	**1,897**
IPI00024175.3	Isoform 1 of Proteasome subunit alpha type-7	**1,948**	**1,551**	**3,020**	1,226	1,030	0,979	1,388
IPI00443909.1	Isoform 1 of Protein canopy homolog 2	0,961	0,870	0,800	0,800	0,926	1,035	0,898
IPI00868973.1	Isoform 1 of Protein PRRC1	**0,631**	0,771	0,951	0,684		1,208	0,771
IPI00072377.1	Isoform 1 of Protein SET	**0,307**	**0,290**	**0,285**	**2,851**	**3,305**	**3,159**	**1,579**
IPI00411680.11	Isoform 1 of Protein-L-isoaspartate(D-aspartate) O-methyltransferase	0,800	0,774	0,724	1,031	1,103	1,019	0,909
IPI01012991.1	Isoform 1 of Putative RNA-binding protein Luc7-	1,099	0,964	1,185	0,810	0,932	0,910	0,948

	like 2							
IPI00013004.1	Isoform 1 of Pyridoxal kinase	0,998	0,953	0,941	0,899	1,070	0,998	0,976
IPI00607591.3	Isoform 1 of Rap1 GTPase-GDP dissociation stimulator 1	0,826	0,768	0,804	0,910	0,951	1,067	0,868
IPI00005719.1	Isoform 1 of Ras-related protein Rab-1A		1,184	0,928	0,963			0,963
IPI00013939.3	Isoform 1 of Replication protein A 32 kDa subunit	0,871	0,829		0,932	0,733	0,895	0,871
IPI00011726.1	Isoform 1 of RNA 3'-terminal phosphate cyclase	0,856	0,966	1,041	1,037	0,879	0,956	0,961
IPI00023556.3	Isoform 1 of RNA polymerase II subunit A C-terminal domain phosphatase SSU72	0,998	1,224	1,131	0,805	0,946	0,975	0,987
IPI00021187.4	Isoform 1 of RuvB-like 1	0,966	1,031	**1,581**	0,931	0,822	0,921	0,949
IPI00301364.3	Isoform 1 of S-phase kinase-associated protein 1	0,874	0,865	0,839	1,112	1,183	1,168	0,993
IPI00782992.3	Isoform 1 of Serine/arginine repetitive matrix protein 2	**0,493**	**0,180**	0,787		1,387	**2,462**	0,787
IPI00012970.1	Isoform 1 of Serine/threonine-protein phosphatase 6 catalytic subunit	**0,665**		0,844	1,019	1,049	1,290	1,019
IPI00168388.1	Isoform 1 of Signal recognition particle 68 kDa protein	**0,588**	0,805	1,390	0,786	**0,483**	**0,509**	0,687
IPI00815770.2	Isoform 1 of Sorting nexin-3	0,830	1,010		0,932	0,765	0,894	0,894
IPI00848161.1	Isoform 1 of Spliceosome RNA helicase BAT1	1,397	1,385	1,329	0,950	0,688	1,146	1,237
IPI00300371.5	Isoform 1 of Splicing factor 3B subunit 3	1,064	1,329	**1,578**	1,268	0,866	0,863	1,166
IPI00301432.3	Isoform 1 of TP53RK-binding protein	1,172	1,060	1,017	0,796	1,046	0,959	1,031
IPI00784161.1	Isoform 1 of Transcription elongation factor SPT6	**0,619**	0,717	0,983	0,766	0,907	1,237	0,837
IPI00438229.2	Isoform 1 of Transcription intermediary factor 1-beta	0,833	0,725	1,119	0,827	0,808	0,721	0,817
IPI00797270.4	Isoform 1 of Triosephosphate isomerase	1,098	1,069	1,009	0,815	0,975	0,907	0,992
IPI00010779.4	Isoform 1 of Tropomyosin alpha-4 chain	1,038	0,960	0,927	0,982	1,063	0,971	0,977
IPI00295400.1	Isoform 1 of Tryptophanyl-tRNA synthetase, cytoplasmic	0,862	0,819	0,747	1,021	1,174	1,155	0,942
IPI00396203.7	Isoform 1 of Tubulin-specific chaperone D	0,937	0,931	1,020	0,770	0,976	1,042	0,957
IPI00420014.2	Isoform 1 of U5 small nuclear ribonucleoprotein 200 kDa helicase	1,451	**2,013**	**4,566**	1,255	0,669	0,976	1,353
IPI00099550.1	Isoform 1 of Ubiquilin-1	**0,628**	**0,605**	0,749	0,880	**1,614**	1,163	0,815
IPI00939174.1	Isoform 1 of Ubiquitin thioesterase OTUB1	0,996	0,855	0,986	0,936	1,073	0,979	0,982
IPI00026965.1	Isoform 1 of Ubiquitin-conjugating enzyme E2 D3	0,800	0,753	0,824	0,910			0,812
IPI00021370.1	Isoform 1 of Ubiquitin-conjugating enzyme E2 K	0,750	0,841	1,002	0,906	1,179	0,921	0,913
IPI00023647.4	Isoform 1 of Ubiquitin-like modifier-activating enzyme 6	0,812	0,898	0,933	0,942	0,971	0,940	0,936
IPI00100775.1	Isoform 1 of UPF0366 protein C11orf67	1,057	0,906	0,879	0,876	1,227	1,044	0,975
IPI00101095.3	Isoform 1 of UPF0687 protein C20orf27	0,739	0,686	**0,625**	1,246	1,487	1,251	0,993
IPI00003923.1	Isoform 1 of Uridine 5'-monophosphate synthase	0,706	0,937	0,882	0,906	0,847	0,872	0,877
IPI00170796.1	Isoform 1 of Vacuolar protein sorting-associated protein 29	1,116	1,151	1,345	0,776	0,761	0,819	0,968
IPI00291175.7	Isoform 1 of Vinculin	0,895	0,879	0,919	0,900	0,967	0,899	0,900
IPI00746165.2	Isoform 1 of WD repeat-containing protein 1	1,048	1,116	1,105	0,889	1,017	0,939	1,032

IPI00886797.1	Isoform 2 of 2',5'-phosphodiesterase 12		0,827	0,839		1,315	1,067	0,953
IPI00456695.1	Isoform 2 of 26S proteasome non-ATPase regulatory subunit 1	1,434	1,324	**2,417**	1,097	0,849	0,892	1,210
IPI00847986.1	Isoform 2 of 40S ribosomal protein S24	**3,666**	**2,962**	**5,243**	**1,771**	0,706	1,029	**2,367**
IPI00746438.2	Isoform 2 of 60S ribosomal protein L11	**2,827**	**1,817**	**2,061**	**2,297**	1,452	**1,707**	**1,939**
IPI00759824.2	Isoform 2 of Acidic leucine-rich nuclear phosphoprotein 32 family member B	0,976	1,024	0,894	0,778	0,902	0,817	0,898
IPI00218988.4	Isoform 2 of Adenylate kinase 2, mitochondrial	0,930	0,972	0,849	0,948	1,057	1,097	0,960
IPI00845377.1	Isoform 2 of ADP-ribosylation factor-like protein 2-binding protein	0,893	0,976	1,005		0,942		0,959
IPI00936002.1	Isoform 2 of Alpha-aminoadipic semialdehyde dehydrogenase	1,128	1,117	1,116	0,962	1,076	1,158	1,116
IPI00220797.1	Isoform 2 of Alpha-endosulfine	0,963	**0,361**	1,024	0,895	1,234	0,940	0,951
IPI00848298.1	Isoform 2 of Apolipoprotein A-I-binding protein	0,700	**0,660**	**0,628**	1,260	**1,589**	1,419	0,980
IPI00180128.4	Isoform 2 of Basic leucine zipper and W2 domain-containing protein 1	0,990	1,197	1,406	1,324		0,984	1,197
IPI00016786.1	Isoform 2 of Cell division control protein 42 homolog	0,748	**0,663**	**0,628**	0,852	1,079	1,400	0,800
IPI00430813.3	Isoform 2 of Cellular nucleic acid-binding protein	1,422	1,132	1,038	0,746	0,747	0,722	0,893
IPI00455383.4	Isoform 2 of Clathrin heavy chain 1	0,688	0,857	1,054	0,917	0,763	0,907	0,882
IPI00646794.1	Isoform 2 of Craniofacial development protein 1	0,891	**0,612**	0,908		0,941	1,016	0,908
IPI00939491.1	Isoform 2 of Cysteinyl-tRNA synthetase, cytoplasmic	0,992	0,870	0,740		1,034	1,157	0,992
IPI00789806.2	Isoform 2 of Cytosol aminopeptidase	1,117	1,151	1,123	0,851	0,965	0,901	1,041
IPI00335930.1	Isoform 2 of DAZ-associated protein 1	1,148		**2,028**	1,450	1,201	1,447	1,447
IPI00375015.3	Isoform 2 of Deoxyuridine 5'-triphosphate nucleotidohydrolase, mitochondrial	0,886	0,815	0,804	1,018	1,213	1,147	0,952
IPI00219865.1	Isoform 2 of Diablo homolog, mitochondrial	0,850	0,897	1,136	0,793	0,766	0,882	0,866
IPI00445401.4	Isoform 2 of E3 ubiquitin-protein ligase HUWE1	**0,544**	**0,665**	1,165	0,911	**0,491**	0,747	0,706
IPI00643286.4	Isoform 2 of Epimerase family protein SDR39U1	0,911	**0,634**	0,935	1,328			0,923
IPI00642256.2	Isoform 2 of F-actin-capping protein subunit beta	1,051	1,008	1,151	0,885	0,999	0,855	1,004
IPI00855957.3	Isoform 2 of Far upstream element-binding protein 2	1,321	1,131	**1,923**	1,054	0,974	1,228	1,179
IPI00302592.2	Isoform 2 of Filamin-A	0,901	0,850	1,434	1,185	0,972	0,991	0,981
IPI00943563.1	Isoform 2 of Filamin-B	0,779	0,804	1,132	0,986	0,922	0,972	0,947
IPI00413958.5	Isoform 2 of Filamin-C	**0,527**	**0,611**	0,861	1,399	1,360	1,389	1,110
IPI00299506.9	Isoform 2 of Glucosamine--fructose-6-phosphate aminotransferase [isomerizing] 1	1,142	1,004	1,077	0,885	1,042	1,007	1,025
IPI00383296.5	Isoform 2 of Heterogeneous nuclear ribonucleoprotein M	**1,920**	**2,543**	**7,716**	1,440	**0,509**	1,043	**1,680**
IPI00647813.1	Isoform 2 of Inosine-5'-monophosphate dehydrogenase 1	**4,013**			**2,309**	**1,711**		**2,309**
IPI00640098.1	Isoform 2 of Inositol-3-phosphate synthase 1	0,983	0,802	0,799	1,096	1,167	1,214	1,040
IPI00385834.3	Isoform 2 of KH domain-containing, RNA-binding, signal transduction-associated protein 1	1,487			**1,544**	**0,587**	0,964	1,225
IPI00900380.1	Isoform 2 of Malignant T cell-amplified sequence 1	**0,619**	**0,601**	1,308		0,679	0,826	0,679

IPI00789428.1	Isoform 2 of Methylcrotonoyl-CoA carboxylase beta chain, mitochondrial	1,074	1,002	1,268	0,903	0,973	0,939	0,988
IPI00220113.1	Isoform 2 of Microtubule-associated protein 4		0,787	1,007	**0,533**	**0,551**	**0,474**	**0,551**
IPI00178861.1	Isoform 2 of N(2),N(2)-dimethylguanosine tRNA methyltransferase	1,047	0,824	0,957		0,952	0,959	0,957
IPI00011454.1	Isoform 2 of Neutral alpha-glucosidase AB	0,986	0,710	0,835	1,328	1,067	**1,534**	1,026
IPI00873590.1	Isoform 2 of NIF3-like protein 1	0,986	0,875	0,873	1,047	1,032	1,163	1,009
IPI00006196.3	Isoform 2 of Nuclear mitotic apparatus protein 1	0,931	1,343	1,202	0,854	**0,587**	**0,634**	0,892
IPI00477179.1	Isoform 2 of Nucleolar RNA helicase 2	**2,441**	**2,250**	**4,872**	**1,997**	0,714	1,106	**2,123**
IPI00220740.1	Isoform 2 of Nucleophosmin	0,760	1,083	1,496	0,967	0,667	0,893	0,930
IPI00216130.8	Isoform 2 of Opioid growth factor receptor		1,069	**0,661**		**1,541**	**1,558**	1,305
IPI00790634.2	Isoform 2 of Partner of Y14 and mago	**1,819**			1,238	0,987		1,238
IPI00604702.1	Isoform 2 of Phosphopantothenoylcysteine decarboxylase		0,849	0,778	0,820			0,820
IPI00903152.1	Isoform 2 of Phosphotriesterase-related protein		0,925		0,873	1,091	1,020	0,973
IPI00410017.1	Isoform 2 of Polyadenylate-binding protein 1	1,406	1,244	**2,641**	0,883	**0,560**	0,789	1,064
IPI00003964.4	Isoform 2 of Probable ubiquitin carboxyl-terminal hydrolase FAF-X	0,920	0,948	1,456	0,806	0,671	0,777	0,863
IPI00171199.5	Isoform 2 of Proteasome subunit alpha type-3	**2,146**	**1,757**	**3,443**	1,240	0,944	0,979	1,499
IPI00607601.2	Isoform 2 of Protein farnesyltransferase/geranylgeranyltransferase type-1 subunit alpha	0,889	0,940	0,865	0,920	1,163	1,070	0,930
IPI00395771.1	Isoform 2 of Protein phosphatase 1 regulatory subunit 7	0,954	0,965	0,957	0,857	0,881	0,922	0,938
IPI00412156.3	Isoform 2 of Protein phosphatase methylesterase 1	**0,510**		0,744	1,118	0,825	0,926	0,825
IPI00735181.2	Isoform 2 of Protein unc-45 homolog A				0,805	**0,532**	**0,654**	**0,654**
IPI00549885.4	Isoform 2 of Pyruvate dehydrogenase E1 component subunit beta, mitochondrial	0,908	0,937	1,354	0,819	**0,629**	0,685	0,864
IPI00217943.3	Isoform 2 of Ras-related protein Rab-6A	0,845	1,052	0,961		1,075	1,035	1,035
IPI00216532.1	Isoform 2 of Regulator of G-protein signaling 10	1,060		0,704	0,902	1,207		0,981
IPI00373788.1	Isoform 2 of Ribulose-phosphate 3-epimerase	0,988	0,928	0,875	0,864	1,148	1,108	0,958
IPI00216659.1	Isoform 2 of RNA-binding protein 8A	0,974	1,031	1,090	1,369	1,299	1,355	1,195
IPI00884890.1	Isoform 2 of Selenocysteine lyase	0,930		**0,589**		1,214	0,930	0,930
IPI00220542.1	Isoform 2 of Serine protease HTRA2, mitochondrial	0,914	0,919	0,817	0,978	1,040	0,964	0,942
IPI00844112.1	Isoform 2 of Sorting nexin-12	0,821	1,036	1,126	0,958	0,903	0,939	0,948
IPI00333015.7	Isoform 2 of Spectrin beta chain, brain 1	0,888	1,046	**1,868**	1,069	**0,515**	**0,659**	0,967
IPI00642393.1	Isoform 2 of Spermine synthase	1,102	1,060	0,951	0,862	0,984	0,942	0,967
IPI00830039.1	Isoform 2 of Splicing factor U2AF 65 kDa subunit	1,010	1,135	**1,741**	1,090	0,831	1,126	1,108
IPI00791573.1	Isoform 2 of Suppressor of G2 allele of SKP1 homolog	**0,583**	0,781	0,772	0,948	0,995	1,009	0,865
IPI00216425.1	Isoform 2 of Testin			**0,463**		1,352	1,219	1,219
IPI00419473.5	Isoform 2 of Transcription factor BTF3	0,915	0,915	0,771	0,963	0,983	0,940	0,927
IPI00843876.1	Isoform 2 of Transportin-1	0,875	1,081	1,327	0,895	0,952	0,924	0,938

IPI00218319.3	Isoform 2 of Tropomyosin alpha-3 chain	1,001	0,945	0,956	0,837	0,993	0,945	0,951
IPI00221178.1	Isoform 2 of Tumor protein D54	1,047	0,969	0,802	0,985	0,862	0,937	0,953
IPI00219512.2	Isoform 2 of Ubiquitin carboxyl-terminal hydrolase isozyme L5	0,705			0,841	0,669	0,750	0,727
IPI00619903.3	Isoform 2 of UDP-glucose:glycoprotein glucosyltransferase 1	0,782	0,896	1,052	0,923	0,933	0,952	0,928
IPI00395676.1	Isoform 2 of UTP--glucose-1-phosphate uridylyltransferase		1,390		0,973	1,001	0,892	0,987
IPI00218467.1	Isoform 2-4 of Alpha-synuclein	0,786	**0,518**		0,714	0,908	0,775	0,775
IPI00940222.2	Isoform 3 of A-kinase anchor protein 12	0,763	**0,499**	0,794	0,706	1,038	1,046	0,779
IPI00549277.2	Isoform 3 of Allograft inflammatory factor 1-like	**0,452**	0,763	**0,403**	1,088	1,231	1,052	0,907
IPI00025333.4	Isoform 3 of Anamorsin	**0,475**	**0,513**		1,173	1,056		0,785
IPI00555743.2	Isoform 3 of Apoptosis inhibitor 5		**1,806**		1,100	**0,562**		1,100
IPI00157908.4	Isoform 3 of Apoptosis-inducing factor 1, mitochondrial	**1,912**	1,457	1,087	1,314	1,307	1,455	1,384
IPI00645320.1	Isoform 3 of Beta-catenin-like protein 1	**0,322**	**0,588**		0,723	**0,468**	0,713	**0,588**
IPI00965290.1	Isoform 3 of Cullin-4B	0,952	1,072	1,302	0,908	0,800	0,812	0,930
IPI00514971.2	Isoform 3 of Dynactin subunit 3	1,049	1,045		0,815	0,790	0,781	0,815
IPI00646605.3	Isoform 3 of E3 ubiquitin-protein ligase UBR4		1,095	**2,167**	1,164	**0,509**	0,703	1,095
IPI00219994.2	Isoform 3 of Exportin-2	**0,658**	1,019	1,384	0,712	**0,478**	**0,632**	0,685
IPI00398214.2	Isoform 3 of FAD synthase		**0,470**	0,706			1,449	0,706
IPI00045498.4	Isoform 3 of Heterogeneous nuclear ribonucleoprotein D-like	**1,503**	**1,670**	**3,261**	0,975	0,704	0,999	1,251
IPI00220684.1	Isoform 3 of Heterogeneous nuclear ribonucleoprotein D0	**1,692**	**1,711**	**2,933**	1,009	0,797	1,101	1,396
IPI00216493.1	Isoform 3 of Heterogeneous nuclear ribonucleoprotein H3	**1,553**	**1,612**	**3,284**	**1,554**	0,716	1,190	**1,553**
IPI00477093.3	Isoform 3 of Integrator complex subunit 3		0,967	1,430	1,171		1,050	1,110
IPI00795292.1	Isoform 3 of Nucleoside diphosphate kinase B	0,964	0,965	0,912	0,951	1,097	1,016	0,965
IPI00783594.3	Isoform 3 of RNA-binding protein with serine-rich domain 1	0,897	1,167		0,805	**0,516**	0,760	0,805
IPI00217296.2	Isoform 3 of Serine/threonine-protein phosphatase 2A activator	1,050	1,038	0,752	0,996	1,171	1,048	1,043
IPI00719345.1	Isoform 3 of Serine/threonine-protein phosphatase 6 regulatory subunit 3		0,830	1,063		0,721	0,911	0,870
IPI00843765.1	Isoform 3 of Spectrin alpha chain, brain	1,193	1,035	**1,628**	0,826	**0,645**	0,755	0,931
IPI00472633.7	Isoform 3 of Transformer-2 protein homolog beta	1,084	1,356	**5,210**	0,776	**0,608**	0,842	0,963
IPI00455127.2	Isoform 3 of Transportin-3	0,733	0,785	0,907	1,212	0,946	0,999	0,927
IPI00885131.1	Isoform 3 of tRNA (adenine-N(1)-)-methyltransferase non-catalytic subunit TRM6	0,824	0,730		0,881	1,046	0,996	0,881
IPI00472498.3	Isoform 3 of Ubiquitin-conjugating enzyme E2 variant 1	**0,528**	0,698	0,669	1,300	**1,531**	1,423	0,999
IPI00646750.2	Isoform 3 of Uncharacterized protein C1orf31	**1,533**	1,067	0,923	1,037	1,279	1,239	1,153
IPI00921488.1	Isoform 4 of COP9 signalosome complex subunit 1		0,670		0,998	0,841	0,872	0,856
IPI00736859.1	Isoform 4 of Heterogeneous nuclear ribonucleoprotein U-like protein 1	1,457	0,875	0,913	1,041	1,268	**2,249**	1,155

IPI00877802.2	Isoform 4 of Histone-binding protein RBBP4	**0,475**	**0,620**	**0,532**	1,240	**1,591**	1,475	0,930
IPI00845510.1	Isoform 4 of Methionine adenosyltransferase 2 subunit beta	1,026	1,050	1,023	0,823	0,899	0,949	0,986
IPI00412714.3	Isoform 4 of Plasminogen activator inhibitor 1 RNA-binding protein	**1,786**	**5,262**	1,198	**1,767**	1,245	1,263	**1,515**
IPI00788826.1	Isoform 4 of Poly(U)-binding-splicing factor PUF60	**0,348**	**5,464**		1,050	**0,555**	1,193	1,050
IPI00889541.2	Isoform 4 of Probable ATP-dependent RNA helicase DDX17	**2,174**	**1,906**	**4,611**	1,270	0,818	1,059	**1,588**
IPI00386118.3	Isoform 4 of Splicing factor 1	0,802	**0,512**	**2,543**	1,106	1,212	1,499	1,159
IPI00816829.2	Isoform 4 of Twinfilin-1		0,927			1,207	1,225	1,207
IPI00219451.1	Isoform 5 of Cytosolic acyl coenzyme A thioester hydrolase	0,714	0,842	0,859	0,885	1,048	1,000	0,872
IPI00219330.2	Isoform 5 of Interleukin enhancer-binding factor 3	**1,804**	1,145	**2,326**	1,270	0,962	1,278	1,274
IPI00554786.5	Isoform 5 of Thioredoxin reductase 1, cytoplasmic	0,803	0,756	**0,592**	0,928	1,337	1,031	0,865
IPI00398776.3	Isoform 7 of Plectin		0,799	**1,645**			0,821	0,821
IPI00010271.3	Isoform A of Ras-related C3 botulinum toxin substrate 1	1,048	0,837	0,672	1,240	**1,798**	1,334	1,144
IPI00465365.4	Isoform A1-A of Heterogeneous nuclear ribonucleoprotein A1	**1,936**	**1,978**	**4,218**	1,130	0,715	0,964	**1,533**
IPI00217816.3	Isoform AGX1 of UDP-N-acetylhexosamine pyrophosphorylase	0,941			0,846	0,966		0,941
IPI00292387.6	Isoform Alpha of Nucleolar and coiled-body phosphoprotein 1		**0,525**	1,383			**0,613**	**0,613**
IPI00465248.5	Isoform alpha-enolase of Alpha-enolase	1,099	1,038	1,028	0,981	1,030	0,996	1,029
IPI00215884.4	Isoform ASF-1 of Serine/arginine-rich splicing factor 1	0,996	1,364	**3,798**	0,792	**0,534**	0,711	0,894
IPI00396378.3	Isoform B1 of Heterogeneous nuclear ribonucleoproteins A2/B1	**1,976**	**2,200**	**4,779**	1,305	0,846	1,090	**1,641**
IPI00218993.1	Isoform Beta of Heat shock protein 105 kDa	1,016	0,978	1,022	0,837	0,969	0,926	0,974
IPI00554556.1	Isoform C of Protein CutA	0,945	0,900	0,872	0,940	1,173	1,012	0,943
IPI00004860.2	Isoform Complexed of Arginyl-tRNA synthetase, cytoplasmic	1,262	1,153	**1,661**	0,990	0,884	0,925	1,071
IPI00759715.1	Isoform Cytoplasmic of Fumarate hydratase, mitochondrial	1,030	1,008	0,895	0,868	0,978	0,931	0,955
IPI00759575.1	Isoform Cytoplasmic of Glutathione reductase, mitochondrial	0,904	0,834	0,780	0,965	1,224	1,164	0,934
IPI00014238.2	Isoform Cytoplasmic of Lysyl-tRNA synthetase	**1,973**	**1,759**	**3,870**	1,047	0,903	0,906	1,403
IPI00745335.7	Isoform Cytoplasmic of Phospholipid hydroperoxide glutathione peroxidase, mitochondrial				1,348	1,233	0,932	1,233
IPI00759663.1	Isoform Cytoplasmic+peroxisomal of Peroxiredoxin-5, mitochondrial	0,993	0,887	0,890	1,150	1,316	0,992	0,992
IPI00010882.3	Isoform DFF45 of DNA fragmentation factor subunit alpha (Fragment)	1,001	0,911	0,921	0,889	1,037	0,987	0,954
IPI00386533.4	Isoform E of Eukaryotic translation initiation factor 4 gamma 1	0,995	0,810	**2,560**	0,916	**0,538**	0,751	0,863
IPI00071059.4	Isoform Epsilon of Apoptosis regulator BAX				1,269	**0,522**	0,766	0,766
IPI00019450.2	Isoform Long of 60 kDa SS-A/Ro ribonucleoprotein	1,018	0,889	0,988	1,000	0,979	0,952	0,984
IPI00024913.2	Isoform Long of ES1 protein homolog,	0,955	0,970	0,882	0,888	0,970	1,073	0,962

	mitochondrial							
IPI00014263.1	Isoform Long of Eukaryotic translation initiation factor 4H	1,000	**0,488**	0,874	1,088	1,051	1,296	1,025
IPI00883857.2	Isoform Long of Heterogeneous nuclear ribonucleoprotein U	**2,047**	**1,782**	**3,166**	1,237	0,907	1,111	**1,510**
IPI00010740.1	Isoform Long of Splicing factor, proline- and glutamine-rich	**2,653**	**3,015**	**37,192**	1,456	**0,430**	0,686	**2,055**
IPI00025273.1	Isoform Long of Trifunctional purine biosynthetic protein adenosine-3	0,838	0,801	0,879	1,022	1,105	1,056	0,950
IPI00479186.7	Isoform M2 of Pyruvate kinase isozymes M1/M2	1,289	1,188	1,084	1,191	1,296	1,030	1,190
IPI00216393.1	Isoform Non-brain of Clathrin light chain A	0,934	0,830	0,958	0,850	1,024	1,050	0,946
IPI00335168.9	Isoform Non-muscle of Myosin light polypeptide 6	1,128	1,102	1,425	1,045	1,067	1,031	1,085
IPI00396056.6	Isoform p18 of 7,8-dihydro-8-oxoguanine triphosphatase	1,020	0,958	0,932	0,871	1,065	1,061	0,989
IPI00022694.3	Isoform Rpn10A of 26S proteasome non-ATPase regulatory subunit 4	1,419	1,295	**2,337**	0,982	0,759	0,890	1,138
IPI00759832.1	Isoform Short of 14-3-3 protein beta/alpha	1,037	1,041	1,017	0,840	0,910	0,886	0,964
IPI00234368.1	Isoform Short of Adenosine kinase	0,981	0,899	0,820	0,974	1,195	1,092	0,978
IPI00873244.1	Isoform Short of Cold shock domain-containing protein E1	0,954	1,094	1,256	0,982	1,001	1,124	1,047
IPI00218547.1	Isoform Short of Delta-1-pyrroline-5-carboxylate synthase	0,931	0,963	1,166	1,046	0,943	1,080	1,004
IPI00289800.7	Isoform Short of Glucose-6-phosphate 1-dehydrogenase	0,936	0,895	0,839	0,992	1,153	1,194	0,964
IPI00218830.1	Isoform Short of Glycylpeptide N-tetradecanoyltransferase 1	1,230			0,974	0,730		0,974
IPI00016832.1	Isoform Short of Proteasome subunit alpha type-1	**2,084**	**1,791**	**3,255**	1,251	1,463	1,039	**1,627**
IPI00375145.1	Isoform Short of Ubiquitin carboxyl-terminal hydrolase 5	0,833	0,876	0,799	0,932	1,109	1,098	0,904
IPI00375513.3	Isoform Soluble of Catechol O-methyltransferase	1,017		1,053	1,386	**1,724**	**1,620**	1,386
IPI00413654.3	Isoform SRP40-4 of Serine/arginine-rich splicing factor 5				0,947	0,680	0,921	0,921
IPI00644127.2	Isoleucyl-tRNA synthetase, cytoplasmic	**1,571**	1,369	**2,733**	1,044	0,810	0,900	1,206
IPI00017283.2	Isoleucyl-tRNA synthetase, mitochondrial	1,255	1,133	1,174	0,771	0,908	1,037	1,085
IPI00012837.1	Kinesin-1 heavy chain	**1,637**	**1,729**	1,083	1,463	1,442	1,353	1,453
IPI00553183.1	kynurenine--oxoglutarate transaminase 3 isoform 2			0,919		1,002	0,899	0,919
IPI00250297.3	L-aminoadipate-semialdehyde dehydrogenase-phosphopantetheinyl transferase	**0,514**	**0,558**	0,912	1,199	1,075	1,167	0,994
IPI00219217.3	L-lactate dehydrogenase B chain	1,076	1,106	1,075	0,854	0,971	0,915	1,023
IPI00220766.5	Lactoylglutathione lyase	1,075	1,037	0,997	0,837	1,029	0,966	1,013
IPI00013976.4	Laminin subunit beta-1	0,902				0,938	0,839	0,902
IPI00793299.2	large proline-rich protein BAG6 isoform c				0,813	**0,604**		0,709
IPI00783271.1	Leucine-rich PPR motif-containing protein, mitochondrial	1,147	1,161	1,178	0,779	0,836	0,879	1,013
IPI00790831.1	LMNB1 protein	**1,892**	1,400	0,951		0,996	1,114	1,114
IPI00009032.1	Lupus La protein	1,118	1,061	1,072	0,816	0,947	0,930	1,004
IPI00007148.1	LYR motif-containing protein 2	1,118	1,121	0,984	0,819	0,919	0,874	0,951

IPI00006979.1	LYR motif-containing protein 4	1,086			1,103	1,118	1,076	1,094
IPI00329321.3	LYR motif-containing protein 7	1,162	1,121	0,981	**0,653**	0,802	0,727	0,891
IPI00293088.7	Lysosomal alpha-glucosidase	1,132	0,900	1,009		1,095	0,989	1,009
IPI00293276.10	Macrophage migration inhibitory factor	0,830	0,807	1,023	1,120	1,285	1,218	1,072
IPI00916111.3	Malate dehydrogenase, cytoplasmic	1,025	1,026	1,033	0,867	1,028	0,940	1,026
IPI00291006.2	Malate dehydrogenase, mitochondrial	1,118	1,110	1,097	1,090	1,269	1,114	1,112
IPI00556579.3	maleylacetoacetate isomerase isoform 1	0,913	0,835	0,804	0,978	1,215	1,135	0,945
IPI00641181.5	MARCKS-related protein	**1,664**	0,986	0,683	**1,902**	**2,304**	**2,107**	**1,783**
IPI00017297.1	Matrin-3	1,333	**1,506**	**3,659**	1,488	0,732	1,057	1,411
IPI00220739.3	Membrane-associated progesterone receptor component 1	1,274	1,427		**1,906**	1,173	1,329	1,329
IPI00980165.2	Mesencephalic astrocyte-derived neurotrophic factor	**1,912**	**1,771**	1,268	0,801	1,006	0,818	1,137
IPI00008240.2	Methionyl-tRNA synthetase, cytoplasmic	**1,643**	1,436	**2,795**	1,270	1,073	1,151	1,353
IPI00012202.1	Methylosome protein 50	1,299	1,282	1,471	0,887	0,860	0,829	1,085
IPI00017596.3	Microtubule-associated protein RP/EB family member 1	1,219	1,092	0,834	1,243	**1,691**	1,114	1,167
IPI00151462.3	Microtubule-associated proteins 1A/1B light chain 3 beta 2				1,352	1,167	1,108	1,167
IPI00877948.1	Minichromosome maintenance complex component 5	**1,616**	1,325	1,300	1,024	1,038	0,996	1,169
IPI00007052.6	Mitochondrial fission 1 protein	1,321				1,118	1,319	1,319
IPI00001589.1	Mitochondrial import inner membrane translocase subunit Tim13	1,209	1,168	1,054	1,015	0,972	0,987	1,035
IPI00028376.1	Mitochondrial import inner membrane translocase subunit Tim8 A	1,178	1,036	1,074	0,946	1,070	0,977	1,053
IPI01015642.1	Mitochondrial import inner membrane translocase subunit Tim8 B	1,062	0,905	1,144	0,726	0,806	0,812	0,859
IPI00024976.5	Mitochondrial import receptor subunit TOM22 homolog	**2,195**	**2,117**		**1,852**	0,933	1,144	**1,852**
IPI00166749.3	Mitochondrial-processing peptidase subunit alpha	0,931	0,922	0,936	0,934	1,058	1,085	0,935
IPI00927892.1	Mitochondrial-processing peptidase subunit beta	1,171	1,082	1,052	0,713	0,890	0,816	0,971
IPI00973093.1	Mitogen-activated protein kinase 9 isoform JNK2 gamma 2	0,817		0,700	1,067	**1,625**	1,195	1,067
IPI00012369.1	Mitotic spindle assembly checkpoint protein MAD2A	**0,474**	**0,594**	0,747	1,009	0,863	1,074	0,805
IPI00007024.1	Mitotic spindle-associated MMXD complex subunit MIP18	0,722	**0,629**	0,871	0,930	1,246	1,269	0,900
IPI00219365.3	Moesin	1,197	1,068	0,718	1,228	1,305	1,189	1,193
IPI00002968.1	Molybdopterin synthase sulfur carrier subunit	1,088	1,103	1,066	0,799	0,978	0,920	1,022
IPI00217223.1	Multifunctional protein ADE2	1,174	1,076	1,261	1,066	1,179	0,999	1,125
IPI00220573.4	Myosin regulatory light chain 12A	1,216	1,170	**1,526**	1,102	0,976	0,972	1,136
IPI00924816.1	Myotrophin	0,957	0,903	0,907	0,974	1,071	1,054	0,966
IPI00219301.7	Myristoylated alanine-rich C-kinase substrate	1,420	**0,570**	0,690	**2,136**	**2,714**	**2,139**	**1,778**
IPI00955394.1	N(4)-(beta-N-acetylglucosaminyl)-L-asparaginase isoform 2 preproprotein				0,965	0,989	0,967	0,967

IPI00910124.1	N(G),N(G)-dimethylarginine dimethylaminohydrolase 1 isoform 2	0,671	0,866	0,987	1,313	1,438	1,105	1,046
IPI00003527.5	Na(+)/H(+) exchange regulatory cofactor NHE-RF1	0,756	**0,659**	**0,580**	1,203	1,421	1,252	0,980
IPI00011201.1	NAD-dependent malic enzyme, mitochondrial	1,373			0,985	1,338	0,859	1,162
IPI00515016.1	NAD(P)H dehydrogenase, quinone 2	**0,626**	0,688	0,880				0,688
IPI00554681.2	NADH dehydrogenase [ubiquinone] 1 alpha subcomplex subunit 5	**1,741**	**1,988**	**2,251**	**2,282**	**2,576**	**2,380**	**2,266**
IPI00291328.3	NADH dehydrogenase [ubiquinone] flavoprotein 2, mitochondrial	1,175	1,244	1,173	1,317	1,324	1,269	1,256
IPI00023748.3	Nascent polypeptide-associated complex subunit alpha	0,925	**2,033**	0,768	0,909	0,853	0,890	0,900
IPI00375533.5	NEDD8-activating enzyme E1 catalytic subunit isoform 2	0,953	0,868	0,868	0,979	1,143	1,075	0,966
IPI00604676.1	NEDD8-activating enzyme E1 regulatory subunit isoform b	0,860	0,877	0,926	0,960	1,132	1,081	0,943
IPI00022597.1	NEDD8-conjugating enzyme Ubc12	**0,649**	0,790	0,840	1,208	1,017	1,135	0,929
IPI00980337.1	NEDD8-MDP1 protein	0,739	0,806	0,749	1,065	1,194	1,223	0,935
IPI00002525.3	Neudesin	1,154	0,990	0,970	0,758	0,921	0,930	0,950
IPI00022640.1	Neurogranin	**0,286**	**0,406**	0,786			**5,263**	**0,596**
IPI00019472.4	Neutral amino acid transporter B(0)	**1,869**	**1,515**		1,319			**1,515**
IPI00160021.2	NFU1 iron-sulfur cluster scaffold homolog, mitochondrial isoform 1	0,955	0,835	0,941		0,969	0,984	0,955
IPI00026167.5	NHP2-like protein 1	1,255	**1,501**	**3,373**	1,022	**0,583**	0,849	1,138
IPI00018873.1	Nicotinamide phosphoribosyltransferase	1,022	0,926	0,821	1,023	1,190	1,006	1,014
IPI00411540.3	Non-histone chromosomal protein			**1,920**		0,939	1,255	1,255
IPI00304596.3	Non-POU domain-containing octamer-binding protein	**2,178**	**3,118**	**18,663**	1,135	**0,423**	0,682	**1,656**
IPI00019380.1	Nuclear cap-binding protein subunit 1	0,732	1,179	**2,086**	0,940	0,694	0,954	0,947
IPI00550746.4	Nuclear migration protein nudC	**0,616**	0,801	0,855	0,863	0,880	0,983	0,859
IPI00783781.2	Nuclear pore complex protein Nup205				0,835	**0,373**	**0,533**	**0,533**
IPI00791711.1	Nuclear receptor 2C2-associated protein	1,081	1,096	1,021	0,861	0,945	0,883	0,983
IPI00009901.1	Nuclear transport factor 2	0,908	0,878	0,855	0,989	1,175	1,163	0,949
IPI00031812.3	Nuclease-sensitive element-binding protein 1	1,131	0,924	1,221	1,341	1,163	1,343	1,192
IPI00411937.4	Nucleolar protein 56	**1,714**	**1,679**	**6,117**	1,386	**0,501**	1,008	**1,533**
IPI00006379.1	Nucleolar protein 58	1,096	**2,011**		1,125	**0,545**	0,827	1,096
IPI00604620.3	Nucleolin	1,072	0,901	**1,885**	0,845	**0,628**	0,873	0,887
IPI00005615.1	Nucleolysin TIAR			**1,703**	1,297	0,898	1,053	1,175
IPI00026496.3	Nucleoplasmin-3	**0,609**	0,897	1,081	0,773	**0,531**	0,808	0,790
IPI00742943.3	Nucleoporin Nup43	0,922	0,871	0,870	0,931	1,065	1,066	0,926
IPI00742682.2	Nucleoprotein TPR	1,114	1,032	1,052	1,009	0,984	0,926	1,020
IPI00023860.1	Nucleosome assembly protein 1-like 1	0,791	0,809	0,873	0,977	1,031	1,053	0,925
IPI00941463.1	Nucleosome assembly protein 1-like 4	0,805	0,770	0,897	0,995	1,057	1,081	0,946
IPI00103142.1	NudC domain-containing protein 2	0,901	0,951	0,850	0,875	0,921	0,961	0,911

IPI00549467.3	Omega-amidase NIT2	0,866	0,795	0,840	1,044	1,204	1,240	0,955
IPI00022334.1	Ornithine aminotransferase, mitochondrial	1,060	0,900	0,921	0,881	1,036	0,965	0,943
IPI00414836.6	Osteoclast-stimulating factor 1	1,041	1,094	0,899				1,041
IPI00103884.3	Ovarian cancer-associated gene 2 protein	0,725	0,735	0,672		**2,065**		0,730
IPI00300659.4	Parafibromin		**12,697**	1,436	0,908		0,868	1,172
IPI00010414.4	PDZ and LIM domain protein 1	0,711	**0,609**	**0,561**	1,088	1,135	1,236	0,900
IPI00018235.3	Peflin	**0,408**	0,900	**2,183**	0,935	0,818	0,909	0,905
IPI00419585.9	Peptidyl-prolyl cis-trans isomerase A	1,115	1,131	0,977	0,952	1,057	0,938	1,017
IPI00646304.4	Peptidyl-prolyl cis-trans isomerase B	1,192	1,386	1,235	1,077	0,922	1,030	1,135
IPI00003927.5	Peptidyl-prolyl cis-trans isomerase D	0,904	0,938	0,795	1,006	1,012	0,923	0,931
IPI00026519.1	Peptidyl-prolyl cis-trans isomerase F, mitochondrial	**2,043**	1,348	1,260	1,386	1,025	1,177	1,304
IPI00303300.3	Peptidyl-prolyl cis-trans isomerase FKBP10		**0,584**	0,827	0,800	0,795	0,813	0,800
IPI00002535.2	Peptidyl-prolyl cis-trans isomerase FKBP2	1,167	1,040	0,867	1,098	1,413	1,118	1,108
IPI00024157.1	Peptidyl-prolyl cis-trans isomerase FKBP3		**3,978**		1,179	**0,476**	**0,644**	0,912
IPI00219005.3	Peptidyl-prolyl cis-trans isomerase FKBP4	0,879	0,927	0,918	0,995	1,094	1,020	0,961
IPI00007346.1	Peptidyl-prolyl cis-trans isomerase H	0,740	0,810	0,934	1,094	1,061	1,021	0,978
IPI00013723.3	Peptidyl-prolyl cis-trans isomerase NIMA-interacting 1	1,075	1,112	1,064	0,944	1,016	1,032	1,048
IPI00007019.1	Peptidyl-prolyl cis-trans isomerase-like 1	1,259	1,440		1,156	1,094	1,054	1,156
IPI00106668.5	perilipin-3 isoform 3	**0,638**	**0,640**	0,711	0,770	**0,592**	0,752	0,675
IPI00000874.1	Peroxiredoxin-1	0,908	0,909	0,926	1,107	1,170	1,156	1,016
IPI00027350.3	Peroxiredoxin-2	0,878	1,013	0,954	1,012	1,379	1,116	1,013
IPI00011937.1	Peroxiredoxin-4	0,980	0,960	0,940	0,932	1,084	1,040	0,970
IPI00220301.5	Peroxiredoxin-6	0,877	0,875	0,869	0,958	1,162	1,092	0,917
IPI00790305.2	PEST proteolytic signal containing nuclear protein, isoform CRA_a		1,237	0,707		**1,608**		1,237
IPI00005511.1	PHD finger-like domain-containing protein 5A	**1,575**	1,110	1,318	0,904	0,982	0,896	1,046
IPI00219446.5	Phosphatidylethanolamine-binding protein 1	0,769	0,746	0,683	1,163	1,436	1,320	0,966
IPI01015282.1	Phosphatidylserine receptor, isoform CRA_d	1,159	1,038	1,009	0,829	0,909	0,900	0,959
IPI00941001.1	Phosphoacetylglucosamine mutase	0,813	0,795	0,769	0,942	1,277	0,916	0,864
IPI00550364.8	Phosphoglucomutase-2	0,999	0,901	0,940	0,969	1,102	0,942	0,956
IPI00169383.3	Phosphoglycerate kinase 1	0,984	0,961	0,870	1,025	1,181	1,054	1,005
IPI00549725.6	Phosphoglycerate mutase 1	0,882	0,843	0,828	1,020	1,229	1,148	0,951
IPI00177008.1	Phosphoglycolate phosphatase	0,734	0,822	0,913	0,902	1,146	0,967	0,908
IPI00218465.10	Phospholipase A-2-activating protein	**0,526**	**0,665**	0,823				**0,665**
IPI00004534.5	Phosphoribosylformylglycinamidine synthase	0,984	0,890	0,917	0,876	1,096	0,999	0,950
IPI00001734.3	Phosphoserine aminotransferase	0,996	1,013	0,895	0,964	1,000	0,968	0,982
IPI00019178.2	Phosphoserine phosphatase	**0,664**	0,807	0,766	1,025	1,408	1,329	0,916
IPI00032304.2	Plastin-1	**0,540**	0,877	0,996	1,035	0,945	0,998	0,970

IPI00216694.3	Plastin-3	0,952	0,955	0,978	0,844	0,972	0,933	0,954
IPI00026546.1	Platelet-activating factor acetylhydrolase IB subunit beta	0,928	0,947	0,831	0,973	1,169	1,080	0,960
IPI00014808.1	Platelet-activating factor acetylhydrolase IB subunit gamma	0,872	0,799	0,765	1,101	1,187	1,171	0,987
IPI00642944.1	Poly(A) binding protein, cytoplasmic 4 (Inducible form), isoform CRA_e	1,261	0,957	**1,845**	1,040	0,713	0,757	0,998
IPI00016610.2	Poly(rC)-binding protein 1	0,781	0,946	1,117	1,090	0,795	1,028	0,987
IPI00470509.3	poly(rC)-binding protein 2 isoform c	0,859	1,000	1,292	1,093	0,780	1,041	1,020
IPI00032827.1	Pre-mRNA branch site protein p14	**1,526**	**1,987**	**4,475**	1,174	**0,556**	0,909	1,350
IPI00007928.4	Pre-mRNA-processing-splicing factor 8	**1,717**	**2,000**	**5,799**	1,348	0,720	0,989	**1,532**
IPI00006052.3	Prefoldin subunit 2	1,041	0,973	1,069	0,800	0,898	0,867	0,936
IPI00015891.1	Prefoldin subunit 4		1,149		0,744	0,833		0,833
IPI00015361.1	Prefoldin subunit 5	1,001	1,084	1,170	0,726	0,799	0,794	0,900
IPI00005657.1	Prefoldin subunit 6	0,954	1,073	1,148	0,789	0,895	0,904	0,929
IPI00030320.4	Probable ATP-dependent RNA helicase DDX6				**1,730**	1,120	1,483	1,483
IPI00006907.1	Probable fructose-2,6-bisphosphatase TIGAR			0,940	0,878		0,896	0,896
IPI00015809.1	Probable tRNA threonylcarbamoyladenosine biosynthesis protein OSGEP		0,879			1,072	1,041	1,041
IPI00216691.5	Profilin-1	1,030	1,012	0,976	0,860	0,996	0,948	0,986
IPI00246058.10	Programmed cell death 6-interacting protein	**0,520**	0,832	0,927	0,919	**0,656**	0,745	0,789
IPI00298558.2	Programmed cell death protein 10		1,006	1,109	1,069			1,069
IPI00023640.3	Programmed cell death protein 5	1,056	1,078	**1,956**	0,788	0,737	0,746	0,922
IPI00025277.5	Programmed cell death protein 6	**0,240**	0,984	**4,455**	0,781	**0,652**	0,727	0,754
IPI00017334.1	Prohibitin	**4,307**		**8,009**	**4,289**			**4,307**
IPI00021700.3	Proliferating cell nuclear antigen	1,095	0,959	0,986	0,873	0,984	0,885	0,972
IPI00299000.5	Proliferation-associated protein 2G4	**3,158**	**2,262**	1,450	**1,656**	0,866	1,176	**1,553**
IPI00016346.2	Proline synthetase co-transcribed homolog (Bacterial), isoform CRA_b	1,106	1,005	0,803	1,226	1,369	1,203	1,154
IPI00008164.2	Prolyl endopeptidase	0,899	1,038	0,919	1,021	1,149	1,167	1,030
IPI00105598.3	Proteasome 26S non-ATPase subunit 11 variant (Fragment)	1,311	1,344	**2,373**	1,111	0,775	0,928	1,211
IPI00479722.2	Proteasome activator complex subunit 1	**2,052**	1,246	**3,043**	1,269	1,153	1,146	1,257
IPI00031106.1	Proteasome assembly chaperone 3	1,028	0,944	0,962	0,922	1,040	1,082	0,995
IPI00552375.3	proteasome assembly chaperone 4 isoform c	1,043	1,017	1,026	0,935	1,015	0,953	1,016
IPI00219622.3	Proteasome subunit alpha type-2	**1,970**	**1,683**	**2,928**	1,362	1,084	1,118	**1,522**
IPI00299155.5	Proteasome subunit alpha type-4	**2,052**	**1,785**	**2,977**	1,251	1,053	0,984	**1,518**
IPI00291922.2	Proteasome subunit alpha type-5	**1,583**	**1,544**	**2,467**	1,172	1,151	0,981	1,358
IPI00029623.1	Proteasome subunit alpha type-6	**2,236**	**1,890**	**3,739**	1,183	1,025	0,948	**1,537**
IPI00025019.3	Proteasome subunit beta type-1	**2,298**	**1,889**	**3,989**	1,221	1,055	1,024	**1,555**
IPI00028006.1	Proteasome subunit beta type-2	**1,781**	**1,569**	**2,941**	1,298	1,218	1,170	1,434
IPI00028004.2	Proteasome subunit beta type-3	**2,223**	**1,967**	**3,795**	1,197	0,985	0,993	**1,582**

IPI00555956.2	Proteasome subunit beta type-4	**2,181**	**1,695**	**3,826**	1,379	1,164	1,119	**1,537**
IPI00479306.1	Proteasome subunit beta type-5	**2,229**	**1,898**	**3,936**	1,246	1,007	0,982	**1,572**
IPI00000811.2	Proteasome subunit beta type-6	**2,048**	**1,872**	**3,645**	1,331	1,114	1,105	**1,601**
IPI00003217.3	Proteasome subunit beta type-7	**2,353**	**1,788**	**3,799**	1,323	1,254	1,174	**1,556**
IPI00157790.7	proteasome-associated protein ECM29 homolog	**3,038**	**2,569**	**5,396**	**1,678**	0,842	1,039	**2,124**
IPI00983987.1	Protein	0,756	0,912	1,017	1,263	1,263	1,139	1,078
IPI01014883.1	Protein	1,097	1,087	0,978	0,985	1,105	0,949	1,036
IPI00853455.1	Protein	0,798	0,968	0,813	1,130	1,189	1,070	1,019
IPI00978875.1	Protein	0,895	1,065	0,796	0,864	1,221	1,184	0,980
IPI00657874.1	Protein	**0,630**	0,848	0,911	0,848	1,195	1,102	0,880
IPI00926799.1	Protein	0,719	0,923	1,023			0,795	0,859
IPI00441473.3	Protein arginine N-methyltransferase 5	1,076	1,002	1,282	0,960	1,056	1,047	1,051
IPI00016925.1	Protein C10	0,825	0,809	0,789	0,912	1,191	1,210	0,869
IPI00878073.1	Protein C17orf37	0,770				1,104	1,064	1,064
IPI00010796.1	Protein disulfide-isomerase	1,039	1,021	0,997	0,825	0,940	0,910	0,968
IPI00009904.1	Protein disulfide-isomerase A4	0,893	0,911	0,847	0,973	1,086	1,114	0,942
IPI00298547.3	Protein DJ-1	1,028	0,939	0,846	0,956	1,164	1,150	0,992
IPI00008991.1	Protein Dr1	1,006	0,891	0,955	0,884		0,985	0,955
IPI00011919.1	Protein FADD	0,993		0,911			0,938	0,938
IPI00816474.1	Protein FAM127A	**0,505**	0,694			0,802	1,062	0,748
IPI00303722.5	Protein FAM136A	1,128	1,131	1,056	0,747	0,968	0,937	1,012
IPI00303318.2	Protein FAM49B	0,791	0,788	0,795	1,049	1,180	1,114	0,922
IPI00939707.1	Protein KIAA0664			0,814		0,897	0,997	0,897
IPI00063234.1	Protein kinase, cAMP-dependent, regulatory, type II, alpha, isoform CRA_b	0,935	1,008	0,940		0,905	0,918	0,935
IPI00019997.1	Protein lin-7 homolog C		1,274	1,061		0,718		1,061
IPI01011745.1	Protein LZIC	0,950	0,954	0,929	0,882	1,074	0,928	0,939
IPI00219306.1	Protein mago nashi homolog	1,257	1,343	1,428	1,037	0,812	0,884	1,147
IPI00398922.4	Protein phosphatase 1 regulatory subunit 14B	0,667	**0,472**	**0,468**	**1,765**	1,432	1,435	1,049
IPI00291412.1	Protein phosphatase 1F	0,786	0,828	0,852	1,042	1,165		0,852
IPI00006167.1	Protein phosphatase 1G	0,744	**0,496**	0,680	1,149	1,348	1,243	0,946
IPI00013895.1	Protein S100-A11	0,779	1,007	**2,047**	0,912	0,997	1,069	1,002
IPI00016179.1	Protein S100-A13	0,882	0,930	1,042	0,880	0,932	0,939	0,931
IPI00789755.1	protein SEC13 homolog isoform 2		0,815		1,076	0,888	0,963	0,926
IPI00788849.1	protein TFG isoform 2	**0,570**	**2,505**	0,852	0,930	1,340	1,017	0,974
IPI00429538.1	Protein yippee-like 5	1,054	1,000	**1,579**	0,993	0,919	0,916	0,996
IPI00044761.4	Pseudouridylate synthase 7 homolog	0,678	0,753	1,156	1,006	0,672		0,753
IPI00218568.7	Pterin-4-alpha-carbinolamine dehydratase	0,919	0,976	0,871	0,869	1,104	0,995	0,947
IPI00062860.2	Putative ataxin-7-like protein 3B	**0,381**	0,868	**0,450**	**1,799**	**1,697**		0,868

IPI00003870.1	Putative ATP-dependent Clp protease proteolytic subunit, mitochondrial	1,044	0,913	0,791		1,104		0,979
IPI00796213.2	Putative uncharacterized protein	**1,588**		**2,004**	1,275	1,132	1,256	1,275
IPI00893035.1	Putative uncharacterized protein CAD	**1,712**	1,486	**3,227**	1,405	1,126	1,176	1,446
IPI00965753.1	Putative uncharacterized protein DKFZp564F123	1,037	0,935	0,905	1,015	1,089	1,095	1,026
IPI00477803.4	Putative uncharacterized protein DKFZp781L0540 (Fragment)	**2,255**			1,281	1,249		1,281
IPI00025340.3	Pyridoxal phosphate phosphatase	0,838	**0,662**	0,668	1,340	1,335	1,345	1,086
IPI00955815.2	pyruvate dehydrogenase E1 component subunit alpha, somatic form, mitochondrial isoform 4 precursor	1,067		1,444	0,723	**0,650**	**0,626**	0,723
IPI00215974.2	Queuine tRNA-ribosyltransferase	0,904	0,760	0,910	0,934	1,029	0,999	0,922
IPI00647366.1	quinone oxidoreductase isoform b	0,732			1,257	1,055	1,286	1,156
IPI00010154.3	Rab GDP dissociation inhibitor alpha	0,741	0,828	**0,648**	1,128	1,308	1,267	0,978
IPI00940148.1	Rab GDP dissociation inhibitor beta	0,899	0,941	0,864	1,049	1,213	1,108	0,995
IPI00480056.8	RAB4A, member RAS oncogene family variant			0,995		1,272	1,331	1,272
IPI00903145.1	Radixin	1,301	1,456	**1,619**	1,105	1,137	0,915	1,219
IPI00030919.3	Ragulator complex protein LAMTOR3	0,843	0,841	0,845		1,181	1,072	0,845
IPI00009342.1	Ras GTPase-activating-like protein IQGAP1	0,939	0,937	1,386	0,962	0,964	0,939	0,951
IPI00377066.1	ras suppressor protein 1 isoform 2				1,042	**1,579**	0,971	1,042
IPI01011983.1	Ras-related protein R-Ras2	1,032	0,930	0,859		0,987	0,999	0,987
IPI00016513.5	Ras-related protein Rab-10	1,108	1,262	1,166	1,113	1,068		1,113
IPI00020436.4	Ras-related protein Rab-11B	1,209	1,184	1,017	0,934	1,029	1,025	1,027
IPI00291928.8	Ras-related protein Rab-14	1,183	1,163	0,943	1,046	1,013	0,997	1,029
IPI00014577.1	Ras-related protein Rab-18		0,914			0,978	1,070	0,978
IPI00008964.3	Ras-related protein Rab-1B	0,841	0,996	0,922	0,833	0,778	1,327	0,882
IPI00007755.3	Ras-related protein Rab-21	1,246	1,136	1,043	1,304			1,191
IPI00031169.1	Ras-related protein Rab-2A	1,113	1,062	1,066	0,925	0,913	0,861	0,994
IPI00016339.4	Ras-related protein Rab-5C	1,226	1,053	0,907	1,274	1,246	0,887	1,140
IPI00016342.1	Ras-related protein Rab-7a	1,074	1,085	0,969	1,015	0,981	0,994	1,004
IPI00028481.1	Ras-related protein Rab-8A	1,382	1,378	1,158	1,058	1,002	1,107	1,133
IPI00016372.1	Ras-related protein Rab-9A	0,915	1,041	0,779	0,974	0,921	0,886	0,918
IPI00009607.1	Ras-related protein Rap-2c	1,445	1,274		0,931		0,796	1,103
IPI00009659.3	Regulation of nuclear pre-mRNA domain-containing protein 1B	**0,655**	**0,536**		1,012	0,875	0,984	0,875
IPI00017373.1	Replication protein A 14 kDa subunit	1,037	0,918	1,333	0,760	0,764	0,868	0,893
IPI00020127.1	Replication protein A 70 kDa DNA-binding subunit	1,114	0,847	**1,850**	0,855	0,758	0,852	0,854
IPI00015842.1	Reticulocalbin-1	0,896	1,114	0,969	0,674	0,888	1,079	0,933
IPI00029628.1	Reticulocalbin-2	0,834	**0,490**	0,831		1,059	0,865	0,834
IPI01011430.2	retinal dehydrogenase 2 isoform 4				1,038	1,006	1,123	1,038
IPI00015161.1	Retinal rod rhodopsin-sensitive cGMP 3',5'-cyclic	0,931	1,023	0,906	0,903	0,990	0,965	0,948

	phosphodiesterase subunit delta							
IPI00003815.3	Rho GDP-dissociation inhibitor 1	0,934	0,908	0,856	0,947	1,102	1,111	0,940
IPI00550069.3	Ribonuclease inhibitor	0,818	0,828	0,883	0,939	0,983	0,973	0,911
IPI00005038.1	Ribonuclease UK114	1,027	0,916	0,893	0,983	1,036	0,973	0,978
IPI00013871.1	Ribonucleoside-diphosphate reductase large subunit	1,368	1,457	1,266	0,977	1,249	0,893	1,258
IPI00946732.1	Ribonucleoside-diphosphate reductase subunit M2	**0,193**	**0,443**	**0,386**	**1,812**	0,932	0,913	0,678
IPI00219616.7	Ribose-phosphate pyrophosphokinase 1	**1,682**	1,403	**2,410**	1,052	0,894	0,866	1,228
IPI00867533.1	Ribosomal protein L6		**13,671**		**8,728**			**11,199**
IPI00478896.3	Ribosomal protein L7a	**3,976**	**3,250**		**5,262**			**3,976**
IPI00304232.1	Ribosome biogenesis protein WDR12	0,957	0,767	0,895	1,129	1,290	1,216	1,043
IPI00642213.1	RNA binding protein, autoantigenic	**1,707**			1,183	**0,441**	0,991	1,087
IPI00815843.1	RPL14 protein (Fragment)	**24,233**	**49,776**		**8,224**			**24,233**
IPI00978180.1	RPS10-NUDT3 protein	0,705	**0,644**		0,971	**1,721**	1,403	0,971
IPI00025039.1	rRNA 2'-O-methyltransferase fibrillarin	1,322	**1,773**		1,283	**0,567**	1,061	1,283
IPI00009104.7	RuvB-like 2	0,960	0,982	**1,717**	0,850	0,750	0,832	0,905
IPI00010157.1	S-adenosylmethionine synthase isoform type-2	0,929	0,894	0,920	0,885	1,084	1,017	0,924
IPI00411706.1	S-formylglutathione hydrolase	0,908	0,803	0,727	0,969	1,167	1,151	0,938
IPI00719256.2	SART3 protein	0,951	1,155	**1,582**	1,014	0,944	1,095	1,054
IPI00335385.4	Scavenger mRNA-decapping enzyme DcpS			0,739	1,483	1,248	1,484	1,366
IPI00289862.5	Secernin-1	0,875	0,744	0,725	1,078	1,346	1,332	0,976
IPI00017469.1	Sepiapterin reductase	0,803	0,883	0,829	1,026	1,213	1,152	0,955
IPI00789370.3	serine hydroxymethyltransferase, mitochondrial isoform 3	1,118	1,102	1,124	0,818	0,925	0,860	1,014
IPI00941907.1	Serine-threonine kinase receptor-associated protein	1,087	1,122	1,145	0,904	0,956	0,935	1,021
IPI01014578.1	Serine/threonine-protein phosphatase (Fragment)	0,949	1,004	1,003	0,809	1,017	0,946	0,976
IPI00332511.5	Serine/threonine-protein phosphatase 2A 55 kDa regulatory subunit B alpha isoform	1,137	1,187	1,112		0,993		1,125
IPI00008380.1	Serine/threonine-protein phosphatase 2A catalytic subunit alpha isoform	0,853	0,931	0,907	1,023	1,187	1,092	0,977
IPI00012833.1	Serine/threonine-protein phosphatase 4 catalytic subunit	**1,985**	0,834	0,968	**1,611**	1,432	1,100	1,266
IPI00550451.1	Serine/threonine-protein phosphatase PP1-alpha catalytic subunit	0,935	1,240		1,204			1,204
IPI00413451.3	Serpin B6	0,914	0,889	0,915	0,835	1,042	0,961	0,914
IPI00220637.5	Seryl-tRNA synthetase, cytoplasmic	1,440	1,352	0,879	1,187	1,384	1,299	1,325
IPI00013789.5	SET and MYND domain-containing protein 5			1,048		0,870	0,913	0,913
IPI00641957.4	SFRS11 protein	**0,591**	**0,493**		1,215			**0,591**
IPI00514669.1	SH3 domain binding glutamic acid-rich protein like 3	1,000	0,988	0,903	0,894	1,067	0,973	0,980
IPI00025318.1	SH3 domain-binding glutamic acid-rich-like protein	1,070	1,068	1,009	0,806	1,055	0,918	1,032
IPI00412272.2	SH3 domain-binding glutamic acid-rich-like protein 2		1,053	1,082		1,098	0,924	1,068

IPI00147874.1	Sialic acid synthase	0,852	0,826	0,818	0,971	1,194	1,106	0,912
IPI00293434.2	Signal recognition particle 14 kDa protein	1,211	1,174	1,384	0,934	0,835	0,996	1,085
IPI00295889.2	Signal recognition particle 19 kDa protein	0,761	0,880	1,207	0,863	**0,660**	0,770	0,816
IPI00215888.4	Signal recognition particle 72 kDa protein	**0,581**	0,725	1,428	0,727	**0,484**	**0,547**	**0,653**
IPI00642816.2	Signal recognition particle 9 kDa protein	1,126	1,059	1,233	1,102	0,895	1,066	1,084
IPI00788723.2	Similar to Eukaryotic translation initiation factor 4E				1,101	1,174	1,083	1,101
IPI00738042.1	similar to proteasome 26S ATPase subunit 4	1,151	1,113	**2,066**	1,155	0,917	0,953	1,132
IPI00029744.1	Single-stranded DNA-binding protein, mitochondrial	**1,759**	1,167	**1,733**	0,775	0,790	0,799	0,983
IPI00014437.4	Sjoegren syndrome nuclear autoantigen 1	1,005	1,068	1,028	0,812	0,936	0,860	0,971
IPI00013949.1	Small glutamine-rich tetratricopeptide repeat-containing protein alpha	0,818	0,915	0,900	0,915	0,952	0,882	0,907
IPI00029266.1	Small nuclear ribonucleoprotein E	1,155	1,270	**2,012**	1,096	0,866	0,934	1,126
IPI00220528.6	Small nuclear ribonucleoprotein F	1,339	1,455	**2,343**	0,956	0,742	0,852	1,148
IPI00302850.4	Small nuclear ribonucleoprotein Sm D1	1,122	1,223	**1,966**	1,098	0,851	0,998	1,110
IPI00017963.1	Small nuclear ribonucleoprotein Sm D2	1,136	1,250	**2,007**	1,107	0,822	0,890	1,121
IPI00220360.2	Small nuclear ribonucleoprotein-associated protein N	**1,577**	**6,031**	**3,405**	1,183	0,702	0,835	1,380
IPI00303105.3	Small ubiquitin-related modifier 1	0,691	1,285		0,876		1,331	1,080
IPI00745893.2	small ubiquitin-related modifier 2 isoform b precursor	0,709	1,076	1,000	0,873	0,955	0,991	0,973
IPI00924895.1	SNRPG protein	1,273	**1,500**	**2,525**	0,898	0,748	0,818	1,086
IPI00977640.1	sodium/potassium-transporting ATPase subunit alpha-1 isoform d	**1,591**	**1,718**	**2,227**	1,318	0,922	0,689	1,455
IPI00216057.6	Sorbitol dehydrogenase	1,038	0,917	0,966	1,239	**1,672**	1,130	1,084
IPI00292020.3	Spermidine synthase	0,942	1,009	0,909	0,857	1,039	1,027	0,975
IPI00026089.4	Splicing factor 3B subunit 1	1,304	**1,515**	**4,498**	1,148	**0,596**	1,266	1,285
IPI00010404.1	Splicing factor 3B subunit 5	0,986	1,399	0,960	**2,113**	0,881	0,874	0,973
IPI00291643.4	SPRY domain-containing protein 4	1,114	1,011	0,987	0,725		0,878	0,987
IPI00009922.3	SRA stem-loop-interacting RNA-binding protein, mitochondrial	1,158	1,080	1,012	0,966	1,018	1,066	1,042
IPI00029601.6	Src substrate cortactin	0,787	**4,449**	1,030	**0,575**	1,146	0,953	0,991
IPI00479997.4	Stathmin	0,886	**0,657**	0,875	1,007	1,059	1,095	0,947
IPI00479934.1	sterol carrier protein 2 isoform 2 precursor	1,258	1,304	1,146	0,916	1,096	1,024	1,121
IPI00334190.4	Stomatin-like protein 2	1,432	1,262	1,115	**1,717**			1,347
IPI00013894.1	Stress-induced-phosphoprotein 1	0,966	1,008	1,244	0,890	0,947	1,041	0,987
IPI00096066.2	Succinyl-CoA ligase [GDP-forming] subunit beta, mitochondrial	1,084	0,937	1,028	0,707	0,817	0,809	0,877
IPI00026516.1	Succinyl-CoA:3-ketoacid-coenzyme A transferase 1, mitochondrial	1,126	0,958	0,991	0,858	0,865	1,068	0,975
IPI00168554.1	Sulfiredoxin-1	0,788	**0,550**	0,902		0,998	0,931	0,902
IPI00033130.3	SUMO-activating enzyme subunit 1	0,908	0,874	0,872	0,922	1,182	1,240	0,915
IPI00023234.3	SUMO-activating enzyme subunit 2	0,925	0,882	0,851	0,930	1,150	1,155	0,928

IPI00032957.1	SUMO-conjugating enzyme UBC9	0,713	0,827	0,729	1,305	1,243	1,279	1,035
IPI00218733.6	Superoxide dismutase [Cu-Zn]	1,067	1,024	0,956	0,847	1,003	0,954	0,980
IPI00022314.1	Superoxide dismutase [Mn], mitochondrial	1,153	1,066	1,017	0,790	0,938	0,905	0,978
IPI00059242.3	Synapse-associated protein 1	**0,441**		0,816	**0,656**	**0,630**	**0,655**	**0,655**
IPI00156689.3	Synaptic vesicle membrane protein VAT-1 homolog	0,959	0,686	0,845	1,037	0,898	1,076	0,929
IPI00032831.4	Synaptosomal-associated protein 29	1,260	1,236	0,954	1,404	**2,158**	1,275	1,267
IPI00290566.1	T-complex protein 1 subunit alpha	**2,177**	**1,707**	**3,662**	1,264	0,996	1,081	1,485
IPI00297779.7	T-complex protein 1 subunit beta	**2,113**	**1,729**	**3,682**	1,190	0,936	1,038	1,459
IPI00302927.6	T-complex protein 1 subunit delta	**2,298**	**1,967**	**3,645**	1,420	1,057	1,256	**1,694**
IPI00010720.1	T-complex protein 1 subunit epsilon	**1,732**	1,405	**2,593**	1,160	0,887	0,993	1,282
IPI00018465.1	T-complex protein 1 subunit eta	**2,213**	**1,767**	**3,670**	1,326	1,127	1,213	**1,546**
IPI00553185.2	T-complex protein 1 subunit gamma	**1,986**	**1,681**	**3,728**	1,384	1,107	1,133	**1,532**
IPI00784090.2	T-complex protein 1 subunit theta	**1,764**	1,447	**2,776**	1,163	0,921	0,956	1,305
IPI00027626.3	T-complex protein 1 subunit zeta	**2,223**	**1,683**	**3,621**	1,279	0,983	1,093	1,481
IPI00298994.6	Talin-1	0,759	0,934	1,117	0,942	0,846	0,900	0,917
IPI00639819.1	TAR DNA binding protein	1,047	1,271	**2,455**	1,055	0,795	1,100	1,077
IPI00032911.3	TATA box-binding protein-like protein 1	0,822	0,869	0,866	0,889	1,050	1,023	0,879
IPI00016912.1	Tetratricopeptide repeat protein 1	0,706	0,782	0,833		0,929	1,105	0,833
IPI00550644.2	Tetratricopeptide repeat protein 38			**0,491**		1,005	0,840	0,840
IPI00175096.1	Tetratricopeptide repeat protein 9C	0,752	0,902	0,982	0,855	0,966	1,082	0,934
IPI00549189.4	Thimet oligopeptidase	0,993	1,019	0,892	0,902	1,004	0,996	0,994
IPI00216298.6	Thioredoxin	0,966	0,899	0,939	0,834	0,984	1,022	0,952
IPI00026328.3	Thioredoxin domain-containing protein 12	0,891	0,875	0,851	0,944	1,099	1,081	0,918
IPI00646689.1	Thioredoxin domain-containing protein 17	0,953	0,912	0,869	1,061	1,098	1,036	0,994
IPI00939560.1	thioredoxin domain-containing protein 5 isoform 3	1,082	1,119	1,027	0,702	0,877	0,849	0,952
IPI00374151.1	thioredoxin-dependent peroxide reductase, mitochondrial isoform b	0,952	1,057	0,993	0,906	0,975	1,017	0,984
IPI01010794.1	THO complex subunit 4	**2,168**	1,217	**5,423**	1,127	**0,537**	0,888	1,172
IPI00329633.5	Threonyl-tRNA synthetase, cytoplasmic	0,963	1,017	1,094	0,880	0,964	0,987	0,975
IPI00299214.7	Thymidine kinase, cytosolic	**0,597**	**1,530**	0,806	**2,646**	**2,609**	1,432	1,481
IPI00013862.7	Thymidylate kinase	1,148	1,049	0,985	0,798	1,039	0,920	1,012
IPI00104050.3	Thyroid hormone receptor-associated protein 3	0,844	**0,526**	**4,378**	**0,593**	0,720	0,708	0,714
IPI00013829.1	TP53-regulated inhibitor of apoptosis 1	0,933	0,947	0,831	0,849	1,092	0,912	0,923
IPI00744692.1	Transaldolase	1,061	1,014	0,947	0,830	0,988	0,916	0,968
IPI00002895.1	Transcription elongation factor SPT4	**0,482**	**0,611**	0,859	1,052	0,878	0,998	0,868
IPI00412792.2	Transcription factor BTF3 homolog 4	0,858	0,699	0,747	1,050	1,181	1,233	0,954
IPI00004353.1	Transcription initiation factor IIA subunit 2	0,888		0,892	0,766	0,962	0,710	0,888
IPI00478231.2	Transforming protein RhoA	1,066	1,024	1,052	0,857	0,915	0,874	0,969

IPI00550363.3	Transgelin-2	0,894	0,940	0,915	0,954	1,215	0,964	0,947
IPI00022774.3	Transitional endoplasmic reticulum ATPase	0,952	1,007	**1,565**	0,961	0,902	0,934	0,957
IPI00001159.11	Translational activator GCN1		1,272	**2,596**	**2,691**	0,851	**1,518**	**1,518**
IPI00550900.1	Translationally-controlled tumor protein	**1,514**	**1,506**	1,083	1,334	1,188	0,915	1,261
IPI00293350.3	Translin-associated protein X	0,889	0,830	0,866	0,985	1,091	1,060	0,937
IPI00028055.4	Transmembrane emp24 domain-containing protein 10	**2,840**	**3,241**	**4,527**	**2,457**		1,431	**2,840**
IPI00031522.2	Trifunctional enzyme subunit alpha, mitochondrial	1,071	1,136	**1,686**	0,924	**0,655**	0,815	0,997
IPI00306369.3	tRNA (cytosine-5-)-methyltransferase NSUN2	0,753	0,744	0,934	0,875	0,994	0,968	0,905
IPI00009010.3	tRNA methyltransferase 112 homolog	0,854	1,124	0,930	0,967	0,945	0,831	0,937
IPI00005087.1	Tropomodulin-3		**0,587**	0,707		1,246	1,169	0,938
IPI00027107.5	Tu translation elongation factor, mitochondrial precursor	1,047	0,970	0,948	0,880	1,012	0,992	0,981
IPI00646779.2	TUBB6 protein		0,846	0,778	1,364	1,325	**1,830**	1,325
IPI00180675.4	Tubulin alpha-1A chain	0,775	1,041	0,896	1,035	1,072	1,232	1,038
IPI00930688.1	Tubulin alpha-1B chain	0,817	**1,653**	0,869	1,037	1,130	1,277	1,084
IPI00218343.4	Tubulin alpha-1C chain	0,854	1,103	0,912	0,906	1,029	1,128	0,970
IPI00909140.8	Tubulin beta chain	0,948	1,171	0,990	0,942	0,928	1,082	0,969
IPI00031370.3	Tubulin beta-2B chain		0,980	0,848	0,867		1,102	0,924
IPI00007752.1	Tubulin beta-2C chain	1,013	1,149	0,980	1,008	1,029	1,007	1,011
IPI00013683.2	Tubulin beta-3 chain	0,752	0,861	**0,581**		1,362	1,478	0,861
IPI00023598.2	Tubulin beta-4 chain	0,929	1,010	0,863	0,891	1,121	1,202	0,970
IPI00879002.1	Tubulin tyrosine ligase-like family, member 12	0,860	0,968	0,884	0,958	1,100	1,053	0,963
IPI00018402.1	Tubulin-specific chaperone E	0,815	0,918		0,861	1,174	1,160	0,918
IPI00007074.5	Tyrosyl-tRNA synthetase, cytoplasmic	0,954	1,007	1,120	0,984	1,075	1,071	1,039
IPI00012382.3	U1 small nuclear ribonucleoprotein A	**1,543**	**5,777**	**2,705**	1,010	**0,620**	0,792	1,276
IPI00013396.3	U1 small nuclear ribonucleoprotein C	1,418	1,090	**4,785**	1,210		0,901	1,210
IPI00297477.3	U2 small nuclear ribonucleoprotein A'	1,362	1,138	**2,203**	1,051	0,829	0,932	1,095
IPI00004436.1	U6 snRNA-associated Sm-like protein LSm1	1,096	1,132	1,293	0,931	0,907	0,936	1,016
IPI00032460.3	U6 snRNA-associated Sm-like protein LSm2	0,932	0,963	1,112	1,100	1,021	1,075	1,048
IPI00219229.3	U6 snRNA-associated Sm-like protein LSm3	0,771	0,834	0,934	1,171	1,045	1,097	0,990
IPI00294955.3	U6 snRNA-associated Sm-like protein LSm4	0,911	0,904	1,227	1,120	1,002	1,073	1,037
IPI00001146.1	U6 snRNA-associated Sm-like protein LSm6	1,073	1,092	1,339	0,919	0,824	0,888	0,996
IPI00007163.1	U6 snRNA-associated Sm-like protein LSm7	1,132	1,173	1,337	0,868	0,855	0,894	1,013
IPI00184533.1	Ubiquitin carboxyl-terminal hydrolase 11	**0,476**				1,288	1,012	1,012
IPI00018352.1	Ubiquitin carboxyl-terminal hydrolase isozyme L1	1,011	0,970	0,928	0,866	1,070	0,973	0,971
IPI00011250.3	Ubiquitin carboxyl-terminal hydrolase isozyme L3	0,786	0,916	0,812	0,987	1,156	1,130	0,952
IPI00179330.6	Ubiquitin-40S ribosomal protein S27a	0,845	1,240	1,022	1,067	0,891	0,865	0,957

IPI00013002.1	Ubiquitin-conjugating enzyme E2 C	**0,566**	0,767	**0,614**	1,175	1,285	1,097	0,932
IPI00021347.1	Ubiquitin-conjugating enzyme E2 L3	**0,596**	**0,637**	**0,555**	**1,531**	**1,757**	**1,665**	1,084
IPI00003949.1	Ubiquitin-conjugating enzyme E2 N	0,713	0,709	0,780	1,234	1,231	1,090	0,935
IPI00783378.3	Ubiquitin-conjugating enzyme E2 O	**0,633**	**0,560**	0,871	0,803	0,881	0,973	0,837
IPI00019600.3	Ubiquitin-conjugating enzyme E2 variant 2	0,961	1,025	**0,643**	0,838	0,851	1,475	0,906
IPI00010207.1	Ubiquitin-fold modifier 1	**0,630**	0,750	0,695	1,464	1,287	1,290	1,018
IPI00294495.5	Ubiquitin-fold modifier-conjugating enzyme 1	0,791	1,214	0,836		0,917	0,884	0,884
IPI00645078.1	Ubiquitin-like modifier-activating enzyme 1	0,876	0,881	0,840	0,988	1,132	1,091	0,934
IPI00005658.3	Ubiquitin-like protein 4A	0,822			1,063	0,743	0,864	0,843
IPI00013241.1	Ubiquitin-like protein 5	1,082	1,126	1,074	0,836	0,907	0,964	1,019
IPI00219953.5	UMP-CMP kinase isoform a	0,996	0,978	0,896	0,878	1,066	1,087	0,987
IPI00794746.1	Uncharacterized protein	**32,659**	**18,071**	**28,898**	**9,044**			**23,485**
IPI00927458.1	Uncharacterized protein	**12,465**			**5,303**		**2,227**	**5,303**
IPI00980350.1	Uncharacterized protein	**5,157**	**4,576**	**7,940**	**3,279**	0,872	1,289	**3,928**
IPI00983316.1	Uncharacterized protein	**4,757**	**4,646**	**4,137**	**2,808**	0,959	**1,676**	**3,472**
IPI00514399.1	Uncharacterized protein	**3,228**	**2,375**	**5,819**	**3,621**	1,270		**3,228**
IPI00975727.1	Uncharacterized protein	**1,990**	**2,316**				1,002	**1,990**
IPI00983214.1	Uncharacterized protein	**2,061**	**1,615**	**2,246**	**1,505**	0,673	0,732	**1,560**
IPI00791426.2	Uncharacterized protein	**1,908**	**1,880**	**2,162**	1,207	0,791	0,925	**1,544**
IPI00964686.1	Uncharacterized protein	**1,749**	**1,752**	**2,830**	1,221	0,865	1,166	1,485
IPI00642046.1	Uncharacterized protein	**2,037**		**4,495**	1,480	**0,585**	1,021	1,480
IPI00917605.1	Uncharacterized protein	**1,870**	**1,627**	1,427	**1,527**	1,378	1,251	1,477
IPI00943181.1	Uncharacterized protein	**1,977**	**1,591**	**2,670**	1,248	1,133	1,254	1,423
IPI01015591.2	Uncharacterized protein	1,406	**1,842**	**2,154**	1,367	1,164	1,054	1,387
IPI00965327.1	Uncharacterized protein	**2,205**			1,144	1,269		1,269
IPI00925656.2	Uncharacterized protein				1,392	1,038	1,254	1,254
IPI00644108.3	Uncharacterized protein				**1,557**	1,247	1,126	1,247
IPI00966700.1	Uncharacterized protein	1,127	1,348		1,418	0,852	1,231	1,231
IPI01011421.2	Uncharacterized protein	1,146	1,296	1,116	1,094	1,007	0,998	1,105
IPI00927109.2	Uncharacterized protein	0,841			1,016	1,271	1,182	1,099
IPI00966182.1	Uncharacterized protein	0,721	**0,574**	0,858	1,267	1,277	1,238	1,048
IPI00945719.1	Uncharacterized protein	1,248	1,220	1,101	0,838	0,993	0,912	1,047
IPI00984352.1	Uncharacterized protein	1,180	1,144	1,237	0,795	0,868	0,927	1,036
IPI00646978.4	Uncharacterized protein	**0,436**			**1,596**	0,989	1,066	1,028
IPI00924545.1	Uncharacterized protein	1,141	1,200	1,256	0,821	0,910	0,904	1,025
IPI01013402.2	Uncharacterized protein	1,225	1,214	1,404	0,791	0,804	0,834	1,024
IPI00788871.1	Uncharacterized protein	1,088	0,988	0,919	1,056	1,218	0,954	1,022
IPI00470394.4	Uncharacterized protein	0,935	1,014	1,042		1,082	0,948	1,014

IPI01009513.2	Uncharacterized protein	0,958	1,246	**2,856**	1,061	**0,503**	0,732	1,010
IPI00794194.1	Uncharacterized protein	1,020	0,994	0,997	1,068	1,207	0,986	1,008
IPI00641550.3	Uncharacterized protein		1,000	1,136	0,718		0,991	0,995
IPI00798211.1	Uncharacterized protein	1,054	0,970	1,016	0,800	1,052	0,975	0,995
IPI00974249.1	Uncharacterized protein	0,999	0,994	1,202	0,746	0,827		0,994
IPI00741317.2	Uncharacterized protein	0,766	0,947	1,049	1,022	0,839	1,042	0,985
IPI00967106.1	Uncharacterized protein	1,247	0,969	0,879	0,867	1,000	1,059	0,985
IPI00878669.2	Uncharacterized protein		0,729	0,932	1,087		1,025	0,978
IPI00640089.1	Uncharacterized protein	1,069	1,158	1,092	0,886	0,884	0,873	0,978
IPI00917694.1	Uncharacterized protein	1,039	0,977	0,969	0,853	0,985	0,967	0,973
IPI00981739.1	Uncharacterized protein	1,036	0,991	0,950	0,850	0,985	0,944	0,968
IPI00795892.1	Uncharacterized protein	1,056	1,025	1,009	0,792	0,923	0,919	0,966
IPI00946351.1	Uncharacterized protein	0,864	0,762	0,935	1,439	1,176	0,992	0,963
IPI00946824.1	Uncharacterized protein	0,988	0,945	0,819	0,840	1,033	0,973	0,959
IPI00982700.1	Uncharacterized protein		1,033			0,933	0,957	0,957
IPI00976265.2	Uncharacterized protein	0,967	0,816	0,839	0,940	1,291	1,033	0,954
IPI00978387.1	Uncharacterized protein	0,982	0,925	0,904	0,897	1,064	1,022	0,954
IPI01013193.2	Uncharacterized protein	0,745		0,721		1,160	1,243	0,953
IPI00793985.2	Uncharacterized protein	0,948	0,975	0,881	1,086	0,929	0,955	0,951
IPI00924705.1	Uncharacterized protein	0,942		0,959		0,862	1,204	0,951
IPI00981694.1	Uncharacterized protein	0,879	0,893	0,829	0,974	1,047	0,968	0,931
IPI01010773.2	Uncharacterized protein	0,888	**0,489**	0,972	**0,628**	0,984	0,962	0,925
IPI00982721.1	Uncharacterized protein	0,816	0,851	0,826	1,044	1,020	0,988	0,920
IPI00965964.3	Uncharacterized protein	1,141	0,958	**2,150**	0,879	0,696	0,855	0,918
IPI00893242.1	Uncharacterized protein				0,939	0,834	0,914	0,914
IPI01014262.2	Uncharacterized protein	**0,643**	**0,662**	0,913		1,034	1,438	0,913
IPI00926560.1	Uncharacterized protein	0,957	0,910	0,779				0,910
IPI00646055.3	Uncharacterized protein	0,730	0,894	1,058	0,972	0,698	0,920	0,907
IPI00983716.1	Uncharacterized protein	1,079	0,813	**2,677**	0,923	0,804	0,869	0,896
IPI00924791.1	Uncharacterized protein	0,732			1,005	0,953	0,833	0,893
IPI00946099.1	Uncharacterized protein	0,876	0,970	1,114	0,817	0,896	0,869	0,886
IPI00978664.1	Uncharacterized protein	**0,654**	0,790	0,762	1,012	1,104	0,958	0,874
IPI01018647.1	Uncharacterized protein	1,016	0,778	1,267	0,890	0,838	0,779	0,864
IPI00552365.7	Uncharacterized protein	0,825		0,857	0,792	1,003	0,925	0,857
IPI00893449.3	Uncharacterized protein			**2,317**		0,856	0,846	0,856
IPI00916480.1	Uncharacterized protein	1,098	0,855	0,992	**0,586**		0,779	0,855
IPI00968174.1	Uncharacterized protein				0,852	0,790	0,905	0,852
IPI00927101.1	Uncharacterized protein	0,977	0,832	1,047	0,856	**0,624**	0,686	0,844

IPI00984941.1	Uncharacterized protein	**0,579**	**0,616**	0,710	0,898	0,946	1,136	0,804
IPI00647126.2	Uncharacterized protein	1,482	0,908		0,719	**0,595**	0,795	0,795
IPI00977701.1	Uncharacterized protein	0,755	0,780	0,698	1,203		1,153	0,780
IPI00966815.3	Uncharacterized protein	0,724	1,372		0,904	**0,551**	**0,649**	0,724
IPI00980443.1	Uncharacterized protein	0,825	**0,523**	**5,008**	**0,500**	**0,596**	0,748	0,672
IPI00384745.4	Uncharacterized protein		**0,492**	**0,597**		**1,558**		**0,597**
IPI00410091.3	Uncharacterized protein C11orf73	0,816	0,933	0,980	0,754	0,794	0,828	0,822
IPI00430803.3	Uncharacterized protein C2orf79	0,886	0,861	0,826	1,012	1,169	1,160	0,949
IPI00029444.2	UPF0160 protein MYG1, mitochondrial	0,929	0,857	0,798	1,194	1,222	1,110	1,020
IPI00002270.3	UPF0364 protein C6orf211	1,160	0,979	0,973	0,832	1,034	1,017	0,998
IPI00001655.1	UPF0468 protein C16orf80	0,996	1,010	1,116	0,966	0,969	0,904	0,983
IPI00170972.2	UPF0553 protein C9orf64	0,976	1,077	0,881	0,850	1,066	0,995	0,986
IPI00056357.3	UPF0556 protein C19orf10	1,137	1,009	0,905	0,755	1,149	0,999	1,004
IPI00006980.1	UPF0568 protein C14orf166	**1,724**	1,453	**2,312**	1,212	0,769	0,865	1,333
IPI00016605.3	UPF0587 protein C1orf123	1,088	0,940	0,976	1,007	1,117	1,108	1,047
IPI00301489.3	Uroporphyrinogen decarboxylase	0,890	0,807	0,816	1,148	1,277	1,236	1,019
IPI00008219.1	UV excision repair protein RAD23 homolog A	0,709	0,691	0,812	1,358	**1,701**	1,366	1,085
IPI00008223.3	UV excision repair protein RAD23 homolog B	0,692	0,706	0,740	0,896	1,231	1,132	0,818
IPI00007812.1	V-type proton ATPase subunit B, brain isoform	0,749	0,766	0,797	1,344	1,297	1,375	1,047
IPI00004488.2	V-type proton ATPase subunit F	1,067	0,972	1,031	0,914	0,998	1,000	0,999
IPI00018931.6	Vacuolar protein sorting-associated protein 35	0,932	1,006	1,303	0,832	0,739	0,773	0,882
IPI00031655.1	Vacuolar protein-sorting-associated protein 25			1,242	1,009	0,870	0,949	0,979
IPI00000873.3	Valyl-tRNA synthetase	0,753	0,935	1,062	1,095	0,896	1,028	0,981
IPI00549343.3	Vesicle-associated membrane protein 3	**2,407**		**3,168**	**1,723**		0,961	**2,065**
IPI00030911.2	Vesicle-associated membrane protein 8				**1,538**	0,727	0,914	0,914
IPI00006865.4	Vesicle-trafficking protein SEC22b	**1,591**	**1,964**		1,463	0,859	1,109	1,463
IPI00022228.2	Vigilin		1,115	**1,746**	1,275	0,935	1,134	1,134
IPI00418471.6	Vimentin	0,737	0,871	0,948	0,882	0,973	0,892	0,887
IPI00334159.6	von Hippel-Lindau binding protein 1, isoform CRA_b	0,940	0,961	1,046	0,807	0,974	0,901	0,950
IPI00019269.3	WD repeat-containing protein 61	1,207	1,211	0,971	0,884	0,959	0,946	0,965
IPI00220834.8	X-ray repair cross-complementing protein 5	1,258	1,134	**1,930**	0,998	0,805	0,907	1,066
IPI00644712.4	X-ray repair cross-complementing protein 6	1,012	1,092	**1,844**	1,189	0,955	1,059	1,076
IPI00645898.2	xaa-Pro aminopeptidase 1 isoform 1	0,920	0,849	0,746	1,090	1,365	1,302	1,005
IPI00257882.7	Xaa-Pro dipeptidase	0,886	0,841	0,786	1,089	1,212	1,107	0,987
IPI01011409.1	zinc phosphodiesterase ELAC protein 2 isoform 2	0,683	0,690	0,740	1,106	1,208	1,210	0,923
IPI00926625.1	Zyxin			**0,585**	1,136	**1,517**		1,136

TABLE 6: Proteins Identified and Quantified in SILAC HEK 293 T - Phosphoproteome Analysis

ACCESSION	DESCRIPTION	Heavy Treat/Light Ctrl Replicate 1	Heavy Treat/Light Ctrl Replicate 2	Heavy Treat/Light Ctrl Replicate 3	Light Treat/Heavy Ctrl Replicate 1	Light Treat/Heavy Ctrl Replicate 2	Light Treat/Heavy Ctrl Replicate 3	MEDIAN
IPI00965616.1	11 kDa protein		0,660					0,660
IPI00916597.1	12 kDa protein		2,497	1,920			3,493	2,497
IPI00879281.1	12 kDa protein		0,966					0,966
IPI00978197.1	13 kDa protein			0,804			0,974	0,889
IPI00983145.1	14 kDa protein	0,222	0,230	0,293	3,987	4,163	3,400	1,846
IPI00893541.1	14 kDa protein		0,942				0,970	0,956
IPI00977372.1	14 kDa protein			0,313				0,313
IPI00018146.1	14-3-3 protein theta	0,825	0,867	0,892			0,933	0,879
IPI00021263.3	14-3-3 protein zeta/delta		0,888	0,911			1,021	0,911
IPI00921408.1	2-oxoglutarate dehydrogenase-like, mitochondrial isoform b			0,694				0,694
IPI00792209.1	20 kDa protein					1,288		1,288
IPI00978582.1	20 kDa protein			1,184				1,184
IPI01014011.1	21 kDa protein					2,235	1,444	1,840
IPI00644531.1	21 kDa protein		0,868	0,897	1,518	1,147	1,246	1,147
IPI00893658.1	22 kDa protein	0,765	0,907	1,221	1,254	1,274	1,433	1,237
IPI00947254.1	25 kDa protein			0,635	1,698	0,260		0,635
IPI00013297.1	28 kDa heat- and acid-stable phosphoprotein		1,643	1,316	0,803	0,499	1,589	1,316
IPI01010378.1	28 kDa protein			1,050	1,665	2,585		1,665
IPI00975917.1	30 kDa protein			0,873			1,111	0,992
IPI00976548.1	33 kDa protein			0,765				0,765
IPI01009205.1	35 kDa protein	0,382	0,337	0,377	2,454	2,380	2,099	1,241
IPI00044724.4	37 kDa protein	0,797						0,797
IPI00013296.3	40S ribosomal protein S18		2,145				1,407	1,776
IPI00719622.1	40S ribosomal protein S28		1,624					1,624
IPI00008433.4	40S ribosomal protein S5		1,617	1,669		0,674	1,358	1,487
IPI00643522.1	40S ribosomal protein S6						1,632	1,632
IPI00646374.1	52 kDa protein		1,046	2,063			1,543	1,543
IPI00747810.3	52 kDa protein			0,766			1,180	0,973
IPI01016072.1	52 kDa protein			0,614				0,614
IPI01012417.1	59 kDa protein	0,336	0,245	0,279	2,445	2,372	2,587	1,354
IPI00893366.1	6 kDa protein				1,701	1,052		1,377
IPI01014055.1	6-phosphofructo-2-kinase/fructose-2, 6-bisphosphatase 2 transcript variant 3				0,535			0,535
IPI00784154.1	60 kDa heat shock protein, mitochondrial	0,901	0,762	0,854	1,113	1,274	0,968	0,935
IPI00008529.1	60S acidic ribosomal protein P2	0,922	0,936	0,878	0,960	1,247	1,148	0,948

IPI00925323.1	60S ribosomal protein L14				2,620			**2,620**
IPI00413324.6	60S ribosomal protein L17	1,855	4,863	6,033	4,203	12,367	18,292	**5,448**
IPI00219153.4	60S ribosomal protein L22		1,177					1,177
IPI00021266.1	60S ribosomal protein L23a	1,786		1,704	1,281		1,725	**1,715**
IPI01022095.1	7 kDa protein		**0,243**	**0,432**		**2,312**	1,575	1,004
IPI00970935.1	71 kDa protein	0,470	0,437	0,527	1,312	1,302	1,162	0,844
IPI00939705.2	76 kDa protein			0,545				**0,545**
IPI00003362.3	78 kDa glucose-regulated protein		0,939			0,881	1,049	0,939
IPI00021320.2	7SK snRNA methylphosphate capping enzyme	0,612	0,461	0,476	1,126	0,884	1,078	0,748
IPI00965771.1	8 kDa protein					2,954		**2,954**
IPI00916507.1	8 kDa protein		0,305		1,516			0,910
IPI00927819.3	80 kDa protein	0,491	0,352	1,006	1,283	1,667	2,076	1,145
IPI00902970.4	88 kDa protein			2,152				**2,152**
IPI00982334.1	9 kDa protein			2,254			2,035	**2,145**
IPI00025849.1	Acidic leucine-rich nuclear phosphoprotein 32 family member A	0,682	0,929	0,796	0,938	1,092	1,299	0,933
IPI00640833.1	acidic leucine-rich nuclear phosphoprotein 32 family member E isoform 3	0,622	0,731	0,836		0,838	1,157	0,836
IPI00743594.2	Actin-binding protein anillin						2,846	**2,846**
IPI00021439.1	Actin, cytoplasmic 1	0,520	0,729	0,769	1,911	1,007	1,209	0,888
IPI00221222.7	Activated RNA polymerase II transcriptional coactivator p15		0,650	0,766		**0,425**	1,125	0,708
IPI00935818.1	adenosylhomocysteinase isoform 2		0,850	0,899				0,874
IPI01009563.1	Adenylyl cyclase-associated protein	0,529	0,270	0,355	3,306	2,843	3,217	**1,686**
IPI01014668.1	afadin			**0,467**	1,651			1,059
IPI00431688.1	AKAP12 protein (Fragment)			0,675				0,675
IPI00027442.4	Alanyl-tRNA synthetase, cytoplasmic			0,867			0,964	0,915
IPI00413641.7	Aldose reductase		0,810					0,810
IPI00470779.2	Alpha-taxilin	0,433	0,442	0,549	3,380	3,020	3,118	**1,784**
IPI00023051.3	Alpha-tectorin					2,511		**2,511**
IPI00033907.1	Anaphase-promoting complex subunit 1		0,776	0,823				0,800
IPI00218918.5	Annexin A1		1,122				2,111	**1,616**
IPI00021290.5	ATP-citrate synthase	1,403	1,001	1,144	1,439	1,554	1,413	1,408
IPI00844578.1	ATP-dependent RNA helicase A		0,983	1,395			1,628	1,395
IPI00641582.1	BAG family molecular chaperone regulator 3		0,340	0,508			1,317	**0,508**
IPI00788953.3	band 4.1-like protein 2 isoform b						1,172	1,172
IPI00003269.1	Beta-actin-like protein 2						**2,180**	**2,180**
IPI00013452.1 1	Bifunctional aminoacyl-tRNA synthetase	1,251	0,488	0,525	2,872	2,102	3,348	**1,676**
IPI00397721.1	Biogenesis of lysosome-related organelles complex 1 subunit 3	**0,345**	**0,256**		**2,374**	**2,714**		1,360

IPI00797574.3	Biorientation of chromosomes in cell division protein 1-like		0,508	0,875			1,636	0,875
IPI00909739.1	box C/D snoRNA protein 1 isoform 2			0,804			1,226	1,015
IPI00002186.5	Brefeldin A-inhibited guanine nucleotide-exchange protein 2		0,694		0,745			0,719
IPI00060715.1	BTB/POZ domain-containing protein KCTD12	0,502	0,393	0,404	2,316	2,226	2,038	1,270
IPI00939535.2	C19orf2 protein			0,669				0,669
IPI00333010.9	Calcium homeostasis endoplasmic reticulum protein				2,758	2,541		**2,649**
IPI00304409.3	Calcium-regulated heat stable protein 1	0,441	0,489	0,499	2,404	2,515	2,395	1,447
IPI00020599.1	Calreticulin		0,786	1,010		1,115	0,955	0,982
IPI00966751.1	CaM kinase II isoform		0,108	0,179			3,215	**0,179**
IPI00021831.1	cAMP-dependent protein kinase type I-alpha regulatory subunit	0,295	0,205	0,221	3,336	3,370	4,104	**1,816**
IPI00010865.1	Casein kinase II subunit beta		0,438	0,445			1,226	**0,445**
IPI00289819.5	Cation-independent mannose-6-phosphate receptor					1,034		1,034
IPI00807498.1	CCDC6 protein (Fragment)		0,527	0,706		2,164		0,706
IPI00006103.1	CD2 antigen cytoplasmic tail-binding protein 2	0,681	0,483	0,524	2,300	1,978	2,084	1,329
IPI00015894.1	Cdc42 effector protein 4			**0,353**				**0,353**
IPI00012073.2	cDNA FLJ10339 fis, clone NT2RM2000740, weakly similar to POSSIBLE GLOBAL TRANSCRIPTION ACTIVATOR SNF2L		1,124	0,944			0,952	0,952
IPI00984351.1	cDNA FLJ10364 fis, clone NT2RM2001319		0,578	0,759			1,187	0,759
IPI00902580.1	cDNA FLJ11050 fis, clone PLACE1004564, highly similar to Cleavage and polyadenylation specificity factor 100 kDa subunit		0,525	0,865				0,695
IPI00646339.1	cDNA FLJ14104 fis, clone MAMMA1001198, highly similar to Epidermal growth factor receptor substrate 15-like 1	0,510	0,446	0,555	1,735	1,434	1,333	0,944
IPI01010189.1	cDNA FLJ16143 fis, clone BRAMY2038516, highly similar to Protein disulfide-isomerase A6	0,423	0,734	0,668	1,687	1,183	0,901	0,817
IPI00307369.1	CDNA FLJ25155 fis, clone CBR07976				1,116			1,116
IPI00902551.1	cDNA FLJ30200 fis, clone BRACE2001455, highly similar to HEAT SHOCK FACTOR PROTEIN 1	0,322	0,231	0,224	1,467	1,466	4,233	0,894
IPI00102313.3	cDNA FLJ30398 fis, clone BRACE2008402, highly similar to Steroid receptor RNA activator 1	0,367	0,245	0,282	3,978	3,603	3,861	**1,985**
IPI00385786.3	cDNA FLJ35170 fis, clone PLACE6012942, highly similar to SPLICING FACTOR, ARGININE/SERINE-RICH 2	0,949	0,665	0,778	1,278	1,360	1,265	1,107
IPI00902976.1	cDNA FLJ37504 fis, clone BRAWH2017103, highly similar to ATPase WRNIP1		0,349	0,747			1,384	0,747
IPI00939558.2	cDNA FLJ38696 fis, clone KIDNE2001931, highly similar to HETEROGENEOUS NUCLEAR RIBONUCLEOPROTEIN G				1,188	0,895		1,042
IPI00903079.1	cDNA FLJ43156 fis, clone DFNES2011239, highly similar to Protein FAM57A			0,735				0,735
IPI01009627.1	cDNA FLJ46798 fis, clone TRACH3031660, highly similar to cAMP-dependent protein kinase type II-beta regulatory subunit	0,731	0,558	0,627	1,355	1,255	1,160	0,945

IPI00922847.1	cDNA FLJ50115, moderately similar to Membrane-associated progesterone receptor component 1	1,062	0,868	1,133	1,933	1,483	3,006	1,308
IPI00337602.4	cDNA FLJ50345, highly similar to Zinc finger protein 326						1,684	**1,684**
IPI01014228.1	cDNA FLJ50986, highly similar to DNA topoisomerase 2-beta		0,575	0,779	**3,078**	**2,750**	**8,482**	**2,750**
IPI01010287.1	cDNA FLJ51031, highly similar to ATP-dependent RNA helicase DDX1						1,590	**1,590**
IPI00908746.1	cDNA FLJ51535, highly similar to Phosphatidylethanolamine-binding protein 1						0,742	0,742
IPI00908319.1	cDNA FLJ51570, highly similar to Thioredoxin domain-containing protein 1	1,865						**1,865**
IPI00937211.1	cDNA FLJ51571, moderately similar to Mediator of DNA damage checkpoint protein 1			0,973	1,396	1,002		1,002
IPI00976971.1	cDNA FLJ51637, highly similar to Metastasis-associated protein MTA2		0,323	0,434				**0,378**
IPI00910350.1	cDNA FLJ52068, highly similar to Microtubule-associated protein RP/EB family member 1		0,807	0,940			1,493	0,940
IPI00910779.1	cDNA FLJ52141, highly similar to 14-3-3 protein gamma			0,900			1,015	0,957
IPI01014477.1	cDNA FLJ52592, highly similar to Acetyl-CoA carboxylase 1		**37,238**					**37,238**
IPI00909530.1	cDNA FLJ52843, highly similar to Histone H3.3		1,001	1,912			1,072	1,072
IPI00908710.1	cDNA FLJ52854, highly similar to Sequestosome-1		0,472	0,598				**0,535**
IPI00910113.1	cDNA FLJ52902, highly similar to Rab GDP dissociation inhibitor alpha		0,672	0,776			1,204	0,776
IPI00909971.1	cDNA FLJ53024, highly similar to Ubiquitin carboxyl-terminal hydrolase 10						1,862	**1,862**
IPI00922843.1	cDNA FLJ53114, highly similar to Neural cell adhesion molecule 2		0,020					**0,020**
IPI01015635.1	cDNA FLJ53176, highly similar to Nuclear autoantigenic sperm protein	1,450	0,833	0,856	**2,696**	**2,156**	1,586	**1,518**
IPI00975695.1	cDNA FLJ53373, highly similar to SAPS domain family member 3	0,904	0,743	0,952	1,259	1,145		0,952
IPI00910164.1	cDNA FLJ53381, highly similar to Monocarboxylate transporter 1			1,349				1,349
IPI00337396.4	cDNA FLJ53414, highly similar to Nuclear pore complex protein Nup98-Nup96precursor			1,065				1,065
IPI00981395.1	cDNA FLJ53442, highly similar to Poly (ADP-ribose) polymerase 1			1,347			1,046	1,196
IPI00977669.1	cDNA FLJ53512, highly similar to Homo sapiens centrosomal protein 170 kDa (CEP170), transcript variant alpha, mRNA (Fragment)			1,302			7,054	**4,178**
IPI01009448.1	cDNA FLJ53521, highly similar to Pumilio homolog 2		0,683	0,820	1,557	1,215		1,017
IPI00884400.1	cDNA FLJ53537				0,733	0,990		0,861
IPI00743469.2	cDNA FLJ53635, highly similar to Homo sapiens tumor protein D52-like 2 (TPD52L2), transcript variant 6, mRNA	0,522	1,536	1,435			**3,456**	1,485
IPI00643908.3	cDNA FLJ53700, highly similar to Hepatoma-derived growth factor	0,575	0,666	0,682	1,594	1,737	1,495	1,088
IPI00921920.1	cDNA FLJ53909, moderately similar to Calpastatin	**0,341**	0,277	0,400	2,440	2,963	2,508	1,420
IPI00910447.1	cDNA FLJ53938	2,143						**2,143**

IPI00908727.1	cDNA FLJ53983, highly similar to IWS1 homolog	1,000	0,787	0,933	1,069	1,057	1,030	1,015
IPI00964952.1	cDNA FLJ53999, highly similar to GRB2-associated-binding protein 1			0,258			2,114	1,186
IPI00644224.2	cDNA FLJ54020, highly similar to Heterogeneous nuclear ribonucleoprotein U	1,746	0,995	1,329	2,079	1,561	2,422	**1,653**
IPI01015887.1	cDNA FLJ54066, highly similar to Drebrin-like protein			**0,469**				**0,469**
IPI00911096.1	cDNA FLJ54127, highly similar to Heterogeneous nuclear ribonucleoproteins C			2,213				**2,213**
IPI00908945.1	cDNA FLJ54147, highly similar to Zinc-finger protein ubi-d4			1,121	1,889	1,606	1,625	**1,616**
IPI01014869.1	cDNA FLJ54148, highly similar to 26S proteasome non-ATPase regulatory subunit 3		1,134	1,037	1,477		1,698	1,305
IPI01014543.1	cDNA FLJ54186, highly similar to Nuclear receptor-binding protein	**0,326**		**0,455**				**0,390**
IPI01008919.1	cDNA FLJ54222, highly similar to Glycylpeptide N-tetradecanoyltransferase 1	0,712	1,103	1,193	1,213	1,031	1,145	1,124
IPI00965501.2	cDNA FLJ54242, highly similar to Calnexin	1,265	1,025	1,398	1,315	1,057	1,919	1,290
IPI00908538.1	cDNA FLJ54293			1,248		1,205	2,365	1,248
IPI01013654.1	cDNA FLJ54323						1,679	**1,679**
IPI00911039.1	cDNA FLJ54408, highly similar to Heat shock 70 kDa protein 1		0,812	0,841		0,911	1,393	0,876
IPI00910497.1	cDNA FLJ54652, highly similar to Homo sapiens podocan (PODN), mRNA						1,723	**1,723**
IPI00922127.1	cDNA FLJ54708, highly similar to 150 kDa oxygen-regulated protein					0,868		0,868
IPI00910714.1	cDNA FLJ54754, highly similar to Protein FAM61A	0,698	0,563	0,501	1,993	1,984	2,596	1,341
IPI00910650.1	cDNA FLJ54979, highly similar to Homo sapiens cyclin-dependent kinase 2 (CDK2), transcript variant 2, mRNA	1,443	1,003	1,588	0,992	0,898	1,419	1,211
IPI00922590.3	cDNA FLJ55014, highly similar to ADP-ribosylation factor GTPase-activating protein 1						1,196	1,196
IPI01011997.1	cDNA FLJ55368, highly similar to Epsin-1				3,250	5,322		**4,286**
IPI01010195.1	cDNA FLJ55629, highly similar to Transcription elongation factor SPT5			0,630				**0,630**
IPI00873286.2	cDNA FLJ55750, highly similar to Eukaryotic translation initiation factor 3 subunit 8	1,510	0,790	0,971	0,780	0,583	1,036	0,881
IPI00893216.2	cDNA FLJ55994, highly similar to RNA-binding protein Luc7-like 2		1,117	1,725				1,421
IPI00798145.2	cDNA FLJ56210, highly similar to Zinc phosphodiesterase ELAC protein 2	**0,493**	**0,410**	**0,397**	1,803	1,921		**0,493**
IPI00910298.1	cDNA FLJ56236, highly similar to Exportin-2		0,946	1,344		1,063		1,063
IPI00926081.1	cDNA FLJ56359, highly similar to Homo sapiens SH3-binding domain protein 5-like (SH3BP5L), mRNA	1,048	1,086	1,224	0,352	0,985		1,048
IPI00641592.3	cDNA FLJ56618, highly similar to Ribosomal protein S6 kinase alpha-3		0,253	0,385			2,425	**0,385**
IPI00793098.2	cDNA FLJ57117, highly similar to Charged multivesicular body protein 2b	0,415	0,408	0,612	0,617	0,542	0,532	**0,537**
IPI01010852.1	cDNA FLJ57121, highly similar to Heterogeneous nuclear ribonucleoprotein F		0,974			1,005	1,492	1,005
IPI00910326.1	cDNA FLJ57288, highly similar to ELL-associated factor 1		0,276	0,405	2,235		2,459	1,320

IPI00911120.1	cDNA FLJ57453	0,235	0,207	0,273	3,383	3,390	2,748	**1,511**
IPI01014021.1	cDNA FLJ57529, highly similar to Helicase SKI2W	**2,914**	**2,070**	**2,275**	1,493	1,147	1,974	**2,022**
IPI00908891.1	cDNA FLJ57803, highly similar to Homo sapiens RNA pseudouridylate synthase domain containing 2 (RPUSD2), mRNA	**0,380**			1,721			1,051
IPI00298070.8	cDNA FLJ57814, highly similar to cAMP-specific 3',5'-cyclic phosphodiesterase 4C		0,764					0,764
IPI00908888.1	cDNA FLJ57836, highly similar to Myb-binding protein 1A						4,064	**4,064**
IPI00982472.1	cDNA FLJ57988, highly similar to Transaldolase		0,667	0,925			0,968	0,925
IPI00945725.1	cDNA FLJ58035, highly similar to Homo sapiens eukaryotic translation initiation factor (eIF) 2A (eIF2A), mRNA		0,668	0,671	3,241	2,268	3,621	**2,268**
IPI00909890.1	cDNA FLJ58049, highly similar to RNA-binding protein FUS			1,692				**1,692**
IPI00643519.3	cDNA FLJ58183, highly similar to Junctophilin-3			0,149				**0,149**
IPI01013941.1	cDNA FLJ58196, highly similar to Zinc finger CCCH domain-containing protein 11A			**2,640**				**2,640**
IPI01009186.1	cDNA FLJ58476, highly similar to Poly(rC)-binding protein 2		0,264	0,450	1,081	0,673	1,382	0,673
IPI00909015.2	cDNA FLJ58500, highly similar to Cytoplasmic dynein 1 light intermediate chain 1		0,460	0,757	1,723	1,483	2,805	1,483
IPI00647060.2	cDNA FLJ58603, highly similar to Actin-binding LIM protein 1		0,410	0,998	1,512	1,473	1,119	1,119
IPI00976057.1	cDNA FLJ58618, highly similar to Poly(A)-specific ribonuclease PARN		0,479	0,674		0,973	1,236	0,823
IPI00964879.1	cDNA FLJ58701, highly similar to SWI/SNF-related matrix-associated actin-dependent regulator of chromatin subfamily A containing DEAD/H box 1		0,763	0,606				0,685
IPI00644506.1	cDNA FLJ58756, highly similar to Nuclear pore complex protein Nup93						1,360	1,360
IPI00909509.1	cDNA FLJ59138, highly similar to Annexin A2		0,406	0,806			0,919	0,806
IPI00910507.1	cDNA FLJ59352, highly similar to Brain-specific angiogenesis inhibitor1-associated protein 2			2,181				**2,181**
IPI00909010.1	cDNA FLJ59356, highly similar to N-acetylserotonin O-methyltransferase-like protein		**0,326**	**0,243**		1,655	0,858	**0,592**
IPI01012981.1	cDNA FLJ59361, highly similar to Protein disulfide-isomerase		0,610	0,672		1,641	1,180	0,926
IPI00794673.2	cDNA FLJ59382, highly similar to T-complex protein 1 subunit theta						1,631	**1,631**
IPI00909427.1	cDNA FLJ59384, highly similar to Striatin-4			0,809		1,106		0,958
IPI01013474.1	cDNA FLJ59392, highly similar to CTP synthase 1	0,792	0,683	0,735	1,621	1,628	1,804	1,207
IPI00910983.1	cDNA FLJ59402, highly similar to Eukaryotic translation initiation factor 4B	**0,420**	0,543	1,038	2,425	1,719	2,052	1,378
IPI00922939.1	cDNA FLJ59521, moderately similar to Zinc finger and SCAN domain-containing protein 2		0,639	1,089	1,398	1,343	1,595	1,343
IPI01008719.1	cDNA FLJ59858, moderately similar to Nuclear valosin-containing protein-like				0,976			0,976
IPI00908647.1	cDNA FLJ59942, highly similar to Prostaglandin E synthase 3		0,840	0,870	1,199		1,090	0,980
IPI00939291.1	cDNA FLJ60207, highly similar to PHD finger protein 6	1,026	0,651	0,869	0,895	0,908	1,503	0,901

IPI00909543.1	cDNA FLJ60283, highly similar to Protein CASC3		0,853	0,963	1,485	1,134	1,525	1,134
IPI00909207.1	cDNA FLJ60461, highly similar to Peroxiredoxin-2	0,507	0,597	0,746		1,144		0,672
IPI00909184.1	cDNA FLJ60601, highly similar to Methylosome protein 50	0,528	0,391	0,451	2,306	2,312	2,340	1,417
IPI00604452.3	cDNA FLJ60912, highly similar to Vinexin		0,403	0,497				**0,450**
IPI01015197.1	cDNA FLJ61114, highly similar to Homo sapiens intersex-lik (IXL), mRNA	0,969	0,843	1,034	0,945		0,989	0,969
IPI00980056.1	cDNA FLJ61415, highly similar to Protein kinase C and casein kinase substratein neurons protein 3			0,221				**0,221**
IPI00892653.2	cDNA FLJ61481, highly similar to PAS domain-containing serine/threonine-protein kinase		0,791					0,791
IPI00328293.3	cDNA FLJ61739, highly similar to Serine/arginine repetitive matrix protein 1	0,892	0,475	0,667	1,985	1,519	2,237	1,205
IPI00792607.1	cDNA FLJ75425, highly similar to Homo sapiens small nuclear ribonucleoprotein polypeptide A', mRNA			1,344				1,344
IPI00043678.3	cDNA FLJ78567						**3,042**	**3,042**
IPI01010145.1	cDNA FLJ90464 fis, clone NT2RP3002281, highly similar to RNA-binding protein 12	0,838			1,047		1,025	1,025
IPI01012004.1	cDNA PSEC0175 fis, clone OVARC1000169, highly similar to Protein disulfide-isomerase A3		0,923	1,022			0,818	0,923
IPI00926316.1	cDNA, FLJ79126, highly similar to Zyxin	**0,495**	0,307	0,474	1,704	2,302	2,494	1,099
IPI00885017.1	cDNA, FLJ79527, moderately similar to Uroporphyrinogen decarboxylase			0,856			1,293	1,074
IPI01015342.1	cDNA, FLJ79540, highly similar to Serine-threonine kinase receptor-associatedprotein		0,547	0,755		**2,539**		0,755
IPI00885107.1	cDNA, FLJ79545, highly similar to Eukaryotic translation initiation factor 3subunit 4	0,338	0,211	0,228	3,660	2,635	4,161	1,486
IPI00184458.2	CDNA: FLJ23312 fis, clone HEP11874		0,139					**0,139**
IPI00005277.4	Cell cycle checkpoint control protein RAD9A		0,265	0,311				**0,288**
IPI00556426.3	Cell division cycle 2-like 2 isoform 4 variant (Fragment)	1,282	0,846	1,170	1,186	0,929		1,170
IPI00009862.4	Cerebellar degeneration-related protein 2		0,896	0,911	0,828	1,223		0,904
IPI00395463.3	Charged multivesicular body protein 7				1,192			1,192
IPI00010896.3	Chloride intracellular channel protein 1		0,557	0,497	1,737			**0,557**
IPI00011857.1	Chromatin assembly factor 1 subunit B	0,454	0,391	0,368	2,187	2,492	4,145	1,321
IPI00793392.1	chromatin complexes subunit BAP18 isoform 3	**0,449**	**0,431**	**0,441**	1,840		**2,244**	**0,449**
IPI00297579.4	Chromobox protein homolog 3		0,573	0,653		0,642	1,088	**0,648**
IPI00641008.1	Chromosome 20 open reading frame 172			1,203			1,291	1,247
IPI00889780.1	Chromosome 22 open reading frame 9						1,628	**1,628**
IPI00852984.3	Cingulin				1,894			**1,894**
IPI00012011.6	Cofilin-1	0,864	0,857	0,760	1,269	1,245	1,146	1,005
IPI00306471.1	Coiled-coil domain-containing protein 94				2,625			**2,625**
IPI00061777.4	Coiled-coil domain-containing protein 97			0,218			4,718	**2,468**
IPI00006442.1	Coilin				1,191			1,191
IPI00844090.1	Collagen alpha-1(V) chain						3,449	**3,449**

IPI00014230.1	Complement component 1 Q subcomponent-binding protein, mitochondrial		0,945	1,068			0,603	0,945
IPI00975725.1	Conserved hypothetical protein	1,048	0,902	0,716	1,869	**2,138**	1,503	1,275
IPI00976447.1	Conserved hypothetical protein					0,931		0,931
IPI00982737.1	Conserved hypothetical protein	0,590	0,611	0,644	1,259	1,328	1,209	0,926
IPI00022977.1	Creatine kinase B-type	0,995	0,895	1,010	1,035	1,107	1,020	1,015
IPI00783502.1	CREB-regulated transcription coactivator 2				1,427			1,427
IPI00645702.1	CTP synthase 2	1,019		0,787		1,313		1,019
IPI00940642.2	CUB and Sushi multiple domains 1 variant				1,072			1,072
IPI00001564.1	Cyclin-dependent kinase 4 inhibitor C			1,004			0,850	0,927
IPI00152692.2	D-tyrosyl-tRNA(Tyr) deacylase 1		0,357	0,384	0,777	0,615	0,602	**0,602**
IPI00012197.1	dCTP pyrophosphatase 1						1,814	**1,814**
IPI00894081.1	DEAH (Asp-Glu-Ala-His) box polypeptide 16	1,695	0,616		0,794	0,924	1,161	0,924
IPI00018117.3	Death-associated protein 1	0,310	0,282	0,360	1,980	2,435	2,457	1,170
IPI00657658.1	Dedicator of cytokinesis 8		0,941					0,941
IPI00883655.2	dihydropyrimidinase-related protein 2 isoform 1	0,636	0,490	0,552	1,884	2,052	1,917	1,260
IPI01010750.1	DNA ligase (Fragment)	0,440	0,385	1,231		0,681		**0,560**
IPI00010141.4	DNA polymerase epsilon subunit 3		0,800	0,927			1,149	0,927
IPI00184330.5	DNA replication licensing factor MCM2	1,004	0,741	0,831	1,234	1,152	1,262	1,078
IPI00031517.1	DNA replication licensing factor MCM6				1,488			1,488
IPI00031627.4	DNA-directed RNA polymerase II subunit RPB1			0,647				**0,647**
IPI00003783.1	Dual specificity mitogen-activated protein kinase kinase 2	0,879				1,771		1,325
IPI00304945.2	E3 ubiquitin-protein ligase NEDD4-like isoform 6		0,499	0,640				**0,570**
IPI00382804.1	EEF1A protein (Fragment)	1,315	1,515	1,721			1,517	**1,516**
IPI00060181.1	EF-hand domain-containing protein D2						1,207	1,207
IPI00940851.1	ELAV-like protein 1			0,930			1,486	1,208
IPI00186290.6	Elongation factor 2	1,190	0,956	1,153	3,060	1,917	1,376	1,283
IPI00027107.5	elongation factor Tu, mitochondrial precursor		0,524	**0,475**				**0,500**
IPI00644418.3	endophilin-A2 isoform 3				2,090	7,698		**4,894**
IPI00027230.3	Endoplasmin		0,716					0,716
IPI00024993.4	Enoyl-CoA hydratase, mitochondrial		0,897					0,897
IPI00385325.2	Epidermal growth factor receptor pathway substrate 15		0,649				**2,013**	1,331
IPI00010951.2	Epiplakin			1,275			2,354	**1,815**
IPI01011926.1	ESF1 protein (Fragment)		0,609	1,050	0,957	0,706	1,121	0,957
IPI00011689.2	Eukaryotic elongation factor 2 kinase	0,689						0,689
IPI00002569.3	Eukaryotic translation initiation factor 4E-binding protein 1	**0,405**	**0,433**	**0,407**	**2,086**	**2,049**	**2,243**	1,241
IPI00002570.1	Eukaryotic translation initiation factor 4E-binding protein 2	0,617	0,592	0,571	1,325	1,188	1,548	0,903

IPI00299254.4	Eukaryotic translation initiation factor 5B	0,737	0,785	1,462	1,245	1,003	1,326	1,124
IPI00005154.1	FACT complex subunit SSRP1		**0,395**	0,594			1,033	**0,594**
IPI00917117.1	FAM129B protein (Fragment)	**0,161**		**0,157**	**4,452**	**2,946**	**4,173**	**2,946**
IPI00026781.3	Fatty acid synthase			0,440			2,105	1,273
IPI00644576.1	Filamin A, alpha			0,494		1,213		0,854
IPI01013798.1	Formin binding protein 1			0,818			1,542	1,180
IPI00016250.7	Fragile X mental retardation syndrome-related protein 2					0,453		**0,453**
IPI00465439.5	Fructose-bisphosphate aldolase A		0,944	0,914			1,605	0,944
IPI00514843.3	FtsJ methyltransferase domain containing 2		2,964					**2,964**
IPI00069232.4	G-protein coupled receptor-associated sorting protein 2			0,478				**0,478**
IPI00160901.4	G2 and S phase-expressed protein 1			0,421				**0,421**
IPI00955973.1	GC-rich promoter binding protein 1-like 1, isoform CRA_a					6,022		**6,022**
IPI00219757.13	Glutathione S-transferase P	0,651	0,671	0,809	1,707	1,629	1,086	0,948
IPI00219018.7	Glyceraldehyde-3-phosphate dehydrogenase	1,191	0,784	1,032	1,525	1,220	1,381	1,205
IPI00943894.1	glycogen phosphorylase, liver form isoform 2			1,106				1,106
IPI00983220.1	Golgi-specific brefeldin A-resistance guanine nucleotide exchange factor 1 isoform 3				1,385			1,385
IPI00921612.1	GPN-loop GTPase 1 isoform d		0,522	0,876	1,553	1,267	1,080	1,080
IPI00337348.2	Growth differentiation factor 7					4,073		**4,073**
IPI01013009.1	GTF3C1 protein	1,013	0,897			1,041	0,924	0,969
IPI00643041.3	GTP-binding nuclear protein Ran		0,963	1,003		0,955	1,112	0,983
IPI00010463.5	GTP-binding protein 1	0,765	0,648	0,729		0,871	1,331	0,765
IPI00853447.3	GTPase activating protein and VPS9 domains 1	**0,497**		0,918	0,977		1,096	0,947
IPI00892665.1	Guanine nucleotide binding protein-like 1	0,663	0,690	0,827		1,110	1,482	0,827
IPI00915274.1	H/ACA ribonucleoprotein complex subunit 4 isoform 2	**2,794**	0,859	1,233	0,933	0,607	1,291	1,083
IPI00976830.2	HCG1820375, isoform CRA_a		0,749	1,266	1,428	0,994	1,581	1,266
IPI00002966.2	Heat shock 70 kDa protein 4	0,957	0,726	**0,339**		0,926	**2,434**	0,926
IPI00339269.1	Heat shock 70 kDa protein 6		**0,495**					**0,495**
IPI00414676.6	Heat shock protein HSP 90-beta	0,913	0,728	0,829	0,965	0,964	1,232	0,939
IPI00944522.2	heparanase isoform 2 precursor				2,212			**2,212**
IPI00910614.1	heterogeneous nuclear ribonucleoprotein R isoform 4		1,439					1,439
IPI00555868.1	Histone deacetylase 2 variant (Fragment)	0,933	0,837	0,960	1,005	0,938	1,120	0,949
IPI00217466.3	Histone H1.3						1,028	1,028
IPI00021924.1	Histone H1x			1,406		0,608	1,587	1,406
IPI00081836.3	Histone H2A type 1-H		0,929	1,077		0,845		0,929
IPI00003935.6	Histone H2B type 2-E		1,042	1,298		0,844		1,042
IPI00013788.1	HIV Tat-specific factor 1	0,860	0,837	0,668	1,113	1,131	1,905	0,987

IPI00939221.2	HLA-B associated transcript 1						1,245	1,245
IPI00792708.1	HLA-B associated transcript 3			0,327				**0,327**
IPI00981203.2	HMGA2d'		0,487	0,485				**0,486**
IPI00013122.1	Hsp90 co-chaperone Cdc37		0,427					**0,427**
IPI00983633.1	HSPE1-MOBKL3 protein	1,023	1,022			0,971		1,022
IPI00935143.1	hypothetical protein LOC100286939			0,897				0,897
IPI00985448.1	hypothetical protein LOC100509542		0,366					**0,366**
IPI00152407.3	hypothetical protein LOC147339 isoform b	1,055	0,915	1,055	1,659	1,812	1,730	1,357
IPI00954120.1	hypothetical protein LOC79886 isoform 2			1,672				**1,672**
IPI00218493.7	Hypoxanthine-guanine phosphoribosyltransferase		0,919	1,016				0,968
IPI00925196.2	IMP dehydrogenase 2					1,759		**1,759**
IPI00002214.1	Importin subunit alpha-2	**0,418**	**0,240**	**0,442**	0,879	1,054	1,224	**0,661**
IPI00299033.1	Importin subunit alpha-3	0,502	**0,490**	**0,491**				**0,491**
IPI00012578.1	Importin subunit alpha-4			1,165			1,181	1,173
IPI00001639.2	Importin subunit beta-1		0,804	0,791			1,684	0,804
IPI00015018.1	Inorganic pyrophosphatase		0,690	0,816			1,028	0,816
IPI00020729.1	Insulin receptor substrate 4	0,682	0,559	0,623	1,972	1,462	2,674	1,072
IPI00008557.6	Insulin-like growth factor 2 mRNA-binding protein 1	1,894	0,899	1,139	1,858	1,269	2,071	**1,563**
IPI00645608.2	Interferon regulatory factor 2-binding protein 1		0,302	0,663				**0,482**
IPI00395667.3	Interferon-related developmental regulator 2, isoform CRA_b						1,867	**1,867**
IPI00556364.1	Interleukin enhancer binding factor 3 isoform c variant (Fragment)		0,866	0,860			2,018	0,866
IPI00005198.2	Interleukin enhancer-binding factor 2		1,131					1,131
IPI00304589.5	Isoform 1 of 182 kDa tankyrase-1-binding protein	**0,412**	0,348	0,693	2,220	3,532	1,465	1,079
IPI00020042.2	Isoform 1 of 26S protease regulatory subunit 6B						1,317	1,317
IPI00024933.3	Isoform 1 of 60S ribosomal protein L12			1,379	1,824			**1,602**
IPI00237884.4	Isoform 1 of A-kinase anchor protein 12	0,413	0,606	0,894	1,368	0,694	1,366	0,794
IPI00024024.4	Isoform 1 of A-kinase anchor protein 17A	1,106					3,905	**2,506**
IPI00007423.1	Isoform 1 of Acidic leucine-rich nuclear phosphoprotein 32 family member B		0,936	1,083		1,066	0,865	1,001
IPI00797397.1	Isoform 1 of Ankyrin repeat and KH domain-containing protein 1		0,386	0,612		1,398		**0,612**
IPI00409671.3	Isoform 1 of ATP-dependent RNA helicase DDX42			0,871				0,871
IPI00879999.1	Isoform 1 of ATP-dependent RNA helicase DDX54	**3,267**		**2,299**			**2,300**	**2,300**
IPI00184821.1	Isoform 1 of Bifunctional coenzyme A synthase		**0,139**	**0,215**			**3,632**	**0,215**
IPI00220445.4	Isoform 1 of Collagen alpha-1(XX) chain		0,832	0,936				0,884
IPI00003406.4	Isoform 1 of Drebrin	0,939	**0,296**	0,643	1,291	1,117	1,792	1,028
IPI00394738.5 ;IPI00944963. 1	Isoform 1 of Dual specificity protein phosphatase 7		0,734	0,998			1,672	0,998

IPI00025156.4	Isoform 1 of E3 ubiquitin-protein ligase CHIP	0,771	0,612	0,610	1,645	1,445	1,601	1,108
IPI00376317.4	Isoform 1 of Enhancer of mRNA-decapping protein 4	0,821	0,343	0,803	1,365	1,086	1,833	0,954
IPI00479786.5	Isoform 1 of Far upstream element-binding protein 2						1,133	1,133
IPI00170778.5	Isoform 1 of Formin-binding protein 4		0,784	1,239	0,969	0,922	0,815	0,922
IPI00028570.2	Isoform 1 of Glycogen synthase kinase-3 beta	1,224	0,396	0,808	1,369	0,968	1,742	1,096
IPI00941614.1	Isoform 1 of Golgi reassembly-stacking protein 2	0,445	0,355	0,393	1,750	1,525	2,068	0,985
IPI00784295.2	Isoform 1 of Heat shock protein HSP 90-alpha	0,729	0,779	0,796	1,342	1,160	1,075	0,935
IPI00216049.1	Isoform 1 of Heterogeneous nuclear ribonucleoprotein K	0,801	0,653	0,933	1,321	1,259	1,610	1,096
IPI00304875.2	Isoform 1 of HIRA-interacting protein 3	0,879	0,455	0,607	0,932	0,922	0,909	0,894
IPI00294398.2	Isoform 1 of Hydroxyacyl-coenzyme A dehydrogenase, mitochondrial		1,387	1,398				1,392
IPI00604711.3	Isoform 1 of Kinesin-like protein KIF1A	**0,296**			**2,766**			**1,531**
IPI00217966.9	Isoform 1 of L-lactate dehydrogenase A chain		0,758	0,955			0,905	0,905
IPI00185919.3	Isoform 1 of La-related protein 1	1,177	0,745	0,656	1,338	1,038	1,849	1,108
IPI00220766.5	Isoform 1 of Lactoylglutathione lyase		0,557					**0,557**
IPI00107745.3	Isoform 1 of Luc7-like protein 3	3,355	0,561	0,688		0,484	1,099	0,688
IPI00396171.4	Isoform 1 of Microtubule-associated protein 4	1,307	0,614	0,761	1,048	1,513	1,968	1,177
IPI00293746.2	Isoform 1 of Multiple myeloma tumor-associated protein 2						3,920	**3,920**
IPI00397526.3	Isoform 1 of Myosin-10	1,442	0,658	0,887	1,040	1,079		1,040
IPI00019502.3	Isoform 1 of Myosin-9	1,064	0,801	1,040	1,318	1,272	1,400	1,168
IPI00442299.1	Isoform 1 of Neurexin-1-alpha				0,973			0,973
IPI00171475.2	Isoform 1 of NFATC2-interacting protein		0,518	0,657			1,403	**0,657**
IPI00022145.6	Isoform 1 of Nuclear ubiquitous casein and cyclin-dependent kinases substrate	0,597	0,540	0,527	1,303	1,398	1,182	0,889
IPI00549248.4	Isoform 1 of Nucleophosmin	1,112	0,549	1,006	1,104	0,818	1,147	1,055
IPI00026260.1	Isoform 1 of Nucleoside diphosphate kinase B	0,861	0,798	0,873		1,198	1,014	0,873
IPI00171176.3	Isoform 1 of Pantothenate kinase 2, mitochondrial				1,229	1,402	1,872	1,402
IPI00784233.2	Isoform 1 of PERQ amino acid-rich with GYF domain-containing protein 2		0,678	1,087			2,521	1,087
IPI00219526.6	Isoform 1 of Phosphoglucomutase-1	0,623	0,645	0,659	1,451	1,596	1,492	1,055
IPI00789041.2	Isoform 1 of Pinin		0,542	0,743	1,129	0,709	1,455	0,743
IPI00171390.2	Isoform 1 of Pre-mRNA-splicing factor 38A		0,646	1,048				0,847
IPI00220302.1	Isoform 1 of Pre-mRNA-splicing regulator WTAP	0,515	0,369	0,533	1,323	1,294	1,468	0,914
IPI00549786.5	Isoform 1 of Proline-rich AKT1 substrate 1	0,068	0,454	0,633	1,056	1,244	1,977	0,844
IPI00443909.1	Isoform 1 of Protein canopy homolog 2			1,039			0,975	1,007
IPI00883930.3	Isoform 1 of Protein FAM189A1						0,792	0,792
IPI00177937.6	Isoform 1 of Protein MICAL-3		0,303	0,334			2,212	**0,334**
IPI00033600.1	Isoform 1 of Protein phosphatase 1 regulatory subunit 7	0,575	0,588	0,931		0,757	1,041	0,757

IPI00970956.1	Isoform 1 of Protein PRRC2B			4,004				**4,004**
IPI00072377.1	Isoform 1 of Protein SET	0,618		**0,167**				**0,392**
IPI00036742.6	Isoform 1 of Protein virilizer homolog	1,095			1,076	0,550	**2,103**	1,085
IPI00293009.4	Isoform 1 of Rab GTPase-binding effector protein 1		0,825	0,721				0,773
IPI00004273.6	Isoform 1 of RNA-binding protein 25	**3,358**	**0,255**	0,726	0,766		1,461	0,766
IPI00782992.3	Isoform 1 of Serine/arginine repetitive matrix protein 2	1,163	0,401	0,561	1,099	1,062	1,398	1,081
IPI00479997.4	Isoform 1 of Stathmin	0,773	0,596	0,654	1,553	1,768	1,472	1,123
IPI00024214.1	Isoform 1 of Telomeric repeat-binding factor 2			1,280				1,280
IPI00301503.8	Isoform 1 of Transformer-2 protein homolog beta		0,766	1,241			1,344	1,241
IPI00797270.4	Isoform 1 of Triosephosphate isomerase	0,887	0,869	0,842	1,113	1,910	1,344	1,000
IPI00010779.4	Isoform 1 of Tropomyosin alpha-4 chain		0,827	0,830			1,060	0,830
IPI00029778.3	Isoform 1 of Tumor suppressor p53-binding protein 1	0,443	0,392	0,519	1,757	1,760	1,916	1,138
IPI00000728.3	Isoform 1 of Ubiquitin carboxyl-terminal hydrolase 15		**0,368**	**0,498**			**2,145**	**0,498**
IPI00782974.1	Isoform 1 of Uncharacterized protein C17orf85			0,403				**0,403**
IPI00291401.5	Isoform 1 of UPF0690 protein C1orf52	0,673	0,596	0,769	1,234	1,261	1,097	0,933
IPI00470483.19	Isoform 1 of WD repeat-containing protein 62		0,350	0,479	1,751		2,251	1,115
IPI00375330.6	Isoform 1 of Wings apart-like protein homolog	0,649		0,712	2,671	1,590		1,151
IPI00328929.4	Isoform 1 of Zinc finger CCCH domain-containing protein 18	2,556	0,354	0,613	0,919	0,626	1,115	0,772
IPI00944518.1	Isoform 10 of Histone deacetylase 7	**0,446**			**2,441**	**2,122**		**2,122**
IPI00886797.1	Isoform 2 of 2',5'-phosphodiesterase 12	**0,182**						**0,182**
IPI00456695.1	Isoform 2 of 26S proteasome non-ATPase regulatory subunit 1			0,499			3,572	**2,036**
IPI00336094.5	Isoform 2 of 3-hydroxyacyl-CoA dehydrogenase type-2					0,913		0,913
IPI00788157.1	Isoform 2 of 5'-3' exoribonuclease 2	1,252	0,953	1,048	1,359	0,986	2,052	1,150
IPI00216622.1	Isoform 2 of Actin-like protein 6A			0,848	1,920		0,726	0,848
IPI00477035.2	Isoform 2 of Arginine/serine-rich protein PNISR	1,379	0,723	0,407	1,042	0,832	0,931	0,882
IPI00410716.1	Isoform 2 of Bromodomain-containing protein 3				1,714			**1,714**
IPI00455383.4	Isoform 2 of Clathrin heavy chain 1	0,847	0,545	0,682	1,173	0,928	1,263	0,888
IPI00179057.6	Isoform 2 of Cullin-4B	0,598	**0,498**	0,731			1,146	**0,664**
IPI00878006.2	Isoform 2 of CWF19-like protein 2		1,016	1,675				1,345
IPI00375015.3	Isoform 2 of Deoxyuridine 5'-triphosphate nucleotidohydrolase, mitochondrial	0,421	0,408	0,434	1,974	2,068	1,747	1,090
IPI00006419.7	Isoform 2 of Diphthine synthase			0,977			0,700	0,838
IPI00552037.1	Isoform 2 of DNA polymerase eta				1,047			1,047
IPI00219251.1	Isoform 2 of Dual specificity tyrosine-phosphorylation-regulated kinase 1A	0,900	0,960	1,153	0,947	0,870	0,961	0,954
IPI00445401.4	Isoform 2 of E3 ubiquitin-protein ligase HUWE1	0,827	0,381	0,549	0,584	0,390	0,987	**0,567**
IPI00376283.1	Isoform 2 of E3 ubiquitin-protein ligase RBBP6						3,440	**3,440**

IPI00172474.3	Isoform 2 of E3 ubiquitin-protein ligase ZFP91	0,387	0,279	0,386	3,346		3,957	**0,387**
IPI00216201.1	Isoform 2 of Endophilin-A3	1,686						**1,686**
IPI00305013.4	Isoform 2 of FGFR1 oncogene partner		**0,357**	**0,367**	**2,186**		**2,158**	1,262
IPI00413958.5	Isoform 2 of Filamin-C	1,797	0,681	1,074	1,014	1,220	1,510	1,147
IPI00855962.1	Isoform 2 of FK506-binding protein 15			0,748	0,604			0,676
IPI00807514.1	Isoform 2 of Forkhead box protein K1				1,688	1,156		1,422
IPI00942874.1	Isoform 2 of G patch domain-containing protein 8		0,576	0,958	1,191			0,958
IPI00744232.2	Isoform 2 of G protein-regulated inducer of neurite outgrowth 1		0,612	0,499				**0,556**
IPI00411594.1	Isoform 2 of General transcription factor 3C polypeptide 3			0,560		0,466		**0,513**
IPI00293242.1	Isoform 2 of General transcription factor II-I				1,369	1,285		1,327
IPI00299506.9	Isoform 2 of Glucosamine--fructose-6-phosphate aminotransferase [isomerizing] 1	1,060	0,897	0,999	1,513	1,609	1,444	1,252
IPI00013290.5	Isoform 2 of Hepatoma-derived growth factor-related protein 2	0,788	0,612	0,838	1,063	1,093	1,083	0,951
IPI00219326.2	Isoform 2 of Host cell factor 1					4,533		**4,533**
IPI00937471.1	Isoform 2 of Importin-5			0,751			0,988	0,869
IPI00015103.2	Isoform 2 of Leucine-rich repeat flightless-interacting protein 2		0,735	0,924	0,605			0,735
IPI00552546.1	Isoform 2 of Mini-chromosome maintenance complex-binding protein		0,414	0,442	1,611		1,377	0,910
IPI00218498.3	Isoform 2 of Misshapen-like kinase 1		0,101					**0,101**
IPI00045729.5	Isoform 2 of MPN domain-containing protein					1,729		**1,729**
IPI00215844.1	Isoform 2 of N-acylethanolamine-hydrolyzing acid amidase			0,594				**0,594**
IPI00470922.2	Isoform 2 of N-alpha-acetyltransferase 50, NatE catalytic subunit			0,737				0,737
IPI00026466.9	Isoform 2 of Nipped-B-like protein						1,761	**1,761**
IPI00006196.3	Isoform 2 of Nuclear mitotic apparatus protein 1	0,597	0,311	0,978	1,680	1,063	2,253	1,020
IPI00477179.1	Isoform 2 of Nucleolar RNA helicase 2	1,810	0,793	1,440	1,542	0,994	2,284	1,491
IPI00940013.1	Isoform 2 of OTU domain-containing protein 5		**0,182**	**0,153**		**5,040**	**3,153**	**1,668**
IPI00827706.2	Isoform 2 of PHD and RING finger domain-containing protein 1		0,732			1,044	1,341	1,044
IPI00165547.1	Isoform 2 of Phosphatidylinositol 4-kinase beta						1,319	1,319
IPI00470497.3	Isoform 2 of Plasminogen activator inhibitor 1 RNA-binding protein	0,927	**3,585**	**2,509**	**7,138**		**2,772**	**2,772**
IPI00171199.5	Isoform 2 of Proteasome subunit alpha type-3		1,550	1,528			1,724	**1,550**
IPI00796836.2	Isoform 2 of Protein DDI1 homolog 2		0,550	0,668				**0,609**
IPI00148820.2	Isoform 2 of Protein deltex-3	0,034		0,028		35,150		**0,034**
IPI00410408.3	Isoform 2 of Protein FAM53B				0,785	0,781		0,783
IPI00760958.3	Isoform 2 of Protein PAT1 homolog 1			0,904	1,962		1,796	**1,796**
IPI00797421.3	Isoform 2 of Protein SDA1 homolog			0,732			1,576	1,154
IPI00301311.1	Isoform 2 of Protein SET		0,766	0,841				0,803
IPI00220716.2	Isoform 2 of Putative RNA-binding protein 15		1,242	2,637			3,477	**2,637**

IPI00410116.1	Isoform 2 of Ras-related protein Rab-36					1,127		1,127
IPI00743517.1	Isoform 2 of Receptor-type tyrosine-protein phosphatase S			0,785				0,785
IPI00154162.5	Isoform 2 of RNA polymerase-associated protein LEO1	0,631	0,476	0,592	0,946	0,947	0,819	0,725
IPI00915253.1	Isoform 2 of RNA-binding protein 10			0,475	1,908		4,704	**1,908**
IPI00061758.1	Isoform 2 of RNA-binding protein 33		1,111	2,047				**1,579**
IPI00216659.1	Isoform 2 of RNA-binding protein 8A						1,335	1,335
IPI00788942.1	Isoform 2 of RuvB-like 1		0,899	0,898			0,929	0,899
IPI00943982.1	Isoform 2 of SAM domain and HD domain-containing protein 1			0,661			2,464	**1,563**
IPI00412643.1	Isoform 2 of Serine/arginine-rich splicing factor 10			1,347			0,834	1,090
IPI00220552.1	Isoform 2 of Short transient receptor potential channel 6				0,628			**0,628**
IPI00843849.1	Isoform 2 of Small G protein signaling modulator 1		0,486					**0,486**
IPI00830039.1	Isoform 2 of Splicing factor U2AF 65 kDa subunit	1,341	0,649	0,843	1,075	0,811	1,312	0,959
IPI00654594.3	Isoform 2 of Striatin	0,794	0,747	1,008			1,053	0,901
IPI00150057.6	Isoform 2 of SWI/SNF complex subunit SMARCC2			0,298			3,385	**1,842**
IPI00926241.1	Isoform 2 of TBC1 domain family member 4	1,951	0,733	1,041	0,744	0,571	1,096	0,892
IPI00759607.1	Isoform 2 of Transcription elongation factor A protein-like 6	0,711	**0,311**					**0,511**
IPI00419473.5	Isoform 2 of Transcription factor BTF3	0,526	0,549	0,560	1,549	1,450	1,482	1,005
IPI00438230.3	Isoform 2 of Transcription intermediary factor 1-beta	0,687	0,492	0,849	1,027	0,960	1,402	0,905
IPI00177938.2	Isoform 2 of Transducin-like enhancer protein 3	0,695	**0,240**	**0,480**	1,218	0,964		0,695
IPI00655718.1	Isoform 2 of Transmembrane channel-like protein 8		0,360	0,666				**0,513**
IPI00640947.2	Isoform 2 of tRNA-dihydrouridine synthase 3-like		0,328	0,386				**0,357**
IPI00896474.3	Isoform 2 of Tumor protein D52	0,818	0,695	1,503	1,145	2,049	3,061	1,324
IPI00908769.1	Isoform 2 of U6 snRNA-associated Sm-like protein LSm5			0,706				0,706
IPI00607830.1	Isoform 2 of Uncharacterized protein CXorf38	0,388						**0,388**
IPI00398012.8	Isoform 2 of Uncharacterized protein KIAA1109	0,780						0,780
IPI00855947.1	Isoform 2 of UPF0485 protein C1orf144	**0,500**	0,486	0,467	2,480	2,508	2,410	1,455
IPI00760714.1	Isoform 2 of WD repeat and FYVE domain-containing protein 3	1,269	1,492				4,309	1,492
IPI00872729.1	Isoform 2 of WD repeat-containing protein 44	0,741	0,687	0,782	1,393	1,425	1,223	1,002
IPI00376222.1	Isoform 2 of YTH domain-containing protein 1	1,731	0,703	0,986	1,014	0,736	1,352	1,000
IPI00016472.4	Isoform 2 of Zinc finger CCCH domain-containing protein 13		1,152	2,208	1,612	0,968	1,927	**1,612**
IPI00219866.2	Isoform 2 of Zinc finger Ran-binding domain-containing protein 2	0,878	0,816	0,804	1,049	1,067	1,063	0,963
IPI00025333.4	Isoform 3 of Anamorsin	0,421	0,302	0,371	1,733	1,535	1,584	0,978
IPI00465449.3	Isoform 3 of Bifunctional protein NCOAT		0,289	0,431				**0,360**

IPI00910708.1	Isoform 3 of BRISC and BRCA1-A complex member 1		0,464	0,617				**0,541**
IPI00879552.1	Isoform 3 of C-Jun-amino-terminal kinase-interacting protein 4	0,772	0,601	0,803	2,024	1,317	1,056	0,929
IPI00979393.2	Isoform 3 of Calpastatin	0,459	0,423	0,616	1,435	1,589	1,465	1,025
IPI00915755.1	Isoform 3 of Coiled-coil domain-containing protein 66		0,648					**0,648**
IPI00185371.5	Isoform 3 of Cyclin-Y-like protein 1				1,008	0,724	0,674	0,724
IPI00411461.1	Isoform 3 of Disks large-associated protein 4			0,566			1,299	0,932
IPI00646605.3	Isoform 3 of E3 ubiquitin-protein ligase UBR4	1,725	0,481	0,772	1,237	0,843	1,725	1,040
IPI00477401.4	Isoform 3 of F-box/WD repeat-containing protein 9		0,427					**0,427**
IPI00015580.3	Isoform 3 of Formin-binding protein 1-like				0,498			**0,498**
IPI00045498.4	Isoform 3 of Heterogeneous nuclear ribonucleoprotein D-like			2,093				**2,093**
IPI00402391.3	Isoform 3 of Heterogeneous nuclear ribonucleoprotein U-like protein 1		0,442	0,676			1,390	0,676
IPI00759822.1	Isoform 3 of Heterogeneous nuclear ribonucleoproteins C1/C2		1,405	2,114	1,226	1,003		1,315
IPI00382733.2	Isoform 3 of Leucine-rich repeat flightless-interacting protein 1	**0,433**		0,752		1,573		0,752
IPI00220466.1	Isoform 3 of LIM domain and actin-binding protein 1	**2,255**	0,442	0,528	1,490	1,414	2,495	1,452
IPI00008449.1	Isoform 3 of Pre-mRNA 3'-end-processing factor FIP1		0,701	0,588	1,482	0,339	1,823	0,701
IPI00168431.1	Isoform 3 of Probable RNA-binding protein 23		0,333				2,604	1,469
IPI00304540.9	Isoform 3 of Protein FAM40A		**0,215**	**0,365**	1,559	1,383	1,643	1,383
IPI00982445.1	Isoform 3 of Remodeling and spacing factor 1	1,296	0,361	0,474	1,470	0,710	1,689	1,003
IPI00329545.7	Isoform 3 of RNA-binding protein 26			1,160			1,649	1,405
IPI00940890.1	Isoform 3 of RNA-binding protein 4		1,035	1,154				1,094
IPI00297407.6	Isoform 3 of Solute carrier family 45 member 4					1,357		1,357
IPI00923553.1	Isoform 3 of Spastin					0,810		0,810
IPI00929688.1	Isoform 3 of tRNA (guanine-N(7)-)-methyltransferase subunit WDR4			0,512				**0,512**
IPI00654621.1	Isoform 3 of Twinkle protein, mitochondrial		0,561					**0,561**
IPI00643818.2	Isoform 3 of UPF0667 protein C1orf55			0,221				**0,221**
IPI00386806.1	Isoform 3 of Zinc finger protein 503			0,327				**0,327**
IPI01009016.1	Isoform 4 of Cellular tumor antigen p53	0,971	0,570	0,682	2,102	1,888	2,191	1,430
IPI00921488.1	Isoform 4 of COP9 signalosome complex subunit 1						1,657	**1,657**
IPI00478744.3	Isoform 4 of DENN domain-containing protein 4C			1,346				1,346
IPI00956562.1	Isoform 4 of G-protein-signaling modulator 1		0,622	0,753	1,247	2,069	1,776	1,247
IPI00157364.2	Isoform 4 of Heparanase-2	1,781						**1,781**
IPI00470504.2	Isoform 4 of Inorganic pyrophosphatase 2, mitochondrial	0,733	0,790	0,816	1,224	1,283	1,121	0,969
IPI00376404.3	Isoform 4 of Nucleosome-remodeling factor subunit BPTF		0,308					**0,308**

IPI00446175.2	Isoform 4 of Protein FAM122B	0,614	0,587	0,659	1,866	2,267	2,130	1,262
IPI00941061.1	Isoform 4 of Protein kinase C-binding protein 1			0,728				0,728
IPI00384121.2	Isoform 4 of Protein NDRG2	0,851	0,895	0,934	1,102	1,086	0,817	0,915
IPI00397730.3	Isoform 4 of Protein phosphatase 1 regulatory subunit 12A				**4,749**			**4,749**
IPI00556406.1	Isoform 4 of Rab11 family-interacting protein 1			0,709		5,897		**3,303**
IPI00179121.4	Isoform 4 of Ran-binding protein 3	0,515	0,527	0,563	1,569	1,532	1,333	0,948
IPI00412748.4	Isoform 4 of Serine/threonine-protein kinase WNK1			0,403			2,020	1,211
IPI00514920.3	Isoform 4 of Serologically defined colon cancer antigen 3		0,622					**0,622**
IPI00654613.1	Isoform 4 of Tight junction-associated protein 1	**0,380**		1,168	**2,280**	1,868	1,585	**1,585**
IPI00219485.1	Isoform 4 of U1 small nuclear ribonucleoprotein 70 kDa	**2,825**	0,669	1,421	1,291	1,160	1,116	1,225
IPI00946257.1	Isoform 4 of Ubiquitin-associated protein 2-like	0,805	0,698	0,771	1,444	1,180	1,760	0,992
IPI00604660.4	Isoform 4 of Vacuolar protein sorting-associated protein 13A				7,695			**7,695**
IPI00651628.1	Isoform 4 of WD repeat domain phosphoinositide-interacting protein 2	0,710			1,062	1,125		1,062
IPI00922165.1	Isoform 5 of Adenylate kinase 2, mitochondrial		0,689	1,285				0,987
IPI00645818.2	Isoform 5 of Cdc42-interacting protein 4	**0,397**						**0,397**
IPI00216720.3	Isoform 5 of ELKS/Rab6-interacting/CAST family member 1				0,991			0,991
IPI00017290.4	Isoform 5 of Serine/threonine-protein phosphatase 4 regulatory subunit 3A			0,459				**0,459**
IPI00927582.2	Isoform 5 of Serrate RNA effector molecule homolog	0,784	0,250	0,399	2,562	1,812	2,724	1,298
IPI00386120.3	Isoform 6 of Splicing factor 1		**0,378**	**0,474**	**3,486**		**3,566**	**1,980**
IPI00953907.2	Isoform 6 of Tetratricopeptide repeat protein 21A					1,627		**1,627**
IPI00940810.2	Isoform 6 of Transcriptional regulator ATRX			1,090				1,090
IPI00165041.5	Isoform 6 of Treacle protein	0,665	0,514	0,844	1,583	1,159	1,626	1,002
IPI00396977.2	Isoform 7 of Nesprin-1	0,947						0,947
IPI00856046.1	Isoform 7 of Palladin		0,506					**0,506**
IPI00921857.1	Isoform 7 of Shootin-1		0,566			1,959		1,263
IPI00911101.1	Isoform 9 of Dysferlin		0,679					0,679
IPI00465365.4	Isoform A1-A of Heterogeneous nuclear ribonucleoprotein A1			1,881		0,731	1,216	1,216
IPI00414696.1	Isoform A2 of Heterogeneous nuclear ribonucleoproteins A2/B1		1,592	**2,179**	1,397	0,909	1,273	1,397
IPI00292387.6	Isoform Alpha of Nucleolar and coiled-body phosphoprotein 1	0,812	0,754	0,578	0,938	1,160	1,742	0,875
IPI00477001.3	Isoform Alpha of Striatin-3	0,738		0,646	1,368	1,216		0,977
IPI00215884.4	Isoform ASF-1 of Serine/arginine-rich splicing factor 1	2,144	0,598	0,919	1,331	0,946	1,622	1,139
IPI00215716.1	Isoform B of Band 4.1-like protein 3	0,605	0,612	0,758	1,483	1,613		0,758
IPI00179890.2	Isoform B of Ras GTPase-activating protein-binding protein 2		0,237	0,405			7,558	**0,405**

IPI00000156.3	Isoform Beta of DNA ligase 3		0,687	0,737			1,439	0,737
IPI00218993.1	Isoform Beta of Heat shock protein 105 kDa	0,832	0,771	0,839	1,316	1,315	1,220	1,029
IPI00233796.2	Isoform C of Oxysterol-binding protein-related protein 1				1,097			1,097
IPI00554556.1	Isoform C of Protein CutA			0,563			1,779	1,171
IPI00794625.1	Isoform C of Xin actin-binding repeat-containing protein 1	0,083						**0,083**
IPI00413075.1	Isoform C5 of CMP-N-acetylneuraminate-beta-1,4-galactoside alpha-2,3-sialyltransferase				3,093			**3,093**
IPI00607674.1	Isoform D2 of DNA damage-binding protein 2	2,155	0,766		1,661		2,842	**1,908**
IPI00010882.3	Isoform DFF45 of DNA fragmentation factor subunit alpha (Fragment)	0,467	0,398	0,455	1,902	1,911	1,811	1,139
IPI00386533.4	Isoform E of Eukaryotic translation initiation factor 4 gamma 1	1,801	0,783	2,147	0,630	0,426	1,353	1,068
IPI00218621.2	Isoform E of Protein SON	1,735	0,653	1,041	1,348	1,221	1,628	1,285
IPI00942246.1	Isoform Ex1B-2-3 of AMP deaminase 2	0,918	1,422	1,137	1,535	1,854	1,245	1,333
IPI00220031.2	Isoform Gamma of Paxillin		0,206					**0,206**
IPI00179700.3	Isoform HMG-I of High mobility group protein HMG-I/HMG-Y	**2,231**	0,658	1,310	3,009	0,508	1,004	1,157
IPI00005614.6	Isoform Long of Spectrin beta chain, brain 1	0,823	0,475	0,524	1,197	0,973	1,640	0,898
IPI00013891.1	Isoform Long of Transformer-2 protein homolog alpha			0,861			1,697	1,279
IPI00432416.4	Isoform LYN B of Tyrosine-protein kinase Lyn			1,185				1,185
IPI00479186.7	Isoform M2 of Pyruvate kinase isozymes M1/M2	0,836	0,794	1,144		1,795	1,998	1,144
IPI00759806.1	Isoform MBP-1 of Alpha-enolase		0,846	0,751			1,340	0,846
IPI00216393.1	Isoform Non-brain of Clathrin light chain A	1,044	0,822	0,921	0,996	1,140		0,996
IPI00216472.1	Isoform Non-brain of Clathrin light chain B					1,271		1,271
IPI00335168.9	Isoform Non-muscle of Myosin light polypeptide 6						1,564	**1,564**
IPI00337465.6	Isoform P of Kinesin light chain 1	1,184	1,207	1,844	1,630	2,014	1,696	**1,663**
IPI00218185.3	Isoform p69 of 2'-5'-oligoadenylate synthase 2		0,971					0,971
IPI00940182.1	Isoform PML-6 of Protein PML				3,369			**3,369**
IPI00759832.1	Isoform Short of 14-3-3 protein beta/alpha		0,893	0,721			0,811	0,811
IPI00020194.1	Isoform Short of TATA-binding protein-associated factor 2N	**2,668**	**2,140**	**2,210**		0,815	0,889	**2,140**
IPI00335824.5	Isoform Short of Tight junction protein ZO-1						1,426	1,426
IPI00218408.1	Isoform Short of Trifunctional purine biosynthetic protein adenosine-3		0,579					**0,579**
IPI00375145.1	Isoform Short of Ubiquitin carboxyl-terminal hydrolase 5				1,414	2,596	1,004	1,414
IPI00009598.1	Isoform SMN-delta57 of Survival motor neuron protein	1,484	1,534	1,512		0,784		1,498
IPI00413654.3	Isoform SRP40-4 of Serine/arginine-rich splicing factor 5	1,955	0,697	0,897	1,457		1,843	1,457
IPI00012345.2	Isoform SRP55-1 of Serine/arginine-rich splicing factor 6	0,789	0,452	0,659	1,415	1,106	1,672	0,947
IPI00974544.1	Isoform SV of 14-3-3 protein epsilon		0,773	0,867			1,191	0,867

IPI00759817.1	Isoform TAFII15 of Transcription initiation factor TFIID subunit 12			0,915			2,328	**1,621**
IPI00306749.8	Kanadaptin	0,814	0,798	0,897	1,137	0,979	1,016	0,938
IPI01013038.1	kinesin-like protein KIF21A isoform 4				1,268	1,299		1,283
IPI00219217.3	L-lactate dehydrogenase B chain		0,963	0,687			1,108	0,963
IPI00514141.2	La ribonucleoprotein domain family, member 5		0,469	0,680			2,308	0,680
IPI00395536.4	La-related protein 7	0,718	0,654	0,692	1,104	1,343	1,635	0,911
IPI00217975.4	Lamin-B1	**0,230**		**0,274**	0,964	1,021		**0,619**
IPI00884965.1	Leucine zipper protein 6				0,902			0,902
IPI00783271.1	Leucine-rich PPR motif-containing protein, mitochondrial		1,010	1,105			0,964	1,010
IPI00069309.6	Leucine-rich repeat and WD repeat-containing protein 1			0,652				**0,652**
IPI00024292.2	Low-density lipoprotein receptor-related protein 2		0,923					0,923
IPI00658031.1	LUC7-like			1,075				1,075
IPI00009032.1	Lupus La protein	0,702	0,673	0,634	1,201	1,221	1,077	0,889
IPI00293276.10	Macrophage migration inhibitory factor			1,148			1,053	1,101
IPI00291006.2	Malate dehydrogenase, mitochondrial		0,783	1,076		1,225	1,122	1,099
IPI00641181.5	MARCKS-related protein	0,625	1,040	1,187	1,647	**2,653**	**3,076**	1,417
IPI00006108.3	Mastermind-like protein 1		0,027					**0,027**
IPI01015100.1	Membrane-associated progesterone receptor component 2		0,846	0,897	**2,036**	1,803	**2,122**	**1,803**
IPI00008240.2	Methionyl-tRNA synthetase, cytoplasmic		1,193	0,832			2,160	1,193
IPI00004795.1	Methylosome subunit pICln	0,614	0,526	0,606	1,522	1,573	1,461	1,037
IPI00022790.2	Microfibrillar-associated protein 1	1,123	0,751	0,892	1,062	0,851	1,012	0,952
IPI00008868.4	Microtubule-associated protein 1B	0,622	0,579	0,584	1,621	1,596	2,200	1,109
IPI00977503.1	midline-1 isoform 5			0,681		1,175	2,014	1,175
IPI00163729.8	MKL1 protein		0,423	0,369				**0,396**
IPI00873776.1	MORC family CW-type zinc finger 2, isoform CRA_a		0,489					**0,489**
IPI00386826.1	Mutant internexin alpha						2,112	**2,112**
IPI00924816.1	Myotrophin		0,992	1,070			0,970	0,992
IPI00219301.7	Myristoylated alanine-rich C-kinase substrate	**0,497**	0,835	0,621	3,629	4,799	4,445	**2,232**
IPI00000760.1	N(G),N(G)-dimethylarginine dimethylaminohydrolase 2		**0,450**					**0,450**
IPI00003527.5	Na(+)/H(+) exchange regulatory cofactor NHE-RF1	**0,466**	**0,307**	**0,461**	1,386	1,541	1,439	0,926
IPI00016802.1	NAD-dependent deacetylase sirtuin-1	0,436	0,259	0,321	1,799	1,709	1,878	1,073
IPI00953272.1	NADH dehydrogenase [ubiquinone] 1 alpha subcomplex subunit 11 isoform 2					2,847		**2,847**
IPI00604676.1	NEDD8-activating enzyme E1 regulatory subunit isoform b			0,779			1,285	1,032
IPI00868727.1	neurofilament medium polypeptide isoform 2	0,378	0,378	0,460	2,413	2,192	2,123	1,291
IPI00296934.3	NF-kappa-B-activating protein	1,086	0,992	1,180	2,027	2,213	2,308	**1,603**

IPI00257910.8	NHS-like protein 2	1,587						**1,587**
IPI00295022.6	NK-tumor recognition protein		0,834		0,843			0,838
IPI00002349.2	Nuclear fragile X mental retardation-interacting protein 2			**2,781**				**2,781**
IPI00031812.3	Nuclease-sensitive element-binding protein 1	1,233	0,978	0,963	1,433	1,099	1,561	1,166
IPI00411886.5	Nucleolar complex protein 2 homolog	**2,966**		1,552	0,796		1,799	**1,676**
IPI00015808.3	Nucleolar GTP-binding protein 2			1,145				1,145
IPI00303813.5	Nucleolar protein 11		0,848					0,848
IPI00411937.4	Nucleolar protein 56		0,773	0,933	0,256		1,258	0,853
IPI00006379.1	Nucleolar protein 58	2,092	0,508	1,066	1,250	1,031	1,949	1,158
IPI00604620.3	Nucleolin	1,096	0,743	0,897	1,015	0,845	1,113	0,956
IPI00023860.1	Nucleosome assembly protein 1-like 1	0,689	0,618	0,663	1,159	1,215	1,451	0,924
IPI00941463.1	Nucleosome assembly protein 1-like 4	0,735	0,619	0,642	1,153	1,151	1,106	0,920
IPI00449112.3	OGFR protein	**0,484**	0,452	0,474	1,573	1,426	1,520	0,955
IPI00168954.1	Olfactory receptor 2Z1			1,449				1,449
IPI00955490.1	ornithine aminotransferase, mitochondrial isoform 2		0,951				1,047	0,999
IPI00024971.1	Oxysterol-binding protein 1	0,615	1,098					0,856
IPI00032970.2	Oxysterol-binding protein-related protein 11			0,690		0,846	1,121	0,846
IPI00815656.1	Parathymosin (Fragment)		0,755	0,510				**0,632**
IPI00001600.1	PAXIP1-associated protein 1	**0,281**	**0,320**	**0,173**	**2,034**	1,958		**0,320**
IPI00010414.4	PDZ and LIM domain protein 1						1,039	1,039
IPI00419585.9	Peptidyl-prolyl cis-trans isomerase A	0,787	0,887	0,956		1,177	1,209	0,956
IPI00219005.3	Peptidyl-prolyl cis-trans isomerase FKBP4	0,871	0,804	1,000	1,043	1,151	1,067	1,022
IPI00642862.1	Peptidyl-prolyl cis-trans isomerase-like 4	0,334	0,249	0,366	3,789	3,153	3,709	**1,759**
IPI00917094.1	periphilin-1 isoform 8					0,726		0,726
IPI00000874.1	Peroxiredoxin-1	0,762	0,802	1,031		1,039	1,119	1,031
IPI00011937.1	Peroxiredoxin-4		1,046	1,023			0,780	1,023
IPI00220301.5	Peroxiredoxin-6			0,993		1,095	0,835	0,993
IPI00169383.3	Phosphoglycerate kinase 1	0,613	0,694	0,656	1,571	1,698	1,257	0,976
IPI00549725.6	Phosphoglycerate mutase 1	0,864	0,734	0,689	1,034	1,517	1,265	0,949
IPI00004534.5	Phosphoribosylformylglycinamidine synthase	0,818		0,858	1,264	1,087	1,527	1,087
IPI00216694.3	Plastin-3		0,839	0,896			1,042	0,896
IPI00016610.2	Poly(rC)-binding protein 1	1,140	0,466	0,829		1,144	1,531	1,140
IPI00556157.1	Polypyrimidine tract-binding protein 1 isoform c variant (Fragment)		1,029		1,275		1,532	1,275
IPI00007928.4	Pre-mRNA-processing-splicing factor 8						2,164	**2,164**
IPI00177381.9	Pre-mRNA-splicing factor CWC22 homolog					0,633		**0,633**
IPI00329791.20;IPI00329791.18	Probable ATP-dependent RNA helicase DDX46		0,655	1,109			1,448	1,109

IPI00006907.1	Probable fructose-2,6-bisphosphatase TIGAR			0,505	1,008			0,757
IPI00216691.5	Profilin-1	0,877	0,761	0,837		1,219	1,103	0,877
IPI00647084.2	programmed cell death protein 4 isoform 3	0,746	0,322	0,279	0,475	0,345	0,746	**0,410**
IPI00023640.3	Programmed cell death protein 5		1,088	0,885				0,987
IPI00021700.3	Proliferating cell nuclear antigen	0,959	0,974	0,844		1,193	0,711	0,959
IPI00871914.1	Proline/serine-rich coiled-coil 1			0,853				0,853
IPI00645836.1	Protein	3,331						**3,331**
IPI00983370.1	Protein			0,112			4,963	**2,538**
IPI00917894.1	Protein	3,782	1,689	2,326	0,966	0,574		**1,689**
IPI01015406.1	Protein	**3,133**	1,750	**2,002**	1,372	0,972	0,648	**1,561**
IPI00982610.1	Protein			1,409			1,545	1,477
IPI00965916.1	Protein	0,596		0,568	1,563	1,453	1,636	1,453
IPI00916835.1	Protein			1,289		1,224	**2,329**	1,289
IPI00977382.1	Protein		1,656		0,881			1,269
IPI00965503.1	Protein		1,248	1,604			0,994	1,248
IPI00978820.1	Protein	**0,166**	1,200		**4,734**			1,200
IPI01011358.1	Protein		0,831	1,123	1,003	1,255	1,456	1,123
IPI00974117.1	Protein			0,953				0,953
IPI00966209.1	Protein	0,736	0,443	0,498	1,501	1,158	1,452	0,947
IPI00946758.1	Protein					0,920		0,920
IPI00924569.2	Protein	0,835						0,835
IPI00968281.1	Protein	0,720		0,833				0,777
IPI00981611.1	Protein		0,694	0,824				0,759
IPI00984011.1	Protein			0,699				0,699
IPI00926623.1	Protein			0,643				**0,643**
IPI00979197.1	Protein			0,639				**0,639**
IPI00915964.1	Protein		0,509	0,582				**0,545**
IPI00743454.2	Protein ACN9 homolog, mitochondrial		1,047	0,941			0,774	0,941
IPI00328702.2	Protein C9orf140				1,157	0,741		0,949
IPI00009904.1	Protein disulfide-isomerase A4			0,795				0,795
IPI00298547.3	Protein DJ-1		0,883	0,881				0,882
IPI00061087.3	Protein FAM122A	**0,412**	0,430	0,602	2,628	3,237	1,307	0,955
IPI00746221.2	Protein FAM195B						0,812	0,812
IPI00009900.1	Protein FAM53C				0,922	1,014	0,824	0,922
IPI00887373.1	Protein kinase C delta VIII (Fragment)						3,667	**3,667**
IPI01012363.1	Protein kinase C, alpha variant (Fragment)				1,275		1,569	1,422
IPI00398998.3	Protein lin-52 homolog				1,022			1,022
IPI00746326.1	Protein phosphatase 1G variant (Fragment)			1,190				1,190

IPI00244512.2	Protein shisa-2 homolog			1,323				1,323
IPI00220835.7	Protein transport protein Sec61 subunit beta			2,291	5,000		14,783	**5,000**
IPI00643781.1	PSIP1 protein		1,591	1,843		0,929	1,145	1,368
IPI00749509.4	Putative 3-phosphoinositide-dependent protein kinase 2	0,924			1,137	0,921		0,924
IPI00745182.1	Putative uncharacterized protein DKFZp434N101 (Fragment)						0,838	0,838
IPI01014299.1	Putative uncharacterized protein DKFZp667D2317			0,901				0,901
IPI00477803.4	Putative uncharacterized protein DKFZp781L0540 (Fragment)	1,110	0,781	0,967			1,354	1,039
IPI00955815.2	pyruvate dehydrogenase E1 component subunit alpha, somatic form, mitochondrial isoform 4 precursor		0,368	0,308			0,365	**0,365**
IPI00009544.3	RalA-binding protein 1	**0,494**	**0,431**	**0,449**			**2,297**	**0,471**
IPI00294879.1	Ran GTPase-activating protein 1	**0,253**		**0,283**	**4,365**	**3,383**		**1,833**
IPI00012442.1	Ras GTPase-activating protein-binding protein 1	1,834	0,935	1,260	1,274	0,831	1,686	1,267
IPI00410411.4	regulatory-associated protein of mTOR isoform 2		0,410	0,568		1,386	1,702	0,977
IPI00883897.1	RELA protein			0,498			1,714	1,106
IPI00241238.3	retinal dehydrogenase 2 isoform 3			0,954			1,317	1,135
IPI00647914.6	Retinoblastoma binding protein 7			0,608			1,590	1,099
IPI00003815.3	Rho GDP-dissociation inhibitor 1		0,876	0,916		1,525		0,916
IPI00000077.1	Ribonuclease H1		0,686	0,758				0,722
IPI00293331.3	Ribonucleases P/MRP protein subunit POP1	1,533	1,230		1,487	1,272		1,380
IPI00946732.1	Ribonucleoside-diphosphate reductase subunit M2			0,245				**0,245**
IPI00795224.1	Ribosomal protein S27					1,089		1,089
IPI00028276.5	RING finger protein unkempt homolog	0,611	0,556	0,607		1,757		**0,609**
IPI00556514.1	RNA binding motif protein 14 variant (Fragment)		1,245	1,696	1,241	0,285	2,442	1,245
IPI00873171.2	RNA polymerase II, heptapeptide repeat, eukaryotic containing protein			0,281				**0,281**
IPI00477468.1	RNA polymerase-associated protein CTR9 homolog	0,884	0,529	0,605	1,015	0,863	1,828	0,874
IPI00556485.2	RPLP0 protein		2,526	2,749				**2,637**
IPI00642046.1	RSL1D1 protein	1,731	0,761	0,667	0,842	0,620	1,334	0,802
IPI00300631.3	Scaffold attachment factor B1			1,737	2,279	1,968	0,954	**1,852**
IPI01009380.1	SEC16A protein (Fragment)	0,647	0,757	1,013	1,587		1,336	1,013
IPI00929107.1	Seipin isoform 1			0,712	1,956	1,648	2,703	**1,802**
IPI00909681.1	Serine hydroxymethyltransferase	1,037	0,875	0,854			1,094	0,956
IPI00003176.1	Serine protease HTRA1					1,384		1,384
IPI00942141.1	Serine/arginine-rich splicing factor 12			0,859				0,859
IPI00010204.1	Serine/arginine-rich splicing factor 3	2,763	0,816	1,228	0,865	0,664	1,077	0,971
IPI00000015.2	Serine/arginine-rich splicing factor 4		0,522	0,656	1,415	0,741	1,495	0,741
IPI00012340.1	Serine/arginine-rich splicing factor 9		0,338	0,468	0,742	0,603	1,439	**0,603**

IPI00304742.5	Serine/threonine-protein kinase 10			1,400	1,360		1,826	1,400
IPI00303797.3	Serine/threonine-protein kinase B-raf	0,705	0,521	0,631	1,466	1,377	1,852	1,041
IPI00031410.1	Serine/threonine-protein kinase mTOR	1,026	0,602		1,047		1,079	1,036
IPI00171336.3	Serine/threonine-protein kinase RIO1			0,815				0,815
IPI00479399.3	Serine/threonine-protein kinase ULK2		0,602					**0,602**
IPI00304493.5	Serum response factor-binding protein 1		0,851	1,099	1,776	1,352	1,831	1,352
IPI00737869.3	Similar to RNA-binding protein with serine-rich domain 1		0,428	0,648			1,364	**0,648**
IPI00739666.2	Similar to Splicing factor, arginine/serine-rich, 46kD				0,704		1,212	0,958
IPI00844203.1	Similar to t-complex 1		1,467					1,467
IPI00744563.1	Similar to X-linked retinopathy protein protein	**3,196**						**3,196**
IPI00607645.5	Sin3 histone deacetylase corepressor complex component SDS3			0,093	3,790		3,303	**3,303**
IPI00029744.1	Single-stranded DNA-binding protein, mitochondrial			1,119			0,904	1,011
IPI00154515.3	Smad nuclear-interacting protein 1		0,296	0,477	1,387	1,226	1,630	1,226
IPI00013949.1	Small glutamine-rich tetratricopeptide repeat-containing protein alpha		**0,464**	0,507	1,813	1,937	1,371	1,371
IPI00029266.1	Small nuclear ribonucleoprotein E			1,161			1,172	1,167
IPI00745893.2	small ubiquitin-related modifier 2 isoform b precursor	0,727	0,745	1,084	0,873	0,832	0,847	0,840
IPI00909967.1	Soluble PDGFRb variant 1					1,125		1,125
IPI00398431.2	Splice variant of four and a half LIM domain protein 2			0,121				**0,121**
IPI00303343.8	Splicing factor, arginine/serine-rich 19	0,415	0,393	0,541	3,597	3,161	4,043	**1,851**
IPI00009922.3	SRA stem-loop-interacting RNA-binding protein, mitochondrial			0,964	0,999			0,981
IPI00013894.1	Stress-induced-phosphoprotein 1		0,773	0,795	1,103		1,311	0,949
IPI00032957.1	SUMO-conjugating enzyme UBC9			0,771				0,771
IPI00218733.6	Superoxide dismutase [Cu-Zn]		0,826	0,965			0,982	0,965
IPI00018037.3	Surfeit locus protein 2		0,248	0,547			1,132	**0,547**
IPI00059242.3	Synapse-associated protein 1	0,563	0,476	0,442	1,296	1,289	1,212	0,887
IPI00329332.1	Syntaxin-12	1,033			1,090			1,061
IPI00297779.7	T-complex protein 1 subunit beta		1,516	1,427		1,012	1,744	1,472
IPI01015038.1	T-complex protein 1 subunit delta					0,966		0,966
IPI00952607.1	T-complex protein 1 subunit eta isoform d		1,643	1,552	2,407	1,025	2,179	**1,643**
IPI00549516.3	Target of EGR1 protein 1	**2,419**	0,904	1,202	**2,790**	**2,371**		**2,371**
IPI00008961.1	Telomeric repeat-binding factor 2-interacting protein 1	0,547	0,325	0,433	0,991	0,920	1,035	0,733
IPI00016912.1	Tetratricopeptide repeat protein 1	0,925			1,219		1,268	1,219
IPI00018208.2	Tetratricopeptide repeat protein 33		0,492	0,580			1,372	**0,580**
IPI00374151.1	thioredoxin-dependent peroxide reductase, mitochondrial isoform b		0,817			1,117		0,967
IPI00550243.2	THUMP domain-containing protein 1	0,867	0,689	0,747	1,186	1,284	1,126	0,997

IPI00830089.1	Thymopoietin zeta isoform	1,233	0,368	0,695		1,154		0,924
IPI00220827.5	Thymosin beta-10		0,632					**0,632**
IPI00555619.1	Thyroid hormone receptor interactor 3 variant (Fragment)		0,380					**0,380**
IPI00104050.3	Thyroid hormone receptor-associated protein 3	2,956	0,557	0,745	1,006	0,743	1,049	0,876
IPI00940872.2	Titin, isoform CRA_a	**0,110**		1,220		0,571		**0,571**
IPI00009146.4	TRAF-type zinc finger domain-containing protein 1	**0,486**	0,346	0,497	1,779	1,406	1,466	0,952
IPI00008965.1	Transcription factor AP-1	1,138	0,883	0,882	0,911	1,460	1,493	1,024
IPI00844417.2	transcription factor BTF3 homolog 4 isoform 2	**0,473**	**0,472**	**0,479**			1,932	**0,476**
IPI00002135.1	Transforming acidic coiled-coil-containing protein 3	**0,293**	**0,207**	**0,278**			**3,396**	**0,285**
IPI00556200.1	Transforming growth factor, beta 2 variant (Fragment)			0,120				**0,120**
IPI00022774.3	Transitional endoplasmic reticulum ATPase		0,595					**0,595**
IPI00942979.1	Transketolase			1,429			1,191	1,310
IPI00001159.11	Translational activator GCN1	0,862						0,862
IPI00000171.1	TSC22 domain family protein 4		**0,249**	**0,439**			1,693	**0,439**
IPI00930688.1	Tubulin alpha-1B chain		0,639	0,965		1,497	1,156	1,060
IPI00007752.1	Tubulin beta-2C chain	0,971	**0,498**	0,993			1,033	0,982
IPI00007074.5	Tyrosyl-tRNA synthetase, cytoplasmic		0,849	0,792			1,181	0,849
IPI00914628.2	Ubiquitin carboxyl-terminal hydrolase	0,919	**0,376**		0,687	**0,431**	1,460	0,687
IPI00030915.1	Ubiquitin carboxyl-terminal hydrolase 8				4,204			**4,204**
IPI00305442.3	Ubiquitin-associated domain-containing protein 1						2,005	**2,005**
IPI00783378.3	Ubiquitin-conjugating enzyme E2 O	0,383	0,276	0,446	2,780	2,100	1,971	1,209
IPI00793209.1	Ubiquitin-like 7 (Bone marrow stromal cell-derived), isoform CRA_a			0,593				**0,593**
IPI00645078.1	Ubiquitin-like modifier-activating enzyme 1	0,809	0,703	0,731	1,162	1,253	1,310	0,985
IPI00048500.14	UBX domain-containing protein 2B			0,461				**0,461**
IPI00909419.2	UMP-CMP kinase isoform b		0,741	0,950	1,018		1,058	0,984
IPI00979280.1	Uncharacterized protein		**0,100**	**0,161**	**8,409**	**11,271**	**7,018**	**7,018**
IPI00965354.1	Uncharacterized protein				3,490			**3,490**
IPI00644832.1	Uncharacterized protein						3,332	**3,332**
IPI00915766.1	Uncharacterized protein					3,038		**3,038**
IPI00793175.1	Uncharacterized protein			2,861	2,041	3,282	2,930	**2,896**
IPI00964419.1	Uncharacterized protein	**0,431**				5,058		**2,745**
IPI01013081.1	Uncharacterized protein					2,524		**2,524**
IPI00966126.1	Uncharacterized protein			1,482			2,907	**2,194**
IPI00983195.2	Uncharacterized protein	2,171	0,943	1,181	2,343		3,564	**2,171**
IPI00658205.1	Uncharacterized protein				2,086	1,718		**1,902**
IPI00927261.2	Uncharacterized protein			0,640			3,151	**1,896**

IPI00794746.1	Uncharacterized protein						1,806	**1,806**
IPI01013392.1	Uncharacterized protein						1,802	**1,802**
IPI00944900.1	Uncharacterized protein				**2,051**	1,450		**1,751**
IPI00893035.1	Uncharacterized protein	1,941	0,897	0,839	1,869	1,595	2,178	**1,732**
IPI00514557.4;IPI01014263.1	Uncharacterized protein	1,636	1,220		1,714	1,999	**3,358**	**1,714**
IPI00946858.1	Uncharacterized protein	1,460	0,468	0,636	2,447	1,867	2,330	**1,663**
IPI00967721.1	Uncharacterized protein	**2,203**	1,016	1,418	1,763	1,124	2,409	**1,591**
IPI00643790.1	Uncharacterized protein	0,644			1,649	1,585		**1,585**
IPI00792186.4	Uncharacterized protein		0,557	0,729	3,277	1,584	3,814	**1,584**
IPI00926886.2	Uncharacterized protein	1,572						**1,572**
IPI00642023.2	Uncharacterized protein				1,444	1,699		**1,571**
IPI00926274.2	Uncharacterized protein	1,569	1,464	1,847	1,642		1,485	**1,569**
IPI01012872.1	Uncharacterized protein		0,602	0,735	1,566	1,638	2,118	**1,566**
IPI00844501.3	Uncharacterized protein						1,522	**1,522**
IPI00939811.2	Uncharacterized protein	2,527	0,760	0,649	1,742	1,289	3,552	**1,515**
IPI00976589.1	Uncharacterized protein	1,500	0,929	1,084	1,668	1,435	2,028	1,467
IPI00967112.1	Uncharacterized protein			1,522			1,356	1,439
IPI00514496.2	Uncharacterized protein	1,878	0,752	1,026	1,584	1,276	1,915	1,430
IPI00940393.3	Uncharacterized protein	1,067	1,427	1,636		1,269	1,609	1,427
IPI00552198.1	Uncharacterized protein	0,621	1,126	0,964	1,625	2,624	2,017	1,375
IPI00894514.1	Uncharacterized protein			1,226			1,459	1,342
IPI01013778.1	Uncharacterized protein		0,626	1,331			1,789	1,331
IPI00940315.1	Uncharacterized protein			1,326	1,259			1,293
IPI00797536.1	Uncharacterized protein	0,434	0,321	0,413	2,211	2,147	2,555	1,290
IPI00965952.1	Uncharacterized protein	1,916	1,204	1,183	1,374	1,083	1,422	1,289
IPI00878409.4	Uncharacterized protein					1,269		1,269
IPI00983716.1	Uncharacterized protein		0,710	0,832	1,304	1,268	1,375	1,268
IPI00964686.1	Uncharacterized protein		1,239					1,239
IPI01012543.1	Uncharacterized protein	0,687	0,881	0,935	1,681	2,274	1,516	1,225
IPI00982782.1	Uncharacterized protein	1,148	0,807	0,955	1,591	1,300	1,758	1,224
IPI00741317.2	Uncharacterized protein						1,210	1,210
IPI00965022.1	Uncharacterized protein			1,142	1,252	1,382	1,011	1,197
IPI00927696.1	Uncharacterized protein	1,194	0,952	1,186	1,314	1,101	1,546	1,190
IPI01010871.1	Uncharacterized protein		1,189	1,385			0,878	1,189
IPI00924637.1	Uncharacterized protein						1,181	1,181
IPI00872495.3	Uncharacterized protein	1,406	0,661	0,977	1,355	1,167		1,167
IPI00412260.3	Uncharacterized protein	1,154	0,753	0,940		1,553	2,643	1,154

IPI00644764.1	Uncharacterized protein	1,325	0,409	0,682	1,511	0,977	1,936	1,151
IPI00386569.3	Uncharacterized protein	0,559	0,488	0,554	1,781	1,850	1,732	1,146
IPI00945081.1	Uncharacterized protein			0,484			1,804	1,144
IPI00964519.2	Uncharacterized protein				1,129			1,129
IPI00385434.2	Uncharacterized protein	1,404	1,140	1,341	1,025	0,980	1,094	1,117
IPI00644786.3	Uncharacterized protein	0,286	0,255	0,315	1,900	2,377	2,063	1,107
IPI00981537.1	Uncharacterized protein						1,092	1,092
IPI01009237.1	Uncharacterized protein	**0,420**	0,843	0,984	1,682	1,654	1,185	1,085
IPI00945873.1	Uncharacterized protein	0,359	0,446	0,434	2,922	1,997	1,711	1,078
IPI00916861.1	Uncharacterized protein					1,066		1,066
IPI00440719.2	Uncharacterized protein	0,591	0,627	0,659	1,577	1,455	1,524	1,057
IPI00975678.1	Uncharacterized protein	0,729	0,563	0,721	1,694	1,374	1,579	1,051
IPI00399306.1	Uncharacterized protein		1,037	1,024		1,608		1,037
IPI00915772.1	Uncharacterized protein				1,033			1,033
IPI00981208.1	Uncharacterized protein	0,922		0,930	1,067	1,028	1,304	1,028
IPI00917908.1	Uncharacterized protein	2,277	0,451	0,885	1,159	0,744	1,360	1,022
IPI00981271.2	Uncharacterized protein	0,719	0,764	0,777	1,259	1,256	1,464	1,017
IPI00063234.1	Uncharacterized protein	0,598	0,504	0,597	1,549	1,435	1,761	1,017
IPI00981943.1	Uncharacterized protein	1,015	0,931	1,041	0,781	1,015	1,120	1,015
IPI00789576.1	Uncharacterized protein		1,010	0,877			1,781	1,010
IPI00645452.1	Uncharacterized protein	0,848	0,706	0,965	1,509	1,249	1,045	1,005
IPI00917313.1	Uncharacterized protein	0,893	0,947	1,008	1,135	1,227	0,991	1,000
IPI00925387.1	Uncharacterized protein	0,965	0,801	0,839	1,022	1,324	1,387	0,993
IPI00924436.1	Uncharacterized protein	0,980	0,597	0,982	1,000	1,103	1,205	0,991
IPI00910594.2	Uncharacterized protein			1,008			0,953	0,980
IPI01010320.1	Uncharacterized protein	1,153	0,830	0,992	0,952	0,885	0,970	0,961
IPI00641842.1	Uncharacterized protein	1,178	0,527	0,861	1,139	0,876	1,034	0,955
IPI00968273.1	Uncharacterized protein					0,954		0,954
IPI00966664.1	Uncharacterized protein			0,822			1,082	0,952
IPI00945782.1	Uncharacterized protein			0,951		1,269	0,880	0,951
IPI00879132.1	Uncharacterized protein	0,716	0,520	0,626	1,186	1,203	1,449	0,951
IPI00915960.1	Uncharacterized protein		0,459	0,824	1,676	0,944	1,574	0,944
IPI00979937.1	Uncharacterized protein		0,904	1,765	0,956	0,921		0,938
IPI00908669.2	Uncharacterized protein		0,656			1,216		0,936
IPI01014177.1	Uncharacterized protein	0,642	0,867	1,035	0,969	0,899	0,971	0,934
IPI01013377.1	Uncharacterized protein		0,692	0,933	1,469			0,933
IPI00979898.1	Uncharacterized protein	0,880	0,734	0,784	1,411	0,972	1,126	0,926
IPI00975879.1	Uncharacterized protein	0,739	0,638	0,724	1,187	1,249	1,111	0,925

IPI01014561.1	Uncharacterized protein	0,924	0,531	0,746		1,077	1,153	0,924
IPI00552768.1	Uncharacterized protein	0,847	0,845	0,900	0,934	0,996	1,030	0,917
IPI00916480.1	Uncharacterized protein	0,892	0,857	0,910		1,111	0,985	0,910
IPI00981414.1	Uncharacterized protein	0,652	0,593	0,559	1,216	1,355	1,157	0,904
IPI00976642.1	Uncharacterized protein	**2,809**	0,573	0,806	0,990	0,728	1,102	0,898
IPI00927947.1	Uncharacterized protein	0,527	0,501	0,593	1,194	1,304	1,108	0,850
IPI00893301.1	Uncharacterized protein		0,843	0,702	1,019	0,660	1,624	0,843
IPI00791836.2	Uncharacterized protein	0,894	0,420	0,558	1,084	0,788	1,087	0,841
IPI00964945.1	Uncharacterized protein		0,782	0,960			0,823	0,823
IPI00981739.1	Uncharacterized protein	0,764	0,826	0,805			1,058	0,815
IPI00964635.1	Uncharacterized protein		0,696	0,815		1,346		0,815
IPI00924536.1	Uncharacterized protein		0,682				0,924	0,803
IPI01012731.1	Uncharacterized protein		0,791					0,791
IPI00396183.3	Uncharacterized protein			0,789				0,789
IPI00965923.1	Uncharacterized protein			0,785				0,785
IPI00925601.1	Uncharacterized protein		0,849	0,720				0,785
IPI00964123.1	Uncharacterized protein	0,625	0,485	0,555	0,933	0,998	1,091	0,779
IPI00967963.1	Uncharacterized protein		0,657	0,765			1,278	0,765
IPI00470523.6	Uncharacterized protein	0,757	0,749		1,804			0,757
IPI00877996.1	Uncharacterized protein	0,751		0,599			1,236	0,751
IPI00925085.1	Uncharacterized protein		0,749	0,693				0,721
IPI00925813.1	Uncharacterized protein	0,714	0,416	0,447		2,567	3,057	0,714
IPI01010953.1	Uncharacterized protein		0,702					0,702
IPI00980240.1	Uncharacterized protein		0,693					0,693
IPI00953224.1	Uncharacterized protein	0,680		0,609		1,300		0,680
IPI00797126.4;IPI00797126.2	Uncharacterized protein	0,585	0,679	0,685				0,679
IPI00927677.1	Uncharacterized protein					0,676		0,676
IPI00981738.1	Uncharacterized protein	0,645	0,617	0,648	1,419	0,871		**0,648**
IPI00973989.1	Uncharacterized protein	1,031	0,466	0,666	0,625	0,571	1,038	**0,646**
IPI00927101.1	Uncharacterized protein		0,633					**0,633**
IPI00979793.1	Uncharacterized protein		0,445	0,712		0,518	1,104	**0,615**
IPI00982231.1	Uncharacterized protein		0,471	0,708				**0,590**
IPI00853290.2	Uncharacterized protein	0,553	0,300	0,588		1,480	1,829	**0,588**
IPI00827831.3	Uncharacterized protein		0,201	0,561			1,532	**0,561**
IPI00947525.1	Uncharacterized protein	0,284	0,334	0,510	0,671	0,631	0,605	**0,557**
IPI00926736.1	Uncharacterized protein			0,512	0,595	0,597	0,458	**0,553**
IPI00916489.1	Uncharacterized protein			0,553				**0,553**

IPI01013635.1	Uncharacterized protein	0,692	**0,220**	**0,307**	0,652	0,722	**0,450**	**0,551**
IPI00178047.7	Uncharacterized protein		0,326	0,519			2,462	**0,519**
IPI00984156.1	Uncharacterized protein	0,479	0,448	0,452	2,096	1,824		**0,479**
IPI00968125.1	Uncharacterized protein			0,477				**0,477**
IPI00945303.1	Uncharacterized protein			0,475				**0,475**
IPI00892609.2	Uncharacterized protein	0,439						**0,439**
IPI00964116.1	Uncharacterized protein		0,410					**0,410**
IPI01015928.1	Uncharacterized protein		**0,270**	**0,397**			1,391	**0,397**
IPI00894075.1	Uncharacterized protein	**0,353**						**0,353**
IPI01012252.1	Uncharacterized protein	0,184	0,124	0,191			3,463	**0,188**
IPI00642131.2	Uncharacterized protein			0,169				**0,169**
IPI00106955.3	Uncharacterized protein C11orf84	0,299	0,210	0,332	2,350	2,054	1,852	1,092
IPI00032506.2	Uncharacterized protein C14orf142	0,736	0,644	0,708			1,301	0,722
IPI00166692.3	Uncharacterized protein C2orf57						1,380	1,380
IPI00398117.7	Uncharacterized protein C6orf222						2,242	**2,242**
IPI00550191.2	Uncharacterized protein C9orf78	0,379	0,407	0,521	2,497	3,020	3,141	**1,509**
IPI00410618.4	Uncharacterized protein KIAA1143	**0,321**	0,528	0,534			**2,816**	**0,531**
IPI00107104.1	UPF0368 protein Cxorf26		0,631					**0,631**
IPI00008219.1	UV excision repair protein RAD23 homolog A	**0,354**		**0,496**	**2,691**	**2,846**	1,710	**1,710**
IPI00021396.1	Vascular endothelial growth factor receptor 2	0,013						**0,013**
IPI00418471.6	Vimentin	0,791	0,783	0,851	1,015	0,858	1,042	0,855
IPI00513835.1	WD repeat and HMG-box DNA-binding protein 1 isoform 2						1,917	**1,917**
IPI00640954.2	WD repeat domain 42A	0,608	**0,500**	0,530		1,519	1,697	**0,608**
IPI00220834.8	X-ray repair cross-complementing protein 5			0,868				0,868
IPI01012297.1	XPO4 protein		0,418					**0,418**
IPI00009326.2	Yes-associated protein beta			2,355				**2,355**
IPI00384180.4	YrdC domain-containing protein, mitochondrial			0,257			3,832	**2,045**
IPI00555885.1	ZFYVE19 protein variant (Fragment)	**0,456**	**0,315**	0,548	0,897	1,193		**0,548**
IPI00187011.4	Zinc finger CCCH domain-containing protein 4		**0,195**	0,630		**5,759**	**5,671**	**3,151**
IPI00917827.2	Zinc finger E-box binding homeobox 2					0,688		0,688
IPI00064212.2	Zinc finger protein 828			1,191				1,191
IPI00043565.4	Zinc finger protein 830		1,161					1,161